



UNIVERSIDAD DE SEVILLA

CONSEJO SUPERIOR DE INVESTIGACIONES CIENTÍFICAS

Departamento de Química Inorgánica

Instituto de Investigaciones Químicas

**Synthesis, Structure and Some Catalytic
Applications of Platinum Complexes with Terphenyl
Phosphine Ligands**

Laura Ortega Moreno

Tesis Doctoral

Sevilla 2016

Synthesis, Structure and Some Catalytic Applications of Platinum Complexes with Terphenyl Phosphine Ligands

Por

Laura Ortega Moreno

Trabajo presentado para aspirar
al Título de Doctora en Química
Sevilla, 2016

Laura Ortega Moreno

Directores de Tesis:

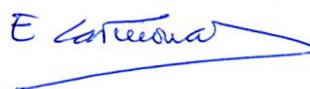


Riccardo Peloso

Profesor Ayudante de Doctor

Química Inorganica

Universidad Sevilla



Ernesto Carmona Guzmán

Catedrático

Química Inorganica

Universidad de Sevilla

A la madre que me ciclometaló

A mi padre

A mi hermano

ACKNOWLEDGEMENTS

We gratefully acknowledge the following contributions to this Thesis:

- ^{195}Pt NMR studies by Prof. Juan Forniés, University of Zaragoza (Spain).
- Support on catalytic assays by Dr. Andrés Suárez, Consejo Superior de Investigaciones Científicas (Sevilla).
- X-ray diffraction studies by Dr. Celia Maya, University of Sevilla.
- Support on DFT calculations and NMR experiments by Joaquín López-Serrano, University of Sevilla.

Se acaba la etapa del doctorado para mí. Muchos dicen que es una de las etapas de la vida más bonitas y entrañables que recordar. Si echo la vista atrás, a mí no me cabe ninguna duda, puesto que no solo ha sido un aprendizaje a nivel académico o profesional sino también a nivel personal durante los últimos 4 años. He pulido mi carácter, a veces un tanto brusco, y he aprendido a controlar mis impulsos, a pensar dos veces antes de abrir la boca y a empatizar con el resto de personas que me rodean. Todo esto se lo debo agradecer a todas y cada una de las maravillosas personas que he conocido aquí en Sevilla y que de una manera u otra son partícipes de esta Tesis.

En primer lugar me gustaría plasmar mi agradecimiento al Prof. Ernesto Carmona, uno de mis directores de Tesis, puesto que fue él el que sin apenas conocerme me ofreció la posibilidad de empezar un nuevo proyecto de investigación en su grupo. Le agradezco no solo la confianza depositada en mí, sino también las palabras de ánimo y cariño que siempre he escuchado de él. Le agradezco también el tiempo dedicado a esta tesis puesto que siempre tenía una nueva idea o enfoque para la química que he desarrollado, demostrando una vez más su dedicación absoluta a la investigación. Por todo ello, GRACIAS Ernesto!

A la tarea de director de tesis se sumó algo más tarde Riccardo Peloso. A él le agradezco todos los consejos tanto fuera como dentro del laboratorio y estando siempre con una sonrisa en la cara e irradiando felicidad y positivismo. Ha sabido compaginar los esfuerzos en la investigación en el laboratorio con las recompensas fuera de él. Siempre me voy a acordar de las noches de charlas con rissotto en tu casa y las correcciones de la Tesis mordisqueadas por su conejo. Eres grande y único. Gracias Ric!

Pese a que no ha sido uno de mis directores de Tesis le agradezco todos los esfuerzos por intentar entender mi química a Manolo Poveda. Gracias por todos esos momentos a mi lado cogiendo papel y bolígrafo para explicarme cualquier duda que me surgiera y por hacerme “pensar” de vez en cuando. También quiero agradecerle los intentos por endulzarme el humor a base de Ferrero-Rocher, pipas peladas y quicos.

Es inevitable echar una vista atrás y recordar a todos los compañeros de laboratorio que estaban aquí cuando llegué y que fueron acabando y desperdigándose por el mundo en el periodo de mi Tesis. Voy a empezar por agradecer a los antiguos habitantes del Laboratorio 9: Marta, Jesús, Orestes, Crispín y Ana Zamorano, puesto que ese fue mi primer “hábitat” al llegar a Sevilla. Gracias por crear un ambiente tan bueno de trabajo y por amenizarlo todo con unas risas y una cerveza al salir del instituto. Del Laboratorio 1-2 tengo que agradecer todos los momentos compartidos a Giovanni (un italiano la mar de “salao”), Mario, Ana Lozano, Irene (mi flamenca achinada), Yohar y Ángela (la niña de mis ojos). No me puedo olvidar de las niñas del 10-11 Conchi y Mónica.

Ahora sí que sí, toca agradeceros vuestra paciencia “máxima” a todos y cada uno de mis compañeros. Empezaré por los del Laboratorio 1-2. Me gustaría empezar este repaso con Carlos, o también conocido como “Papote Malote”, dado que el laboratorio no es lo mismo sin ti y sin tus bromas y buen rollo. Juanjo, su ojito derecho y unas de las últimas incorporaciones al laboratorio. Mi “Morrocan Queen” (también conocida como Natalia para el resto) que es todo corazón y que no hay cosa con la que no te ayude. Mi Marifé, la primera persona que conocí, incluso antes de llegar a Sevilla, y que hemos trabajado codo a codo en el laboratorio y hasta incluso vivido juntas durante más de un año. A ella le agradezco su comprensión en mis malos momentos y las alegrías compartidas.

Quiero agradecer también a los doctorandos del laboratorio 3-4. Entre ellos se encuentra John (el colombiano más bailongo y simpático que jamás haya conocido), Carmen (la chica que supo compaginar una tesis con ponerse en forma en el gimnasio), Elena (la dulzura personificada) y Astrid (mi granadina favorita y una técnica que vale para todo dentro y fuera del laboratorio, una todo terreno).

Siguiendo el recorrido por los laboratorios tengo que pararme en el Lab 9 y 10-11 donde se han incorporado nuevas adquisiciones del grupo en los que se encuentran Martín, Félix, Práxedes (o también conocido como “miarma”), Pablo y Leonardo. Agradeceros el apoyo y los ánimos recibidos, sobretudo en esta etapa final de la Tesis. Como olvidarme de Eire y Pedro, que aunque estuvieron solo unos pocos meses de estancia en nuestro centro han dejado mella en todos nosotros.

Este grupo también cuenta con los mejores jefes y PostDocs que me gustaría agradecer su participación tanto en la tesis como en la mejoría de mi estancia estos años aquí en Sevilla. Salva y Amor, como decirlo?... Sois increíbles fuera y dentro del laboratorio. Os agradezco mucho la confianza depositada en mí. A Patricia, Nuria y Laura deciros que sois un ejemplo a seguir y agradeceros enormemente vuestra simpatía y ganas de ayudar al prójimo tanto en lo que se refiere a burocracia, como a la química como fuera de los menesteres de la investigación. A Margarita Paneque gracias por cuidar de cada uno de nosotros incluso cuando hay volantes de trajes de flamenca por en medio. A Joaquín le tengo que agradecer todos los consejos y ayuda no solo en cálculos y RMN (que no es poco) sino también por su tiempo fuera del laboratorio. A Luis Sánchez, gran experto de gases del grupo, le agradezco enormemente su ayuda en todo lo relacionado con manorreductores, conexiones y sistemas de secado de gases.

No me puedo olvidar de los técnicos de los equipos del instituto. En primer lugar le agradezco a Flo por los esfuerzos titánicos realizados en sacar los análisis elementales de los compuestos sensibles y también por las visitas exprés a la casa rural junto a su familia. A Fran por su inestimable ayuda tanto en todo lo que se refiere a los problemas con los programas informáticos (licencias) como con el gases-masas. A Margarita, la secretaria, le agradezco su destreza con todo lo que se refiere a burocracia y su simpatía constante.

Ampliando las fronteras de la química organometálica debo agradecer también a mis compañeros de los laboratorios orgánicos (Ainhoa, Rocío, Javi, José Juan, Pedro, Abel, Rute, M^a José, Ana, Pepe, Arcadio) por hacer que esa frontera sea cada vez más difusa y por el buen ambiente creado en los comedores y en las cenas de navidad.

Porque la tesis no es solo el laboratorio sino que también es un momento para abrir la mente en todos los sentidos y disfrutar de la vida, quiero también mostrar mi agradecimiento a esas extrañas personitas que me han hecho mucho más llevadera la estancia aquí en Sevilla fuera del instituto. Estoy pensando en Lilian, mi mejicana favorita, a los niños de Jerez, Miriam y Javi que tienen todo el arte que le corre por las venas, a Miguel, que aunque seas del Madrid no eres malo del todo, y a Andrea! Muchas gracias chicos por compartir vuestro tiempo conmigo.

Estos agradecimientos no se entenderían sin mencionar a mis amigas de Pineda y cercanías, que pese a estar tanto tiempo distanciadas siempre hemos encontrado un momento para seguir en contacto y transmitirnos el afecto mutuo que tenemos. Estoy refiriéndome a Deby, Rosa, Lorena y Sara. Sois increíbles amigas y mejores personas. Gracias por vuestras llamadas y cariño (incluida alguna que otra escapadita al sur).

Estos agradecimientos no tendrían ningún sentido si no incluyera también a mi familia. Mis padres y hermano han sido siempre un pilar fundamental en mi vida, pero el hecho de vivir lejos de ellos durante este periodo de tiempo me ha hecho apreciarlos aún más si cabe. Ellos me han hecho tal y como soy, se lo debo absolutamente todo a ellos. Gracias por el apoyo, los ánimos y vuestro incondicional amor. Me gustaría también agradecer a mis abuelos el cariño recibido no solo en esta etapa sino en todas las de mi vida. GRACIAS FAMILIA!

TABLE OF CONTENTS

Abbreviations	1
Consideraciones Generales	5
Publications	11
Summary of Compounds	13
Abstract	17
 Chapter I.	
I.1. INTRODUCTION	23
<i>I.1.1. A brief historical preface</i>	23
<i>I.1.2. Introductory comments</i>	31
I.2. RESULTS AND DISCUSSION	45
<i>I.2.1. Pt(II) Complexes of the o-Xylyl Substituted</i> <i>PMe₂Ar^{Xyl}₂ Ligand</i>	45
I.2.1.1. Bis(phosphine) Pt(II) Complexes	46
I.2.1.2. Mono(phosphine) Pt(II) Platinacycles.	
Synthesis and Reactivity	58
I.2.1.3. Protonation of Complexes 2 and 3	63
<i>I.2.2. Pt(II) Complexes of the terphenylphosphines</i> <i>PMe₂Ar^{Dipp}₂ and PMe₂Ar^{Tipp}₂</i>	68
I.2.2.1. Neutral Pt(II) Complexes with Bidentate (κ^1 -P, η^1 -arene) Phosphine Coordination	69
Dichloro Complexes	69

Dimethyl Complexes [PtMe ₂ (PMe ₂ Ar')]	
Methyl Chloride Species [PtMe(Cl)(PMe ₂ Ar ^{Dipp2})]	72
The Diphenyl Complex [PtPh ₂ (PMe ₂ Ar ^{Dipp2})]	80
Silyl Hydride Complexes	82
Recapitulation of Structural Data Pertaining	
Neutral Pt(II) Complexes with Bidentate	
Phosphine Coordination	89
I.2.2.2. Forcing Monodentate P-Coordination of the	
Phosphine. Reactivity Towards Lewis Bases	92
The Allyl Platinum(II) Complex	
[Pt(η ³ -C ₃ H ₅)Br(PMe ₂ Ar ^{Dipp2})]	98
I.2.2.3. Cationic Unsaturated Pt(II) Complexes that Exhibit	
Bidentate (κ ¹ -P, η ¹ -arene) Phosphine Coordination	101
· Cationic Monochloride and Related	
· Dicationic Complexes	101
· Cationic Complexes with Platinum to Carbon	
Sigma Bonds. Methyl and Phenyl Derivatives	114
· Reactivity of <i>cis</i> -[PtMe(PMe ₂ Ar ^{Dipp2})] ⁺ (20·S)	
towards dihydrogen	134
· The Phenyl Cationic Complex	
[PtPh(py)(PMe ₂ Ar ^{Dipp2})][BArF] (22)	139
· Reactivity of <i>cis</i> -[PtMe(S)(PMe ₂ Ar ^{Dipp2})] ⁺ (20·S)	
towards <i>cis</i> -[PtMe ₂ (PMe ₂ Ar ^{Dipp2})] (8)	141

I.2.2.4. Reactivity of the Cationic Platinum(II) Methyl Complex [PtMe(PMe ₂ Ar ^{Dipp} ₂)(S)] ⁺ (20•S) towards C ₂ H ₄ and C ₂ H ₂ . A Combined Experimental and Computational Study.	146
I.2.2.5. Some Catalytic studies	167
Hydroarylation of alkynes	167
Hydroamination of terminal alkynes	170
I.3. EXPERIMENTAL SECTION	173
<i>I.3.1. General Considerations</i>	173
<i>I.3.2. Synthesis and Characterisation of the New Complexes Obtained</i>	174
<i>I.3.3. Kinetic Studies on the Cyclometallation of Complex 2</i>	243
<i>I.3.4. Reaction of complexes 2 and 3 with [H(Et₂O)₂][BAr_F]</i>	244
<i>I.3.5. Characterisation of detected intermediates in the formation of complex 24</i>	244
<i>I.3.6. Reaction of 20•S with H₂ and D₂</i>	246
<i>I.3.7. Computational Details</i>	246
<i>I.3.8. 1D Selective EXSY Experiments</i>	248
<i>I.3.9. General Method for Catalytic Hydroarylation of Alkynes</i>	256
<i>I.3.10. General Method for Catalytic Hydroamination of Alkynes</i>	256
I.4. BIBLIOGRAPHY	257
 Chapter II	
II.1. PREFACE	273
II.2. INTRODUCTION	277

II.3. RESULTS AND DISCUSSION	289
<i>II.3.1. Synthesis of Pt(0)-olefin Complexes</i>	289
<i>II.3.2. Reactivity of Pt(0)-olefin Complexes</i>	312
II.3.2.1. Reactivity towards CO	312
II.3.2.2. Reactivity towards Protonation	315
II.3.2.3. Oxidative Addition of Allylbromides	319
<i>II.3.3. Catalytic Hydrosilylation of Alkynes</i>	322
II.4. EXPERIMENTAL SECTION	329
<i>II.4.1. General Considerations</i>	329
<i>II.4.2. Synthesis and Characterisation of the New Complexes</i>	
<i>Obtained</i>	330
<i>II.4.3. General Method for Catalytic Hydrosilylation of Alkynes</i>	347
II.5. BIBLIOGRAPHY	349
 Conclusiones	 355

ABBREVIATIONS

Me	methyl, -CH ₃
Et	ethyl, -CH ₂ CH ₃
ⁱ Pr	<i>iso</i> -propyl, CH(CH ₃) ₂
^t Bu	<i>tert</i> -butyl, -C(CH ₃) ₃
Ph	phenyl, -C ₆ H ₅
Dipp	2,6-diisopropylphenyl, 2,6- ⁱ Pr ₂ C ₆ H ₃
Tipp	2,4,6-triisopropylphenyl, 2,4,6- ⁱ Pr ₃ C ₆ H ₂
Xyl	xylyl, 2,6-(CH ₃) ₂ C ₆ H ₃
Ar'	aryl
Ar ^{Xyl} ₂	2,6-Xyl ₂ C ₆ H ₃
Ar ^{Dipp} ₂	2,6-Dipp ₂ C ₆ H ₃
Ar ^{Tipp} ₂	2,6-Tipp ₂ C ₆ H ₃
THF	tetrahydrofuran, C ₄ H ₈ O
Et ₂ O	diethyl ether, CH ₃ CH ₂ OCH ₂ CH ₃
CH ₃ CN	acetonitrile
NHC	N-heterocyclic carbene
L	2 electron donor ligand
κ	ligand hapticity
η	number of atoms of carbon directly bound to a metal center
ν	infrared vibrational frequency (cm ⁻¹)
h	hours
min	minutes
equiv.	equivalents

atm	atmospheres
K_{eq}	equilibrium constant
k	rate constant
$t_{1/2}$	half-life
Anal. Calc.	analysis calculated
Exp.	Experimental
d_n	number of deuterium atoms in a molecule
g	grams
mmol	millimol
mL	millilitre
cm	centimetre
Å	Angstrom
°	degree
C	Celsius
K	Kelvin
M	molar concentration
Ref.	reference
p	page
vol	volume
ORTEP	crystallographic representation (Oak Ridge Thermal Ellipsoid Program)
IR	infrared
e^-	electron
HRMS	high resolution mass spectrometry
ESI	electrospray

NMR Abbreviations

NMR	Nuclear Magnetic Resonance
δ	chemical shift
ppm	parts per million
NOESY	Nuclear Overhauser Enhancement Spectroscopy
COSY	^1H - ^1H correlation spectroscopy
HSQC	Correlation spectroscopy (Heteronuclear Single Quantum Coherence)
HMBC	Correlation spectroscopy (Heteronuclear Multiple Bond Correlation)
S	singlet
d	doublet
t	triplet
q	quartet
setp	septet
m	multiplet
<i>o</i>	<i>ortho</i>
<i>m</i>	<i>meta</i>
<i>p</i>	<i>para</i>
br	broad
$^nJ_{\text{AB}}$	coupling constant between A and B nuclei separated by n bonds
Hz	Hertz

CONSIDERACIONES GENERALES

La investigación científica tiene como misión fundamental generar nuevo conocimiento, en las fronteras de la ciencia actual, que conduzca a una mejor comprensión de la naturaleza y que además contribuya a solucionar las necesidades presentes y futuras de la sociedad.

La investigación química, en particular, se enfrenta en nuestro tiempo a grandes retos, puesto que su actuación se extienda a múltiples y muy variadas parcelas de la vida ordinaria, en las que debe desarrollar procesos y tecnologías sostenibles, es decir, transformaciones limpias y eficaces, de bajo consumo energético que produzcan ínfimas cantidades de residuos. Así, la investigación química presente no se circunscribe a áreas estrictamente relacionadas con esta disciplina, a saber, a la síntesis química inorgánica u orgánica y a las aplicaciones directas de estas moléculas o materiales, sino que se adentra en campos como la agricultura, la cosmética, los productos farmacéuticos, los nuevos materiales de importantes aplicaciones prácticas, o la búsqueda de fuentes alternativas de energía, entre otros trascendentes desafíos.

Una de las grandes campos de actuación de la Química moderna es la química organometálica, que se centra en el estudio del metal-carbono, y que por ello se sitúa en la divisoria, en la región fronteriza, de los dos grandes territorios clásicos de esta ciencia, la química inorgánica y la orgánica. Aunque la disciplina es en rigor mucho más antigua, el

desarrollo real de la química organometálica que propició su extraordinario avance hasta alcanzar la posición preferente que la caracteriza en nuestros días, se produjo en los primeros años de la década de 1950, y estuvo fuertemente influido por los trabajos pioneros de las escuelas de E.O. Fischer y G. Wilkinson, como se reconoció en el Premio Nobel de Química de 1973, concedido a estos dos grandes investigadores “*for their pioneering work, performed independently, on the chemistry of the organometallic, so called sandwich compounds*”. En fechas recientes (2009), un muy destacado representante de la química organometálica del último cuarto del siglo XX, el profesor Helmut Werner de la Universidad de Würzburg (Alemania), ha publicado una rigurosa, al tiempo que amena, monografía, de lectura muy recomendable, que ilustra el desarrollo y la evaluación de la química organometálica durante el pasado siglo hasta nuestros días, y su influencia en otras áreas de la Química y en la industria química: “*Landmarks in Organo-Transition Metal Chemistry, A Personal View*” (Springer Science, 2009).

En la actualidad se conocen infinidad de compuestos organometálicos de naturaleza muy diversa, muchos de los cuales exhiben reactividad química sin precedentes, que en no pocos casos ha llevado al desarrollo de procesos industriales que, en última instancia, han contribuido de forma notoria a mejorar la calidad de nuestra vida. Existen asimismo múltiples aplicaciones de los compuestos organometálicos en procesos relacionados con la vida, en la denominada química bioinorgánica, o en su variante bioorganometálica, como agentes antitumorales o con otros fines biológicos, así como en el desarrollo de nuevos materiales y en otras importantes áreas de la química actual. Su influencia en el desarrollo de la catálisis homogénea ha sido de tal transcendencia que tres grandes campos de esta disciplina han sido

distinguidos por *The Royal Swedish Academy of Sciences* con la concesión de otros tantos Premios Nobel:

- 2001 a W. S. Knowles, R. Noyori and K. B. Sharples, “*for their work on chirally catalysed hydrogenation and oxidation reactions*”
- 2005 a Y. Chauvin, R. H. Grubbs and R. R. Schrock, “*for the development of the metathesis method in organic synthesis*”
- 2010 a R. F. Heck, E. Negishi and A. Suzuki, “*for palladium-catalysed cross coupling in organic synthesis*”

En esta memoria se presentan y discuten resultados que por su naturaleza se encuadran en las líneas de investigación que desarrolla el grupo de Química Organometálica y Catálisis Homogénea del Instituto de Investigaciones Químicas (Centro mixto Universidad de Sevilla – Consejo Superior de Investigaciones Científicas), y en particular en la que se concierne al estudio de la activación de moléculas pequeñas y de enlaces C—H mediante complejos de metales de la mena del platino, considerándose en esta Tesis exclusivamente este metal noble. Como se analiza con el debido detalle en secciones posteriores, la atención investigadora se concentra en compuestos organometálicos de platino que contienen ligandos auxiliares de tipo fosfina terciaria con gran impedimento estérico, como resultado de la presencia de un radical terfenilo muy voluminoso unido directamente al átomo de fósforo. Estos ligandos permiten estabilizar estructuras complejas de bajo número de coordinación y como consecuencia con una importante insaturación electrónica. Además de los propios complejos de platino se describen los pertinentes estudios de reactividad, y los de caracterización estructural, estos últimos por aplicación de técnicas espectroscópicas (RMN de ^1H , ^{13}C y ^{31}P , mono y bidimensionales) o de difracción de rayos X, que se han

completado mediante determinaciones analíticas, bien de análisis elemental o de espectrometría de masas de alta resolución. Las determinaciones cristalográficas se han llevado a cabo de manera independiente a este trabajo por la Dra. Celia Maya (Universidad de Sevilla).

La Tesis consta de dos capítulos, cada uno de los cuales se estructura de la forma habitual: introducción, resultados y discusión y parte experimental. Para facilitar su lectura, la bibliografía aparece tanto a pie de página como al final de cada uno de los capítulos, de forma independiente. La numeración de esquemas, figuras, tablas y la numeración de los compuestos es asimismo independiente en cada uno de ellos.

Como parte del programa del programa de Formación del Personal Investigador (FPI), he realizado una estancia de cuatro meses de duración (de junio a octubre de 2013) en la Universidad de Oxford bajo la supervisión del Profesor Andrew S. Weller. El interés que he tenido siempre por la catálisis homogénea me llevó a considerar que esta estancia podría ser muy beneficiosa para mi formación científica. Durante estos cuatro meses, desarrollé trabajos de investigación sobre la hidroboración de alquenos con fosfinoboranos, empleando el fragmento Rh-Xantphos como catalizador.

La mencionada estancia es un prerequisite para optar a la mención de Doctor Internacional (RD99/2011, BOE-10-02-2011, Art. 15). Con objeto de obtener dicha mención, la mayor parte de la Tesis debe redactarse en un idioma extranjero. Por esta razón, los Capítulos 1 y 2 se han escrito en inglés, mientras que las Consideraciones Generales y las Conclusiones, se han redactado en español.

Una parte comparativamente menor de los resultados obtenidos se ha publicado ya, mientras que otras secciones están todavía inéditas. La relación de los artículos derivados del presente trabajo se presenta en la

sección *Publications*. A esta parte le sigue una relación de compuestos (*Summary of Compounds*) obtenidos y caracterizados a lo largo de esta Tesis.

PUBLICATIONS

Reactivity of cationic agostic and carbene structures derived from platinum (II) metallacycles. Campos, J.; Ortega-Moreno, L.; Conejero, S.; Peloso, R.; Lopez-Serrano, J.; Maya, C.; Carmona, E. *Chem. Eur. J.* **2015**, *21*, 8883-8896.

Platinum (0) olefin complexes of a bulky terphenylphosphine ligand. Synthetic, structural and reactivity studies. Ortega-Moreno, L.; Peloso, R.; Maya, C.; Suárez, A.; Carmona, E. *Chem. Commun.* **2015**, *51*, 17008-17011.

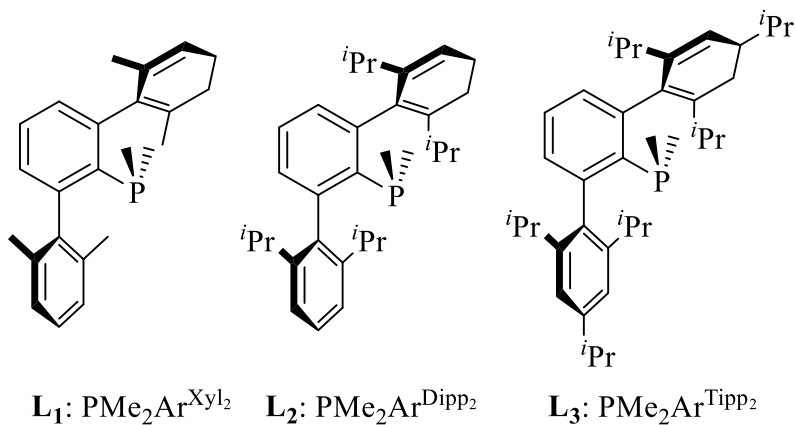
Synthesis, Properties, and Some Rhodium, Iridium, and Platinum Complexes of a Series of Bulky m-Terphenylphosphine Ligands. Ortega-Moreno, L.; Fernández-Espada, M.; Moreno, J. J.; Navarro-Gilabert, C.; Campos, J.; Conejero, S.; López-Serrano, J.; Maya, C.; Peloso, R.; Carmona, E. *Polyhedron*, **2016**, Accepted.

Other Research Articles not Directly Related with the PhD Thesis

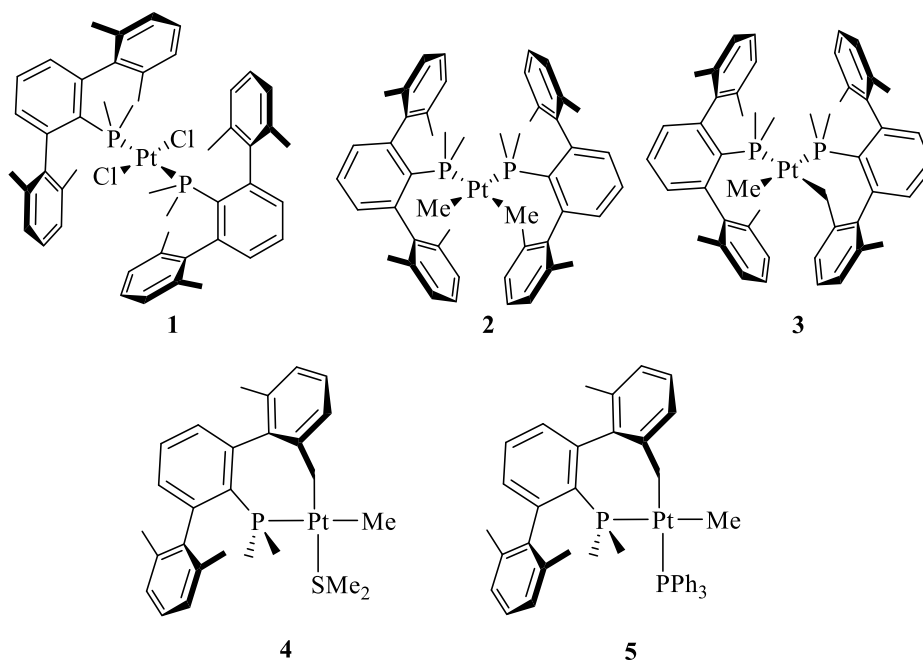
NH₂ as a directing group: from the cyclopalladation of amino estersto preparation of benzolactams by palladium(II)-catalyzed carbonylation of N-unprotected aryethylamines. Albert, J.; Ariza, X.; Calvet, T.; Font-Bardia, M.; Garcia, J.; Granell, J.; Lamela, A.; López, B.; Martinez, M.; Ortega, L.; Rodriguez, A.; Santos, D. *Organometallics*, **2013**, *32*, 649-659.

Exploring the mechanism of the hydroboration of alkenes by amine-boranes catalysed by [Rh(xantphos)]⁺. Johnson, H. C.; Torry-Harris, R.; Ortega, L.; Theron, R.; McIndoe, J. S.; Weller, S. A.; *Catal. Sci. Technol.*, **2014**, *4*, 3486-3494.

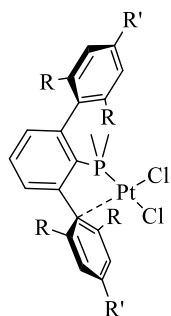
LIGANDS



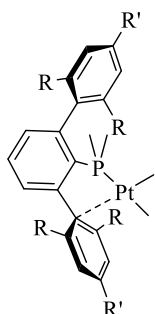
CHAPTER I



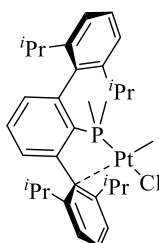
CHAPTER I (cont.)



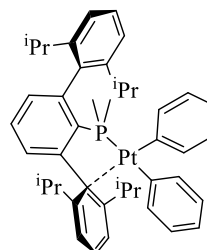
6: R = *i*Pr, R' = H
7: R = R' = *i*Pr



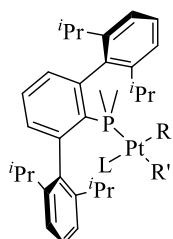
8: R = *i*Pr, R' = H
9: R = R' = *i*Pr



10



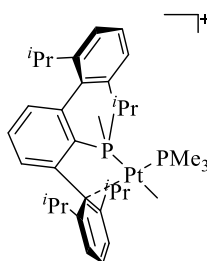
11



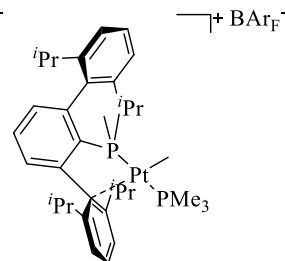
6·L (L = CO, PPh₃): R=R'=Cl

8·L (L = CO, PMe₃): R=R'=Me

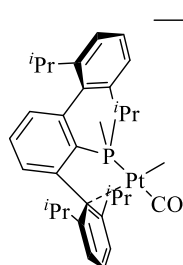
10·L (L = CO, PPh₃): R=Me, R'=Cl



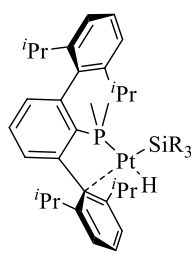
Cis-8·PMe₃⁺



Trans-8·PMe₃⁺



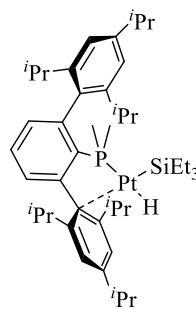
8·CO⁺



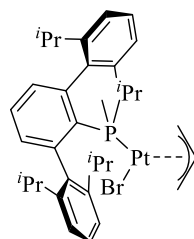
12a: R₃ = Et₃

12b: R₃ = Ph₃

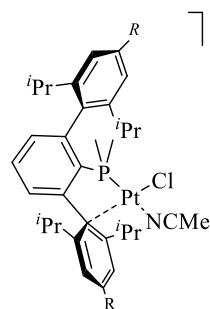
12c: R₃ = MePh₂



13

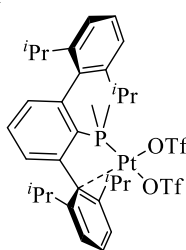


14



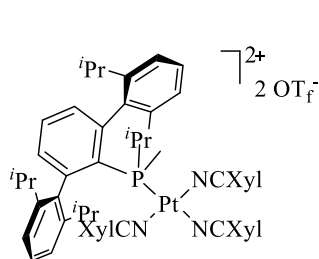
15·NCMe: R = H, X = SbF₆

16·NCMe: R = *i*Pr, X = BAr_F

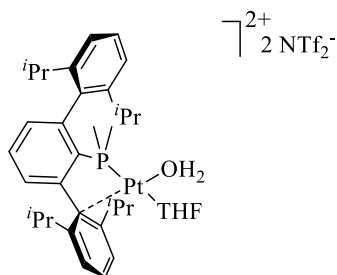


17

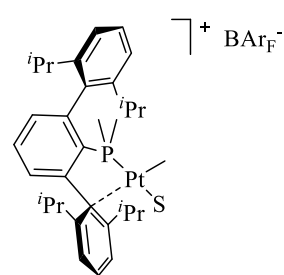
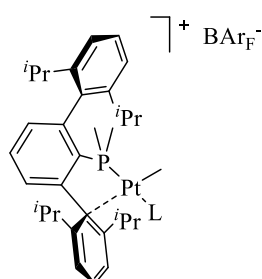
CHAPTER I (cont.)



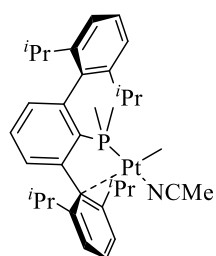
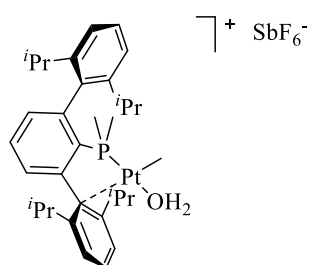
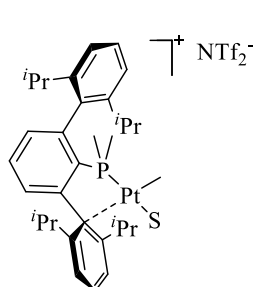
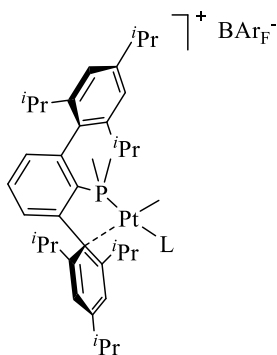
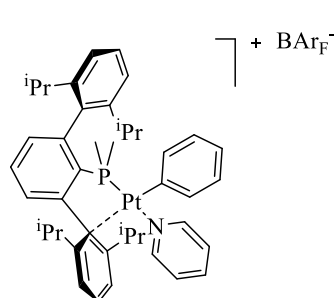
18



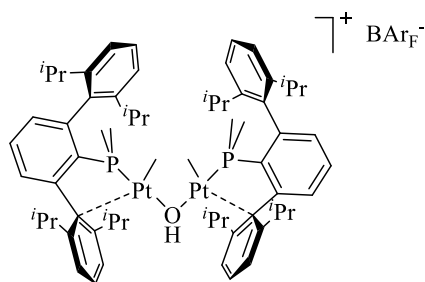
19

20·S
S = Et₂O, CH₂Cl₂, H₂O

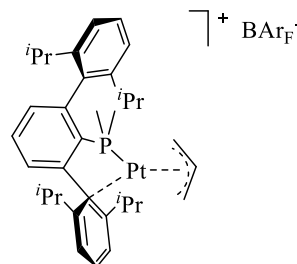
20·L

L = THF, NCMe, C₂H₄, SMe₂20·NCMe-PF₆20·H₂O-SbF₆20·S-NTf₂
S = CH₂Cl₂, NTf₂⁻21·L
L = CO, NCMe

22

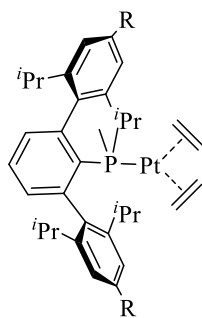


23



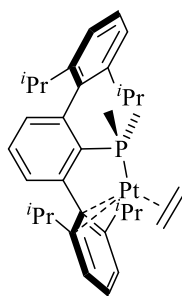
24

CHAPTER II

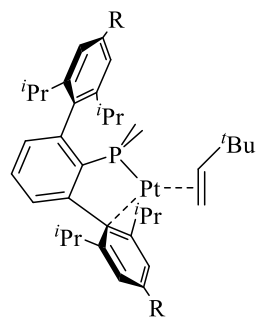


1: R=H

2: R=*i*Pr

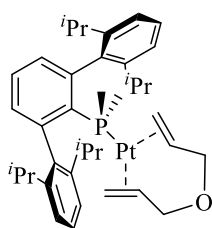


1'

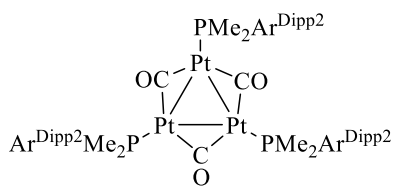


3: R=H

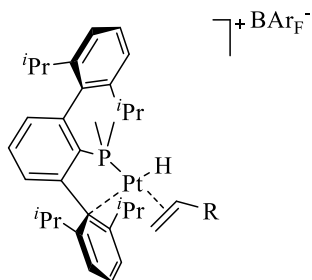
4: R=*i*Pr



5

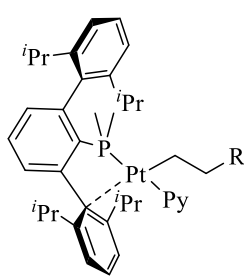


6



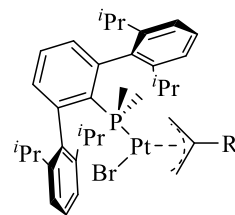
7: R = H

8: R = *t*Bu



9: R = H

10: R = *t*Bu



11: R = H

12: R = Me

ABSTRACT

Chapter I contains synthetic, structural and reactivity studies on Pt(II) complexes bearing the bulky dimethylterphenylphosphines $\text{PMe}_2\text{Ar}^{\text{Xyl}_2}$ (**L**₁), $\text{PMe}_2\text{Ar}^{\text{Dipp}_2}$ (**L**₂) or $\text{PMe}_2\text{Ar}^{\text{Tipp}_2}$ (**L**₃) (see page 13 for the structural formulae of these phosphines). It comprises two main sections. The first is dedicated to compounds of the xylyl substituted terphenylphosphine (**L**₁). Despite the bulkiness of this ligand, bis(phosphine) Pt(II) complexes could be synthesised. Since the ligand contains ζ -C-H bonds, cyclometallation reactions could be achieved to form seven-membered platinacycles. Kinetic studies on the cyclometallation reaction were also developed. Two different Pt(II) precursors were used in this section, namely *cis*-[PtCl₂(COD)] and *cis*-[PtMe₂(SMe₂)₂]. The newly prepared complexes included bis(chloride) and bis(methyl derivatives with different molecular geometry, *i.e.* *trans*-[PtCl₂(PMe₂Ar^{Xyl}₂)₂] and *cis*-[PtMe₂(PMe₂Ar^{Xyl}₂)₂], as well as some cyclometallated complexes. The protonation reactions of some of these platinum organometallics were investigated by variable temperature NMR spectroscopy.

The second section of Chapter I describes a variety of Pt(II) complexes of ligands **L**₂ and **L**₃. These ligands are able to stabilize low-coordinated species that feature formally a 14-electron count. In order to counterbalance the metal coordinative and electronic unsaturation, these compounds feature a relatively weak Pt...C_{arene} interaction with the *ipso* carbon atom of a flanking aryl ring of the terphenyl group of the phosphine.

A series of neutral Pt(II) complexes were characterized by common techniques (NMR spectroscopy and single crystal X-ray diffraction) for a variety of monoanionic ligands, such as Me^- , Cl^- , H^- and SiR_3^- . New compounds in this section comprised the methyl derivatives *cis*-[PtMe₂(PMe₂Ar')] of ligands **L**₂ and **L**₃, as well as the chloro-methyl species *cis*-[Pt(Me)Cl(PMe₂Ar^{Dipp2})] and some hydride-silyl complexes, *cis*-[Pt(H)(SiR₃)(PMe₂Ar')], among others. The secondary interaction offered by the phosphine was easily replaced by various Lewis bases alike CO or PR₃. In addition, cationic complexes were also investigated. The important steric protection provided by the bulky terphenylphosphines allowed abstraction of one or the two chloride ligands of the complex *cis*-[PtCl₂(PMe₂Ar^{Dipp2})] with formation of mono- and bis-cationic complexes with weakly bound molecules of poorly coordinating solvents completing the metal coordination sphere. Some of the Pt(II) cations investigated were generated by protonation of *cis*-[PtMe₂(PMe₂Ar^{Dipp2})], among them the dication *cis*-[Pt(PMe₂Ar^{Dipp2})(S)₂]²⁺, isolated as the bis(triflimidate) salt (NTf₂⁻). This complex contains only one firmly bound κ^2 -P,C phosphine ligand and two molecules of poor donor solvents like dichloromethane, diethylether or water (adventitious), and may be therefore viewed as a source of the [Pt(PMe₂Ar^{Dipp2})]²⁺ fragment. Another, in our opinion interesting complex that was fully characterised in this work is the monocation *cis*-[PtMe(S)(PMe₂Ar^{Dipp2})]⁺ (the analogous PMe₂Ar^{Tipp2} derivative was also studied although only for comparative structural analysis). We studied the reactivity of PMe₂Ar^{Dipp2} complex towards some small inorganic and organic molecules. Specifically, the reaction with C₂H₂ yielded the four-coordinate allyl complex [Pt(η^3 -C₃H₅)(PMe₂Ar^{Dipp2})]⁺ through a reactive vinylidene intermediate, as demonstrated by isotopic labelling studies using C₂D₂. Computational

studies on this reaction and on the related process involving C_2H_4 were also developed. To complete this section, we deemed appropriate some catalytic studies using these cations as catalyst precursors. The reactions embraced a variety of alkyne hydroarylations, along with the hydroamination of some terminal alkynes.

Chapter II is dedicated to the study of Pt(0) complexes of the terphenylphosphine ligands L_2 and L_3 . Since it is well known that Pt(0)- PR_3 complexes are one of the most important families of organometallic catalysts, it was though mandatory disclosing the structural and reactivity properties of Pt(0) derivatives of these bulky phosphines, including some catalytic applications.

The core of these investigations are Pt(0)- PMe_2Ar' -olefin complexes of the types $[Pt(C_2H_4)_n(PMe_2AR^{Dipp_2})]$, where $n = 1$ or 2 . Since the mono(ethylene) complexes feature relatively poor thermal stability, the analogous complexes $[Pt(CH_2=CH^tBu)(PMe_2Ar')]$ of the bulkier 3,3-dimethylbut-1-ene olefin were prepared and characterized. As discussed in a forthcoming section of this Thesis, these complexes were generated by two different methods. The first consisted in the Zn powder reduction of the corresponding *cis*- $[PtCl_2(PMe_2Ar')]$ precursor in the presence of the alkene, while the second involved reductive elimination of $HSiEt_3$ from the hydride.silyl predecessor induced by the olefin. A chelating alkene such as bis(allyl)ether, $(CH_2=CHCH_2)_2O$, as also utilised successfully to generate complexes of this kind.

Besides the structural characterization of the new compounds, some reactivity studies were carried out, in particular the reaction with CO, that yielded an interesting triplatinum cluster, namely $[Pt_3(\mu-CO)_3(PMe_2AR^{Dipp_2})_3]$, demonstrating that the Pt(0)- PMe_2Ar' -olefin complexes are a useful source of the reactive $[Pt(PMe_2Ar')]$ fragment. Low

temperature protonation studies made evident the formation of *cis*-[Pt(H)(olefin)(PMe₂Ar')]⁺ species, which rearranged by migratory insertion of the olefin into the Pt—H bond and behave as precatalysts for olefin dimerization reactions. In addition, the Pt(0)-PMe₂Ar' complexes were shown to undergo oxidative addition reactions. This reactivity was demonstrated with the formation of platinum(II) allyl complexes when complex [Pt(C₂H₄)₂(PMe₂Ar^{Dipp2})] was treated with BrCH₂C(R)=CH₂ (R = H, Me).

In the same way as in Chapter I, Chapter II ends with catalytic studies based on some of the new Pt(0) complexes as precatalysts for the hydrosilylation of terminal alkynes. As discussed later, the hydrosilylation of alkyl-substituted terminal alkynes was accomplished with high activity and *E*-selectivity, while for arylacetylenes a strong dependence of the catalytic activity with electronic effects on the *para*-substituents was disclosed.

CHAPTER I

I.1. INTRODUCTION

I.1.1. A brief historical preface

This Doctoral Thesis is devoted to the study of platinum complexes that contain coordinated tertiary phosphine ligands. Doubtless, this is a classical area of research in modern Inorganic and Organometallic Chemistry, and as such has been intensively investigated in the past decades. Therefore, progress over the years has been collected in many textbooks and specialised monographs, as well as in countless review articles, and in readily accessible encyclopaedia like *Comprehensive Coordination Chemistry*¹ and *Comprehensive Organometallic Chemistry*.² The first editions of these collective works were published in 1987 and 1982, respectively. Despite this extensive literature coverage, we believe that a brief historical survey on phosphine ligands and their metal complexes with emphasis placed on platinum is appropriate.

¹ *Comprehensive Coordination Chemistry*, 2nd ed. (Eds.: J. A. McCleverty, T. J. Meyer), Elsevier, **2004**. First edition published in 1987

² *Comprehensive Organometallic Chemistry*, 3rd ed. (Ed.: R. H. Crabtree), Elsevier, **2007**. First edition published in 1982.

The simplest alkyl phosphines, PMe_3 and PEt_3 , were prepared in the mid-nineteenth century by P. Thénard (1847) and F. Bérle (1855), respectively. The highly reactive alkyl phosphines attracted the interest of the great A. W. Hofmann and his co-workers, particularly A. Cahours in the 1860s. The syntheses of these compounds were fraught with so many difficulties and experimental obstacles that, according to Chatt,^{3a} defeated some inorganic and organic chemists even in the 1950s, and delayed the extensive study of tertiary phosphine complexes for a whole century.

Aromatic phosphines, including some dialkylphenylphosphines and triphenylphosphine, were first synthesised around 1885 by the school of Michaelis. The development of aromatic phosphines rapidly overtook that of their aliphatic analogues. In fact, some 75 years after its discovery, PPh_3 became one of the most important phosphines in the development of homogeneous catalysis by phosphine metal complexes. Great impetus to the synthesis of bi- and poly-dentate phosphine and related arsine and stibine ligands came from the recognition of their novel and influential coordination chemistry in the 1950s and 1960s. The preparation of these multidentate ligands may be contemplated in perspective as something of an art,⁴ and found leading protagonists in the schools of Nyholm, Venanzi, Sacconi, Meek, King and their co-workers.

Serious investigations on platinum phosphine complexes took already place in the second half of the nineteenth century with the preparation of $[\text{PtCl}_2(\text{PMe}_3)_2]$, $[\text{PtCl}_2(\text{PEt}_3)_2]$ and other complexes with diverse tertiary phosphines and arsines, mainly by the groups of Hofmann

³ a) See *Historical Introduction* by J. Chatt in Chapter 1 of reference 3b. b) L. H. Pignolet, *Homogeneous Catalysis with Metal Phosphine Complexes*, Ed. Plenum Press, New York, **1983**.

⁴ C. A. McAuliffe, W. Levason, *Phosphine, Arsine and Stibine Complexes of the Transition Elements*, Elsevier Scientific Pub. Co., Amsterdam, **1999**.

and Cahours.⁵ After the second World War, K. A. Jensen determined the dipole moments of many complex compounds, comprising coordination compounds such as *cis*-[PtCl₂(PR₃)₂] for which he found values of around 11 Debye units, showing that, contrary to previous thoughts, all those platinum(II) complexes, except the ammines, have a *cis* configuration. In the years around 1950, the chemistry of these compounds experienced an explosive development that was highly influenced by fundamental research from the school of Chatt and coworkers.⁵ Many relevant areas of coordination and organometallic chemistry were investigated during those years with the aid of platinum phosphine complexes. The following will be briefly discussed as a representative selection, while others will be presented in forthcoming sections of this Thesis.

(i) The coordination of alkenes and alkynes to platinum(II) and other metal centres that led the now well-known and widely utilised Dewar-Chatt-Duncanson model (DCD) for the bonding interactions between unsaturated hydrocarbons and transition metals.⁶ The revolutionary idea that olefins could donate their π -electrons to form a dative bond was advanced by Dewar in 1945 to explain the *trans* addition of an electrophilic reagent such as Br₂ to olefins through the intermediacy of a bromonium-olefin cation. In 1951, Dewar clarified using molecular orbital theory^{6a} the notion of the olefin-metal bond in olefin complexes of the silver(I) cation, Ag⁺, with 4d¹⁰ electronic configuration. He proposed that the metal-olefin bond was divided in a σ - and a π -component. The first could arise from overlap of the filled bonding π -orbital of the olefin with

⁵ For an informative discussion on the development of phosphine metal complexes (also compounds with arsine and stibine ligands) focused on research from the 1950s and early 1960s, see: G. Booth, *Adv. Inorg. Chem. Radiochem.* **1964**, 6, 1-69.

⁶ a) M. J. S. Dewar, *Bull. Soc. Chim. Fr.* **1951**, 18, C71-C79; b) J. Chatt, L. A. Duncanson, *J. Chem. Soc.* **1953**, 2939-2947.

the empty s-orbital of Ag^+ , whereas the second was considered to implicate a filled d-orbital of the metal and the vacant antibonding orbital of the olefin.

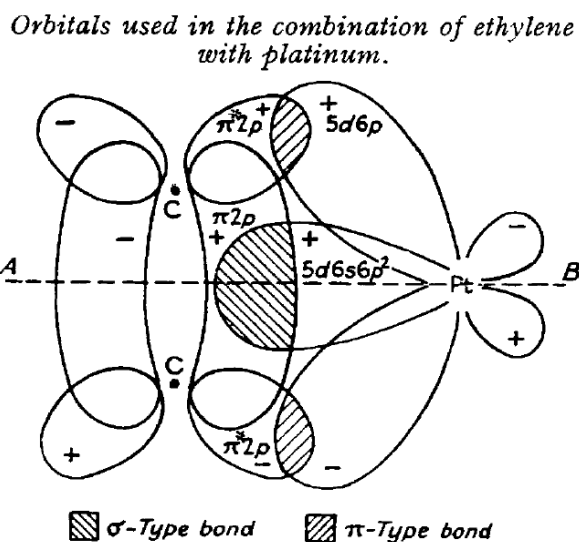


Figure 1: Alkene-metal bonding. Original from reference 6b.

Two years later, with reference to Dewar's model, Chatt and Duncanson,^{6b} in an article that collected infrared spectroscopic studies on a range of olefin platinum(II) complexes, proposed (Figure 1) that the σ -type bond would be formed between a vacant dsp^2 (5d, 6s and 6p) hybrid orbital of the platinum atom and the filled π -orbital of the olefin. In turn, the π -component of the bond will result from overlap of a filled dp hybrid orbital of the metal and the empty π^* -orbital of the olefin. Furthermore, Chatt and Duncanson illustrated how the model could be used to interpret not only the physical properties of the olefin platinum compounds, such as the spectroscopic data and dipole moments, but also their reactivity and their superior stability compared to the olefin silver salts.⁷

⁷ H. Werner, *Landmarks in Organo-Transition Metal Chemistry*, Springer, **2003**.

(ii) The stabilization of σ Pt-C bonds in heteroleptic platinum alkyl and aryl complexes. The most stable transition metal alkyls prepared in the late 1950s and early 1960s were those of platinum bearing tertiary phosphine ligands, thanks to the pioneering studies carried out by Chatt and Shaw.⁸ With the knowledge of the intrinsic instability of simple, homoleptic MR_2 and MR_3 alkyl and aryl derivatives of the transition metals, these authors foresaw that *ligands causing large splittings of the d-energy levels should stabilise planar and octahedral alkyl and aryl metal complexes of d^3 - d^8 types.*^{8a} They also noted that tertiary phosphines form very stable $[MX_2(PR_3)_2]$ complexes ($M = Ni, Pd, Pt$; $X = \text{halogen}$) of square-planar configuration and prepared a series of methyl complexes of the types *trans*- $[Pt(Me)X(PR_3)_2]$ and *cis*- $[PtMe_2(PR_3)_2]$, utilising methyl lithium or methyl Grignard reagents.^{7,8} These compounds were *remarkably inert* and were *not hydrolysed by dilute acids or oxidised in moist air*. They moreover prepared dimethyl platinum(IV) complexes of formula $[Pt(Me)_2X_2(PR_3)_2]$ in different isomeric forms by oxidative addition of MeI or Cl_2 to *trans*- $[PtMe(I)(PR_3)_2]$ and *cis*- $[PtMe_2(PR_3)_2]$.

(iii) The study of the *trans* effect of phosphine and other ligands like hydride, alkyl or aryl groups.⁹ Indeed, the high *trans* effect of phosphine ligands, along with their steric bulk, explained that only one or two monophosphine ligands could coordinate strongly to a metal ion or atom. Complexes with three or more phosphine ligands usually undergo dissociation, providing a vacant coordination site for the activation of reactant molecules.

⁸ a) J. Chatt, B. L. Shaw, *J. Chem. Soc.* **1959**, 705-716; b) J. Chatt, B. L. Shaw, *J. Chem. Soc.* **1959**, 4020-4033.

⁹ a) T. G. Appleton, H. C. Clark, L. E. Manzer, *Coord. Chem. Rev.* **1973**, *10*, 335-422; b) F. R. Hartley, *Chem. Soc. Rev.* **1973**, *2*, 163-179; c) L. J. Manojlovic-Muir, K. W. Muir, *Inorg. Chim. Acta* **1974**, *10*, 47-49.

(iv) The internal metallation of tertiary phosphine ligands leading to platinacycles that contain a chelating [Pt(P[^]C)] linkage. This reactivity was pioneered by the group of Shaw, who demonstrated the importance of steric hindrance and the preference for the formation of five-membered rings.¹⁰ Transition metal metallacycles are now ubiquitous and encompass not only metallated P[^]C ligands, but also related P[^]X structures, where X represents a monoanionic heteroatom like O, S, N, etc.¹¹ Furthermore, they find plentiful applications in different areas of research, comprising catalysis, medicinal chemistry and material science.¹²

(v) The applications of phosphine metal complexes in homogeneous catalysis,^{3b} that started to flourish in the 1950s and was based mainly on platinum-group metals, notably ruthenium and rhodium.^{3a} Platinum catalysts containing PPh₃ were, however, successful, in combination with SnCl₂, for the hydrogenation of ethylene and acetylene at room temperature and atmospheric pressure,^{13a} and also for the hydrogenation of methyl linolenate and other fatty acid methyl esters.^{13b} Despite limited applications at the early stages, the capacity of Pt(II) complexes, particularly of cationic species, to activate alkenes and alkynes on coordination, has caused in the last two decades a tremendous growth of platinum-catalysed reactions that involve the electrophilic activation of C=C and C≡C bonds towards the attack by a variety of nucleophiles, including protic oxygen, nitrogen and carbon nucleophiles, as well as

¹⁰ a) A. J. Cheney, B. E. Mann, B. L. Shaw, R. M. Slade, *J. Chem. Soc., Chem. Commun.* **1970**, 1176-1177; b) A. J. Cheney, B. E. Mann, B. L. Shaw, R. M. Slade, *J. Chem. Soc., A* **1971**, 3833-3842; c) A. J. Cheney, B. L. Shaw, *J. Chem. Soc., Dalton Trans.* **1972**, 754-763.

¹¹ See for example: J. Campos, L. Ortega-Moreno, S. Conejero, R. Peloso, J. López-Serrano, C. Maya, E. Carmona, *Chem. Eur. J.* **2015**, *21*, 8883-8896.

¹² For leading references see: J. Campos, M. F. Espada, J. López-Serrano, E. Carmona, *Inorg. Chem.* **2013**, *52*, 6694-6704.

¹³ a) R. D. Cramer, E. L. Jenner, R. V. Lindsey, U. G. Stolberg, *J. Am. Chem. Soc.* **1963**, *85*, 1691-1692; b) E. Frankel, E. Emken, H. Itatani, J. J. Bailar, *J. Org. Chem.* **1967**, *32*, 1447-1452.

arenes and C=C bonds.¹⁴ These and other catalytic properties of platinum(0) and platinum(II) complexes shall be discussed further in forthcoming sections of this Thesis.

¹⁴ a) A. R. Chianese, S. J. Lee, M. R. Gagné, *Angew. Chem. Int. Ed.* **2007**, *46*, 4042-4059;
b) A. Fürstner, P. W. Davies, *Angew. Chem. Int. Ed.* **2007**, *46*, 3410-3449.

I.1.2. Introductory comments

As noted in the previous section, phosphines and related P(III) phosphorus ligands, PR_3 , are one of the most widely used classes of ligands in coordination and organometallic chemistry, as they usually form inert and stable bonds with the majority of the transition metals. They are particularly useful because their electronic and steric properties can be altered in a systematic and predictable way by varying the R groups, which do not have to be necessarily identical, but can range within a variety of inorganic and organic radicals such as hydrogen, halide, hydrocarbyl, alkoxy, amide, etc. Phosphine ligands are able to stabilize a broad range of metal oxidation states and are of exceptional industrial interest because of their ability to promote diverse catalytic reactions in combination with transition metals. Indeed, their crucial role in the stabilization of reactions intermediates is well-known.¹⁵ The introduction of elements of chirality in the molecular structure of mono or polydentate phosphines and related

¹⁵ a) M. Bochmann, *Organometallics and Catalysis. An Introduction.*, Oxford University Press, Oxford, UK, **2015**; b) R. H. Crabtree, *The Organometallic Chemistry of the Transition Metals*, 6th ed., John Wiley & Sons, Inc., Hoboken, **2014**; c) J. Hartwig, *Organotransition Metal Chemistry: From Bonding to Catalysis*, Sausalito, **2010**; d) R. H. Crabtree, *J. Organomet. Chem.* **2005**, 690, 5451-5457; e) C. A. Tolman, *Chem. Rev.* **1977**, 77, 313-348.

ligands, and their application in asymmetric catalysis represented one of the landmark discoveries of the chemical community in the last century.¹⁶

A key feature of PR_3 ligands is that electronic properties can be easily varied without any major change in steric features (*e.g.*, by moving from PBu_3 to $\text{P}(\text{O}^i\text{Pr})_3$), and *vice versa* (*i.e.* upon changing PPh_3 by $\text{P}(\text{o-tolyl})_3$). While the variation of the donor-acceptor abilities of the ligand can perturb oxidative and reductive catalytic steps favouring higher or lower oxidation states of the metals, the steric bulk is expected to stabilize low-coordination-number species, which are known to be particularly relevant in catalysis.¹⁷

In recent years bulky phosphines with unprecedented properties, such as those reported by Beller¹⁸, Buchwald¹⁹, Fu²⁰, and Hartwig²¹ have been widely utilised for the synthesis of transition metal complexes and the development of challenging catalytic processes (Figure 2).

¹⁶ a) R. Noyori, *Angew. Chem. Int. Ed.* **2002**, *41*, 2008-2022; b) W. S. Knowles, *Angew. Chem. Int. Ed.* **2002**, *41*, 1998-2007.

¹⁷ a) J. Halpern, *Inorg. Chim. Acta* **1981**, *50*, 11-19; b) C. P. Casey, G. T. Whiteker, M. G. Melville, L. M. Petrovich, J. A. Gavney, D. R. Powell, *J. Am. Chem. Soc.* **1992**, *114*, 5535-5543; c) L. H. Shultz, D. J. Tempel, M. Brookhart, *J. Am. Chem. Soc.* **2001**, *123*, 11539-11555; d) Z. Liu, E. Somsook, C. B. White, K. A. Rosaaen, C. R. Landis, *J. Am. Chem. Soc.* **2001**, *123*, 11193-11207.

¹⁸ A. Zapf, A. Ehrentraut, M. Beller, *Angew. Chem. Int. Ed.* **2000**, *39*, 4153-4155.

¹⁹ a) J. P. Wolfe, R. A. Singer, B. H. Yang, S. L. Buchwald, *J. Am. Chem. Soc.* **1999**, *121*, 9550-9561; b) A. Aranyos, D. W. Old, A. Kiyomori, J. P. Wolfe, J. P. Sadighi, S. L. Buchwald, *J. Am. Chem. Soc.* **1999**, *121*, 4369-4378; c) J. P. Wolfe, S. Wagaw, J.-F. Marcoux, S. L. Buchwald, *Acc. Chem. Res.* **1998**, *31*, 805-818; d) R. Martin, S. L. Buchwald, *Acc. Chem. Res.* **2008**, *41*, 1461.

²⁰ A. F. Littke, G. C. Fu, *Angew. Chem. Int. Ed.* **2002**, *41*, 4176-4211.

²¹ a) Q. Shelby, N. Kataoka, G. Mann, J. Hartwig, *J. Am. Chem. Soc.* **2000**, *122*, 10718-10719; b) G. Mann, C. Incarvito, A. L. Rheingold, J. F. Hartwig, *J. Am. Chem. Soc.* **1999**, *121*, 3224-3225; c) J. F. Hartwig, *Angew. Chem. Int. Ed.* **1998**, *37*, 2046-2067.

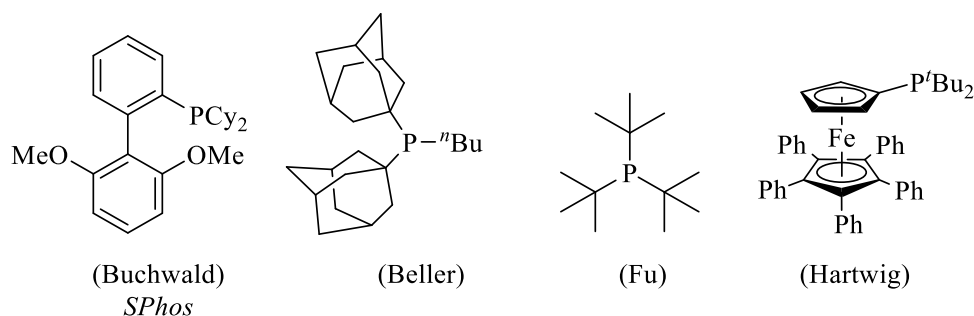
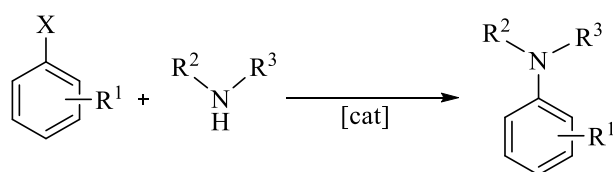


Figure 2. Some representative phosphines studied by Buchwald, Beller, Fu, Hartwig and their co-workers.

In particular, the dialkylbiaryl phosphines reported by Buchwald have acquired great importance and are amply used in a variety of catalytic organic transformations mediated by transition metals. Notably, the Pd-catalysed arylation of nitrogen nucleophiles using this ligand type has undergone considerable development, which has been driven by innovations in ligand design and by optimization of reaction conditions. As a result, the reactions can often be employed with complex substrates and low catalyst loadings (Scheme 1).^{19,22}



Scheme 1: Pd-catalysed amination of aryl halides using dialkylbiaryl phosphines.

²² a) D. S. Surry, S. L. Buchwald, *Chem. Sci.* **2011**, 2; b) T. J. Maimone, P. J. Milner, T. Kinzel, Y. Zhang, M. K. Takase, S. L. Buchwald, *J. Am. Chem. Soc.* **2011**, 133, 18106-18109; c) B. P. Fors, D. A. Watson, M. R. Biscoe, S. L. Buchwald, *J. Am. Chem. Soc.* **2008**, 130, 13552-13554; d) T. E. Barder, S. L. Buchwald, *J. Am. Chem. Soc.* **2007**, 129, 12003-12010; e) T. E. Barder, S. D. Walker, J. R. Martinelli, S. L. Buchwald, *J. Am. Chem. Soc.* **2005**, 127, 4685-4696.

In a Perspective article,^{22a} Surry and Buchwald have recently summarized the key variables that affect the success of this reaction.

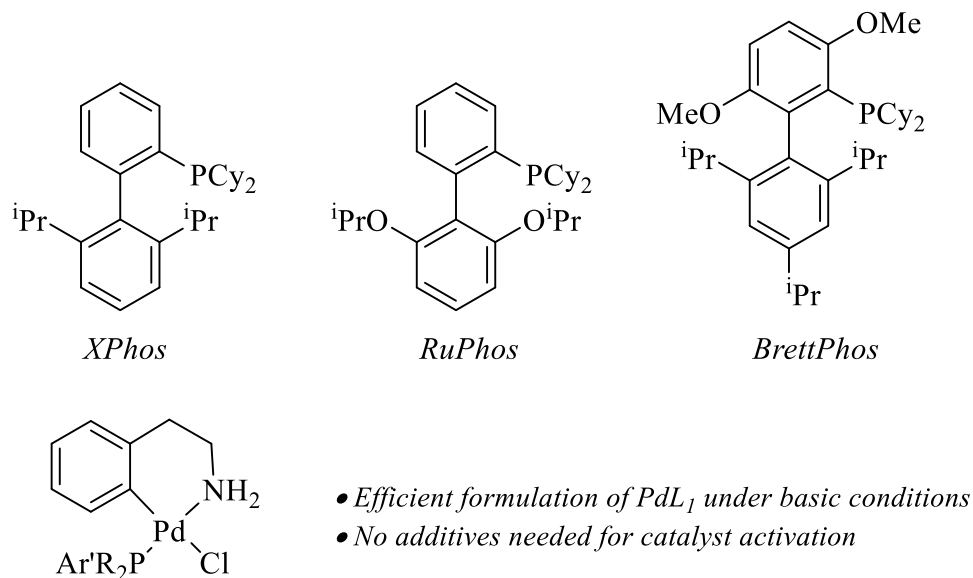


Figure 3. Some dialkylbiaryl phosphines (top) and Pd(II) catalyst precursors (bottom) for amination reactions ($\text{R} = \text{Cy}$ or tBu ; $\text{Ar}' = \text{biaryl}$; adapted from Reference 22.

Basically, the structures of the amine and the electrophile determine the choice of the essential reaction parameters of ligand, palladium precursor, base and solvent. Since this Thesis concentrates attention on platinum complexes of related dialkylterphenyl phosphines we deem proper summarizing the influence of the phosphine in a given palladium catalysed amination reaction.

The key feature is doubtless the structure of the ligand (the one represented in Figure 2 is named *SPhos*). The original studies made use of ligands *DavePhos* and *JohnPhos* for amination reactions,^{22a} but a major breakthrough came with the discovery of *XPhos* and *RuPhos* (Figure 3), which yielded improved reactivity in a variety of demanding amination

reactions. More recently, *BrettPhos* (Figure 3) was introduced, and appears to date as the most generally useful ligand for the arylation of primary amines, whereas *RuPhos* is the phosphine of choice for the arylation of secondary amines.^{22a}

Monophosphine Pd(0) complexes of this type are highly reactive towards oxidative addition. In accordance with this observation, for simple substrates the ideal metal to ligand ratio is 1:1. Often an extra equivalent of the ligand is, however, needed to stabilize the catalyst in highly demanding transformations that require long reaction times or when a high TON (*Turn-Over Number*) is desirable. It should be noted that due to the bulkiness of Buchwald's phosphines, even in the presence of a protective extra equivalent of the ligand the monophosphine species can still be dominant in solution. Moreover, biarylphosphines are able to stabilise low-coordinate palladium centres by means of weak bonding interactions usually involving the *ipso* carbon atom of the pending aryl ring.^{19d,22} The efficiency with which the active catalyst [Pd(PR₂Ar')] is formed is also a pivotal factor. In this regard, we point out that cyclometallated amine complexes (N[^]C) of the type represented in Figure 3 have proven ideal to generate [Pd(PR₂Ar')] under reaction the conditions.^{22a} Some of these precatalysts are commercially available, but they are not possible for all PR₂Ar' ligands.

Bulky phosphines with aryl substituents often act as hemilabile ligands,²³ as the coordination to the metal can occur through the phosphine and also through the weakly coordinating π -system of the arene. The arene interaction can lead to η^6 -binding or to lower hapticity such as η^1 or η^2 -coordination. As a result, the substituents of the phosphine provide steric

²³ a) P. Braunstein, F. Naud, *Angew. Chem. Int. Ed.* **2001**, 40, 680-699; b) H. Grützmacher, *Angew. Chem. Int. Ed.* **2008**, 47, 1814-1818; c) H. Werner, *Dalton Trans.* **2003**, 3829-3837; d) H. Werner, G. Canepa, K. Ilg, J. Wolf, *Organometallics* **2000**, 19, 4756-4766.

shielding, protecting the phosphorus and metal atoms towards oxidation, and contribute to the stabilization of unsaturated reaction intermediates. There are examples of such stabilization in late transition metal complexes of biarylphosphines, not only on palladium,^{22b-e} but also on Rh, Ir, Pt and Au complexes.²⁴

Besides phosphines of the types represented in Figure 1, a diversity of mono- and polydentate phosphine ligands have been developed in recent years, and their late transition metal complexes investigated in numerous stoichiometric and catalytic transformations. Reference 25 collects some representative work with leading citations to different aspects of this field of research. In addition, it is pertinent to mention some recent, interesting advancements in the use of electron-poor phosphine ligands, which find ample use in the chemistry of Pt(II) and Au(I), and in their applications in catalysis.²⁵

A somewhat classical strategy for the synthesis of P-donors with overall acceptor properties implies the use of perfluoro-alkyl or -aryl substituents on phosphorus. Ligands of this kind encompass monodentate phosphines (for instance $\text{PR}(\text{C}_2\text{F}_5)_2$, R = alkyl or aryl radical), bidentate donors like $(\text{C}_2\text{F}_5)_2\text{PCH}_2\text{CH}_2\text{P}(\text{C}_2\text{F}_5)_2$ (dfepe), and pincer ligands alike 1,3- $\text{C}_6\text{H}_4(\text{CH}_2\text{P}(\text{CF}_3)_2)_2$, 1,3- $\text{C}_6\text{H}_4(\text{CH}_2\text{P}(\text{C}_6\text{F}_5)_2)_2$, and related molecules.^{26,27}

²⁴ a) A. R. O'Connor, W. Kaminsky, B. C. Chan, D. M. Heinekey, K. I. Goldberg, *Organometallics* **2013**, 32, 4016-4019; b) A. R. O'Connor, W. Kaminsky, D. M. Heinekey, K. I. Goldberg, *Organometallics* **2011**, 30, 2105-2116; c) A. DeAngelis, V. W. Shurtleff, O. Dmitrenko, J. M. Fox, *J. Am. Chem. Soc.* **2011**, 133, 1650-1653; d) A. Grirrane, H. Garcia, A. Corma, E. Álvarez, *ACS Catal.* **2011**, 1, 1647-1653; e) Y. Wang, K. Ji, S. Lan, L. Zhang, *Angew. Chem. Int. Ed.* **2012**, 51, 1915-1918; f) E. Herrero-Gómez, C. Nieto-Oberhuber, S. López, J. Benet-Buchholz, A. M. Echavarren, *Angew. Chem. Int. Ed.* **2006**, 45, 5455-5459.

²⁵ a) R. J. Lundgren, M. Stradiotto, *Aldrichimica Acta* **2012**, 45, 59-65; b) M. Albrecht, M. M. Lindner, *Dalton Trans.* **2011**, 40, 8733-8744; c) C. A. Fleckenstein, H. Plenio, *Chem. Soc. Rev.* **2010**, 39, 694-711; d) A. J. Kendall, C. A. Salazar, P. F. Martino, D. R. Tyler, *Organometallics* **2014**, 33, 6171-6178; e) J. Keller, C. Schlierf, C. Nolte, P. Mayer, B. F. Straub, *Synthesis* **2006**, 2006, 354-365.

²⁶ a) J. J. Adams, A. Lau, N. Arulsamy, D. M. Roddick, *Inorg. Chem.* **2007**, 46, 11328-11334; b) S. Basu, N. Arulsamy, D. M. Roddick, *Organometallics* **2008**, 27, 3659-3665;

36

The electron-poor nature of their cationic platinum (II) complexes is attested by the high $\bar{\nu}(\text{CO})$ values recorded, for instance around 2170 cm^{-1} in $[\text{PtMe}(\text{CO})(\text{dfepe})]^+$, 2150 cm^{-1} for *trans*- $[\text{PtMe}(\text{CO})(\text{PMe}(\text{C}_2\text{F}_5)_2)_2]$ and around 2110 and 2150 cm^{-1} in the analogous derivatives of the above mentioned fluorinated pincer ligands.^{26,27}

Recently, an alternative plan of action was put into practice. The new approach envisioned the use of cationic rather than formally neutral radical substituents bonded to the phosphorus atom and led to a variety of carbeniophosphanes embracing P^+, P^+ -chelating bis(imidazoliophosphine) and related P^+CP^+ pincer ligands.²⁸ Recent work from the group of Alcarazo²⁹ has resulted in phosphonium cations of the types represented in Figure 4. The new ligands include some pyridinio-dialkyl or -diaryl phosphines,^{29b} as well as mono-, bis- and tris-(dialkylamino)cyclopropenium substituted phosphines. It is remarkable that the bis(dialkylamino)cyclopropenium disubstituted phosphines have electron-donor properties comparable to those of $\text{P}(\text{CF}_3)_3$.^{29c} It has also been found that in the $[\text{PtCl}_3(\text{L})][\text{ClO}_4]_2$ complex of the tricationic phosphine, the $\text{L} \rightarrow \text{Pt}$ σ -donation is lower than the $\text{Pt(II)} \rightarrow \text{L}$ π -back-donation, that is, the P-ligand removes net electron density from the metal, thereby enhancing the intrinsic π -acidity of Pt(II) .^{29d}

c) J. J. Adams, N. Arulsamy, D. M. Roddick, *Organometallics* **2009**, 28, 1148-1157; d) B. Thapaliya, S. Debnath, N. Arulsamy, D. M. Roddick, *Organometallics* **2015**, 34, 4018-4022.

²⁷ B. G. Anderson, J. L. Spencer, *Chem. Eur. J.* **2014**, 20, 6421-6432.

²⁸ a) C. Barthes, C. Lepetit, Y. Canac, C. Duhayon, D. Zargarian, R. Chauvin, *Inorg. Chem.* **2013**, 52, 48-58; b) Y. Canac, C. Maaliki, I. Abdellah, R. Chauvin, *New J. Chem.* **2012**, 36, 17-27.

²⁹ a) Á. Kozma, T. Deden, J. Carreras, C. Wille, J. Petuškova, J. Rust, M. Alcarazo, *Chem. Eur. J.* **2014**, 20, 2208-2214; b) H. Tinnermann, C. Wille, M. Alcarazo, *Angew. Chem. Int. Ed.* **2014**, 53, 8732-8736; c) J. Carreras, G. Gopakumar, L. Gu, A. Gimeno, P. Linowski, J. Petuškova, W. Thiel, M. Alcarazo, *J. Am. Chem. Soc.* **2013**, 135, 18815-18823; d) J. Carreras, M. Patil, W. Thiel, M. Alcarazo, *J. Am. Chem. Soc.* **2012**, 134, 16753-16758; e) J. Petuškova, M. Patil, S. Holle, C. W. Lehmann, W. Thiel, M. Alcarazo, *J. Am. Chem. Soc.* **2011**, 133, 20758-20760; f) J. J. Weigand, K.-O. Feldmann, F. D. Henne, *J. Am. Chem. Soc.* **2010**, 132, 16321-16323.

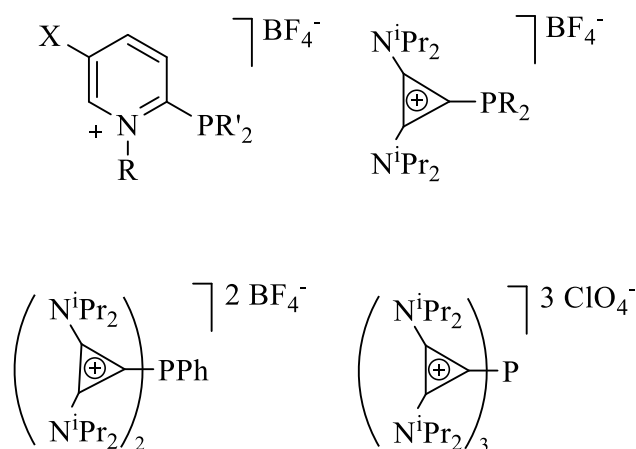


Figure 4. Some newly designed mono and polycationic phosphorus donor ligands (See Reference 29).

Our research group has had a long-standing interest in transition metal complexes of tertiary phosphines and related P-donor ligands.^{30,31} In recent years, terphenyl groups have been employed to stabilize unusual dimolybdenum complexes that contain Mo–Mo quadruple bonds.³² Bearing in mind the extraordinary practical importance of Buchwald’s dialkylbiaryl phosphines, we thought it worthwhile to explore the chemistry of the even bulkier terphenylphosphine ligands, $\text{PR}_2\text{Ar}'$ (see Figure 5; Ar' represents a terphenyl substituted radical) for which there is a scarcity of information in the chemical literature.^{11,33} This chapter deals

³⁰ See for example: a) E. Carmona, F. Gonzalez, M. L. Poveda, J. L. Atwood, R. D. Rogers, *J. Chem. Soc., Dalton Trans.* **1980**, 2108-2116; b) E. Carmona, F. Gonzalez, M. L. Poveda, J. L. Atwood, R. D. Rogers, *J. Chem. Soc., Dalton Trans.* **1981**, 777-782.

³¹ See for example: a) E. Carmona, J. M. Marin, M. L. Poveda, J. L. Atwood, R. D. Rogers, *J. Am. Chem. Soc.* **1983**, *105*, 3014-3022; b) R. Alvarez, E. Carmona, M. L. Poveda, R. Sanchez-Delgado, *J. Am. Chem. Soc.* **1984**, *106*, 2731-2732.

³² a) M. Carrasco, I. Mendoza, E. Álvarez, A. Grirrane, C. Maya, R. Peloso, A. Rodríguez, A. Falceto, S. Álvarez, E. Carmona, *Chem. Eur. J.* **2015**, *21*, 410-421; b) M. Carrasco, I. Mendoza, M. Faust, J. López-Serrano, R. Peloso, A. Rodríguez, E. Álvarez, C. Maya, P. P. Power, E. Carmona, *J. Am. Chem. Soc.* **2014**, *136*, 9173-9180.

³³ a) D. V. Partyka, M. P. Washington, J. B. Updegraff Iii, X. Chen, C. D. Incarvito, A. L. Rheingold, J. D. Protasiewicz, *J. Organomet. Chem.* **2009**, *694*, 1441-1446; b) R. C. Smith, R. A. Woloszynek, W. Chen, T. Ren, J. D. Protasiewicz, *Tetrahedron Lett.* **2004**, *45*, 8327-8330; c) B. Buster, A. A. Diaz, T. Graham, R. Khan, M. A. Khan, D. R. Powell, **38**

with the synthesis and reactivity of a variety of Pt(II) complexes stabilized with the terphenylphosphines $\text{PMe}_2\text{Ar}^{\text{Xyl}_2}$, $\text{PMe}_2\text{Ar}^{\text{Dipp}_2}$, and $\text{PMe}_2\text{Ar}^{\text{Tipp}_2}$ ($\text{Ar}^{\text{Xyl}_2} = \text{C}_6\text{H}_3\text{-2,6-(C}_6\text{H}_3\text{-2,6-Me}_2)_2$; $\text{Ar}^{\text{Dipp}_2} = \text{C}_6\text{H}_3\text{-2,6-(C}_6\text{H}_3\text{-2,6-}^i\text{Pr}_2)_2$; $\text{Ar}^{\text{Tipp}_2} = \text{C}_6\text{H}_3\text{-2,6-(C}_6\text{H}_2\text{-2,4,6-}^i\text{Pr}_3)_2$). Their catalytic activities for hydroamination and hydroarylation of alkynes have also been tested.

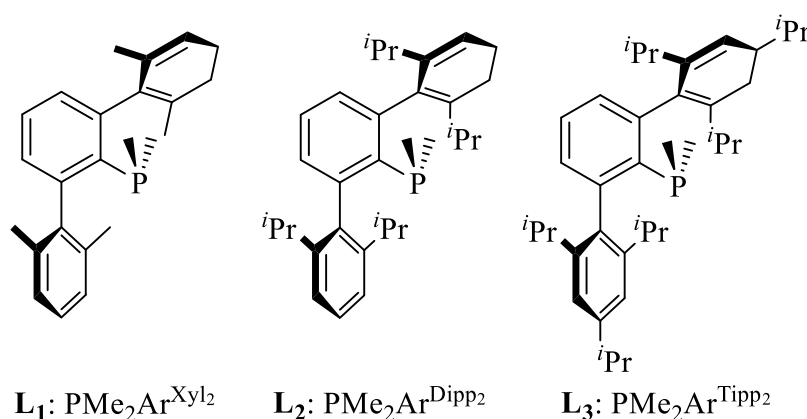


Figure 5. Dimethylterphenylphosphines utilised in this work.

Although four-coordinate square-planar geometries, with a formal count of 16 electrons, are absolutely dominant in isolated Pt(II) compounds, three-coordinate-14 electron Pt(II) complexes are believed to be key intermediates in a number of platinum-mediated organometallic transformations. Most of these unsaturated Pt(II) complexes feature a T-shaped coordination geometry, although a rare example of Y-shaped complex has also been documented.³⁴ In spite of the very small number of three-coordinate Pt(II) complexes that have been isolated and characterized

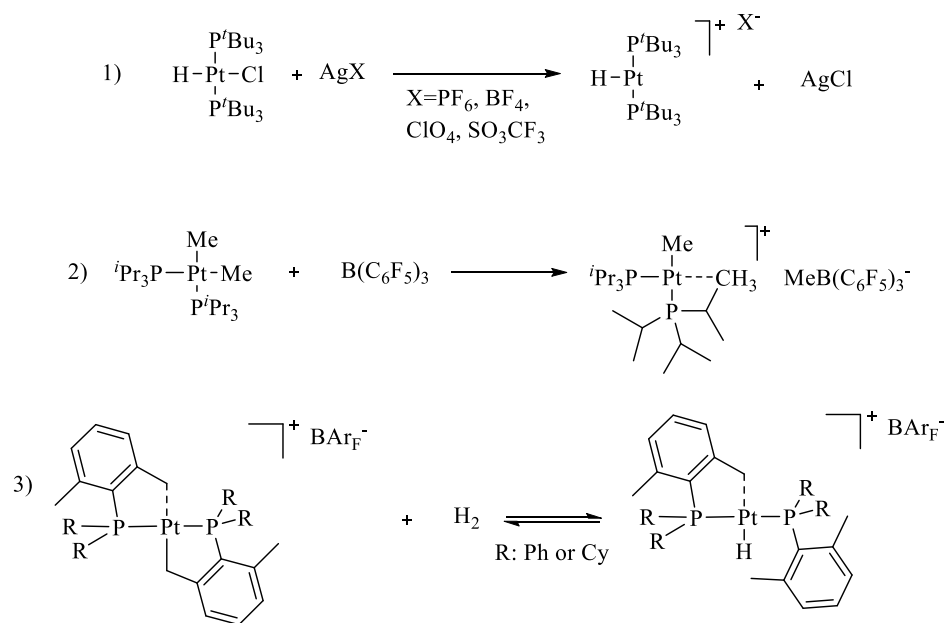
R. J. Wehmschulte, *Inorg. Chim. Acta* **2009**, 362, 3465-3474; d) L. Ortega-Moreno, R. Peloso, C. Maya, A. Suarez, E. Carmona, *Chem. Commun.* **2015**, 51, 17008-17011; e) M. F. Espada, J. Campos, J. López-Serrano, M. L. Poveda, E. Carmona, *Angew. Chem. Int. Ed.* **2015**, 54, 15379-15384.

³⁴ G. Berthon-Gelloz, B. de Bruin, B. Tinant, I. E. Markó, *Angew. Chem. Int. Ed.* **2009**, 48, 3161-3164.

to date,^{11,35} many species can be described as operationally three-coordinate in a kinetic sense. In these compounds the fourth position is occupied by a very weak ligand (agostic bond, solvent molecule or counteranion) which can be easily displaced. Given the electronic and coordinative unsaturated nature of such compounds, they can often be isolated only when the vacant coordination site is blocked to avoid intra- and intermolecular interactions. Steric effects are important in preventing the coordination of a fourth external ligand. The use of bulky species, which hamper the entry of ligands into the platinum coordination sphere, is a good strategy toward this goal. Electronic effects, as well as the involvement of strong electron-donating ligands, also have a stabilizing impact.

Selected examples of the several methods that have been described to prepare coordinatively unsaturated Pt(II) complexes are shown in Scheme 2.

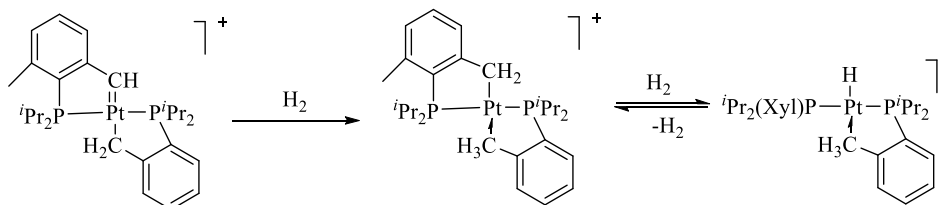
³⁵ a) O. Rivada-Wheelaghan, M. A. Ortuño, J. Díez, A. Lledós, S. Conejero, *Angew. Chem.* **2012**, *124*, 4002-4005; b) O. Rivada-Wheelaghan, B. Donnadieu, C. Maya, S. Conejero, *Chem. Eur. J.* **2010**, *16*, 10323-10326; c) H. Braunschweig, K. Radacki, K. Uttinger, *Chem. Eur. J.* **2008**, *14*, 7858-7866; d) H. Braunschweig, K. Radacki, D. Rais, D. Scheschke, *Angew. Chem. Int. Ed.* **2005**, *44*, 5651-5654; e) M. J. Ingleson, M. F. Mahon, A. S. Weller, *Chem. Commun.* **2004**, 2398-2399; f) W. Baratta, S. Stoccoro, A. Doppiu, E. Herdtweck, A. Zucca, P. Rigo, *Angew. Chem. Int. Ed.* **2003**, *42*, 105-108; g) R. G. Goel, R. C. Srivastava, *Can. J. Chem.* **1983**, *61*, 1352-1359.



Scheme 2: Examples of synthetic methods for unsaturated Pt(II) compounds from references 35g (1), 35e (2), and 35f (3).

In most cases they are obtained by removing a coordinated halogen ligand (Cl, Br, I) by means of a “halogen abstractor” reagent, which is usually an alkali metal salt with a poor coordinating anion, such as PF_6^- , BF_4^- , tetrakis[3,5-bis(trifluoromethyl)phenyl]borate (BAr_F^-), or hexafluoroantimonate.³⁵ Stable T-shaped structures have also been generated by methyl abstraction from the neutral derivative by using highly electrophilic Lewis acids alike $\text{B}(\text{C}_6\text{F}_5)_3$ or $[\text{CPh}_3][1\text{-H-}closo\text{-CB}_{11}\text{Me}_{11}]$.^{35e} H_2 addition across Pt-C alkyl bonds can also lead to electron deficient Pt(II) species stabilized by agostic interactions. Baratta and co-workers studied the addition of H_2 to unsaturated Pt(II) complexes to prepare Pt(II) hydrides.^{35f} Alternatively, our group have recently described that the hydrogenation of a cationic 16-electron Pt(II) carbene bearing a cyclometallated phosphine ligand resulted in the formation of a

cyclometallated complex, which can be further hydrogenated to give a Pt(II) hydride with a δ -agostic interaction (Scheme 3).³⁶

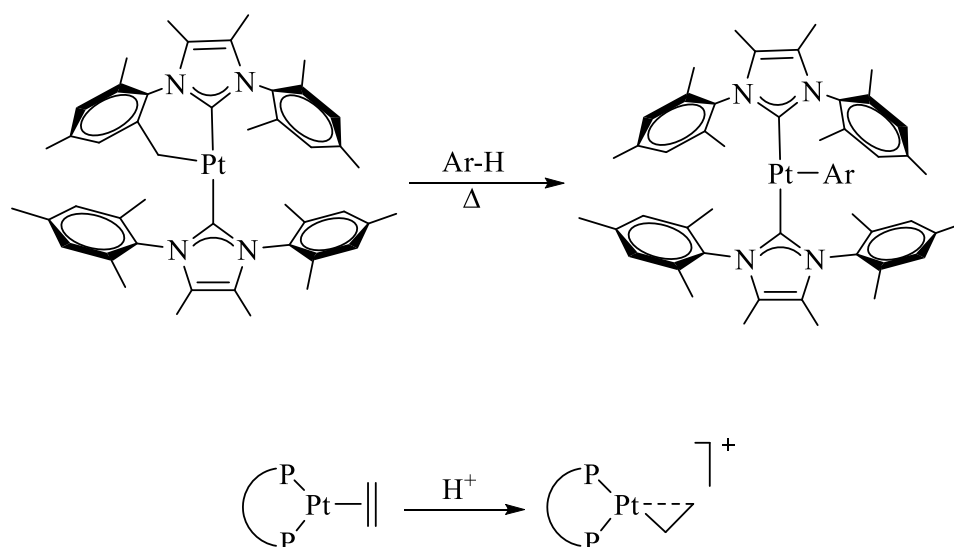


Scheme 3: Hydrogenation of a Pt(II) carbene reported by our group.

Low electron-count species can also be prepared by C-H bond activation reactions from coordinatively unsaturated compounds in a way similar to the addition of H_2 to Pt-C_{alkyl} bonds mentioned above (Scheme 4, top).^{15f} Spencer et al. reported that stable electron-deficient Pt(II) complexes stabilized by strong β -agostic interactions can be accessible by protonation of electron-rich alkene Pt(0) compounds (Scheme 4, bottom).³⁷

³⁶ J. Campos, R. Peloso, E. Carmona, *Angew. Chem. Int. Ed.* **2012**, *51*, 8255-8258.

³⁷ a) N. Carr, B. J. Dunne, L. Mole, A. G. Orpen, J. L. Spencer, *J. Chem. Soc., Dalton Trans.* **1991**, 863-871; b) L. Mole, J. L. Spencer, N. Carr, A. G. Orpen, *Organometallics* **1991**, *10*, 49-52.



Scheme 4. Formation of unsaturated Pt(II) complexes from references 35a (top) and 37 (bottom).

I.2. RESULTS AND DISCUSSION

I.2.1. Pt(II) Complexes of the *o*-Xylyl-Substituted $\text{PMe}_2\text{Ar}^{\text{Xyl}_2}$ Ligand

The first section of this chapter is concerned with studies dedicated to organometallic and coordination compounds of Pt(II) stabilised by the bulky, xylyl substituted terphenyl phosphine $\text{PMe}_2\text{Ar}^{\text{Xyl}_2}$, **L₁**, whose molecular structure is depicted in Figure 6.

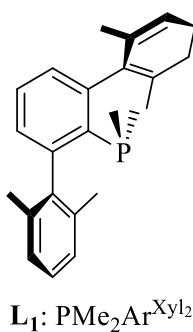
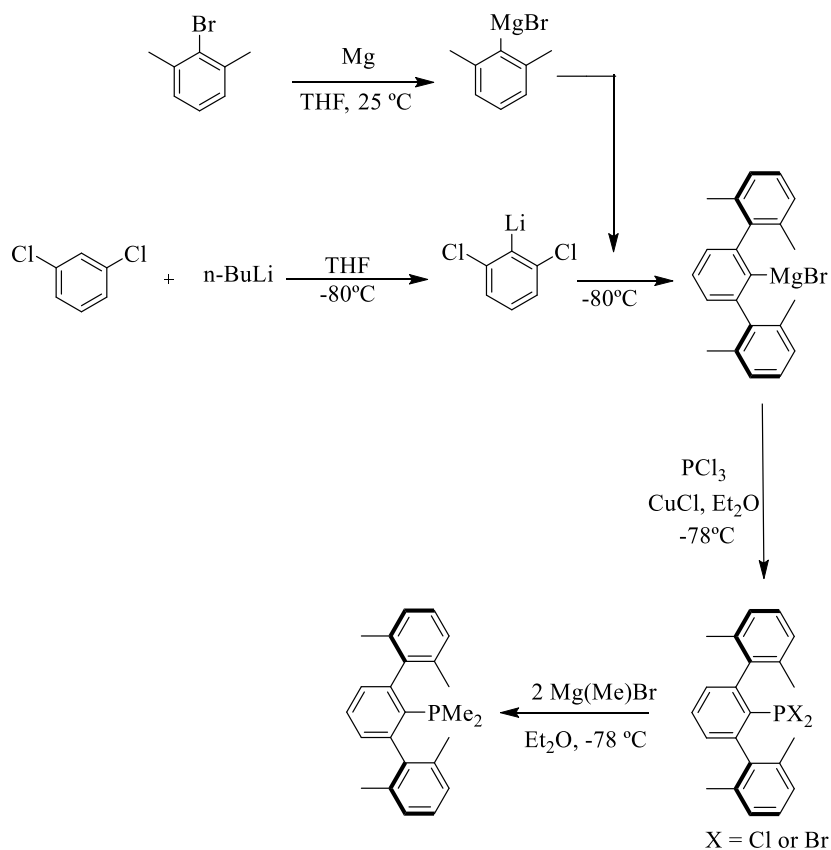


Figure 6: Dimethylterphenylphosphine with xylyl substituents on the pendant aryl groups, **L₁**.

The synthesis of **L₁** is based on the reaction of PCl_3 with the corresponding terphenylmagnesium bromide catalysed by CuCl , and the

subsequent methylation of the resulting dihalo terphenylphosphines with methylmagnesium bromide (Scheme 5). This ligand is a moderately air-stable colourless solid and it was completely characterized by NMR spectroscopy.¹¹

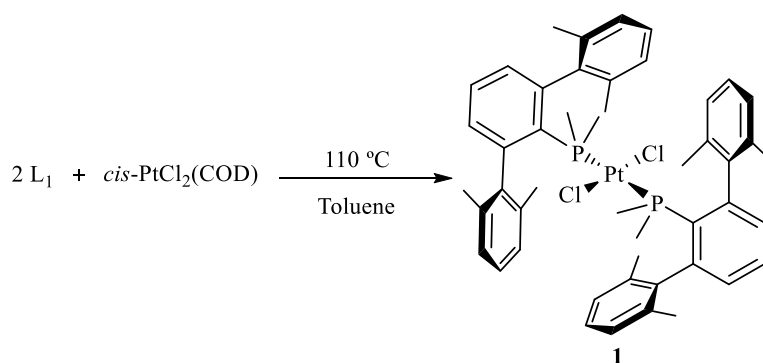


Scheme 5. Synthesis of $\text{PMe}_2\text{Ar}^{\text{Xyl}_2} (\text{L}_1)$

I.2.1.1. Bis(phosphine) Pt(II) Complexes

The phosphine $\text{PMe}_2\text{Ar}^{\text{Xyl}_2}$, L_1 , reacted cleanly (toluene, 110 °C) with the Pt precursor *cis*-[PtCl₂(COD)] (COD = 1,5-cyclooctadiene), in a 2:1 molar ratio to generate complex **1** in high yield (Scheme 6). As can be seen, compound **1** resulted from the substitution of the neutral COD ligand by two molecules of L_1 and concomitant isomerisation to the *trans* isomer.

The isomerisation is probably driven by the steric bulk of the terphenyl phosphine ligand, coupled with the low *trans*-influence of the chloride group.³⁸ Curiously, no evidence for the formation of the mono(phosphine) adduct was found, and consequently, the optimized reaction conditions for the preparation of complex **1** required the already stated 1:2 ratio of Pt:PR₂Ar'.



Scheme 6. Synthesis of *trans*-[PtCl₂(PMe₂Ar^{Xyl})₂], **1**.

Complex **1** is an air-stable colourless solid, highly soluble in common organic solvents such as benzene, toluene, chloroform and dichloromethane. Figure 7 shows the aliphatic region of the HSQC ¹H-¹³C NMR spectrum (300 MHz, CDCl₃, 25 °C) of complex **1**. The eight equivalent methyl groups of the xylyl moieties give rise to a singlet at 2.07 ppm in the ¹H NMR spectrum of **1**. The equivalency of these groups can be ascribed either to the molecular symmetry of the complex or to dynamic processes involving the phosphine ligand facile rotation around C_{ar}-C_{ar} and C_{ar}-P bonds. In addition, the methyl groups directly bound to the P atom appear as a pseudotriplet in the ¹H and ¹³C{¹H} NMR spectra, due to

³⁸ a) T. G. Appleton, M. A. Bennett, *Inorg. Chem.* **1978**, *17*, 738-747; b) E. M. Shustorovich, M. A. Porai-Koshits, Y. A. Buslaev, *Coord. Chem. Rev.* **1975**, *17*, 1-98; c) K. F. Purcell, J. C. Kotz, in *Inorg. Chem.*, W. B. Saunders Co., Philadelphia, **1977**, Chapter 13.

virtual coupling to the ^{31}P nuclei,³⁹ clearly demonstrating the *trans* arrangement of the ligands in this complex. The $^{31}\text{P}\{^1\text{H}\}$ resonance of complex **1** appears as a singlet at -17.3 ppm ($^1J_{\text{PPt}} = 2555$ Hz) with a shift to higher frequencies of 23 ppm with respect to the free phosphine ligand.

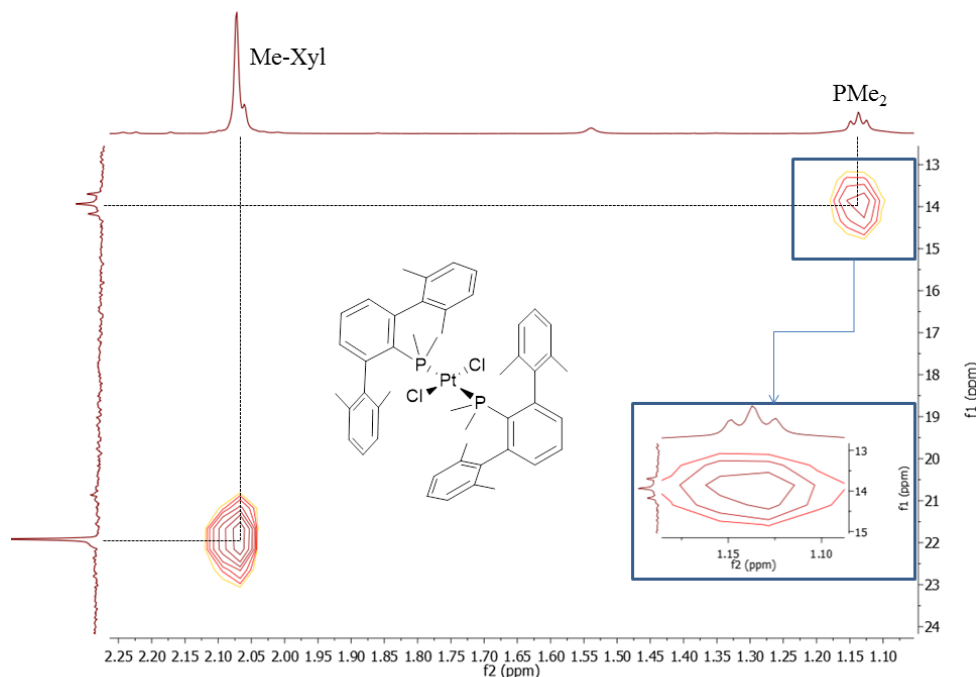
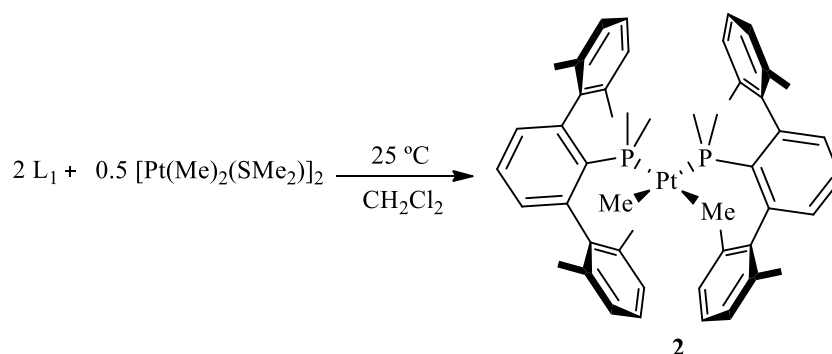


Figure 7. Aliphatic region of the HSQC ^1H - ^{13}C NMR spectrum of complex **1** (300 MHz, CDCl_3 , 25 $^\circ\text{C}$).

The phosphine $\text{PMe}_2\text{Ar}^{\text{Xyl}_2}$, **L**₁, also reacted with the organometallic Pt(II) precursor formed by the mixture of $[\text{Pt}(\text{Me})_2(\mu\text{-SMe}_2)]_2$ and $\text{Pt}(\text{Me})_2(\text{SMe}_2)_2$,⁴⁰ (CH_2Cl_2 , 25 $^\circ\text{C}$) in a 2:1, P:Pt molar ratio, to afford cleanly the neutral mononuclear complex *cis*- $[\text{PtMe}_2(\text{PMe}_2\text{Ar}^{\text{Xyl}_2})_2]$, **2** (Scheme 7).

³⁹ a) R. H. Crabtree, *The Organometallic Chemistry of the Transition Metals*, Vol. Chapter 10, 1st ed., John Wiley & Sons, Inc., **1988**; b) R. K. Harris, *Can. J. Chem.* **1964**, 42, 2275-2281; c) A. Ault, *J. Chem. Educ.* **1970**, 47, 812; d) D. A. Redfield, L. W. Cary, J. H. Nelson, *Inorg. Chem.* **1975**, 14, 50-59.

⁴⁰ J. D. Scott, R. J. Puddephatt, *Organometallics* **1983**, 2, 1643-1648.



Scheme 7: Synthesis of complex **2**.

By contrast with the analogous dichloride derivative **1**, the dimethyl complex **2** features the typical *cis* ligand arrangement found in complexes of this kind,⁴¹ despite the bulkiness of the $\text{PMe}_2\text{Ar}^{\text{Xyl}_2}$ ligands. Since the van der Waals radius of chlorine is similar, if somewhat smaller, to that of the methyl group (1.80 and 2.0 Å, respectively),⁴² it seems probable that observed geometry is a consequence of the strong σ -donor character, and consequently high *trans*-influence of the methyl groups,^{9,38} which tend to avoid each other in opposite coordination positions. The ^1H NMR data for compound **2** are typical of square-planar *cis*- $[\text{PtMe}_2(\text{PR}_3)_2]$ complexes.⁴¹ The platinum bonded methyl groups are equivalent and give rise to a ^{31}P -coupled multiplet centred at 0.0 ppm (Figure 8), with ^{195}Pt satellites of 71 Hz. The corresponding $^{13}\text{C}\{^1\text{H}\}$ resonance is located at δ 1.3 with apparent J_{CP} coupling constants of 105 and 9 Hz, and a one-bond ^{13}C - ^{195}Pt coupling constant of 610 Hz. No attempts were made to compute these spectra.^{41a} The $^{31}\text{P}\{^1\text{H}\}$ spectrum is a sharp singlet placed at -5.3 ppm, with $^1J_{\text{PPt}} = 1773$ Hz. All these parameters are analogous to those reported previously

⁴¹ See for example: a) R. J. Goodfellow, M. J. Hardy, B. F. Taylor, *J. Chem. Soc., Dalton Trans.* **1973**, 2450-2453; b) C. M. Haar, S. P. Nolan, W. J. Marshall, K. G. Moloy, A. Prock, W. P. Giering, *Organometallics* **1999**, *18*, 474-479.

⁴² L. Pauling, *The Nature of the Chemical Bond*, 3rd. ed., Cornell University Press, Cornell University, New York, **1960**.

for similar complexes.

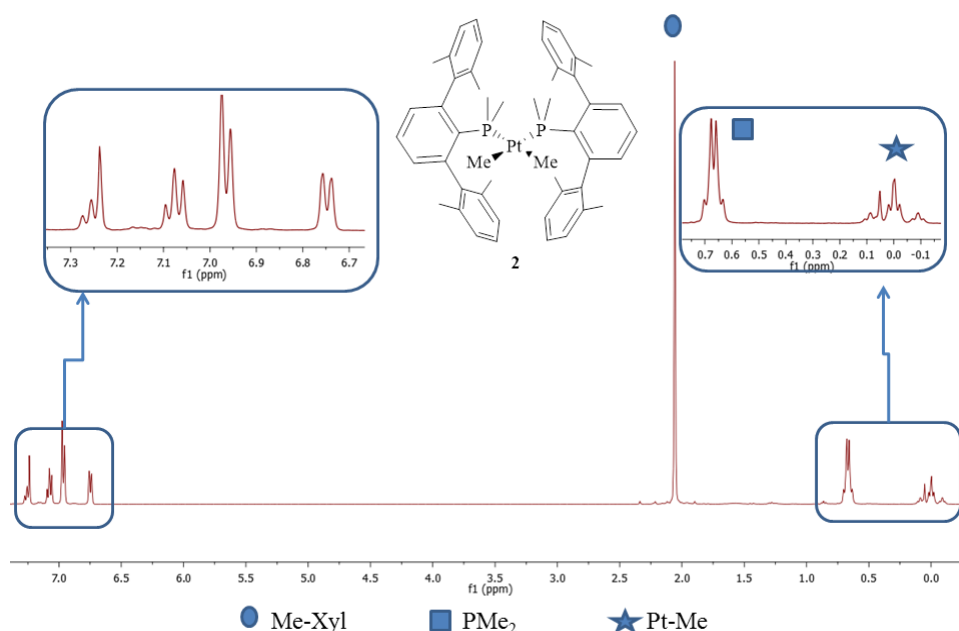


Figure 8: ^1H NMR spectrum of complex **2** (300 MHz, CDCl_3 , 25 $^\circ\text{C}$).

The preparation of complexes **1** and **2** motivated us to search for metallacyclic species derived from these compounds. The historical importance of platinacycles was briefly commented in Section I.1.1 of this Thesis. It was then noted that the fundamental work of Shaw and co-workers demonstrated that steric hindrance, and the feasibility of $\delta\text{-C-H}$ metallation leading to five-membered rings, considerably facilitated the formation of platinacycles.¹⁰ On these grounds, the *o*-tolyl-substituted phosphines, $\text{PPh}(\textit{o}\text{-tolyl})_2$, $\text{P}^t\text{Bu}(\textit{o}\text{-tolyl})_2$ and $\text{P}^t\text{Bu}_2(\textit{o}\text{-tolyl})$ proved particularly useful. In pursuit of such structures, a large number of cyclometallated complexes were prepared in the subsequent decades,⁴³

⁴³ For some early review articles, see: a) G. W. Parshall, *Acc. Chem. Res.* **1970**, 3, 139-144; b) J. Dehand, M. Pfeffer, *Coord. Chem. Rev.* **1976**, 18, 327-352; c) M. I. Bruce, *Angew. Chem. Int. Ed. Engl.* **1977**, 16, 73-86; d) I. Omae, *Coord. Chem. Rev.* **1980**, 32, 235-271.

encompassing a variety of metals and P[^]C, P[^]N, P[^]O, P[^]S, etc., bidentate ligands.^{15d,35f,44-49}

Recent work from our group focused on Pt(II) complexes of the bulky phosphines PⁱPr₂(Xyl) and PMe(Xyl)₂, permitted the synthesis of five-membered bis-metallacycles and the study of their chemical reactivity.³⁶ Milstein and co-workers reported six-membered platinacycles derived from the aryl-monophosphine α^2 -(diisopropylphosphino)isodurene.⁴⁵ However, internal metallation of the terphenylphosphine PMe₂Ar^{Xyl}₂, **L**₁, is not expected to be a facile reaction, since generation of the purported seven-member metallacycle would need the activation of a ζ -C—H bond. In accordance with this hypothesis, while PⁱPr₂(Xyl) and PMe(Xyl)₂ reacted with [PtCl₂(COD)] in the presence of

⁴⁴ a) A. D. Ryabov, *Chem. Rev.* **1990**, 90, 403-424; b) M. E. van der Boom, D. Milstein, *Chem. Rev.* **2003**, 103, 1759-1792; c) M. Albrecht, *Chem. Rev.* **2010**, 110, 576-623; d) I. Omae, *Cyclometalation Reactions*, Springer, Japan, **2014**; e) Y.-F. Han, G.-X. Jin, *Chem. Soc. Rev.* **2014**, 43, 2799-2823; f) F. Mohr, S. H. Privér, S. K. Bhargava, M. A. Bennett, *Coord. Chem. Rev.* **2006**, 250, 1851-1888.

⁴⁵ a) M. E. van der Boom, S.-Y. Liou, L. J. W. Shimon, Y. Ben-David, D. Milstein, *Organometallics* **1996**, 15, 2562-2568; b) M. E. van der Boom, J. Ott, D. Milstein, *Organometallics* **1998**, 17, 4263-4266; c) M. Montag, G. Leitus, L. J. W. Shimon, Y. Ben-David, D. Milstein, *Chem. Eur. J.* **2007**, 13, 9043-9055.

⁴⁶ a) J. Forniés, A. Martín, R. Navarro, V. Sicilia, P. Villarroja, *Organometallics* **1996**, 15, 1826-1833; b) M. Sano, Y. Nakamura, *J. Chem. Soc., Dalton Trans.* **1991**, 417-424.

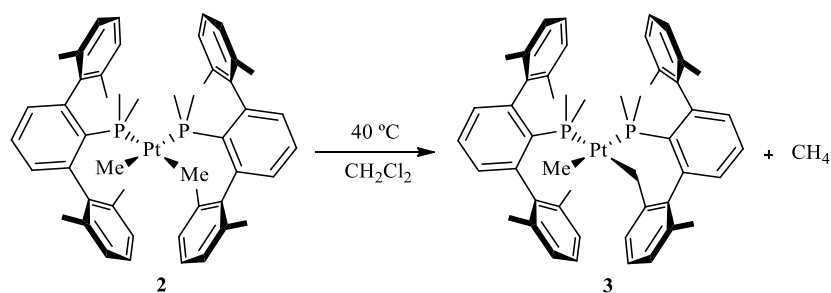
⁴⁷ a) R. Romeo, M. R. Plutino, A. Romeo, *Helv. Chim. Acta* **2005**, 88, 507-522; b) A. Marrone, N. Re, R. Romeo, *Organometallics* **2008**, 27, 2215-2222.

⁴⁸ a) W. Baratta, E. Herdtweck, P. Rigo, *Angew. Chem. Int. Ed.* **1999**, 38, 1629-1631; b) W. Baratta, E. Herdtweck, P. Martinuzzi, P. Rigo, *Organometallics* **2001**, 20, 305-308; c) W. Baratta, C. Mealli, E. Herdtweck, A. Ienco, S. A. Mason, P. Rigo, *J. Am. Chem. Soc.* **2004**, 126, 5549-5562; d) W. Baratta, A. Del Zotto, G. Esposito, A. Sechi, M. Toniutti, E. Zangrando, P. Rigo, *Organometallics* **2004**, 23, 6264-6272; e) W. Baratta, M. Ballico, A. Del Zotto, E. Zangrando, P. Rigo, *Chem. Eur. J.* **2007**, 13, 6701-6709.

⁴⁹ a) A. Zucca, G. L. Petretto, S. Stoccoro, M. A. Cinellu, G. Minghetti, M. Manassero, C. Manassero, L. Male, A. Albinati, *Organometallics* **2006**, 25, 2253-2265; b) A. Zucca, G. L. Petretto, S. Stoccoro, M. A. Cinellu, M. Manassero, C. Manassero, G. Minghetti, *Organometallics* **2009**, 28, 2150-2159; c) G. L. Petretto, J. P. Rourke, L. Maidich, S. Stoccoro, M. A. Cinellu, G. Minghetti, G. J. Clarkson, A. Zucca, *Organometallics* **2012**, 31, 2971-2977; d) L. Maidich, G. Zuri, S. Stoccoro, M. A. Cinellu, M. Masia, A. Zucca, *Organometallics* **2013**, 32, 438-448; e) L. Maidich, G. Zuri, S. Stoccoro, M. A. Cinellu, A. Zucca, *Dalton Trans.* **2014**, 43, 14806-14815; f) A. Zucca, L. Maidich, L. Canu, G. L. Petretto, S. Stoccoro, M. A. Cinellu, G. J. Clarkson, J. P. Rourke, *Chem. Eur. J.* **2014**, 20, 5501-5510.

K_2CO_3 to afford the expected platinacycles,¹¹ the reaction of $\text{PMe}_2\text{Ar}^{\text{Xyl}_2}$ under otherwise identical conditions resulted in an intractable mixture of products. Use of isolated complex **1** and a diversity of bases (K_2CO_3 , KO^tBu , 2,2,6,6-tetramethylpiperidine) made no improvement.

At variance with these observations, the dimethyl complex **2** underwent cyclometallation under mild conditions to originate the desired seven-member platinacycle **3** (Scheme 8), accompanied by liberation of methane. This result was not unforeseen since it has long been known that the existence of Pt-Me bonds (in general Pt-alkyl bonds) facilitates considerably the cyclometallation reaction.^{45,47}



Scheme 8: Synthesis of complex **3**.

Compound **3** was characterized by microanalysis, solution NMR spectroscopy and X-ray crystallography. As expected, and as a consequence of the lower symmetry of **3** compared to **2**, five singlets due to the benzylic CH_3 protons appear in the ^1H NMR spectrum of complex **3** between *ca.* δ 1.90 and 2.45 ppm (Figure 9).

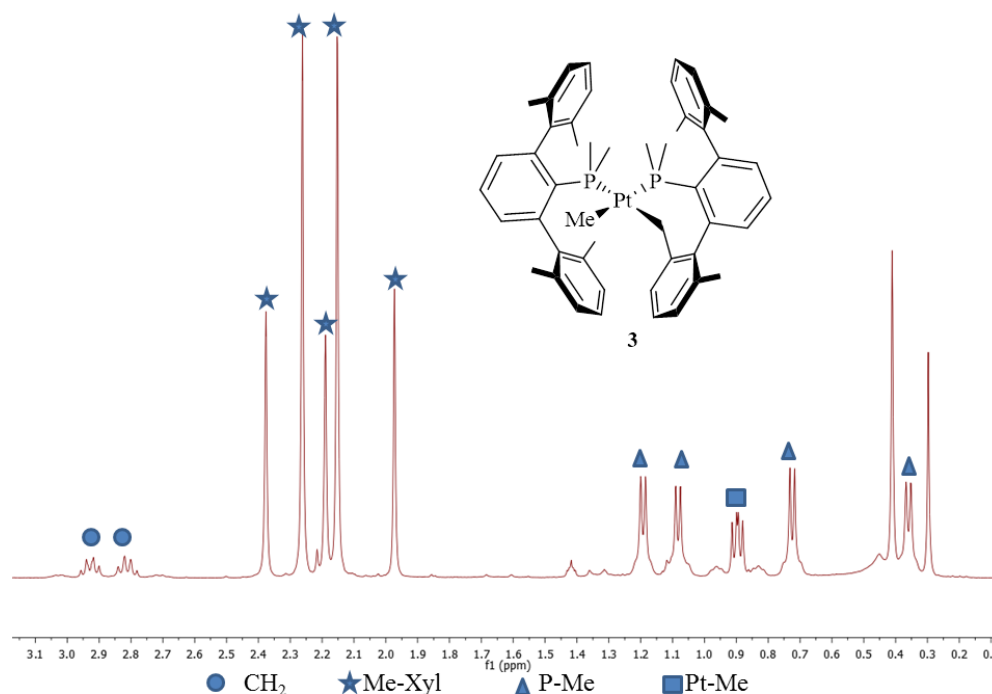


Figure 9: ^1H NMR spectrum of complex **3** (300 MHz, C_6D_6 , 25 $^\circ\text{C}$).

In addition, the platinum-bound methylene protons are diastereotopic and resonate at 2.81 and 2.93 ppm as deceptively simple doublets of doublets, with apparent J_{PH} coupling constants of 19.5 and 8.8 Hz, also showing Pt satellites with a large $^2J_{\text{HPt}}$ coupling constant of about 100 Hz. As regards the $^{13}\text{C}\{^1\text{H}\}$ spectrum of **3**, the methylene carbon nucleus gives also rise to a seemingly simple doublet of doublets, with apparent ^{13}C - ^{31}P coupling constants of 95 and 6 Hz, $^1J_{\text{PtC}} = 549$ Hz. The inequivalency of the two phosphorus atoms is reflected in the $^{31}\text{P}\{^1\text{H}\}$ spectrum of complex **3**, which consists of two doublets centred at -7.9 and -4.3 ppm with a small ^{31}P - ^{31}P coupling of 6 Hz, and ^{195}Pt - ^{31}P constants of 1748 Hz and 1985 Hz, respectively, the latter two in the range normally expected for complexes of this type.

As anticipated, the solid structure of compound **3** was also confirmed by single crystal X-ray diffraction studies (Figure 10). The Pt(II) atom is four-coordinate and lies in a distorted square-planar environment. The angle between the two planes defined by atoms C49, Pt1, and C1, and P1, Pt1, and P2, is actually of 10.88°. This notable distortion is reasonable to ascribe to the crowded coordination environment and to the rigidity of the 7-membered platinacycle.

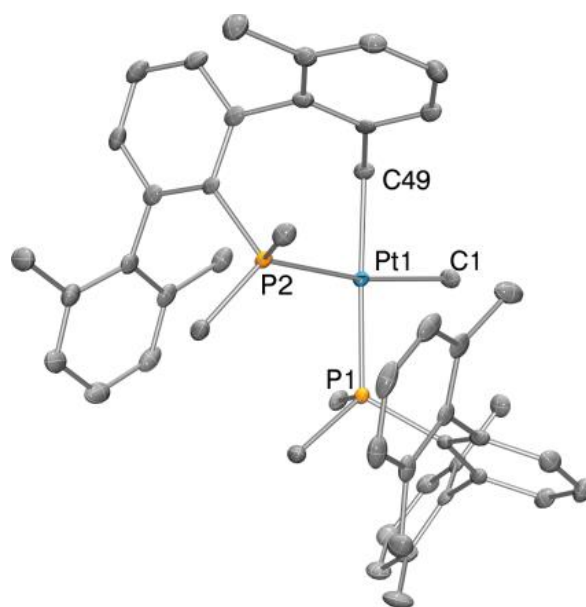


Figure 10. ORTEP view of complex **3**; hydrogen atoms are excluded for clarity and thermal ellipsoids are set at 50% level of probability. Selected bond distances (Å) and angles(°): Pt1–P1 2.3000(7), Pt1–C1 2.107(3), Pt1–P2 2.2943(7), Pt1–C49 2.126(3), P1–Pt1–C1 86.05(8), P1–Pt1–P2 103.62(2), P2–Pt1–C49 86.29(7), C49–Pt1–C1 84.6(1).

The mechanism of the cycloplatination reaction was thoroughly investigated by the group of Romeo and Re with the aid of extensive experimental kinetic studies, complemented with computational work.⁴⁷ The results of these investigations, based on the complex *cis*-[PtMe₂(dmsO)(P(*o*-tolyl)₃)], supported a mechanism initiated by reversible dissociation of dmsO and formation of a three-coordinate, T-shaped species. We monitored the cyclometallation reaction that converts complex

2 into **3** by ^1H and $^{31}\text{P}\{^1\text{H}\}$ NMR spectroscopy at 55 °C, using C_6D_6 as the solvent (Figure 11). Similarly to Romeo and Re's results, our monitoring of the cycloplatination reaction revealed the presence of only the starting (bottom spectra in Figures 11a and 11b) and the final cyclometallated complexes (top spectra) with no evidence for the formation of detectable amounts of any intermediate species. As shown in Figures 11 and 12, the reaction went to completion in about 90 minutes at 55 °C (*ca.* six half-lives) and followed first-order kinetics. An Eyring representation of kinetic data measured at 40, 45, 50, 55, and 60 °C (Figure 12 bottom) yielded ΔH^\ddagger and ΔS^\ddagger values of $31 \pm 1 \text{ kcal}\cdot\text{mol}^{-1}$ and $22 \pm 4 \text{ cal}\cdot\text{K}^{-1}\cdot\text{mol}^{-1}$, with ΔG^\ddagger $25 \pm 3 \text{ kcal}\cdot\text{mol}^{-1}$ (at 25 °C).

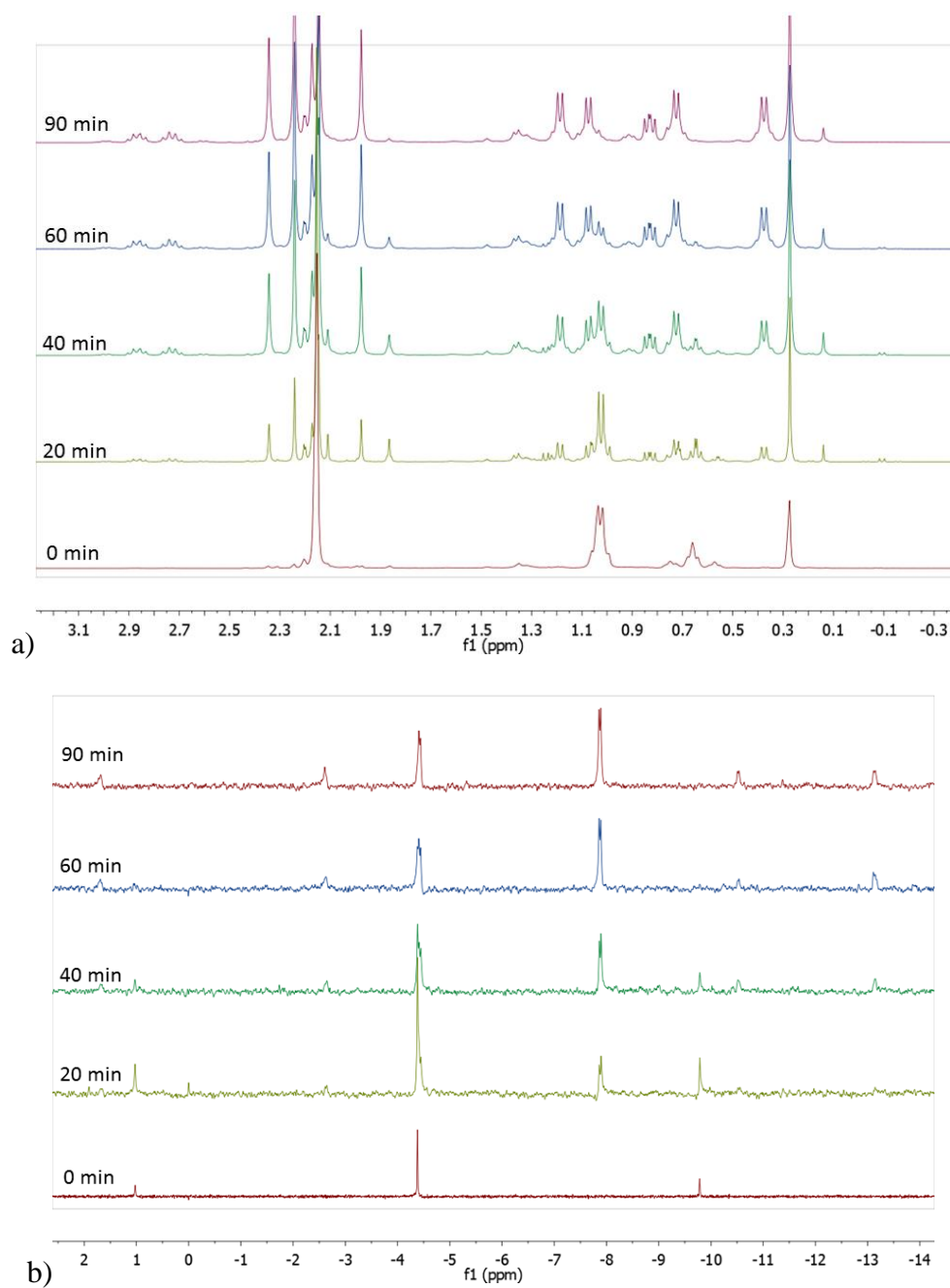


Figure 11. Aliphatic area of 1H (a) and $^{31}P\{^1H\}$ NMR (b) spectra at 55 °C in C_6D_6 , showing the conversion of **2** into **3**. The first spectrum (bottom, $t = 0$ min) corresponds to pure **2**, the last one (top, $t = 90$ min) to complex **3**.

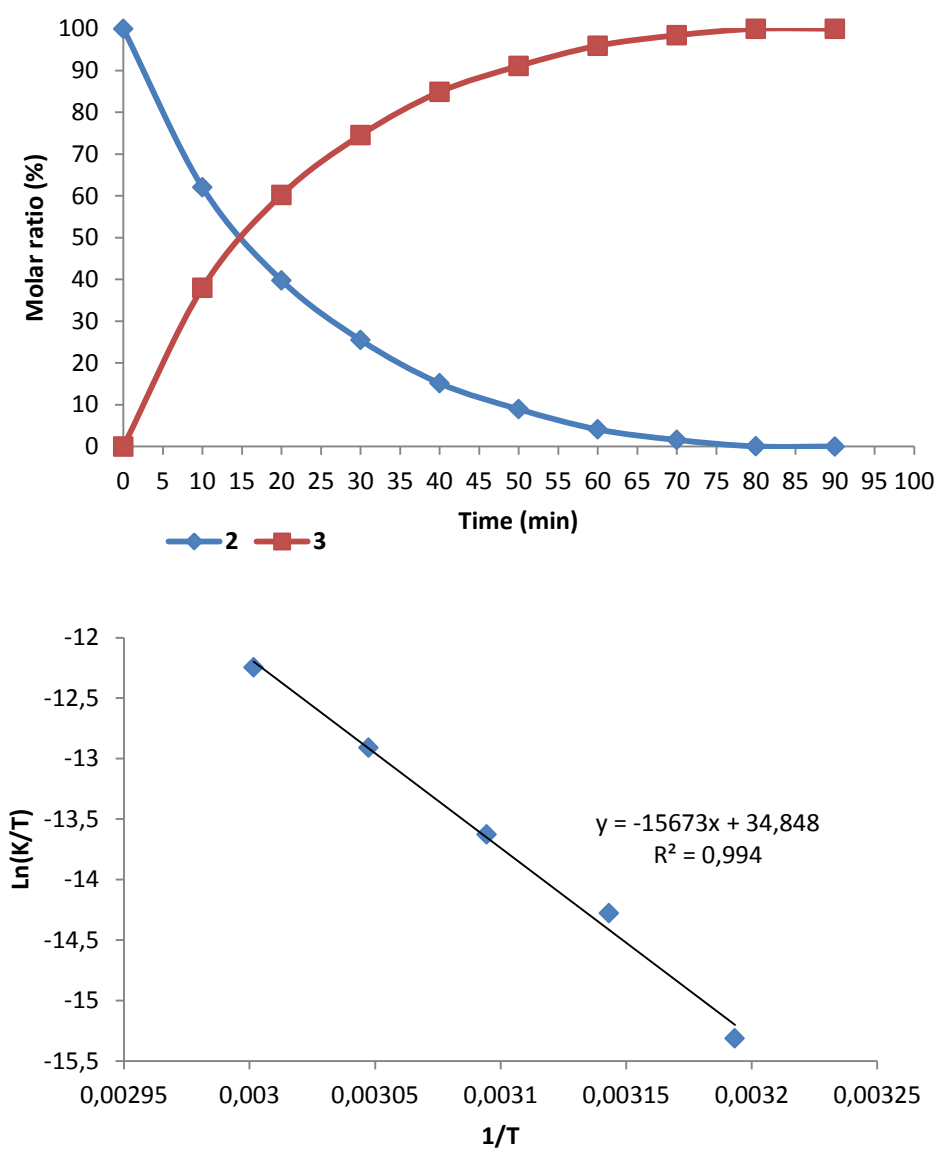
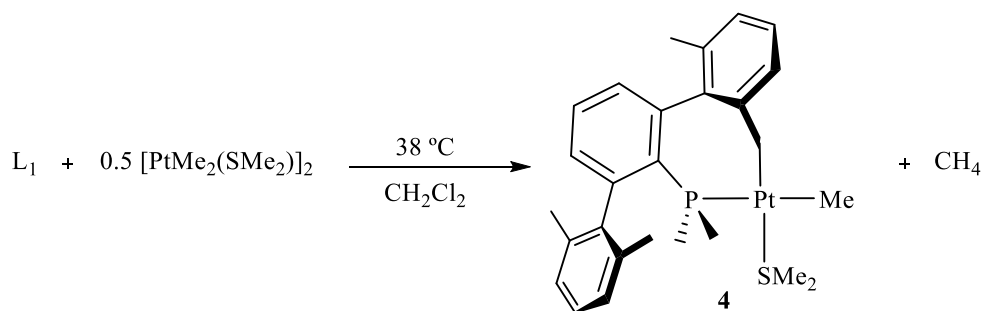


Figure 12: Concentration vs. time (top) and Eyring (bottom) representations for the conversion of complex **2** into **3**. Kinetic data were recorded in C_6D_6 at the temperatures specified in the text, *i.e.* 55 °C (top) and 40, 45, 50, 55 and 60 °C (Eyring plot).

I.2.1.2. Mono(phosphine) Pt(II) Platinacycles. Synthesis and Reactivity.

The tendency of platinum (II) methyl complexes to undergo cyclometallation already alluded to, suggested that a mono(phosphine) metallacycle could be readily obtained. Treatment of the platinum precursor $[\text{PtMe}_2(\text{SMe}_2)]_2$ with the phosphine $\text{PMe}_2\text{Ar}^{\text{Xyl}_2}$ (**L**₁) in a 1:1 platinum:phosphine ratio (CH_2Cl_2 , 38 °C) cleanly yielded the platinacycle **4** (Scheme 9).



Scheme 9. Synthesis of complex **4**.

The aliphatic area of the ^1H NMR spectrum of complex **4** between *ca.* 0.2 and 2.7 ppm is shown in Figure 13. The two diastereotopic methyl groups of the phosphine give rise to two different resonances at 0.57 and 0.62 ppm; similarly, the benzylic methyl protons resonate as two sharp singlets at *ca.* 2.1 (6H) and 2.4 (3H) ppm. In contrast, the CH_3 groups of the coordinated dimethylsulphide are equivalent, probably due to fast rotation along the Pt-S bond, and show a three-bond Pt-H coupling constant of 24.7 Hz. The Pt-Me group resonates at 0.57 ppm as a doublet ($^3J_{\text{HPt}} = 7.2$ Hz, $^2J_{\text{HPt}} = 65.9$ Hz). In the $^{31}\text{P}\{^1\text{H}\}$ NMR spectrum, a singlet at -7.7 ppm, with a $^1J_{\text{PPt}}$ of 1950 Hz was observed.

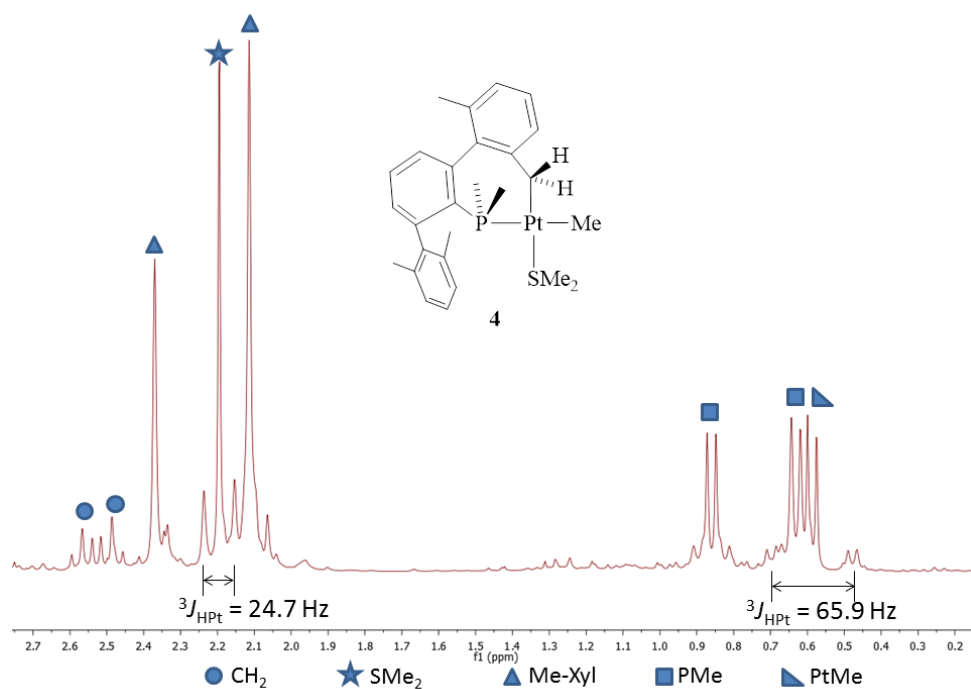


Figure 13. Aliphatic area of the ^1H NMR spectra of complex **4** (300 MHz, CDCl_3 , 25 °C).

Figure 14 shows an ORTEP view of the solid-state molecular structure of complex **4**. This square-planar Pt(II) complex features Pt-C and Pt-P bond distances similar to those of **2**, but the distortion appears somehow reduced in this monophosphine complex, perhaps due to the reduced steric hindrance exerted by the coordination environment.

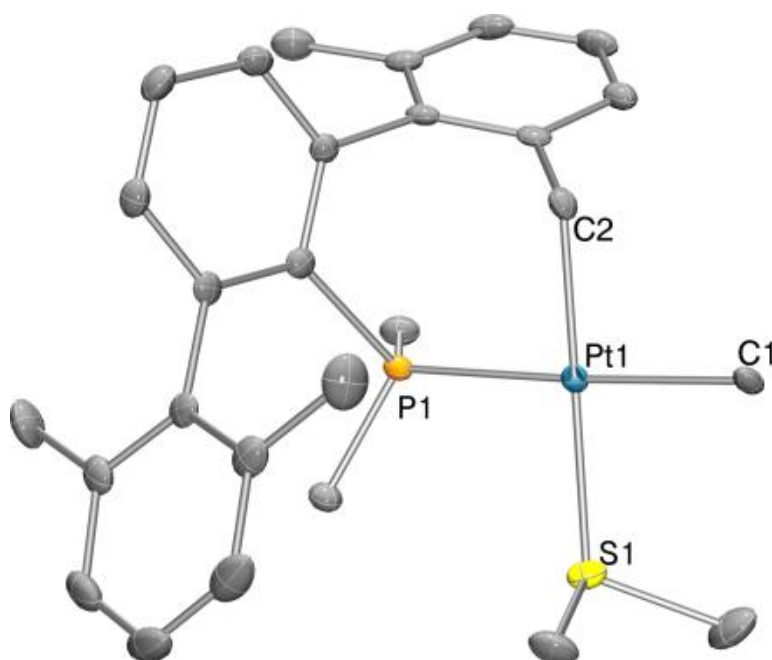


Figure 14. ORTEP view of the solid structure of **4** with ellipsoids drawn at the 50% probability level. Selected bond distances [Å] and angles [°]: Pt1–P1 2.3545(9), Pt1–C2 2.085(2), Pt1–C1 2.162 (2), Pt1–S1 2.3577(9), P1–Pt1–C2 88.48(7), C2–Pt1–C1 88.69(9), C1–Pt1–S1 90.50(6), S1–Pt1–P1 92.34(2).

Taking advantage of the lability of the SMe_2 ligand, we performed the reaction of complex **4** with PPh_3 in CH_2Cl_2 at 25 °C. $^{31}\text{P}\{^1\text{H}\}$ NMR spectroscopy of the crude reaction mixture made clear that under these conditions, a mixture of *cis* and *trans* isomers in a ca. 4:1 molar ratio was formed (Figure 15). Although substitution reactions in square planar platinum(II) complexes usually occur through an associative mechanism, which implies retention of stereochemistry, the partial formation of the *trans* isomer in the present case seems to indicate the participation of a dissociative pathway⁵⁰ favoured by steric hindrance, which could give rise to the mixture of *cis*-**5** and *trans*-**5** according to Scheme 10. The minor *trans* complex could be removed by washing with small portions of

⁵⁰ G. Faraone, V. Ricevuto, R. Romeo, M. Trozzi, *Inorg. Chem.* **1969**, 8, 2207-2211.

pentane, allowing the isolation of the *cis* isomer as a pure air-stable white solid, that was fully characterized by NMR spectroscopy (See Figure 16 and the Experimental Section).

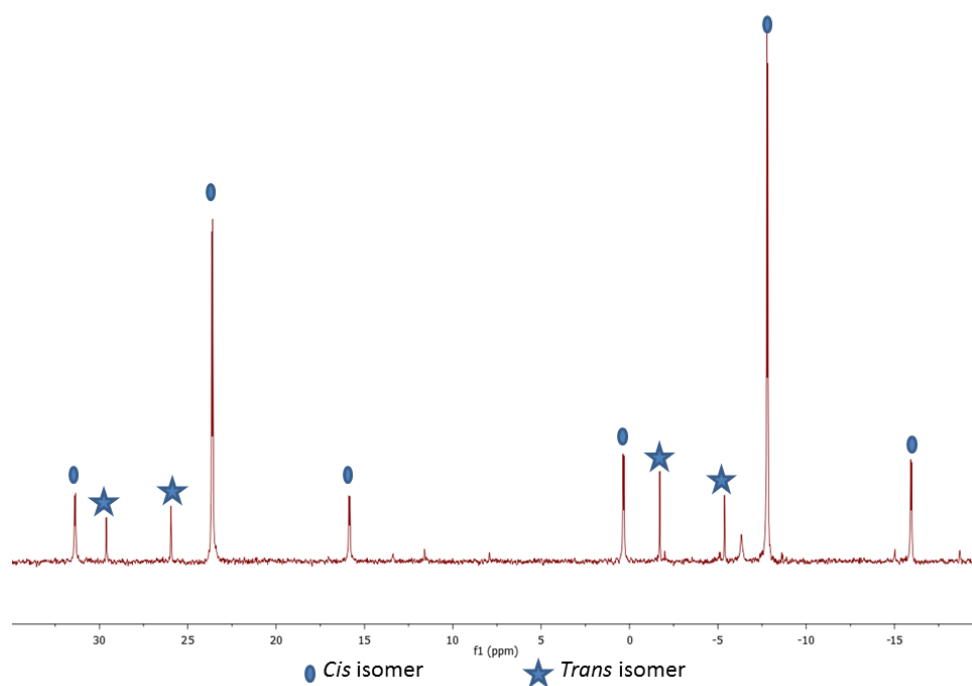
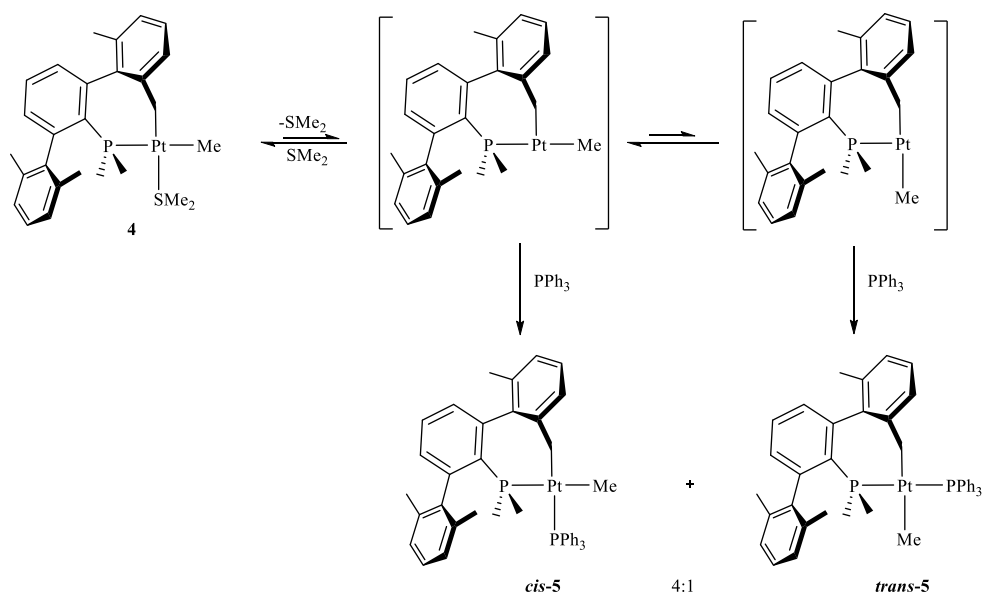


Figure 15. $^{31}\text{P}\{^1\text{H}\}$ NMR spectrum of the crude for the formation of *cis* and *trans* isomers of complex **4** (300 MHz, CD_2Cl_2 , 25 °C).



Scheme 10. Formation of the PPh_3 complexes **5**.

The *cis* geometry proposed for this complex is definitely deduced from its $^{31}\text{P}\{^1\text{H}\}$ NMR spectrum, that contains two doublets at δ -7.8 and 23.8 ppm, with an unquestionably *cis* $^2J_{\text{PP}}$ coupling of only 7 Hz. The two signals are escorted by ^{195}Pt satellites of 1978 and 1886 Hz, respectively, in agreement with their phosphorus atoms being part of *trans*-P—Pt—C arrangements. By similarity with what was observed for the also cyclometallated complexes **3** and **4**, the platinum bonded methylene protons are diastereotopic and give rise to ^{31}P - and ^{195}Pt -coupled multiplets located at 2.59 and 2.31 ppm (Figure 16). The corresponding $^{13}\text{C}\{^1\text{H}\}$ signal appears as a first-order doublet of doublets at 33.6 ppm, with *trans* and *cis* couplings to the ^{31}P nuclei of 89 and 5 Hz, respectively.

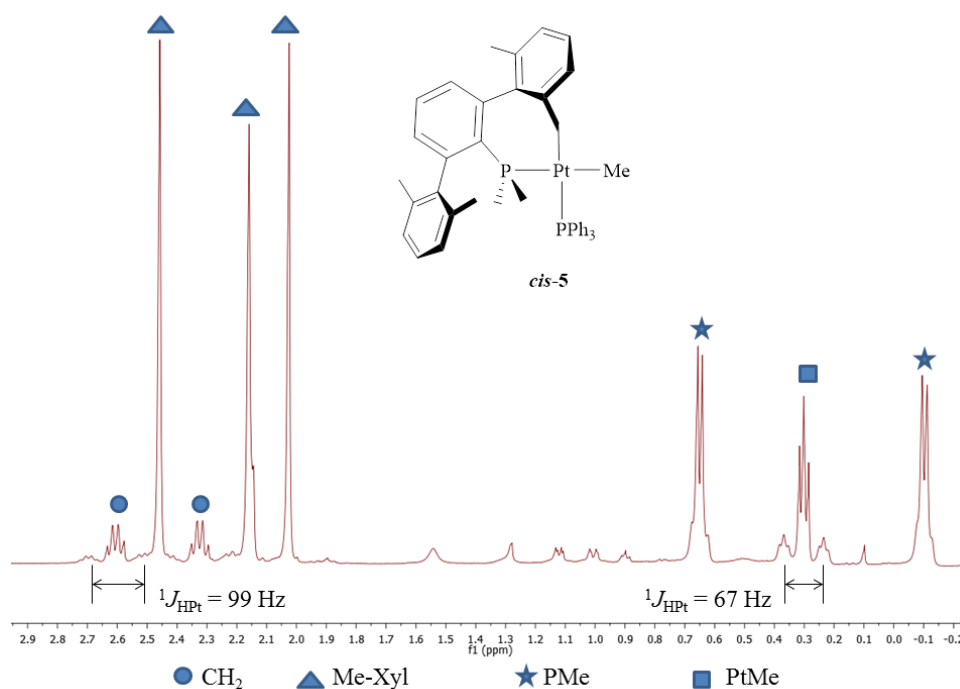


Figure 16: Aliphatic region of the ¹H NMR spectrum of complex *cis-5* (500 MHz, CD₂Cl₂, 25 °C).

1.2.1.3. Protonation of Complexes 2 and 3

To investigate the possibility of generating three-coordinate T-shaped Pt(II) cationic species stabilized by ligand **L**₁, we studied the protonation of complexes **2** and **3** with [H(Et₂O)₂][BAr_F] ([BAr_F] = [B(3,5-(CF₃)₂C₆H₃)₄]), which may accurately be viewed as a non-coordinating acid. It is worth recalling that this is a common synthetic method for the production of low-coordinated species that feature agostic interactions. Moreover, a similar procedure was utilised by Goldberg, Brookhart and co-workers for the successful low-temperature characterisation of the first transition metal methane complex.⁵¹

⁵¹ W. H. Bernskoetter, C. K. Schauer, K. I. Goldberg, M. Brookhart, *Science* **2009**, 326, 553-556.

The protonation of complex **2** by $[\text{H}(\text{Et}_2\text{O})_2][\text{BAr}_\text{F}]$ (1 equiv) was brought about at $-80\text{ }^\circ\text{C}$ (CD_2Cl_2) and the progress of the reaction monitored by ^1H and $^{31}\text{P}\{^1\text{H}\}$ NMR spectroscopy. Figure 17 contains variable temperature $^{31}\text{P}\{^1\text{H}\}$ spectra in the temperature interval from -80 ° to $50\text{ }^\circ\text{C}$. At the lowest temperature studied, a mixture of two complexes appears to exist. The major one contains two doublets centred at -8.4 and 24.9 ppm that correspond to an AX spin system with a *cis*-AX coupling of 11 Hz . The higher frequency signal features $J_{\text{PPt}} = 4760\text{ Hz}$, whereas for the other, the one bond $^{31}\text{P}\text{-}^{195}\text{Pt}$ coupling constant amounts 2200 Hz . We suggest that these parameters correspond to the formally three coordinate complex **A** (see Figure 17) in which the phosphorus atom responsible for the -8.4 resonance is *trans* to a weakly bound molecule of solvent (not represented in Figure 17), whereas the other is *trans* to the methyl group. The value of 2200 Hz found the $^{31}\text{P}\text{-}^{195}\text{Pt}$ coupling for this phosphorus nucleus is comparable to others found for *trans*- $\text{P}\text{---Pt---C}_{\text{alkyl}}$ units reported in this Thesis. In turn, the minor species appears as a singlet at -5.8 ppm and features a $^{31}\text{P}\text{-}^{195}\text{Pt}$ coupling of 2980 Hz , typical for *trans*- $\text{P}\text{---Pt---P}$ units (structure **B** in Figure 17).

As represented in Figure 17, at $0\text{ }^\circ\text{C}$ the *trans* complex **B** became the major product at the expense of the *cis* isomer, most probably to avoid steric repulsions between the phosphine ligands of the latter. No other significant change was detected, although upon warming at $25\text{ }^\circ\text{C}$ two new structures **C** and **D** appeared with accompanying loss of **A** and **B**. We propose that the new compounds result from facile cycloplatination of one of the $\text{PMe}_2\text{Ar}^{\text{Xyl}_2}$ ligands (*vide supra*), with liberation of CH_4 (detected by ^1H NMR). Complex **C** is proposed to contain a *trans* distribution of the non-equivalent phosphorus nuclei, as hinted by the observation of an AB quartet, characterized by $\delta_\text{A} = 2.0\text{ ppm}$, $\delta_\text{B} = 17.2\text{ ppm}$ and $^2J_{\text{AB}} = 386\text{ Hz}$ along with $^2J_{\text{P}_\text{A}\text{Pt}}$ and $^2J_{\text{P}_\text{B}\text{Pt}}$ values of 3119 and 3078 Hz , respectively.

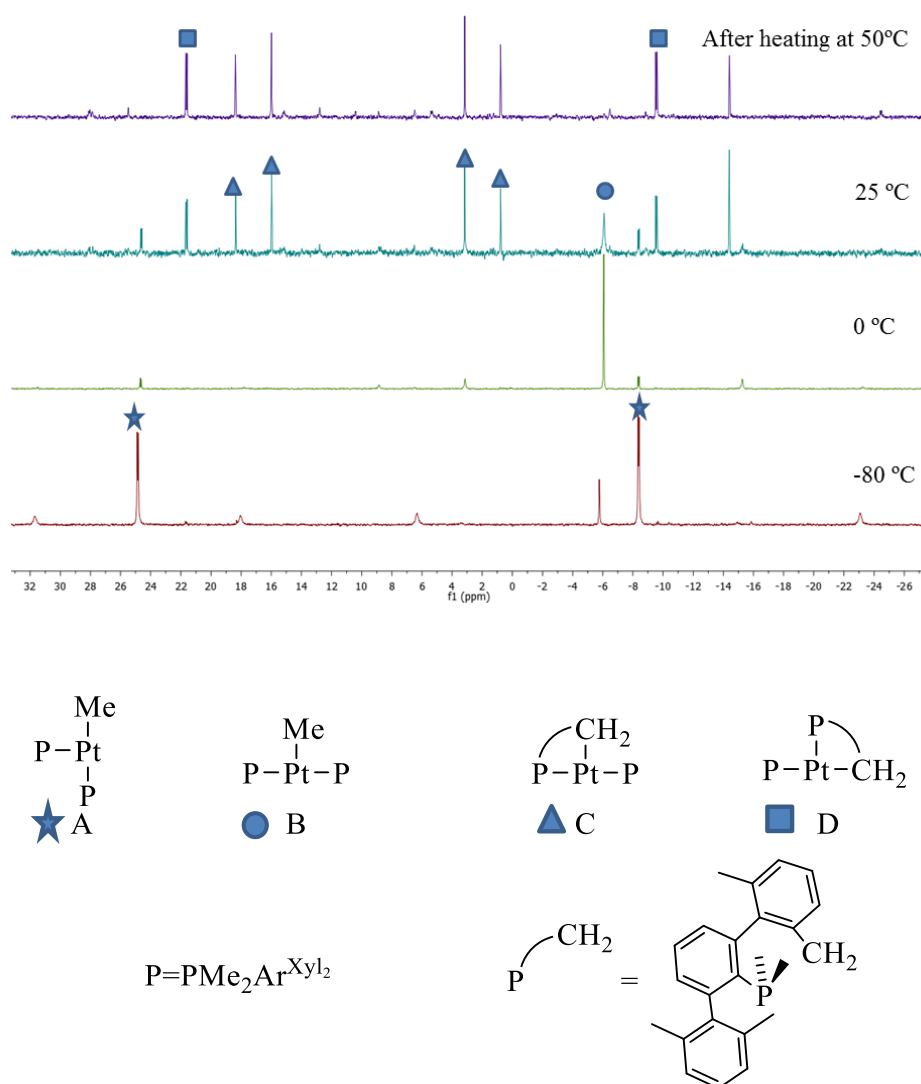


Figure 17. Variable temperature $^{31}\text{P}\{^1\text{H}\}$ NMR spectra recorded for the protonation of complex **2** with $[\text{H}(\text{Et}_2\text{O})_2][\text{BAR}_\text{F}]$ (161.9 MHz, CD_2Cl_2). The fourth platinum coordination position is proposed to be occupied by a molecule of CD_2Cl_2 .

As for **D**, a *cis* arrangement of the phosphorus atoms is considered, as insinuated by the observation of two doublets with δ -9.6 and 21.6 ppm, and $^2J_{\text{PP}}$ equal to 14 Hz. These ^{31}P resonances are further characterised by $^1J_{\text{PPt}}$ couplings of 4831 and 2087 Hz, in accordance with the proposed structure. Besides signals due to the *cis* and *trans* isomers, a singlet at -14.4

ppm is observed for an unidentified product. Heating at 50 °C for 22 h results in full consumption of the initial reaction products, complexes **A** and **B**, with no other relevant variation relative to the room temperature spectrum.

Similar intermediates and final products were also expected to form in the protonation of complex **3**. Interestingly, this species contains two different Pt-C bonds and therefore there are two alternative positions for the proton to attack, that is the cyclometallated Pt-CH₂ linkage and the Pt-Me bond. In fact, the ³¹P{¹H} NMR spectrum of the crude reaction mixture that emanates from the protonation of complex **3** at low temperatures (-80 °C) reveals the formation of the four possible structures that could derive from H⁺ addition at the two Pt-C sites, followed by *cis*-to-*trans* isomerisation of the corresponding T-shaped intermediates. Upon increasing the temperature to room temperature, the mixture evolves to afford as the main products of the protonation reaction the cyclometallated isomers detected for compound **2**, that is, complexes **C** and **D**, characterised by resonances at 21.6 and -9.6 ppm (²J_{PP} = 14 Hz) for the *cis* isomer, and at 17.2 and 2.0 ppm (²J_{PP} = 386 Hz, ¹J_{PPt} = 3078 and 3119 Hz, respectively) for the *trans* one (Figure 18).

In agreement with these observations, the protonation of complexes **2** and **3** can be proposed to occur as summarized in Scheme 11.

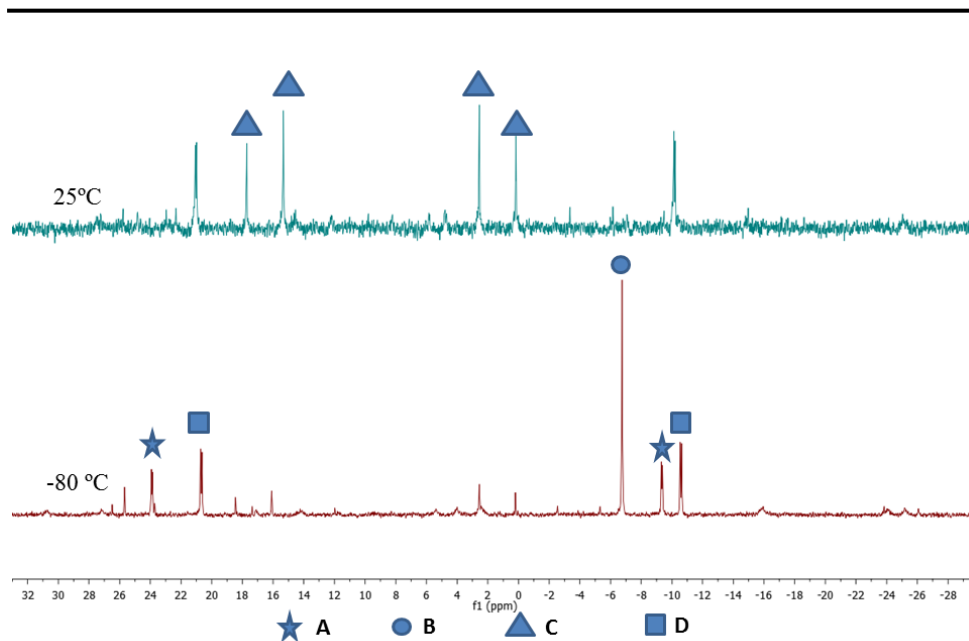
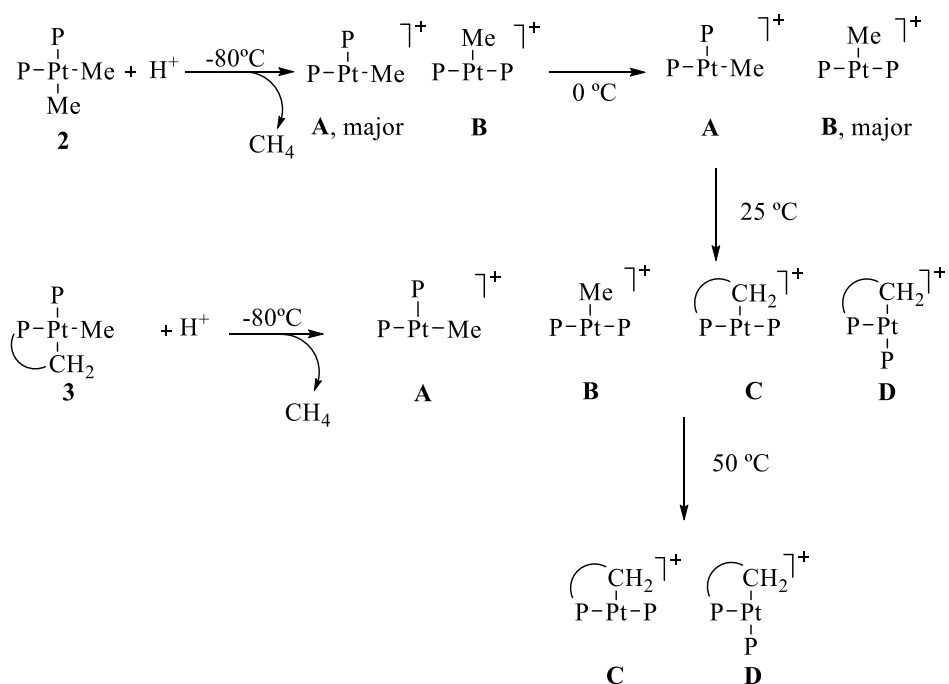


Figure 18: Variable temperature $^{31}\text{P}\{^1\text{H}\}$ NMR spectra of the protonation of complex **3** with $[\text{H}(\text{Et}_2\text{O})_2][\text{BAr}_\text{F}]$ (129.5 MHz, CD_2Cl_2).



Scheme 11. Proposed product manifold for the protonation of complexes **2** and **3** with $[\text{H}(\text{Et}_2\text{O})_2][\text{BAr}_\text{F}]$. As in Figure 17, the fourth platinum coordination site in structures **A-D** is proposed to be occupied by a molecule of CD_2Cl_2 .

I.2.2. Pt(II) Complexes of the Terphenylphosphines $\text{PMe}_2\text{Ar}^{\text{Dipp}_2}$ and $\text{PMe}_2\text{Ar}^{\text{Tipp}_2}$

In this section new results concerning the synthesis, characterisation, reactivity and catalytic properties of neutral and cationic complexes of Pt(II) containing the terphenylphosphine ligands $\text{PMe}_2\text{Ar}^{\text{Dipp}_2}$ (L_2), and $\text{PMe}_2\text{Ar}^{\text{Tipp}_2}$ (L_3), are described (Figure 19).

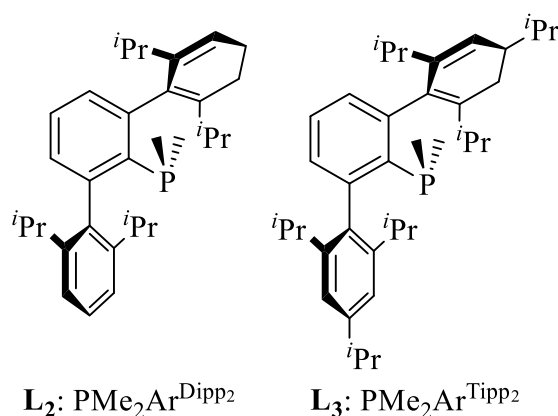


Figure 19: Dimethylterphenylphosphines L_2 and L_3 .

The synthetic routes used for the preparation of L_2 and L_3 are analogous to that employed for L_1 . The two phosphines are pale yellow solids, soluble in common organic solvents such as pentane, benzene, or dichloromethane, and exhibit good stability towards air, particularly in the solid state.

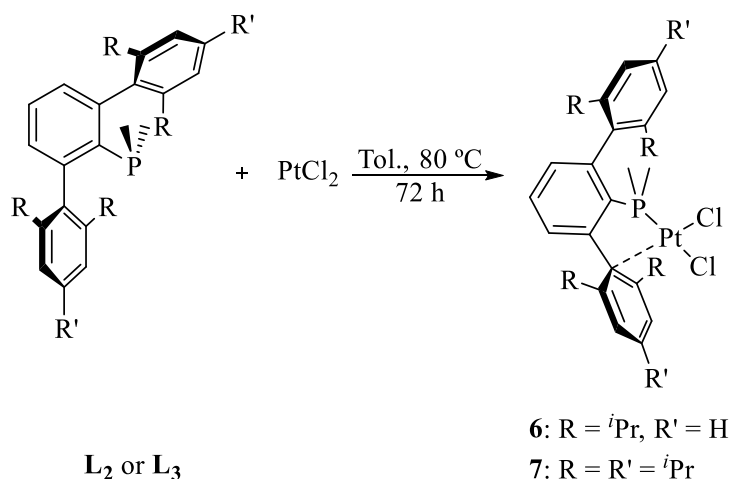
The majority of the new compounds reported contain ligand L_2 , although some derivatives of L_3 were also prepared for comparative purposes. As noted above, some are neutral species, but others are cationic, with one or two positive charges on the Pt(II) centre. Some of the complexes are coordination compounds in a classical sense (e.g. halide- or hydride-phosphine complexes) whereas others are truly organometallic, actually hydrocarbyl species, comprising methyl, phenyl and allyl

derivatives. In many of the complexes the phosphine ligand binds to platinum in a bidentate fashion, through the phosphorus atom and the *ipso* carbon atom of one of the aryl substituents of the terphenyl group, while in others monodentate P-coordination was imposed by action of other Lewis bases.

I.2.2.1. Neutral Platinum(II) Complexes with Bidentate (κ^1 -P, η^1 -arene) Phosphine Coordination

Dichloro Complexes

Phosphines **L**₂ and **L**₃ reacted cleanly (toluene, 80 °C) with one equivalent of the commercially available Pt precursor PtCl₂, to generate complexes **6** and **7** in high yield (Scheme 12), that contain *cis* chloride ligands.



Scheme 12. Synthesis of the complexes [PtCl₂(PMe₂Ar')], **6** and **7**.

Formally in complexes **6** and **7** there are only three ligands in the metal coordination sphere and therefore they might be viewed as T-shaped 14-electron species. Notwithstanding, to counterbalance this unsaturation,

the phosphine acts as a bidentate ligand with a κ^1 -P, η^1 -arene coordination mode, as revealed by X-ray studies to be discussed later. Because of this unusual aryl phosphine binding, the symmetry of the terphenyl group changes compared with that of the free ligand, and this variation becomes evident by NMR spectroscopy. In the ^1H NMR spectra of both complexes (Figure 20), four different doublet resonances for the methyl groups of the *i*Pr substituents at the 2,6-aryl positions are detected and, in the case of complex **7**, two additional doublets for the 4-*i*Pr methyl groups are also observed. These spectroscopic data reveal the non-equivalent nature of the flanking aryl rings. The $^{31}\text{P}\{^1\text{H}\}$ NMR resonances and $^1J_{\text{PPt}}$ values for both complexes are very similar (10.9 ppm and 3189 Hz for **6** and 10.6 ppm and 3226 Hz for **7**).

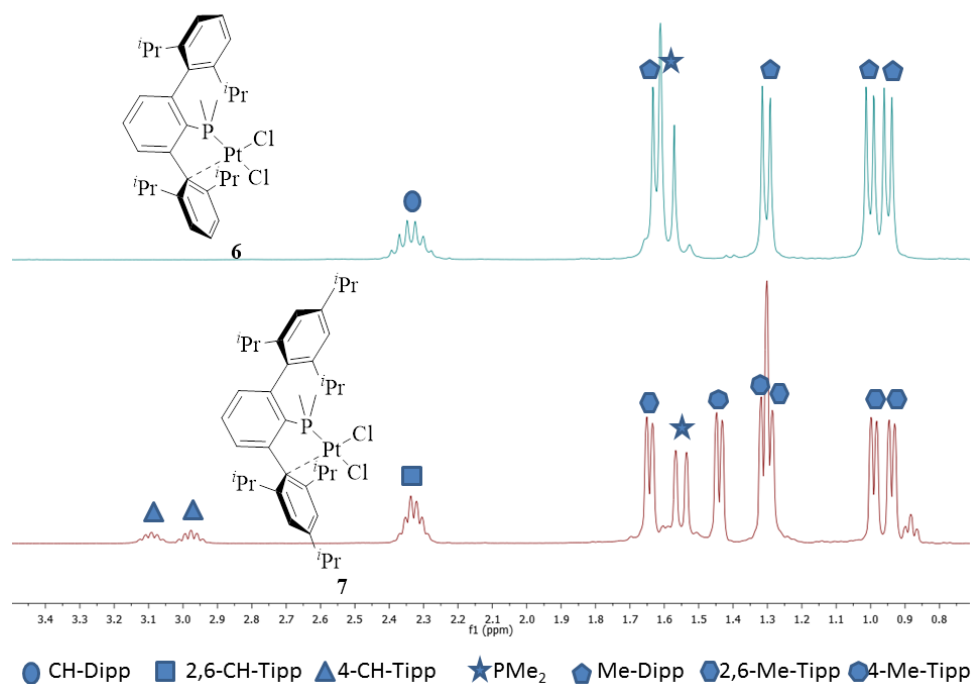


Figure 20. The ^1H NMR spectra of complexes **6** and **7** (CD_2Cl_2 , 300 MHz (top), 400 MHz (bottom), 25°C) in the chemical shift range *ca.* 0.80 - 3.50 ppm.

The molecular structure of complex **6** was determined in the solid state by single crystal X-ray diffraction studies (Figure 21). In accordance with the NMR data already analysed, the phosphine acts as a bidentate κ^1 -P, η^1 -C_{ipso} ligand with Pt—P and Pt—C_{ipso} contacts of 2.215(1) and 2.228(5) Å, respectively. The latter distance denotes significant Pt—C_{arene} bonding interaction.⁵² It is, however, longer than the Pt(II)-olefinic carbon bonds in Zeise's salt (roughly 2.16 Å)⁵³, in accordance with the partial unsaturated character of these complexes, which can be envisioned as a source of [PtCl₂(PMe₂Ar')] fragments. Congruent with these considerations the Pt1A-Cl1 bond *trans* to the Carene (C1 in Figure 21) at 2.350(1) Å is shorter than the Pt1A-Cl2 bond placed *trans* with respect to the phosphine ligand (2.401(1) Å).^{9,38}

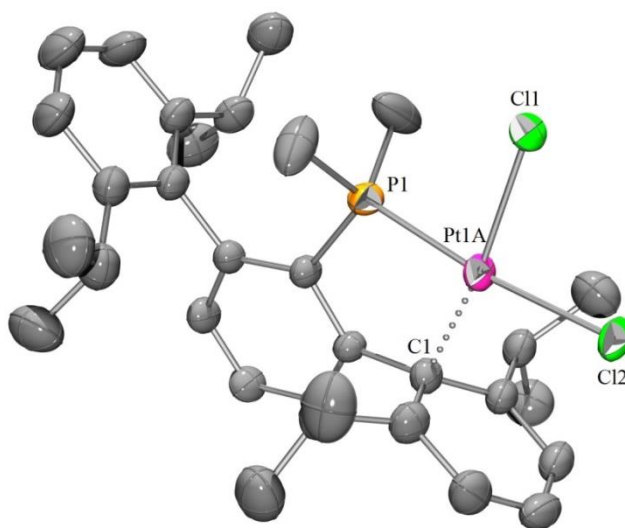


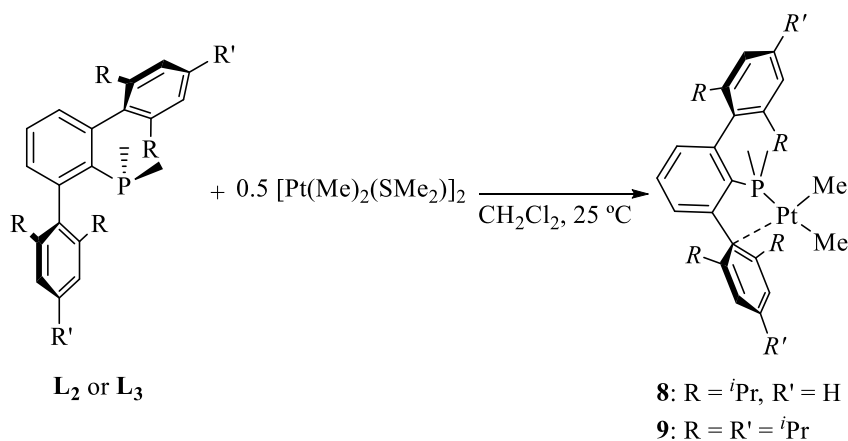
Figure 21: ORTEP view of complex **6**; hydrogen atoms are excluded for clarity and thermal ellipsoids are set at 50 % level probability. Selected bond distances (Å) and angles (°): Pt1A-P1 2.215(1), Pt1A-Cl1 2.350(1), Pt1A-Cl2 2.401(1), Pt1A-C1 2.228(5), P1-Pt1A-Cl1 85.66(4), Cl1-Pt1A-Cl2 87.01(4), Cl2-Pt1A-C1 104.6(1), C1-Pt1A-P1 82.8(1).

⁵² A. Falceto, E. Carmona, S. Alvarez, *Organometallics* **2014**, 33, 6660-6668.

⁵³ M. Black, R. H. B. Mais, P. G. Owston, *Acta Crystall. B* **1969**, 25, 1753-1759.

Dimethyl Complexes [PtMe₂(PMe₂Ar')] and the Mixed Methyl Chloride species [Pt(Me)Cl(PMe₂Ar^{Dipp}₂)]

The phosphines PMe₂Ar^{Dipp}₂, **L**₂, and PMe₂Ar^{Tipp}₂, **L**₃, reacted cleanly (CH₂Cl₂, 25 °C) with one molar equivalent (phosphine to platinum ratio of 1:1) of the mixture formed by [Pt(Me)₂(μ-SMe₂)]₂ and [Pt(Me)₂(SMe₂)₂]⁴⁰, to generate complexes **8** and **9** respectively, in high yield (Scheme 13).



Scheme 13. Synthesis of complexes **8** and **9**.

The formulation proposed for these complexes is in agreement with solution NMR spectroscopic studies, and was further corroborated by X-ray crystallography. Figure 22 shows the *ca.* 2.8 to -0.5 ppm region of the ¹H NMR spectrum of complex **8**. As can be observed, the number of resonances corresponding to the aliphatic protons of the terphenyl fragment suggests the non-equivalence of the two flanking aryl groups and therefore that the phosphine acts as κ¹-P, η¹-C_{arene} bidentate ligand.

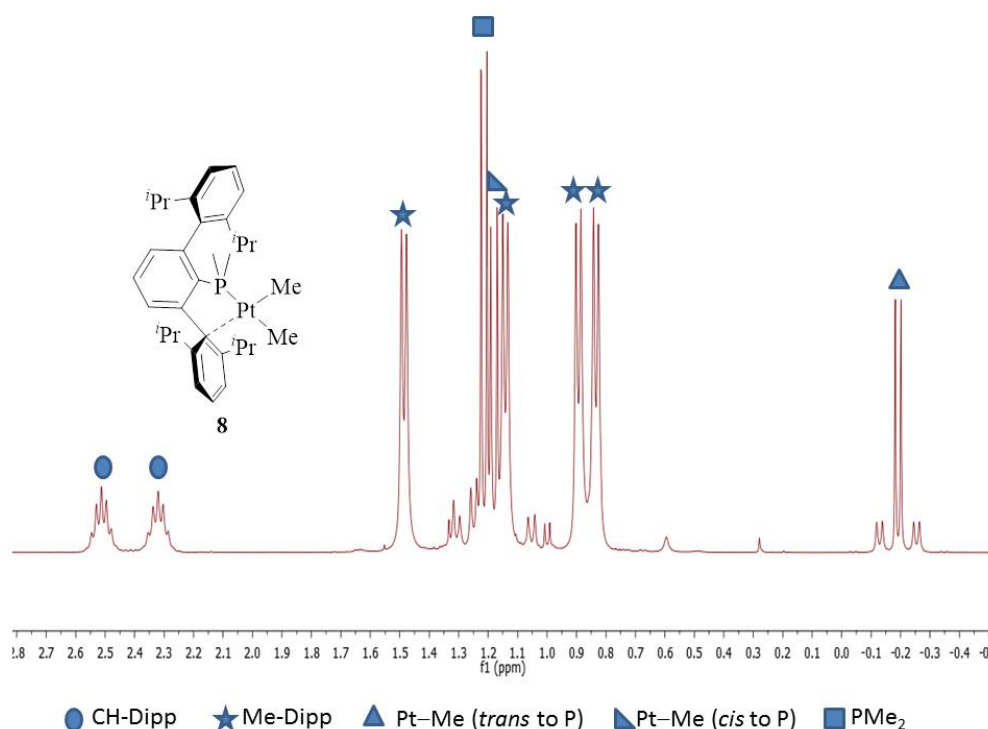


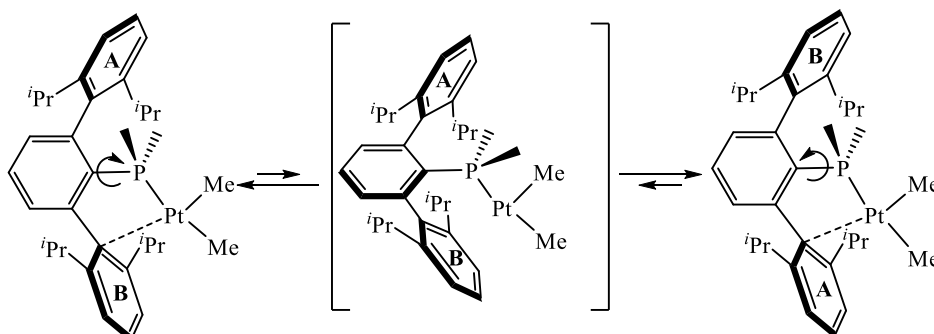
Figure 22. Partial ^1H NMR spectrum of complex **8** (C_6D_6 , 400 MHz, 25 $^\circ\text{C}$).

The NMR data recorded for the two complexes are collected in the Experimental Section. For the sake of simplicity, we analyse below data for the $\text{PMe}_2\text{Ar}^{\text{Dipp}_2}$ complex **8**, focusing the discussion mainly on the Pt—Me resonances. In the ^1H NMR spectrum (Figure 22) the two methyl groups resonate with well differentiated chemical shifts of 1.18 and -0.19 ppm, and appear as doublets with not really different $^3J_{\text{PH}}$ values of 8.9 and 7.7 Hz, respectively. They, however, exhibit distinct $^2J_{\text{HPt}}$ coupling constants of 101.3 and 50.3 Hz respectively, that suggest that the former is *trans* to the Pt $\cdots\text{C}_{\text{ar}}$ bond, while the latter occupies the *trans* position with respect to the phosphorus atom. In the $^{13}\text{C}\{^1\text{H}\}$ NMR spectrum the corresponding resonances appear at δ 27.1 ($^2J_{\text{CP}} = 107$, $^1J_{\text{CPt}} = 627$ Hz) and -11.0 ppm ($^2J_{\text{CP}} = 5$, $^1J_{\text{CPt}} = 915$ Hz), respectively. We have been unable to locate the $^{13}\text{C}\{^1\text{H}\}$ resonance of the *ipso* carbon atom directly bonded to

platinum. The $^{31}\text{P}\{^1\text{H}\}$ NMR spectrum of complex **8** contains the expected singlet signal that features ^{195}Pt satellites resulting from $^1J_{\text{Pt}} = 2010$ Hz, in accordance with the ^{31}P nuclei being *trans* with respect to a methyl group. All these data are comparable to those already in the literature for related complexes.^{11,45-48,54}

C_6D_6 solutions of complex **8** were studied by ^1H NMR spectroscopy at higher temperatures (up to 75 °C), with the expectation of unveiling a fluxional behaviour that could exchange the roles of the two flanking rings of the terphenylphosphine substituent. As represented in Figure 23 such a process does indeed take place. Mild heating (35 °C) already causes significant broadening of the resonances due to the methyne protons of the *iso*-propyl substituents of the terphenyl group. The two signals practically coalesce at roughly 60 °C, to merge as a broad hump at 65 °C and above. No attempts were made to reach the fast-exchange limit. Using the slow-exchange approximation a rate constant of 211 s^{-1} was calculated at the coalescence temperature of 60 °C, with an associated free energy of activation, $\Delta G^\ddagger = 16\text{ kcal mol}^{-1}$. These data strongly reinforce the notion of complex **8** (and by analogy **9**) as an unsaturated T-shaped Pt(II) derivative, with the weak $\text{Pt(II)}\cdots\text{C}_{\text{arene}}$ secondary interaction partly compensating the low coordination and electron count of the metal. Scheme 14 depicts the molecular motions that permit the interchange of the two Dipp rings.

⁵⁴ a) P. S. Pregosin, *NMR in Organometallic Chemistry*, Wiley-VCH, Weinheim, **2012**; b) J. G. Verkade, *Phosphorus-31 NMR spectroscopy in stereochemical analysis: organic compounds and metal complexes*, VCH, Deerfield Beach, FL, **1987**; c) S. O. Grim, R. L. Keiter, W. McFarlane, *Inorg. Chem.* **1967**, *6*, 1133-1137.



Scheme 14. Proposed fluxional behaviour mechanism of complex **8**.

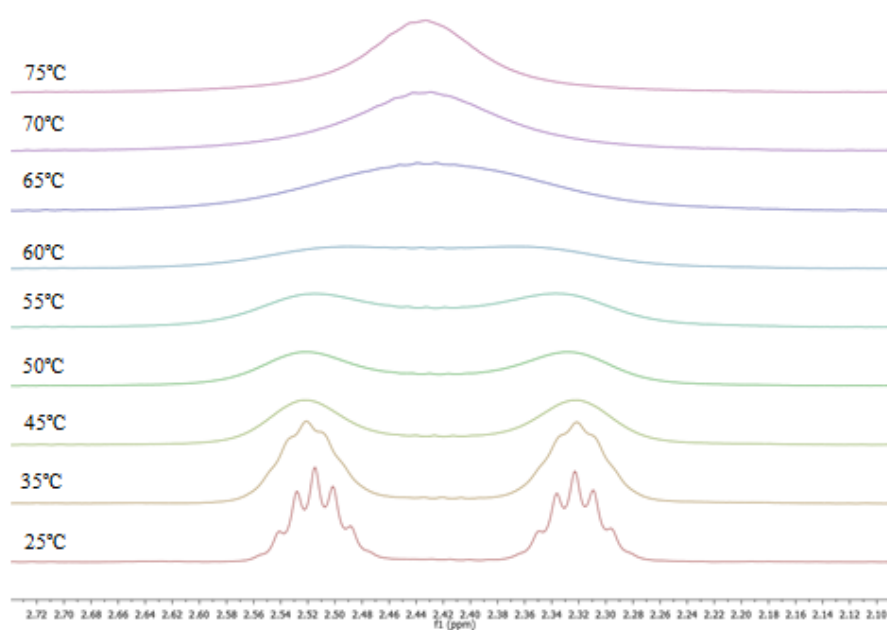


Figure 23. Variable temperature ^1H NMR spectra of complex **10** showing the resonances of the isopropyl CH protons (500 MHz, C_6D_6).

As noted already, complexes **8** and **9** were also characterized by single-crystal X-ray crystallography. Figure 24 shows the solid-state molecular structures of the two compounds, the Pt(II) centres of which lie in slightly distorted square-planar environments. Bond angles within the coordination plane sum for the two compounds nearly exactly the ideal

360° value. The Pt-P bonds of the two complexes are nearly identical at *ca.* 2.25 Å. This length is normal, in the range of the Pt-PR₃ distances listed in the Cambridge Structural Database (CSD).⁵⁵ The two different Pt-Me bonds also have normal values, with the one *trans* to the C_{ar} donor atom being somewhat shorter than the other (*ca.* 2.05 *vs.* 2.08 Å), evidently as a reflection of the higher *trans*-influence of PMe₂Ar', relative to the π-C_{ar} ligand. In accordance with the NMR data already discussed, the Pt-Car bonds of **8** and **9** are long, and therefore weak, with Pt...C_{ar} contacts of roughly 2.33 Å in **8** (to C23, Figure 26) and 2.31 Å in **9** (C11). It is pertinent to highlight that in the already discussed *cis*-[PtCl₂(PMe₂Ar^{Dipp}₂)] complex **6**, the corresponding Pt...C_{ar} contact of 2.23 Å is significantly shorter than in **8**, once more as a reflection of the electronic influence of the *trans* ligand (chloride in **6** and methyl in **8**).

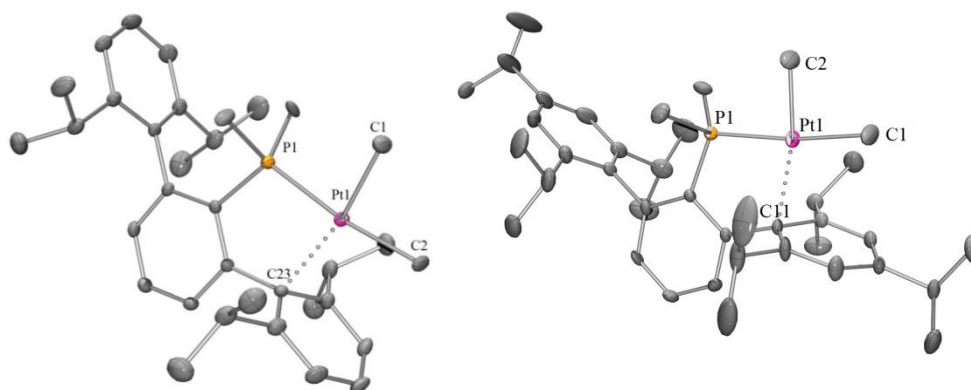
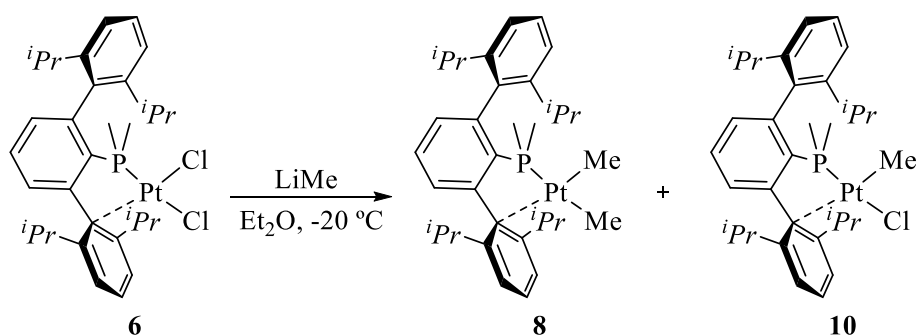


Figure 24. ORTEP view of the complex **8** (left) and **9** (right); hydrogen atoms are excluded for clarity and thermal ellipsoids are set to 50 % level of probability. Selected bond distances (Å) and angles (°): **8**: Pt1-P1 2.2484(4), Pt1-C1 2.054(2), Pt1-C2 2.108(2), Pt1-C23 2.334(2), P1-Pt1-C1 89.30(6), C1-Pt1-C2 82.84(8), C2-Pt1-C23 106.76(7), C23-Pt1-P1 81.23(4); **9**: Pt1-P1 2.248(1), Pt1-C2 2.053 (6), Pt1-C1 2.084(5), Pt1-C11 2.312(4), P1-Pt1-C2 89.3(1), C2-Pt1-C1 83.5(2), C1-Pt1-C11 106.0(2), C11-Pt1-P1 81.06(9).

⁵⁵ F. Allen, O. Kennard, *Chemical Design Automation News* **1993**, 8, 31-37.

The dimethyl complex **8** was alternatively obtained by alkylation of the dichloride **6**, employing commercial solutions of LiMe as the methylating reagent (Scheme 15). The reaction occurs in a step-wise manner, through the intermediacy of the methyl-chloride complex **10**. In fact, the use of a 1:1 ratio of the dichloro complex **6** to LiMe yields a mixture of the mono- and dimethyl complexes **10** and **8**, respectively, as illustrated by $^{31}\text{P}\{^1\text{H}\}$ NMR studies of the crude reaction product (Figure 25)



Scheme 15: Stepwise methylation of *cis*-[PtCl₂(PMe₂Ar^{Dipp}₂)], **6**.

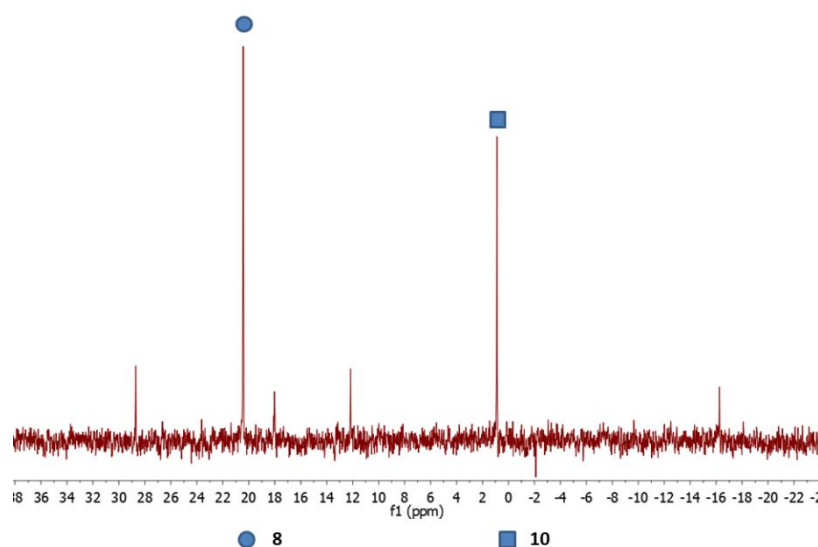
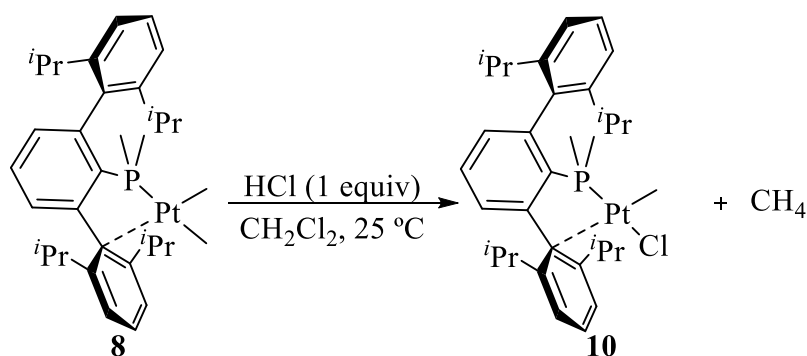


Figure 25: $^{31}\text{P}\{^1\text{H}\}$ NMR spectra of the crude of reaction depicted in Scheme 15 (C₆D₆, 121.4 MHz, 25 °C).

Compound **10** results also from a comproportion reaction between dichloride **6** and dimethyl **8**, but the most convenient synthetic procedure for the isolation of analytically pure samples of the mixed methyl-chloride complex **10** consists in the protonation of the dimethyl derivative **8** with a 1 M ether solution of HCl, according to Scheme 16. Two different isomers could form in this reaction but protonation seemed to occur selectively at the Pt-Me bond *trans* to the phosphine ligand, affording complex **10** quantitatively (by ^1H NMR), with elimination of CH_4 . A detailed mechanistic study of this reaction was not attempted.



Scheme 16. Synthesis of complex **10**.

Complex **10** was fully characterized by solution NMR spectroscopy studies and by X-ray crystallography. Once more, structural data are consistent with a bidentate $\kappa^1\text{-P}$, $\eta^1\text{-C}_{\text{arene}}$ coordination mode of the phosphine ligand, both in solution and in the solid state. The mutually *cis* distribution of the methyl and phosphine ligands is unambiguously inferred from ^1H and $^{13}\text{C}\{^1\text{H}\}$ NMR data. Thus, the Pt—Me linkage is responsible for a doublet ^1H resonance (Figure 26) at δ 0.87 ppm ($^2J_{\text{PtH}} = 86$, $^3J_{\text{PH}} = 4.3$ Hz) and for a $^{13}\text{C}\{^1\text{H}\}$ signal at -11.3 ppm, that exhibits $^1J_{\text{PtC}}$ and $^2J_{\text{PC}}$ couplings of 771 and 6 Hz, respectively. The $^{31}\text{P}\{^1\text{H}\}$ NMR spectrum is the expected singlet, characterized by δ 0.4 ppm and $^1J_{\text{PPt}} = 4300$ Hz.

Although the magnitude of this coupling appears unusually large in comparison with other *trans*-P—Pt—Cl linkages studied in this work, it is comparable to the 4179 Hz value found for $^1J_{\text{Pt}} \text{ trans}$ to chloride in the somewhat related compound *cis*-[Pt(Me)Cl(PEt₃)₂].⁵⁶

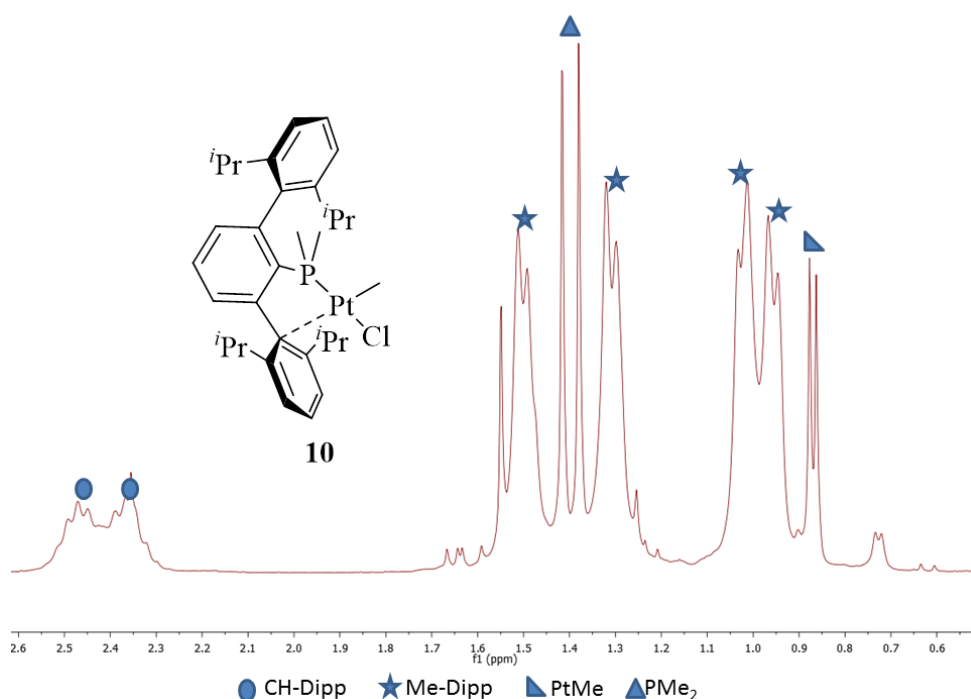


Figure 26. Aliphatic area of ^1H NMR spectrum of complex **10** (300MHz, CDCl₃, 25 °C).

With the identification by X-ray studies of the structure of complex **10** (Figure 27), we complete in this Thesis an interesting set of *cis*-[Pt(X)(Y)(PMe₂Ar^{Dipp2})] structures, X and Y being methyl and/or chloride ligands, namely *cis*-[PtCl₂(PMe₂Ar^{Dipp2})] (**6**), *cis*-[PtMe₂(PMe₂Ar^{Dipp2})] (**8**), and *cis*-[Pt(Me)Cl(PMe₂Ar^{Dipp2})] (**10**). The solid state structure of the molecules **6**, **8**, and **10** are similar, although they reveal the variations expected upon changing the chloride ligands by methyl groups. For

⁵⁶ F. H. Allen, A. Pidcock, *J. Chem. Soc., A* **1968**, 2700-2704.

instance, in the present complex **10**, the Pt—P bond (2.215(1) Å) is shorter than in **8** (2.248(4) Å), while the Pt—Me bond remains essentially invariant at roughly 2.05 Å. The Pt···C_{ar} interaction in **10** appears to be somewhat longer than in **8** (*ca.* 2.37 vs. 2.33 Å), a variation that finds no simple justification on electronic grounds.

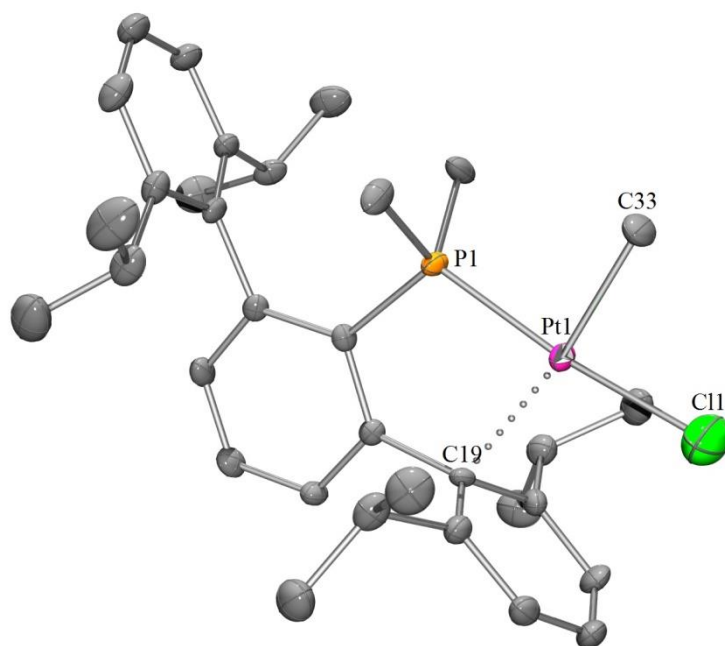
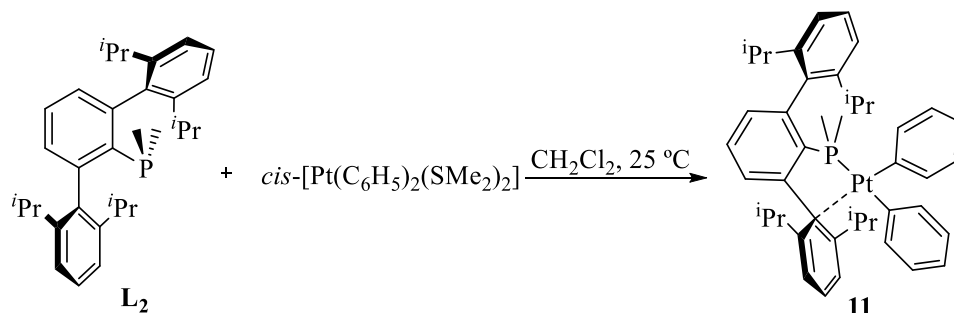


Figure 27. ORTEP view of the complex **10**; hydrogen atoms are excluded for clarity and thermal ellipsoids are set at 50 % level of probability. Selected bond distances (Å) and angles (°): Pt1-P1 2.215(1), Pt1-C33 2.053(5), Pt1-Cl1 2.280(2), Pt1-C19 2.368(4), P1-Pt1-C33 88.8(1), C33-Pt1-Cl1 84.1 (1), Cl1-Pt1-C19 105.4(1), C19-Pt1-P1 87.77(9).

The Diphenyl Complex *cis*-[Pt(Ph)₂(PMe₂Ar^{Dipp2})₂]

The preparative procedure utilised for the isolation of the dimethyl complex **8** was successfully applied to obtain the analogous bis(phenyl) complex **11**. Thus, as depicted in Scheme 17, the terphenylphosphine **L₂**

reacted cleanly (CH_2Cl_2 , 25 °C) with one equivalent (with reference to the P:Pt ratio) of the mixture formed by $[\text{Pt}(\text{Ph})_2(\mu\text{-SMe}_2)]_2$ and $[\text{Pt}(\text{Ph})_2(\text{SMe}_2)_2]$ ⁵⁷, to generate complex **11**, in which the phosphine also exhibits a $\kappa^1\text{-P}$, $\eta^1\text{-C}_{\text{arene}}$ coordination mode.



Scheme 17. Synthesis of complex **11**.

Figure 29 shows the ^1H and $^1\text{H}\{^{31}\text{P}\}$ NMR spectra (300 MHz, CD_2Cl_2 , 25 °C) of the new complex in the region from *ca.* 0.7 to 2.7 ppm. Once more, the methyl groups of the phosphine *iso*-propyl substituents appear as four doublets at 0.98, 1.01, 1.29 and 1.84 ppm, in accord with the existence of a $\text{Pt}\cdots\text{C}_{\text{arene}}$ interaction. The $^{31}\text{P}\{^1\text{H}\}$ resonance of this complex appears as a singlet at 12.8 ppm ($^1J_{\text{PPt}} = 1930$ Hz).

⁵⁷ M.-E. Moret, P. Chen, *Organometallics* **2008**, 27, 4903-4916.

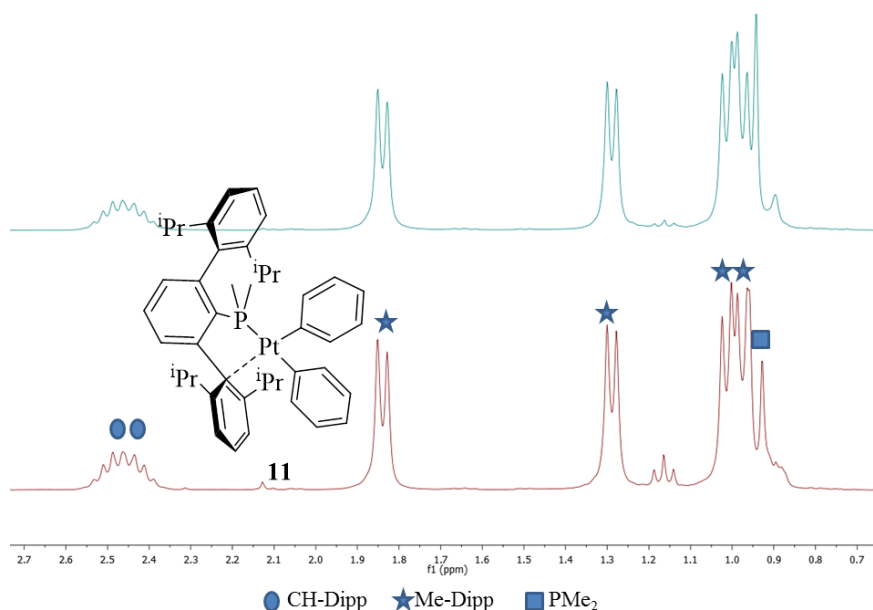


Figure 29. Partial ^1H (bottom) and $^1\text{H}\{^{31}\text{P}\}$ (top) NMR spectra of complex **11** (300 MHz, CD_2Cl_2 , 25 °C).

Silyl Hydride Complexes

Transition-metal silyl chemistry has experienced an enormous growth over the past decades.⁵⁸ This is due mainly to the influential chemical role of hydrosilanes, $\text{SiR}_{4-n}\text{H}_n$ ($n = 1-3$), which represent one of the most important families of reagents in organic synthesis,⁵⁹ as they are able to add catalytically to C—C, C—O and C—N multiple bonds, in the well-known, widely utilised hydrosilylation reaction.^{60,61} Platinum

⁵⁸ J. Y. Corey, J. Braddock-Wilking, *Chem. Rev.* **1999**, 99, 175-292.

⁵⁹ F. Alonso, I. P. Beletskaya, M. Yus, *Chem. Rev.* **2002**, 102, 4009-4092.

⁶⁰ a) B. Marciniec, *Silicon Chemistry* **2002**, 1, 155-174; b) A. K. Roy, in *Adv. Organomet. Chem.*, Vol. Volume 55 (Eds.: A. F. H. Robert West, J. F. Mark), Academic Press, **2007**, 1-59; c) E. Calimano, T. D. Tilley, *J. Am. Chem. Soc.* **2009**, 131, 11161-11173.

⁶¹ a) R. Malacea, R. Poli, E. Manoury, *Coord. Chem. Rev.* **2010**, 254, 729-752; b) R. H. Morris, *Chem. Soc. Rev.* **2009**, 38, 2282-2291.

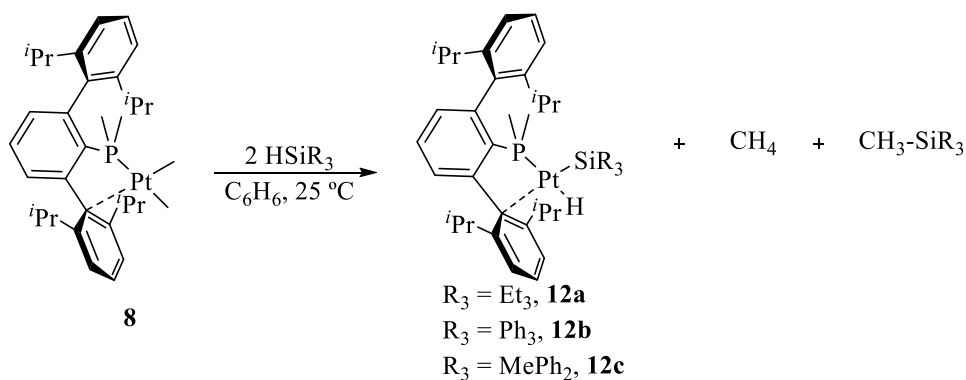
complexes are overwhelmingly preferred as catalysts.^{62,63} Two of them, namely the Speir catalyst, $\text{H}_2\text{PtCl}_6/\text{PrOH}$, and the Kardstedt catalyst, $[\text{Pt}_2(\text{CH}_2=\text{CHSi}(\text{Me})_2\text{OSi}(\text{Me})_2\text{CH}=\text{CH}_2)_3]$ have found ample use in the silicone industry.⁶² We therefore considered appropriate to study the formation of platinum(II)-silyl complexes and envisioned that the dimethyl derivatives *cis*- $[\text{PtMe}_2(\text{PMe}_2\text{Ar}')] \text{ (8) and (9)}$ could be suitable starting materials yielding silyl complexes by means of a combination of oxidative addition and reductive elimination reactions.

In this section, the synthesis and structural characterisation of a series of hydride silyl complexes of composition *cis*- $[\text{Pt}(\text{H})(\text{SiR}_3)(\text{PMe}_2\text{Ar}')] \text{ is reported. As for other complexes already considered, the terphenylphosphine ligand, } \text{PMe}_2\text{Ar}^{\text{Dipp}_2} \text{ or } \text{PMe}_2\text{Ar}^{\text{Tipp}_2}, \text{ acts as bidentate, coordinating to Pt(II) through the phosphorus atom and through an } ipso \text{ carbon atom of a lateral terphenyl aromatic ring. Further platinum-silyl chemistry, this time catalytic involving hydrosilylation reactions, will be discussed in an ensuing section devoted to the chemistry of Pt(0) complexes of these terphenylphosphines.}$

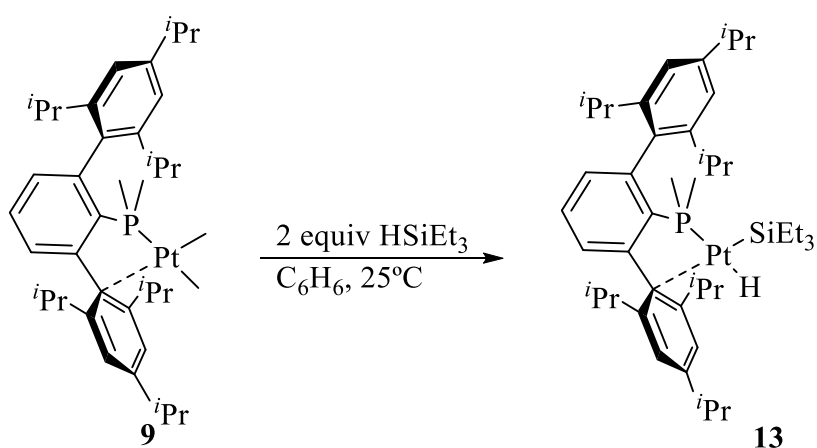
When complex **8** was treated with 2 mol-equiv of the tertiary silanes HSiR_3 , in benzene at room temperature (Scheme 18), the neutral hydride silyl species *cis*- $[\text{Pt}(\text{H})(\text{SiR}_3)(\text{PMe}_2\text{Ar}^{\text{Dipp}_2})] \text{ (12) were obtained (SiR}_3 = \text{SiEt}_3 \text{ 12a, SiPh}_3 \text{ 12b, SiMePh}_2 \text{ 12c). The triethylsilyl complex } cis\text{-}[\text{Pt}(\text{H})(\text{SiEt}_3)(\text{PMe}_2\text{Ar}^{\text{Tipp}_2})] \text{ (13), was also prepared by a similar procedure (Scheme 19).}$

⁶² For leading work and references see: I. E. Markó, S. Stérin, O. Buisine, G. Mignani, P. Branlard, B. Tinant, J. Declercq, *Science* **2002**, 298, 204-206.

⁶³ See for example: a) D. A. Rooke, E. M. Ferreira, *Angew. Chem. Int. Ed.* **2012**, 51, 3225-3230; b) S. E. Parker, J. Börgel, T. Ritter, *J. Am. Chem. Soc.* **2014**, 136, 4857-4860.



Scheme 18. Synthesis of complexes **12a**, **12b** and **12c**.



Scheme 19. Synthesis of complex **13**.

The newly prepared hydride silyl complexes **12a-12c** and **13** were fully characterized with the aid of conventional analytical and spectroscopic techniques. The SiEt_3 derivative **12a**, was additionally investigated by X-ray crystallography. Before pertinent structural data are explained and interpreted, it is worth mentioning that the formation of the hydride silyl derivatives from the *cis*-[PtMe₂(PMe₂Ar')] precursors took

place with concurrent elimination of CH₄ and MeSiR₃, as convincingly indicated by ¹H NMR studies of the reaction leading to complex **12a** (Figure 30). One may speculate with the reaction being triggered by oxidative addition of HSiEt₃ to *cis*-[PtMe₂(PMe₂Ar^{Dipp})₂], followed by reductive elimination of CH₄ (expected to be kinetically favoured relative to MeSiEt₃ elimination) to yield an undetected mixed methyl silyl platinum(II) complex. Somewhat analogous *cis*-[Pt(Me)(SiPh₃)(PR₃)₂] complexes are known to eliminate readily MeSiPh₃ in solution.⁶⁴ Therefore, the unobserved methyl silyl intermediate could experience reductive elimination of MeSiEt₃, followed by oxidative addition of HSiEt₃ to the resulting Pt(0) complex. The last step constitutes a well-known procedure for the synthesis of Pt(II) hydride silyl complexes. For example, Duckett, Perutz and others, reported recently a series of platinum hydride silyl complexes *cis*-[Pt(H)(SiR₂R')(PCy₃)₂] that were obtained by reaction of [Pt(PCy₃)₂] with the appropriate silane, HSiR₂R'.⁶⁵

⁶⁴ a) F. Ozawa, T. Hikida, T. Hayashi, *J. Am. Chem. Soc.* **1994**, *116*, 2844-2849; b) F. Ozawa, *J. Organomet. Chem.* **2000**, *611*, 332-342; c) F. Ozawa, T. Hikida, K. Hasebe, T. Mori, *Organometallics* **1998**, *17*, 1018-1024; d) K. Hasebe, J. Kamite, T. Mori, H. Katayama, F. Ozawa, *Organometallics* **2000**, *19*, 2022-2030.

⁶⁵ D. Chan, S. B. Duckett, S. L. Heath, I. G. Khazal, R. N. Perutz, S. Sabo-Etienne, P. L. Timmins, *Organometallics* **2004**, *23*, 5744-5756.

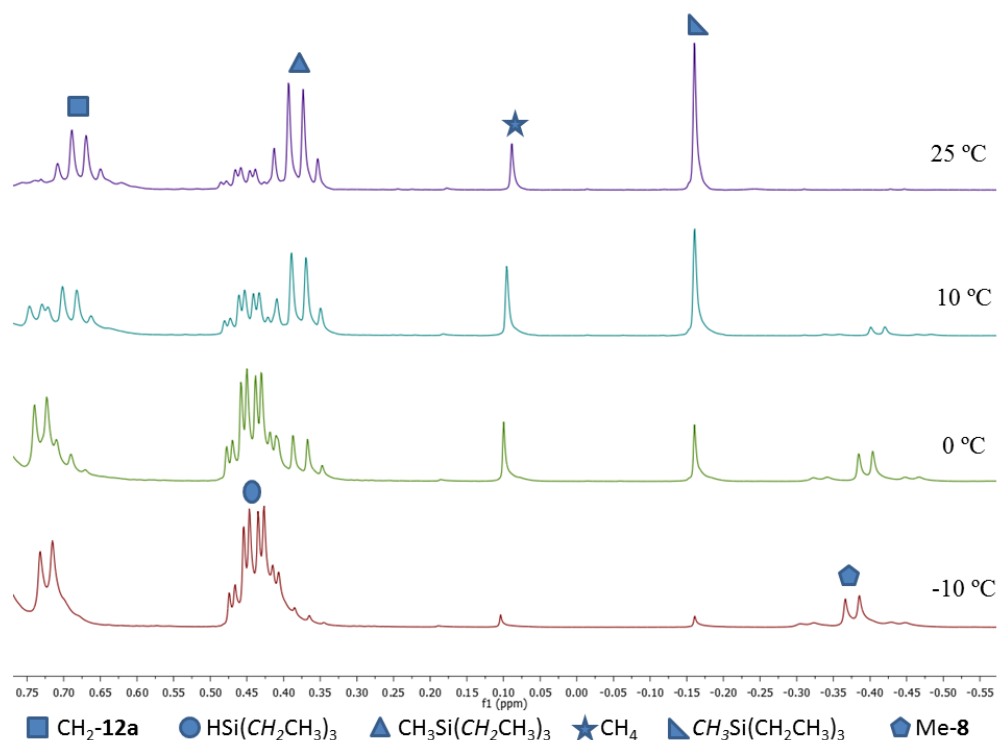


Figure 30: Aliphatic region of ^1H NMR spectra of the reaction of complex **8** with HSiEt_3 at different temperatures (400 MHz, C_6D_6)

At room temperature the ^1H NMR spectra of the four hydride silyl complexes contain some broad signals that witness the non-rigidity of their structures. The solution dynamics concerns, however, only with signals due to the terphenylphosphine substituents, clearly pointing out the interchange of the flanking aryl rings. Figure 31 contains variable temperature (-60 to 25 °C) ^1H NMR data for complex **12a** in the aliphatic and hydride region of the spectra (from *ca.* 2.7 to -2.7 ppm). With reference, for the sake of simplicity, to the methine protons of the *iso*-propyl substituents two septets are discerned at -60 °C, with δ 2.29 and 2.40 ppm, that convert into a broad unresolved signal at 0 °C and a poorly resolved septet at 25 °C. Using the slow-exchange approximation, a value of 102 s^{-1} can be estimated for the rate of the exchange at the coalescence temperature (*ca.* -10 °C), which leads to a ΔG^\ddagger value of $12.9\text{ kcal}\cdot\text{mol}^{-1}$.

The hydride resonance appears in the four complexes in the rather narrow chemical shift range from -1.7 to -1.2 ppm, and it is characterized by a $^2J_{\text{HP}}$ coupling to the *trans* ^{31}P nucleus of *ca.* 170 Hz and by $^1J_{\text{HPt}}$ of *ca.* 1000 Hz. The $^{31}\text{P}\{^1\text{H}\}$ NMR spectra of compounds **12a-c** shows a singlet at 23-25 ppm, with $^1J_{\text{PPt}}$ coupling constants comprised between 2348 and 2544 Hz. All these NMR parameters compare well with those already reported for analogous complexes.⁶⁵ For instance, complex *cis*-[Pt(H)(SiEt₃)(PCy₃)₂] features a hydride signal at δ -3.6 ppm, with $^2J_{\text{HP}}(\text{trans}) = 146$ and $^1J_{\text{HPt}} = 823$ Hz. The ^{31}P nucleus *trans* to the hydride exhibits $^1J_{\text{PPt}} = 2721$ Hz, whereas for that *trans* to SiEt₃, the corresponding coupling is significantly smaller, 1368 Hz.

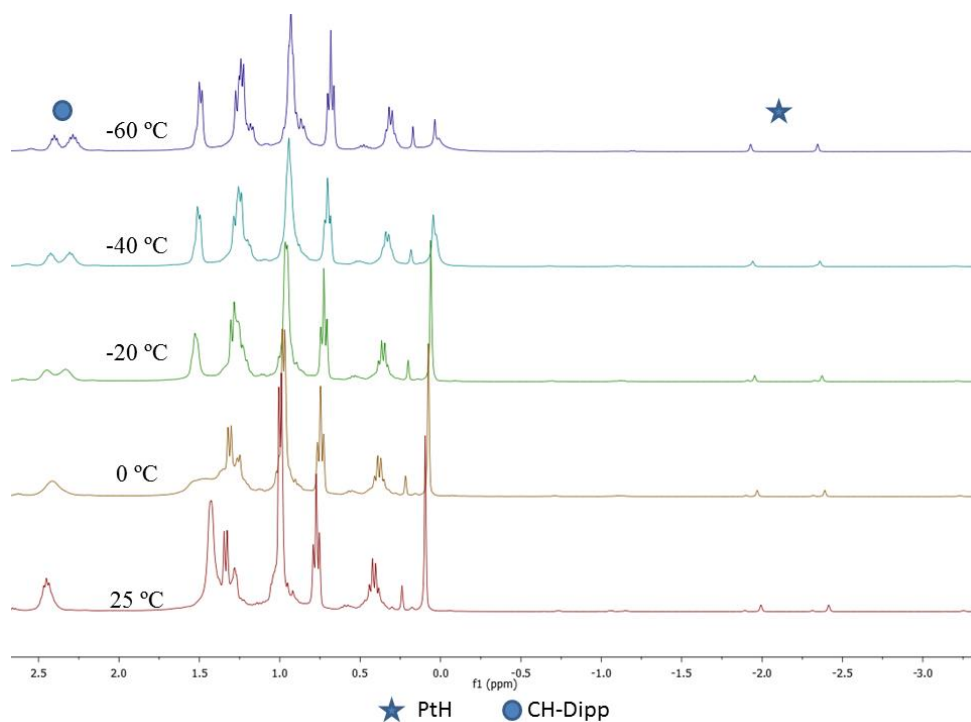


Figure 31. Variable temperature aliphatic area of ^1H NMR spectra of complex **12a** (CD_2Cl_2 , 400 MHz).

Crystals of complex **12a** suitable for X-ray studies were obtained by cooling its solutions in diethylether at -20 °C. Figure 32 shows an

ORTEP view of the molecules of the complex and reveals that its geometry is close to planar, although bond angles deviate significantly from the ideal 90° of a square-planar geometry. In particular the P1-Pt1-Si1 angle is 101.30(3)°, possibly due to steric repulsions between the bulky SiEt₃ and PMe₂Ar' ligands. Nonetheless, the SiEt₃ group is nearly *trans* to the *ipso* carbon atom C21 (bond angle of roughly 183°) and the hydride practically *trans* to the phosphorus atom (*ca.* 174°). The Pt-H distance of 1.69(4) Å is only slightly longer than the average of 1.61 Å found by neutron diffraction in terminal platinum hydrides⁶⁶ and comparable to values reported for the cationic hydrides *trans*-[Pt(H)(XR)(P^{*i*}Pr₃)₂][BAr_F] where XR represents a monodentate halocarbon (for example, ClCH₂Cl).⁶⁷ In the somewhat related *cis*-[PtH(SiPh₂H)(PCy₃)₂] complex, the Pt-H distance is 1.44(3) Å. In our compound, the Pt-Si distance is 2.3062(9) Å, similar to the 2.3311(9) Å reported for the latter species.⁶⁵ Finally, the Pt-P distance in **12a** of 2.2750(7) Å is also shorter than the 2.3127(8) Å value found for the PCy₃ ligand *trans* to hydride in the latter complex. A final comparison which is worthy of note involves the already discussed *cis*-[PtMe₂(PMe₂Ar'^{Dipp2})] complex **8**, where the Pt-P bond length is 2.2484(4) Å. These data are consistent with comparable, albeit slightly higher *trans* influence for the hydride ligand than for methyl.^{9,38}

⁶⁶ R. Bau, M. H. Drabnis, *Inorg. Chim. Acta* **1997**, 259, 27-50.

⁶⁷ M. D. Butts, B. L. Scott, G. J. Kubas, *J. Am. Chem. Soc.* **1996**, 118, 11831-11843.

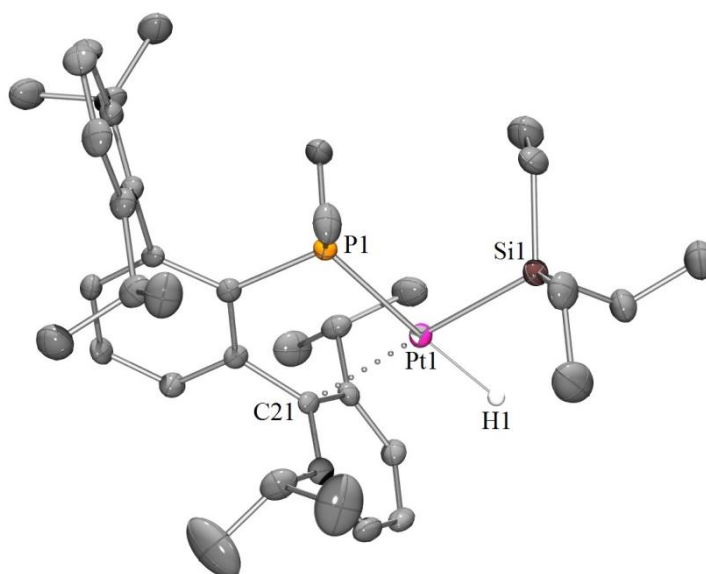


Figure 32. ORTEP view of the complex **12a**; hydrogen atoms are excluded for clarity and thermal ellipsoids are set to 50% level probability. Selected bond distances (Å) and angles (°): Pt1-H1 1.69(4), Pt1-Si1 2.3062(9), Pt1-P1 2.2750(7), Pt1-C21 2.421(3), H1-Pt1-Si1 73(1), Si1-Pt1-P1 101.30(3), P1-Pt1-C21 81.53(6), C21-Pt1-H1 105(1).

Recapitulation of Structural Data Pertaining Neutral Pt(II) Complexes with Bidentate Phosphine Coordination

Having prepared and structurally characterised by NMR spectroscopy, and in many cases by X-ray analysis, a set of neutral Pt(II) complexes that contain a $[\text{Pt}(\text{P}^{\wedge}\text{C}_{\text{ar}})]$ moiety bonded to two monoanionic X and Y ligands (Cl^- , Me^- , Ph^- , H^- and R_3Si^-), we believe that a brief discussion of relevant structural data for these complexes is appropriate. We focus our comments on the values of the one-bond ^{31}P -to- ^{195}Pt coupling constants found for the five types of complex studied (Figure 33) and on bond distances and angles measured for the complexes that were authenticated by X-ray crystallography (Figure 34).

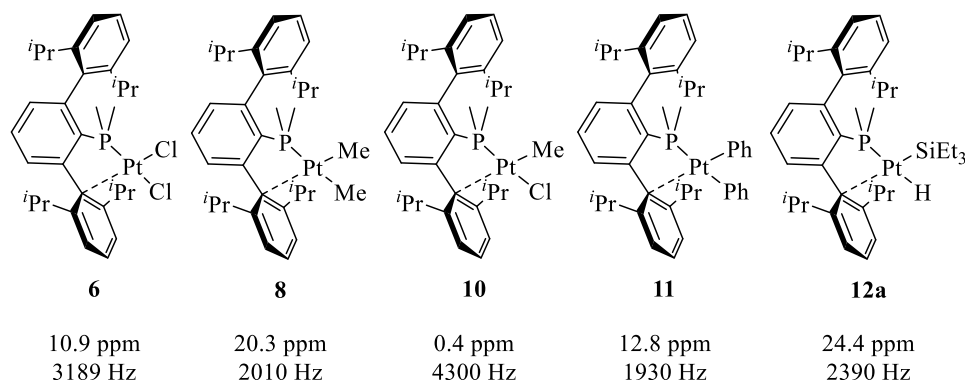


Figure 33: Some $^{31}\text{P}\{^1\text{H}\}$ NMR parameters for the neutral Pt(II) complexes **6**, **8**, **10**, **11**, and **12a**.

In complexes **6**, **8**, **10**, **11** and **12a**, the phosphine ligand occupies a *trans* coordination position relative to Cl^- (complexes **6** and **10**), Me^- (**8**), Ph^- (**11**) and H^- (**12a**). Figure 33 contains structural formulae for these compounds and includes the corresponding magnitude of the $^1J_{\text{PPt}}$ coupling constant (δ values have been added for informative purposes). These data are in good harmony with those already in the literature⁵⁴ for related platinum (II) complexes. With reference to the *trans* influence exerted by these donor ligands, the order is $\text{Ph}^- > \text{Me}^- > \text{H}^- > \text{Cl}^-$. It has been proposed that the variation in $^1J_{\text{PPt}}$ upon changing the X ligand *trans* to phosphorus reflects primarily the change in 6s character of the Pt—X bond at the expense of the *trans* Pt—P bond, which uses the same s-d hybrid orbital. Weaker X donor ligands exercise smaller *trans* influences and give rise to larger values of $^1J_{\text{PPt}}$ and viceversa,^{9,38} which explains the commonly found $\text{Ph}^- > \text{Me}^- > \text{Cl}^-$ sequence. The 2390 Hz ^{31}P - ^{195}Pt coupling recorded for the hydride silyl complex **12a** is possibly a bit larger than expected in comparison with the methyl group. While it is not easy to rationalize such a small variation, it could be argued that this may be a consequence of the dominating *trans*-influence role of the silyl coligand, which results in a high 6s character for the orthogonal Pt-H and Pt-P bonds, in comparison with the Pt-Si and Pt-C_{ar} interactions. In fact the $^1J_{\text{HPt}}$ value of 1007 Hz is 90

larger than found for *cis*-[Pt(H)(SiR₂R')(PCy₃)₂] (between *ca.* 780 and 960 Hz).⁶⁵

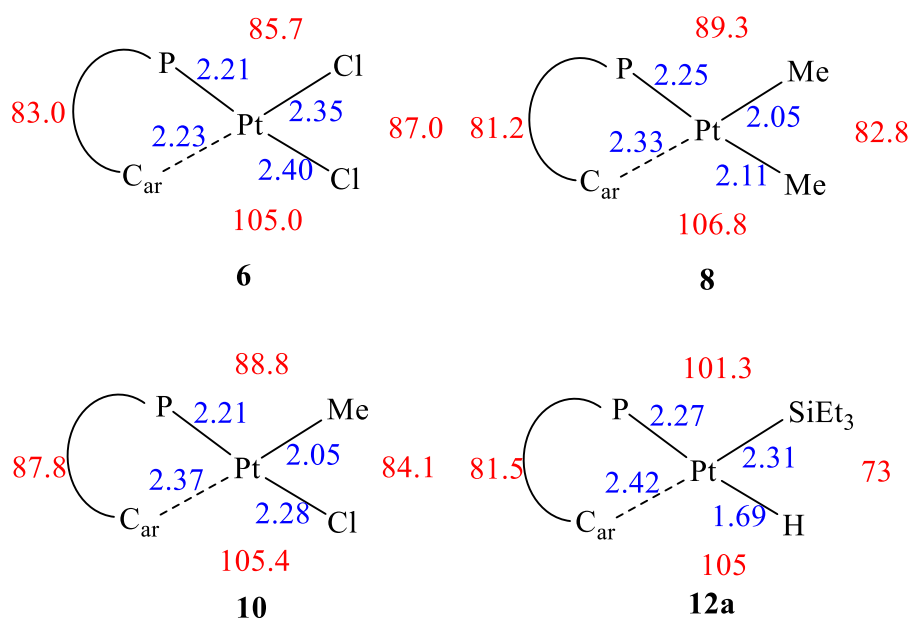


Figure 34: Some bond lengths (Å, blue) and angles (°, red) for the neutral Pt(II) complexes **6**, **8**, **10**, and **12a**. For simplicity, bond distances have been rounded up to the second decimal figure and bond angles to the first.

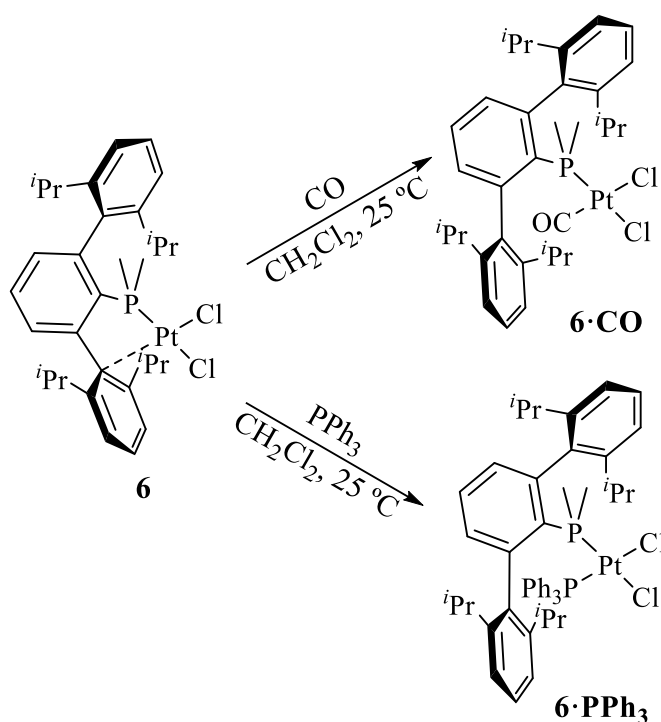
As already indicated, we think that it is also appropriate bringing together relevant X-ray data, firstly to highlight the similarity of the molecular structures of the new complexes, and then to analyse specific differences in bond lengths caused by ligands with high *trans*-influence. Figure 34 collects data considered of interest for this scrutiny. The four complexes exhibit a distorted square-planar geometry, with the sum of the four angles in the molecular plane approaching closely the ideal 360° (only for the methyl chloride derivative **10** the sum of the angles is somewhat larger at 366°). For complexes **6**, **8** and **10** three of the bond angles are smaller than, although close or relatively close to, the ideal 90°, with the fourth, namely the Cl—Pt—Cl in **6** or the C_{ar}—Pt—X in **8** (X = Me) and

10 (X = Cl), compensating for the deviation. In the hydride silyl compound **12a**, there are two acute and two obtuse angles (Figure 34).

In the two chloride complexes, **6** and **10**, the Pt—P distance (*trans* to chloride) is *ca.* 2.21 Å, whereas in the dimethyl **8** and hydride silyl **12a**, this bond length becomes somewhat longer at roughly 2.25 and 2.27 Å respectively. From this variation the sequence for *trans*-influence is $\text{Cl}^- < \text{Me}^- < \text{H}^-$. Regarding the secondary $\text{Pt} \cdots \text{C}_{\text{ar}}$ interaction, it increases from 2.23 Å (*trans* to Cl^- , **6**) to 2.33 or 2.37 Å (*trans* to Me^- , Me/Me, **8**, and Me/Cl, **10**) and 2.42 Å (*trans* to SiEt_3^- , **12a**), giving a *trans*-influence series $\text{Cl}^- < \text{Me}^- < \text{SiEt}_3^-$. Clearly all of these compounds may be seen as T-shaped, three-coordinate 14-electron complexes, with the $\text{Pt} \cdots \text{C}_{\text{ar}}$ interaction counterbalancing the metal unsaturation, at least in part.

1.2.2.2. Forcing Monodentate P-Coordination of the Phosphine Ligand. Reactivity Towards Lewis Bases.

The relatively weak $\text{Pt(II)} \cdots \text{C}_{\text{ar}}$ interaction observed in the neutral complexes described in the previous section was expected to be labile and therefore easily substituted by various Lewis bases. In accordance with this supposition, it was found that complex *cis*-[PtCl₂(PMe₂Ar^{Dipp2})] (**6**) reacted with CO and PPh₃, to generate the corresponding adducts *cis*-[PtCl₂(PMe₂Ar^{Dipp2})(L)], **6**•CO and **6**•PPh₃, respectively (Scheme 20). The new compounds are truly four-coordinate species with the usual monodentate P-binding of the phosphine ligand.



Scheme 20. Synthesis of adducts **6·CO** and **6·PPh₃**.

Spectroscopic characterisation of **6·CO** was straightforward. In the IR spectrum a strong absorption at 2114 cm^{-1} is found due to the stretching vibration of the multiple carbon-oxygen bond of the carbonyl ligand. The observed wavenumber value is in the region expected for Pt(II) carbonyl complexes^{27,68} and denotes reduced metal-to-ligand π -back donation. For comparison, free CO absorbs at 2143 cm^{-1} and *cis*-[PtCl₂(CO)₂] shows bands⁶⁹ at 2170 and 2130 cm^{-1} . Compared to the parent compound **6**, the $^{31}\text{P}\{^1\text{H}\}$ resonance of **6·CO** is significantly displaced towards lower frequency regions, appearing at -16.6 ppm . This is probably a consequence

⁶⁸ a) H. A. Zhong, J. A. Labinger, J. E. Bercaw, *J. Am. Chem. Soc.* **2002**, *124*, 1378-1399; b) L. Johansson, O. B. Ryan, C. Rømming, M. Tilset, *J. Am. Chem. Soc.* **2001**, *123*, 6579-6590; c) S. Reinartz, P. S. White, M. Brookhart, J. L. Templeton, *Organometallics* **2000**, *19*, 3854-3866; d) J. C. Thomas, J. C. Peters, *Inorg. Chem.* **2003**, *42*, 5055-5073; e) S. Martínez-Salvador, B. Menjón, J. Forniés, A. Martín, I. Usón, *Angew. Chem. Int. Ed.* **2010**, *49*, 4286-4289; f) S. Martínez-Salvador, J. Forniés, A. Martín, B. Menjón, *Chem. Eur. J.* **2011**, *17*, 8085-8097.

⁶⁹ F. Canziani, P. Chini, A. Quarta, A. Di Martino, *J. Organomet. Chem.* **1971**, *26*, 285-292.

of the coordination of the new ligand, that frees the $\text{Pt}\cdots\text{C}_{\text{arene}}$ interaction of **6**. The one-bond ^{31}P - ^{195}Pt coupling in **6**·**CO** is, however, comparable to that of **6** (2970 vs. 3190 Hz) and therefore a *cis* geometry is proposed for this compound (Scheme 20).

Despite the larger cone angle of PPh_3 relative to CO (145° vs. *ca* 95°)^{15e} a *cis* structure is also suggested in Scheme 20 for the triphenylphosphine adduct **6**·**PPh₃**. This proposition is unmistakingly confirmed by the two-bond ^{31}P - ^{31}P coupling of 13 Hz observed in the $^{31}\text{P}\{^1\text{H}\}$ NMR spectrum of **6**·**PPh₃** (doublets at 8.3 (PPh_3) and -20.9 ppm, with $^1J_{\text{PPt}} = 3857$ and 3566 Hz, respectively). It is, nonetheless, interesting to note that while in complex **6**·**CO** the two flanking aryl rings of the terphenylphosphine substituent are equivalent and give rise to only one septet and two doublets for the methane and methyl protons of the four *iso*-propyl substituents (Figure 35), in adduct **6**·**PPh₃** two septets (δ 3.51 and 2.22) and four doublets (between approximately 1.7 and 0.65 ppm) are recorded. A reasonable explanation for this difference is that the bulkiness of PPh_3 impedes free rotation around P-C_{ar} and $\text{C}_{\text{ar}}\text{-C}_{\text{ar}}$ bonds within the terphenylphosphine ligand.

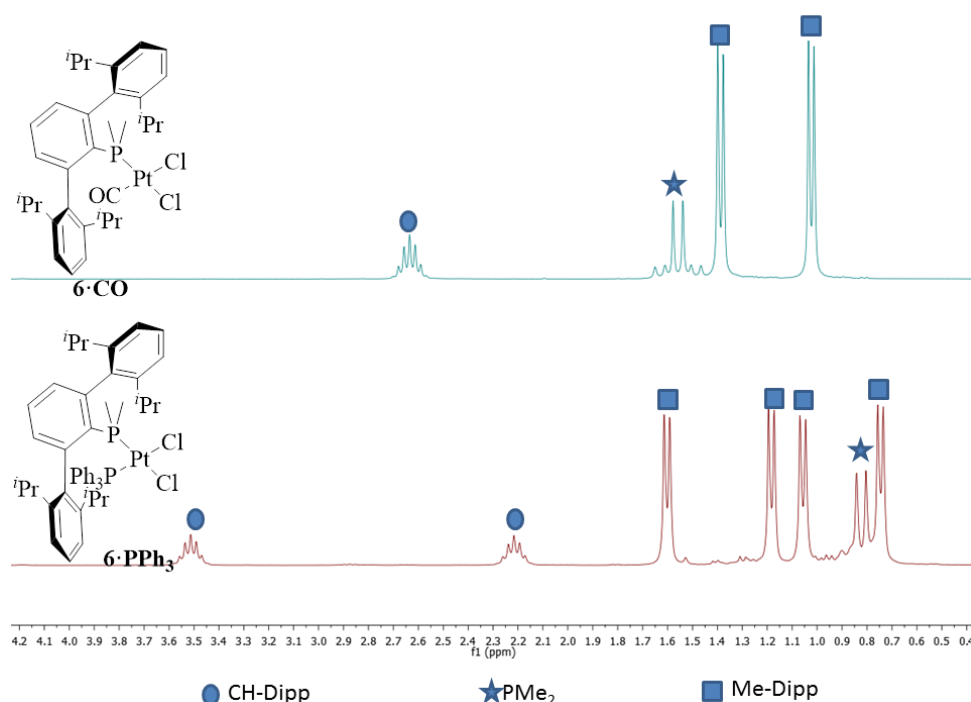
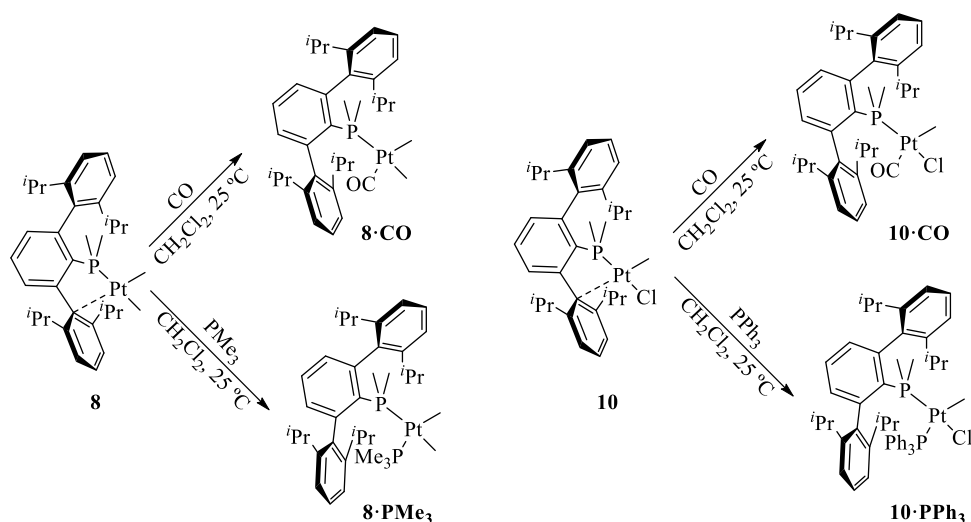


Figure 35: Aliphatic region of the ^1H NMR spectra of adducts **6·CO** (top) and **6·PPh₃** (bottom) (300 MHz, CD_2Cl_2 , 25 °C).

By analogy with previous finding on the parent dichloride complex $\text{cis-}[\text{PtCl}_2(\text{PMe}_2\text{Ar}^{\text{Dipp}_2})]$ (**6**), we expected the η^1 -arene interaction in compounds **8** and **10** to be labile, and consequently easily substituted by a Lewis base such as CO or another phosphine ligand. In this way we generated the corresponding adducts **8·CO** and **8·PMe₃**, and **10·CO** and **10·PPh₃** respectively. As can be seen in Scheme 21, **8·CO** and **8·PMe₃** possess *cis* methyl groups. Similarly, in **10·CO** and **10·PPh₃** the anionic ligands Me^- and Cl^- occupy adjacent coordination sites.



Scheme 21. Synthesis of adducts **8·CO**, **8·PMe₃**, **10·CO** and **10·PPh₃**.

The two carbonyl and the two phosphine adducts represented in Scheme 21 were characterized in solution by multinuclear 1D and 2D NMR studies. The molecular structure of **8·CO** was also elucidated by single crystal X-ray diffraction studies. For the two carbonyl complexes, the Pt—CO resonance appears in the $^{13}\text{C}\{^1\text{H}\}$ NMR spectrum in the proximity of 180 ppm as a doublet, with a $^2J_{\text{CP}}$ value of 5 Hz, indicating that the carbonyl ligand simply replaces the $\text{Pt}\cdots\text{C}_{\text{ar}}$ interaction of **8** and places itself in a *cis* position with respect to the phosphine ligand. The $^{31}\text{P}\{^1\text{H}\}$ resonances of the two complexes are the expected singlets, with chemical shifts -13.1 (**8·CO**) and -18.2 ppm (**10·CO**), and $^1J_{\text{PPt}}$ coupling constants of 1603 and 3938 Hz, respectively, the latter in accordance with the proposed *trans*-P—Pt—Me and *trans*-P—Pt—Cl arrangements. Other NMR data for these compounds are collected in the Experimental Section and are also in agreement with the proposed structures. It is worth remarking that the two complexes feature strong IR bands in the carbonyl region, characterised by $\bar{\nu}(\text{CO})$ values of 2031 and 2092 cm^{-1} , respectively. If one recalls that for the parent $[\text{PtCl}_2(\text{CO})(\text{PMe}_2\text{Ar}^{\text{Dipp}_2})]$ complex **6·CO**,

$\bar{\nu}(\text{CO})$ appears at 2114 cm^{-1} , it becomes evident that replacement of one or the two chloride ligands in **6** by electron-rich methyl groups increases the electron density at the Pt(II) centre thereby augmenting π -back donation to the strong π -acceptor carbon monoxide ligand.

In these two compounds as well as in the phosphine adducts, the two Dipp substituents of the terphenylphosphine become equivalent and give rise to only one septet and two doublets for, respectively, the methine and methyl protons of the *iso*-propyl substituents. This can be seen in Figure 36 that contains the ^1H NMR spectrum of complex **8**·PMe₃ in the aliphatic region, from *ca.* -0.3 to 3.1 ppm (bottom spectrum). The top representation corresponds to the ^{31}P -decoupled proton NMR spectrum.

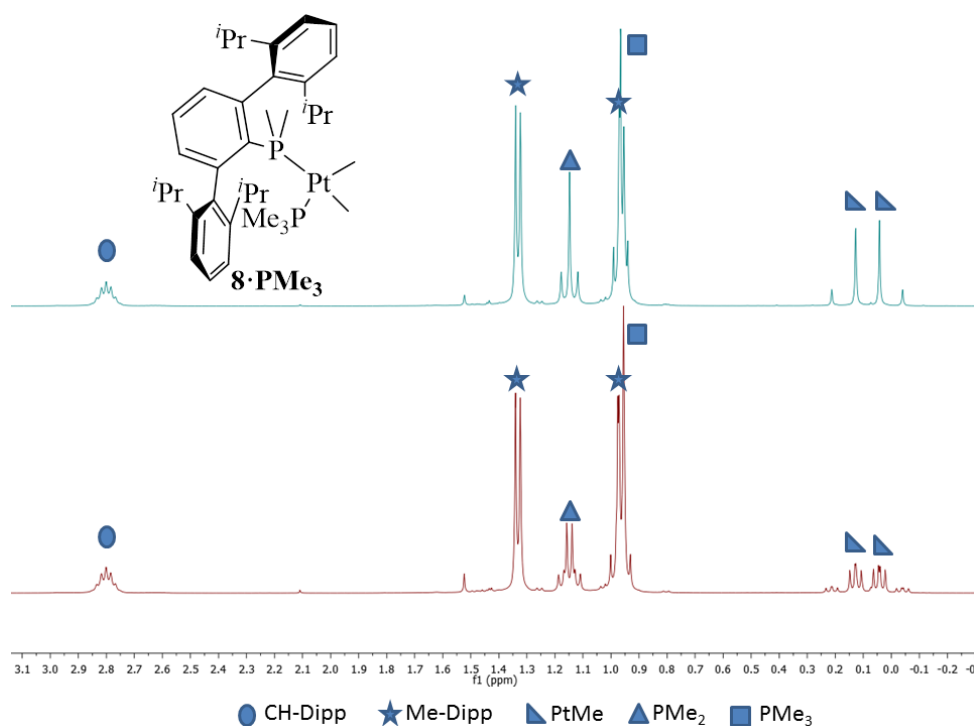


Figure 36. Aliphatic area of ^1H NMR spectrum (bottom) and $^1\text{H}\{^{31}\text{P}\}$ NMR spectrum (top) of complex **8**·PMe₃ (400 MHz, CD_2Cl_2 , 25 °C).

As commented above, complex **8**·CO was further characterized by X-ray diffraction analysis (Figure 37). Its molecular structure confirms the

κ^1 -P coordination mode of the phosphine. The Pt1-C33 bond *trans* to CO has a distance of approximately 2.08 Å, that is comparable, if slightly longer, to the Pt—Me bond *trans* to the secondary C_{ar} interaction in complexes **8** and **10** (*ca.* 2.05 Å). In turn, the Pt—Me bond *trans* to phosphorus, with a length of 2.096(5) Å (Pt1-C34 in Figure 37) is very similar to the analogous bond in compound **8** (2.108(2) Å).

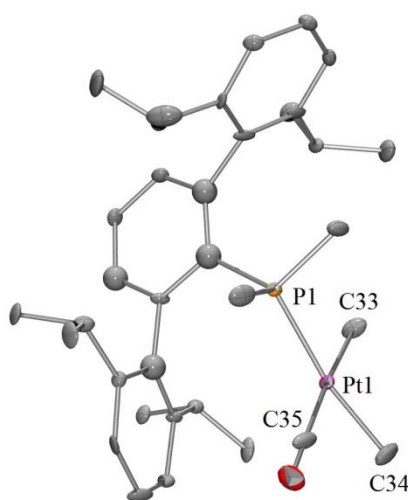


Figure 37. ORTEP view of the complex **8**·CO; hydrogen atoms are excluded for clarity and thermal ellipsoids are set at 50 % level of probability. Selected bond distances (Å) and angles (°): Pt1-P1 2.319(1), Pt1-C33 2.076(5), Pt1-C34 2.096(5), Pt1-C35 1.891(5), P1-Pt1-C33 87.1(1), C33-Pt1-C34 86.6 (2), C34-Pt1-C35 88.6(2), C35-Pt1-P1 97.8(1).

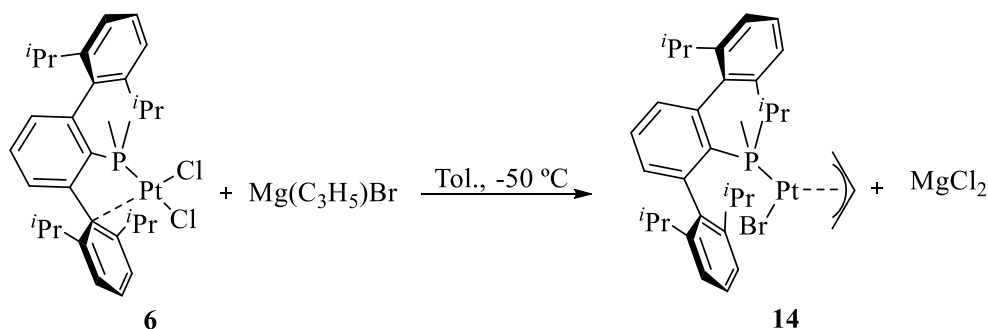
The Allyl Platinum(II) Complex [Pt(η^3 -C₃H₅)Br(PMe₂Ar^{Dipp2})]

Transition metal allyl complexes have been studied extensively and have a long history.^{15a-c,70} A classical route to compounds of this kind involves allylation of a metal halide precursor, employing a lithium or Grignard-allyl reagent. An alternative method is based on the oxidative

⁷⁰ C. Elschenbroich, *Organometallics*, 3rd ed., **2006**.

addition of an allyl transfer reagent, for instant an allyl halide, to suitable Pt(0) complex precursors.⁷¹

These two procedures have been utilised in this Thesis. Here, in Chapter I, we describe the synthesis of complex $[\text{Pt}(\eta^3\text{-C}_3\text{H}_5)\text{Br}(\text{PMe}_2\text{Ar}^{\text{Dipp}2})]$ (**14**), by reaction of *cis*- $[\text{PtCl}_2(\text{PMe}_2\text{Ar}^{\text{Dipp}2})]$ (**6**) with $\text{Mg}(\text{C}_3\text{H}_5)\text{Br}$, while in Chapter II the oxidative addition of $\text{CH}_2=\text{CHCH}_2\text{Br}$ to $[\text{Pt}(\text{C}_2\text{H}_4)_2(\text{PMe}_2\text{Ar}^{\text{Dipp}2})]$ will be reported. In addition, in a coming section of this chapter, formation of the cationic allyl platinum(II) complex $[\text{Pt}(\eta^3\text{-C}_3\text{H}_5)(\text{PMe}_2\text{Ar}^{\text{Dipp}2})]^+$ (**24**) will be discussed as resulting from a C—C bond forming reaction between *cis*- $[\text{PtMe}(\text{S})(\text{PMe}_2\text{Ar}^{\text{Dipp}2})]$ (**20·S**) and C_2H_2 , through the intermediacy of a vinylidene species (See I.2.2.4 Section, page 147)



Scheme 22. Synthesis of complex **14**.

As depicted in Scheme 22, treatment of the dichloride complex **6** with an small excess of $\text{Mg}(\text{C}_3\text{H}_5)\text{Br}$ afforded selectively and cleanly the new bromo-allyl complex **14**, with monodentate P-coordinated terphenylphosphine ligand. The new compound was isolated as a yellow solid, soluble in common organic solvents like CH_2Cl_2 , C_6H_6 or $\text{C}_4\text{H}_8\text{O}$, and was fully characterised by NMR spectroscopy. Figure 38 shows its ^1H

⁷¹ J. Forniés, E. Lalinde, in *Comprehensive Organometallic Chemistry III* (Ed.: R. H. Crabtree), Elsevier, Oxford, **2007**, 8.09, 611-673.

NMR spectrum in the region 4.6-0.9 ppm, approximately. Consistent with the proposed non-symmetric structure, the two P-bonded methyl groups, $\text{PMe}_2\text{Ar}'$, are diastereotopic and yield two doublets at 1.47 and 1.35 ppm, with the same $^2J_{\text{HP}} = 10.5$ Hz, and somewhat different $^3J_{\text{HPt}}$ couplings of 46.0 and 39.5 Hz, respectively. The Dipp_2 rings of the phosphine yield two partially superimposed septets centred at 2.85 and 2.80 ppm plus four doublets (4.17, 3.91, 2.54 and 2.44 ppm). These resonances are attributed to the four *iso*-propyl substituents of the aromatic rings, which become equivalent two by two, probable as a consequence of fast rotation around the aryl connecting C—C bonds. The five allylic protons are non-equivalent. They originate signals at 1.34 (masked by isopropyl methyl resonances), 2.44, 2.54, 3.91, and 4.17 ppm. In the $^{13}\text{C}\{^1\text{H}\}$ NMR spectrum, the ^{13}C allylic nuclei resonate at 108.3 ($^1J_{\text{CPt}} = 47$ Hz), 64.3 ($^2J_{\text{CP}} = 35$ Hz, $^1J_{\text{CPt}} = 53$ Hz) and 44.7 ($^1J_{\text{CPt}} = 259$ Hz) ppm. Finally, the $^{31}\text{P}\{^1\text{H}\}$ NMR resonance is the expected singlet at -10.0 ppm, with a ^{31}P - ^{195}Pt coupling constant of 4370 Hz. All of these NMR data are in agreement with those reported for other allyl complexes of platinum(II).^{54a}

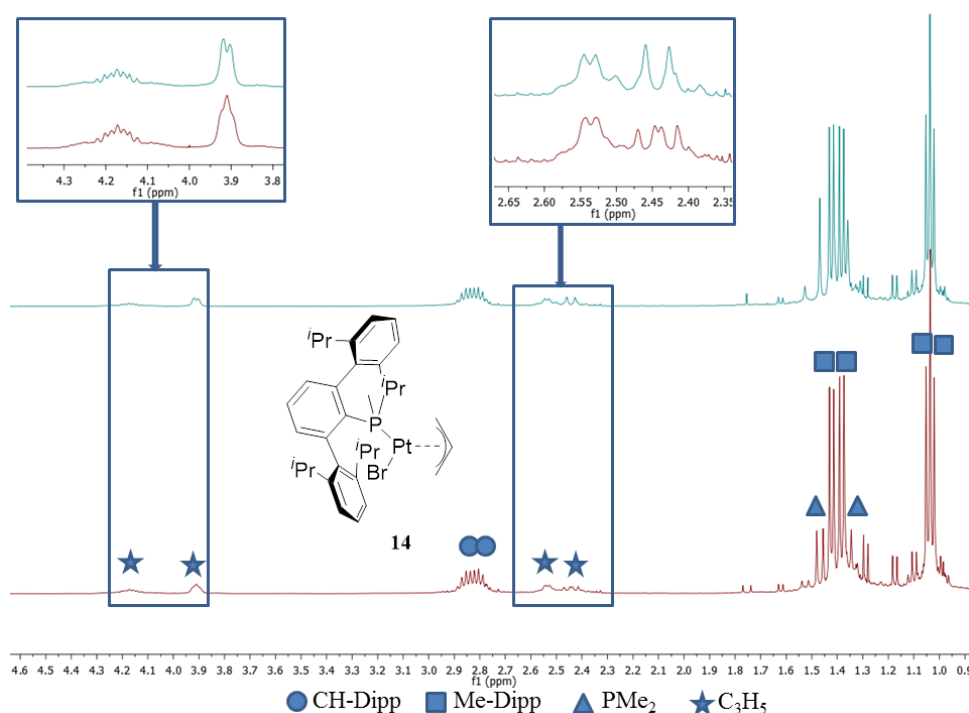


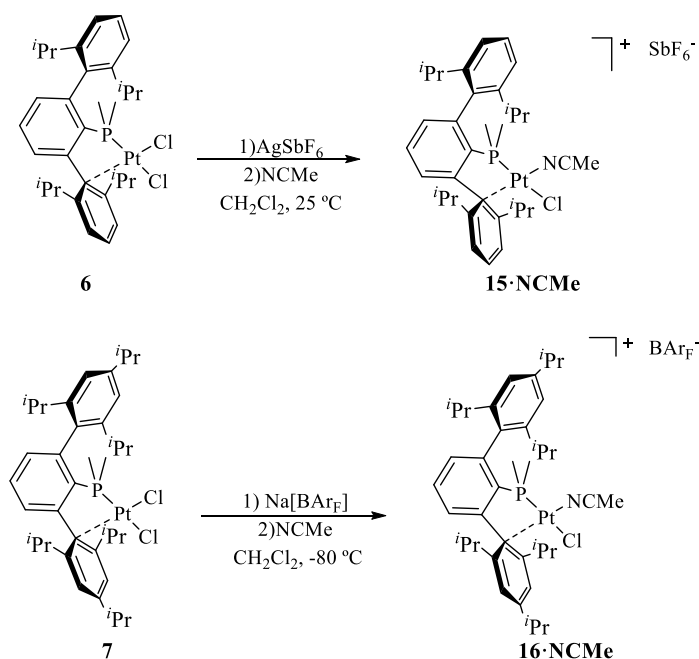
Figure 38. Aliphatic area of $^1\text{H}\{^{31}\text{P}\}$ (top) and ^1H (bottom) NMR of complex **14** (400 MHz, CD_2Cl_2 , 25 °C).

I.2.2.3. Cationic Unsaturated Platinum(II) Complexes that Exhibit Bidentate ($\kappa^1\text{-P}$, $\eta^1\text{-arene}$) Phosphine Coordination

Cationic Monochloride and Related Dicationic Complexes

As mentioned briefly earlier, one of the objectives of this Thesis was the generation of low-coordinate, unsaturated Pt(II) complexes, taking advantage of the large steric requirements of terphenylphosphines and of the protection they provide to metals bonded to a small number of ligands. We therefore decided to perform the reactions of the neutral dichloride complexes *cis*-[PtCl₂(PMe₂Ar')] **6** and **7**, with Ag[SbF₆] or Na[BAr_F], as chloride abstracting reagents. The corresponding reactions were carried out in CH₂Cl₂ and occurred quantitatively by NMR spectroscopy, to afford the

expected cationic complexes $[\text{PtCl}(\text{PMe}_2\text{Ar}')(\text{S})]^+$, in which a molecule of the solvent ($\text{S}=\text{CH}_2\text{Cl}_2$) occupies the place of the leaving chloride ligand.⁶⁷ The newly formed species provided, however, very broad NMR signals, undoubtedly due to dynamic processes facilitated by the lability of the coordinated molecule of CH_2Cl_2 . Treatment of the crude reaction products with acetonitrile neatly generated the corresponding adducts, **15·NCMe** and **16·NCMe**, that were isolated as pale yellow solids (Scheme 23).



Scheme 23: Synthesis of complexes **15·NCMe** and **16·NCMe**.

Formally the new compounds could be envisioned as two-coordinate cationic $[\text{PtCl}(\text{PMe}_2\text{Ar}')]^+$ species, with one of the lateral terphenyl rings partly offsetting the coordination and electronic unsaturation of the Pt(II) ion by means of a secondary $\text{Pt} \cdots \text{C}_{\text{ar}}$ interaction, and a molecule of CH_2Cl_2 or NCMe completing the distorted tetracoordinate geometry. The analysis of the NMR data does not sustain an unequivocal structural proposal although it firmly buttresses the *trans*-

P—Pt—Cl arrangement represented in Scheme 24 for the NCMe complexes **15·NCMe** and **16·NCMe**. In fact, the anticipated κ^1 -P, η^1 -C bidentate bonding of the phosphine is strongly supported by the inequivalency of the flanking aryl rings. In the ^1H NMR spectrum of **15·NCMe**, they give rise to two septets and four doublets for the $i\text{Pr}$ substituents (Figure 39, bottom), whereas in that of **16·NCMe** four CHMe_2 septets and six CHMe_2 doublets are clearly discerned (Figure 39, top spectrum). The $^{31}\text{P}\{^1\text{H}\}$ NMR spectrum of these compounds shows the expected singlet at 7.5 (**15·NCMe**) and 7.7 ppm (**16·NCMe**). These resonances are accompanied by ^{195}Pt satellites that lead to $^1J_{\text{PPt}}$ values of 3335 and 3395 Hz, respectively, which are not very different from the *ca.* 3200 Hz value found in the parent compounds **6** and **7** (*vide supra*). Since in the also cationic NCMe adduct $[\text{PtMe}(\text{PMe}_2\text{Ar}^{\text{Dipp}_2})(\text{NCMe})]^+$, to be discussed in a forthcoming section, that features *trans* phosphine and NCMe ligands, the corresponding coupling amounts 4304 Hz, the *trans*-P-Pt-Cl ligand distribution shown in Scheme 23 is proposed for these compounds. In agreement with this proposal, we additionally note that the above $^1J_{\text{PPt}}$ values are very similar to those reported for *cis*- $[\text{PtCl}_2(\text{PR}_3)_2]$ complexes, which were found to vary between *ca* 3500 and 3640 Hz.^{54c}

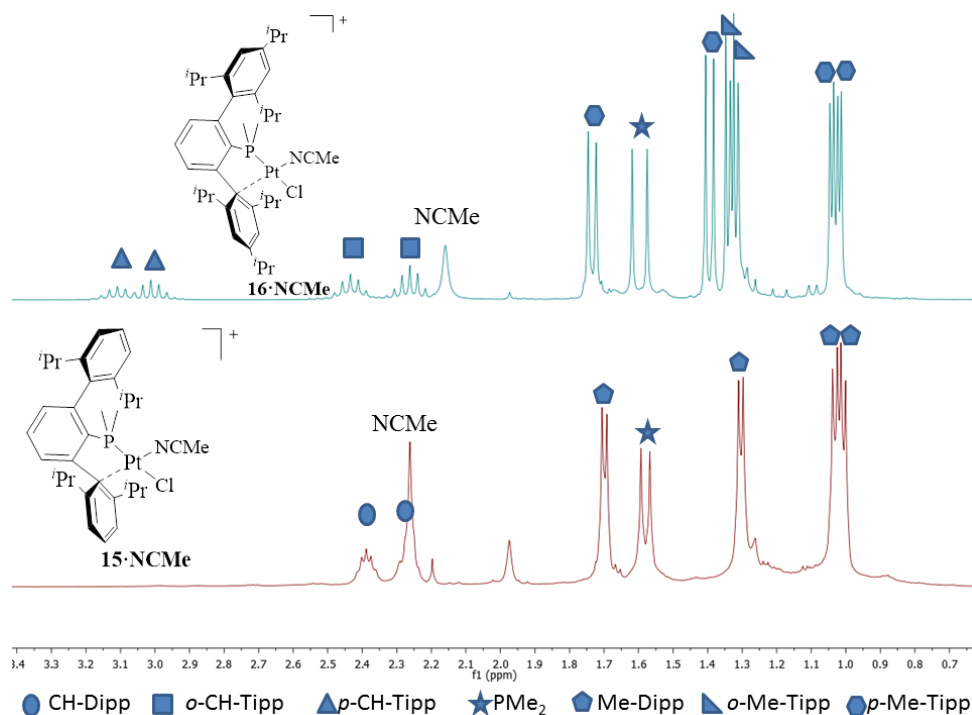
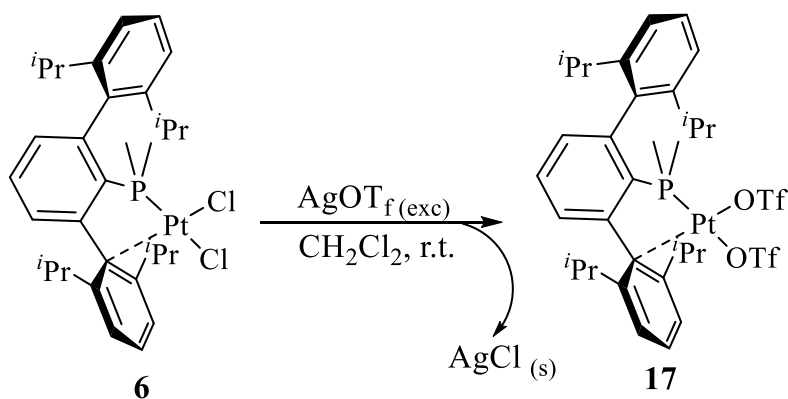


Figure 39. Aliphatic area of ^1H NMR spectra for complexes **15·NCMe** (bottom, CD_2Cl_2 , 500 MHz, 25 °C) and **16·NCMe** (top, CD_2Cl_2 , 300 MHz, 25 °C).

We also found that the dichloride complex $\text{cis-}[\text{PtCl}_2(\text{PMe}_2\text{Ar}^{\text{Dipp}_2})]$ (**6**), reacted readily with a slight excess of AgOTf in dichloromethane, to produce the new compound, $\text{cis-}[\text{Pt}(\text{OTf})_2(\text{PMe}_2\text{Ar}^{\text{Dipp}_2})]$ (**17**), as a result of chloride displacement by triflate (Scheme 24). Triflate complexes of platinum are a well-known family of compounds⁷² and some bis(triflate) complexes have found applications as catalysts for hydroarylations and

⁷² a) M. Lersch, M. Tilset, *Chem. Rev.* **2005**, *105*, 2471-2526; b) H. Heiberg, L. Johansson, O. Gropen, O. B. Ryan, O. Swang, M. Tilset, *J. Am. Chem. Soc.* **2000**, *122*, 10831-10845; c) N. Oberbeckmann-Winter, X. Morise, P. Braunstein, R. Welter, *Inorg. Chem.* **2005**, *44*, 1391-1403; d) P. Nilsson, G. Puxty, O. F. Wendt, *Organometallics* **2006**, *25*, 1285-1292.

hydroaminations of alkenes⁷³ and other important reactions of unsaturated hydrocarbons.¹⁴



Scheme 24: Synthesis of the neutral complex **17**.

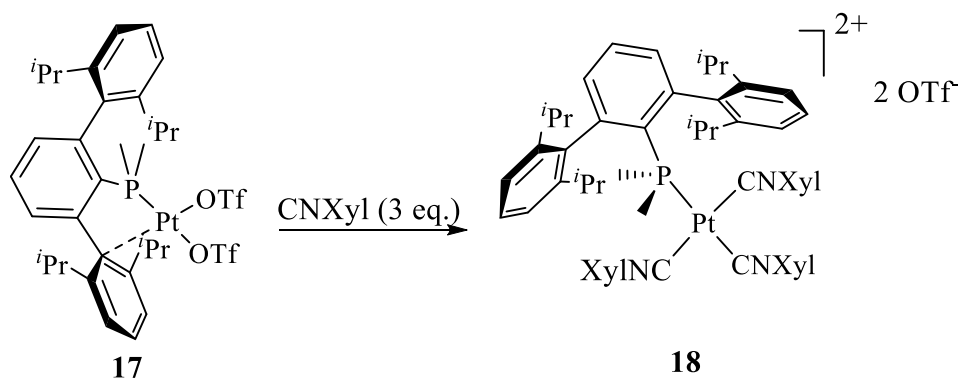
Our bis(triflate) complex **17** presents dynamic behaviour in solution, very likely due to facile triflate dissociation in dichloromethane. Nevertheless, its ^1H NMR spectrum recorded in CD_2Cl_2 exhibits two septets and four doublets for the methine and methyl protons, respectively, of the terphenyl *iso*-propyl substituents, in agreement with the expected bidentate $\text{P},\text{C}_{\text{ar}}$ -coordination of the phosphine ligand. The room temperature $^{31}\text{P}\{^1\text{H}\}$ NMR spectrum is a broad resonance centred at 12.2 ppm, with $^1J_{\text{PPt}} = 3531$ Hz.

Similar to other triflate, and in general cationic Pt(II) complexes, compound **17** is moisture sensitive,^{73,74} which made difficult isolation in a crystalline state. Treatment of its CH_2Cl_2 solution with 3 equiv of NCXyl yielded, however, the dicationic compound **18** (Scheme 25), which was

⁷³ a) D. Karshtedt, A. T. Bell, T. D. Tilley, *Organometallics* **2004**, 23, 4169-4171; b) D. Karshtedt, A. T. Bell, T. D. Tilley, *J. Am. Chem. Soc.* **2005**, 127, 12640-12646; c) J. L. McBee, A. T. Bell, T. D. Tilley, *J. Am. Chem. Soc.* **2008**, 130, 16562-16571.

⁷⁴ a) M. P. Brown, S. J. Cooper, A. A. Frew, L. Manojlovic-Muir, K. W. Muir, R. J. Puddephatt, K. R. Seddon, M. A. Thomson, *Inorg. Chem.* **1981**, 20, 1500-1507; b) P. K. Monaghan, R. J. Puddephatt, *Organometallics* **1984**, 3, 444-449; c) K. R. Pellarin, M. S. McCready, R. J. Puddephatt, *Dalton Trans.* **2013**, 42, 10444-10453.

isolated as a crystalline solid and was fully characterised by NMR spectroscopy and X-ray crystallography.



Scheme 25: Synthesis of the dicationic compound **18**.

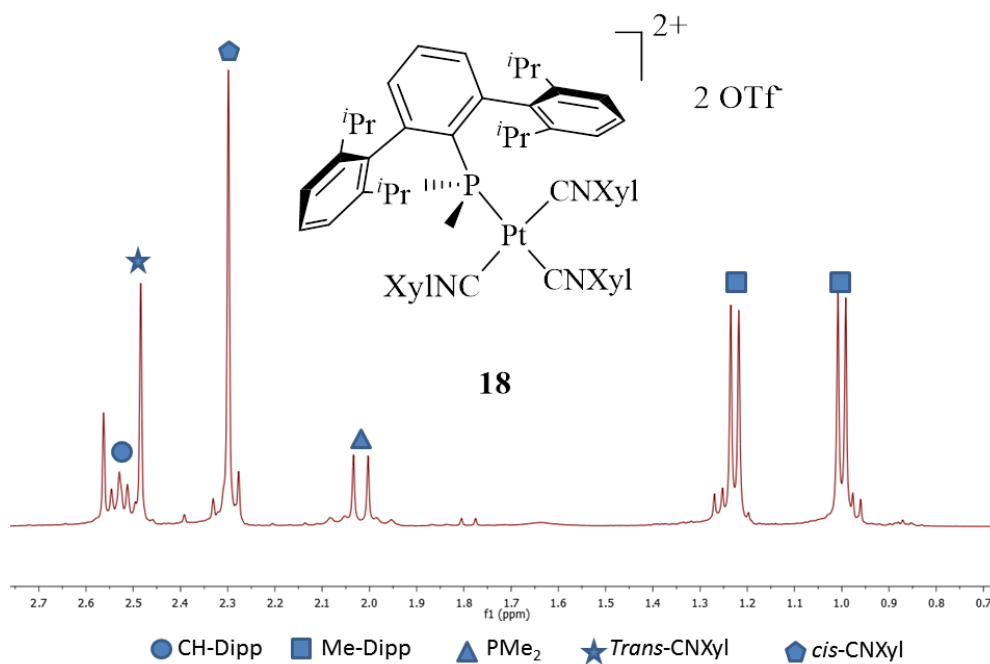
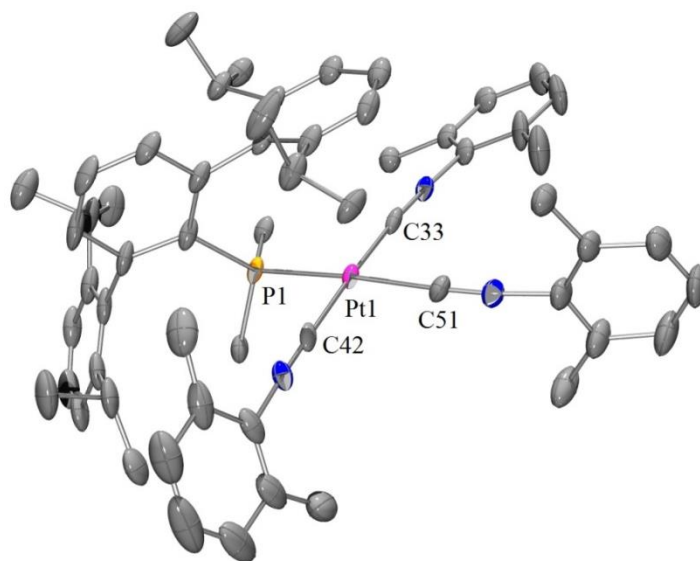


Figure 40: Aliphatic zone of the ^1H NMR spectra of complex **18**.
(400 MHz, CD_2Cl_2 , 25 °C).

A single-crystal X-ray investigation of the triflate salt of this dication confirmed these predictions (Figure 41). The two *trans* Pt-C bonds (Pt1-C33 and Pt1-C42) have similar lengths of about 1.95 Å, whereas the Pt1-C51 distance is longer (*ca.* 2.03 Å) reflecting the higher *trans*-influence of the phosphine ligand.



C51–Pt1–C42 85.37(17), C42–Pt1–P1 93.75(12).

Dicationic platinum(II) complexes are rare, and have recently gained increasing interest due to their promising reactivity toward hydrocarbon substrates. In Pt and Au catalysis, strong Lewis acidity is often required²⁹ and an obvious way of increasing the metal π -acidity implies incrementing the positive complex charge. In this way, a coordinated C-C multiple bond becomes highly activated towards attack by even weak nucleophiles, allowing the formation of new C—C, C—N and C—O bonds.⁷⁵ Hahn, Vitagliano and co-workers have used dicationic Pt(II) complexes stabilised by tridentate PNP pincer ligands to activate alkenes and alkynes towards nucleophilic attack.^{75,76} The reactivity of these systems is, however, limited by the coordination of the tridentate pincer ligand, that leaves only one accessible coordination site. Employing diimine ligands, Labinger, Bercaw⁷⁷ and Tilset⁷⁸ have generated a variety of complexes with a $[\text{Pt}(\text{N}^{\wedge}\text{N})]^{2+}$ framework, with weakly bound alcohols in the remaining coordination positions, that are capable to activate C-H bonds.⁷⁷ Truly tricoordinate dicationic platinum(II) complexes were recently described by Braunschweig and coworkers, as resulting from halide abstraction from cationic base-stabilised borylene complexes.⁷⁹ The same year, work from Bowring, Bergman and Tilley resulted in a

⁷⁵ a) C. Hahn, *Organometallics* **2010**, 29, 1331-1338; b) C. Hahn, P. Morvillo, E. Herdtweck, A. Vitagliano, *Organometallics* **2002**, 21, 1807-1818; c) C. Hahn, M. E. Cucciolito, A. Vitagliano, *J. Am. Chem. Soc.* **2002**, 124, 9038-9039; d) M. E. Cucciolito, A. D'Amor, A. Vitagliano, *Organometallics* **2005**, 24, 3359-3361; e) M. E. Cucciolito, A. D'Amora, A. Tuzi, A. Vitagliano, *Organometallics* **2007**, 26, 5216-5223; f) M. E. Cucciolito, A. Vitagliano, *Organometallics* **2008**, 27, 6360-6363; g) W. D. Kerber, J. H. Koh, M. R. Gagné, *Org. Lett.* **2004**, 6, 3013-3015; h) J. A. Feducia, A. N. Campbell, M. Q. Doherty, M. R. Gagné, *J. Am. Chem. Soc.* **2006**, 128, 13290-13297; i) C. Hahn, *Chem. Eur. J.* **2004**, 10, 5888-5899.

⁷⁶ M. E. Cucciolito, A. D'Amora, A. Vitagliano, *Organometallics* **2010**, 29, 5878-5884.

⁷⁷ a) T. J. Williams, A. J. M. Caffyn, N. Hazari, P. F. Oblad, J. A. Labinger, J. E. Bercaw, *J. Am. Chem. Soc.* **2008**, 130, 2418-2419; b) T. G. Driver, T. J. Williams, J. A. Labinger, J. E. Bercaw, *Organometallics* **2007**, 26, 294-301; c) A. G. Wong-Foy, L. M. Henling, M. Day, J. A. Labinger, J. E. Bercaw, *J. Mol. Catal. A: Chem.* **2002**, 189, 3-16.

⁷⁸ J. Parmene, A. Krivokapic, M. Tilset, *Eur. J. Inorg. Chem.* **2010**, 2010, 1381-1394.

⁷⁹ H. Braunschweig, P. Brenner, R. D. Dewhurst, J. O. C. Jimenez-Halla, T. Kupfer, D. Rais, K. Uttinger, *Angew. Chem. Int. Ed.* **2013**, 52, 2981-2984.

dicationic platinum salt with composition $[\text{Pt}(\text{}^t\text{Bu}_2\text{bpy})(\text{solvent})_2][\text{NTf}_2]_2$, that was characterised by X-ray studies as the pentafluoropyridine bis(solvate).^{80a}

Inspired by this work, we reacted a benzene solution of dimethyl complex *cis*- $[\text{PtMe}_2(\text{PMe}_2\text{Ar}^{\text{Dipp}_2})]$ (**8**) with a slight excess of triflimide, HNTf₂, at room temperature, for a period of 12 h. Following removal of the solvent under vacuum, the resulting oily residue was washed with cold pentane (*ca.* -40 °C) to produce a pale-brown solid that was crystallised from CH₂Cl₂-pentane solvent mixtures and was identified as the complex *cis*- $[\text{Pt}(\text{PMe}_2\text{Ar}^{\text{Dipp}_2})(\text{S})_2][\text{NTf}_2]_2$ (**19**), where S represents a molecule of a poor donor solvent like CH₂Cl₂, THF or adventitious water. In fact, the crystals obtained were shown by ¹H NMR and X-ray crystallography to contain one molecule of THF and another of water coordinated to platinum. The THF was subsequently ascertained as an impurity of the CH₂Cl₂ used for crystallization.

⁸⁰ a) M. A. Bowring, R. G. Bergman, T. D. Tilley, *Organometallics* **2013**, 32, 5266-5268; b) M. A. Bowring, R. G. Bergman, T. D. Tilley, *J. Am. Chem. Soc.* **2013**, 135, 13121-13128.

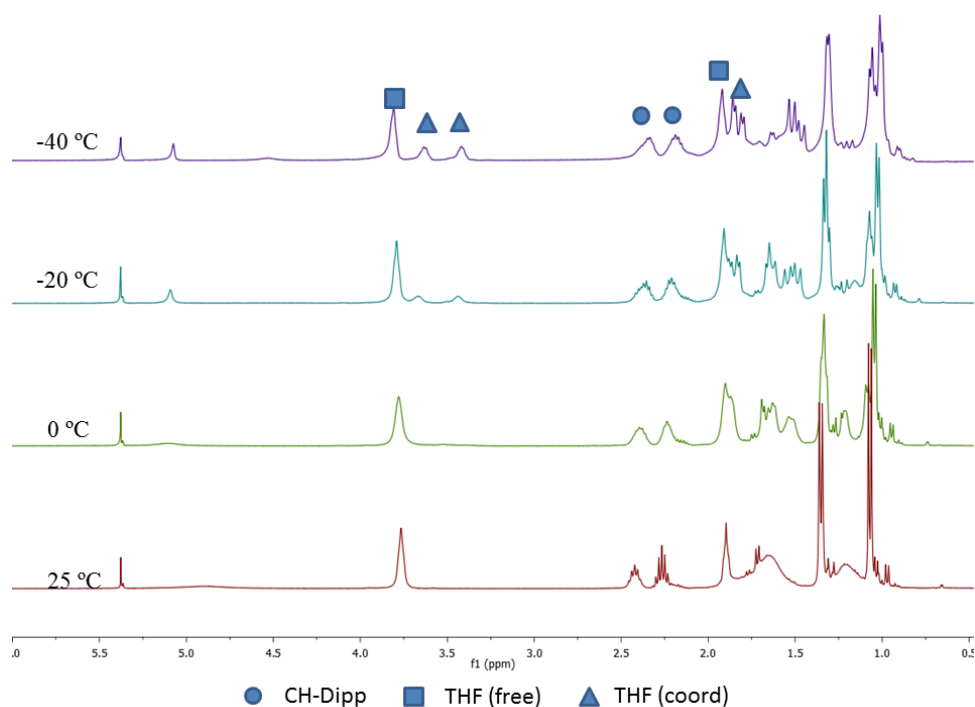


Figure 42: Aliphatic area of variable temperature ^1H NMR spectrum of compound **19** (CH_2Cl_2 , 400 MHz).

Figure 42 shows variable temperature ^1H NMR spectra of complex **19** in the chemical shift range *ca.* 6.0-0.5 ppm. Although the spectrum is rather complicated, particularly in the region 2.0-1.0 ppm, and therefore little informative, the observation of two septets (2.26 and 2.42 ppm) for the ^iPr methine protons is in agreement with the foreseen bidentate coordination of the phosphine ligand. Furthermore, in the room temperature spectrum there are two rather broad resonances with δ 1.89 and 3.76 ppm that can be attributed to the CH_2 and CH_2O protons of tetrahydrofuran. These signals have relative intensities that denote a $\text{THF}:\text{PMe}_2\text{Ar}'$ molar ratio of *ca.* 2.5:3 and suggest fast exchange between bonded and free THF at this temperature. Upon cooling, the resonance at 3.76 becomes broader (See Figure 42, spectrum recorded at 0 °C) and at -

20 °C splits, giving rise to an unresolved signal at δ 3.79 due to free THF⁸¹ and to two broad peaks with δ 3.67 and 3.44 ppm, which can be tentatively attributed to the diastereotopic CH₂O protons of a coordinated molecule of THF. Lowering the temperature to -40 °C intensifies these changes (Figure 42). A similar variation can be detected for the 1.89 ppm THF resonance, although the existence in this region of the spectrum of other resonances makes the assignment less accurate. Finally, and perhaps somewhat speculatively, the broad ¹H resonance discernible in the room temperature ¹H NMR spectrum at *ca.* 4.86 ppm may be due to the presence of water. Upon cooling it converts into a broad singlet at 5.09 ppm (-20 °C) which splits into two resonances centred at 5.07 and 4.52 ppm. A reasonable, if somewhat adventurous, explanation is that small amounts of adventitious water compete with THF for one of the two available coordination sites at the dicationic metal centre of the [Pt(PMe₂Ar^{Dipp}₂)]²⁺ unit. Besides these uncertainties, the possibility of NTf₂⁻ coordination adds further complications (*vide infra*).

To complete the discussion of the NMR data, two additional comments could be made. At -40 °C, the ¹⁹F NMR spectrum of compound **19** recorded in CD₂Cl₂ contains a sharp singlet at *ca.* -79 ppm and a very broad resonance that is nearly hidden under the base line, centred at about -70 ppm. Following Bergman and Tilley^{80b} the first may be attributed to the free, dissociated counteranion, while the second is due to platinum-bonded NTf₂⁻, that is, to a Pt-NTf₂ linkage. Thus, in addition to the intricate solution dynamics due to the lability of the coordinated molecules of H₂O and THF, NTf₂⁻ coordination and dissociation adds further complexity. Secondly, in accordance with the above ¹H and ¹⁹F NMR data, the ³¹P{¹H} spectrum of complex **19**, recorded at room temperature in a solution in

⁸¹ G. R. Fulmer, A. J. M. Miller, N. H. Sherden, H. E. Gottlieb, A. Nudelman, B. M. Stoltz, J. E. Bercaw, K. I. Goldberg, *Organometallics* **2010**, 29, 2176-2179.

CD_2Cl_2 is a broad signal centred at *ca.* 13.7 ppm. Cooling at 0 °C converts this resonance into a well-defined singlet with essentially the same chemical shift (Figure 43) whereas additional cooling first at -20 °C and then at -40 °C, originates two singlet resonances of similar relative intensities. It is evident from all these data that at low temperatures two main species exist in CD_2Cl_2 solutions and it seems that one of them may contain a bound NTf_2^- counteranion, while the other could consist of the true $[\text{Pt}(\text{PMe}_2\text{Ar}^{\text{Dipp}_2})(\text{S})_2]^{2+}$ dications, with non-bonded NTf_2^- counteranions. As for the nature of S, water, tetrahydrofuran and perhaps CD_2Cl_2 may compete for the vacant coordination sites in the two closely related isomeric complex salts.

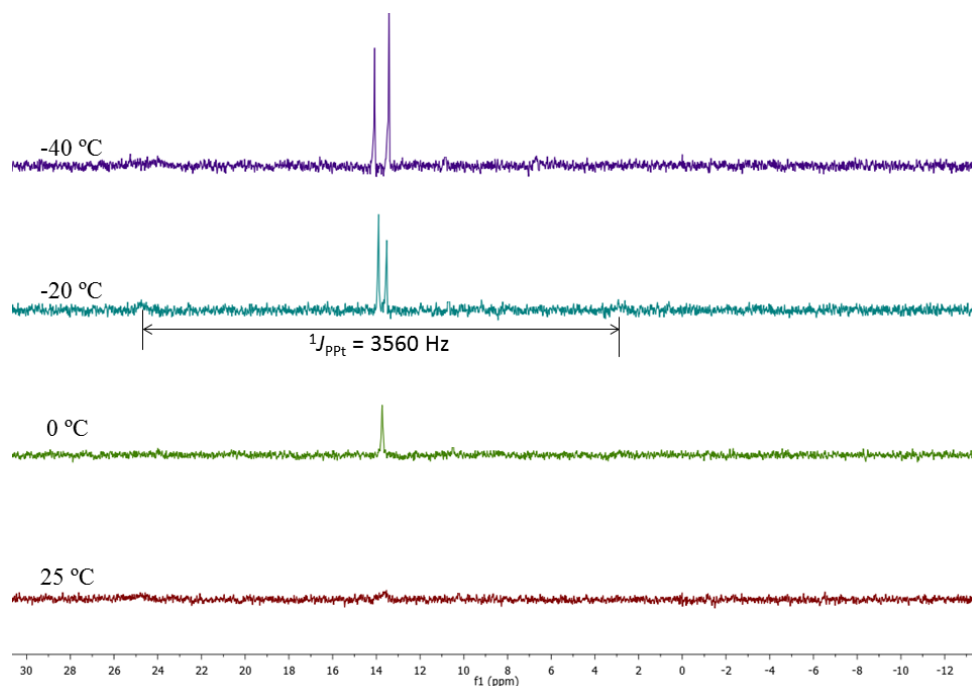


Figure 43: Variable temperature $^{31}\text{P}\{^1\text{H}\}$ NMR spectra of complex **19** (CD_2Cl_2 , 161.9 MHz)

The above conjectures find strong support in the crystallographic analysis of single crystals of this compound. The solid-state structure of its

molecules was determined at -100 °C and can be observed in Figure 44 in the form of ORTEP representation. The complex exhibits the expected distorted square-planar geometry, but the coordination polygon is made of the terphenylphosphine, which binds to the platinum dication in a κ^1 -P, η^2 -arene fashion, and of two actually poor donor ligands, viz a molecule of tetrahydrofuran and a molecule of water.

Surprisingly, complex **19** represents the first structurally characterized Pt(II) complex that contains coordinated molecules of H₂O and THF. The Pt—O distances are 2.072(4) Å for the Pt—OH₂ bond and 2.118(4) Å for the Pt—OC₄H₈ bond. The Pt—OC₄H₈ distance is significantly shorter than in *trans*-[Pt(H)(THF)(P^{*i*}Pr₃)₂]⁺ (2.224(7) Å)⁶⁷ and comparable to the 2.142(4) Å value found in a related Pt(II) complex of a chelating Ph₂PCH₂C₄H₇O ligand that incorporates a molecule of tetrahydrofuran.⁸² The Pt—OH₂ bond is also comparatively short. For instance, in some cationic aryl complexes *trans*-[Pt(Ar)(H₂O)(PR₃)₂]⁺, the Pt—OH₂ distance was found in the 2.175-2.190 Å range,⁸³ while in a recently reported [Pt(PCP)(H₂O)]⁺ complex^{26c} it amounts 2.145(2) Å. By contrast to other PMe₂Ar' complexes described in this Thesis, complex **19** features an η^2 (rather than η^1) bonding interaction with one of the lateral aryl rings of the terphenylphosphine ligand (see Figure 44 for appropriate Pt—C distances). Moreover, this interaction can be defined as strong if Pt—C_{ar} separations are used as criterium for robustness. Thus, The Pt1-C27 distance is 2.168(6) Å. Not only is this contact the shortest of the Pt...C_{ar} interactions described in this Thesis, besides, it is comparable to the olefinic Pt—C bonds in Zeise's salt (*ca.* 2.16 Å).⁵³ As already mentioned, there is another Pt...C_{ar} distance which can be judged as

⁸² N. W. Alcock, A. W. G. Platt, P. G. Pringle, *J. Chem. Soc., Dalton Trans.* **1989**, 2069-2072.

⁸³ a) Y. K. Kryshchenko, S. R. Seidel, D. C. Muddiman, A. I. Nepomuceno, P. J. Stang, *J. Am. Chem. Soc.* **2003**, 125, 9647-9652; b) M. Ito, M. Ebihara, T. Kawamura, *Inorg. Chim. Acta* **1994**, 218, 199-202.

bonding,⁵² namely Pt1-C8 at 2.480(6) Å, which as shown in Figure 44 involves one of the *ortho* carbon atoms of the interacting aryl ring.

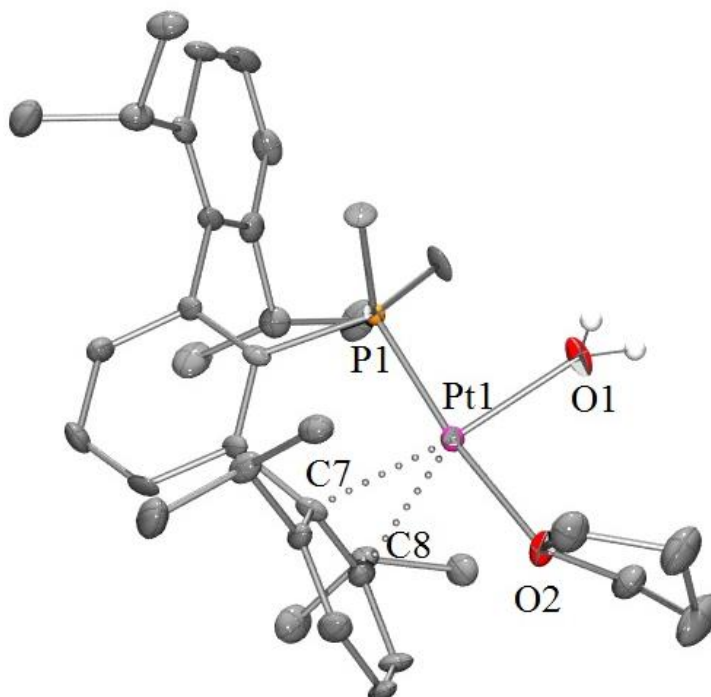


Figure 44: ORTEP view of the complex **19**; selected hydrogen atoms and NTF₂ anions are excluded for clarity and thermal ellipsoids are set to 50% level probability. Selected bond distances (Å) and angles (°): Pt1-P1 2.206(1), Pt1-C7 2.168(6), Pt1-C8 2.480(6), Pt1-O1 2.072(4), Pt1-O2 2.118(4), O1-Pt1-O2 82.0(2), O2-Pt1-C7 102.8(2), C7-Pt1-P1 83.8 (2), P1-Pt1-O1 91.2(1).

Cationic Complexes with Platinum to Carbon Sigma Bonds.

Methyl and Phenyl Derivatives

As stated in preceding sections of this Thesis, cationic organometallic complexes are reactive species that find diverse applications in catalysis, spanning C-C bond formation, enantioselective olefin hydrogenation, olefin polymerisation and alkane C-H bond

activation reactions.^{29d,84-86} Low-coordinate cationic complexes of Pt(II) that contain platinum to carbon sigma bonds such as alkyls and aryls are of special importance, for they combine the existence of readily accessible coordination sites and enhanced electrophilicity of the positively charged metal, with the intrinsic reactivity of the M-C σ -bond.^{35e,35f,72a,87-89}

As a natural extension of the chemistry described in the foregoing sections, we considered of interest to carry out the protonation of *cis*-[PtMe₂(PMe₂Ar^{Dipp2})] (**8**) with [H(Et₂O)₂][BAr_F]. With this reactivity we targeted at the synthesis of the cationic Pt(II) complexes *cis*-[PtMe(S)(PMe₂Ar^{Dipp2})]⁺ (**20•S**), expecting κ^2 -P,C phosphine coordination and therefore the existence of labile Pt...C_{ar} and Pt...S interactions, the latter involving a molecule of a poorly coordinating solvent, like H₂O, Et₂O, THF, etc. The objective of this work was the study of the reactivity of such cationic species **20•S** towards some small inorganic and organic molecules. In particular, we aimed as a major goal to ascertain the

⁸⁴ a) S. D. Ittel, L. K. Johnson, M. Brookhart, *Chem. Rev.* **2000**, *100*, 1169-1204; b) M. Bochmann, *Organometallics* **2010**, *29*, 4711-4740; c) D. S. McGuinness, *Chem. Rev.* **2011**, *111*, 2321-2341.

⁸⁵ a) J. J. Verendel, O. Pàmies, M. Diéguez, P. G. Andersson, *Chem. Rev.* **2014**, *114*, 2130-2169; b) G. S. Chen, J. A. Labinger, J. E. Bercaw, *PNAS* **2007**, *104*, 6915-6920.

⁸⁶ a) R. Dorel, A. M. Echavarren, *Chem. Rev.* **2015**, *115*, 9028-9072; b) I. Braun, A. M. Asiri, A. S. K. Hashmi, *ACS Catal.* **2013**, *3*, 1902-1907; c) C. Hahn, M. Miranda, N. P. B. Chittineni, T. A. Pinion, R. Perez, *Organometallics* **2014**, *33*, 3040-3050.

⁸⁷ a) R. Romeo, *Comments Inorg. Chem.* **2002**, *23*, 79-100; b) R. Romeo, G. D'Amico, E. Sicilia, N. Russo, S. Rizzato, *J. Am. Chem. Soc.* **2007**, *129*, 5744-5755; c) R. J. Puddephatt, *Coord. Chem. Rev.* **2001**, *219-221*, 157-185; d) E. M. Prokopcuk, R. J. Puddephatt, *Organometallics* **2003**, *22*, 787-796.

⁸⁸ a) L. Johansson, M. Tilset, J. A. Labinger, J. E. Bercaw, *J. Am. Chem. Soc.* **2000**, *122*, 10846-10855; b) J. S. Owen, J. A. Labinger, J. E. Bercaw, *J. Am. Chem. Soc.* **2006**, *128*, 2005-2016; c) A. E. Shilov, G. B. Shul'pin, *Chem. Rev.* **1997**, *97*, 2879-2932; d) U. Fekl, K. I. Goldberg, in *Adv. Inorg. Chem., Vol. Volume 54*, Academic Press, **2003**, pp. 259-320,

⁸⁹ a) S. H. Crosby, G. J. Clarkson, J. P. Rourke, *Organometallics* **2011**, *30*, 3603-3609; b) O. Rivada-Wheelaghan, M. Roselló-Merino, M. A. Ortuño, P. Vidossich, E. Gutiérrez-Puebla, A. Lledós, S. Conejero, *Inorg. Chem.* **2014**, *53*, 4257-4268; c) O. Rivada-Wheelaghan, M. Roselló-Merino, J. Díez, C. Maya, J. López-Serrano, S. Conejero, *Organometallics* **2014**, *33*, 5944-5947; d) J. L. Spencer, G. S. Mhinzi, *J. Chem. Soc., Dalton Trans.* **1995**, 3819-3824.

coordination of C_2H_2 and C_2H_4 to these Pt(II) cations and to unveil the ensuing C-C bond forming reactivity that might arise between the existing Pt-Me bond and the coordinated, unsaturated hydrocarbons.

In general, cationic Pt(II) complexes are π -acidic systems that catalyse efficiently (along with Au(I) analogues) a good many electrophilic activations of alkenes and alkynes.^{14,75i} Carbene complexes, including the intriguing subclass of metal-vinylidenes,^{90,91} are often invoked as active intermediates, but in most instances there is no direct evidence for their involvement, and proposed mechanistic paths rely mainly on reaction outcomes and computational data. In fact, while carbene and vinylidene complexes of W, Ru, Os, Rh, and Ir have been widely investigated,^{90,91} little is known about platinum analogues.^{11,36,92} In accordance with these arguments, we investigated by experimental and computational methods the possible implication as reactive intermediates of the cationic carbene structures $[Pt=C(H)Me]^+$ and $[Pt=C=CH_2]^+$, resulting from tautomerisation of C_2H_4 and C_2H_2 , respectively, upon coordination to the Pt(II) centre of **20·S**. Indeed, it was found that the use C_2D_2 provided unequivocal evidence for the participation of a platinum-vinylidene intermediate in the reaction of **20·S** with acetylene.

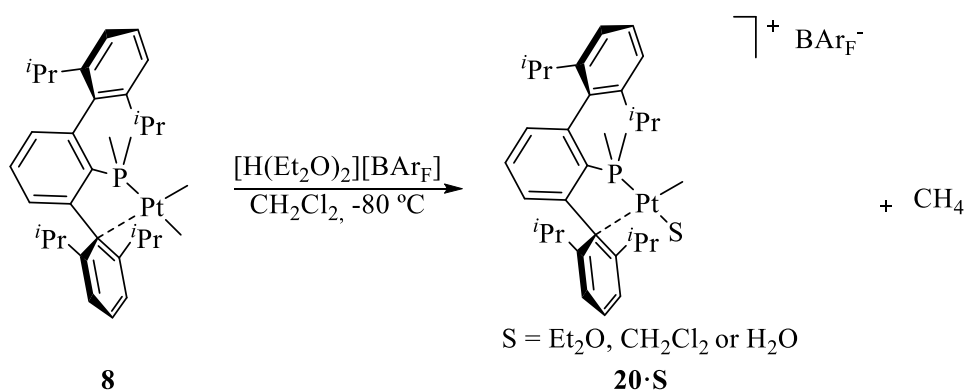
⁹⁰ a) J. Silvestre, R. Hoffmann, *Helv. Chim. Acta* **1985**, 68, 1461-1506; b) M. I. Bruce, *Chem. Rev.* **1991**, 91, 197-257; c) C. Bruneau, P. H. Dixneuf, *Angew. Chem. Int. Ed.* **2006**, 45, 2176-2203.

⁹¹ a) J. M. Lynam, *Chem. Eur. J.* **2010**, 16, 8238-8247; b) O. J. S. Pickup, I. Khazal, E. J. Smith, A. C. Whitwood, J. M. Lynam, K. Bolaky, T. C. King, B. W. Rawe, N. Fey, *Organometallics* **2014**, 33, 1751-1761; c) M. Jiménez-Tenorio, M. C. Puerta, P. Valerga, M. A. Ortuño, G. Ujaque, A. Lledós, *Inorg. Chem.* **2013**, 52, 8919-8932; d) H. Werner, *Coord. Chem. Rev.* **2004**, 248, 1693-1702.

⁹² For early work on mononuclear Pt(II) vinylidenes see: a) U. Belluco, R. Bertani, F. Meneghetti, R. A. Michelin, M. Mozzon, *J. Organomet. Chem.* **1999**, 583, 131-135; b) U. Belluco, R. Bertani, R. A. Michelin, M. Mozzon, *J. Organomet. Chem.* **2000**, 600, 37-55; c) M. Rashidi, R. J. Puddephatt, *J. Am. Chem. Soc.* **1986**, 108, 7111-7112.

To complete this section, the protonation reactions of *cis*-[PtMe₂PMe₂Ar^{Tipp2}]**(9)**, and *cis*-[PtPh₂PMe₂Ar^{Dipp2}]**(11)** were also studied.

Low-temperature protonation (CD₂Cl₂, -80 °C) of complex *cis*-[PtMe₂(PMe₂Ar^{Dipp2})]**(8)** with [H(OEt₂)₂][BAr_F] ([BAr_F] = [B(3,5-(CF₃)₂C₆H₃)₄]) did not permit detection of a transient cationic Pt(II) σ-CH₄ complex.⁵¹ Instead liberation of CH₄ was observed with quantitative formation (by ¹H and ³¹P{¹H} NMR spectroscopy) of the cationic complex [PtMe(S)(PMe₂Ar^{Dipp2})]⁺**(20·S)**. As represented in Scheme 26, protonation occurred formally at the Pt—Me bond *trans* to the P atom and generated a coordination vacancy that was probably occupied by a labile molecule of solvent present in the reaction medium (CH₂Cl₂, OEt₂ or adventitious water). No unequivocal spectroscopic evidence was obtained for solvent coordination (see below) although as discussed later, the X-ray diffraction analysis of a crystalline sample of **20·S** obtained following work-up of the reaction mixture revealed the presence of a molecule of adventitious water directly ligated to the metal centre.



Scheme 26. Synthesis of complex **20·S**.

The NMR data recorded for this complex are in agreement with the structure proposed in Scheme 26. Figure 45 contains the low frequency range of its ^1H NMR spectrum in the δ region 3.7-0.5 ppm. Once again, the observation of two septets between 2.30 and 2.55 ppm and of four doublets, two of them accidentally with the same chemical shift, between *ca.* 1.0 and 1.6 ppm, attributed respectively to the methine and methyl protons of the terphenyl *iso*-propyl substituents, supports bidentate $\kappa^2\text{-P}$, $\eta^1\text{-C}$ coordination of the phosphine ligand. Besides a doublet resonance at 1.55 ppm assigned to the $\text{PMe}_2\text{Ar}'$ protons ($^2J_{\text{HP}} = 10$ Hz, $^3J_{\text{HPt}} = 70$ Hz), the spectrum in Figure 45 contains a slightly broad unresolved signal at 0.76 ppm due to the platinum-bound methyl group along with a triplet at 1.18 and a quartet at 3.55 ppm, which might be due to a coordinated molecule of Et_2O . We note, however, that the differences in these chemical shift values with those of free, uncoordinated diethylether, are almost negligible. In the $^{13}\text{C}\{^1\text{H}\}$ NMR spectrum there is a slightly broad Pt—Me singlet at -6.9 ppm with unresolved ^{13}C - ^{31}P coupling, that shows ^{195}Pt satellites yielding a $^1J_{\text{CPt}}$ value of 769 Hz. The $^{31}\text{P}\{^1\text{H}\}$ NMR spectrum recorded at 25 °C is a broad resonance at -0.5 ppm, probably as a consequence of rapid exchange of the *trans* solvent molecule in the NMR time scale. This signal is characterized by a large $^1J_{\text{PPt}}$ value of 4882 Hz that attests the weakness of the Pt—S bond and the very small *trans*-influence exerted by S.

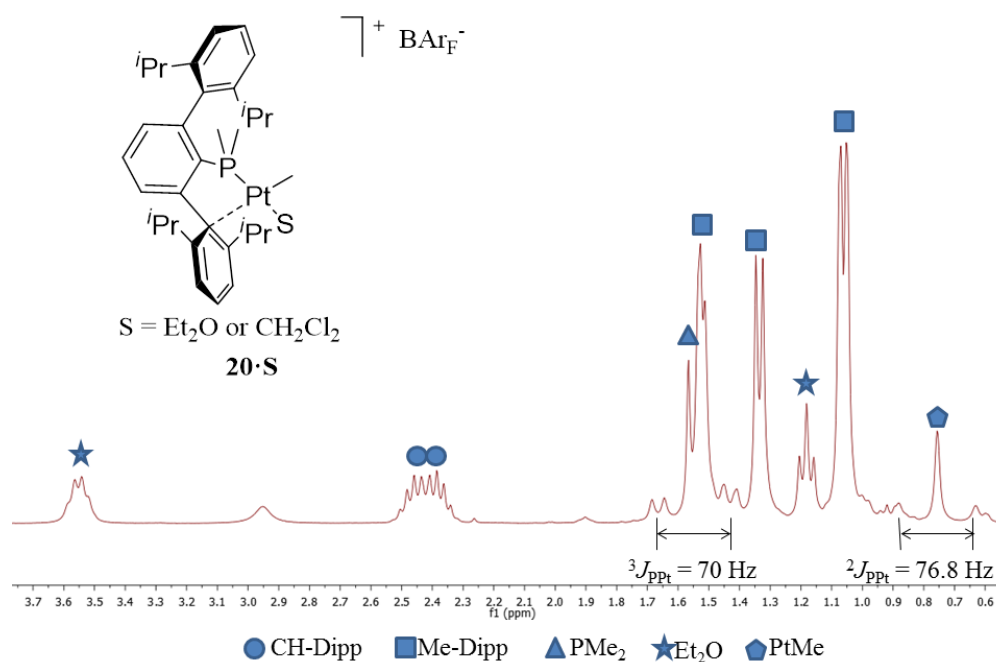


Figure 45. Aliphatic region of ^1H NMR spectrum of complex **20·S** (300 MHz, CD_2Cl_2 , 25 °C).

In addition to facile exchange of the coordinated solvent molecule (*vide infra*), complex **20·S** exhibits in solution a dynamic behaviour that involves the exchange of the flanking aryl ring of the phosphine terphenyl substituents. Figure 46 collects the variations experienced by the resonances due to the *CH* protons of the *iso*-propyl substituents when the temperature is varied between 25 and 115 °C. The spectra were recorded in $\text{C}_2\text{D}_2\text{Cl}_4$. At room temperature two septets at 1.64 and 1.75 ppm can be clearly distinguished. These resonances broaden at higher temperatures and coalesce at about 100 °C, to merge into a broad resonance at 105 °C and yield a discernible septet centred at 1.78 ppm. The calculated rate constant for the exchange at the coalescence temperature is 87.1 s^{-1} , with an associated activation energy, ΔG^\ddagger of $18.7 \text{ kcal}\cdot\text{mol}^{-1}$.

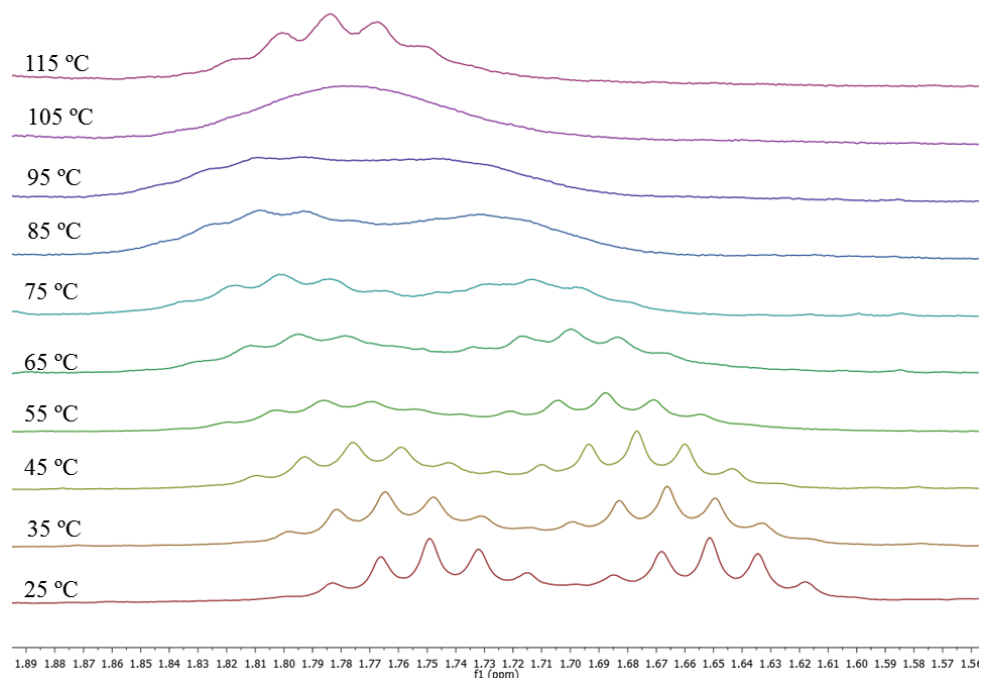


Figure 46: Variable temperature ^1H NMR spectra of complex **20·S** showing the resonances of the *isopropyl* CH protons (400 MHz, $\text{C}_2\text{D}_2\text{Cl}_4$).

The molecular structure of **20·S** was unequivocally determined by X-ray crystallography in the form of the water adduct **20·H₂O**. Although the Et_2O complex **20·Et₂O** was recrystallized from CH_2Cl_2 /pentane solvent mixtures at $-20\text{ }^\circ\text{C}$ for 2-3 days, adventitious water appear to compete successfully to coordinate to the Pt(II) centre and provided crystals of **20·H₂O** in preference to those of **20·Et₂O** or **20·CH₂Cl₂**. Water was reported to displace⁶⁷ coordinated CH_2Cl_2 from *trans*-[Pt(H)(ClCH₂Cl)(P^{*i*}Pr₃)₂]⁺.

The molecular structure of **20·H₂O** is depicted in Figure 47. The coordination environment of the platinum atom may be approximately viewed as T-shaped, consisting of a *trans*-P—Pt—OH₂ linkage with a methyl group *cis* to the phosphine and water ligands. This description is an extreme one, for the coordination and electronic unsaturation of the Pt(II)

centre is partially compensated by a long, and therefore weak Pt \cdots C_{ar} interaction with the *ipso* carbon atom (C22) of an Dipp ring. Overall, there are two relatively short bonds, namely the Pt—Me and the Pt—P bonds (Pt1—C1 and Pt1—P1 in Figure 47) with lengths of 2.034(6) Å, and 2.170(1) Å, respectively, the long Pt \cdots C_{ar} at 2.348(5) Å, and an also weak Pt—OH₂ ligation characterised by a Pt1—O1 distance of 2.143(4) Å. The latter is significantly longer than the corresponding distance in the dicationic complex *cis*-[Pt(PMe₂Ar^{Dipp}₂)(OH₂)(THF)]²⁺, where it has a value of 2.072(4) Å.

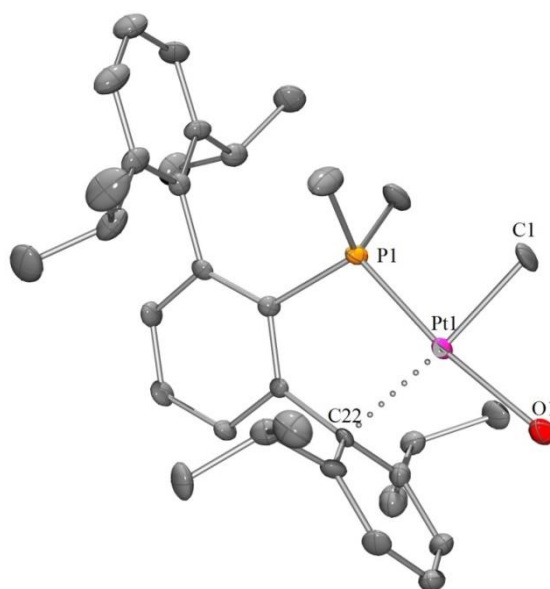
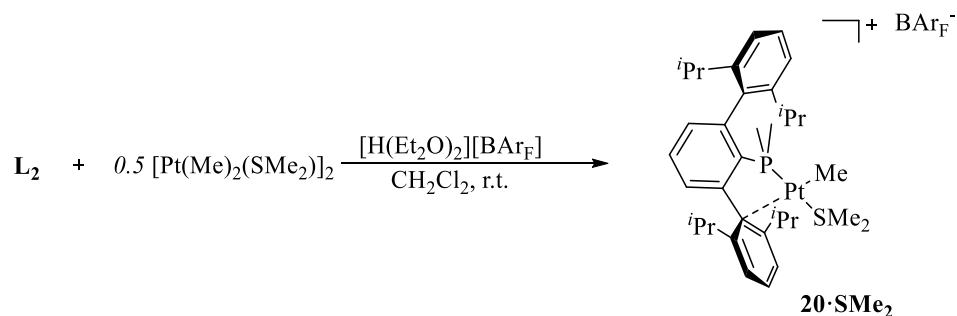


Figure 47. ORTEP view of the cation of complex **20·H₂O**; BAr_F anion and hydrogen atoms are excluded for clarity and thermal ellipsoids are set at 50 % level probability. Selected bond distances (Å) and angles(°): Pt1—O1 2.143(4), Pt1—C1 2.034(6), Pt1—P1 2.170(1), Pt1—C22 2.348(5), O1—Pt1—C1 83.2(2), C1—Pt1—P1 89.6(2), P1—Pt1—C22 83.9(1), C22—Pt1—O1 103.1(2).

We prepared and structurally characterised by NMR spectroscopy and in some cases by X-ray crystallography other **20·S** complexes. For example, adding [H(OEt₂)₂][BAr_F] to a mixture of *cis*-[PtMe₂(SMe₂)₂]₂ and

$\text{PMe}_2\text{Ar}^{\text{Dipp}_2}$ in CH_2Cl_2 (Scheme 27) led preferentially to the SMe_2 adduct *cis*- $[\text{Pt}(\text{Me})(\text{SMe}_2)(\text{PMe}_2\text{Ar}^{\text{Dipp}_2})][\text{BAr}_\text{F}]$.



Scheme 27. Synthesis of adduct **20·SMe₂**.

The NMR data obtained for the **20·SMe₂** cations (see Figure 48 for the ^1H NMR spectrum between 2.6 and 0.5 ppm) are similar to those described for the adduct commented above. The superior ligating properties of SMe_2 compared to Et_2O or H_2O leads to a well-resolved spectrum where the Pt—Me resonance appears as a doublet with δ 0.73 ppm, $^3J_{\text{HPt}} = 4$ and $^2J_{\text{HPt}} = 82.2$ Hz. Similarly, the Pt—SMe_2 protons originate a doublet at δ 1.99 ppm, with an observable four-bond $^1\text{H—}^{31}\text{P}$ coupling constant of 3.6 Hz and $^3J_{\text{HPt}} = 32.5$ Hz. The corresponding $^{13}\text{C}\{^1\text{H}\}$ signals appear at -3.5 (Pt—Me , $^2J_{\text{CP}} = 5$ Hz) and 21.4 ppm (Pt—SMe_2 , $^3J_{\text{CP}} = 2$ Hz). The $^{31}\text{P}\{^1\text{H}\}$ NMR spectrum is a singlet at 12.3 ppm with $^1J_{\text{PPt}} = 3730$ Hz, in accordance with the proposed *trans*- $\text{PMe}_2\text{Ar}^{\text{Dipp}_2}\text{—Pt—SMe}_2$ distribution.

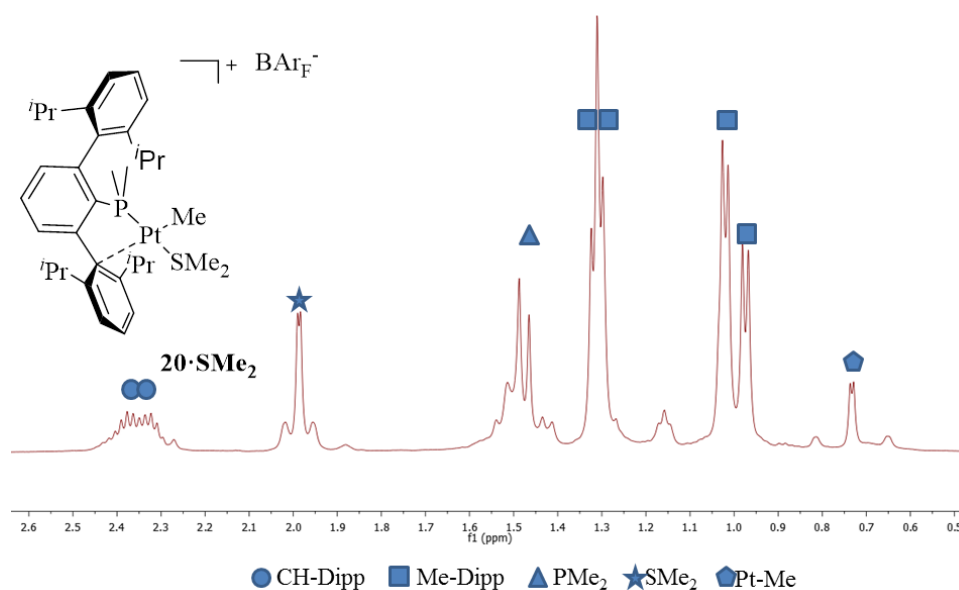


Figure 48. High field area of ^1H NMR spectrum of adduct $20 \cdot \text{SMe}_2$ (500 MHz, CD_2Cl_2 , 25 $^\circ\text{C}$).

Complex $20 \cdot \text{SMe}_2$ was further characterized as the BAr_F salt by single crystal X-ray diffraction studies (Figure 49). The structure is similar to that found previously for complex $20 \cdot \text{H}_2\text{O}$. Nevertheless, the Pt—P distance in the SMe_2 adduct is longer (2.239(1) Å) compared to the water analogue (2.170(1) Å) in accordance with the increased *trans* influence of the S donor ligand. The Pt—Me bond has a similar length (2.062(3) Å) and the Pt $\cdots\text{C}_\text{ar}$ interaction is also comparable to that reported for $20 \cdot \text{H}_2\text{O}$ (2.357(2) Å).

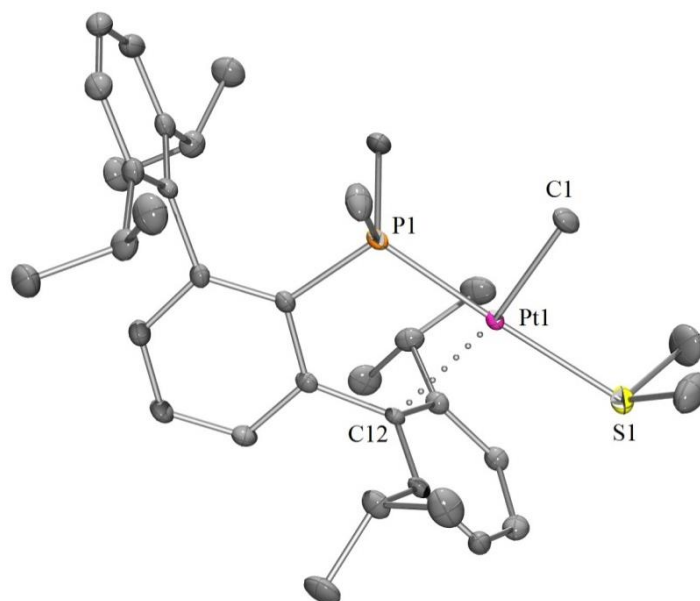
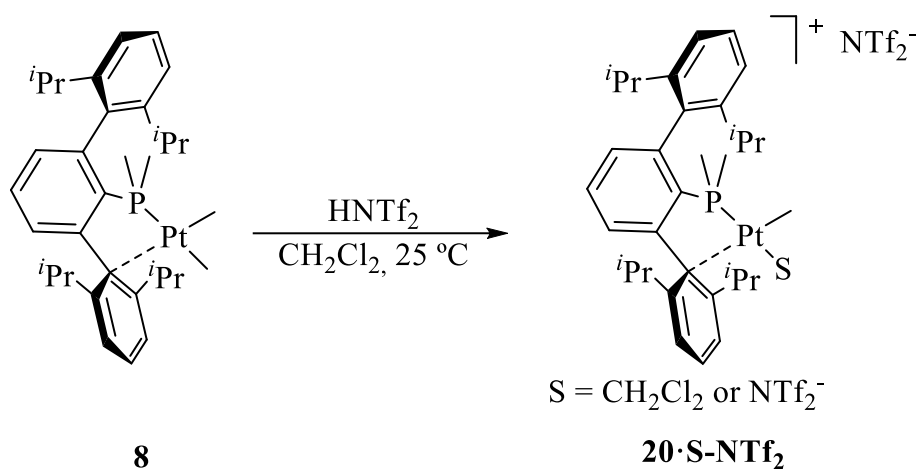


Figure 49. ORTEP view of the cation of complex **20·SMe₂**; BAr_F[−] anion and hydrogen atoms are excluded for clarity and thermal ellipsoids are set at 50 % level probability. Selected bond distances (Å) and angles(°): Pt1-S1 2.359(1), Pt1-C1 2.062(3), Pt1-P1 2.239(1), Pt1-C12 2.357(2), S1-Pt1-C1 88.9(1), C1-Pt1-P1 87.2(1), P1-Pt1-C12 82.22(7), C12-Pt1-S1 101.42(7).

To ascertain if the poorly coordinating triflimidate anion, NTf₂[−], could compete with the solvent for the readily available coordination position of the Pt(II) centre of **20·S**, the protonation of complex *cis*-[PtMe₂(PMe₂Ar^{Dipp2})] (**8**), was carried out with 1 mol-equiv of triflimide HNTf₂. The reaction gave rise to the expected complex represented in a simplified maner as **20·S-NTf₂**, (Scheme 28) which was shown by NMR spectroscopy and X-ray crystallography to exist principally as the complex salt *cis*-[PtMe(S)(PMe₂Ar^{Dipp2})] [NTf₂], in equilibrium in solution with minor concentrations of the neutral complex [PtMe(NTf₂)(PMe₂Ar^{Dipp2})].



Scheme 28. Synthesis of complex **20·S-NTf₂**.

The new complex exhibits solution dynamic behaviour at room temperature. Thus, at 25 °C, the $^{31}\text{P}\{^1\text{H}\}$ NMR spectrum is a broad signal centred at -2.7 ppm (CD_2Cl_2) with $^1J_{\text{PPt}} = 4928$ Hz, that gives rise to two resonances with different intensity upon lowering the temperature at -30 °C. The more intense signal appears at -2.4 ppm and has $^1J_{\text{PPt}} = 4721$ Hz, while that due to the minor species is found nearby, -3.1 ppm with $^1J_{\text{PPt}} = 5160$ Hz. The $^{19}\text{F}\{^1\text{H}\}$ NMR spectra recorded for these solutions are also informative (Figure 50). At room temperature there is a singlet with δ -78.9 and -71.1 ppm, with relative intensities of approximately 100:4. In agreement with literature data,^{80b} these signals can be respectively assigned to free and coordinated NTf_2^- in the Pt(II) structures depicted in Scheme 29.

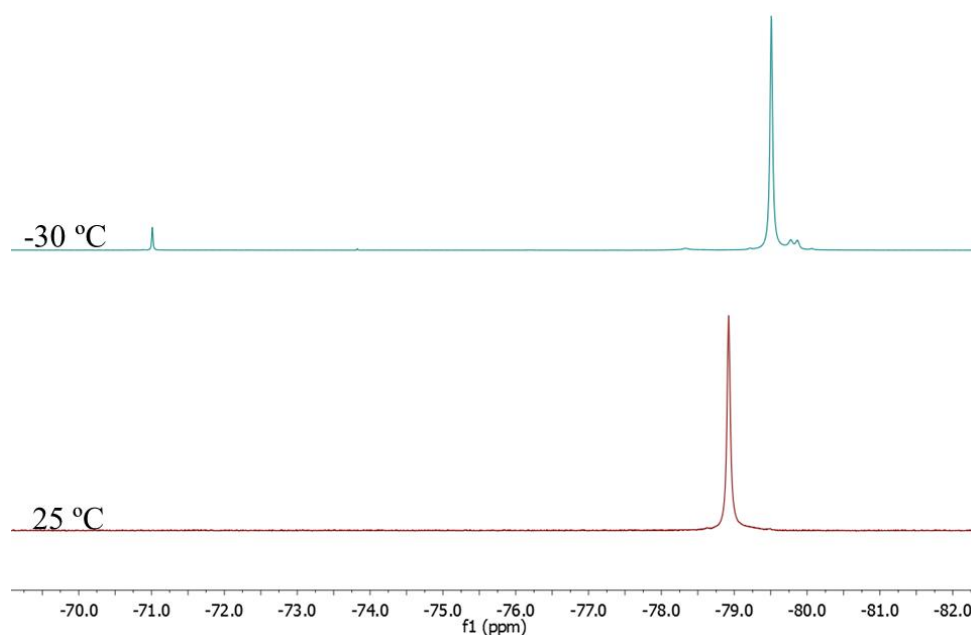
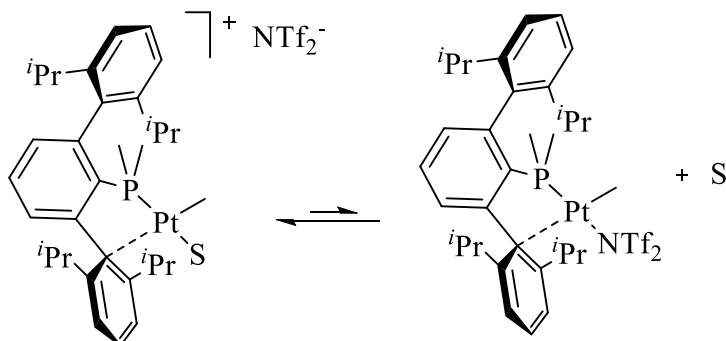


Figure 50. ^{19}F NMR spectrum of complex **20**·**S**-**NTf₂** at 25 °C and -30 °C (376.31 MHz, CD_2Cl_2).



Scheme 29: Equilibrium in solution between cationic and neutral complexes due to triflimide coordination.

Single crystals of **20 S-NTf₂** were obtained when concentrated solutions of the complex in a mixture of dichloromethane and pentane were cooled at -20 °C for three days. Resolution of the X-ray data collected at -100 °C led to the rather intriguing observation that, once again, adventitious water, in rivalry with large concentrations of CH_2Cl_2 , dominated the contest to occupy the fourth platinum coordination site of

cation $[\text{PtMe}(\text{PMe}_2\text{Ar}^{\text{Dipp2}})]^+$ (Figure 51). Therefore, the single crystals of **22·S-NTf₂** utilised for the X-ray diffraction analysis had composition *cis*- $[\text{PtMe}(\text{S})(\text{PMe}_2\text{Ar}^{\text{Dipp2}})][\text{NTf}_2]$, the complex cation being chemically identical to that found in the structure of **20·S** (Figure 47). Metrical parameters for the new compounds are consequently very similar (Figure 51).

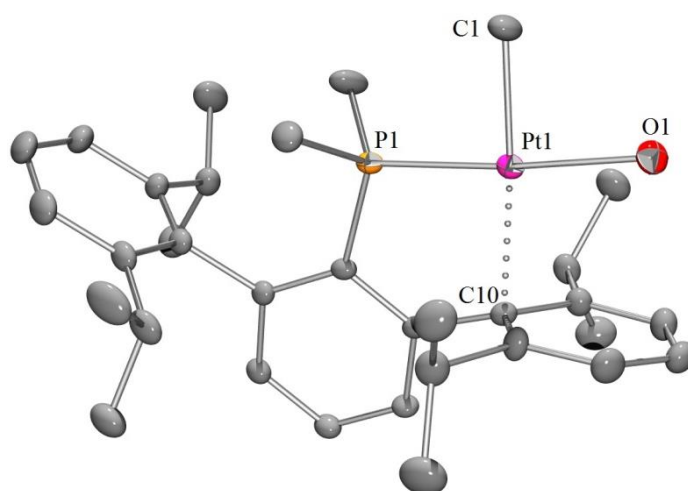


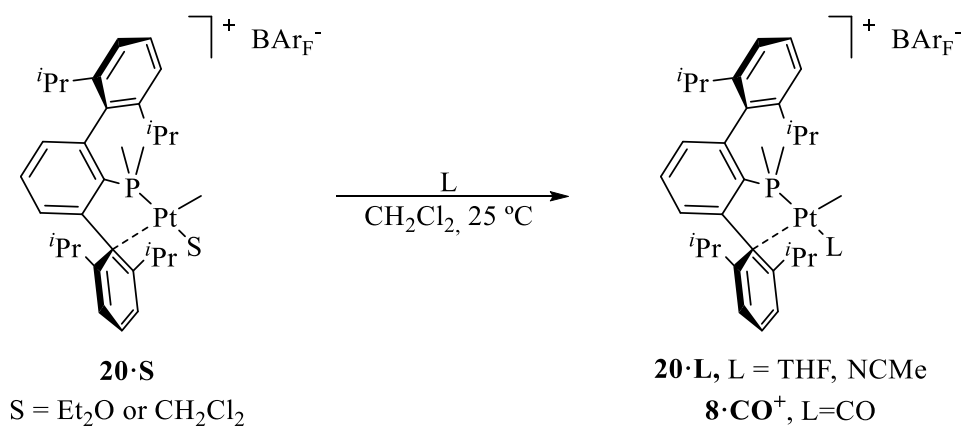
Figure 51. ORTEP view of the cation of complex **20·H₂O-NTf₂**; NTf₂ anion and hydrogen atoms are excluded for clarity and thermal ellipsoids are set at 50 % level probability. Selected bond distances (Å) and angles(°): P1-Pt1 2.1821(7), Pt1-C1 2.046(3), Pt1-O1 2.129(2), Pt1-C10 2.354(2), P1-Pt1-C189.29(9), C1-Pt1-O1 85.9(1), O1-Pt1-C10 101.16(8), C10-Pt1-P1 83.53(5).

Other Cationic Methyl Complexes

Several additional cationic complexes of the type '*cis*- $[\text{PtMe}(\text{L})(\text{PMe}_2\text{Ar}^{\text{Dipp2}})]^+$ ' were also prepared either by displacement of the weakly bonded molecule of the solvent of **20·S** (Scheme 30), by protonation of the neutral complexes **8·CO** and **8·PMe₃** (Scheme 31) or by other procedures discussed later.

The substitution of the molecule of S in **20·S** occurred readily at room temperature in the presence of an excess of the Lewis base (L = THF, NCMe and CO) to afford the expected adducts, as shown in Scheme 30.

Referring to the acetonitrile/adduct **20·NCMe** as a representative example, the ^1H NMR spectrum contains sharp, well-resolved resonances in accordance with the proposed structure, which is rigid under these conditions (Figure 52). This structure implies, once more, bidentate coordination of the terphenylphosphine, and gives rise to $^{31}\text{P}\{^1\text{H}\}$ resonances in the range from approximately -4 to -15 ppm for all the complexes studied, with $^1J_{\text{PPt}}$ values between 3230 and 4640 Hz.



Scheme 30. Synthesis of adducts **20·L**.

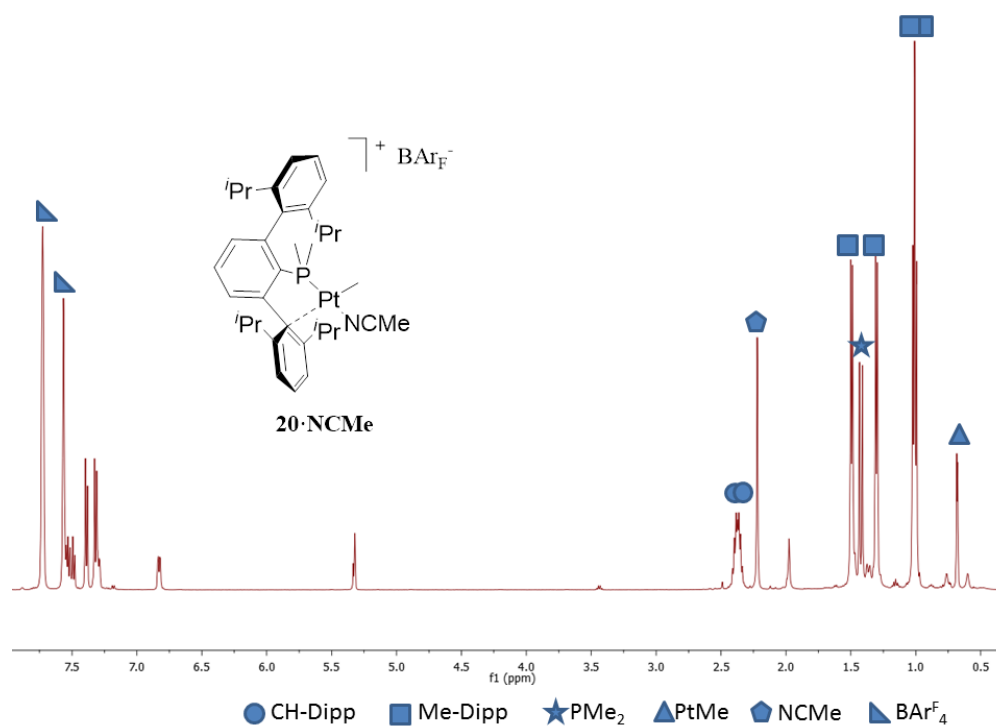
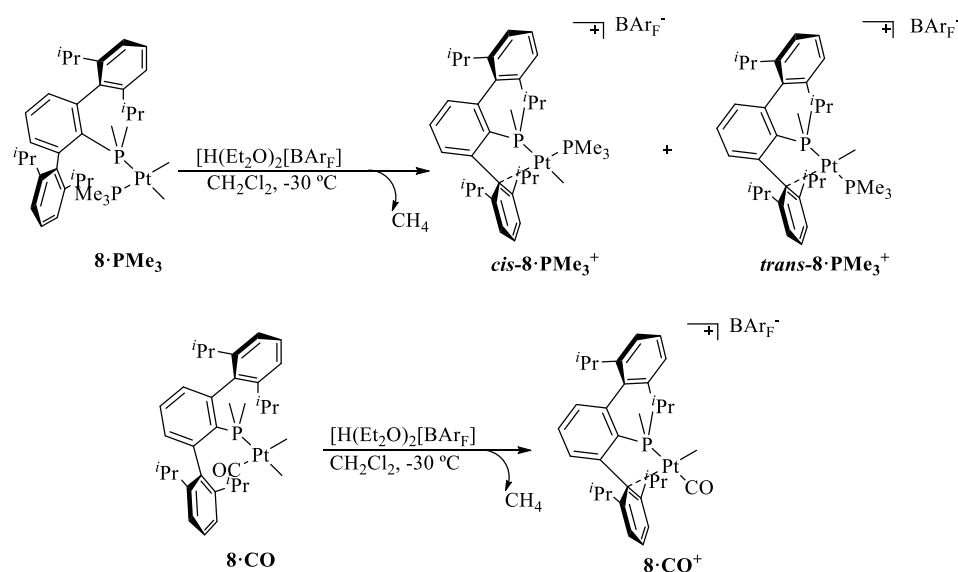


Figure 52. ¹H NMR spectrum of adduct **20·CNMe** (500 MHz, CD₂Cl₂, 25 °C).

Protonation of the dimethyl complexes *cis*-[PtMe₂(L)(PMe₂Ar^{Dipp}₂)], L = CO, **8·CO** and PMe₃, **8·PMe₃** also yielded the expected cationic adducts, **8·CO⁺** and **8·PMe₃⁺**, respectively (Scheme 31).



Scheme 31. Protonation of adducts **8·PMe₃** and **8·CO** with $[H(Et_2O)_2][BAr_F]$.

The synthesis of **8·CO⁺** was of interest as a test for the π -acidity of the $[PtMe(PMe_2Ar^{Dipp_2})]^+$ cationic fragment. The compound was isolated as a pale yellow solid, and features an IR absorption at 2127 cm^{-1} due to the stretching vibration of the coordinated molecule of CO. This $\bar{\nu}(CO)$ value is in the upper part of the region expected for $[Pt(II)—CO]^+$ entities^{11,68a,27} and is close to the 2143 cm^{-1} wavenumber of free CO, albeit slightly smaller. For comparison, we note that for the parent complex *cis*- $[PtMe_2(CO)(PMe_2Ar^{Dipp_2})]$ (**8·CO**), the CO stretching appears at significantly lower wavenumber, at 2030 cm^{-1} .

Somewhat unexpectedly, low-temperature ($-30\text{ }^\circ\text{C}$) protonation of *cis*- $[PtMe_2(PMe_2Ar^{Dipp_2})(PMe_3)]$ (**8·PMe₃**) led to an almost 1:1 mixture of the monomethyl cations **8·PMe₃⁺** (Scheme 31). Although we have not investigated the mechanism of this reaction, it seems probable that protonation leads to a three-coordinate, T-shaped intermediate $[PtMe(PMe_2Ar^{Dipp_2})(PMe_3)]^+$ that undergoes fast isomerisation between the two possible structures, namely with *trans*-P—Pt—P' and *trans*-P—Pt—

Me linkages (see Section I.2.1.3, page 63), prior to η^1 coordination of one of the terphenyl phosphine pendant aryl rings.

In the ^1H NMR spectrum of the mixture of *cis*- and *trans*- **8**• PMe_3^+ , two low-frequency resonances are recorded with δ -1.04 and 0.69 ppm, that exhibit very different $^2J_{\text{HPt}}$ coupling constants of 29.5 and 82.5 Hz, respectively, as expected for methyl groups *trans* to phosphine and to a weak C_{ar} donor ligand. The corresponding $^{13}\text{C}\{^1\text{H}\}$ signals appear at 27.5 and -6.2 ppm, for the *cis* and *trans* isomers, respectively.

$^{31}\text{P}\{^1\text{H}\}$ NMR spectroscopy of this solution mixture of *cis* and *trans*-**8**• PMe_3^+ isomers proved most informative (Figure 53). Thus two almost first-order doublets were observed for each complex, one with a reduced $^2J_{\text{PP}}$ constant of 13 Hz, and the other with a much larger ^{31}P - ^{31}P coupling constant of 413 Hz, corresponding respectively to the *cis* and *trans* isomeric structures.

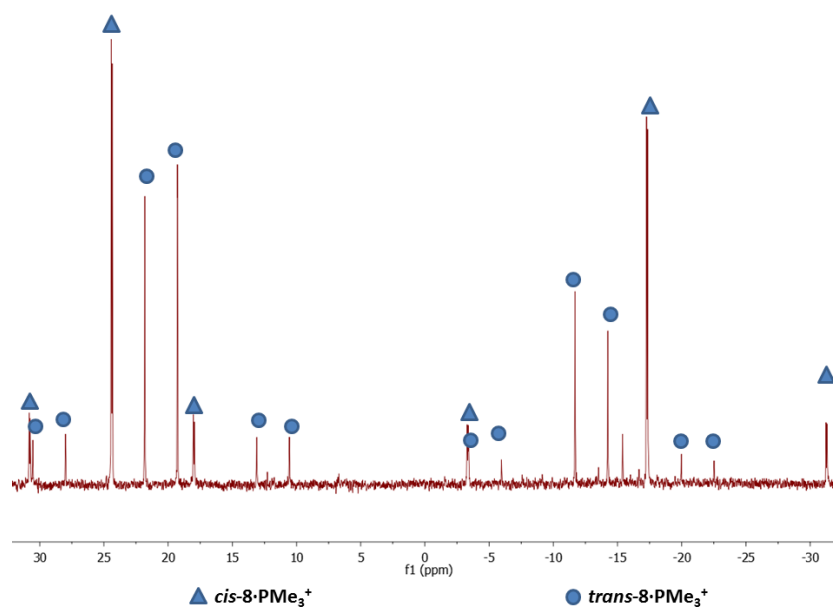


Figure 53. $^{31}\text{P}\{^1\text{H}\}$ NMR spectrum of isomers *cis*- and *trans*-**8**• PMe_3^+ (CD_2Cl_2 , 161.9 MHz, 25 °C).

We succeeded in separating these isomers by slow diffusion of hexane in a dichloromethane solution of the two compounds at $-23\text{ }^{\circ}\text{C}$, which allowed isolation of small amounts of the *cis* isomer as a crystalline solid. The solid state molecular structure of *cis*-**8**· PMe_3^+ was determined by single crystal X-ray diffraction studies (Figure 54). This analysis revealed a significant difference of nearly $0.08\text{ }\text{\AA}$ in the lengths of the two Pt—P bonds (see Figure 54 for the metrical parameters), in agreement with the poor *trans* influence that exerts the η^1 -arene interaction, compared to the methyl ligand.

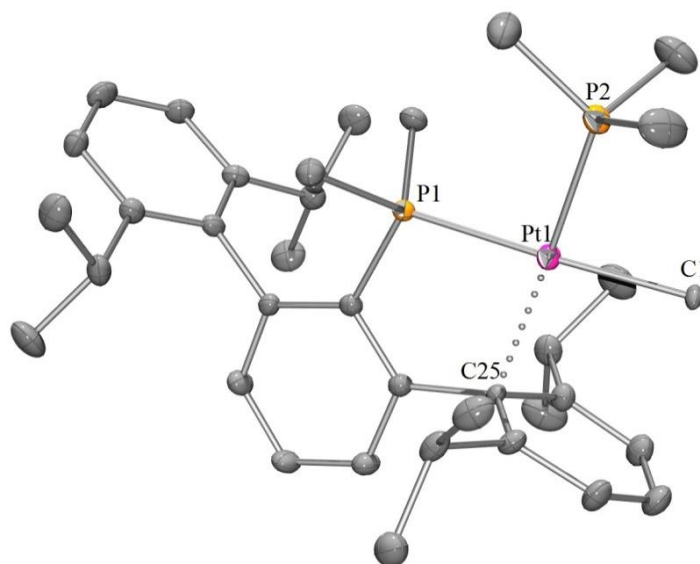
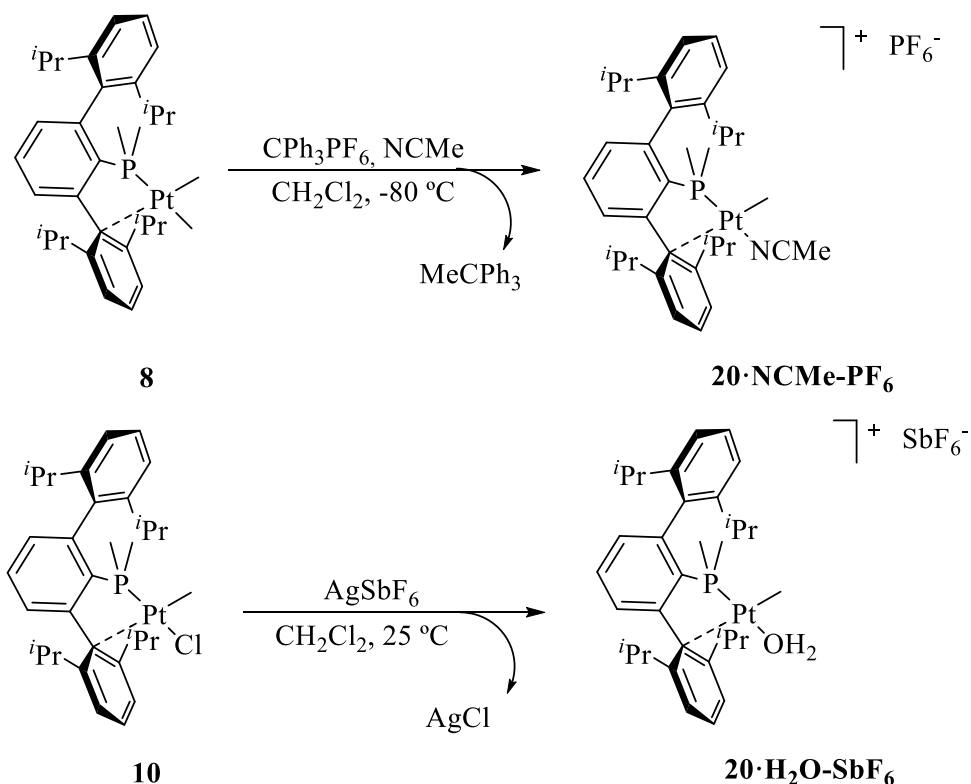


Figure 54: ORTEP view of the cation of complex *cis*-**8**· PMe_3^+ ; BAr_F anion and hydrogen atoms are excluded for clarity and thermal ellipsoids are set at 50 % level probability. Selected bond distances (\AA) and angles($^{\circ}$): P1-Pt1 2.3090(7), P2-Pt1 2.2307(6), C1-Pt1 2.159(3), C25-Pt1 2.353(2), P1-Pt1-P2 98.33(2), P2-Pt1-C1 81.08(6), C1-Pt1-C25 100.37(8), C25-Pt1-P1 80.31(6).

To complete this discussion on *cis*- $[\text{PtMe}(\text{L})(\text{PMe}_2\text{Ar}^{\text{Dipp}_2})]^+$ complexes it should be noted that they could be alternatively generated by other procedures commonly used for the synthesis of such compounds (Scheme 32). Thus, treatment of dimethyl complex **8** with $[\text{CPh}_3][\text{PF}_6]$ in the presence of NCMe , provided adduct **20**· NCMe , isolated as the PF_6^-

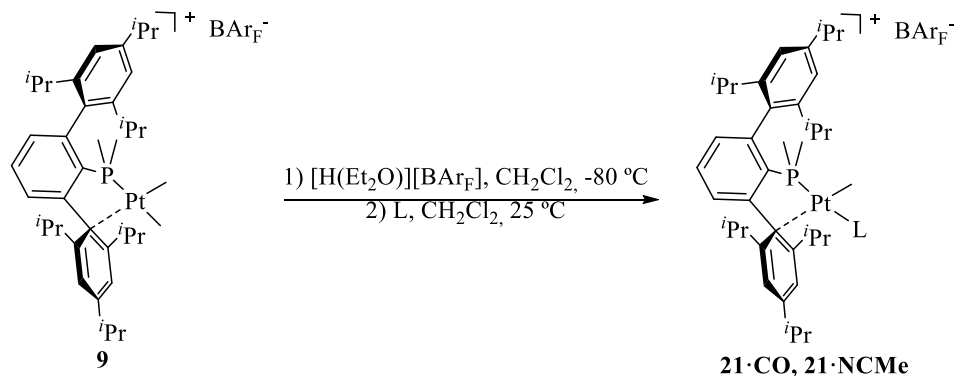
salt, with elimination of MeCPh_3 . Similarly, chloride abstraction with AgSbF_6 from *cis*- $[\text{PtMe}(\text{Cl})(\text{PMe}_2\text{Ar}^{\text{Dipp}_2})]$ (**10**), using CH_2Cl_2 as reaction solvent, resulted one more time in the crystallization of the *aqua* complex *cis*- $[\text{PtMe}(\text{H}_2\text{O})(\text{PMe}_2\text{Ar}^{\text{Dipp}_2})][\text{SbF}_6]$, isolated on this occasion as the SbF_6^- salt.



Scheme 32. Alternative synthetic methods to form unsaturated methyl cationic complexes

Finally, the dimethyl platinum complex of the $\text{PMe}_2\text{Ar}^{\text{Tipp}_2}$ ligand *cis*- $[\text{PtMe}_2(\text{PMe}_2\text{Ar}^{\text{Tipp}_2})]$ (**9**), was also protonated with $[\text{H}(\text{Et}_2\text{O})_2][\text{BAr}_\text{F}]$ in the presence of CO and NCMe (Scheme 33). The reactions proceeded quantitatively by ^1H NMR and yielded adducts **21·CO** and **21·NCMe**, which were fully characterized by spectroscopy. Infrared and NMR data

are similar to those recorded for the analogous $\text{PMe}_2\text{Ar}^{\text{Dipp}_2}$ complexes (see Experimental Section).



Scheme 33. Synthesis of cationic adducts **21·CO** and **21·CNMe** derived from $\text{PMe}_2\text{Ar}^{\text{Tipp}_2}$.

Reactivity of $\text{cis-}[\text{Pt}(\text{Me})(\text{S})(\text{PMe}_2\text{Ar}^{\text{Dipp}_2})]^+$ (20·S**) towards Dihydrogen**

To assess further the electrophilicity of the platinum(II) centre of the title complex, we studied its reactivity toward H_2 .^{67,93} No new complexes were detected by ^1H and $^{31}\text{P}\{^1\text{H}\}$ NMR spectroscopy between -80 and -20 °C, and upon warming at room temperature methane liberation was observed by ^1H NMR. Extensive decomposition of the Pt(II) complex **20·S** took also place, as evidenced by formation of a finely divided black solid, probably platinum metal.

It seems likely that H_2 replaced the weakly bonded solvent molecule, forming an undetected cationic $\sigma\text{-H}_2$ complex, $[\text{PtMe}(\text{H}_2)(\text{PMe}_2\text{Ar}^{\text{Dipp}_2})]^+$. This species then underwent intramolecular heterolysis of the Pt—Me bond with elimination of methane and formed an

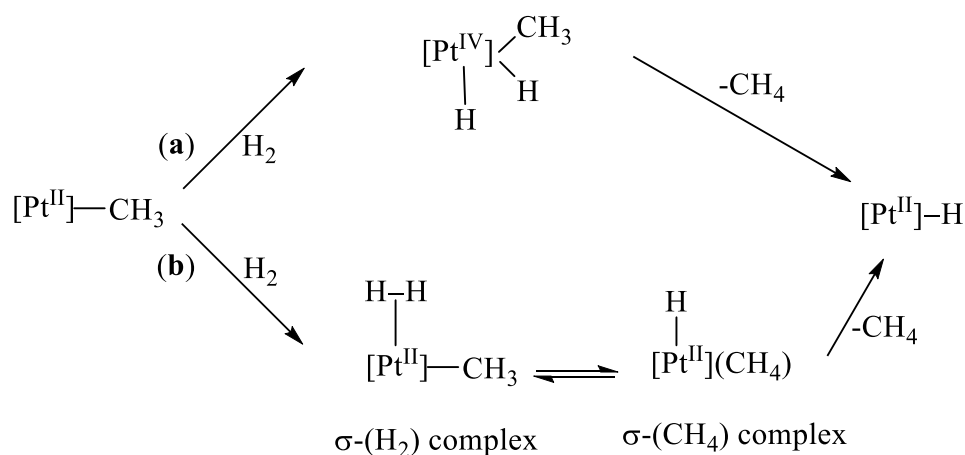
⁹³ a) S. S. Stahl, J. A. Labinger, J. E. Bercaw, *Inorg. Chem.* **1998**, *37*, 2422-2431; b) K. Q. Almeida Lenero, Y. Guari, P. C. J. Kamer, P. W. N. M. van Leeuwen, B. Donnadieu, S. Sabo-Etienne, B. Chaudret, M. Lutz, A. L. Spek, *Dalton Trans.* **2013**, *42*, 6495-6512; c) D. G. Gusev, J. U. Notheis, J. R. Rambo, B. E. Hauger, O. Eisenstein, K. G. Caulton, *J. Am. Chem. Soc.* **1994**, *116*, 7409-7410.

also undetected cationic hydride, $[\text{PtH}(\text{S})(\text{PMe}_2\text{Ar}^{\text{Dipp}_2})]^+$, which presumably decomposed under the reaction conditions. In fact, as discussed in Chapter II of this Thesis, related cationic hydrides generated by protonation of $\text{Pt}(0)\text{-PMe}_2\text{Ar}^{\text{Dipp}_2}$ complexes are unstable and decompose readily under conditions similar to those above.

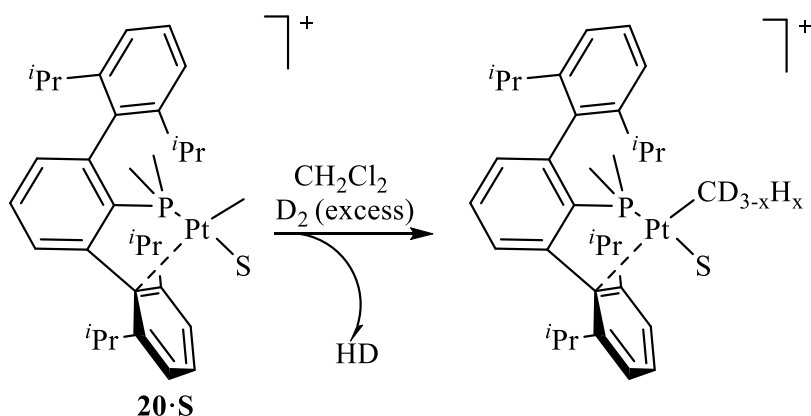
Hydrogenolysis of metal-alkyl bonds is an important reaction for both early and late transition metal alkyls.⁹⁴ For late transition metal systems, the hydrogenolysis of a M-Me bond may occur through two possible pathways, as represented in Scheme 34 for a $[\text{Pt}^{\text{II}}]\text{-Me}$ linkage. Route **a** implies oxidative addition of H_2 to form a Pt(IV) methyl bis(hydride) intermediate that renders the final Pt(II) hydride product by reductive elimination of CH_4 . By contrast, path **b** involves the formation of a $\sigma\text{-H}_2$ complex, conversion to a $\sigma\text{-CH}_4$ complex and dissociation of methane. The latter reaction route, in which there is no higher-oxidation-state intermediate, has been termed by Perutz and Sabo-Etienne σ -complex-assisted metathesis ($\sigma\text{-CAM}$).⁹⁵

⁹⁴ a) J. Campos, S. Kundu, D. R. Pahls, M. Brookhart, E. Carmona, T. R. Cundari, *J. Am. Chem. Soc.* **2013**, *135*, 1217-1220; b) J. R. Webb, C. Munro-Leighton, A. W. Pierpont, J. T. Gurkin, T. B. Gunnoe, T. R. Cundari, M. Sabat, J. L. Petersen, P. D. Boyle, *Inorg. Chem.* **2011**, *50*, 4195-4211; c) D. Stern, M. Sabat, T. J. Marks, *J. Am. Chem. Soc.* **1990**, *112*, 9558-9575.

⁹⁵ R. N. Perutz, S. Sabo-Etienne, *Angew. Chem. Int. Ed.* **2007**, *46*, 2578-2592.



Scheme 34: Possible reaction paths for the hydrogenolysis of a $\text{Pt}^{\text{II}}\text{—Me}$ bond.



Scheme 35: Reaction of complex **20·S** with D_2 . Deuterium exchange with the methyl protons.

To gain further insight into the hydrogenolysis of the Pt—Me bond of complex **20·S**, D_2 was utilised in place of H_2 . This experiment proved valuable, for ^1H NMR studies of the reaction demonstrated the generation at 20 °C of H_2 and HD , evinced by appearance of a singlet at 4.64 ppm and an isotopically shifted triplet at 4.61 ppm, due to free H_2 and HD , respectively (Figure 55). The latter triplet was characterised by a $^1J_{\text{HD}}$ coupling constant of 43 Hz practically identical to the experimental and

calculated value for the HD molecule.⁹⁶ Furthermore, in the proximity of 0 ppm, a complex pattern of resonances was found that resembled the set of signals expected for CH₄ and its CH_{4-n}D_n isotopologues.^{72a-b,97,98} Loss of methane was irreversible, as addition of CD₄ to the reaction mixture did not reverse to isotopic scrambling. The observed H/D exchanges suggest, however that coordination of H₂^{67,93} and subsequent generation of a σ -CH₄ complex without losing methane were reversible reactions (Scheme 36).^{72a-b,98}

The analysis of the 4.80-4.40 ppm region of the spectrum disclosed liberation to the reaction medium (Figure 55) of *ca.* 1 molecule of H₂ per 4 molecules of HD. This result suggests that scrambling between the coordinated molecule of D₂ (or HD or H₂) and the [Pt]⁺—CH_{3-n}D_n linkage (Scheme 36a, steps from left to right) is competitive with dihydrogen and methane dissociation (in their respective isotopologue forms) in the putative σ -dihydrogen and σ -methane complexes (the latter represented in Scheme 36a in the fully protio form, structure **A**). In Scheme 36b, some of the individual steps that may lead to the liberation of CH_{4-n}D_n have been represented, specifically those for which substitution of the Pt-coordinated molecules of HD (or H₂) by excess D₂ allows D-enrichment at the Pt—CH₃ sites and subsequent dissociation of deuterated methanes.

⁹⁶ J. Oddershede, J. Geertsen, G. E. Scuseria, *The Journal of Physical Chemistry* **1988**, 92, 3056-3059.

⁹⁷ F. A. L. Anet, D. J. O'Leary, *Tetrahedron Lett.* **1989**, 30, 2755-2758.

⁹⁸ a) S. S. Stahl, J. A. Labinger, J. E. Bercaw, *J. Am. Chem. Soc.* **1996**, 118, 5961-5976; b) M. W. Holtcamp, L. M. Henling, M. W. Day, J. A. Labinger, J. E. Bercaw, *Inorg. Chim. Acta* **1998**, 270, 467-478; c) J. A. Labinger, J. E. Bercaw, *Nature* **2002**, 417, 507-514; d) R. Romeo, G. D'Amico, *Organometallics* **2006**, 25, 3435-3446.

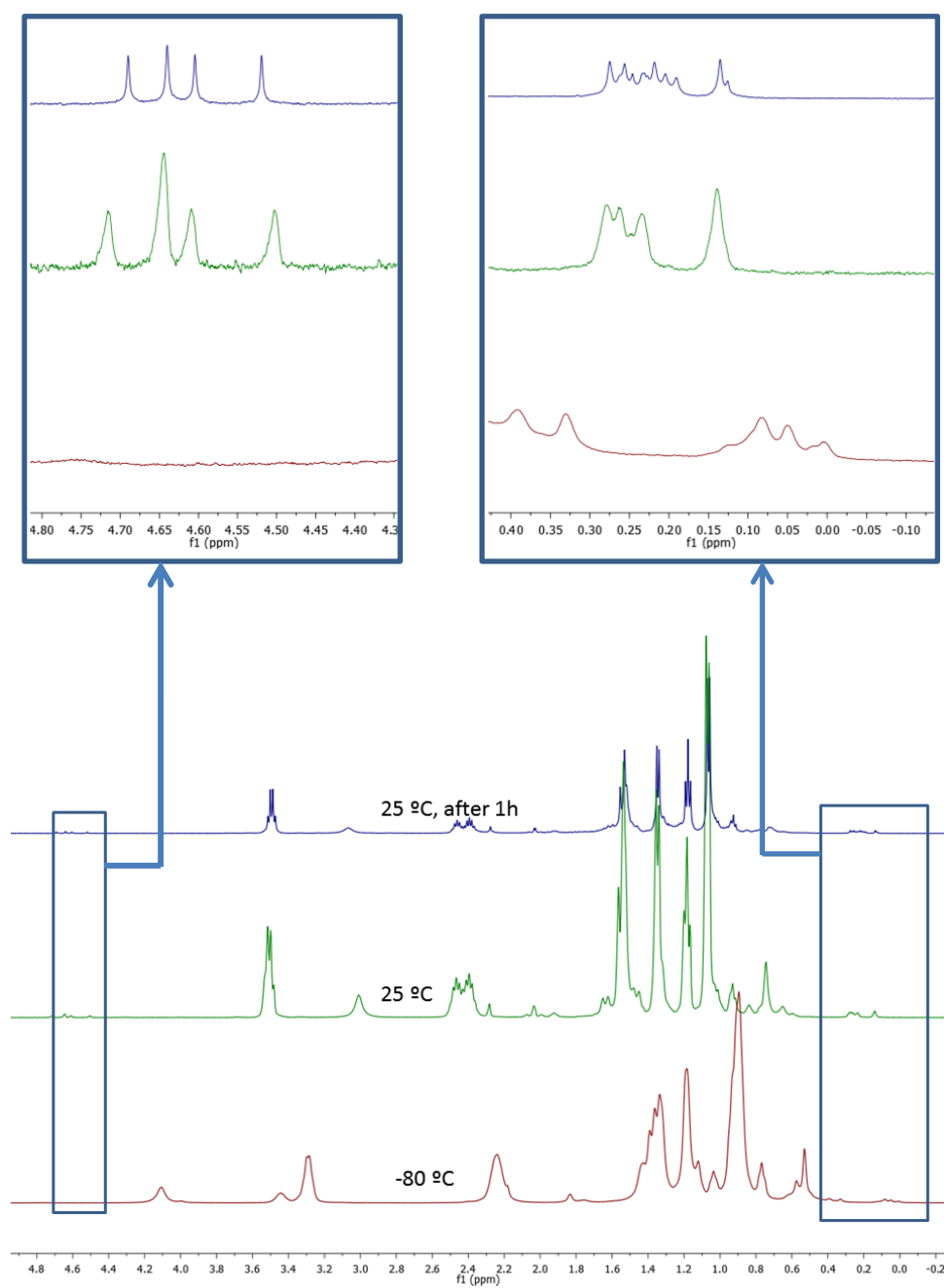
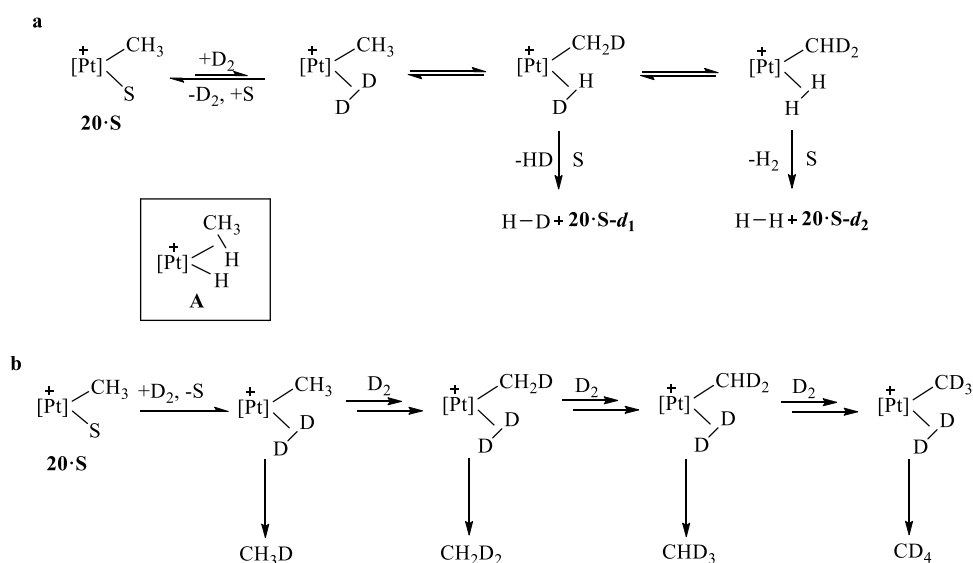


Figure 55. Evolution of the reactivity of **20·S** towards D_2 . Aliphatic zone of ^1H NMR spectra (500 MHz, CD_2Cl_2 , 25 °C).



Scheme 36: Simplified reaction outlines for the formation of H₂ and HD (**a**), and of the methane isotopologues CH_{4-n}D_n (**b**), in the reaction of the cationic complex **20·S** with D₂. See text for details.

The Phenyl Cationic Complex *cis*-[PtPh(py)(PMe₂Ar^{Dipp2})] [BAr_F] (22)

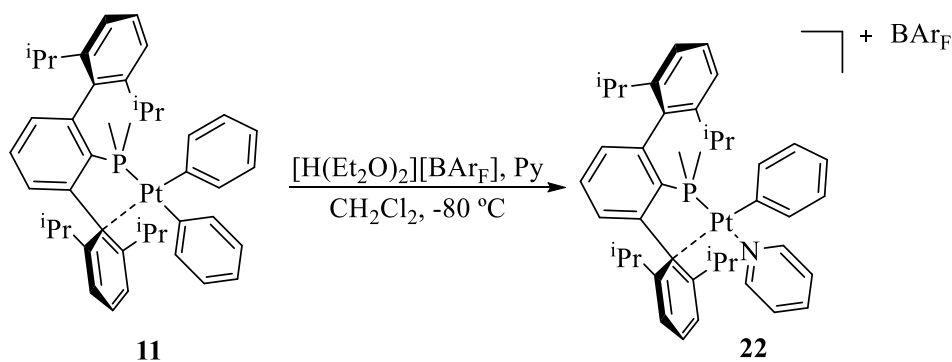
Aromatic C-H bond activation reactions promoted by platinum complexes have been intensively investigated in recent years and mechanistic insights gained by looking at the key step of its microscopic reverse reaction, namely the protonation of Pt(II) phenyl complexes.^{72a,78c,85b,88a,99,100} In this respect, the most commonly studied compounds contain neutral, bidentate N-donor ligands such as variously substituted 1,4-diaza-1,3-butadiene entities, bipyridines and bipyrimidines (see for instance references 78, 88a, 100 and references therein). In some

⁹⁹ C. M. Morris, J. L. Templeton, in *Activation and Functionalization of C-H Bonds* (Eds.: K. I. Goldberg, A. S. Goldman), ACS Symposium Series 885, Washington, DC, **2004**, pp. 303-318,

¹⁰⁰ J. Parmene, I. Ivanović-Burmazović, M. Tilset, R. van Eldik, *Inorg. Chem.* **2009**, *48*, 9092-9103.

of these systems Pt(IV) hydrides of the type $[\text{PtPh}_2(\text{N}^{\wedge}\text{N})(\text{H})(\text{NCMe})]^+$ or related complexes stabilised by other donor solvents were characterised at low temperatures, and were found to eliminate benzene with formation of $[\text{PtPh}(\text{N}^{\wedge}\text{N})(\text{NCMe})]^+$ or $[\text{PtPh}(\text{N}^{\wedge}\text{N})(\eta^2\text{-C}_6\text{H}_6)]^+$ when the protonation was effected in a weakly donor solvent.^{72a,78c,85b,88a,99,100}

Our complex $\text{cis-}[\text{PtPh}_2(\text{PMe}_2\text{Ar}^{\text{Dipp}_2})]$ (**11**) reacted with $[\text{H}(\text{Et}_2\text{O})_2][\text{BAr}_\text{F}]$ in CD_2Cl_2 (-80°C to 20°C) to afford a cationic phenyl complex that could be tentatively formulated as $\text{cis-}[\text{PtPh}(\text{S})(\text{PMe}_2\text{Ar}^{\text{Dipp}_2})]^+$, containing a coordinated molecule of Et_2O or CH_2Cl_2 . Our efforts to isolate this species in crystalline or microcrystalline form were, however, fruitless and therefore we decided to stabilise this cationic species by coordination of a molecule of pyridine (Scheme 37). Following the procedure described in the Experimental Section, the desired complex, **22**, was isolated as a pale yellow solid in high yields (*ca.* 90%).



Scheme 37. Synthesis of cationic complex **22**.

Figure 58 shows the ^1H NMR spectrum of this complex. The coordinated pyridine ligand originates slightly broad resonances at 8.86, 7.79 and 7.33 ppm, whereas the aromatic protons of the phenyl group resonate at 7.28, 7.05 and 6.79 ppm, also as slightly broad signals. The poor resolution of these resonances may be due to restricted rotation around the Pt—C bond due to steric hindrance. The low frequency signals (between 140

ca. 3.0 and 0.5 ppm, Figure 58) are in accordance with the proposed bidentate coordination of the phosphine ligand.

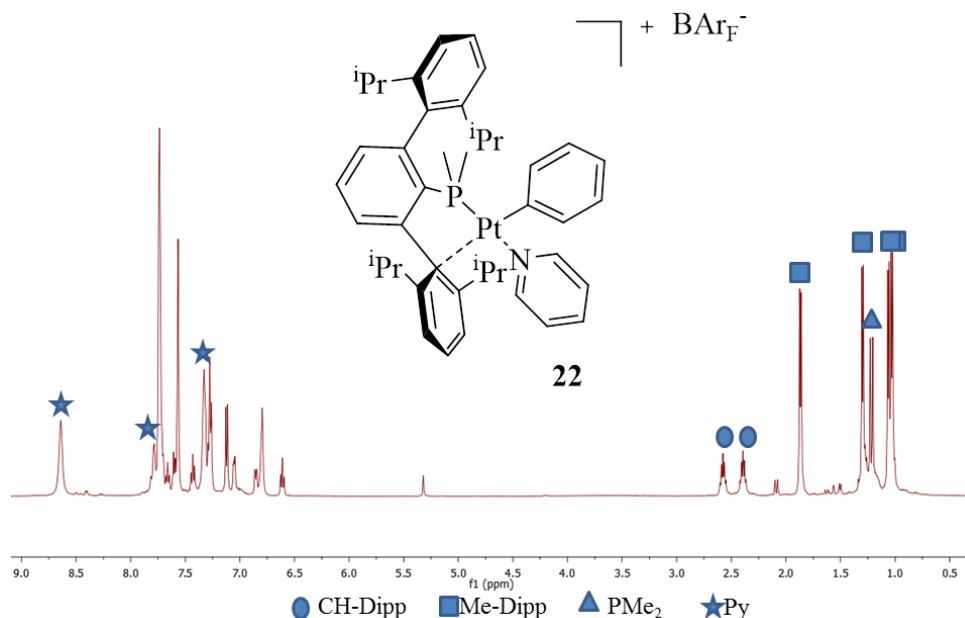


Figure 58: ^1H NMR spectrum of complex **22** (500 MHz, CD_2Cl_2 , 25 °C).

Reactivity of $\text{cis-}[\text{PtMe}(\text{S})(\text{PMe}_2\text{Ar}^{\text{Dipp}2})]^+$ (20-S**) towards $\text{cis-}[\text{PtMe}_2(\text{PMe}_2\text{Ar}^{\text{Dipp}2})]$ (**8**)**

The neutral dimethyl complex **8** may be envisaged as a Lewis base, being capable to act as a methyl transfer agent in transmetallation reactions.^{101,102} On the other hand, the chemical reactivity of the cationic Pt(II) complex **20-S** discussed in the foregoing sections evinces beyond any doubt its electrophilicity. We therefore considered of interest studying

¹⁰¹ a) M.-E. Moret, in *Higher Oxidation State Organopalladium and Platinum Chemistry* (Ed.: J. A. Canty), Springer Berlin Heidelberg, Berlin, Heidelberg, **2011**, pp. 157-184, ; b) D. Serra, M.-E. Moret, P. Chen, *J. Am. Chem. Soc.* **2011**, *133*, 8914-8926; c) M.-E. Moret, D. Serra, A. Bach, P. Chen, *Angew. Chem. Int. Ed.* **2010**, *49*, 2873-2877.

¹⁰² a) J. delPozo, D. Carrasco, M. H. Pérez-Temprano, M. García-Melchor, R. Álvarez, J. A. Casares, P. Espinet, *Angew. Chem. Int. Ed.* **2013**, *52*, 2189-2193; b) A. R. Petersen, R. A. Taylor, I. Vicente-Hernández, J. Heinzer, A. J. P. White, G. J. P. Britovsek, *Organometallics* **2014**, *33*, 1453-1461.

their direct reaction, having in mind, in particular, the possibility of accessing a bridging methyl structure of type $[\text{Pt}(\mu\text{-Me})\text{Pt}]^+$.

In contrast to bridging hydride derivatives, transition metal complexes with bridging methyl groups are uncommon, although a variety of structures that include three-centre two-electron agostic interactions, are possible.^{103,104} In fact, a recent search in the Cambridge Structural Database for bimetallic transition metal complexes with bridging methyl ligands¹⁰⁴ produced only 75 results. It is worth remarking that most compounds featured early transition metals. The first methyl-bridged digold(I) complex was recently described by our group,^{33e} and whereas a $\text{Cu}^{\text{I}}(\mu\text{-Me})\text{Pt}^{\text{II}}$ species relevant to transmetallation processes is known^{101c} the simple homobimetallic $[\text{Pt}_2(\mu\text{-Me})]^+$ structure seems to be unknown.

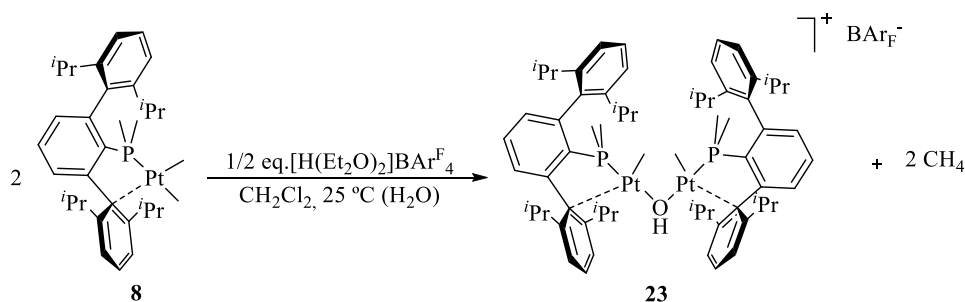
Early work from Puddephatt and others attempted the generation of a trimethyldiplatinum complex with an “A-frame” structure $[\text{Pt}_2\text{Me}_2(\mu\text{-Me})(\text{dppm})_2]^+$, where $\text{dppm} = \text{Ph}_2\text{PCH}_2\text{PPh}_2$.^{74a} The complex was considered of unlikely existence, for it would contain an electron-deficient $[\text{Pt}_2(\mu\text{-Me})]^+$ bridge. Indeed, the desired complex was isolated but X-ray crystallography demonstrated the existence of a direct $\text{Pt}(\text{II}) \rightarrow \text{Pt}(\text{II})$ donor-acceptor bond, of length 2.769(1) Å, between a donor $[\text{PtMe}_2\text{P}_2]$ unit and an acceptor $[\text{PtMeP}_2]^+$ fragment, and only terminal Pt—Me bonds.^{74a}

In accordance with these and other literature precedents, the reaction between neutral dimethyl platinum(II) complex **8** and the cationic unsaturated species **20•S** did not allow isolation of the target $[\text{Pt}(\mu\text{-Me})\text{Pt}]^+$ structure. Instead, it yielded the binuclear, hydroxo-bridged complex $\{[\text{PtMe}(\text{PMe}_2\text{Ar}^{\text{Dipp}_2})]_2(\mu\text{-OH})\}^+$, that was isolated as the BAR_F^- salt

¹⁰³ a) J. Holton, M. F. Lappert, R. Pearce, P. I. W. Yarrow, *Chem. Rev.* **1983**, 83, 135-201; b) P. Braunstein, N. M. Boag, *Angew. Chem. Int. Ed.* **2001**, 40, 2427-2433; c) J. C. Green, M. L. H. Green, G. Parkin, *Chem. Commun.* **2012**, 48, 11481-11503; d) M. L. H. Green, G. Parkin, in *Struct. Bond.*, Springer, Berlin, Heidelberg, **2016**, pp. 1-61,

¹⁰⁴ J. Campos, J. López-Serrano, R. Peloso, E. Carmona, *Chem. Eur. J.* **2016**. doi: 10.1002/chem.201504483

(Scheme 38). The reacting mixture of **8** plus **20·S** was attained either by mixing equimolar amounts of the two complexes, or alternatively it was generated *in situ* by protonation of *cis*-[PtMe₂(PMe₂Ar^{Dipp}₂)] (**8**), with half-an-equivalent of the acid (Scheme 38). It seems probable that the desired bridging methyl complex formed in this reaction, but it reacted instantly with adventitious water that we could not exclude completely, despite our precautions. Monitoring of the reaction by ¹H and ³¹P{¹H} NMR spectroscopy from -80 °C to room temperature permitted detection of only the initial and the final complexes, as well as the production of methane.



Scheme 38. Synthesis of the hydroxo-bridged binuclear complex **23**.

The new OH-bridged diplatinum complex was fully characterised by NMR spectroscopy and by High Resolution ElectroSpray Ionisation Mass Spectrometry (ESI-HR-MS). The *cis*-P—Pt—Me distribution proposed for this complex is unequivocally deduced from NMR data. For example, the equivalent Pt—CH₃ units of **23** give rise to ¹H and ¹³C{¹H} NMR doublets at 0.5 and -0.8 ppm, respectively (see Figure 59 for ¹H NMR data) with ³J_{HP} = 2.7 and ²J_{CP} = 3 Hz. In the ³¹P{¹H} NMR spectrum the two equivalent ³¹P nuclei of complex **23** resonate as a singlet at -3.2 ppm, with a one-bond ³¹P-¹⁹⁵Pt coupling constant of 4270 Hz, that clearly

indicates *trans*-P—Pt—OH, rather than *trans*-P—Pt—Me arrangements.^{38a,105}

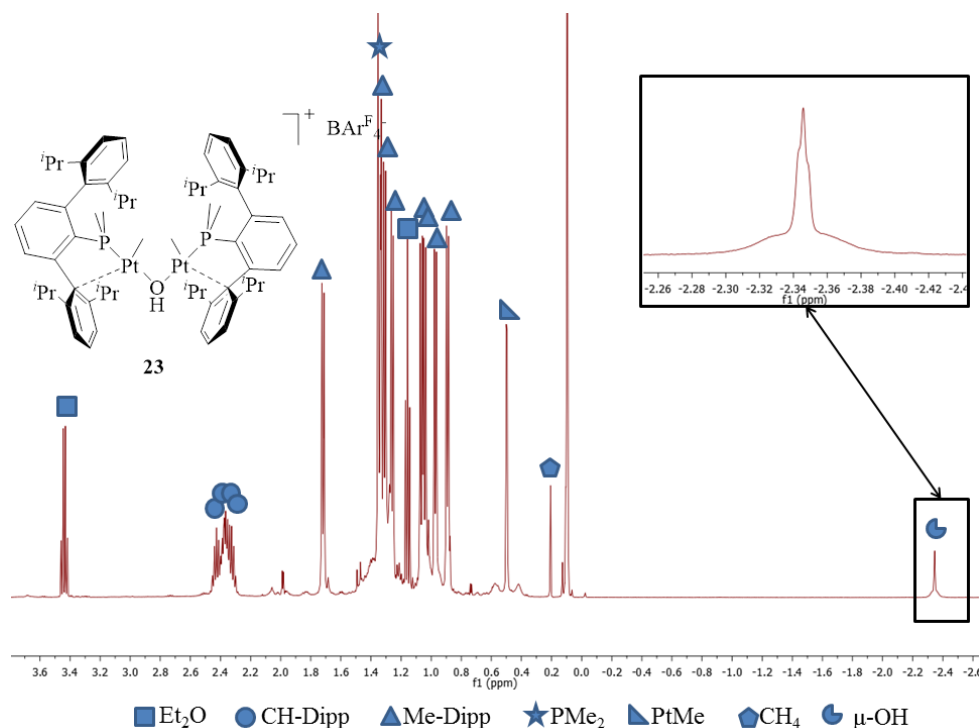


Figure 59. Aliphatic region of ^1H NMR spectrum of complex **23** (500 MHz, CD_2Cl_2 , 25 °C).

The hydroxo proton appears at -2.35 ppm as a broad, partially unresolved triplet ($^3J_{\text{HP}} = 1.5$ Hz) with platinum satellites ($^2J_{\text{HPt}} = 23.5$ Hz). All of these data compare well with NMR parameters already reported for Pt(II)-OH complexes.^{38a,105, 106} The IR spectrum (KBr and nujol mull) shows the $\bar{\nu}(\text{OH})$ band around 3420 cm^{-1} , which is in the range of absorptions reported for diplatinum complexes with bridging OH ligands.¹⁰⁷ The

¹⁰⁵ a) U. Anandhi, P. R. Sharp, *Inorg. Chem.* **2004**, 43, 6780-6785; b) U. Belluco, R. Bertani, S. Coppetti, R. A. Michelin, M. Mozzon, *Inorg. Chim. Acta* **2003**, 343, 329-334.

¹⁰⁶ a) T. L. Lohr, W. E. Piers, M. J. Sgro, M. Parvez, *Dalton Trans.* **2014**, 43, 13858-13864; b) T. L. Lohr, W. E. Piers, M. Parvez, *Dalton Trans.* **2013**, 42, 14742-14748; c) T. L. Lohr, W. E. Piers, M. Parvez, *Inorg. Chem.* **2012**, 51, 4900-4902.

¹⁰⁷ a) J. J. Li, W. Li, P. R. Sharp, *Inorg. Chem.* **1996**, 35, 604-613; b) J. J. Li, P. R. Sharp, *Inorg. Chem.* **1994**, 33, 183-184; c) J. J. Li, W. Li, A. J. James, T. Holbert, T. P. Sharp, P. 144

structure of complex **23** resembles that proposed for the somewhat related¹⁰⁸ phenyl derivative $\{[\text{PtPh}(\text{cod})]_2(\mu\text{-OH})\}^+$. For informative purposes, Figure 60 contains the ESI-HR-MS of this complex and provides in addition a comparison of the observed and simulated molecular ion peak.

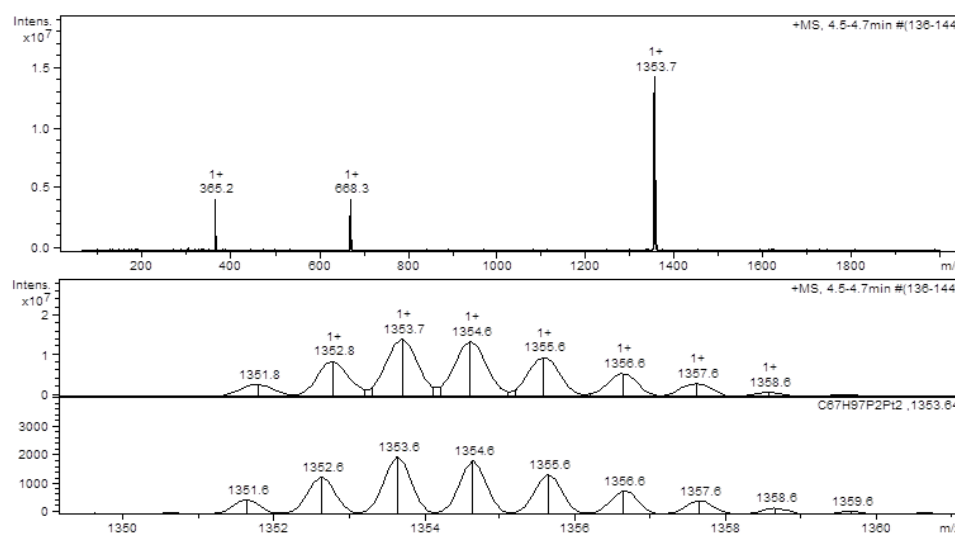


Figure 60: ESI-HR-MS of compound **23** (top) and comparison of the molecular peak and its simulation (bottom).

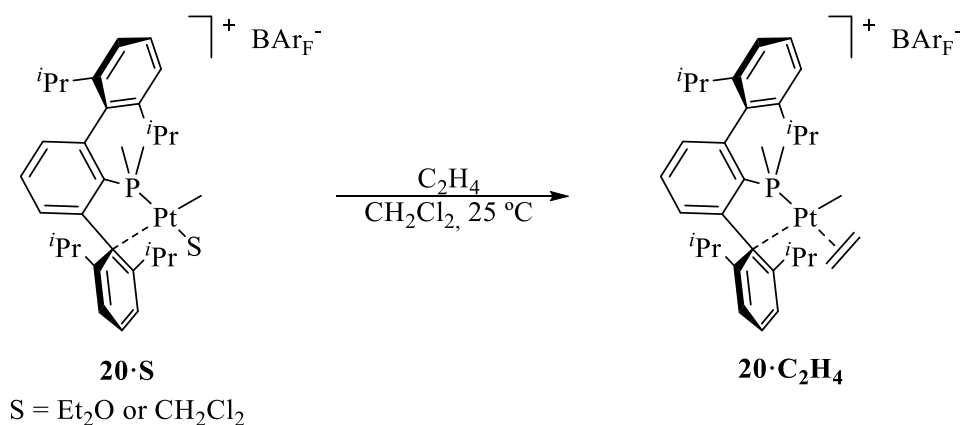
R. Sharp, *Inorg. Chem.* **1999**, 38, 1563-1572; d) S. Kannan, A. J. James, P. R. Sharp, *Polyhedron* **2000**, 19, 155-163.

¹⁰⁸ a) Y. Suzuki, K. Osakada, *Organometallics* **2006**, 25, 3251-3258; b) Y. Suzuki, K. Osakada, *Organometallics* **2004**, 23, 5081-5084.

I.2.2.4. Reactivity of the Cationic Platinum(II) Methyl Complex $[\text{PtMe}(\text{PMe}_2\text{Ar}^{\text{Dipp}_2})(\text{S})]^+$ (**20-S**) towards C_2H_4 and C_2H_4 . A Combined Experimental and Computational Study.

Experimental studies

Formation of the acetylene adduct $[\text{PtMe}(\text{L})(\text{PMe}_2\text{Ar}^{\text{Dipp}_2})][\text{BAr}_\text{F}]$, **20·C₂H₄** was accomplished by adding C_2H_4 to the dichloromethane solutions of complex **20·S** at room temperature (Scheme 39).



Scheme 39. Synthesis of adducts **20·C₂H₄**.

The behaviour in solution of the ethylene adduct, **20·C₂H₄**, was studied by NMR techniques. At room temperature, the coordinated molecule of ethylene rotates fast around the Pt-alkene bond, as the four protons resonate at 3.88 ppm as a broad singlet with platinum satellites ($^2J_{\text{HPt}} = 34.6$ Hz). At -80 °C, although NOESY experiments demonstrated that rotation is still present (vide infra), the rate constant of this process becomes considerably slower and the C_2H_4 protons resonate as two doublets at 3.18 and 4.30 ppm ($^3J_{\text{HP}} = 15.7$ Hz). Coalescence is observed around -25 °C (Figure 61).

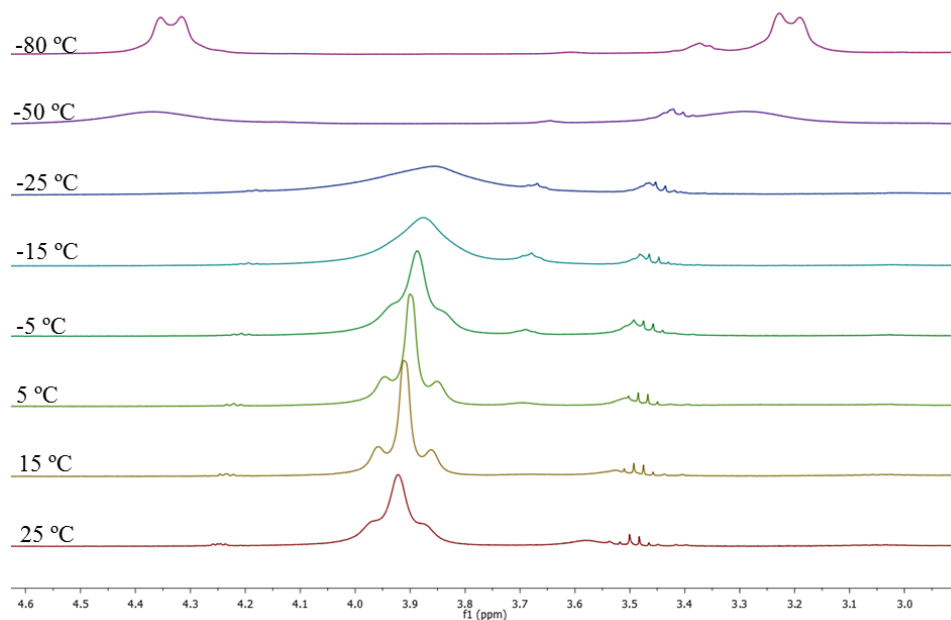


Figure 61: Variable temperature ¹H NMR spectra of **20**·C₂H₄ showing the resonances of the olefinic protons (400 MHz, CD₂Cl₂).

Thermodynamic parameters for the exchange reaction of ethylene within the coordination sphere of the metal centre were calculated by NMR experiments. Thus, in the presence of free ethylene fast exchange of the alkene at room temperature was detected by NOESY and 1D EXSY NMR experiments in the range between 25 – 0 °C (Figure 62). The ΔH^\ddagger , ΔS^\ddagger and ΔG^\ddagger values associated to this process are $17.6 \pm 0.8 \text{ kcal}\cdot\text{mol}^{-1}$, $7 \pm 3 \text{ cal}\cdot\text{mol}^{-1}\cdot\text{K}^{-1}$, and $16 \pm 2 \text{ kcal}\cdot\text{mol}^{-1}$, respectively.

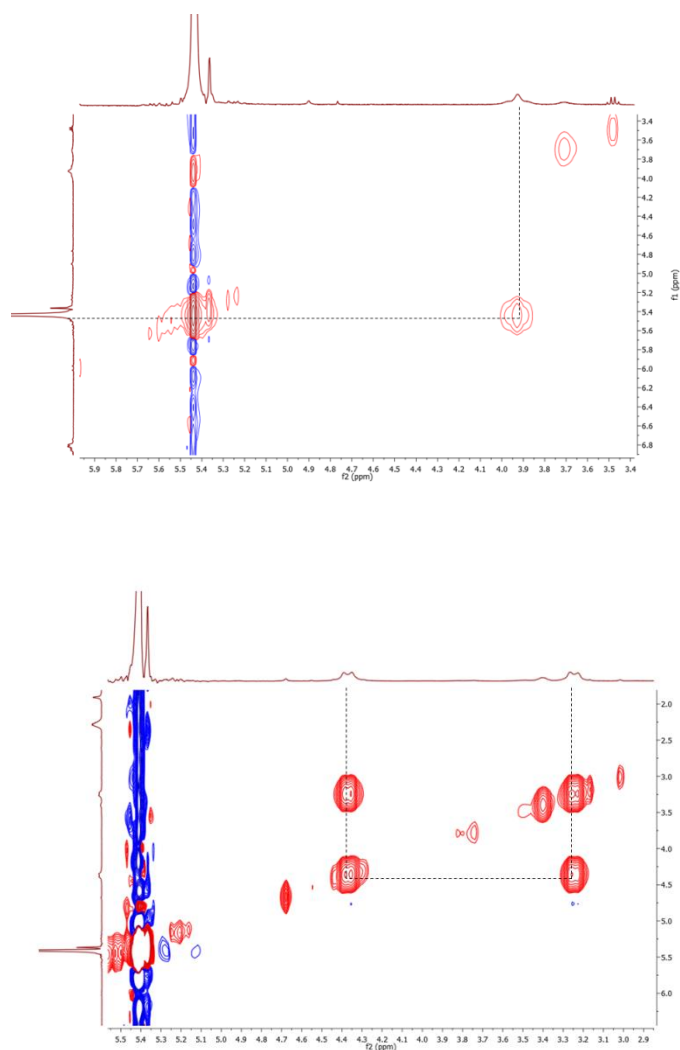
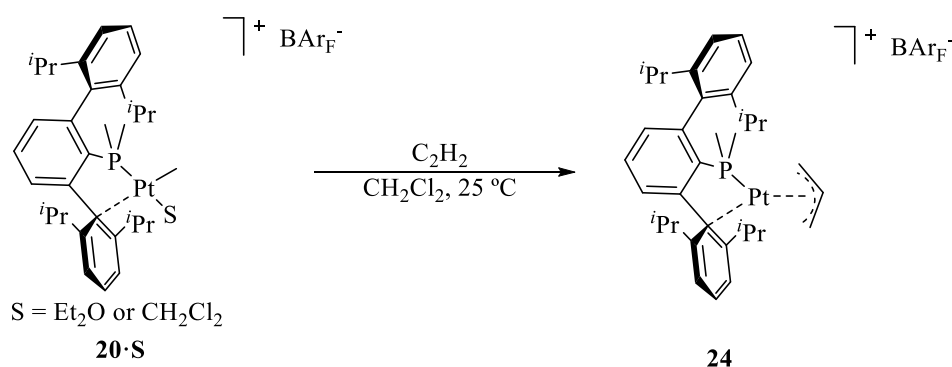


Figure 62: NOESY experiments at 25 °C (top) and at -80 °C (bottom) of complex $20 \cdot C_2H_4$ (400 MHz, CD_2Cl_2).

Preliminary studies suggested that compound $20 \cdot C_2H_4$ catalyzes ethylene dimerization when its solutions in dichloromethane are heated at 50 °C under 2 bars ethylene. Indeed, GC analyses of the volatile fraction of the reaction demonstrated the formation of the three isomers of butene (1-butene, *E*-2-butene, *Z*-2-butene).

Compound $20 \cdot S$ is a rare example of a stable transition metal complex which exhibits a vacant coordination site in conjunction with a

very labile ligand, that is a solvent molecule such as dichloromethane or ether. These peculiar characteristics make it an exceptional candidate for reactivity studies. Aiming to explore its behaviour towards insertion of unsaturated organic species, solutions of complex **20**·**S** were treated with acetylene (2 bar C₂H₂, CH₂Cl₂, 25 °C), which allowed for the formation of a cationic η^3 -allyl Pt(II) complex, **24** (Scheme 40).



Scheme 40. Synthesis of cationic allylic complex **24**.

The isopropyl ¹H NMR resonances corresponding to the terphenyl phosphine are in accordance to a κ^1 -P, η^1 -C_{arene} coordination that has been already discussed for related three-coordinate complexes (Figure 63). Furthermore, the lack of a symmetry plane due to the allyl ligand makes diastereotopic the P bonded CH₃ groups, which resonate as doublets at 1.61 and 1.48 ppm. The ¹H and ¹³C resonances of the allyl ligand show coupling with the ³¹P and ¹⁹⁵Pt nuclei demonstrating the coordination of this fragment. The ³¹P{¹H} NMR spectrum exhibits singlet at 18.6 ppm (¹J_{Pt} = 4078 Hz).

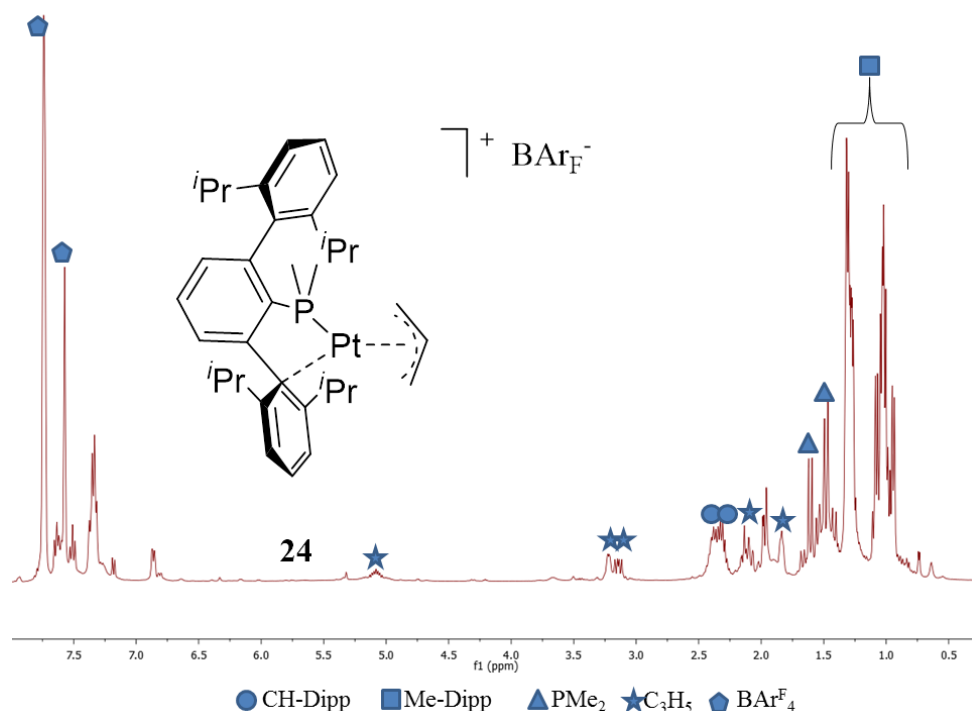
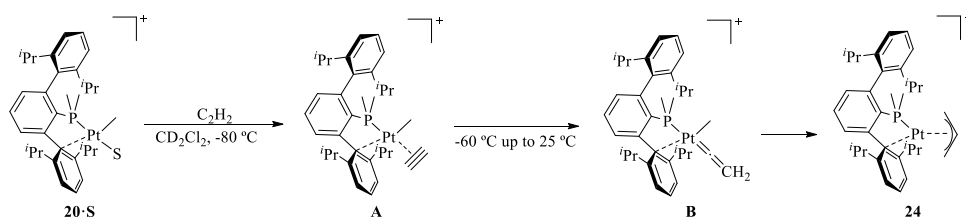


Figure 63. ^1H NMR spectrum of compound **24** (400 MHz, CD_2Cl_2 , 25 °C).

Low-temperature NMR experiments of the reaction of **20·S** with acetylene permitted the detection of two reaction intermediates prior to the formation of the final product **24** (Scheme 41).



Scheme 41: Intermediates found in the formation of the cationic allylic complex **24**.

Coordination of acetylene takes place even at -80 °C forming intermediate **A** which features a $^{31}\text{P}\{^1\text{H}\}$ NMR resonance at 11.5 ppm with a $^1J_{\text{PPt}}$ value of 4282 Hz (Figure 64). The proposed molecular structure of

this intermediate is based on the unambiguous identification of the NMR resonances corresponding to the Pt-Me fragment and to a coordinated acetylene molecule. Thus the Pt-Me protons resonate at 0.60 ppm as a doublet ($^3J_{\text{PH}} = 3 \text{ Hz}$, $^2J_{\text{HPt}} = 76 \text{ Hz}$) whereas the C_2H_2 gives rise to a doublet at 3.08 ppm ($^3J_{\text{HP}} = 4 \text{ Hz}$, $^2J_{\text{HPt}} = 50 \text{ Hz}$) in the ^1H NMR spectrum of the reaction mixture and to a doublet of doublets centered at 77.7 ppm in the ^{13}C spectrum ($^1J_{\text{CH}} = 263 \text{ Hz}$, $^2J_{\text{CH}} = 44 \text{ Hz}$, $^2J_{\text{CP}} = 12 \text{ Hz}$).

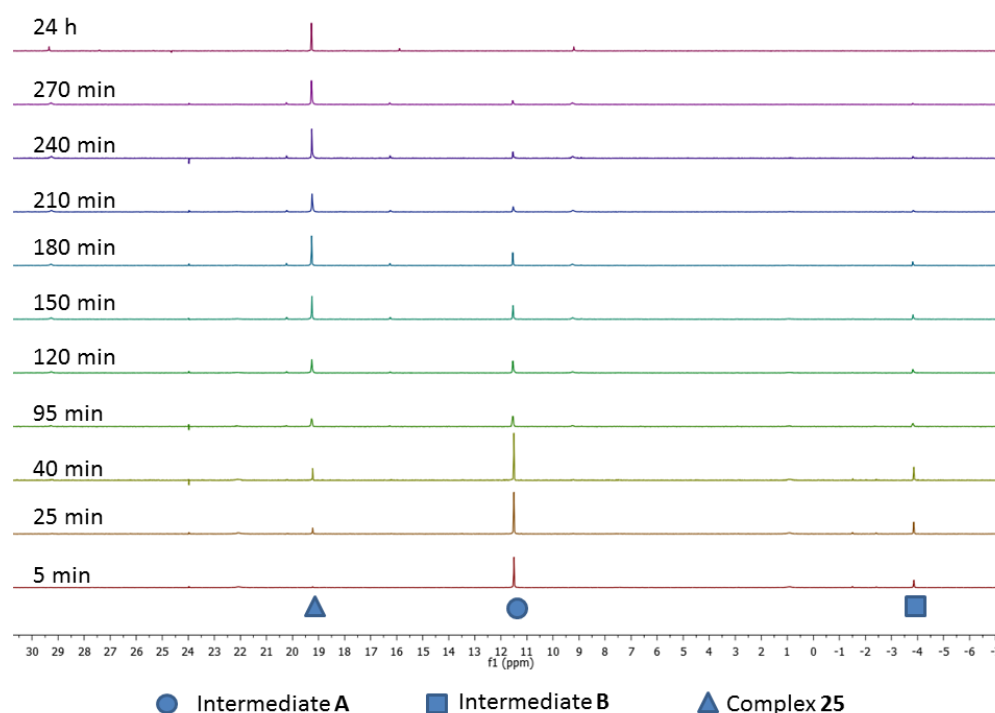


Figure 64 $^{31}\text{P}\{^1\text{H}\}$ NMR spectra of reaction between acetylene and complex **20·S** at room temperature recorded at -60°C (161.9 MHz, CD_2Cl_2)

The second intermediate, **B**, which forms above -60°C and is also detected for a short period of time at room temperature, converts slowly into the final product **24**. This second intermediate shows a $^{31}\text{P}\{^1\text{H}\}$ resonance at -4.3 ppm characterized by a large $^1J_{\text{PPt}}$ value of 4611 Hz , which appears quite broad at room temperature. Therefore, its NMR

characterisation was best performed at $-20\text{ }^{\circ}\text{C}$. The proposed methyl vinylidene structure of complex **B** is in agreement with i) a singlet at 0.43 ppm ($^2J_{\text{HPt}} = 74\text{ Hz}$) in ^1H NMR spectra assigned to the Pt-CH₃ protons with the corresponding $^{13}\text{C}\{^1\text{H}\}$ resonance at -6.6 ppm ($^2J_{\text{CP}} = 6\text{ Hz}$), ii) a very low-field ^{13}C resonance at 221.2 typical of a C=Pt carbon nucleus (figure 65). Intermediate **B** is the result of the isomerization of a coordinated acetylene molecule to a vinylidene ligand.

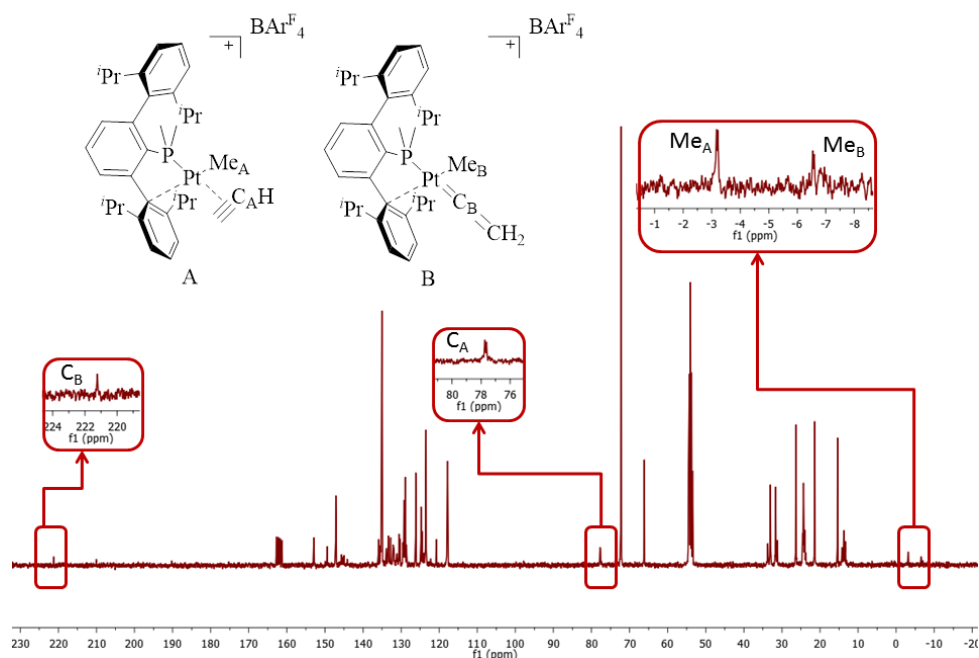


Figure 65: $^{13}\text{C}\{^1\text{H}\}$ NMR spectra of the mixture of two intermediates **A** and **B** (CD_2Cl_2 , $-20\text{ }^{\circ}\text{C}$, 100.6 MHz).

We also studied the exchange process of the coordinated acetylene molecule in the intermediate **A** with the free alkyne in the range of -35 to $-20\text{ }^{\circ}\text{C}$ by 1D EXSY NMR experiments. The calculated activation parameters for this process (ΔH^\ddagger , ΔS^\ddagger , and $\Delta G^\ddagger_{298\text{K}}$) are $15.3 \pm 0.4\text{ kcal}\cdot\text{mol}^{-1}$, $4 \pm 1\text{ cal}\cdot\text{mol}^{-1}\cdot\text{K}^{-1}$, and $14.0 \pm 0.8\text{ kcal}\cdot\text{mol}^{-1}$, respectively. These values are very similar to those found for the ethylene exchange.

Single-crystal X-ray studies confirmed the molecular structure of complex **24**. An ORTEP view of the cation is shown in Figure 66. The secondary $\text{Pt}\cdots\text{C}_{\text{arene}}$ interaction features a distance of 2.271 Å. The allyl ligand is not symmetrically bound to the platinum atom with a variation of the Pt—C distances in accord with different *trans* influences corresponding to the P donor and to the weak $\text{Pt}\cdots\text{C}$ interaction.

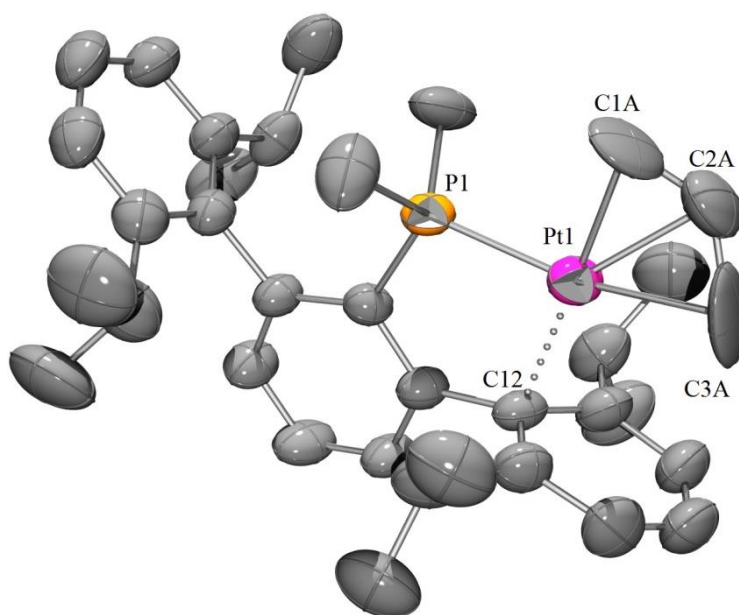
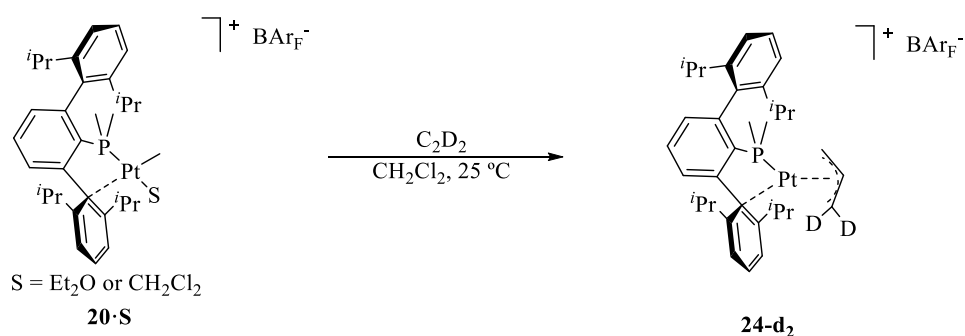


Figure 66: ORTEP view of the cation of complex **24**; BAr_F anion and hydrogen atoms are omitted for clarity and thermal ellipsoids are set at 50 % level probability. Selected bond distances (Å) and angles($^\circ$): Pt1-P1 2.238(1), Pt1-C1A 2.13(2), Pt1-C2A 2.11(2), Pt1-C3A 2.20(2), Pt1-C12 2.271(4), C1A-C2A-C3A 121(2), P1-Pt1-C12 83.7(1).

Mechanistic Insights

The mechanistic pathway for the above transformation proposed in the previous section is based on deuteration experiments and theoretical (DFT) calculations.

Thus, the reaction of **20·S** with C_2D_2 , generated *in situ* by reacting CaC_2 with D_2O , yielded compound **24-d₂** (Scheme 42), in which the newly formed allyl fragment bears two D atoms bound to a terminal carbon, as evidenced by the lack of the corresponding resonances in the 1H NMR spectrum (Figure 67). This fact implies an isomerization of the coordinated alkyne molecule to give a vinylidene intermediate followed by the methyl insertion into the $Pt=CCD_2$ bond to form compound **24**.



Scheme 42. Synthesis of compound **24-d₂**.

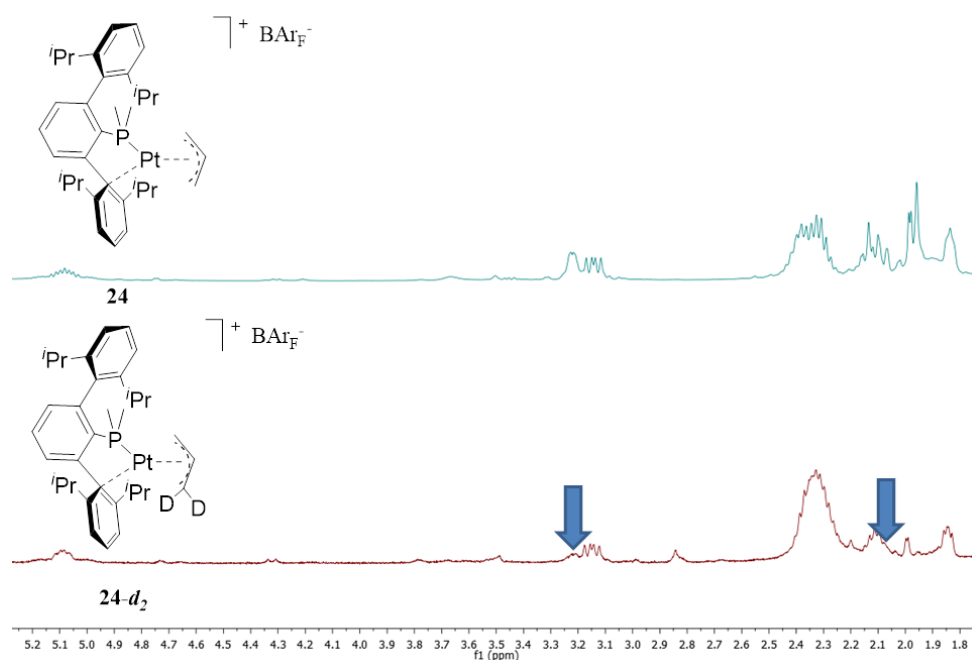


Figure 67. Aliphatic area of ^1H NMR spectra of complex **24** (top) and deuterated derivative **24-d₂** (400 MHz, CD_2Cl_2 , 25 $^\circ\text{C}$).

These hypotheses are supported by DFT calculations on a model system in which the only simplification with respect to the real system is that diethylether has been substituted by a molecule of dimethylether. We considered two different mechanistic pathways: a) the classic migratory insertion of the alkyne into the Pt—Me bond; and b) the isomerization of the alkyne ligand to vinylidene prior to carbene migratory insertion. According to the calculations, the substitution of the ether molecule by an η^2 -coordinated acetylene is thermodynamically favoured by $2.18 \text{ kcal}\cdot\text{mol}^{-1}$ (ΔG^0 in gas phase). In our calculations, we arbitrarily set the energy of the acetylene adduct, **20**·**C₂H₂**, to 0 and we took into account the effect of the reaction solvent (dichloromethane) by including a continuum solvation model (SMD).¹⁰⁹

¹⁰⁹ A. V. Marenich, C. J. Cramer, D. G. Truhlar, *The Journal of Physical Chemistry B* **2009**, *113*, 6378-6396.

The overall reaction is, according to the calculations, exergonic by $40.9 \text{ kcal}\cdot\text{mol}^{-1}$ (ΔG^{DCM}). The calculated Gibbs energy profile for the first mechanistic pathway is shown in Figure 68. Migratory insertion of the acetylene into the Pt-CH₃ bond takes place through an energy barrier of $24.9 \text{ kcal}\cdot\text{mol}^{-1}$. The resulting vinyl intermediate **A**, which exhibits an agostic C-H interaction with the Pt centre, is thermodynamically more stable than the acetylene adduct, **20**·C₂H₄, by $1.3 \text{ kcal}\cdot\text{mol}^{-1}$. Then, C-H activation of the C-terminal of the alkenyl ligand gives hydride **B** and has an energy barrier of $16.7 \text{ kcal}\cdot\text{mol}^{-1}$. Reductive C-H elimination from the latter, formally a Pt(IV) intermediate, is almost barrierless and yields the allyl product **24**.

Although the higher calculated energetic barrier for this reaction pathway ($24.9 \text{ kcal}\cdot\text{mol}^{-1}$) is in the upper limit for a process which occurs at room temperature, this mechanism is not in accordance with the observations obtained from the deuteration experiments, as it does not place both acetylenic protons on the same terminal C atom of the allyl ligand of the final product. Moreover, the calculated intermediates do not match with those observed in the variable temperature NMR experiments.

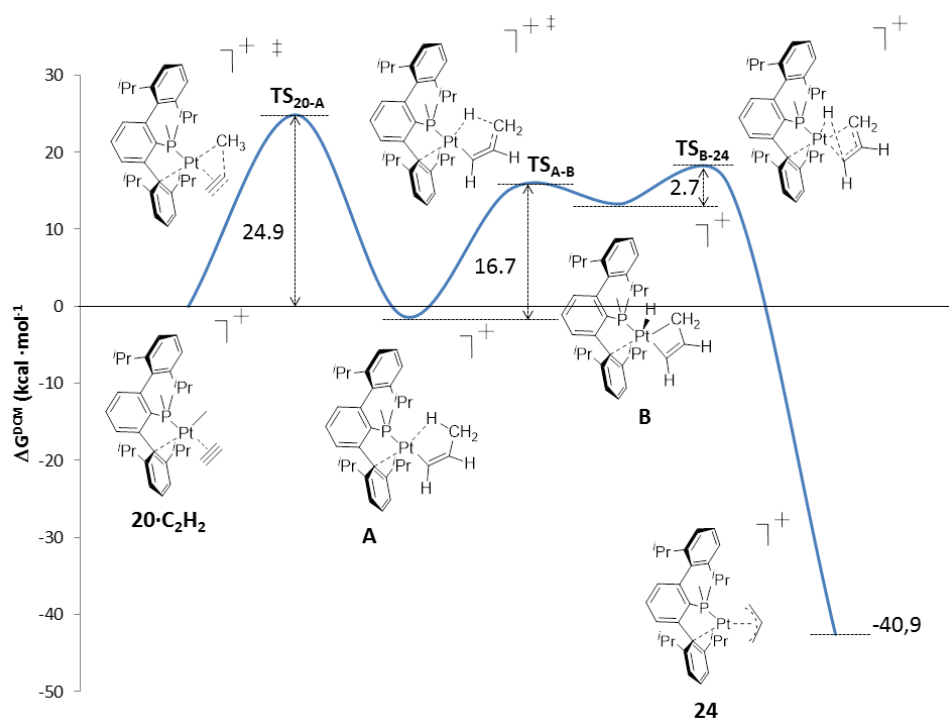


Figure 68: Calculated Gibbs Energies for the migratory insertion mechanism for the formation of complex **24**.

The second mechanistic proposal (Figure 69) begins with the tautomerization of the η^2 -coordinated acetylene to a vinylidene ligand via 1,2-H-shift with an energetic barrier of $19.4 \text{ kcal}\cdot\text{mol}^{-1}$. The resulting intermediate **A** is $6.4 \text{ kcal}\cdot\text{mol}^{-1}$ less stable than its precursor. This first intermediate undergoes a methyl insertion into the Pt=C bond, with a low energy barrier of $5.9 \text{ kcal}\cdot\text{mol}^{-1}$, giving a second intermediate, **B**, which features an agostic CH interaction with the Pt center. Direct proton migration from the terminal CH_3 to the central C atom possesses a calculated energy barrier of $21.5 \text{ kcal}\cdot\text{mol}^{-1}$, which is in the upper limit for processes that occur at room temperature. Nevertheless, Pt-assisted proton migration can originate firstly the hydride-allene intermediate **C** with an energy barrier of $4.9 \text{ kcal}\cdot\text{mol}^{-1}$. Formation of **24** from **C** takes place as a

formal migratory insertion of the hydride ligand into the Pt-allene bond with a low energy barrier of 5.4 kcal·mol⁻¹.

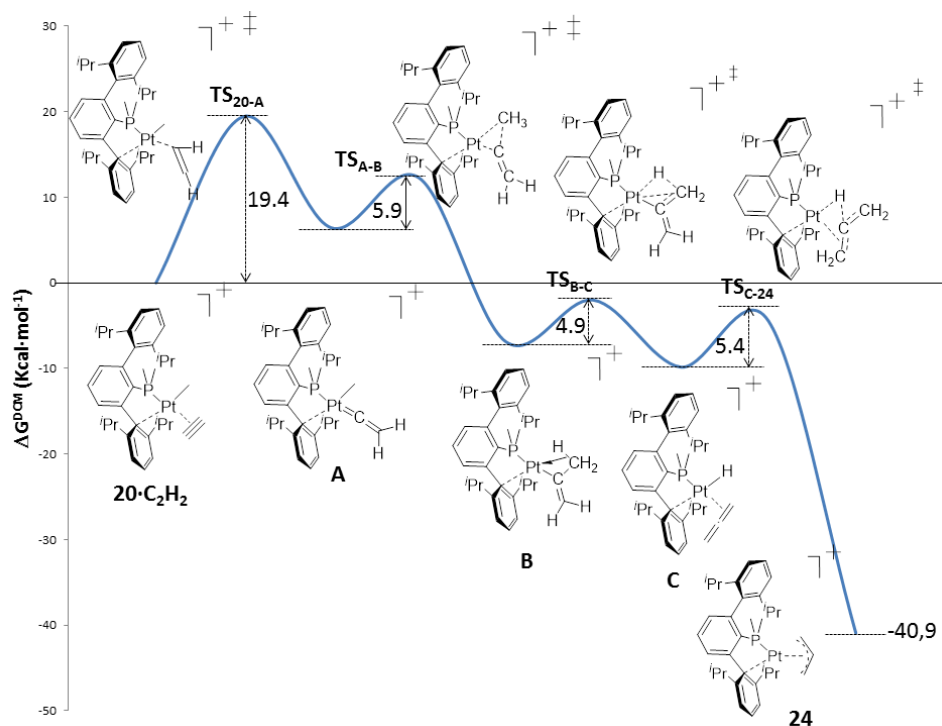


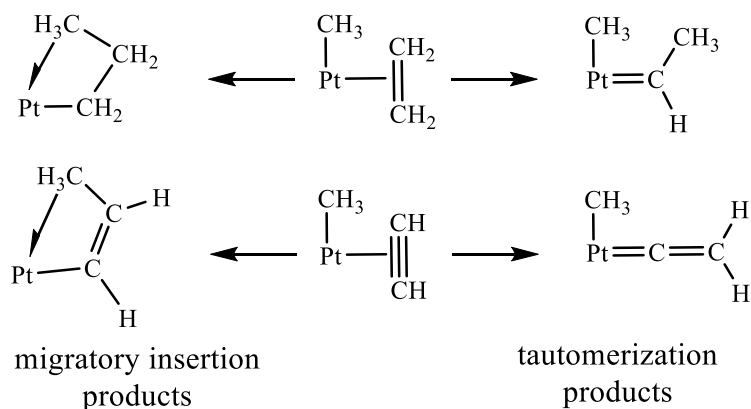
Figure 69. Calculated Gibbs energies for the isomerization mechanism of the formation of **24**.

The mechanism illustrated in figure 69 is in agreement both with the deuteration experiments and with the NMR studies previously discussed. It should be noted, however, that the low calculated energy barrier for the conversion of **A** into **B** should not allow for its NMR detection even at low temperatures.

Ethylene vs. acetylene

DFT calculations were also been used to rationalize the different reactivity of **20·S** with acetylene and ethylene. In particular, experimental observations demonstrated that, while the platinum cation $[[(\text{PMe}_2\text{Ar}^{\text{Dipp}_2})\text{PtMe}(\text{C}_2\text{H}_4)]^+$ is stable within a wide range of temperatures

(*vide supra*), the analogous acetylene complex $[(\text{PMe}_2\text{Ar}^{\text{Dipp}_2})\text{PtMe}(\text{C}_2\text{H}_2)]^+$ is only detectable at low temperatures and rapidly converts into other species. Similarly to the analysis described in the previous section, we decided to study two possible reaction pathways which would transform these adducts into i) the corresponding tautomers, that is an alkylidene complex from the ethylene adduct and a vinylidene one for the acetylene analogue, or ii) the products of migratory insertions, that is an alkyl complex for the ethylene adduct and an alkenyl for the acetylene analogue (Scheme 43).



Scheme 43. Possible transformations for tautomerization or migratory insertion of ethylene (top) and acetylene (bottom) adducts.

As shown in figure 70, both kinetically and thermodynamically the isomerization is much more disfavoured for the ethylene complex than for the acetylene analogue. The same conclusion can be drawn looking to the calculated reaction profiles for the migratory insertion (Figure 71).

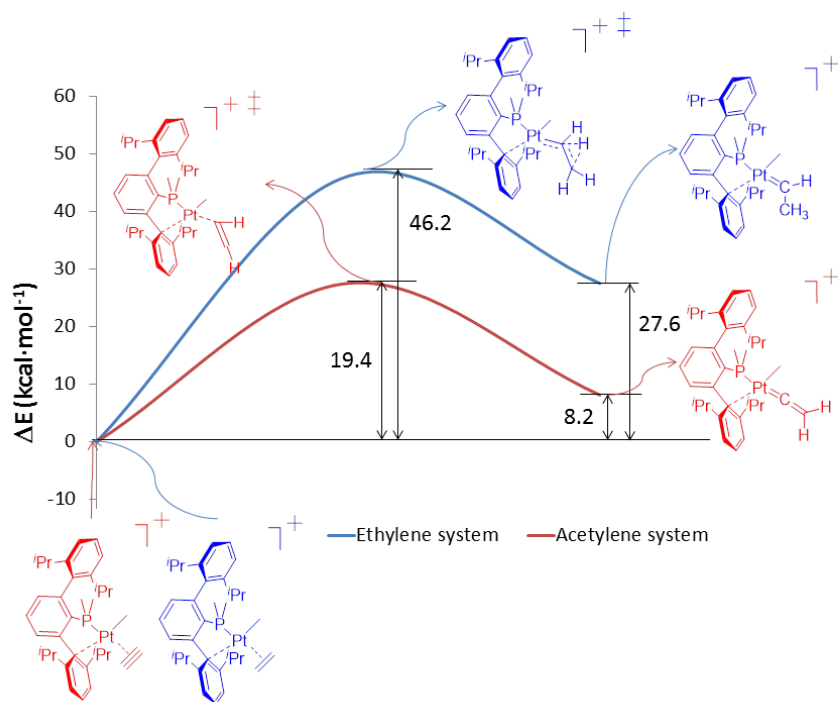


Figure 70: Comparison the Pt-assisted isomerization of ethylene and acetylene to the corresponding metal alkylidene and vinylidene, respectively.

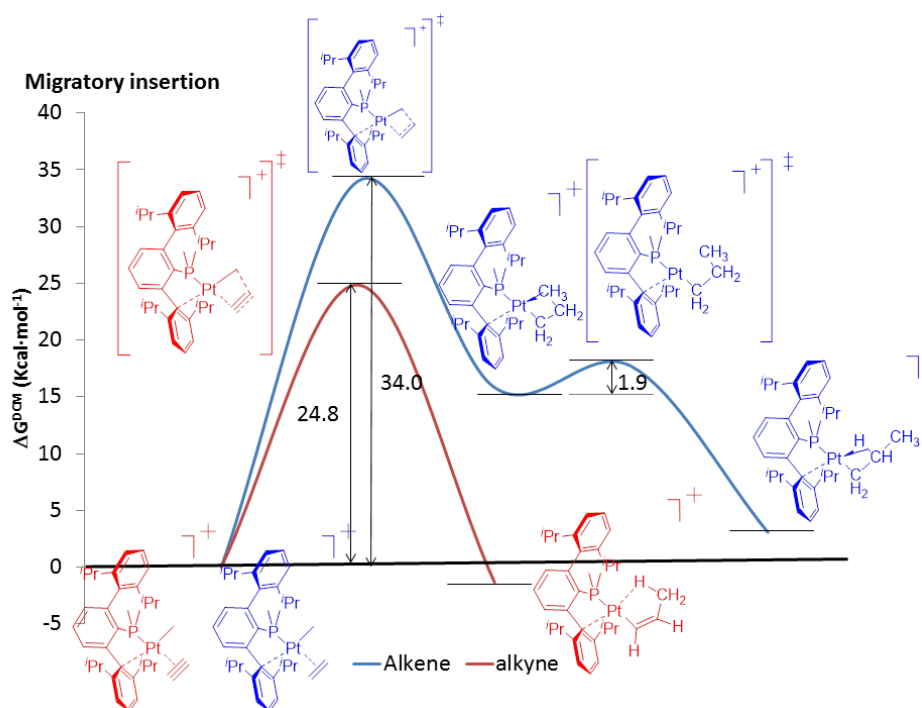


Figure 71: First step of the migratory insertion mechanism for acetylene (red) and ethylene (blue) species.

To gain a deeper understanding of the different reactivity of **20·S** with ethylene and acetylene, we performed some calculations on the systems **20·C₂H₄** and **20·C₂H₂** to compare the nature of the bond (σ and π components) between the organometallic fragment $[\text{PtMe}(\text{PMe}_2\text{Ar}^{\text{Dipp}_2})]^+$ and ethylene or acetylene. As already discussed, the bonding between transition metals and alkenes or alkynes is usually described with the aid of the Dewar, Chatt, and Duncanson model (DCD), which assumes σ donation from a π bond of the hydrocarbon to an empty metal d orbital, complemented by π back-bonding from a filled metal d orbital to an antibonding π^* orbital of the unsaturated hydrocarbon.⁶ NBO analysis¹¹⁰ of adducts **20·C₂H₄** and **20·C₂H₂** was done in order to rationalize the observed thermodynamic preference for alkene coordination. Analysis of

¹¹⁰ A. E. Reed, L. A. Curtiss, F. Weinhold, *Chem. Rev.* **1988**, 88, 899-926.

the second-order perturbation energies reveals that σ donation from the alkene and alkyne ligands is more important than π back-donation in both cases. These results are summarized below.

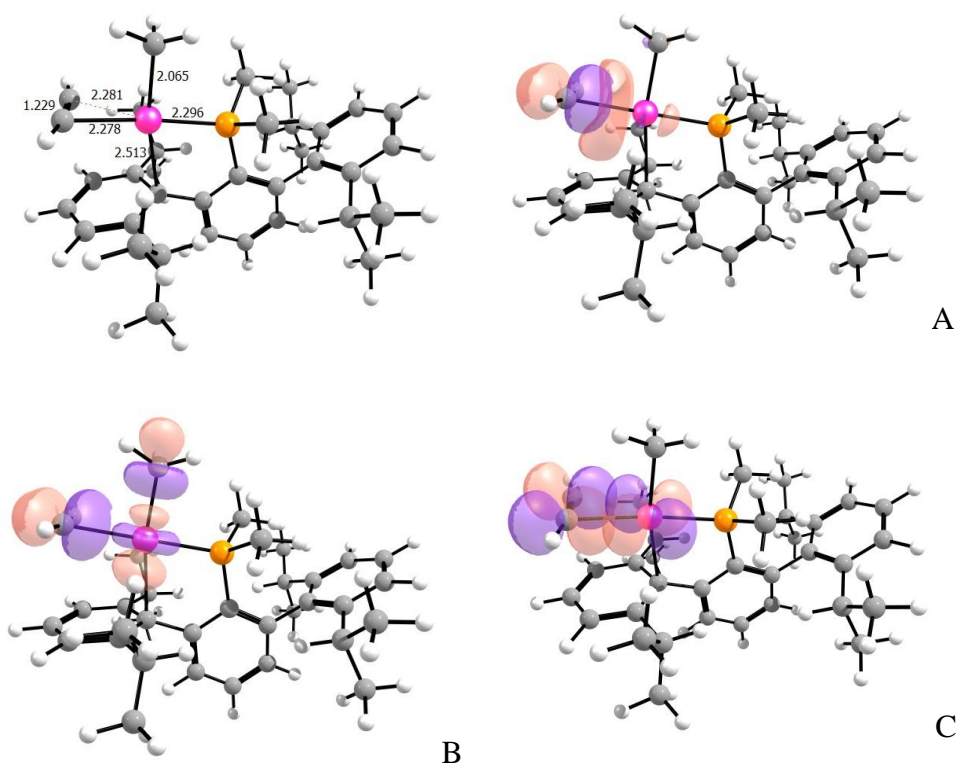


Figure 72: DFT free optimized geometry of $20 \cdot C_2H_2$ (top) and relevant donor-acceptor interactions based on NBO analysis.

					2 nd Order Perturbation Theory analysis (delocalization energies)		
	NBO	Type	Occupation	E (a.u.)	Acceptor Orbital (j)	Type	ΔE_{ij}^a (kcal·mol ⁻¹)
A	95	π_{CC}	1.75245	-0.50213	146	σ donation	33.21
B	95	π_{CC}	1.75245	-0.50213	688	σ donation	40.60
C	145	LP _{Pt}	1.85352	-0.39516	782	π back donation	22.00
	146	LP* _{Pt}	0.14526	0.26572			
	688	BD* _{PtP}	0.26495	0.20190			
	782	$\pi^* CC$	0.11925	0.01587			
Table 1: Relevant NBOs and donor acceptor interactions of 20·C₂H₂ (free optimized in the gas phase). LP = lone pair; *antibonding/empty. ^a ΔE_{ij} is the stabilization energy associated with the donor –acceptor (i-j) interaction.							

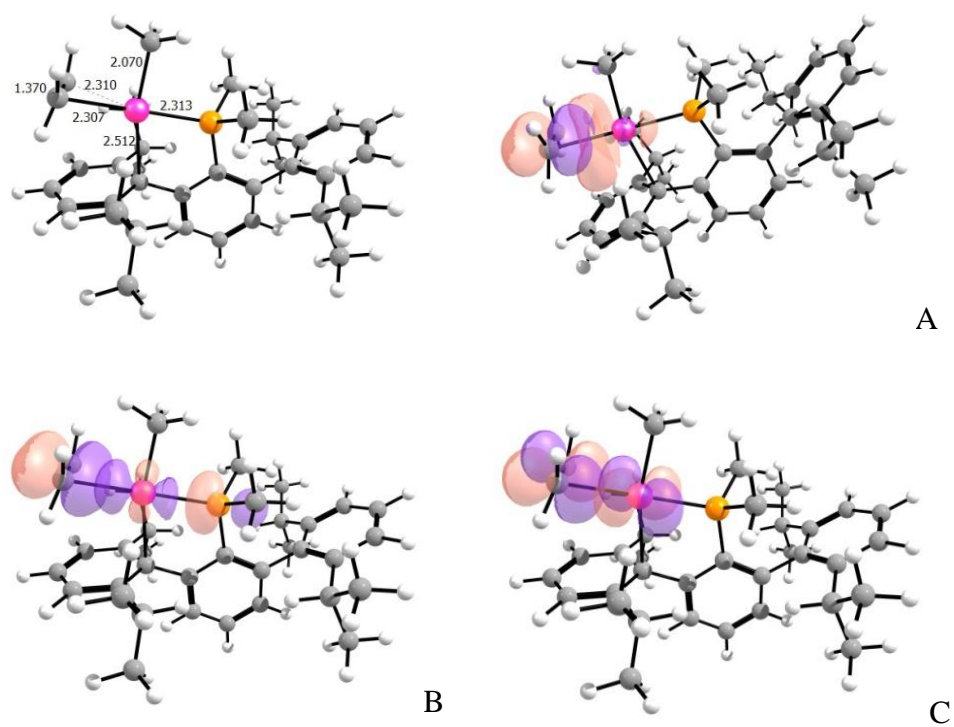


Figure 73: DFT free optimized geometry of $20 \cdot C_2H_4$ and relevant donor-acceptor interactions based on NBO analysis.

					2 nd Order Perturbation Theory Analysis (delocalization energies)		
	NBO	Type	Occupation	E (a.u.)	Acceptor Orbital (j)	Type	$\Delta E_{i,j}^a$ (kcal·mol ⁻¹)
A	94	π_{CC}	1.72111	-0.44148	147	σ donation	29.83
B	94	π_{CC}	1.72111	-0.44148	697	σ donation	44.73
C	146	LP _{Pt}	1.84240	-0.39185	790	π back donation	28.47
	147	LP* _{Pt}	0.14940	0.34146			
	697	BD* _{PPt}	0.28323	0.51076			
	790	BD* _{CC}	0.13675	-0.08129			
Table 2: Relevant NBOs and donor acceptor interactions of 20·C₂H₄ (free optimized in the gas phase). LP = lone pair; *antibonding/empty. ^a $\Delta E_{i,j}$ is the stabilization energy associated with the donor –acceptor (i-j) interaction.							

Analysis of the second order perturbation theory for the acetylene and ethylene adducts reveals the existence of three donor-acceptor contributions to the bonding between the organic ligand and the [PtMe(PMe₂Ar^{Dipp2})] fragment, two of them of the σ type (A and B) and one of the π type, corresponding to π -back donation from a filled d orbital of the platinum atom to a π^* orbital of the unsaturated organic molecule (C).

Analysis of the delocalized molecular orbitals of both adducts reveals, in the case of the alkyne adduct, an antibonding interaction between the occupied π_{\perp} orbital of the acetylene and an occupied d orbital of the Pt centre (Figure 74). Such interaction is absent in the alkene adduct and may account for the slightly higher thermodynamic stability of the

latter complex ($1 \text{ kcal}\cdot\text{mol}^{-1}$) which was calculated from the difference of the optimized energies between the products and reagents of the formation of both species from $20\cdot\text{Me}_2\text{O}$.

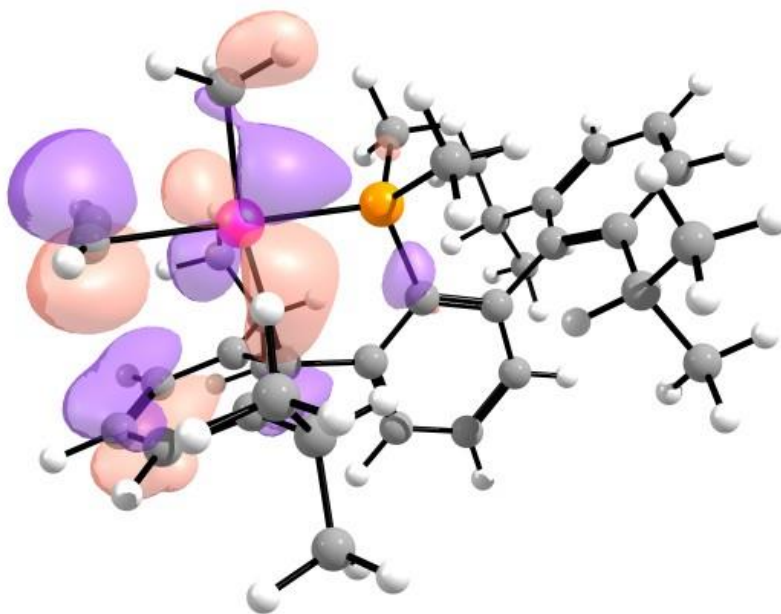


Figure 74: Antibonding interaction between the acetylene and $[\text{PtMe}(\text{PMe}_2\text{Ar}^{\text{Dipp}_2})]$ fragments of $20\cdot\text{C}_2\text{H}_2$.

1.2.2.5. Some Catalytic Studies

a) Hydroarylation of alkynes

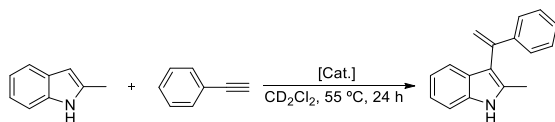
Transition-metal (TM)-catalyzed hydroarylation reactions of alkynes have received much attention,¹¹¹ because they enable the net insertion of alkyne C–C triple bonds into C–H bonds of aromatic precursors, resulting in regio- and stereo-selective formation of synthetically useful arylalkenes. Taking advantage of this feature, TM-catalyzed alkyne hydroarylations have been successfully used for the synthesis of heterocycles^{73a,112,113}. In general, highly electrophilic complexes based on Pt and other metals have shown wide applicability in these reactions.

In general, two possible pathways are followed for this kind of reactions. On one hand, the reaction of carbonyl complexes, $[M(CO)_6]$ ($M = Mo, W, Cr$) and certain Ru(II) complexes with terminal alkynes or with alkynes with migrating groups could proceed via vinylidene metal complexes. On the other hand, electrophilic metal salts or complexes prefer the alkyne coordination to facilitate electrophilic substitution on the arene. However, previous direct metalation followed by insertion of the alkyne into the σ -M-C bond of $Ar-ML_n$ species can also compete in certain cases.^{111d}

¹¹¹ a) T. Kitamura, *Eur. J. Org. Chem.* **2009**, 2009, 1111-1125; b) Y. Yamamoto, *Chem. Soc. Rev.* **2014**, 43, 1575-1600; c) P. d. Mendoza, A. M. Echavarren, *Pure Appl. Chem.* **2010**, 82, 801-820; d) C. Nevado, A. M. Echavarren, *Synthesis* **2005**, 2, 167-182.

¹¹² a) S. Bhuvaneshwari, M. Jeganmohan, C.-H. Cheng, *Chem. Eur. J.* **2007**, 13, 8285-8293; b) J. Oyamada, T. Kitamura, *Tetrahedron* **2009**, 65, 3842-3847.

¹¹³ a) C. Ferrer, H. M. A. Catelijne, A. M. Echavarren, *Chem. Eur. J.* **2007**, 13, 1358-1373; b) X. Hu, D. Martin, M. Melaimi, G. Bertrand, *J. Am. Chem. Soc.* **2014**, 136, 13594-13597; c) J. S. Yadav, B. V. S. Reddy, B. Padmavani, M. K. Gupta, *Tetrahedron Lett.* **2004**, 45, 7577-7579; d) T. Tsuchimoto, H. Matsubayashi, M. Kaneko, Y. Nagase, T. Miyamura, E. Shirakawa, *J. Am. Chem. Soc.* **2008**, 130, 15823-15835.

Table 3. Optimization of the catalyst for the coupling of 2-Methylindole and Phenylacetylene *

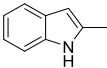
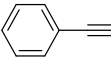
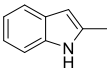
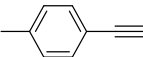
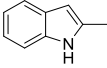
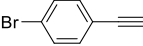
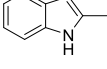

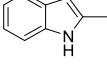

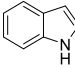
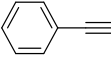
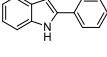
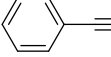
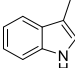
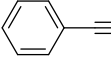
Entry	Catalyst	NMR Yield (%)
1	20·S	27
2	6 + AgSbF ₆	30
3	6 + 2 AgSbF ₆	47
4 ^a	6 + 2 AgSbF ₆	37
5 ^b	6 + 2 AgSbF ₆	20
6	6 + NaBAr _F	30
7	6 + 2 NaBAr _F	60

*Unless otherwise noted reactions were carried out using 0.17 mmol of 2-methylindole, 0.17 mmol of phenylacetylene and 0.007 mmol of Pt catalyst (4 mol%) in CD₂Cl₂ at 55 °C for 24 h.. Yield was determined by ¹H NMR spectroscopy. ^aMolar ratio 2-methylindole:phenylacetylene is 1:2. ^bMolar ratio 2-methylindole:phenylacetylene is 2:1.

(entry 2). But surprisingly, if the amount of the silver salt is increased (entry 3), the yield is considerably increased up to 47%. It is interesting to mention that when the molar ratio between the two substrates is not equimolar (2-methylindole:phenylacetylene is 1:2 and 2:1, entries 4 and 5 respectively) the catalyst activity decreased compared to that found for equimolar conditions. Finally, when the halide abstractor is changed to Na[BAr_F], the catalytic system appear to be more efficient (entries 6 and 7).

We tested the catalytic activity of some electrophilic Pt(II) cationic complexes in order to catalyse the reaction of 2-methylindole with phenylacetylene (Table 3). When using the cationic complex [Pt(PMe₂Ar^{Dipp})Me(S)][BAr_F], **22·S**, the desired product is formed in 27% yield (entry 1), and when using as catalyst the chloride derivative **6** with one equivalent of AgSbF₆ the yield increased up to 30%

Table 4. Substrate Scope for the Hydroarylation of alkynes^a.

Entry	Indole	Alkyne	NMR Yield (%)
1			75
2			84
3			70
4			69
5			0
6			26
7			>99
8			0

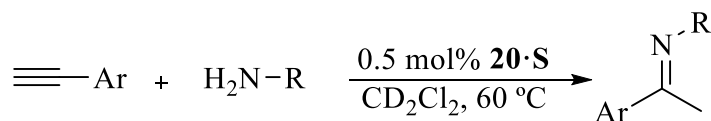
^aReactions were performed using the mixture **6** + 2 NaBAR_F as catalyst with loading of 5%, 0.17 mmol of indole, 0.17 mmol of alkyne in CD₂Cl₂ (0.5 mL) at 55 °C for 24 h. Yield was determined by ¹H NMR spectroscopy.

Next, a series of alkynes and indoles were tested in this reaction using the best catalytic system (5% of **6** + 2 NaBAR_F) in CD₂Cl₂ at 55 °C (Table 4). The introduction of electron-withdrawing groups in the aromatic ring of the substrate slightly decreased the catalyst activity (entries 1-4), whereas no conversion into the desired C—C coupling product was observed when using an internal alkyne (entry 5). With regard to the indole partner (entries 1 and 6-8), use of an unsubstituted indole provided a lower conversion (entry 6), while substitution of the

methyl group at 2 position by an aromatic ring increased markedly the product yield (entry 7). Finally, reaction of 3-methylindole with phenylacetylene did not proceed.

b) Hydroamination of terminal alkynes

Catalytic additions of ammonia or primary and secondary amines to non-activated alkenes and alkynes are called hydroaminations. These reactions of fundamental simplicity represent the most atom efficient processes for the formation of amines, enamines and imines, which are important bulk and fine chemicals or building blocks in organic synthesis¹¹⁴. Consequently, the development of corresponding hydroamination reactions has received much attention and great progresses have been achieved for alkyne hydroaminations of alkynes over the past decade¹¹⁴⁻¹¹⁵. In the bibliography there are several examples of hydroamination or hydroamidation reactions catalysed by Pt species,^{73,116} including simple PtBr₂¹¹⁷.



Scheme 44. Hydroamination of terminal alkynes with primary amines.

Based on these precedents, we examined the activity of the cationic Pt unsaturated complex **20·S** in the addition of anilines to terminal alkynes. Initial catalytic tests were performed using the benchmark reaction of phenylacetylene with aniline at 60 °C with 0.5 mol% catalyst loading in in dichloromethane-d₂, demonstrating the hability of this complex to catalyze

¹¹⁴ L. Huang, M. Arndt, K. Gooßen, H. Heydt, L. J. Gooßen, *Chem. Rev.* **2015**, *115*, 2596-2697.

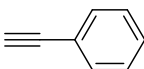
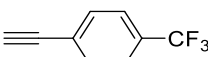
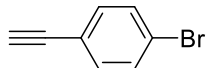
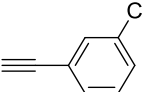
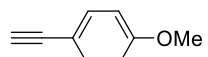
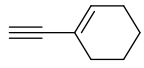
¹¹⁵ a) R. Severin, S. Doye, *Chem. Soc. Rev.* **2007**, *36*, 1407-1420; b) T. E. Müller, K. C. Hultsch, M. Yus, F. Foubelo, M. Tada, *Chem. Rev.* **2008**, *108*, 3795-3892.

¹¹⁶ a) J. M. Hoover, A. DiPasquale, J. M. Mayer, F. E. Michael, *J. Am. Chem. Soc.* **2010**, *132*, 5043-5053; b) H. Qian, R. A. Widenhoefer, *Org. Lett.* **2005**, *7*, 2635-2638; c) C. Liu, C. F. Bender, X. Han, R. A. Widenhoefer, *Chem. Commun.* **2007**, 3607-3618; d) C. Tsukano, S. Yokouchi, A.-L. Girard, T. Kuribayashi, S. Sakamoto, T. Enomoto, Y. Takemoto, *Organic & Biomolecular Chemistry* **2012**, *10*, 6074-6086.

¹¹⁷ J.-J. Brunet, N. C. Chu, O. Diallo, S. Vincendeau, *J. Mol. Catal. A: Chem.* **2005**, *240*, 245-248.

the reaction with good activity (*ca.* 80 % conversion). Moreover, the product derived from Markovnikov addition of the N-H bond to the acetylene was selectively obtained (Scheme 41).

Table 5. Hydroamination of alkynes with aniline catalysed by **20·S**^[a]

Entry	Alkyne	Conversion (% (time))
1		80 (4 h)
2		17 (5 h)
3		33 (4 h)
4		10 (5 h)
5		92 (4 h)
6		81 (5 h)

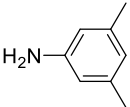
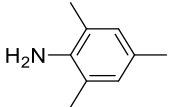
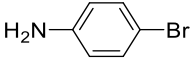
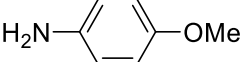
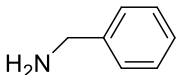
[a] Reactions were carried out at 60 °C in CD₂Cl₂ using 0.13 mmol of alkyne ([alkyne] = 0.26 M), 0.13 mmol of amine, 0.01 mmol of 1,3,5-tris(*ter*-butyl)benzene (internal standard) and 0.5 mol% of **20·S**. Conversion and selectivity were determined by ¹H NMR spectroscopy.

alkynes containing an additional C=C bond was also examined (entry 6). Selective N-H addition to the acetylenic bond took place leaving the C=C functionality unaltered.

Next, the hydroamination of a series of alkynes with aniline was studied under the optimized reaction conditions (Table 5). A significant dependence of the catalytic activity on the electronic characteristics of the substituents was evidenced (entries 1-5). Thus, the reaction rate of the *p*-bromophenylacetylene was lower than that of the phenyl and *p*-methoxyphenylacetylene.

The hydroamination of

Table 6. Hydroamination of phenylacetylene with primary amines catalysed by **20·S**^[a]

Entry	Amine	Conversion (%)
1		63 (4 H)
2		55 (6 H)
3		82 (4 H)
4		31 (4 H)
5		0 (6 H)

[a] Reactions were carried out at 60 °C in CD₂Cl₂ using 0.13 mmol of alkyne ([alkyne] = 0.26 M), 0.13 mmol of amine, 0.01 mmol of 1,3,5-tris(*ter*-butyl)benzene (internal standard) and 0.5 mol% of **20·S**. Conversion and selectivity were determined by ¹H NMR spectroscopy.

conversion was detected when the amine contains an electron poor ring (entry 3-4). It is important to mention that, this catalytic system is limited to aryl amines, being inactive for benzylamine.

Finally, a number of primary amines were tested in this reaction with phenylacetylene in the presence of the catalyst **22·S** (Table 6). Again, both steric and electronic effects were detected. For example, when the substituents are located in the *ortho* positions (entry 2), the activity is lower than when these groups are in the *meta* positions. Moreover, a great enhancement of the

I.3. EXPERIMENTAL SECTION

I.3.1. General Considerations

All operations were performed under a nitrogen atmosphere using standard Schlenk techniques, employing dry solvents and glassware. Microanalyses were performed by the Microanalytical Service of the Instituto de Investigaciones Químicas. Infrared spectra were recorded on a Bruker Vector 22 spectrometer.

The NMR experiments were carried out on Bruker DRX-500, DRX-400, Advance^{III}-400/R and DRX-300 spectrometers. Spectra were referenced to external SiMe₄ (δ : 0 ppm) using residual proton solvent peaks as internal standards (¹H NMR experiments), or the characteristic resonances of the solvent nuclei (¹³C NMR experiments), while ³¹P and ¹⁹F were referenced to external H₃PO₄ and CFCI₃, respectively. Spectral assignments were made by routine one- and two-dimensional NMR experiments (¹H, ¹H{³¹P}, ¹³C, ¹³C{¹H}, COSY, NOESY, HSQC, and HMBC).

I.3.2. Synthesis and Characterisation of the New Complexes Obtained

Synthesis and Characterisation of $\text{PMe}_2\text{Ar}^{\text{Xyl}_2}$ (L_1)

A solution of 38.2 mmol of the Grignard reagent $\text{Mg}(\text{Ar}^{\text{Xyl}_2})\text{Br}$ in THF (*ca.* 60 mL) was added dropwise to a solution of PCl_3 (3.7 mL, 42 mmol) in THF (40 mL) at -80°C in the presence of CuCl (575 mg, 6.25 mmol). The reaction mixture was allowed to reach slowly the room temperature and was stirred overnight. All volatiles were removed by evaporation at reduced pressure and the solid residue was extracted three times with pentane (3×50 mL). The combined organic fractions were dried under vacuum giving a mixture of the three possible dihalidephosphines, $\text{PX}_2\text{Ar}^{\text{Xyl}_2}$ ($\text{X} = \text{Cl}, \text{Br}$), which was redissolved in THF (50 mL). A 3 M solution of $\text{Mg}(\text{Me})\text{Br}$ in Et_2O (25.5 mL, 76.5 mmol) was added dropwise at -80°C , and the mixture was allowed to reach slowly the room temperature, and stirred overnight. The volatiles were removed under reduced pressure and the solid residue was extracted with pentane (3×50 mL). The solution was concentrated under reduced pressure to *ca.* 25 mL and stored at -23°C . Pale yellow crystals of **I** separated out and were collected by filtration and dried *under vacuum* (7.9 g, 60%).

^1H NMR (300 MHz, C_6D_6 , 25°C): δ 7.15-7.03 (m, 3H, *p*-Xyl and *p*- C_6H_3), 7.0 (d, $^3J_{\text{HH}} = 7.6$ Hz, 2H, *m*-Xyl), 6.75 (dd, 2H, $^3J_{\text{HH}} = 7.6$ Hz, $^4J_{\text{PH}} = 2.0$ Hz, *m*- C_6H_3), 2.11 (s, 12H, Ar-CH_3), 0.71 (d, 6H, $^2J_{\text{PH}} = 4.9$ Hz, P-CH_3) ppm.

$^{13}\text{C}\{^1\text{H}\}$ NMR (100.5 MHz, C_6D_6 , 25°C): δ 145.8 (d, $^2J_{\text{PC}} = 14.0$ Hz, *o*- C_6H_3), 142.5 (s), 137.0 (d, $^1J_{\text{PC}} = 30.7$ Hz, PC), 136.0 (s), 129.3 (s), 128.4 (s), 127.3 (s), 21.1 (s, CH_3 Xyl), 13.3 (d, $^1J_{\text{PC}} = 15.9$ Hz, PCH_3) ppm.

$^{31}\text{P}\{^1\text{H}\}$ NMR (202.4 MHz, CDCl_3 , 25°C): δ -40.44 (s) ppm.

Synthesis and Characterisation of $\text{PMe}_2\text{Ar}^{\text{Dipp}_2}(\text{L}_2)$

A solution of 35 mmol the Grignard reagent $\text{Mg}(\text{Ar}^{\text{Dipp}_2})\text{Br}$ in THF (*ca.* 60 mL) was added dropwise to a solution of PCl_3 (3 mL, 35 mmol) in THF (40 mL) at -80°C in the presence of CuCl (340 mg, 3.5 mmol). The reaction mixture was allowed to reach slowly the room temperature and was stirred overnight. All volatiles were removed under vacuum and the solid residue was extracted with pentane (4×50 mL). The combined organic fractions were dried under vacuum giving a mixture of the three possible dihalophosphine $\text{PX}_2\text{Ar}^{\text{Dipp}_2}$ ($\text{X} = \text{Cl}, \text{Br}$), which was redissolved in THF (50 mL). A 3 M solution of $\text{Mg}(\text{Me})\text{Br}$ in Et_2O (16.7 mL, 50 mmol) was added dropwise at -80°C , and the mixture was allowed to reach slowly the room temperature, and stirred overnight. The volatiles were removed under reduced pressure and the solid residue was extracted with pentane (4×50 mL). The solution was concentrated under reduced pressure to *ca.* 25 mL and stored at -23°C . Pale yellow crystals of II separated out and were collected by filtration and dried *under vacuum* (9.08 g, 56.6%).

Anal. Calc. for $\text{C}_{32}\text{H}_{43}\text{P}$: C, 83.8; H, 9.5. **Found:** C, 83.8; H, 9.9.

^1H NMR (300 MHz, 25°C , CDCl_3): δ 7.36 (t, 2H, $^3J_{\text{HH}} = 7.7$ Hz, *p*-Dipp), 7.30 (t, 1H, $^3J_{\text{HH}} = 7.6$ Hz, *p*- C_6H_3), 7.19 (d, 4H, $^3J_{\text{HH}} = 7.7$ Hz, *m*-Dipp), 7.05 (dd, 2H, $^3J_{\text{HH}} = 7.6$ Hz, $^4J_{\text{HP}} = 2.0$ Hz, *m*- C_6H_3), 2.66 (hept, 4H, $^3J_{\text{HH}} = 6.8$ Hz, *CH*-Dipp), 1.25 (d, 12H, $^3J_{\text{HH}} = 6.8$ Hz, Me-Dipp), 1.05 (d, 12H, $^3J_{\text{HH}} = 6.8$ Hz, Me-Dipp), 0.70 (d, 6H, $^2J_{\text{HP}} = 5.0$ Hz, PMe_2) ppm.

$^{13}\text{C}\{^1\text{H}\}$ NMR (100 MHz, 25°C , CD_2Cl_2): δ 147.1 (s, *o*-Dipp), 145.2 (d, $^2J_{\text{CP}} = 15$ Hz, *o*- C_6H_3), 140.4 (d, $^3J_{\text{CP}} = 4$ Hz, *ipso*-Dipp), 138.4 (d, $^1J_{\text{CP}} = 28$ Hz, *ipso*- C_6H_3), 131.2 (d, $^3J_{\text{CP}} = 2$ Hz, *m*- C_6H_3), 128.3 (s, *p*-Dipp), 127.0 (s, *p*- C_6H_3), 122.8 (s, *m*-Dipp), 31.2 (s, *CH*-Dipp), 25.7 (s, Me-Dipp), 22.6 (s, Me-Dipp), 13.7 (d, $^1J_{\text{CP}} = 14$ Hz, PMe_2) ppm.

$^{31}\text{P}\{^1\text{H}\}$ NMR (160 MHz, 25°C , CD_2Cl_2): δ -41.3(s) ppm.

Synthesis and Characterisation of $\text{PMe}_2\text{Ar}^{\text{Tipp}_2}$ (L_3)

A solution of 45 mmol of the Grignard reagent $\text{Mg}(\text{Ar}^{\text{Tipp}_2})\text{Br}$ in THF (*ca.* 60 mL) was added dropwise to a solution of PCl_3 (3.9 mL, 45 mmol) in THF (40 mL) at -80°C in the presence of CuCl (445 mg, 4.5 mmol). The reaction mixture was allowed to reach slowly the room temperature and was stirred overnight. All volatiles were removed by evaporation under reduced pressure and the solid residue was extracted three times with pentane (3×50 mL). The combined organic fractions were dried under vacuum giving a mixture of the three possible dihalidephosphines, $\text{PX}_2\text{Ar}^{\text{Tipp}_2}$ ($\text{X} = \text{Cl}, \text{Br}$), which was redissolved in THF (50 mL). A 3 M solution of $\text{Mg}(\text{Me})\text{Br}$ in Et_2O (20 mL, 27.5 mmol) was added dropwise at -80°C , the mixture was allowed to reach slowly the room temperature, and stirred overnight. The volatiles were removed under reduced pressure and the solid residue was extracted with pentane (3×50 mL). The solution was concentrated under reduced pressure to *ca.* 25 mL and stored at -23°C . Pale yellow crystals of III separated out and were collected by filtration and dried under vacuum (13.2 g, 54.3%).

Anal. Calc. for $\text{C}_{38}\text{H}_{55}\text{P}$: C, 84.0; H, 10.2. **Found:** C, 84.4; H, 10.4.

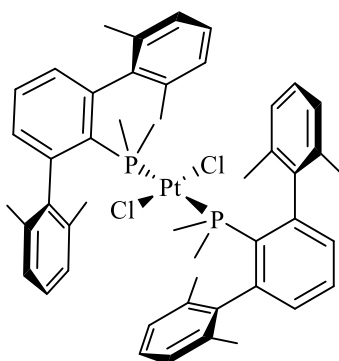
^1H NMR (300 MHz, 25°C , CDCl_3): δ 7.23 (t, 1 H, $^3J_{\text{HH}} = 7.6$ Hz, *p*- C_6H_3), 7.02 (dd, 2 H, $^3J_{\text{HH}} = 7.6$ Hz, $^4J_{\text{HP}} = 1.5$ Hz, *m*- C_6H_3), 6.99 (s, 4 H, *m*-Tipp), 2.91 (hept, 2 H, $^3J_{\text{HH}} = 6.7$ Hz, *p*-CH-Tipp), 2.64 (hept, 4 H, $^3J_{\text{HH}} = 6.6$ Hz, *o*-CH-Tipp), 1.27 (d, 12 H, $^3J_{\text{HH}} = 7.0$ Hz, *p*-Me-Tipp), 1.22 (d, 12 H, $^3J_{\text{HH}} = 6.9$ Hz, *o*-Me-Tipp), 1.02 (d, 12 H, $^3J_{\text{HH}} = 6.8$ Hz, *o*-Me-Tipp), 0.63 (d, 6 H, $^2J_{\text{HP}} = 4.6$ Hz, PMe_2) ppm.

$^{13}\text{C}\{^1\text{H}\}$ NMR (125 MHz, 25°C , CD_2Cl_2): δ 148.0 (s, *p*-Tipp), 146.1 (s, *o*-Tipp), 144.7 (d, $^1J_{\text{CP}} = 15$ Hz, *o*- C_6H_3), 138.6 (d, $^1J_{\text{CP}} = 27$ Hz, $\text{C}_{\text{ipso}}\text{-C}_6\text{H}_3$), 137.4 (d, $^3J_{\text{CP}} = 4$ Hz, $\text{C}_{\text{ipso}}\text{-Tipp}$), 130.8 (s, *m*- C_6H_3), 126.3 (s, *p*- C_6H_3), 120.4 (s, *m*-Tipp), 34.2 (s, *p*-CH-Tipp), 30.8 (s, *o*-CH-Tipp), 25.7 (s, *o*-Me-Tipp), 24.2 (s, *p*-Me-Tipp), 22.6 (s, *o*-Me-Tipp), 13.5 (d, $^3J_{\text{HP}} = 14$ Hz, PMe_2) ppm.

$^{31}\text{P}\{^1\text{H}\}$ NMR (160 MHz, 25°C , CD_2Cl_2): δ -40.7 (s) ppm.

Synthesis and Characterisation of Complex $trans\text{-}[\text{PtCl}_2(\text{PMe}_2\text{Ar}^{\text{Xyl}2})_2]$,**1**

$\text{PtCl}_2(\text{COD})$ (40 mg, 0.11 mmol) and $\text{PMe}_2\text{Ar}^{\text{Xyl}2}$ (75 mg, 0.22 mmol) were stirred overnight in toluene at 110 °C. The solvent was removed by evaporation under reduced pressure to obtain the compound as a colourless solid (98 mg, 95%).



Anal. Calc. for $\text{C}_{48}\text{H}_{54}\text{Cl}_2\text{P}_2\text{Pt}$: C, 60.1; H, 5.8. **Found:** C, 60.1; H, 5.7.

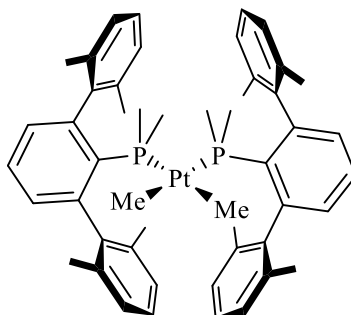
^1H NMR (300 MHz, 25 °C, CDCl_3): δ 7.39 (t, 2H, $^3J_{\text{HH}} = 7.6$ Hz, $p\text{-C}_6\text{H}_3$), 7.1 (m, 4H, $p\text{-Xyl}$), 6.99 (d, 8H, $^3J_{\text{HH}} = 7.5$ Hz, $m\text{-Xyl}$), 6.88 (d, 4H, $^3J_{\text{HH}} = 7.6$ Hz, $m\text{-C}_6\text{H}_3$), 2.07 (s, 24H, Me-Xyl), 1.14 (t, 12H, $^2J_{\text{PH}} = 3.6$ Hz, PMe_2) ppm.

$^{13}\text{C}\{^1\text{H}\}$ NMR (75.4 MHz, 25 °C, CDCl_3): δ 146.5 (s, $o\text{-C}_6\text{H}_3$), 141.9 (s, $\text{C}_{\text{ipso-Xyl}}$), 136.5 (s, $o\text{-Xyl}$), 130.9 (s, $m\text{-C}_6\text{H}_3$), 130.4 (s, $p\text{-C}_6\text{H}_3$), 128.5 (s, $\text{C}_{\text{ipso-C}_6\text{H}_3}$), 127.7 (s, $m\text{-Xyl}$), 127.5 (s, $p\text{-Xyl}$), 21.1 (s, Me-Xyl), 13.9 (t, $^1J_{\text{PC}} = 19$ Hz, PMe_2) ppm.

$^{31}\text{P}\{^1\text{H}\}$ NMR (121.4 MHz, 25 °C, CDCl_3): δ -17.3 ($^1J_{\text{PPt}} = 2555$ Hz) ppm.

Synthesis and Characterisation of Complex *cis*- [Pt(Me)₂(PMe₂Ar^{Xyl})₂]₂

A mixture of [Pt(Me)₂(μ-SMe₂)]₂ and Pt(Me)₂(SMe₂)₂ (150 mg, 0.465 mmol based on Pt) and **L**₁ (0.324 mg, 0.93 mmol) was placed in a Schlenk flask and dissolved in CH₂Cl₂ (5 mL). After stirring at room temperature overnight the volatiles were removed by evaporation under reduced pressure. The product was washed with pentane (3 × 10 mL) at room temperature. Pure samples of complex **2** were obtained by crystallization from toluene/pentane (1:1) at −20 °C (130 mg, 40%).



Anal. Calc. for C₅₀H₆₀P₂Pt: C, 65.4; H, 6.6. **Found:** C, 65.7; H, 6.3.

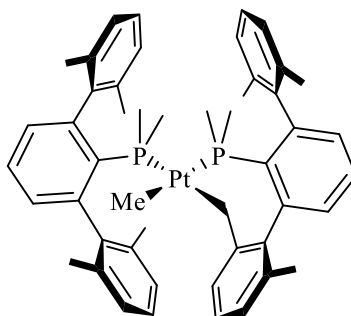
¹H NMR (300 MHz, 25 °C, CDCl₃): δ 7.26 (m, 2H, p-C₆H₃), 7.08 (m, 4H, p-Xyl), 6.96 (d, 8H, ³J_{HH} = 7.4 Hz, m-Xyl), 6.74 (dd, 4H, ⁴J_{PH} = 1.9 Hz, ³J_{HH} = 7.76 Hz, m-C₆H₃), 2.06 (s, 24H, Me-Xyl), 0.67 (d, 12H, ²J_{PH} = 7.5 Hz, ³J_{PH} = 20.8 Hz, PMe₂), 0.00 (m, 6H, ³J_{PH} = 6.9 Hz, ³J_{PH} = 9.4 Hz, ²J_{PH} = 70.7 Hz, PtMe₂) ppm.

¹³C{¹H} NMR (75.4 MHz, 25°C, CDCl₃): δ 146.3 (s, o-C₆H₃), 136.9 (s, o-Xyl), 131.6 (s, ipso-C₆H₃), 143.2 (s, ipso-Xyl), 130.8 (s, m-C₆H₃), 129.0 (s, p-C₆H₃), 127.6 (s, m-Xyl), 21.8 (s, Me-Xyl), 18.1 (d, ¹J_{PC} = 28 Hz, ²J_{PC} = 21 Hz, PMe₂), 1.3 (dd, ²J_{PC} = 105 Hz, ²J_{PC} = 9 Hz, ¹J_{PC} = 610 Hz, PtMe₂) ppm.

³¹P{¹H} NMR (121.4 MHz, 25°C, CDCl₃): δ −5.3 (¹J_{PtP} = 1773 Hz) ppm.

Synthesis and Characterisation of Complex $[\text{Pt}(\kappa^2\text{-P,C-PMe}_2\text{Ar}^{\text{Xyl}})_2\text{Me}(\text{PMe}_2\text{Ar}^{\text{Xyl}})]_3$

Complex **2** (40 mg, 0.043 mmol) was heated in CH₂Cl₂ (2 mL) at 40 °C overnight. After elimination of the volatiles by evaporation under reduced pressure, the product was obtained as a colourless powder and dried for 3 h under vacuum (39 mg, 100%).



Anal. Calc. for C₄₉H₅₆P₂Pt: C, 63.2; H, 6.3. **Found:** C, 63.1; H, 6.3.

¹H NMR (500 MHz, 25 °C, C₆D₆): δ 7.30 (d, 1H, ³J_{HH} = 7.5 Hz, H_{ar}), 7.18 (m, 1H, H_{ar}), 7.08 (t, 1H, ³J_{HH} = 7.5 Hz, H_{ar}), 6.89-7.02 (m, 10H, H_{ar}), 6.87 (d, 1H, ³J_{HH} = 7.5 Hz, H_{ar}), 7.62-7.71 (m, 4H, H_{ar}), 2.93 (dd, 1H, ²J_{HH} = 8.7 Hz, ³J_{PH} = 19.7 Hz, ²J_{PtH} = 99.8 Hz, CH₂Pt), 2.81 (dd, 1H, ²J_{HH} = 8.8 Hz, ³J_{PH} = 19.5 Hz, ²J_{PtH} = 101.2 Hz, PtCH₂), 2.38 (s, 3H, Me-Xyl), 2.26 (s, 6H, Me-Xyl), 2.19 (s, 3H, Me-Xyl), 2.15 (s, 6H, Me-Xyl), 1.97 (s, 3H, Me-Xyl), 1.19 (d, 3H, ²J_{PH} = 7.6 Hz, ⁴J_{PtH} = 16.1 Hz, PMe), 1.08 (d, 3H, ²J_{PH} = 7.4 Hz, ⁴J_{PtH} = 25.1 Hz, PMe), 0.90 (dd, 3H, ³J_{PH} = 9.9 Hz, ³J_{PH} = 6.8 Hz, ²J_{PtH} = 65.9 Hz, PtMe), 0.72 (d, 3H, ²J_{PH} = 7.4 Hz, ⁴J_{PtH} = 20.0 Hz, PMe), 0.36 (d, 3H, ²J_{PH} = 7.6 Hz, ⁴J_{PtH} = 15.8 Hz, PMe) ppm.

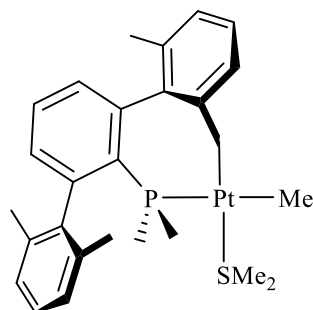
$^{13}\text{C}\{^1\text{H}\}$ NMR (125.72 MHz, 25 °C, CD_2Cl_2): δ 146.9 (d, $J_{\text{PC}} = 10$ Hz), 146.6 (d, $J_{\text{PC}} = 9$ Hz), 143.6 (s), 142.8 (d, $J_{\text{PC}} = 4$ Hz), 142.6 (d, $J_{\text{PC}} = 6$ Hz), 137.9 (s), 137.4 (4), 137.2 (s), 137.0 (d, $J_{\text{PC}} = 6$ Hz), 136.6 (s), 135.2 (s), 134.0 (d, $^1J_{\text{PC}} = 35$ Hz, *ipso*- C_6H_3), 132.6 (d, $^1J_{\text{PC}} = 29$ Hz, *ipso*- C_6H_3), 131.5 (d, $J_{\text{PC}} = 6$ Hz), 131.2 (d, $J_{\text{PC}} = 7$ Hz), 129.7 (s), 129.5 (d, $J_{\text{PC}} = 6.2$ Hz), 129.1 (s), 128.2 (s), 127.9 (s), 127.8 (s), 127.7 (s), 126.0 (d, $J_{\text{PC}} = 3$ Hz), 124.4 (d, $J_{\text{PC}} = 3$ Hz), 29.7 (dd, $^2J_{\text{PC}} = 95$ Hz, $^2J_{\text{PC}} = 6$ Hz, $^1J_{\text{PtC}} = 549$ Hz, PtCH_2), 22.6 (s, Me-Xyl), 22.4 (s, Me-Xyl), 22.3 (s, Me-Xyl), 21.8 (s, Me-Xyl), 21.7 (s, Me-Xyl), 19.9 (d, $^1J_{\text{PC}} = 22$ Hz, PMe), 18.9 (d, $^1J_{\text{PC}} = 24$ Hz, PMe).

Hz, PMe), 18.5 (d, $^1J_{\text{PC}} = 31$ Hz, PMe), 17.9 (d, $^1J_{\text{PC}} = 30$ Hz, PMe), 5.7 (dd, $^2J_{\text{PC}} = 8$ Hz, $^2J_{\text{PC}} = 95$ Hz, $^1J_{\text{PtC}} = 630$ Hz, PtMe) ppm.

$^{31}\text{P}\{^1\text{H}\}$ NMR (161.9 MHz, 25 °C, CD_2Cl_2): δ -7.9 (d, $^2J_{\text{PP}} = 6.1$ Hz, $^1J_{\text{PPt}} = 1748$ Hz), -4.3 (d, $^2J_{\text{PP}} = 6.1$ Hz, $^1J_{\text{PPt}} = 1985$ Hz) ppm.

Synthesis and Characterisation of Complex $[\text{Pt}(\kappa^2\text{-P,C-PMe}_2\text{Ar}^{\text{Xyl}_2})\text{Me}(\text{SMe}_2)]$, **4**

A mixture of $[\text{Pt}(\text{Me})_2(\mu\text{-SMe}_2)]_2$ and $\text{Pt}(\text{Me})_2(\text{SMe}_2)_2$ (90 mg, 0.28 mmol based on Pt) and **L**₁ (0.97 mg, 0.28 mmol) was placed in a Schlenk tube and dissolved in CH_2Cl_2 (5 mL). After stirring at room temperature overnight the reaction mixture was heated at 38 °C during 20 hours. The volatiles were removed under vacuum and the resulting solid residue was washed with Et_2O (3×5 mL). Pure complex **4** was obtained by crystallization from CH_2Cl_2 /pentane (1:1) at −20 °C (80 mg, 47%).



Anal. Calc. for $\text{C}_{27}\text{H}_{35}\text{P}_2\text{PtS}$: C, 52.5; H, 5.7; S, 5.2. **Found:** C, 52.3; H, 5.6; S: 5.1.

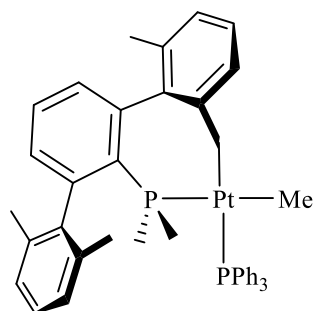
^1H NMR (300 MHz, 25 °C, CDCl_3): δ 6.87–7.44 (m, 9H, H_{ar}), 2.51 (m, 2H, PtCH_2), 2.36 (s, 3H, Me-Xyl), 2.18 (s, 6H, $^3J_{\text{PtH}} = 24.7$ Hz, SMe_2), 2.10 (s, 6H, Me-Xyl), 0.85 (d, 3H, $^3J_{\text{HP}} = 7.5$ Hz, PMe), 0.62 (d, 3H, $^3J_{\text{HP}} = 7.5$ Hz, PMe), 0.57 (d, 3H, $^3J_{\text{HP}} = 7.2$ Hz, $^2J_{\text{HPt}} = 65.9$ Hz, PtMe) ppm.

$^{13}\text{C}\{^1\text{H}\}$ NMR (75.4 MHz, 25 °C, CDCl_3): δ 149.5 (s), 145.9 (d, $^2J_{\text{PC}} = 11$ Hz, o- C_6H_3), 142.7 (s, o-Xyl), 141.9 (s, o- C_6H_3), 137.5 (s, ipso-Xyl'), 136.2 (s, ipso-Xyl), 135.4 (s), 131.1 (d, $^3J_{\text{PC}} = 7$ Hz, m- C_6H_3), 129.9 (d, $^1J_{\text{PC}} = 5$ Hz, ipso- C_6H_3), 129.1 (d, $^3J_{\text{PC}} = 6$ Hz, m- C_6H_3), 129.0 (s, p- C_6H_3), 127.6 (s, m-Xyl'), 127.4 (s, o-Xyl), 127.0 (d, $^2J_{\text{PC}} = 5$ Hz, m-Xyl'), 126.1 (s), 124.5 (s), 11.6 (d, $^1J_{\text{PC}} = 27$ Hz, PMe_2), 3.8 (d, $^1J_{\text{PC}} = 103$ Hz, $^1J_{\text{PtC}} = 649$ Hz, PtMe) ppm.

$^{31}\text{P}\{^1\text{H}\}$ NMR (121.4 MHz, 25 °C, CDCl_3): δ −7.7 ($^1J_{\text{Ppt}} = 1950$ Hz) ppm.

Synthesis and Characterisation of Complex [Pt(PMe₂Ar^{Xyl})₂Me(PPh₃)], **5**

CH₂Cl₂ (2 mL) was added to a solid mixture of **4** (30 mg, 0.05 mmol) and PPh₃ (13 mg, 0.05 mmol). The reaction mixture was stirred for 2 h at room temperature. The solvent was evaporated under reduced pressure and the solid residue was washed with pentane (3 mL) to obtain the *cis* complex **5** as a white solid (22 mg, 55%).



Anal. Calc. for C₄₃H₄₄P₂Pt: C, 63.2; H, 5.4. **Found:** C, 63.5; H, 5.2.

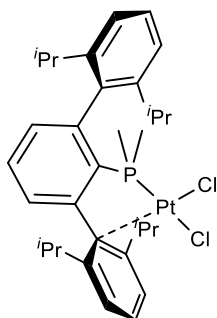
¹H NMR (500 MHz, 25 °C, CD₂Cl₂): δ 6.86-7.48 (m, 24H, H_{ar}), 2.59 (dd, 1H, ³J_{PH} = 9.3 Hz, ²J_{HH} = 8.4 Hz, ²J_{PtH} = 89.8 Hz, PtCH₂), 2.46 (s, 3H, Me-Xyl), 2.31 (dd, 1H, ³J_{PH} = 9.3 Hz, ²J_{HH} = 8.2 Hz, ²J_{PtH} = 99.0 Hz, PtCH₂), 2.16 (s, 3H, Me-Xyl), 2.02 (s, 3H, Me-Xyl), 0.63 (d, 3H, ²J_{PH} = 8.0 Hz, ³J_{PtH} = 20.0 Hz, PMe), 0.30 (t, 3H, ³J_{PH} = 7.6 Hz, ²J_{PtH} = 67.0 Hz, PtMe), -0.10 (d, 3H, ²J_{PH} = 8.1 Hz, ³J_{PtH} = 17.0 Hz, PMe) ppm.

¹³C{¹H} NMR (125.72 MHz, 25°C, CD₂Cl₂): δ 150.2 (s) ppm, 147.2 (s), 143.4 (s), 136.6 (s), 136.3 (s), 134.8 (s), 134.7 (d, ²J_{PC} = 12 Hz, *o*-PPh₃), 132.7 (d, J_{PC} = 38 Hz), 131.3 (d, J_{PC} = 7 Hz), 129.9 (s, *p*-PPh₃), 129.3 (s), 128.5 (s), 128.4 (s), 128.2 (d, ³J_{PC} = 10 Hz, *m*-PPh₃), 127.7 (s), 127.7 (s), 127.6 (s), 127.5 (s), 125.7 (s), 124.3 (s), 33.6 (dd, ²J_{PC} = 89 Hz, ²J_{PC} = 5 Hz, PtCH₂), 22.2 (s, Me-Xyl), 21.6 (s, Me-Xyl), 15.6 (d, ¹J_{PC} = 30 Hz, PMe), 13.9 (d, ¹J_{PC} = 27 Hz, PMe), 5.6 (dd, ²J_{PC} = 94 Hz, ²J_{PC} = 8 Hz, PtMe) ppm.

³¹P{¹H} NMR (200 MHz, 25°C, CD₂Cl₂): -7.8 (d, ²J_{PP} = 7.3 Hz, ¹J_{PtP} = 1978 Hz), 23.7 (d, ²J_{PP} = 7.1 Hz, ¹J_{PtP} = 1886 Hz) ppm.

Synthesis and Characterisation of *cis*-[PtCl₂(PMe₂Ar^{Dipp2})], **6**

- 1) Commercial PtCl₂ (300 mg, 1.13 mmol) was placed in an ampoule under nitrogen and dissolved in dry toluene (10 ml). A solution of the ligand **L**₂ (570 mg, 1.24 mmol) in toluene (10 ml) was prepared in another ampoule under nitrogen and was transferred to the previous one at room temperature. The reaction mixture was heated at 80°C for 3 days. After this period of time the colour of the solution changed from the initial brown to final red. All volatiles were removed under vacuum and the residue was washed with pentane (3x20 mL), giving the product as an orange powder (0.729 g, 89%).
- 2) A solution of HCl 1M in Et₂O (0.90 mL, 0.09 mmol) was added under argon to a solution of complex **10** (30 mg, 0.044 mmol) in dichlorometane at room temperature. The reaction mixture was stirred at this temperature for 4 h and the product was obtained as an orange solid when all volatiles were removed under vacuum.



Anal. Calc. for C₃₂H₄₃Cl₂PPt: C, 53.0; H, 6.0. **Found:** C, 52.9; H, 6.0.

¹H NMR (300 MHz, 25 °C, CD₂Cl₂): δ 7.88 (t, 1 H, ³J_{HH} = 8 Hz, *p*-C₆H₃), 7.50 (m, 2H, *p*-Dipp), 7.31 (d, 2 H, ³J_{HH} = 8.2 Hz, *m*-Dipp), 7.23 (m, 3 H, *m*-C₆H₃ and *m*-Dipp'), 6.75 (d, 1 H, ³J_{HH} = 7.7 Hz, *m*-Dipp'), 2.34 (hept, 4 H, ³J_{HH} = 6.6 Hz, CH-Dipp), 1.63 (d, 6 H, ³J_{HH} = 7.1 Hz, Me-Dipp), 1.51 (d, 6 H, ²J_{HP} = 12.0 Hz, ⁴J_{HPt} = 26.4 Hz, PMe₂), 1.31 (d, 6 H, ³J_{HH} = 7.1 Hz, Me-Dipp), 1.01 (d, 6 H, ³J_{HH} = 7.1 Hz, Me-Dipp), 0.96 (d, 6 H, ³J_{HH} = 6.6 Hz, Me-Dipp) ppm.

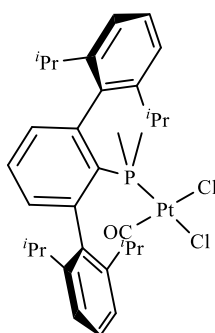
¹³C{¹H} NMR (75.4 MHz, 25°C, CD₂Cl₂): δ 148.5 (s), 147.5 (s), 138.1 (s, ⁵J_{CPt} = 34 Hz, *p*-C₆H₃), 133.3 (d, ³J_{CP} = 7 Hz, *m*-Dipp'), 132.3 (s, *p*-Dipp'), 131.2 (d, J_{CP} = 15 Hz, *m*-Dipp'), 130.5 (s, *p*-Dipp'), 126.6 (s, ⁴J_{CPt} = 25 Hz, *m*-C₆H₃), 123.6 (s, *m*-Dipp), 34.6 (s, CH-Dipp), 31.7 (s, CH-Dipp), 26.6 (s, Me-Dipp), 25.4 (s, ⁴J_{CPt} = 18.3 Hz, Me-Dipp), 24.2 (s, ⁴J_{CPt}

= 22 Hz, Me-Dipp), 21.7 (s, Me-Dipp), 13.4 (d, $^1J_{\text{CP}} = 45$ Hz, $^2J_{\text{CPt}} = 26$ Hz, PMe₂) ppm.

$^{31}\text{P}\{^1\text{H}\}$ NMR (121.4 MHz, 25°C, CD₂Cl₂): δ 10.9 (s, $^1J_{\text{PPt}} = 3189$ Hz) ppm.

Synthesis and Characterisation of *cis*-[PtCl₂(CO)(PMe₂Ar^{Dipp}₂)], **6**·CO

In a Young's NMR tube, complex **6** (15 mg, 0.04 mmol) was dissolved in CD₂Cl₂ (0.6 ml) under nitrogen. The system was degassed (3 freeze-pump-thaw cycles) and charged with CO (2 atm) at room temperature. After 4 hours, the sample was analysed by NMR spectroscopy. The product was obtained as a white solid when all volatiles were removed under vacuum (14 mg, 90 %).



Anal. Calc. for C₃₃H₄₃Cl₂OPPt: C, 52.7; H, 5.8. **Found:** C, 52.2; H, 5.7.

IR (Nujol): $\bar{\nu}(\text{CO}) = 2114 \text{ cm}^{-1}$.

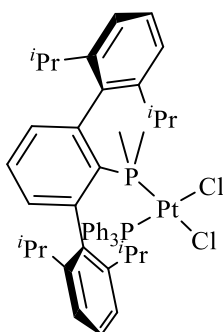
¹H NMR (300 MHz, 25 °C, CD₂Cl₂): δ 7.60 (td, 1 H, ³*J*_{HH} = 7.8 Hz, ⁵*J*_{HP} = 1.7 Hz, *p*-C₆H₃), 7.49 (t, 2 H, ³*J*_{HH} = 7.7 Hz, *p*-Dipp), 7.35 (dd, 2 H, ³*J*_{HH} = 7.7 Hz, ⁴*J*_{HP} = 3.9 Hz, *m*-C₆H₃), 7.32 (d, 4 H, ³*J*_{HH} = 7.7 Hz, *m*-Dipp), 2.63 (hept, 4 H, ³*J*_{HH} = 6.6 Hz, CH-Dipp), 1.56 (d, 6 H, ²*J*_{HP} = 12.1 Hz, ³*J*_{HPt} = 43.2 Hz, PMe₂), 1.39 (d, 12 H, ³*J*_{HH} = 6.6 Hz, Me-Dipp), 1.02 (d, 12 H, ³*J*_{HH} = 6.6 Hz, Me-Dipp) ppm.

¹³C{¹H} NMR (75.4 MHz, 25 °C, CD₂Cl₂): δ 184.6 (s, CO), 147.6 (s, *o*-Dipp), 145.1 (s, *o*-C₆H₃), 138.5 (s, C_{ipso}-Dipp), 134.2 (s, *m*-C₆H₃), 130.3 (s, *p*-Dipp), 130.1 (s, *p*-C₆H₃), 124.2 (s, *m*-Dipp), 31.7 (s, CH-Dipp), 26.5 (s, CH₃-Dipp), 22.9 (s, Me-Dipp), 19.3 (d, ¹*J*_{CP} = 44 Hz, PMe₂) ppm.

³¹P{¹H} NMR (121.4 MHz, 25 °C, CD₂Cl₂): δ -16.6 (s, ¹*J*_{Pt} = 2970 Hz) ppm.

Synthesis and Characterisation of *cis*-[PtCl₂(PPh₃)(PMe₂Ar^{Dipp}₂)], 6-PPh₃

Complex **6** (20 mg, 0.027 mmol) and triphenylphosphine (7.2 mg, 0.027 mmol) were dissolved in an ampoule under nitrogen in dichloromethane at room temperature. The reaction mixture was stirred overnight. All volatiles were removed under vacuum and the product was analysed in NMR spectroscopy in CD₂Cl₂.



Anal. Calc. for C₃₈H₅₅P: C, 60.9; H, 5.9. **Found:** C, 60.6; H, 6.1.

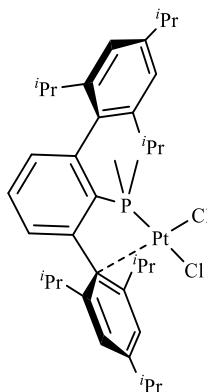
¹H NMR (300 MHz, 25 °C, CD₂Cl₂): δ 7.30-7.50 (m, 21 H, H_{ar}), 7.20-7.40 (m, 3 H, *p*-PPh₃), 3.51 (hept, 2 H, ³J_{HH} = 7.1 Hz, CH-Dipp), 2.22 (hept, 2 H, ³J_{HH} = 7.4 Hz, CH-Dipp), 1.60 (d, 6 H, ³J_{HH} = 7.7 Hz, Me-Dipp), 1.18 (d, 6 H, ³J_{HH} = 7.7 Hz, Me-Dipp), 1.06 (d, 6 H, ³J_{HH} = 7.7 Hz, Me-Dipp), 0.82 (d, 6 H, ²J_{HP} = 11.0 Hz, ³J_{HPt} = 37.6 Hz, PMe₂), 0.75 (d, 6 H, ³J_{HH} = 7.7 Hz, Me-Dipp) ppm.

¹³C{¹H} NMR (75.4 MHz, 25 °C, CD₂Cl₂): δ 149.1 (s, *o*-Dipp), 147.4 (s, *o*-Dipp), 144.4 (s), 139.9 (s, C_{ipso}-Dipp), 135.4 (d, ³J_{CP} = 11 Hz, *m*-PPh₃), 133.3 (d, ⁴J_{CP} = 9 Hz, *p*-PPh₃), 131.3 (s), 129.4 (s, *p*-Dipp), 128.6 (d, ²J_{CP} = 11 Hz, *o*-PPh₃), 128.2 (s), 125.1 (s, *m*-Dipp), 122.5 (s, *m*-Dipp), 31.6 (s, CH-Dipp), 31.3 (s, CH-Dipp), 27.5 (s, Me-Dipp), 25.9 (s, Me-Dipp), 24.39 (s, Me-Dipp), 21.67 (s, Me-Dipp), 17.63 (d, ¹J_{CP} = 40 Hz, PMe₂) ppm.

³¹P{¹H} NMR (121.4 MHz, 25 °C, CD₂Cl₂): δ 8.6 (d, ²J_{PP} = 13 Hz, ¹J_{PPt} = 3857 Hz, PPh₃), -20.9 (d, ²J_{PP} = 13 Hz, ¹J_{PPt} = 3566 Hz, PMe₂Ar^{Dipp}₂) ppm.

Synthesis and Characterisation of *cis*-[PtCl₂(PMe₂Ar^{Tipp}₂)], 7

Commercial PtCl₂ (90 mg, 0.34 mmol) was placed in an ampoule under nitrogen and dissolved in dry toluene (5 ml). A solution of the ligand **L**₃ (200 mg, 0.37 mmol) in toluene (5 ml) was prepared in another ampoule under nitrogen and was transferred to the previous one at room temperature. The reaction mixture was heated at 80°C for 3 days. After this period of time the colour of the solution changed from the initial brown to final red. All volatiles were removed under vacuum and the residue was washed with pentane (3 x 20 mL), giving the product as an orange powder (0.233 g, 85%).



Anal. Calc. for C₃₈H₅₅Cl₂PPt·CH₂Cl₂: C, 52.4; H, 6.4. **Found:** C, 52.2; H, 6.7.

¹H NMR (400 MHz, 25 °C, CD₂Cl₂): δ 7.44 (t, 1 H, ³J_{HH} = 7.6 Hz, *p*-C₆H₃), 7.19 (d, 1 H, ³J_{HH} = 7.2 Hz, *m*-C₆H₃), 7.14 (s, 2 H, *m*-Tipp), 7.06 (s, 2 H, *m*-Tipp'), 6.68 (d, 1 H, ³J_{HH} = 7.7 Hz, *m*-C₆H₃), 3.09 (hept, 1 H, ³J_{HH} = 6.6 Hz, *p*-CH-Tipp), 2.98 (hept, 1 H, ³J_{HH} = 6.9 Hz, *p*-CH-Tipp), 2.34 (hept, 2 H, ³J_{HH} = 6.5 Hz, *o*-CH-Tipp), 2.32 (hept, 2 H, ³J_{HH} = 6.5 Hz, *o*-CH-Tipp), 1.64 (d, 6 H, ³J_{HH} = 6.6 Hz, *o*-Me-Tipp), 1.55 (d, 6 H, ²J_{HP} = 12.5 Hz, ³J_{HPt} = 26.3 Hz, PMe₂), 1.44 (d, 6 H, ³J_{HH} = 6.6 Hz, *p*-Me-Tipp), 1.31 (d, 6 H, ³J_{HH} = 6.5 Hz, *p*-Me-Tipp'), 1.29 (d, 6 H, ³J_{HH} = 6.5 Hz, *o*-Me-Tipp), 0.99 (d, 6 H, ³J_{HH} = 6.4 Hz, *o*-Me-Tipp), 0.94 (d, 6 H, ³J_{HH} = 6.5 Hz, *o*-Me-Tipp) ppm.

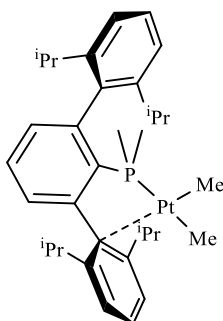
¹³C{¹H} NMR (96.6 MHz, 25°C, CD₂Cl₂): δ 163.7 (s, *p*-Tipp), 151.9 (s, *o*-Tipp), 151.14 (s, *p*-Tipp'), 148.4 (d, ²J_{CP} = 21 Hz, *o*-C₆H₃), 147.3 (s, *o*-Tipp'), 144.9 (d, ²J_{CP} = 2 Hz, *o*-C₆H₃), 135.4 (d, ¹J_{CP} = 58 Hz, C_{ipso}-C₆H₃), 133.7 (d, ³J_{CP} = 3 Hz, C_{ipso}-Tipp'), 133.2 (d, ³J_{CP} = 7 Hz, *m*-C₆H₃), 132.0

(d, $^3J_{\text{CP}} = 3$ Hz, *p*-C₆H₃), 131.0 (s, *m*-C₆H₃), 124.6 (s, *m*-Tipp'), 121.4 (s, *m*-Tipp), 97.4 (d, $^3J_{\text{CP}} = 3$ Hz, C_{ipso}-Tipp), 35.9 (s, *p*-CH-Tipp), 35.0 (s, *p*-CH-Tipp), 34.79 (s, *o*-CH-Tipp), 31.7 (s, *o*-CH-Tipp), 26.7 (s, *o*-Me-Tipp), 25.6 (s, *o*-Me-Tipp), 25.3 (s, *p*-Me-Tipp), 24.4 (s, *p*-Me-Tipp), 24.3 (s, *o*-Me-Tipp), 21.8 (s, *o*-Me-Tipp), 13.4 (d, $^1J_{\text{CP}} = 44$ Hz, PMe₂) ppm.

$^{31}\text{P}\{^1\text{H}\}$ NMR (161.9 MHz, 25 °C, CD₂Cl₂): δ 10.6 (s, $^1J_{\text{PPt}} = 3226$ Hz) ppm.

Synthesis and Characterisation of Complex *cis*-[PtMe₂(PMe₂Ar^{Dipp}₂)], **8**

A mixture of [Pt(Me)₂(μ-SMe₂)]₂ and Pt(Me)₂(SMe₂)₂ (100 mg, 0.195 mmol based on Pt) and **L**₂ (154 mg, 0.195 mmol) were placed in a Schlenk flask and dissolved in CH₂Cl₂ (5 mL) under inert atmosphere. After stirring at room temperature for 4 hours the volatiles were removed under vacuum giving the product as a yellow powder. For further purification the complex can be crystallized from hexane at −23 °C, providing analytically pure samples of the desired product (73 mg, 55%).



Anal. Calc. for C₃₄H₄₉PPt: C, 59.7; H, 7.7. **Found:** C, 59.4; H, 7.3.

¹H NMR (400 MHz, 25 °C, C₆D₆) δ: 7.27 (t, 1H, ³J_{HH} = 7.7 Hz, *p*-Dipp), 7.10 (d, 2H, ³J_{HH} = 7.8 Hz, *m*-Dipp), 7.46 (t, 1H, ³J_{HH} = 7.5 Hz, *p*-Dipp'), 6.91 (d, ³J_{HH} = 7.4 Hz, 2H, *m*-Dipp'), 6.93 (d, 1H, ³J_{HH} = 7.6 Hz, *m*-C₆H₃), 6.88 (td, 1H, ³J_{HH} = 7.5 Hz, ⁵J_{PH} = 2.1 Hz, *p*-C₆H₃), 6.52 (d, 1H, ³J_{HH} = 7.6 Hz, *m*-C₆H₃), 2.51 (hept, 2H, ³J_{HH} = 6.8 Hz, CH-Dipp), 2.32 (sept, 2H, ³J_{HH} = 6.7 Hz, CH-Dipp'), 1.49 (d, 6H, ³J_{HH} = 6.8 Hz, Me-Dipp'), 1.14 (d, 6H, ³J_{HH} = 6.7 Hz, Me-Dipp), 1.18 (d, 3H, ³J_{PH} = 8.9 Hz, ²J_{PtH} = 101.3 Hz, Pt-Me *cis* to P), 0.89 (d, 6H, ³J_{HH} = 6.6 Hz, Me-Dipp), 0.83 (d, 6H, ³J_{HH} = 6.7 Hz, Me-Dipp'), −0.19 (d, 3H, ³J_{PH} = 7.7 Hz, ²J_{PtH} = 50.3 Hz, Pt-Me *trans* to P) ppm.

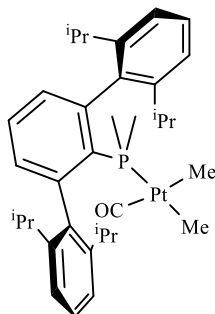
¹³C{¹H} NMR (100.6 MHz, 25 °C, C₆D₆): δ 148.5 (d, ²J_{CP} = 36 Hz, *o*-C₆H₃), 145.5 (d, ²J_{CP} = 2 Hz, *o*-C₆H₃), 147.2 (s, *o*-Dipp'), 141.6 (s, *o*-Dipp), 141.6 (d, ¹J_{CP} = 34 Hz, C_{ipso}-C₆H₃), 137.7 (s, C_{ipso}-Dipp'), 132.5 (d, ³J_{CP} = 15 Hz, *p*-C₆H₃), 129.5 (s, *p*-Dipp'), 129.2 (s, *p*-Dipp'), 122.9 (s, *m*-Dipp'), 122.8 (s, *m*-Dipp), 118.8 (d, ²J_{CP} = 3 Hz, C_{ipso}-Dipp'), 33.4 (s, CH-Dipp'), 31.3 (s, CH-Dipp), 27.1 (d, ²J_{CP} = 107 Hz, ¹J_{Cpt} = 627 Hz, Pt-Me *trans* to P), 26.4 (s, Me-Dipp), 24.3 (s, Me-Dipp'), 24.3 (s, Me-Dipp'),

21.6 (s, Me-Dipp), 12.5 (d, $^1J_{\text{CP}} = 28$ Hz, $^2J_{\text{CPt}} = 39$ Hz, PMe_2), -11.0 (d, $^2J_{\text{CP}} = 5$ Hz, $^1J_{\text{CPt}} = 915$ Hz, Pt-Me *cis* to P) ppm.

$^{31}\text{P}\{^1\text{H}\}$ NMR (161.9 MHz, 25 °C, C_6D_6): δ 20.3 (s, $^1J_{\text{PPt}} = 2010$ Hz) ppm.

Synthesis and Characterisation of Complex [PtMe₂(CO)(PMe₂Ar^{Dipp}₂)], 8-CO

In a pressure-resistant vessel, the dimethyl platinum (II) complex **8** (80 mg, 0.12 mmol) was dissolved in CH₂Cl₂ (5 ml). The system was degassed (3 freeze-pump-thaw cycles) and charged with CO (2 atm) at room temperature. After 30 minutes all volatiles were removed under vacuum and the product was isolated as white powder. Slow evaporation of dichloromethane solutions of this compound afforded air-stable, white crystals, suitable for X-ray diffraction.



Anal. Calc. for C₃₅H₄₉OPPt: C, 59.1; H, 6.9. **Found:** C, 58.6; H, 6.9.

IR (Nujol): $\bar{\nu}(\text{CO}) = 2031 \text{ cm}^{-1}$.

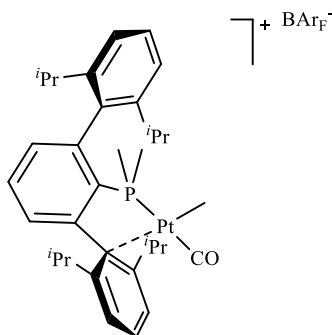
¹H NMR (300 MHz, 25 °C, CD₂Cl₂): δ 7.43 (t, 1H, $^3J_{\text{HH}} = 7.8 \text{ Hz}$, *p*-C₆H₃), 7.40 (t, 2H, $^3J_{\text{HH}} = 7.8 \text{ Hz}$, *p*-Dipp), 7.24 (d, 4H, $^3J_{\text{HH}} = 7.8 \text{ Hz}$, *m*-Dipp), 7.21 (dd, 2H, $^3J_{\text{HH}} = 7.6 \text{ Hz}$, $^4J_{\text{HP}} = 3 \text{ Hz}$, *m*-C₆H₃), 2.69 (sept, 4H, $^3J_{\text{HH}} = 7.1 \text{ Hz}$, CH-Dipp), 1.34 (d, 12H, $^3J_{\text{HH}} = 7.1 \text{ Hz}$, Me-Dipp), 1.20 (d, 6H, $^2J_{\text{HP}} = 8.2 \text{ Hz}$, $^3J_{\text{HPt}} = 23.5 \text{ Hz}$, PMe₂), 1.00 (d, 12H, $^3J_{\text{HH}} = 6.6 \text{ Hz}$, Me-Dipp), 0.49 (d, 3H, $^3J_{\text{HP}} = 7.1 \text{ Hz}$, $^2J_{\text{HPt}} = 73.0 \text{ Hz}$, Pt-Me *trans* to P), 0.14 (d, 3H, $^3J_{\text{HP}} = 10.4 \text{ Hz}$, $^2J_{\text{HPt}} = 70.1 \text{ Hz}$, Pt-Me *cis* to P) ppm.

¹³C{¹H} NMR (100.6 MHz, 25 °C, CD₂Cl₂): δ 181.7 (d, $^2J_{\text{CP}} = 5 \text{ Hz}$, CO), 147.3 (s, *o*-Dipp), 144.3 (d, $^2J_{\text{CP}} = 9 \text{ Hz}$, *o*-C₆H₃), 140.0 (d, $J_{\text{CP}} = 4 \text{ Hz}$, C_{ipso}-Dipp), 133.5 (d, $^3J_{\text{CP}} = 7 \text{ Hz}$, *m*-C₆H₃), 129.1 (s, *p*-Dipp), 128.0 (s, *p*-C₆H₃), 123.3 (s, *m*-Dipp), 31.4 (s, CH-Dipp), 26.0 (s, Me-Dipp), 22.9 (s, Me-Dipp), 17.3 (d, $^1J_{\text{CP}} = 33 \text{ Hz}$, $^2J_{\text{CPt}} = 27 \text{ Hz}$, PMe₂), 2.9 (d, $^2J_{\text{CP}} = 8 \text{ Hz}$, $^1J_{\text{CPt}} = 620 \text{ Hz}$, Pt-Me *cis* to P), -3.7 (d, $^2J_{\text{CP}} = 96 \text{ Hz}$, $^1J_{\text{CPt}} = 469 \text{ Hz}$, Pt-Me *trans* to P) ppm.

³¹P{¹H} NMR (121.4 MHz, 25 °C, CD₂Cl₂): δ -13.1 (s, $^1J_{\text{PPt}} = 1603 \text{ Hz}$) ppm.

Synthesis and Characterisation of Complex [PtMe(CO)(PMe₂Ar^{Dipp}₂)] [BAr_F] 8·CO⁺

- a) Complex **8·CO** (25 mg, 0.035 mmol) and [H(Et₂O)₂][BAr_F] (1.2 eq, 44.5 mg, 0.042 mmol) were dissolved in dry CH₂Cl₂ at –80°C. The reaction mixture was allowed to reach the room temperature overnight. All volatiles were removed under vacuum and the product was washed with pentane (3 x 5 mL). (35 mg, 65%)
- b) In a Young NMR tube, the cationic methyl complex **22·S** (20 mg, 0.012) was dissolved in CD₂Cl₂ (0.5 mL). The system was degassed (3 freeze-pump-thaw cycles) and charged with CO (2 bar) at room temperature. The product was obtained with quantitative spectroscopic yield.



Anal. Calc. for C₆₆H₅₈BF₂₄OPPt: C, 50.82; H, 3.75. **Found:** C, 50.9; H, 3.6.

IR (Nujol): $\bar{\nu}(\text{CO}) = 2127 \text{ cm}^{-1}$.

¹H NMR (500 MHz, 25 °C, CD₂Cl₂): δ 7.77 (d, 2 H, ³J_{HH} = 7.9 Hz, *m*-Dipp), 7.72 (s, 8 H, *o*-BAr_F), 7.64 (t, 1 H, ³J_{HH} = 7.6 Hz, *p*-C₆H₃), 7.56 (s, 4 H, *p*-BAr_F), 7.52 (t, 1 H, ³J_{HH} = 8.0 Hz, *p*-Dipp'), 7.48 (t, 1 H, ³J_{HH} = 8.0 Hz, *p*-Dipp), 7.39 (dd, 1 H, ³J_{HH} = 7.6 Hz, ⁴J_{HP} = 3.2 Hz, *m*-C₆H₃), 7.34 (d, 2 H, ³J_{HH} = 7.8 Hz, *m*-Dipp'), 6.82 (dd, 1 H, ³J_{HH} = 8.0 Hz, ⁴J_{HP} = 3.0 Hz, *m*-C₆H₃), 2.40 (hept, 2 H, ³J_{HH} = 7.0 Hz, CH-Dipp), 2.30 (hept, 2 H, ³J_{HH} = 6.9 Hz, CH-Dipp), 1.55 (d, 6 H, ³J_{HH} = 6.9 Hz, Me-Dipp), 1.44 (d, 6 H, ²J_{HP} = 11.2 Hz, ³J_{HPt} = 45.5 Hz, PMe₂), 1.31 (d, 6 H, ³J_{HH} = 6.9 Hz, Me-Dipp), 1.04 (d, 6 H, ³J_{HH} = 7.1 Hz, Me-Dipp), 1.02 (d, 6 H, ³J_{HH} = 6.8 Hz, Me-Dipp), 0.94 (d, 3 H, ³J_{HP} = 5.9 Hz, ²J_{HPt} = 81.0 Hz, Pt-Me) ppm.

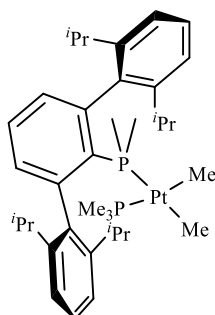
¹³C{¹H} NMR (125.72 MHz, 25 °C, CD₂Cl₂): δ 180.9 (d, ²J_{CP} = 142 Hz, CO), 153.8 (s, *o*-Dipp'), 147.5 (s, *o*-Dipp), 143.5 (d, J_{CP} = 22 Hz), 134.5 (s,

p-Dipp), 134.4 (d, $^3J_{\text{CP}} = 7$ Hz, *m*-C₆H₃), 133.5 (s, *p*-C₆H₃), 132.4 (d, $^3J_{\text{CP}} = 13$ Hz, *m*-C₆H₃), 131.2 (s, *p*-Dipp'), 128.4 (s), 126.8 (s, *m*-Dipp), 126.3 (s), 124.1 (s), 124.0 (s, *m*-Dipp'), 34.1 (s, CH-Dipp), 32.0 (s, CH-Dipp), 26.5 (s, Me-Dipp), 25.3 (s, Me-Dipp), 24.5 (s, Me-Dipp), 21.7 (s, Me-Dipp), 12.4 (d, $^1J_{\text{CP}} = 41$ Hz, $^2J_{\text{CPt}} = 45$ Hz, PMe₂), -11.3 (d, $^2J_{\text{CP}} = 5$ Hz, Pt-Me) ppm.

$^{31}\text{P}\{^1\text{H}\}$ NMR (202.40 MHz, 25 °C, CD₂Cl₂): δ 10.4 (s, $^1J_{\text{Pt}} = 3232$ Hz) ppm.

Synthesis and Characterisation of Complex [PtMe₂(PMe₃)(PMe₂Ar^{Dipp}₂)], 8-PMe₃

Phosphine-dimethyl-platinum(II) complex **8** (30 mg, 0.04mmol) was placed in an ampoule under nitrogen and dissolved in dichloromethane (2mL). PMe₃(4.2 μL, 0.04 mmol) was added at room temperature. After 3 hours of stirring at room temperature, all volatiles were removed under vacuum affording the product as a pale yellow solid.



Anal. Calc. for C₃₇H₅₈P₂Pt: C, 58.5; H, 7.7. **Found:** C, 58.6; H, 7.9.

¹H NMR (400 MHz, 25 °C, CD₂Cl₂): δ 7.33 (t, 2H, ³J_{HH} = 7.7 Hz, *p*-Dipp), 7.32 (t, 1H, ³J_{HH} = 7.8 Hz, *p*-C₆H₃), 7.19 (d, 4H, ³J_{HH} = 7.7 Hz, *m*-Dipp), 7.09 (dd, 2H, ³J_{HH} = 7.5 Hz, ⁴J_{PH} = 2.4 Hz, *m*-C₆H₃), 2.80 (hept, 4H, ³J_{HH} = 6.9 Hz, CH-Dipp), 1.33 (d, 12H, ³J_{HH} = 6.7 Hz, Me-Dipp), 1.15 (d, 6H, ²J_{PH} = 7.6 Hz, ³J_{PtP} = 23.4 Hz, PMe₂), 0.97 (d, 9H, ²J_{PH} = 8 Hz, ³J_{PtH} = 20.3 Hz, PMe₃), 0.96 (d, 12H, ³J_{HH} = 6.5 Hz, Me-Dipp), 0.13 (dd, 3H, ³J_{PH} = 9.0 Hz, ³J_{PH} = 7.3 Hz, ²J_{PtH} = 68 Hz, Pt-Me), 0.04 (dd, 3H, ³J_{PH} = 9.6 Hz, ³J_{PH} = 7.2 Hz, ²J_{PtH} = 66 Hz, Pt-Me) ppm.

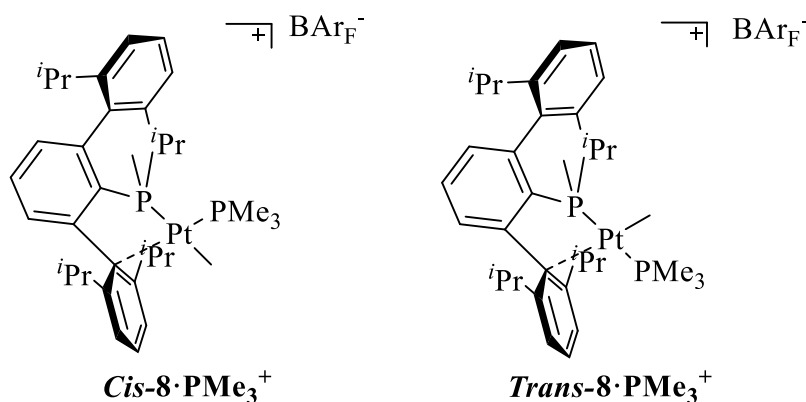
¹³C{¹H} NMR (100.6 MHz, 25°C, CD₂Cl₂): δ 148.0 (s, *o*-Dipp), 144.8 (d, J_{CP} = 9 Hz, *o*-C₆H₃), 140.7 (d, J_{CP} = 3 Hz, C_{ipso}-Dipp), 133.1 (d, ³J_{CP} = 7 Hz, *m*-C₆H₃), 128.9 (s, *p*-Dipp), 126.8 (d, J_{CP} = 2 Hz, *p*-C₆H₃), 123.0 (s, *m*-Dipp), 31.3 (s, CH-Dipp), 26.3 (s, Me-Dipp), 23.0 (s, Me-Dipp), 20.0 (dd, ¹J_{CP} = 28 Hz, ³J_{PC} = 3 Hz, ²J_{CPt} = 25 Hz, PMe₃), 16.9 (dd, J_{CP} = 28 Hz, ³J_{PC} = 2 Hz, ²J_{CPt} = 27 Hz, PMe₂), 2.0 (dd, ²J_{PC} = 40.9 Hz, ²J_{PC} = 8.2 Hz, Pt-Me), 1.0 (dd, ²J_{PC} = 35 Hz, ²J_{PC} = 8 Hz, Pt-Me) ppm.

³¹P{¹H} NMR (161.9 MHz, 25°C, CD₂Cl₂): δ -22.5 (d, ³J_{PP} = 10 Hz, ¹J_{PtP} = 1866 Hz), -6.7 (d, ³J_{PP} = 10 Hz, ¹J_{PtP} = 1803 Hz) ppm.

Synthesis and Characterisation of Complex *cis*- and *trans*-[PtMe(PMe₃)(PMe₂Ar^{Dipp}₂)] [BAr_F], *cis*- and *trans*-8·PMe₃⁺

Complex **8·PMe₃** (56 mg, 0.073 mmol) and [H(Et₂O)₂][BAr_F] (1.1 eq, 80 mg, 0.08 mmol) were dissolved in dry CH₂Cl₂ at -50°C. The reaction mixture was allowed to reach the room temperature overnight. All volatiles were removed under vacuum and the solid residue was washed with pentane (3 x 5 mL) obtaining the mixture of products in a *ca.* 1:1 molar ratio as a pale yellow solid. Small amounts of the *cis* isomer could be crystallized from dichloromethane: hexane (1:1 by vol.) mixture at -20 °C. (59 mg, 50%)

The NMR characterisation was performed using a 1:1 mixture of both isomers. Only the ¹H and ¹³C NMR resonances due to the Pt-Me groups of the two isomers are provided.



Anal. Calc. for C₆₈H₆₇BF₂₄P₂Pt: C, 50.79; H, 4.20. **Found:** C, 50.5; H, 4.1.

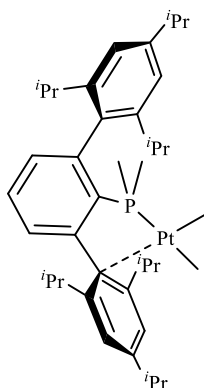
¹H NMR (400 MHz, 25 °C, CD₂Cl₂): δ 0.69 (dd, ³J_{HP} = 9.1 Hz, ³J_{HP} = 6.9 Hz, ²J_{HPt} = 81.9 Hz, Pt-Me *trans* isomer), -1.04 (dd, ³J_{HP} = 6.5 Hz, ³J_{HP} = 2.7 Hz, ²J_{HPt} = 29.7 Hz, Pt-Me *cis* isomer) ppm.

¹³C{¹H} NMR (100.6 MHz, 25 °C, CD₂Cl₂): δ 27.5 (dd, ²J_{CP} = 75.6 Hz, ²J_{CP} = 11.0 Hz, Pt-Me *cis* isomer), -6.2 (dd, ²J_{PC} = 6.6 Hz, ²J_{PC} = 5.7 Hz, ¹J_{CPt} = 713.3 Hz, Pt-Me *trans* isomer) ppm.

$^{31}\text{P}\{^1\text{H}\}$ NMR (161.9 MHz, 25 °C, CD_2Cl_2): δ 24.39 (d, $^2J_{\text{PP}} = 12.6$ Hz, $^1J_{\text{PPt}} = 2072.7$ Hz) and -17.3 (d, $^2J_{\text{PP}} = 12.6$ Hz, $^1J_{\text{PPt}} = 4529.9$ Hz) ppm for the *cis* isomer; 20.55 (d, $^2J_{\text{PP}} = 412.6$ Hz, $^1J_{\text{PPt}} = 2824.1$ Hz) and -17.3 (d, $^2J_{\text{PP}} = 412.7$ Hz, $^1J_{\text{PPt}} = 2680.7$ Hz) ppm for the *trans* isomer.

Synthesis and Characterisation of Complex *cis*-[PtMe₂(PMe₂Ar^{Tipp}₂)], **9**

A mixture of [Pt(Me)₂(μ-SMe₂)]₂ and Pt(Me)₂(SMe₂)₂ (300 mg, 0.96 mmol based on Pt) and **L**₃ (520 mg, 0.96 mmol) was dissolved in CH₂Cl₂ (5 mL). After stirring at room temperature overnight, the volatiles were removed under vacuum and the solid residue was extracted with hexane (3 x 15 mL). The volatiles were removed under reduced pressure to obtain **9** as a yellow powder. For further purification the complex was crystallized from a saturated hexane solution at -23 °C, providing an analytically pure sample of the product (287 mg, 39%).



Anal. Calc. for C₄₀H₆₁PPt: C, 62.56; H, 8.01. **Found:** C, 62.3; H, 7.7.

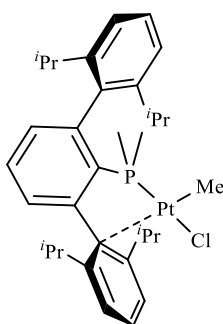
¹H NMR (500 MHz, 25 °C, CD₂Cl₂): 7.32 (td, 1 H, ⁵J_{HP} = 1.8 Hz, ³J_{HH} = 7.5 Hz, *p*-C₆H₃), 7.11 (s, 2 H, *m*-Tipp), 7.09 (d, 1 H, ³J_{HH} = 7.4 Hz, *m*-C₆H₃), 6.86 (s, 2 H, *m*-Tipp'), 6.70 (d, 1 H, ³J_{HH} = 7.0 Hz, *m*-C₆H₃), 3.06 (hept, 1 H, ³J_{HH} = 6.7 Hz, *p*-CH-Tipp), 2.97 (hept, 1 H, ³J_{HH} = 6.8 Hz, *p*-CH-Tipp), 2.48 (hept, 2 H, ³J_{HH} = 6.7 Hz, *o*-CH-Tipp), 2.22 (hept, 2 H, ³J_{HH} = 6.7 Hz, *o*-CH-Tipp), 1.41 (d, 6 H, ³J_{HH} = 6.7 Hz, *p*-Me-Tipp), 1.34 (d, 6 H, ³J_{HH} = 6.8 Hz, *o*-Me-Tipp), 1.31 (d, 6 H, ³J_{HH} = 6.9 Hz, *p*-Me-Tipp), 1.28 (d, 6 H, ³J_{HH} = 6.6 Hz, *o*-Me-Tipp), 1.19 (d, 6 H, ²J_{CP} = 8.1 Hz, ³J_{HPt} = 27.2 Hz, PMe₂), 0.99 (d, 6 H, ³J_{HH} = 6.4 Hz, *o*-Me-Tipp), 0.88 (d, 6 H, ³J_{HH} = 6.5 Hz, *o*-Me-Tipp), 0.55 (d, 3 H, ³J_{HP} = 8.7 Hz, ²J_{HPt} = 101.3 Hz, Pt-Me *cis* to P), -1.08 (d, 3 H, ³J_{HP} = 8.7 Hz, ²J_{HPt} = 50.8 Hz, Pt-Me *trans* to P) ppm.

$^{13}\text{C}\{^1\text{H}\}$ NMR (125.7 MHz, 25 °C, CD_2Cl_2): 152.4 (s, *p*-Tipp'), 150.1 (s, *p*-Tipp), 148.6 (s, *o*- C_6H_3), 147.3 (s, *o*-Tipp), 145.9 (s, *o*- C_6H_3), 142.8 (s, *o*-Tipp'), 141.5 (d, $^1J_{\text{CP}} = 35.0$ Hz, $\text{C}_{\text{ipso}}\text{-C}_6\text{H}_3$), 135.5 (s, $\text{C}_{\text{ipso}}\text{-Tipp}$), 132.6 (s, *m*- C_6H_3), 132.5 (s, *m*- C_6H_3), 129.8 (s, *p*- C_6H_3), 121.3 (s, *m*-Tipp'), 121.2 (s, *m*-Tipp), 116.9 (s, $\text{C}_{\text{ipso}}\text{-Tipp}'$), 35.0 (s, *p*-CH-Tipp), 34.7 (s, *p*-CH-Tipp), 33.5 (s, *o*-CH-Tipp), 31.6 (s, *o*-CH-Tipp), 26.6 (s, *o*-Me-Tipp), 26.0 (s, *p*-Me-Tipp), 24.5 (s, *o*-Me-Tipp), 24.5 (s, *o*-Me-Tipp), 24.3 (s, *p*-Me-Tipp), 23.1 (d, $^2J_{\text{CP}} = 108$ Hz, Pt-Me *trans* to P), 21.95 (s, *o*-Me-Tipp), 12.62 (d, $^1J_{\text{CP}} = 29$ Hz, $^2J_{\text{CPt}} = 39$ Hz, PMe_2), -12.54 (s, $^2J_{\text{CPt}} = 910$ Hz, Pt-Me *cis* to P) ppm.

$^{31}\text{P}\{^1\text{H}\}$ NMR (202.40 MHz, 25 °C, CD_2Cl_2): 19.0 (s, $^1J_{\text{PPt}} = 2036$ Hz) ppm.

Synthesis and Characterisation of Complex [PtMeCl(PMe₂Ar^{Dipp}₂)], 10

A solution of HCl 1M in Et₂O (0.15 mL, 0.15 mmol) was added to a solution of complex **8** (100 mg, 0.15 mmol) in dichloromethane at room temperature. The reaction mixture was stirred for 3 hours and then all volatiles were removed under vacuum. Crystallization from toluene/pentane mixtures under nitrogen at -23°C provided analytically pure samples of the product (60 mg, 73%).



Anal. Calc. for C₃₃H₄₆ClPPt: C, 56.3; H, 6.6. **Found:** C, 56.0; H, 6.8.

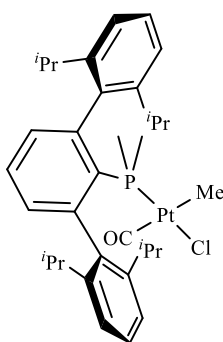
¹H NMR (300 MHz, 25 °C, CDCl₃): δ 7.74 (t, 1 H, *J*_{HH} = 7.5 Hz, H_{ar}), 7.43 (m, 2 H, H_{ar}), 7.27 (m, 3 H, H_{ar}), 7.19 (d, br, 3 H, *J*_{HH} 7.7 Hz, H_{ar}), 6.82 (d, 1 H, *J*_{HH} = 6.7 Hz, H_{ar}), 2.47 (hept, 2 H, ³*J*_{HH} = 6.9 Hz, CH-Dipp'), 2.37 (hept, 2 H, ³*J*_{HH} = 6.3 Hz, CH-Dipp), 1.50 (d, 6H, ³*J*_{HH} = 5.8 Hz, Me-Dipp), 1.40 (d, 6 H, ²*J*_{PH} = 10.8 Hz, PMe₂), 1.31 (d, 6 H, ³*J*_{HH} = 6.4 Hz, Me-Dipp'), 1.02 (d, 6 H, ³*J*_{HH} = 5.9 Hz, Me-Dipp'), 0.96 (d, 6 H, ³*J*_{HH} = 6.3 Hz, Me-Dipp), 0.87 (d, 3 H, ²*J*_{PH} = 86 Hz, ³*J*_{PH} = 4.3 Hz, Pt-Me) ppm.

¹³C{¹H} NMR (75.4 MHz, 25 °C, CDCl₃): δ 147.7 (s, *o*-Dipp), 147.2 (s, *o*-C₆H₃), 147.1 (s, *o*-Dipp'), 143.8 (s, *o*-C₆H₃), 136.7 (s, C_{ipso}-Dipp), 133.4 (s, *p*-Dipp), 132.4 (s, *m*-C₆H₃), 131.6 (s, *m*-C₆H₃), 130.0 (s, *p*-C₆H₃), 129.6 (s, *p*-Dipp'), 126.0 (s), 124.4 (s, *m*-Dipp), 123.0 (s, *m*-Dipp'), 121.7 (s, C_{ipso}-Dipp'), 32.6 (s, CH-Dipp), 31.2 (s, CH-Dipp'), 26.3 (s, Me-Dipp'), 24.5 (s, Me-Dipp), 23.9 (s, Me-Dipp), 21.6 (s, Me-Dipp'), 13.4 (d, ¹*J*_{PC} = 42 Hz, PMe₂), -11.3 (d, ¹*J*_{PtC} = 771 Hz, ²*J*_{PC} = 6 Hz, Pt-Me) ppm.

³¹P{¹H} NMR (121.4 MHz, 25 °C, CDCl₃): δ 0.4 (¹*J*_{PtP} = 4300 Hz) ppm.

Synthesis and Characterisation of Complex [PtMeCl(CO)(PMe₂Ar^{Dipp}₂)], **10**·CO

In a Young NMR tube complex **10** (30 mg, 0.04 mmol) was dissolved in CD₂Cl₂ (0.6 ml). The system was degassed (3 freeze-pump-thaw cycles) and charged with CO (2 atm) at room temperature. After 4 hours the sample was analysed by NMR spectroscopy. Then all volatiles were removed under vacuum and the product was obtained as a white powder (30 mg, 96%).



Anal. Calcd. for C₃₄H₄₆ClO₂Pt: C, 55.8; H, 6.3. **Found:** C, 55.3; H, 6.5.

IR (Nujol): $\bar{\nu}(\text{CO}) = 2092 \text{ cm}^{-1}$.

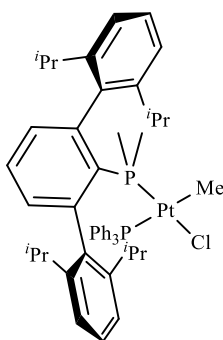
¹H NMR (400 MHz, 25 °C, CD₂Cl₂): δ 7.54 (t, 2 H, ³*J*_{HH} = 7.7 Hz, *p*-C₆H₃), 7.46 (t, 2 H, ³*J*_{HH} = 7.7 Hz, *p*-Dipp), 7.26-7.33 (m, 6 H, *m*-H_{ar}), 2.58 (hept, 4 H, ³*J*_{HH} = 7.0 Hz, CH-Dipp), 1.44 (d, 6 H, ²*J*_{HP} = 11 Hz, ³*J*_{HPt} = 54.1 Hz, PMe₂), 1.39 (d, 12 H, ³*J*_{HH} = 7.0 Hz, Me-Dipp), 1.02 (d, 12 H, ³*J*_{HH} = 7.0 Hz, Me-Dipp), 0.50 (d, 3 H, ³*J*_{HP} = 6.2 Hz, ²*J*_{HPt} = 56.3 Hz, Pt-Me) ppm.

¹³C{¹H} NMR (96.6 MHz, 25 °C, CD₂Cl₂): δ 178.1 (d, ²*J*_{CP} = 5 Hz, ¹*J*_{CPt} = 993 Hz, CO), 147.7 (s, *o*-Dipp), 144.9 (d, ²*J*_{CP} = 10 Hz, ³*J*_{CPt} = 23 Hz, *o*-C₆H₃), 139.1 (d, ³*J*_{CP} = 4 Hz, C_{ipso}-Dipp), 134.1 (d, ³*J*_{CP} = 9 Hz, *m*-C₆H₃), 130.0 (s, *p*-Dipp), 129.4 (d, ⁴*J*_{CP} = 2 Hz, *p*-C₆H₃), 126.4 (d, ¹*J*_{CP} = 58 Hz, ²*J*_{CPt} = 64 Hz, C_{ipso}-C₆H₃), 123.9 (s, *m*-Dipp), 31.7 (s, CH-Dipp), 26.5 (s, CH₃-Dipp), 22.8 (s, Me-Dipp), 19.5 (d, ¹*J*_{CP} = 43 Hz, ²*J*_{CPt} = 44 Hz, PMe₂), 5.0 (d, ²*J*_{CP} = 8 Hz, ¹*J*_{CP} = 505 Hz, Pt-Me) ppm.

³¹P{¹H} NMR (161.9 MHz, 25 °C, CD₂Cl₂): δ -18.2 (s, ¹*J*_{PPt} = 3938 Hz) ppm.

Synthesis and Characterisation of Complex [PtMeCl(PPh₃)(PMe₂Ar^{Dipp}₂)], 10-PPh₃

Complex **10** (30 mg, 0.042 mmol) and triphenylphosphine (11 mg, 0.042 mmol) were dissolved in dichloromethane (2 mL) at room temperature. The reaction mixture was stirred overnight. All volatiles were removed under vacuum to obtain the product as a yellow solid.



Anal. Calc. for C₅₁H₆₁ClP₂Pt: C, 63.4; H, 6.4. **Found:** C, 63.2; H, 6.3.

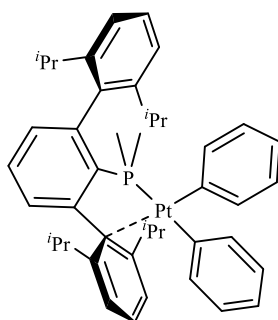
¹H NMR (500 MHz, 25 °C, CD₂Cl₂): δ 7.26-7.43 (m, 20 H, H_{ar}), 7.14-7.18 (m, 4 H, H_{ar}), 3.09 (hept, 2 H, ³J_{HH} = 6.6 Hz, CH-Dipp), 2.30 (hept, 2 H, ³J_{HH} = 6.7 Hz, CH-Dipp), 1.59 (d, 6 H, ³J_{HH} = 6.7 Hz, Me-Dipp), 1.19 (d, 6 H, ³J_{HH} = 6.6 Hz, Me-Dipp), 1.09 (d, 6 H, ³J_{HH} = 6.8 Hz, Me-Dipp), 0.87 (d, 6 H, ²J_{HP} = 10.5 Hz, ³J_{HPt} = 49.4 Hz, PMe₂), 0.75 (d, 6 H, ³J_{HH} = 6.6 Hz, Me-Dipp), 0.65 (dd, 3 H, ³J_{HP} = 5.4 Hz, ³J_{HP} = 7.2 Hz, ²J_{HPt} = 52.2 Hz, Pt-Me) ppm.

¹³C{¹H} NMR (125.7 MHz, 25 °C, CD₂Cl₂) δ: 148.2 (s, *o*-Dipp), 147.6 (s, *o*-Dipp), 140.1 (s, C_{ipso}-Dipp), 135.2 (d, ²J_{CP} = 11 Hz, *o*-C₆H₃), 134.3 (s), 134.2(s), 133.5 (d, ⁴J_{CP} = 8 Hz, *p*-C₆H₃), 130.1 (s), 129.4 (s), 129.3 (s), 129.0 (d, J_{CP} = 4 Hz), 128.4 (d, ³J_{CP} = 10 Hz, *m*-C₆H₃), 128.1 (s), 124.7 (s, *m*-Dipp), 122.6 (s, *m*-Dipp), 31.8 (s, CH-Dipp), 31.4 (s, CH-Dipp), 27.2 (s, Me-Dipp), 25.8 (s, Me-Dipp), 24.4 (s, Me-Dipp), 21.8 (s, Me-Dipp), 19.2 (d, ¹J_{CP} = 39 Hz, ²J_{CPt} = 39 Hz, PMe₂), 5.9 (dd, ²J_{CP} = 93 Hz, ²J_{CP} = 8 Hz, Pt-Me) ppm.

³¹P{¹H} NMR (202.4 MHz, 25 °C, CD₂Cl₂): δ 24.6 (d, ²J_{PP} = 9 Hz, ¹J_{PPt} = 1775 Hz), -17.6 (d, ²J_{PP} = 9 Hz, ¹J_{PPt} = 4352 Hz) ppm.

Synthesis and Characterisation of Complex *cis*-[Pt(PMe₂Ar^{Dipp}₂)Ph₂], 11

A mixture of [Pt(Ph)₂(μ-SMe₂)]₂ and Pt(Ph)₂(SMe₂)₂ (40 mg, 0.095 mmol based on Pt) and **L**₂ (43.8 mg, 0.095 mmol) were dissolved in CH₂Cl₂ (2 mL). After stirring at room temperature for 4 hours the volatiles were removed under vacuum and the residue was washed with pentane (2 x 5mL) to yield the product as a yellow powder. (77 mg, 65%).



Anal. Calc. for C₄₄H₅₃PPt: C, 65.4; H, 6.6. **Found:** C, 64.9; H, 7.1.

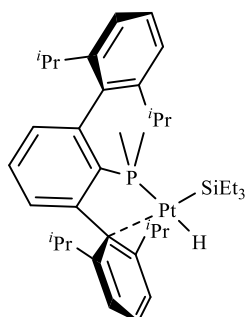
¹H NMR (300 MHz, 25 °C, CD₂Cl₂): δ 7.34-7.45 (m, 3 H, *m*-C₆H₅ and *p*-Dipp'), 7.22 (d, 2 H, ³*J*_{HH} = 7.7 Hz, *m*-Dipp'), 7.15 (m, 1 H, *p*-C₆H₅), 7.12 (d, 2 H, ³*J*_{HH} = 7.4 Hz, ³*J*_{HPt} = 93.0 Hz, *o*-C₆H₅), 6.88 (d, 2 H, ³*J*_{HH} = 7.7 Hz, *m*-Dipp), 6.66-6.82 (m, 6 H, *m*-C₆H₅, *o*-C₆H₅ and *m*-C₆H₃), 6.53-6.63 (m, 2 H, *p*-C₆H₅ and *p*-C₆H₃), 6.38 (t, 1 H, ³*J*_{HH} = 7.6 Hz, *p*-Dipp), 2.49 (hept, 2 H, ³*J*_{HH} = 7.0 Hz, CH-Dipp), 2.44 (hept, 2 H, ³*J*_{HH} = 7.0 Hz, CH-Dipp), 1.84 (d, 6 H, ³*J*_{HH} = 6.9 Hz, Me-Dipp), 1.29 (d, 6 H, ³*J*_{HH} = 6.7 Hz, Me-Dipp), 1.01 (d, 6 H, ³*J*_{HH} = 6.7 Hz, Me-Dipp), 0.98 (d, 6 H, ³*J*_{HH} = 7.3 Hz, Me-Dipp), 0.94 (d, ²*J*_{HP} = 9.4 Hz, 6 H, ³*J*_{HPt} = 27.6 Hz, PMe₂) ppm.

¹³C{¹H} NMR (75.4 MHz, 25 °C, CD₂Cl₂): δ 147.6 (s, *o*-Dipp'), 143.1 (s, *o*-Dipp), 140.4 (s), 137.3 (s, C_{ipso}-Dipp'), 136.0 (d, ³*J*_{CP} = 3 Hz, ²*J*_{CPt} = 47 Hz, *o*-C₆H₅), 132.8 (d, ⁵*J*_{CP} = 4 Hz, *p*-C₆H₅), 132.2 (d, ⁴*J*_{CP} = 14 Hz, *m*-C₆H₅), 130.6 (s, *p*-Dipp), 130.4 (s), 130.4 (s), 129.6 (s, *p*-Dipp'), 127.5 (s), 126.9 (s, *m*-C₆H₃), 126.8 (s, *m*-C₆H₃), 125.5 (s, *m*-Dipp), 123.4 (s, *m*-Dipp'), 121.5 (s, C_{ipso}-Dipp), 121.1 (s, *p*-C₆H₃), 33.4 (s, CH-Dipp), 31.6 (s, CH-Dipp), 26.6 (s, Me-Dipp), 25.3 (s, Me-Dipp), 24.5 (s, Me-Dipp), 21.9 (s, Me-Dipp), 11.8 (d, ¹*J*_{CP} = 33 Hz, ²*J*_{CPt} = 38 Hz, PMe₂) ppm.

³¹P{¹H} NMR (121.4 MHz, 25 °C, CD₂Cl₂): δ 12.8 (s, ¹*J*_{PPt} = 1930 Hz) ppm.

Synthesis and Characterisation of Complex [Pt(PMe₂Ar^{Dipp}₂)H(SiEt₃)], **12a**

Complex **8** (200 mg, 0.29 mmol) was dissolved in benzene (8 mL) and SiHEt₃ (95 μ L) was added at room temperature. After 30 min of stirring, all volatiles were removed under vacuum. The residue was redissolved in the minimum amount of Et₂O and kept in the fridge at -23 °C to induce the precipitation of **12a** as a brown crystalline solid (168 mg, 75%).



Anal. Calc. for C₃₈H₅₉PPtSi: C, 59.3; H, 7.7. **Found:** C, 59.2; H, 8.0.

¹H NMR (300 MHz, 25°C, C₆D₆): δ 7.35 (br, 4 H, H_{ar}), 7.05 (br, 2 H, H_{ar}), 6.76 (br, 2 H, H_{ar}), 6.87 (t, 1 H, ³J_{HH} = 7.5 Hz, H_{ar}), 2.52 (hept, 4 H, ³J_{HH} = 6.6 Hz, CH-Dipp), 1.44 (br, 12 H, Me-Dipp), 1.40 (d, 6 H, ²J_{HP} = 7.7 Hz, ³J_{HPt} = 39.0 Hz, PMe₂), 1.23 (t, 9 H, ³J_{HH} = 8 Hz, CH₃-CH₂-Si), 0.89 (d, 12 H, ³J_{HH} = 6.6 Hz, Me-Dipp), 0.85 (q, 6 H, ³J_{HH} = 7.7 Hz, CH₂-Si), -1.47 (d, 1 H, ²J_{HP} = 172.0 Hz, ¹J_{HPt} = 1008.0 Hz, H-Pt) ppm.

¹H NMR (400 MHz, -60°C, CD₂Cl₂): δ 7.62 (d, 2 H, ³J_{HH} = 7.7 Hz, *m*-Dipp), 7.40 (t, 1 H, ³J_{HH} = 7.8 Hz, *p*-Dipp'), 7.36 (t, 1 H, ³J_{HH} = 7.2 Hz, *p*-C₆H₃), 7.23 (d, 2 H, ³J_{HH} = 7.8 Hz, *m*-Dipp'), 7.09 (d, 1 H, ³J_{HH} = 7.7 Hz, *m*-C₆H₃), 6.84 (t, 1 H, ³J_{HH} = 7.5 Hz, *p*-Dipp), 6.80 (d, 1 H, ³J_{HH} = 7.5 Hz, *m*-C₆H₃), 2.40 (hept, 2 H, ³J_{HH} = 6.4 Hz, CH-Dipp), 2.29 (hept, 2 H, ³J_{HH} = 6.7 Hz, CH-Dipp), 1.49 (d, 6 H, ³J_{HH} = 6.5 Hz, Me-Dipp), 1.27 (d, 6 H, ³J_{HH} = 8.3 Hz, Me-Dipp), 1.23 (d, 6 H, ³J_{HH} = 6.5 Hz, Me-Dipp), 0.94 (d, 6 H, ³J_{HH} = 5.3 Hz, Me-Dipp), 0.68 (t, 9 H, ³J_{HH} = 7.6 Hz, CH₃CH₂-Si), 0.31 (q, 6 H, ³J_{HH} = 7.3 Hz, CH₂-Si), -2.14 (d, 1 H, ²J_{HP} = 166.5 Hz, ¹J_{HPt} = 1007 Hz, Pt-H) ppm.

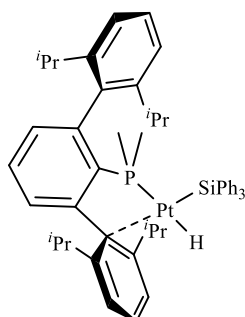
¹³C{¹H} NMR (75.4 MHz, C₆D₆, 25°C): δ 145.9 (s), 134.4 (s), 132.2 (d, J_{CP} = 8 Hz), 129.2 (s), 129.0 (s), 32.3 (s, CH-Dipp), 25.5 (s, Me-Dipp), 23.4 (br, Me-Dipp), 17.0 (d, ¹J_{CP} = 28 Hz, ²J_{CPt} = 74 Hz, PMe₂), 11.4 (d,

$^3J_{\text{CP}} = 4 \text{ Hz}$, $^2J_{\text{CPt}} = 120 \text{ Hz}$, $\text{CH}_2\text{-Si}$), 10.2 (s, $^3J_{\text{CPt}} = 40 \text{ Hz}$, $\text{CH}_3\text{-CH}_2\text{-Si}$) ppm.

$^{31}\text{P}\{^1\text{H}\}$ NMR (121.4 MHz, C_6D_6 , 25°C): δ 24.4 (s, $^1J_{\text{PPt}} = 2390 \text{ Hz}$) ppm.

Synthesis and Characterisation of Complex [Pt(PMe₂Ar^{Dipp})H(SiPh₃)], 12b

Complex **8** (30 mg, 0.043 mmol) and SiHPh₃ (22.4 mg, 0.086 mmol) were dissolved in benzene (2 mL) at room temperature. After stirring overnight, all volatiles were removed under vacuum. The residue was washed with pentane (3 x 2 mL) obtaining the product as a dark brown solid (39 mg, 82%).



Anal. Calc. for C₅₀H₅₉PPtSi: C, 65.7; H, 6.5. **Found:** C, 65.2; H, 6.2.

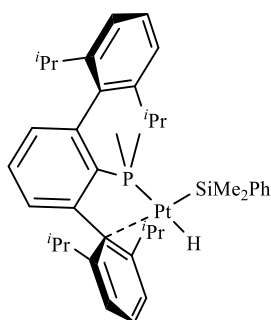
¹H NMR (400 MHz, −20 °C, Toluene-d₈): δ 7.87 (d, 6 H, ³J_{HH} = 7.3 Hz, *o*-Ph), 7.61 (d, 2 H, ³J_{HH} = 7.7 Hz, *m*-Dipp), 7.20 (t, 6 H, ³J_{HH} = 7.4 Hz, *m*-Ph), 7.00-7.15 (m, 5 H, *p*-Dipp, *p*-Ph and *m*-C₆H₃), 6.90 (d, 2 H, ³J_{HH} = 6.5 Hz, *m*-Dipp), 6.76 (t, 1 H, ³J_{HH} = 7.8 Hz, *p*-Dipp), 6.53 (d, 1 H, ³J_{HH} = 6.8 Hz, *m*-C₆H₃), 2.54 (hept, 2 H, ³J_{HH} = 6.6 Hz, CH-Dipp), 2.47 (hept, 2 H, ³J_{HH} = 6.6 Hz, CH-Dipp), 1.82 (d, 6 H, ³J_{HH} = 6.6 Hz, Me-Dipp), 1.08 (d, 6 H, ³J_{HH} = 6.6 Hz, Me-Dipp), 1.00 (d, 6 H, ²J_{HP} = 8.4 Hz, PMe₂), 0.94 (d, 6 H, ³J_{HH} = 6.4 Hz, Me-Dipp), 0.85 (d, 6 H, ³J_{HH} = 6.4 Hz, 6.88 (m, 1 H, *p*-C₆H₃), Me-Dipp), −1.67 (d, 1 H, ²J_{HP} = 163.2 Hz, ¹J_{HPt} = 888.0 Hz, Pt-H) ppm.

¹³C{¹H} NMR (120.8 MHz, −20°C, Toluene-d₈): δ 147.1 (s, *o*-Dipp), 143.6 (s, *o*-Dipp), 137.9 (s, *o*-Ph), 132.4 (s, *m*-C₆H₃), 131.5 (s, *p*-C₆H₃), 129.5 (s, *p*-Dipp), 128.4 (s, *p*-Ph), 127.7 (s, *m*-Ph), 126.9 (s, *m*-Dipp), 123.4 (s, *m*-Dipp), 33.7 (s, CH-Dipp), 31.8 (s, CH-Dipp), 26.7 (s, Me-Dipp), 25.8 (s, Me-Dipp), 25.2 (s, Me-Dipp), 22.0 (s, Me-Dipp), 15.1 (d, ¹J_{CP} = 29 Hz, PMe₂) ppm. (The unmentioned ¹³C peaks are masked by residual solvent signals).

$^{31}\text{P}\{^1\text{H}\}$ NMR (161.9 MHz, -20°C , Toluene- d_8): δ 25.4 (d, $^1J_{\text{PPt}} = 2544$ Hz) ppm.

Synthesis and Characterisation of Complex [Pt(PMe₂Ar^{Dipp2})H(SiPh₂Me)], **12c**

Complex **8** (40 mg, 0.06 mmol) was dissolved in benzene (2 mL), and SiHMe₂Ph (18.2 μ L, 0.12 mmol) was added at room temperature. After stirring overnight at room temperature, all volatiles were removed under vacuum. The residue was redissolved in the minimum amount of Et₂O and kept in the fridge at -23 °C to induce the precipitation of **12c** as a brown crystalline solid (37 mg, 80%).



Anal. Calc. for C₄₀H₅₅PPtSi: C, 60.8; H, 7.0. **Found:** C, 60.5; H, 7.2.

¹H NMR (400 MHz, 25 °C, C₆D₆): δ 7.74 (d, 2 H, $^3J_{\text{HH}} = 7.4$ Hz, H_{ar}), 7.30 (br, 3 H, H_{ar}), 7.18 (m, 3H, H_{ar}), 7.07 (t, 1 H, $^3J_{\text{HH}} = 7.0$ Hz, H_{ar}), 6.99 (br, 2 H, H_{ar}), 6.86 (t, 1 H, $^3J_{\text{HH}} = 7.5$ Hz, H_{ar}), 6.72 (br, 2 H, H_{ar}), 2.48 (hept, 4 H, $^3J_{\text{HH}} = 6.7$ Hz, CH-Dipp), 1.41 (br, 12 H, Me-Dipp), 1.17 (d, 6 H, $^2J_{\text{HP}} = 8.1$ Hz, $^3J_{\text{HPt}} = 39.1$ Hz, PMe₂), 0.88 (d, 12 H, $^3J_{\text{HH}} = 6.6$ Hz, Me-Dipp), 0.74 (s, 6 H, $^3J_{\text{HPt}} = 51.0$ Hz, SiMe₂), -1.25 (d, 1 H, $^2J_{\text{HP}} = 170.8$ Hz, $^1J_{\text{HPt}} = 1012.2$ Hz, Pt-H) ppm.

¹H NMR (400 MHz, -50 °C, CD₂Cl₂): δ 7.65 (d, 2 H, $^3J_{\text{HH}} = 7.7$ Hz, *m*-Dipp'), 7.34 (m, 2 H, *p*-C₆H₃ and *p*-Ph), 7.27 (d, 2 H, $^3J_{\text{HH}} = 6.7$ Hz, *o*-Ph), 7.17 (d, 2 H, $^3J_{\text{HH}} = 7.8$ Hz, *m*-Dipp), 7.10 (m, 3 H, *m*-Ph and *p*-Dipp), 7.03 (d, 1 H, $^3J_{\text{HH}} = 7.4$ Hz, *m*-C₆H₃), 6.85 (t, 1 H, $^3J_{\text{HH}} = 7.7$ Hz, *p*-Dipp'), 6.77 (d, 1 H, $^3J_{\text{HH}} = 7.2$ Hz, *m*-C₆H₃), 2.30 (hept, 6 H, $^3J_{\text{HH}} = 6.4$ Hz, CH-Dipp), 2.23 (hept, 2 H, $^3J_{\text{HH}} = 6.2$ Hz, CH-Dipp), 1.50 (d, 6 H, $^3J_{\text{HH}} = 6.8$ Hz, Me-Dipp), 1.15 (d, 6 H, $^3J_{\text{HH}} = 6.7$ Hz, Me-Dipp), 0.91 (d, 6 H, $^3J_{\text{HH}} = 7.1$ Hz, Me-Dipp), 0.88 (d, 6 H, $^3J_{\text{HH}} = 6.5$ Hz, Me-Dipp), 0.82 (d, 6 H, $^2J_{\text{HP}} = 8.2$ Hz, PMe₂), 0.15 (s, 6 H, SiMe₂), -2.16 (d, 1 H, $^2J_{\text{HP}} = 165.4$ Hz, $^1J_{\text{HPt}} = 1000.2$ Hz, Pt-H) ppm.

¹³C{¹H} NMR (120.8 MHz, -40 °C, CD₂Cl₂): δ 147.3 (s, C_{ipso}-Ph), 146.5 (s, *o*-Dipp), 144.9 (d, $^2J_{\text{CP}} = 32$ Hz, *o*-C₆H₃), 144.4 (s), 143.4 (s, *o*-Dipp),

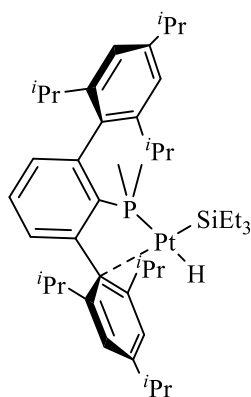
139.1 (d, $^1J_{\text{CP}} = 36$ Hz, $\text{C}_{\text{ipso}}\text{-C}_6\text{H}_3$), 137.0 (s, $\text{C}_{\text{ipso}}\text{-Dipp}'$), 133.2 (s, *o*-Ph), 131.2 (s, *m*- C_6H_3), 131.1 (s, *m*- C_6H_3), 129.4 (s), 128.7 (s), 128.0 (s, *p*-Dipp'), 126.9 (s, *p*-Dipp), 126.8 (s, $\text{C}_{\text{ipso}}\text{-Dipp}$), 125.2 (s, *m*-Dipp'), 122.4 (s, *m*-Dipp), 32.4 (s, CH-Dipp), 30.9 (s, CH-Dipp), 25.8 (s, Me-Dipp), 24.6 (s, Me-Dipp), 24.0 (s, Me-Dipp), 21.0 (s, Me-Dipp), 14.2 (d, $^1J_{\text{CP}} = 30$ Hz, PMe_2), 6.3 (s, SiMe_2) ppm.

$^{31}\text{P}\{^1\text{H}\}$ NMR (161.9 MHz, 25 °C, C_6D_6): δ 24.7 (s, $^1J_{\text{PPt}} = 2348$ Hz) ppm.

$^{31}\text{P}\{^1\text{H}\}$ NMR (202.5 MHz, 25 °C, CD_2Cl_2): δ 23.0 (s, $^1J_{\text{PPt}} = 2355$ Hz) ppm.

Synthesis and Characterisation of Complex [Pt(PMe₂Ar^{Tipp})₂H(SiEt₃)], **13**

Complex **9** (283 mg, 0.37 mmol) was dissolved in benzene (8 mL) and SiHEt₃ (116 μ L) was added at room temperature. After 30 min of stirring at room temperature, all volatiles were removed under vacuum. The residue was redissolved in the minimum amount of Et₂O and kept in the fridge at -23 °C to induce precipitation of **13** as a brown crystalline solid (224 mg, 70%).



¹H NMR (400 MHz, 25 °C, CD₂Cl₂): δ 7.45 (br, 3 H), 7.26 (d br, 2 H), 6.95 (br, 1 H), 6.89 (br, 1 H), 3.04 (hept, 2 H, ³J_{HH} = 6.7 Hz, *p*-CH-Tipp), 2.95 (hept, 2 H, ³J_{HH} = 6.6 Hz, *o*-CH-Tipp), 2.66 (hept, 2 H, ³J_{HH} = 6.8 Hz, *o*-CH-Tipp), 1.54 (br, 12 H, *p*-CH₃-Tipp), 1.52 (d, 6 H, ²J_{HP} = 7.8 Hz, PMe₂), 1.36 (d, 12 H, ³J_{HH} = 7.1 Hz, *o*-Me-Tipp), 1.27 (t, 9 H, ³J_{HH} = 7.8 Hz, CH₃-CH₂-Si), 1.06 (d, 12 H, ³J_{HH} = 6.7 Hz, *o*-Me-Tipp), 0.89 (q, 6 H, ³J_{HH} = 7.8 Hz, CH₂-Si), -1.30 (d, 1 H, ²J_{HP} = 171.6 Hz, ¹J_{HPt} = 1006.4 Hz, Pt-H) ppm.

¹H NMR (500 MHz, -50 °C, CD₂Cl₂): δ 7.35 (m, 2 H, *m*-Dipp), 7.31 (m, 1 H, *p*-C₆H₃), 7.07 (m, 1 H, *m*-C₆H₃), 7.04 (m, 2 H, *m*-Dipp'), 6.79 (m, 1 H, *m*-C₆H₃), 2.87 (m, 1 H, *p*-CH-Dipp), 2.80 (m, 1 H, *p*-CH-Dipp), 2.37 (m, 1 H, *o*-CH-Dipp), 2.25 (m, 1 H, *o*-CH-Dipp), 1.46 (m, 6 H, *p*-Me-Dipp), 1.21 (m, 18 H, *p*-Me-Dipp, *o*-Me-Dipp, PMe₂), 1.10 (m, 6 H, *p*-Me-Dipp), 0.90 (m, 12 H, *o*-Me-Dipp), 0.64 (m, 9 H, CH₃-CH₂-Si), 0.25 (m, 6 H, CH₃-CH₂-Si), -2.16 (d, 1 H, ²J_{HP} = 169.5 Hz, ¹J_{HPt} = 1003 Hz, Pt-H) ppm.

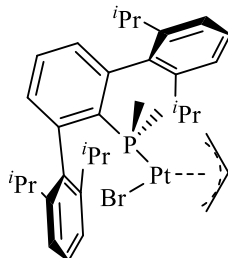
¹³C{¹H} NMR (125.7 MHz, -50 °C, CD₂Cl₂): δ 149.3 (s, *o*-Dipp), 148.0 (s, *p*-Dipp), 146.5 (s, C_{ipso}-Dipp), 146.2 (s, *o*-Dipp), 144.9 (s, *p*-Dipp), 143.3 (s, C_{ipso}-Dipp), 140.5 (d, ¹J_{CP} = 33 Hz, C_{ipso}-C₆H₃), 135.0 (s, *o*-

C₆H₃), 131.9 (s, *m*-C₆H₃), 131.3 (d, ³*J*_{CP} = 9 Hz, *m*-C₆H₃), 129.1 (s, *p*-C₆H₃), 126.8 (s, *o*-C₆H₃), 123.0 (s, *m*-Dipp), 120.4 (s, *m*-Dipp), 34.4 (s, *p*-CH-Dipp), 34.0 (s, *p*-CH-Dipp), 32.44 (s, *o*-CH-Dipp), 31.1 (s, *o*-CH-Dipp), 26.0 (s, *o*-Me-Dipp), 24.4 (s, *p*-Me-Dipp), 24.3 (s, *p*-Me-Dipp), 24.1 (s, *o*-Me-Dipp), 22.8 (s, *o*-Me-Dipp), 21.3 (s, *o*-Me-Dipp), 16.2 (d, ¹*J*_{PC} = 28 Hz, PMe₂), 9.9 (s, CH₃-CH₂-Si), 9.3 (s, CH₃-CH₂-Si) ppm.

³¹P{¹H} NMR (161.9 MHz, 25°C, CD₂Cl₂): δ 24.3 (s, ¹*J*_{Pt} = 2392 Hz) ppm.

Synthesis and Characterisation of Complex [Pt(PMe₂Ar^{Dipp2})Br(η³-C₃H₅)], **14**

- a) [PtCl₂(PMe₂Ar^{Dipp2})], **6**, (100 mg, 0.14 mmol) was dissolved in toluene (10 mL), the resulting solution was cooled at -50 °C and a solution containing a small excess (1.2 equiv) of Mg(C₃H₅)Br (0.17 mL, 1 M, 0.17 mmol) was added dropwise. The reaction mixture was allowed to warm to room temperature while stirring overnight. The suspension was filtered and the volatiles removed in vacuo. The product was extracted in pentane (2 x 5 mL), giving a yellow solid after evaporation of the solvent (48 mg, 44%).
- b) [Pt(C₂H₄)₂(PMe₂Ar^{Dipp2})], **1** from chapter II, (100 mg, 0.14 mmol) was dissolved in CH₂Cl₂ (5 mL). Avoiding the light, allyl bromide (12 μL, 0.14 mmol) was added and the reaction mixture was stirred overnight at room temperature. After removing all volatiles under vacuum, the residue was extracted in pentane (2 x 5 mL), to yield a yellow solid after removal of the solvent under vacuum (68 mg, 62%).



Anal. Calc. for C₃₅H₄₈BrPPt: C, 52.4; H, 5.9. **Found:** C, 52.1; H, 6.4.

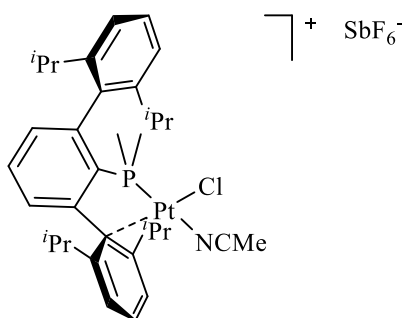
¹H NMR (400 MHz, 25 °C, CD₂Cl₂): δ 7.46 (td, 1 H, ⁵J_{HP} = 1.7 Hz, ³J_{HH} = 7.8 Hz, *p*-C₆H₃), 7.40 (t, 2 H, ³J_{HH} = 7.8 Hz, *p*-Dipp), 7.28 (d br, 2 H, ³J_{HH} = 7.1 Hz, *m*-Dipp), 7.26 (d, br, 2 H, ³J_{HH} = 7.2 Hz, *m*-Dipp), 7.22 (dd, 2 H, ⁴J_{HP} = 3.0 Hz, ³J_{HH} = 7.7 Hz, *m*-C₆H₃), 4.17 (m, 1 H, CH-allyl), 3.91 (t br, 1 H, ³J_{HH} = 6.3 Hz, ³J_{HP} = 5.3 Hz, *anti*-CH₂), 2.85 (hept, 2 H, ³J_{HH} = 6.7 Hz, CH-Dipp), 2.80 (hept, 2 H, ³J_{HH} = 6.7 Hz, CH-Dipp), 2.54 (m, 1 H, ³J_{HH} = 6.5 Hz, *syn*-CH₂), 2.44 (dd, 1 H, ³J_{HH} = 13.2 Hz, ³J_{HP} = 9.5 Hz, *anti*-CH₂), 1.47 (d, 3 H, ²J_{HP} = 10.5 Hz, ²J_{HPt} = 46 Hz, PMe), 1.42 (d, 6 H, ³J_{HH} = 6.7 Hz, Me-Dipp), 1.38 (d, 6 H, ³J_{HH} = 6.7 Hz, Me-Dipp), 1.35 (d, 3 H, ²J_{HP} = 10.8 Hz, ³J_{HPt} = 39.5 Hz, PMe), 1.34 (m, 1 H, *syn*-CH₂), 1.05 (d, 6 H, ³J_{HH} = 6.3 Hz, Me-Dipp), 1.03 (d, 6 H, ³J_{HH} = 6.2 Hz, Me-Dipp) ppm.

$^{13}\text{C}\{^1\text{H}\}$ NMR (96.6 MHz, 25 °C, CD_2Cl_2): δ 147.8 (s, *o*-Dipp), 147.7 (s, *o*-Dipp), 144.8 (d, $^2J_{\text{CP}} = 10$ Hz, $^3J_{\text{CPt}} = 21$ Hz, *o*- C_6H_3), 140.6 (d, $^3J_{\text{CP}} = 3$ Hz, C_{ipso} -Dipp), 133.8 (d, $^3J_{\text{CP}} = 8$ Hz, *m*- C_6H_3), 130.8 (d, $^1J_{\text{CP}} = 43$ Hz, C_{ipso} -P), 129.3 (s, *p*-Dipp), 128.2 (s, *p*- C_6H_3), 123.4 (s, *m*-Dipp), 123.3 (s, *m*-Dipp), 108.3 (s, $^1J_{\text{CPt}} = 47$ Hz, CH-allyl), 64.3 (d, $^2J_{\text{CP}} = 35$ Hz, $^1J_{\text{CPt}} = 53$ Hz, CH_2 transoid to P), 44.7 (s, $^1J_{\text{CPt}} = 259$ Hz, CH_2 cisoid to P), 31.6 (s, CH-Dipp), 31.4 (s, CH-Dipp), 26.3 (s, Me-Dipp), 26.3 (s, Me-Dipp), 23.6 (s, Me-Dipp), 23.5 (s, Me-Dipp), 19.4 (d, $^1J_{\text{CP}} = 37$ Hz, $^2J_{\text{CPt}} = 56$ Hz, PMe), 19.1 (d, $^1J_{\text{CP}} = 36$ Hz, $^2J_{\text{CPt}} = 37$ Hz, PMe) ppm.

$^{31}\text{P}\{^1\text{H}\}$ NMR (161.9 MHz, 25 °C, CD_2Cl_2): δ -10.0 (s, $^1J_{\text{PPt}} = 4370$ Hz) ppm.

Synthesis and Characterisation of [PtCl(NCMe)(PMe₂Ar^{Dipp2})]⁺[SbF₆]⁻, 15·NCMe

Platinum complex [PtCl₂(PMe₂Ar^{Dipp2})], **6**, (100 mg, 0.138 mmol) and AgSbF₆ (49.3 mg, 0.138 mmol) were dissolved in CH₂Cl₂ (2 mL) in an ampoule under N₂ at room temperature. After 30 min of stirring, the resulting suspension was filtered and dry acetonitrile (0.1 mL) was added. After removing all volatiles under vacuum the product was obtained as a yellow solid. Yield: 113 mg (85 %).



Anal. Calc. for C₃₄H₄₆ClF₆NPPtSb: C, 42.3; H, 4.8; N, 1.5. **Found:** C, 42.2; H, 5.0; N, 1.0.

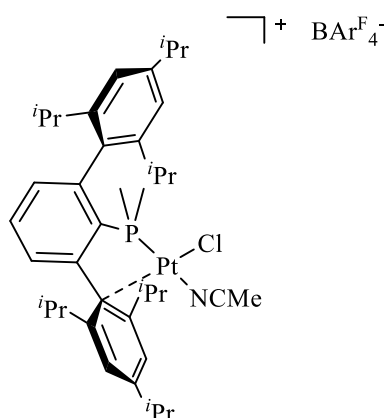
¹H NMR (500 MHz, 25 °C, CD₂Cl₂): δ 7.92 (t, 1 H, ³J_{HH} = 7.9 Hz, *m*-Dipp), 7.62 (td, 1 H, ³J_{HH} = 7.7 Hz, ⁵J_{HP} = 2.4 Hz, *p*-C₆H₃), 7.56 (d, 1 H, ³J_{HH} = 7.8 Hz, *p*-Dipp), 7.52 (t, 1 H, ³J_{HH} = 7.8 Hz, *p*-Dipp'), 7.33 (d, 2 H, ³J_{HH} = 7.7 Hz, *m*-Dipp'), 7.31 (m, 1 H, *m*-C₆H₃), 6.80 (dd, 1 H, ³J_{HH} = 7.7 Hz, ⁴J_{HP} = 2.8 Hz, *m*-C₆H₃), 2.39 (hept, 2 H, ³J_{HH} = 6.4 Hz, CH-Dipp), 2.27 (hept, 2 H, ³J_{HH} = 6.5 Hz, CH-Dipp), 2.26 (s, 3 H, CH₃CN), 1.70 (d, 6 H, ³J_{HH} = 6.8 Hz, Me-Dipp), 1.58 (d, 6 H, ²J_{HP} = 13.0 Hz, PMe₂), 1.30 (d, 6 H, ³J_{HH} = 6.7 Hz, Me-Dipp), 1.03 (d, 6 H, ³J_{HH} = 6.7 Hz, Me-Dipp), 1.01 (d, 6 H, ³J_{HH} = 6.6 Hz, Me-Dipp) ppm.

¹³C{¹H} NMR (125.7 MHz, 25 °C, CD₂Cl₂): δ 152.2 (s, *o*-Dipp), 147.5 (s, *o*-Dipp'), 145.4 (s), 145.3 (s), 145.1 (s), 139.0 (s, *m*-Dipp), 135.0 (s), 133.9 (d, ³J_{CP} = 8 Hz, *m*-C₆H₃), 133.2 (d, ⁴J_{CP} = 2 Hz, *p*-C₆H₃), 131.3 (d, ³J_{CP} = 14 Hz, *m*-C₆H₃), 131.0 (s, *p*-Dipp'), 127.2 (s, *p*-Dipp), 123.9 (s, *m*-Dipp'), 116.7 (s, CH₃CN), 34.9 (s, CH-Dipp), 31.8 (s, CH-Dipp), 26.6 (s, Me-Dipp), 25.8 (s, Me-Dipp), 24.0 (s, Me-Dipp), 21.7 (s, Me-Dipp), 13.7 (d, ¹J_{CP} = 47 Hz, PMe₂), 3.9 (s, CH₃CN) ppm.

³¹P{¹H} NMR (202.4 MHz, 25 °C, CD₂Cl₂): δ 7.5 (s, ¹J_{Pt} = 3335 Hz) ppm.

Synthesis and Characterisation of $[\text{PtCl}(\text{NCMe})(\text{PMe}_2\text{Ar}^{\text{Tipp}_2})][\text{BAr}_\text{F}^-]$, **16-NCMe**

In an ampoule kept under N_2 , the Pt(II) chloride complex **7** (25 mg, 0.031 mmol) and $\text{Na}[\text{BAr}_\text{F}]$ (27.4 mg, 0.031 mmol) were dissolved in CH_2Cl_2 at -80°C . The reaction mixture was allowed to reach room temperature overnight. After that, it was filtered to remove the NaCl that precipitated. Acetonitrile (0.1 mL) was added to the filtrate and after 30 min all volatiles were removed under vacuum providing the desired product as a pale yellow solid. (45 mg, 87%)



Anal. Calc. for $\text{C}_{72}\text{H}_{70}\text{BClF}_{24}\text{PPt}$: C, 51.55; H, 4.21; N, 0.83. **Found:** C, 51.8; H, 4.1; N, 0.7.

^1H NMR (400 MHz, 25°C , CD_2Cl_2): δ 7.72 (s, 8 H, $p\text{-BAr}_\text{F}$), 7.58 (m, 1 H, $p\text{-C}_6\text{H}_3$), 7.57 (s, 4 H, $o\text{-BAr}_\text{F}$), 7.31 (s, 2 H, $m\text{-Tipp}$), 7.30 (m, 1 H, $m\text{-C}_6\text{H}_3$), 7.17 (s, 2 H, $m\text{-Tipp}'$), 6.73 (d, 1 H, $^3J_{\text{HH}} = 7.7$ Hz, $m\text{-C}_6\text{H}_3$), 3.08 (hept, 1 H, $^3J_{\text{HH}} = 7.1$ Hz, $p\text{-CH-Tipp}$), 2.98 (hept, 1 H, $^3J_{\text{HH}} = 7.1$ Hz, $p\text{-CH-Tipp}$), 2.41 (hept, 2 H, $^3J_{\text{HH}} = 7.2$ Hz, $o\text{-CH-Tipp}$), 2.23 (hept, 2 H, $^3J_{\text{HH}} = 6.6$ Hz, $o\text{-CH-Tipp}$), 2.13 (s, 3 H, MeCN), 1.71 (d, 6 H, $^3J_{\text{HH}} = 6.7$ Hz, $o\text{-Me-Tipp}$), 1.57 (d, 6 H, $^2J_{\text{HP}} = 13.0$ Hz, $^3J_{\text{HPt}} = 26$ Hz, PMe_2), 1.37 (d, 6 H, $^3J_{\text{HH}} = 6.8$ Hz, $p\text{-Me-Tipp}$), 1.31 (d, 6 H, $^3J_{\text{HH}} = 5.4$ Hz, $p\text{-Me-Tipp}$), 1.29 (d, 6 H, $^3J_{\text{HH}} = 6.3$ Hz, $o\text{-Me-Tipp}$), 1.00 (t br, 12 H, $o\text{-Me-Tipp}$) ppm.

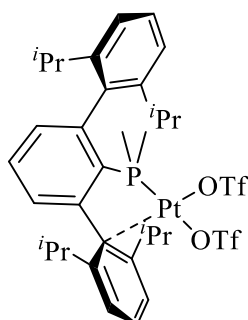
$^{13}\text{C}\{^1\text{H}\}$ NMR (96.6 MHz, 25°C , CD_2Cl_2): δ 162.3 (q, $\text{C}_{\text{ipso-BAr}_\text{F}}$), 162.3 (s, $p\text{-Tipp}'$), 155.1 (s, $o\text{-Tipp}'$), 152.0 (s, $p\text{-Tipp}$), 147.2 (s, $o\text{-Tipp}$), 145.5 (d, $^2J_{\text{CP}} = 15$ Hz, $o\text{-C}_6\text{H}_3$), 145.4 (d, $^2J_{\text{CP}} = 29$ Hz, $o\text{-C}_6\text{H}_3$), 134.1 (d, $^3J_{\text{CP}} = 8$ Hz, $m\text{-C}_6\text{H}_3$), 133.6 (d, $^4J_{\text{CP}} = 2$ Hz, $p\text{-C}_6\text{H}_3$), 132.4 (s, $\text{C}_{\text{ipso-Tipp}}$), 132.4

(d, $^3J_{\text{CP}} = 7$ Hz, $\text{C}_{\text{ipso}}\text{-C}_6\text{H}_3$), 131.0 (d, $^3J_{\text{CP}} = 14$ Hz, $m\text{-C}_6\text{H}_3$), 129.4 (qq, $^1J_{\text{CF}} = 32$ Hz, $^5J_{\text{CF}} = 3$ Hz, CF_3 BAr_F), 126.5 (s, CCF_3 BAr_F), 124.5 (s, $m\text{-Tipp}$), 121.8 (s, $m\text{-Tipp}'$), 118.0 (hept, $^4J_{\text{CF}} = 4$ Hz, $p\text{-BAr}^\text{F}$), 99.4 (d, $^3J_{\text{CP}} = 4$ Hz, $\text{C}_{\text{ipso}}\text{-Tipp}$), 35.3 (s, $p\text{-CH-Tipp}$), 35.0 (s, $p\text{-CH-Tipp}$), 35.0 (s, $o\text{-CH-Tipp}$), 31.9 (s, $o\text{-CH-Tipp}$), 26.6 (s, $o\text{-Me-Tipp}$), 26.0 (s, $o\text{-Me-Tipp}$), 24.3 (s, $p\text{-Me-Tipp}$), 24.1 (s, $o\text{-Me-Tipp}$), 23.8 (s, $p\text{-Me-Tipp}$), 21.7 (s, $o\text{-Me-Tipp}$), 13.80 (d, $^1J_{\text{CP}} = 47$ Hz, PMe_2), 4.2 (s, MeCN) ppm.

$^{31}\text{P}\{^1\text{H}\}$ NMR (161.9 MHz, 25 °C, CD_2Cl_2): δ 7.7 (s, $^1J_{\text{PPt}} = 3395$ Hz) ppm.

Synthesis and Characterisation of *cis*-[Pt(OTf)₂(PMe₂Ar^{Dipp}₂)], 17

In an ampoule, the Pt(II) chloride complex **6** (50 mg, 0.069 mmol) and AgOTf (55 mg, 0.21 mmol) were dissolved in CH₂Cl₂ at room temperature and stirring overnight avoiding the light. After that, it was filtered to remove the AgCl that precipitated and all volatiles were removed under vacuum providing the desired product as an oily orange solid. (46 mg, 70%)



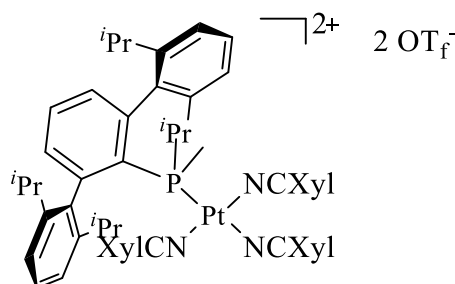
¹H NMR (500 MHz, CD₂Cl₂, 25 °C): δ 8.18 (t, ³J_{HH} = 7.9 Hz, 1 H, *p*-Dipp), 7.67 (t, ³J_{HH} = 8.2 Hz, 1 H, *p*-C₆H₃), 7.54 (t, ³J_{HH} = 8.2 Hz, 1 H, *p*-Dipp), 7.43 (d, ³J_{HH} = 7.9 Hz, 2 H, *m*-Dipp), 7.34 (d, ³J_{HH} = 7.9 Hz, 2 H, *m*-Dipp), 7.30 (d, ³J_{HH} = 8.0 Hz, 1 H, *m*-C₆H₃), 6.86 (d, ³J_{HH} = 7.8 Hz, 1 H, *m*-C₆H₃), 2.35 (sept, ³J_{HH} = 6.7 Hz, 2 H, CH-Dipp), 2.23 (sept, ³J_{HH} = 6.7 Hz, 2 H, CH-Dipp), 1.85 (d, ³J_{HH} = 6.8 Hz, 6 H, Me-Dipp), 1.49 (d, ²J_{HP} = 13.0 Hz, 6 H, PMe₂), 1.31 (d, ³J_{HH} = 7.0 Hz, 6 H, Me-Dipp), 1.04 (d, ³J_{HH} = 7.0 Hz, 6 H, Me-Dipp), 1.01 (d, ³J_{HH} = 6.5 Hz, 6 H, Me-Dipp) ppm.

¹³C{¹H} NMR (125.7 MHz, CD₂Cl₂, 25 °C): δ 154.9 (s, *o*-Dipp), 147.5 (s, *o*-Dipp), 145.4 (*o*-C₆H₃), 143.2 (s, *p*-Dipp), 134.4 (s, *p*-C₆H₃), 134.0 (d, ³J_{CP} = 8.4 Hz, *m*-C₆H₃), 131.3 (s, *p*-Dipp), 130.9 (s, *m*-C₆H₃), 127.4 (s br, *m*-Dipp), 124.0 (s, *m*-Dipp), 92.0 (s, *ipso*-Dipp), 35.0 (s, CH-Dipp), 31.9 (s, CH-Dipp), 26.7 (s, Me-Dipp), 26.5 (s, Me-Dipp), 23.9 (s, Me-Dipp), 21.7 (s, Me-Dipp), 12.5 (d, ¹J_{CP} = 44 Hz, PMe₂) ppm.

³¹P{¹H} NMR (202.4 MHz, CD₂Cl₂, 25 °C): δ 12.2 (s, ¹J_{PPt} = 3531 Hz) ppm.

Synthesis and Characterisation of *cis*-[Pt(NCXyl)₃(PMe₂Ar^{Dipp}₂)](OTf)₂, **18**

In an ampoule, the Pt(II) chloride complex **6** (50 mg, 0.069 mmol) and AgOTf (55 mg, 0.21 mmol) were dissolved in CH₂Cl₂ at room temperature and stirring overnight avoiding the light. After that, it was filtered to remove the AgCl that precipitated. When NCXyl (27 mg, 0.21 mmol) was added to the orange solution it was instantaneously changed to yellow. All volatiles were removed under vacuum and the solid residue was washed with pentane at room temperature providing the desired product as a yellow solid. For further purification, the product could be crystallised from dichloromethane/hexane mixtures (1:1 by vol) at -20 °C. (47 mg, 65%)



¹H NMR (400 MHz, CD₂Cl₂, 25 °C): δ 7.80 (dt, ³J_{HH} = 7.7 Hz, ⁵J_{HP} = 4.0 Hz, 1 H, *p*-C₆H₃), 7.52 (dd, ³J_{HH} = 7.7 Hz, ⁴J_{HP} = 4.0 Hz, 2 H, *m*-C₆H₃), 7.38-7.49 (m, 6 H, H_{ar}-CNXyl and *p*-Dipp), 7.31 (d, ³J_{HH} = 7.8 Hz, 4 H, *m*-Dipp), 7.20-7.26 (m, 5 H, H_{ar}-CNXyl), 2.53 (sept, ³J_{HH} = 6.8 Hz, 4 H, CH-Dipp), 2.48 (s, 6 H, CNXyl), 2.30 (s, 12 H, CNXyl), 2.02 (d, ²J_{HP} = 12.3 Hz, ³J_{HPt} = 39.1 Hz, 6 H, PMe₂), 1.23 (d, ³J_{HH} = 6.9 Hz, 12 H, Me-Dipp), 1.00 (d, ³J_{HH} = 6.6 Hz, 12 H, Me-Dipp) ppm.

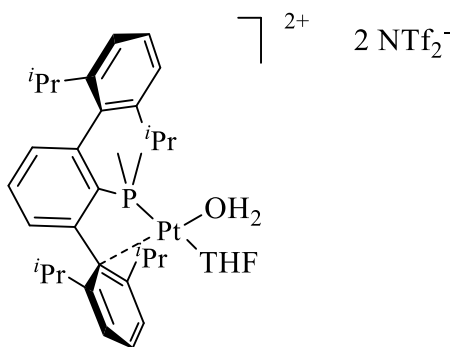
¹³C{¹H} NMR (100.6 MHz, CD₂Cl₂, 25 °C): δ 147.7 (s, *o*-Dipp), 146.3 (d, ²J_{CP} = 10 Hz, *o*-C₆H₃), 137.4 (s, C_{ipso}-Dipp), 134.5 (d, ³J_{CP} = 9.6 Hz, *m*-C₆H₃), 133.3 (s, CNXyl), 133.0 (s, CNXyl), 132.0 (d, ⁴J_{CP} = *p*-C₆H₃), 131.3 (s, *p*-Dipp), 129.7 (s, CNXyl), 129.4 (s, CNXyl), 124.5 (s, *m*-Dipp), 32.3 (s, CH-Dipp), 26.4 (s, Me-Dipp), 22.9 (s, Me-Dipp), 19.1 (s, Me-CNXYl), 19.0 (s, Me-CNXYl), 18.2 (d, ¹J_{CP} = 41.2 Hz, PMe₂) ppm.

$^{31}\text{P}\{^1\text{H}\}$ NMR (161.9 MHz, CD_2Cl_2 , 25 °C): δ -23.4 (s, $^1J_{\text{Pt}} = 2437$ Hz) ppm.

$^{19}\text{F}\{^1\text{H}\}$ NMR (376.3 MHz, CD_2Cl_2 , 25 °C): δ -78.9 (s) ppm.

Synthesis and Characterisation of Complex [Pt(PMe₂Ar^{Dipp}₂)(S)₂][NTf₂]₂, 19

In an ampoule, the Pt(II) dimethyl complex **8** (50 mg, 0.073 mmol) and HNTf₂ (45 mg, 0.2116 mmol) were dissolved in C₆H₆ at room temperature and the reaction mixture was stirred overnight. After that, all volatiles were removed under vacuum and the residue was washed with pentane (3 x 5 mL) at -40 °C obtaining the product as a pale brown solid. In order to obtain crystals suitable for X-ray diffraction the compound could be crystallised from dichloromethane/hexane mixtures (1:1 by vol) at -20 °C. (57 mg, 60%)



¹H NMR (400 MHz, -40 °C, CD₂Cl₂): δ 6.88–8.23 (m, 9H, H_{ar}), 4.53 (br, 2H, H₂O), 3.63 (m, 2H, CH₂O coord), 3.41 (m, 2H, CH₂O coord), 2.34 (sept, ³J_{HH} = 6.7 Hz, 2H, CH-Dipp), 2.19 (sept, ³J_{HH} = 6.9 Hz, 2H, CH-Dipp), 1.85 (d, ²J_{HH} = 6.4 Hz, 2H, CH₂), 1.80 (d, ²J_{HH} = 6.4 Hz, 2H, CH₂), 1.52 (d, ²J_{HP} = 13.0 Hz, 3H, PMe), 1.47 (d, ²J_{HP} = 12.8 Hz, 3H, MeP), 1.31 (d, ³J_{HH} = 5.0 Hz, 6H, Me-Dipp), 1.07 (d, ³J_{HH} = 5.8 Hz, 6H, Me-Dipp), 1.04 (d, ³J_{HH} = 6.2 Hz, 6H, Me-Dipp), 1.00 (d, ³J_{HH} = 5.8 Hz, 6H, Me-Dipp) ppm.

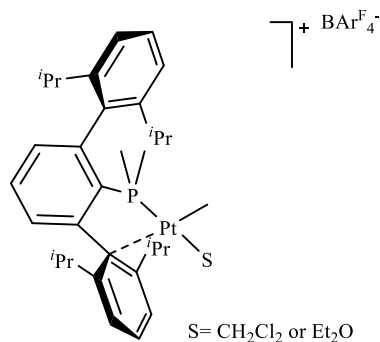
¹³C{¹H} NMR (100.6 MHz, -40 °C, CD₂Cl₂): δ 114.5–157.2 (m, C_{ar}), 74.4 (s, CH₂O coord), 24.1 (br, CH₂), 34.8 (s, CH-Dipp), 31.4 (s, CH-Dipp), 26.6 (s, CH₃-Dipp), 25.5 (s, CH₃-Dipp), 23.6 (s, CH₃-Dipp), 21.0 (s, CH₃-Dipp), 12.3 (d, ¹J_{CP} = 43 Hz, PMe), 11.8 (d, ¹J_{CP} = 45 Hz, PMe) ppm.

$^{31}\text{P}\{^1\text{H}\}$ NMR (161.9 MHz, -40 °C, CD_2Cl_2): δ 13.5, 13.9 ($1\text{JPPt} = 3560$ Hz) ppm.

$^{19}\text{F}\{^1\text{H}\}$ NMR (376.3 MHz, -40 °C, CD_2Cl_2): δ -79.5(s), -70.3 (br) ppm.

Synthesis and Characterisation of [PtMe(S)(PMe₂Ar^{Dipp2})]⁺[BAr_F]⁻, 20-S, 20-THF and 20-NCMe

A solid mixture of [PtMe₂(PMe₂Ar^{Dipp2})] **8**, (150 mg, 0.22 mmol) and [H(Et₂O)₂][BAr_F] (222 mg, 0.22 mmol) was dissolved at -80°C in CH₂Cl₂ (10 mL). The reaction mixture was allowed to warm up in the bath while stirring overnight. The complex was crystalized from CH₂Cl₂/hexane mixtures at -23 °C. (150 mg, 57%). In order to obtain the THF and the CNMe adducts, some crystals of the complex were dissolved in dichloromethane (*ca.* 2 mL) and 0.1 mL of the corresponding Lewis base was added. After removing volatiles under vacuum the compound was obtained with quantitative spectroscopic yield.



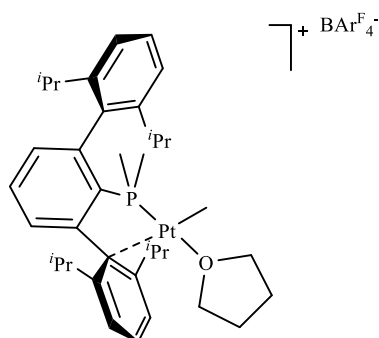
Anal. Calc. for C₆₅H₅₈BF₂₄PPt(CH₂Cl₂ adduct): C, 49.0; H, 3.7. **Found:** C, 49.3; H, 4.06.

¹H NMR (300 MHz, 25 °C, CD₂Cl₂): δ 7.78 (s, 8 H, *o*-BAr_F), 7.75 (m, 1 H, *m*-C₆H₃), 7.65 (t, 1 H, ³*J*_{HH} = 7.6 Hz, *p*-C₆H₃), 7.61 (s, 4 H, *p*-BAr_F), 7.54 (t, 1 H, ³*J*_{HH} = 7.6 Hz, *p*-Dipp), 7.41 (d, 2 H, ³*J*_{HH} = 7.6 Hz, *m*-Dipp), 7.36 (d, 2 H, ³*J*_{HH} = 7.6 Hz, *m*-Dipp), 7.00 (d, 1 H, ³*J*_{HH} = 7.5 Hz, *m*-C₆H₃), 2.46 (hept, 2 H, ³*J*_{HH} = 6.7 Hz, CH-Dipp), 2.38 (hept, 2 H, ³*J*_{HH} = 6.8 Hz, CH-Dipp), 1.55 (d, 6 H, ²*J*_{HP} = 9.9 Hz, ³*J*_{HPt} = 70.0 Hz, PMe₂), 1.52 (d, 6 H, ³*J*_{HH} = 6.8 Hz, Me-Dipp), 1.33 (d, 6 H, ³*J*_{HH} = 6.7 Hz, Me-Dipp), 1.06 (d, 12 H, ³*J*_{HH} = 6.3 Hz, Me-Dipp), 0.76 (s, 3 H, ²*J*_{HPt} = 76.8 Hz, Pt-Me) ppm.

¹³C{¹H} NMR (100.6 MHz, 25 °C, CD₂Cl₂): δ -6.9 (br, ¹*J*_{CPt} = 769 Hz, Pt-Me), 14.1 (d, ¹*J*_{CP} = 47.1 Hz, PMe₂), 21.1 (s, Me-Dipp), 23.5 (s, Me-Dipp), 24.0 (s, Me-Dipp), 25.9 (s, Me-Dipp), 31.3 (s, CH-Dipp), 32.8 (s, CH-Dipp), 117.5 (hept, ⁴*J*_{CF} = 4 Hz, *p*-BAr_F), 122.5 (br, C_{ipso}-Dipp), 123.2 (s, *m*-Dipp), 123.3 (s, *m*-Dipp), 130.3 (s, *p*-Dipp), 130.9 (d, ³*J*_{CP} = 12 Hz, *m*-

C₆H₃), 131.9 (s, *p*-C₆H₃), 133.6 (d, ³*J*_{CP} = 12 Hz, *m*-C₆H₃), 135.0 (s, *o*-BAr_F), 136.1 (s, C_{ipso}-Dipp), 144.35 (br, *o*-C₆H₃), 147.0 (s, *o*-Dipp), 150.2 (s, *o*-Dipp), 162.4 (q, *ipso*-BAr_F), ppm.

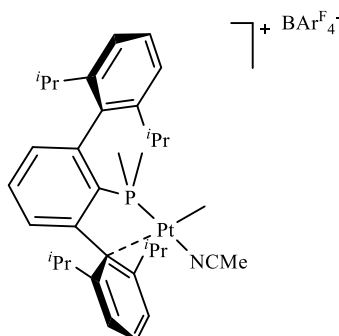
³¹P{¹H} NMR (161.9 MHz, 25 °C, CD₂Cl₂): δ -0.5 (s, ¹*J*_{Pt} = 4882 Hz) ppm.



¹H NMR (300 MHz, 25 °C, CD₂Cl₂): δ 7.72 (s, 8 H, *o*-BAr_F), 7.60 (m, 1 H, *p*-C₆H₃), 7.56 (s, 4 H, *p*-BAr_F), 7.50 (t, 2 H, ³*J*_{HH} = 7.7 Hz, *p*-Dipp and *p*-Dipp'), 7.37 (d, 2 H, ³*J*_{HH} = 8.2 Hz, *m*-Dipp'), 7.32 (d, 2 H, ³*J*_{HH} = 7.7 Hz, *m*-Dipp), 7.30 (m, 1 H, *m*-C₆H₃), 6.89 (d, 1 H, ³*J*_{HH} = 7.7 Hz, *m*-C₆H₃), 3.51 (br, 4 H, (O-CH₂-CH₂)), 2.40 (hept, 2 H, ³*J*_{HH} = 7.4 Hz, CH-Dipp), 2.36 (hept, 2 H, ³*J*_{HH} = 7.4 Hz, CH-Dipp), 1.87 (br, 4 H, O-CH₂-CH₂), 1.56 (d, 6 H, ³*J*_{HH} = 7.7 Hz, CH₃-Dipp), 1.47 (d, 6 H, ²*J*_{HP} = 12.1 Hz, ³*J*_{HPt} = 67.4 Hz, PMe₂), 1.30 (d, 6 H, ³*J*_{HH} = 7.1 Hz, Me-Dipp), 1.02 (d, 12 H, ³*J*_{HH} = 7.7 Hz, Me-Dipp), 0.64 (s, 3 H, ²*J*_{HPt} = 76.1 Hz, Pt-Me) ppm.

¹³C{¹H} NMR (75.4 MHz, 25 °C, CD₂Cl₂): δ 162.4 (q, *ipso*-BAr_F), 150.1 (s, *o*-Dipp'), 147.5 (s, *o*-Dipp), 135.4 (s, *m*-BAr_F), 134.5 (s, *p*-Dipp'), 133.9 (m, C_{ipso}-C₆H₃), 132.3 (s, *p*-C₆H₃), 131.5 (d, ³*J*_{CP} = 13 Hz, *m*-C₆H₃), 130.8 (s, *p*-Dipp), 124.2 (s, *m*-Dipp'), 123.8 (s, *m*-Dipp), 118.05 (hept, ⁴*J*_{CF} = 4 Hz, *p*-BAr_F), 73.9 (s, O-CH₂-CH₂), 33.3 (s, CH-Dipp), 31.9 (s, CH-Dipp), 26.5 (s, Me-Dipp), 26.4 (s, O-CH₂-CH₂), 24.7 (s, Me-Dipp), 24.4 (s, Me-Dipp), 21.8 (s, Me-Dipp), 14.5 (d, ¹*J*_{CP} = 48 Hz, PMe₂), -5.9 (s, Pt-CH₃) ppm.

³¹P{¹H} NMR (121.4 MHz, 25 °C, CD₂Cl₂): δ -4.1 (s, ¹*J*_{Pt} = 4636 Hz) ppm.



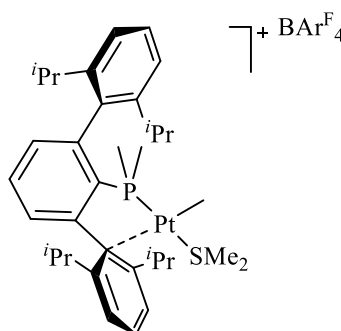
^1H NMR (500 MHz, 25 °C, CD_2Cl_2): δ 7.54 (m, 1 H, *p*- C_6H_3), 7.53 (t, 1 H, $^3J_{\text{HH}} = 7.7$ Hz, *p*-Dipp), 7.49 (t, 1 H, $^3J_{\text{HH}} = 7.6$ Hz, *p*-Dipp'), 7.39 (d, 2 H, $^2J_{\text{HH}} = 7.8$ Hz, *m*-Dipp), 7.32 (d, 2 H, $^3J_{\text{HH}} = 8$ Hz, *m*-Dipp'), 7.30 (dd, 1 H, $^3J_{\text{HH}} = 7.4$ Hz, $^4J_{\text{HP}} = 2$ Hz, *m*-Dipp), 6.83 (dd, 1 H, $^3J_{\text{HH}} = 7.4$ Hz, $^4J_{\text{HP}} = 2$ Hz, *m*- C_6H_3), 2.38 (hept, 2 H, $^3J_{\text{HH}} = 6.8$ Hz, CH-Dipp), 2.36 (hept, 2 H, $^3J_{\text{HH}} = 6.7$ Hz, CH-Dipp), 2.22 (s, 3 H, NCCH_3), 1.49 (d, 6 H, $^3J_{\text{HH}} = 6.9$ Hz, Me-Dipp), 1.42 (d, 6 H, $^2J_{\text{HP}} = 11.4$ Hz, $^3J_{\text{HPt}} = 58.6$ Hz, PMe_2), 1.30 (d, $^3J_{\text{HH}} = 6.8$ Hz, 6 H, Me-Dipp), 1.02 (d, 6 H, $^3J_{\text{HH}} = 7.1$ Hz, Me-Dipp), 1.00 (d, 6 H, $^3J_{\text{HH}} = 7.6$ Hz, Me-Dipp), 0.68 (d, 3 H, $^3J_{\text{HP}} = 3.4$ Hz, $^2J_{\text{HPt}} = 80.8$ Hz, Pt-Me) ppm.

$^{13}\text{C}\{^1\text{H}\}$ NMR (125.7 MHz, 25 °C, CD_2Cl_2): δ 162.4 (q, *ipso*- BAr_F), 150.8 (s, *o*-Dipp), 147.6 (s, *o*-Dipp'), 136.0 (s, C_{ipso} -Dipp'), 135.4 (s, *m*- BAr_F), 133.9 (s, *p*-Dipp), 133.6 (s, *m*- C_6H_3), 132.2 (s, *m*- C_6H_3), 131.9 (d, $^4J_{\text{CP}} = 12$ Hz, *p*- C_6H_3), 126.3 (s), 130.7 (s, *p*-Dipp'), 125.1 (s, *m*-Dipp), 124.1 (s), 123.8 (s, *m*-Dipp'), 121.9 (s, C_{ipso} -Dipp), 118.1 (hept, $^4J_{\text{CF}} = 4$ Hz, *p*- BAr_F), 33.5 (s, CH-Dipp), 31.9 (s, CH-Dipp), 2.5 (s, Me-Dipp), 24.6 (s, Me-Dipp), 24.4 (s, Me-Dipp), 21.8 (s, Me-Dipp), 13.6 (d, $^1J_{\text{CP}} = 45$ Hz, $^2J_{\text{CPt}} = 59$ Hz, PMe_2), 4.1 (s, CH_3CN), -9.2 (d, $^2J_{\text{CP}} = 6$ Hz, Pt-Me) ppm.

$^{31}\text{P}\{^1\text{H}\}$ NMR (202.4 MHz, 25 °C, CD_2Cl_2): δ -2.2 (s, $^1J_{\text{PPt}} = 4304$ Hz) ppm.

Synthesis and Characterisation of [PtMe(SMe₂)(PMe₂Ar^{Dipp}₂)] [BAr^F], **20**·SMe₂

The synthesis is analogous to that employed for complex **20**·S but using an *in situ* prepared sample of [Pt(PMe₂Ar^{Dipp}₂)Me₂] (200 mg, 0.29 mmol), generating by mixing PMe₂Ar^{Dipp}₂ with [PtMe₂(SMe₂)₂]. The product was recrystallized from a CH₂Cl₂/hexane mixture (1:2) at -23 °C as a pale yellow crystalline solid (190 mg, 40%).



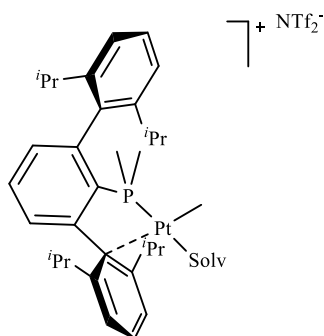
¹H NMR (500 MHz, 25 °C, CD₂Cl₂): δ 7.79 (t, 1 H, ³J_{HH} = 7.8 Hz, *p*-Dipp), 7.57 (m, 1 H, *p*-C₆H₃), 7.50 (t, 1 H, *p*-Dipp), 7.35 (m, 1 H, *m*-C₆H₃), 7.33 (d, 2 H, ³J_{HH} = 7.7 Hz, *m*-Dipp), 7.18 (d, 2 H, ³J_{HH} = 7.7 Hz, *m*-Dipp), 6.80 (d, 1 H, ³J_{HH} = 7.7 Hz, *m*-C₆H₃), 2.38 (hept, 2 H, ³J_{HH} = 6.7 Hz, CH-Dipp), 2.32 (hept, 2 H, ³J_{HH} = 6.7 Hz, CH-Dipp), 1.99 (d, 6 H, ⁴J_{HP} = 3.6 Hz, ³J_{HPt} = 32.5 Hz, SMe₂), 1.48 (d, 6 H, ²J_{HP} = 11.3 Hz, ³J_{HPt} = 52.5 Hz, PMe₂), 1.32 (d, 6 H, ³J_{HH} = 6.6 Hz, Me-Dipp), 1.30 (d, 6 H, ³J_{HH} = 6.5 Hz, Me-Dipp), 1.02 (d, 6 H, ³J_{HH} = 6.5 Hz, Me-Dipp), 0.97 (d, 6 H, ³J_{HH} = 6.8 Hz, Me-Dipp), 0.73 (d, 3 H, ³J_{HP} = 4.1 Hz, ²J_{HPt} = 82.2 Hz, Pt-Me) ppm.

¹³C{¹H} NMR (125.7 MHz, 25 °C, CD₂Cl₂): δ 151.8 (s, *o*-Dipp), 147.6 (s, *o*-Dipp), 145.8 (d, *J*_{CP} = 22 Hz), 135.8 (s, *p*-Dipp), 134.1 (d, ³*J*_{CP} = 7 Hz, *m*-C₆H₃), 132.4 (s, *p*-C₆H₃), 132.2 (d, ³*J*_{CP} = 13 Hz, *m*-C₆H₃), 130.5 (s, *p*-Dipp), 128.4 (s), 126.3 (s), 124.1 (s), 123.9 (s), 123.8 (s, *m*-Dipp), 123.4 (s, *m*-Dipp), 33.6 (s, CH-Dipp), 31.9 (s, CH-Dipp), 26.5 (s, Me-Dipp), 25.1 (s, Me-Dipp), 24.4 (s, Me-Dipp), 21.8 (s, Me-Dipp), 21.4 (d, ³*J*_{CP} = 2 Hz, SMe₂), 13.4 (d, ¹*J*_{CP} = 42 Hz, PMe₂), -3.5 (d, ²*J*_{CP} = 5 Hz, Pt-Me) ppm.

³¹P{¹H} NMR (202.4 MHz, 25 °C, CD₂Cl₂): δ 12.3 (s, ¹*J*_{PPt} = 3730 Hz) ppm.

Synthesis and Characterisation of [Pt(Me)(S)(PMe₂Ar^{Dipp}₂)]N(SO₂CF₃)₂, 20·S-NTf₂, 20·NCMe-NTf₂

[PtMe₂(PMe₂Ar^{Dipp}₂)], **8**, (30 mg, 0.043 mmol) and HNTf₂ (12.3 mg, 0.043 mmol) were dissolved in CH₂Cl₂ (*ca.* 3 mL) at room temperature. After 30 min stirring, all volatiles were removed under vacuum affording the product as a pale yellow solid. In the case of the CNMe adduct, 0.1 mL of this solvent was added to the reaction mixture.



¹H NMR (400 MHz, 25 °C, CD₂Cl₂) δ: 7.75 (br, 1 H, *p*-Dipp'), 7.60 (t, 1 H, ³*J*_{HH} = 7.8 Hz, *p*-C₆H₃), 7.54 (t, 1 H, ³*J*_{HH} = 7.8 Hz, *p*-Dipp), 7.43 (d, 2 H, ³*J*_{HH} = 7.8 Hz, *m*-Dipp'), 7.36 (d, 2 H, ³*J*_{HH} = 7.8 Hz, *m*-Dipp), 7.33 (d, br, 1 H, ³*J*_{HH} = 7.0 Hz, *m*-C₆H₃), 6.96 (d br, 1 H, ³*J*_{HH} = 7.0 Hz, *m*-C₆H₃), 2.43 (hept, 4 H, ³*J*_{HH} = 7.2 Hz, CH-Dipp), 1.59 (br d, 6 H, ³*J*_{HH} = 7.2 Hz, Me-Dipp), 1.53 (d, 6 H, ²*J*_{HP} = 11.9 Hz, ³*J*_{HPt} = 71.4 Hz, PMe₂), 1.36 (d, 6 H, ³*J*_{HH} = 6.8 Hz, Me-Dipp), 1.06 (d, 12 H, ³*J*_{HH} = 6.8 Hz, Me-Dipp), 0.80 (br, 3 H, ²*J*_{HPt} = 76 Hz, Pt-Me) ppm.

¹H NMR (500 MHz, -30 °C, CD₂Cl₂): δ 7.75 (t, 1 H, ³*J*_{HH} = 7.7 Hz, *p*-Dipp'), 7.55 (t, 1 H, ³*J*_{HH} = 7.8 Hz, *p*-C₆H₃), 7.46 (t, 1 H, ³*J*_{HH} = 7.8 Hz, *p*-Dipp'), 7.34 (d, 2 H, ³*J*_{HH} = 7.8 Hz, *m*-Dipp'), 7.28 (d, 2 H, ³*J*_{HH} = 7.8 Hz, *m*-Dipp), 7.26 (d, 1 H, ³*J*_{HH} = 7.0 Hz, *m*-C₆H₃), 6.92 (d, 1 H, ³*J*_{HH} = 7.0 Hz, *m*-C₆H₃), 2.32 (hept, 2 H, ³*J*_{HH} = 6.8 Hz, CH-Dipp), 2.30 (hept, 2 H, ³*J*_{HH} = 6.8 Hz, CH-Dipp), 1.44 (d, 6 H, ³*J*_{HH} = 6.6 Hz, Me-Dipp), 1.42 (d, 6 H, ²*J*_{HP} = 12.1 Hz, PMe₂), 1.26 (d, 6 H, ³*J*_{HH} = 6.6 Hz, Me-Dipp), 0.98 (d, 12 H, ³*J*_{HH} = 6.5 Hz, Me-Dipp), 0.63 (s, 3 H, ²*J*_{HPt} = 72.4 Hz, Pt-Me), ppm.

¹³C{¹H} NMR (96.6 MHz, 25 °C, CD₂Cl₂): δ 149.6 (br, *o*-Dipp'), 147.6 (s, *o*-Dipp), 136.14 (s), 133.7 (d, ⁴*J*_{HP} = 7 Hz, *m*-C₆H₃), 132.0 (d, ⁵*J*_{HP} = 2 Hz, *p*-C₆H₃), 131.6 (d, ⁴*J*_{HP} = 12 Hz, *m*-C₆H₃), 130.6 (s, *p*-Dipp), 124.7 (s, *m*-Dipp'), 123.7 (s, *m*-Dipp), 118.5 (s), 33.3 (s, CH-Dipp), 31.9 (s, CH-Dipp),

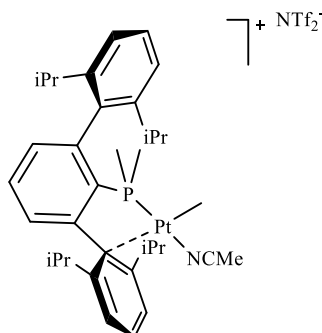
26. 6 (s, Me-Dipp), 24.8 (s, Me-Dipp), 24.1 (s, Me-Dipp), 21.8 (s, Me-Dipp), 14.7 (d, $^1J_{\text{CP}} = 47$ Hz, PMe_2), -6.1 (s br, Pt-Me) ppm.

$^{31}\text{P}\{^1\text{H}\}$ NMR (161.9 MHz, 25 °C, CD_2Cl_2): $\delta -2.7$ (s br, $^1J_{\text{PPt}} = 4928$ Hz) ppm.

$^{31}\text{P}\{^1\text{H}\}$ NMR (202.4 MHz, -30 °C, CD_2Cl_2): $\delta -2.4$ (s, $^1J_{\text{PPt}} = 4721$ Hz, major), -3.1 (s, $^1J_{\text{PPt}} = 5160$ Hz, minor)

$^{19}\text{F}\{^1\text{H}\}$ NMR (376.4 MHz, 25 °C, CD_2Cl_2): $\delta -78.9$ (s, $\text{CF}_3\text{-NTf}_2$)

$^{19}\text{F}\{^1\text{H}\}$ NMR (376.4 MHz, -30 °C, CD_2Cl_2): $\delta -79.5$ (s, $\text{CF}_3\text{-NTf}_2$, major), -71.1 (s, $\text{CF}_3\text{-NTf}_2$, minor) ppm.



^1H NMR (500 MHz, CD_2Cl_2 , 25 °C): δ 7.61 (t, 1 H, $^3J_{\text{HH}} = 7.8$ Hz, p -Dipp'), 7.56 (td, 1 H, $^3J_{\text{HH}} = 7.7$ Hz, $^5J_{\text{HP}} = 2.1$ Hz, $p\text{-C}_6\text{H}_3$), 7.50 (t, 1 H, $^3J_{\text{HH}} = 7.8$ Hz, p -Dipp'), 7.44 (d, 2 H, $^3J_{\text{HH}} = 7.7$ Hz, m -Dipp'), 7.32 (d, 2 H, $^3J_{\text{HH}} = 7.7$ Hz, m -Dipp'), 7.28 (dd, 1 H, $^3J_{\text{HH}} = 7.6$ Hz, $^4J_{\text{HP}} = 3.0$ Hz, $m\text{-C}_6\text{H}_3$), 6.84 (dd, 1 H, $^3J_{\text{HH}} = 7.7$ Hz, $^4J_{\text{HP}} = 2.7$ Hz, $m\text{-C}_6\text{H}_3$), 2.38 (hept, 4 H, $^3J_{\text{HH}} = 6.8$ Hz, CH-Dipp), 2.30 (s, 3 H, CH_3CN), 1.52 (d, 6 H, $^3J_{\text{HH}} = 6.9$ Hz, Me-Dipp), 1.43 (d, 6 H, $^2J_{\text{HP}} = 11.4$ Hz, $^3J_{\text{HPt}} = 58.3$ Hz, PMe_2), 1.31 (d, 6 H, $^3J_{\text{HH}} = 6.8$ Hz, Me-Dipp), 1.02 (d, 12 H, $^3J_{\text{HH}} = 6.8$ Hz, Me-Dipp), 0.70 (d, 3H, $^3J_{\text{PH}} = 3.6$ Hz, $^2J_{\text{HPt}} = 81.4$ Hz, Pt-Me) ppm.

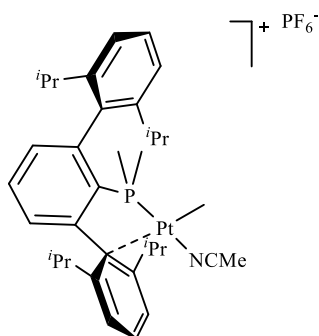
$^{13}\text{C}\{^1\text{H}\}$ NMR (125.7 MHz, CD_2Cl_2 , 25°C): δ 150.6 (s), 147.6 (s), 145.7 (s), 145.6 (s), 145.1 (s), 136.1 (s), 134.0 (s, p -Dipp'), 133.8 (d, $^3J_{\text{CP}} = 8$ Hz, $m\text{-C}_6\text{H}_3$), 132.1 (s, $p\text{-C}_6\text{H}_3$), 131.9 (d, $^3J_{\text{CP}} = 12$ Hz, $m\text{-C}_6\text{H}_3$), 125.2 (s, m -Dipp), 130.6 (s), 123.7 (s, m -Dipp), 115.9 (s, CH_3CN), 33.5 (s, CH-Dipp), 31.8 (s, CH-Dipp), 26.6 (s, Me-Dipp), 24.7 (s, Me-Dipp), 24.4 (s, Me-Dipp), 21.8 (s, Me-Dipp), 13.6 (d, $^1J_{\text{CP}} = 45$ Hz, $^2J_{\text{CPt}} = 60$ Hz, PMe_2), 4.10 (s, CH_3CN), -9.3 (d, $^3J_{\text{HP}} = 6$ Hz, Pt-Me) ppm.

$^{31}\text{P}\{^1\text{H}\}$ NMR (202.4 MHz, CD_2Cl_2 , 25°C): $\delta -2.3$ (s, $^1J_{\text{PPt}} = 4302$ Hz) ppm.

$^{19}\text{F}\{^1\text{H}\}$ NMR (376.4 MHz, CD_2Cl_2 , 25°C): $\delta -79.28$ (s, NTf_2) ppm.

Synthesis and Characterisation of [PtMe(NCMe)(PMe₂Ar^{Dipp}₂)]⁺[PF₆]⁻, 20·NCMe-PF₆

[PtMe₂(PMe₂Ar^{Dipp}₂)], **8**, (27 mg, 0.039 mmol) and [Ph₃C][PF₆] (1 equiv., 15.3 mg, 0.039 mmol) were dissolved in CH₂Cl₂ at -80°C. Acetonitrile was added to the mixture and the temperature was allowed to rise up slowly to the room temperature. After 30 min stirring, volatiles were removed under vacuum obtain the product as a yellow pale solid. (28 mg, 75%)



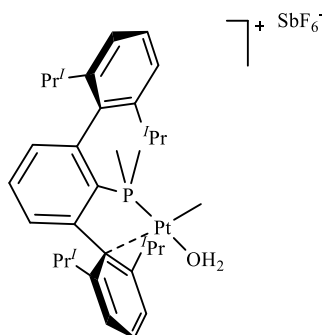
¹H NMR (500 MHz, 25 °C, CD₂Cl₂): δ 7.64 (t, 1 H, ³J_{HH} = 7.8 Hz, *p*-Dipp), 7.55 (td, 1 H, ³J_{HH} = 7.7 Hz, ⁵J_{HP} = 1.9 Hz, *p*-C₆H₃), 7.50 (t, 1 H, ³J_{HH} = 7.8 Hz, *p*-Dipp'), 7.45 (d, 2 H, ³J_{HH} = 7.8 Hz, *m*-Dipp), 7.32 (d, 2 H, ³J_{HH} = 7.8 Hz, *m*-Dipp'), 7.28 (ddd, 1 H, ³J_{HH} = 7.5 Hz, ⁴J_{HH} = 1.0 Hz, ⁴J_{HP} = 3.2 Hz, *m*-C₆H₃), 6.85 (ddd, 1 H, ³J_{HH} = 7.5 Hz, ⁴J_{HH} = 0.9 Hz, ⁴J_{HP} = 2.1 Hz, *m*-C₆H₃), 2.39 (hept, 4 H, ³J_{HH} = 6.6 Hz, CH-Dipp), 2.32 (s, 3 H, CH₃CN), 1.53 (d, 6 H, ³J_{HH} = 6.9 Hz, Me-Dipp), 1.42 (d, 6 H, ²J_{HP} = 11.5 Hz, ³J_{HPt} = 58.3 Hz, PMe₂), 1.32 (d, 6 H, ³J_{HH} = 6.9 Hz, Me-Dipp), 1.03 (d, 12 H, ³J_{HH} = 6.9 Hz, Me-Dipp), 0.71 (d, 3 H, ³J_{HP} = 3.5 Hz, ²J_{HPt} = 81.7 Hz, Pt-Me) ppm.

¹³C{¹H} NMR (125.7 MHz, 25 °C, CD₂Cl₂): δ 150.5 (s, *o*-Dipp), 147.6 (s, *o*-Dipp'), 145.7 (d, ¹J_{CP} = 20 Hz, C_{ipso}-C₆H₃), 145.0 (s), 136.1 (s), 134.1 (s, *p*-Dipp), 133.7 (d, ³J_{CP} = 7 Hz, *m*-C₆H₃), 132.19 (s, *p*-C₆H₃), 131.9 (d, ³J_{CP} = 13 Hz, *m*-C₆H₃), 130.6 (s, *p*-Dipp'), 125.3 (s, *m*-Dipp), 123.7 (s, *m*-Dipp'), 33.58 (s, CH-Dipp), 31.8 (s, CH-Dipp), 26.6 (s, Me-Dipp), 24.7 (s, Me-Dipp), 24.4 (s, Me-Dipp), 21.8 (s, Me-Dipp), 13.6 (d, ¹J_{PC} = 45 Hz, ²J_{CPt} = 61 Hz, PMe₂), 4.0 (s, CH₃CN), -9.35 (d, ²J_{CP} = 6 Hz, ¹J_{CPt} = 720 Hz, Pt-Me) ppm.

³¹P{¹H} NMR (202.40 MHz, 25 °C, CD₂Cl₂): δ -2.3 (s, ¹J_{PPt} = 4301 Hz, P-Pt), 145.19 (hept, ¹J_{PF} = 711 Hz, PF₆) ppm.

Synthesis and Characterisation of $[\text{PtMe}(\text{H}_2\text{O})(\text{PMe}_2\text{Ar}^{\text{Dipp}_2})][\text{SbF}_6]$, $20 \cdot \text{H}_2\text{O} \cdot \text{SbF}_6$

This procedure was performed in the absence of light. $[\text{PtMeCl}(\text{PMe}_2\text{Ar}^{\text{Dipp}_2})]$, **10**, (12.2 mg, 0.017 mmol) and AgSbF_6 (6mg, 0.017 mmol) were dissolved in 1 mL of CH_2Cl_2 . After 30 min of stirring at room temperature, the resulting suspension was filtered. All volatiles of the filtrate were removed under vacuum obtaining the product as a pale yellow solid.



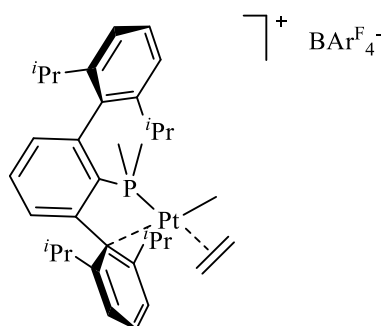
^1H NMR (300 MHz, 25 °C, CD_2Cl_2): δ 7.86 (t, 1 H, $^3J_{\text{HH}} = 7.7$ Hz, *p*-Dipp), 7.57 (td, 1 H, $^3J_{\text{HH}} = 7.8$ Hz, $^5J_{\text{HP}} = 1.8$ Hz, *p*- C_6H_3), 7.50 (t, 1 H, $^3J_{\text{HH}} = 7.8$ Hz, *p*-Dipp'), 7.41 (d, 2 H, $^3J_{\text{HH}} = 7.7$ Hz, *m*-Dipp), 7.32 (d, 2 H, $^3J_{\text{HH}} = 7.7$ Hz, *m*-Dipp'), 7.29 (dd, 1 H, $^4J_{\text{HP}} = 1.8$ Hz, $^3J_{\text{HH}} = 7.6$ Hz, *m*- C_6H_3), 6.92 (dd, 1 H, $^4J_{\text{HP}} = 1.8$ Hz, $^3J_{\text{HH}} = 7.6$ Hz, *m*- C_6H_3), 2.79 (br, 2 H, H_2O), 2.39 (hept, 2 H, $^3J_{\text{HH}} = 6.8$ Hz, CH-Dipp), 2.36 (hept, 2 H, $^3J_{\text{HH}} = 6.8$ Hz, CH-Dipp'), 1.51 (d, 6 H, $^3J_{\text{HH}} = 6.6$ Hz, Me-Dipp), 1.48 (d, 6 H, $^2J_{\text{HP}} = 11.8$ Hz, $^2J_{\text{HPt}} = 66.7$ Hz, PMe_2), 1.30 (d, 6 H, $^3J_{\text{HH}} = 6.6$ Hz, Me-Dipp'), 1.01 (d, 12 H, $^3J_{\text{HH}} = 6.6$ Hz, Me-Dipp), 0.73 (d, 3 H, $^3J_{\text{HP}} = 1$ Hz, $^2J_{\text{HPt}} = 75.5$ Hz, Pt-Me) ppm.

$^{13}\text{C}\{^1\text{H}\}$ NMR (75.4 MHz, 25 °C, CD_2Cl_2): δ 150.2 (s, *o*-Dipp'), 147.6 (s, *o*-Dipp), 133.8 (d, $^3J_{\text{CP}} = 7$ Hz, *m*- C_6H_3), 133.1 (s, *p*-Dipp), 132.1 (s, *p*- C_6H_3), 131.6 (d, $^3J_{\text{CP}} = 12$ Hz, *m*- C_6H_3), 130.4 (s, *p*-Dipp'), 124.6 (s, *m*-Dipp), 123.7 (s, *m*-Dipp'), 33.4 (s, CH-Dipp), 31.9 (s, CH-Dipp'), 26.6 (s, Me-Dipp), 24.7 (s, Me-Dipp), 24.1 (s, Me-Dipp), 21.7 (s, Me-Dipp), 14.6 (d, $^1J_{\text{CP}} = 47$ Hz, $^2J_{\text{CPt}} = 64$ Hz, PMe_2), -6.1 (d, $^2J_{\text{CP}} = 5$ Hz, Pt-Me) ppm.

$^{31}\text{P}\{^1\text{H}\}$ NMR (121.4 MHz, 25 °C, CD_2Cl_2): δ -2.9 (s, $^1J_{\text{PPt}} = 4705$ Hz) ppm.

Synthesis and Characterisation of $[\text{PtMe}(\text{C}_2\text{H}_4)(\text{PMe}_2\text{Ar}^{\text{Dipp}_2})][\text{BAr}^{\text{F}}_4]$, **20**· C_2H_4

In a Young NMR tube, the cationic methyl complex **20**·**S** (30 mg, 0.019 mmol) was dissolved in CD_2Cl_2 at room temperature. The system was degassed (3 freeze-pump-thaw cycles) and charged with ethylene (2 bar). After 5 hours at room temperature, the product was obtained and characterized by NMR spectroscopy with a quantitative spectroscopic yield. After removing all volatiles under vacuum, the product was obtained as a pale yellow solid.



Anal. Calc. for $\text{C}_{67}\text{H}_{62}\text{BF}_{24}\text{PPt}$: C, 51.6; H, 4.061. **Found:** C, 51.7; H, 3.9.

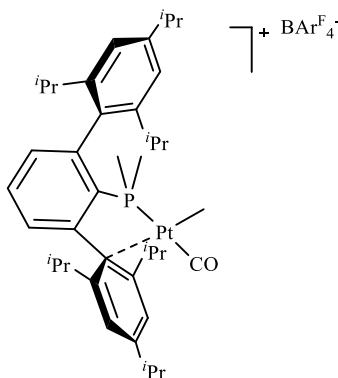
^1H NMR (500 MHz, 25 °C, CD_2Cl_2): δ 7.73 (s, 8 H, $o\text{-BAr}^{\text{F}}$), 7.64 (br t, 1 H, $^3J_{\text{HH}} = 7.6$ Hz, $p\text{-Dipp}$), 7.60 (td, 1 H, $^5J_{\text{HP}} = 2.1$ Hz, $^3J_{\text{HH}} = 7.6$ Hz, $p\text{-C}_6\text{H}_3$), 7.56 (s, 4 H, $p\text{-BAr}^{\text{F}}$), 7.51 (t, 1 H, $^3J_{\text{HH}} = 7.8$ Hz, $p\text{-Dipp}'$), 7.47 (d br, 2 H, $^3J_{\text{HH}} = 7.6$ Hz, $m\text{-Dipp}$), 7.36 (d, 1 H, $^3J_{\text{HH}} = 7.9$ Hz, $m\text{-C}_6\text{H}_3$), 7.34 (d, 2 H, $^3J_{\text{HH}} = 7.8$ Hz, $m\text{-Dipp}'$), 6.77 (d, 1 H, $^3J_{\text{HH}} = 6.7$ Hz, $m\text{-C}_6\text{H}_3$), 3.88 (br, 4 H, $^2J_{\text{HPt}} = 34.6$ Hz, C_2H_4), 2.36 (hept, $^3J_{\text{HH}} = 6.7$ Hz, 2 H, CH-Dipp), 1.49 (d, 6 H, $^2J_{\text{HP}} = 11.2$ Hz, $^3J_{\text{HPt}} = 55.8$ Hz, PMe_2), 1.39 (d, 6 H, $^3J_{\text{HH}} = 6.8$ Hz, Me-Dipp), 1.31 (d, 6 H, $^3J_{\text{HH}} = 6.8$ Hz, Me-Dipp), 1.03 (d, 6 H, $^3J_{\text{HH}} = 6.7$ Hz, Me-Dipp), 0.99 (d, 6 H, $^3J_{\text{HH}} = 6.7$ Hz, Me-Dipp), 0.70 (d, 3 H, $^3J_{\text{HP}} = 4.6$ Hz, $^2J_{\text{HPt}} = 76.2$ Hz, Pt-Me) ppm.

$^{13}\text{C}\{^1\text{H}\}$ NMR (125.7 MHz, 25°C, CD_2Cl_2): δ 162.4 (q, BArF), 149.8 (br, $o\text{-Dipp}$), 147.6 (s, $o\text{-Dipp}'$), 135.6 (br), 135.4 (s, $o\text{-BAr}^{\text{F}}$), 134.5 (br), 133.9 (br, $p\text{-Dipp}$), 133.05 (br, $p\text{-C}_6\text{H}_3$), 132.3 (br, $m\text{-C}_6\text{H}_3$), 131.0 (s, $p\text{-Dipp}'$), 129.5 (q, BArF), 128.5 (s), 126.3 (s), 125.9 (br, $m\text{-Dipp}$), 124.1 (s), 124.0 (s, $m\text{-Dipp}'$), 129.3 (s, free C_2H_4), 118.1 (hept, $^3J_{\text{CF}} = 4$ Hz, $p\text{-BAr}^{\text{F}}$), 102.2 (br, Pt- C_2H_4), 33.6 (s, CH-Dipp), 32.0 (s, CH-Dipp), 26.5 (s, Me-Dipp), 24.5 (s, Me-Dipp), 24.2 (s, Me-Dipp), 21.8 (s, Me-Dipp), 13.5 (m, PMe_2), -1.6 (m, Pt-Me) ppm.

$^{31}\text{P}\{^1\text{H}\}$ NMR (202.4 MHz, 25°C, CD_2Cl_2): δ 14.4 (s, $^1J_{\text{PPt}} = 4042$ Hz) ppm.

Synthesis and Characterisation of [PtMe(CO)(PMe₂Ar^{Tipp2})] [BAr_F], 21·CO

A mixture of the complex [Pt(PMe₂Ar^{Tipp2})Me₂], **9**, (80 mg, 0.10 mmol) and [H(Et₂O)₂][BAr_F] (116 mg, 0.11 mmol) was dissolved in CH₂Cl₂ at –80°C and allowed to reach the room temperature overnight. After that, CO was bubbled into the solution for 10 min at room temperature. All volatiles were removed under vacuum and the product was isolated as a pale yellow solid. (77.5 mg, 90%)



Anal. Calc. for C₇₂H₇₀BF₂₄OPPt: C, 52.60; H, 4.29. **Found:** C, 52.5; H, 4.0.

IR (Nujol): $\bar{\nu}(\text{CO}) = 2118 \text{ cm}^{-1}$.

¹H NMR (400 MHz, 25 °C, CDCl₃): δ 7.73 (m, 8 H, *o*-BAr_F), 7.59 (dt, 1 H, ³*J*_{HH} = 7.2 Hz, ⁴*J*_{HP} = 2.2 Hz, *p*-C₆H₃), 7.58 (s, 2 H, *m*-Dipp), 7.55 (s, 4 H, *p*-BAr_F), 7.38 (ddd, 1 H, ³*J*_{HH} = 7.6 Hz, ⁴*J*_{HH} = 1.1 Hz, ⁴*J*_{HP} = 3.2 Hz, *m*-C₆H₃), 7.18 (s, 2 H, *m*-Dipp), 6.78 (ddd, 1 H, ³*J*_{HH} = 7.8 Hz, ⁴*J*_{HH} = 1.1 Hz, ⁴*J*_{HP} = 3.1 Hz, *m*-C₆H₃), 3.15 (hept, 1 H, ³*J*_{HH} = 6.9 Hz, *p*-CH-Dipp'), 3.01 (hept, 1 H, ³*J*_{HH} = 6.9 Hz, *p*-CH-Dipp), 2.40 (hept, 2 H, ³*J*_{HH} = 6.9 Hz, *o*-CH-Dipp'), 2.29 (hept, 2 H, ³*J*_{HH} = 6.7 Hz, *o*-CH-Dipp), 1.54 (d, 6 H, ³*J*_{HH} = 7.0 Hz, *o*-Me-Dipp'), 1.43 (d, 6 H, ²*J*_{HP} = 11.2 Hz, ³*J*_{HPt} = 45.2 Hz, PMe₂), 1.34 (d, 6 H, ³*J*_{HH} = 6.8 Hz, *p*-Me-Dipp'), 1.33 (d, 6 H, ³*J*_{HH} = 6.9 Hz, *p*-Me-Dipp), 1.31 (d, 6 H, ³*J*_{HH} = 6.8 Hz, *o*-Me-Dipp), 1.04 (d, 6 H, ³*J*_{HH} = 6.6 Hz, *o*-Me-Dipp), 1.03 (d, 6 H, ³*J*_{HH} = 6.8 Hz, *o*-Me-Dipp'), 0.86 (d, 3 H, ³*J*_{HP} = 5.8 Hz, ²*J*_{HPt} = 80.9 Hz, Pt-Me) ppm.

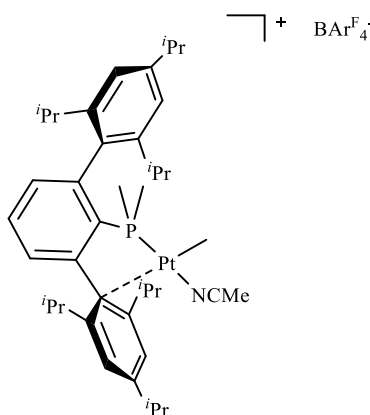
¹³C{¹H} NMR (100.6 MHz, 25 °C, CDCl₃): δ 179.9 (d, ²*J*_{CP} = 141 Hz, CO), 159.6 (s, C_{ipso}-C₆H₃), 156.9 (s, *p*-Dipp), 154.7 (s, *o*-Dipp), 151.6 (s,

p-Dipp), 146.7 (s, *o*-Dipp), 134.8 (s, *o*-BAr_F), 133.8 (d, $^3J_{\text{CP}} = 7$ Hz, *m*-C₆H₃), 133.2 (s, *o*-C₆H₃), 132.6 (d, $^4J_{\text{CP}} = 3$ Hz, *p*-C₆H₃), 131.8 (d, $^3J_{\text{CP}} = 3$ Hz, *m*-C₆H₃), 131.7 (d, $^3J_{\text{CP}} = 2$ Hz, C_{ipso}-Dipp), 128.9 (q, CF₃-BAr_F), 124.0 (s, *m*-Dipp), 121.3 (s, *m*-Dipp), 117.42 (m, *p*-BAr_F), 116.6 (d, $^3J_{\text{CP}} = 5$ Hz, C_{ipso}-Dipp'), 34.4 (s, *p*-CH-Dipp), 33.9 (s, *p*-CH-Dipp), 33.6 (s, *o*-CH-Dipp), 31.4 (s, *o*-CH-Dipp), 26.2 (s, *o*-Me-Dipp), 24.8 (s, *o*-Me-Dipp), 24.0 (s, *o*-Me-Dipp), 23.9 (s, *p*-Me-Dipp), 23.6 (s, *p*-Me-Dipp), 21.3 (s, *o*-Me-Dipp), 11.7 (d, $^1J_{\text{CP}} = 41$ Hz, $^2J_{\text{CPt}} = 43$ Hz, PMe₂), -12.2 (d, $^2J_{\text{CP}} = 5$ Hz, $^1J_{\text{CPt}} = 590$ Hz, Pt-Me) ppm.

$^{31}\text{P}\{^1\text{H}\}$ NMR (161.9 MHz, 25 °C, CDCl₃): δ 11.6 (s, $^3J_{\text{PPt}} = 3212$ Hz) ppm.

Synthesis and Characterisation of [PtMe(NCMe)(PMe₂Ar^{Tipp}₂)] [BAr_F], 21·NCMe

A mixture of the complex [Pt(PMe₂Ar^{Tipp}₂)Me₂], **9**, (40 mg, 0.05 mmol) and [H(Et₂O)₂][BAr_F] (55 mg, 0.05 mmol) was dissolved in CH₂Cl₂ at –80°C and allowed to reach the room temperature overnight. After that, acetonitrile (0.1 mL) was added to the mixture and after 30 min all volatiles were removed under vacuum. The product was obtained as a pale yellow solid. (77.5 mg, 90%)



Anal. Calc. for C₇₃H₇₃BF₂₄NPPt·CH₂Cl₂: C, 52.91; H, 4.44. **Found:** C, 52.7; H, 4.2.

¹H NMR (500 MHz, 25 °C, CD₂Cl₂): δ 7.74 (s, 8 H, *o*-BAr_F), 7.57 (s, 4 H, *p*-BAr_F), 7.52 (td, 1 H, ³*J*_{HH} = 7.6 Hz, ⁵*J*_{HP} = 1.9 Hz, *p*-C₆H₃), 7.28 (m, 3 H, *m*-C₆H₃ and *m*-Tipp), 7.17 (s, 2 H, *m*-Tipp'), 6.79 (dd, 1 H, ³*J*_{HH} = 7.7 Hz, ⁴*J*_{HP} = 2.1 Hz, *m*-C₆H₃), 3.13 (hept, 1 H, ³*J*_{HH} = 6.9 Hz, *p*-CH-Tipp), 2.99 (hept, 1 H, ³*J*_{HH} = 6.6 Hz, *p*-CH-Tipp), 2.40 (hept, 2 H, ³*J*_{HH} = 6.6 Hz, *o*-CH-Tipp), 2.36 (hept, 2 H, ³*J*_{HH} = 6.6 Hz, *o*-CH-Tipp), 2.14 (s, 3H, MeCN), 1.52 (d, 6 H, ³*J*_{HH} = 6.9 Hz, *o*-Me-Tipp), 1.41 (d, 6 H, ²*J*_{HP} = 11.5 Hz, ³*J*_{HPt} = 50.6 Hz, PMe₂), 1.37 (d, 6 H, ³*J*_{HH} = 6.9 Hz, *p*-Me-Tipp), 1.32 (s, 6 H, ³*J*_{HH} = 6.6 Hz, *p*-Me-Tipp), 1.30 (d, 6 H, ³*J*_{HH} = 5.7 Hz, *o*-Me-Tipp), 1.01 (d, 6 H, ³*J*_{HH} = 7.1 Hz, *o*-Me-Tipp), 1.00 (d, 6 H, ³*J*_{HH} = 7.4 Hz, *o*-Me-Tipp), 0.64 (d, 3 H, ³*J*_{HP} = 3.3 Hz, ²*J*_{HPt} = 79.8 Hz, Pt-Me) ppm.

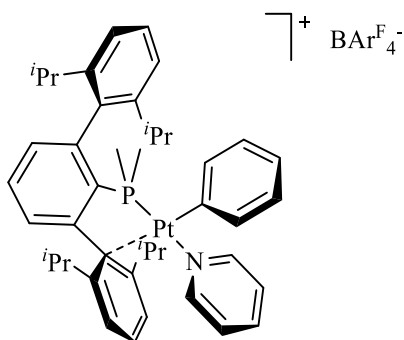
¹³C{¹H} NMR (125.7 MHz, 25 °C, CD₂Cl₂): δ 162.2 (q, BAr_F), 155.8 (s, *p*-Tipp'), 151.4 (s, *o*-Tipp'), 151.2 (s, *p*-Tipp), 147.2 (s, *o*-Tipp), 145.7 (s), 145.5 (s), 145.2 (s), 145.2 (s), 135.2 (s, *o*-BAr_F), 133.7 (s, *m*-C₆H₃), 133.4 (s), 131.9 (s, *p*-C₆H₃), 131.7 (d, ³*J*_{CP} = 12 Hz, *m*-C₆H₃), 129.3 (q, BAr_F),

128.3 (s), 126.12 (s), 123.9 (s), 122.8 (s, *m*-Tipp), 121.8 (s), 121.5 (s, *m*-Tipp'), 117.9 (s, *p*-BAr^F), 34.9 (s, *p*-CH-Tipp), 34.1 (s, *p*-CH-Tipp), 33.4 (s, *o*-CH-Tipp), 31.7 (s, *o*-CH-Tipp), 26.5 (s, *o*-Me-Tipp), 24.5 (s, *p*-Me-Tipp), 24.3 (s, *p*-Me-Tipp), 24.2 (s, *o*-Me-Tipp), 21.6 (s, *o*-Me-Tipp), 13.4 (d, $^1J_{CP} = 46$ Hz, $^2J_{CPt} = 46$ Hz, PMe₂), -9.00 (d, $^2J_{CP} = 6$ Hz, Pt-Me) ppm.

$^{31}\text{P}\{^1\text{H}\}$ NMR (202.40 MHz, 25 °C, CD₂Cl₂): δ -2.3 (s, $^1J_{PPt} = 4318$ Hz) ppm.

Synthesis and Characterisation of Complex [Pt(PMe₂Ar^{Dipp2})Ph(Py)][BAR_F], 22

A solid mixture of complex **11** (20 mg, 0.025 mmol) and [H(Et₂O)₂][BAR_F] (30 mg, 0.029) was dissolved in CH₂Cl₂ at –80 °C. The reaction mixture was allowed to reach room temperature overnight. All volatiles were then removed under vacuum. Pyridine (0.1 mL) was added to the mixture and after 30 min all volatiles were removed under vacuum, obtaining the product as a pale yellow solid (38 mg, 90%).



Anal. Calc. for C₇₅H₆₅BF₄NNPt: C, 53.5; H, 4.0; N, 1.2. **Found:** C, 53.8; H, 4.0; N, 0.8.

¹H NMR (500 MHz, 25 °C, CD₂Cl₂): δ 8.86 (br, 2 H, *o*-Py), 7.79 (br, 1 H, *p*-Py), 7.73 (s, 8 H, *m*-BAR_F), 7.66 (t, 1 H, ³*J*_{HH} = 7.8 Hz, *p*-C₆H₃), 7.60 (dd, 1 H, ³*J*_{HH} = 7.8 Hz, ⁴*J*_{HP} = 2.1 Hz, *m*-C₆H₃), 7.56 (s, 4 H, *p*-BAR_F), 7.43 (t, 1 H, ³*J*_{HH} = 7.9 Hz, *p*-Dipp), 7.33 (br, 2 H, *m*-Py), 7.28 (m, 3 H, *m*-Dipp and *p*-Ph), 7.12 (d, 2 H, ³*J*_{HH} = 7.8 Hz, *m*-Dipp), 7.05 (m, 2 H, *m*-Ph), 6.85 (d br, 1 H, ³*J*_{HH} = 7.8 Hz, ⁴*J*_{HP} = 2.8 Hz, *m*-C₆H₃), 6.79 (br, 2 H, *o*-Ph), 6.61 (t, 1 H, ³*J*_{HH} = 7.8 Hz, *p*-Dipp), 2.58 (hept, 2 H, ³*J*_{HH} = 7.1 Hz, CH-Dipp), 2.39 (hept, 2 H, ³*J*_{HH} = 6.3 Hz, CH-Dipp), 1.87 (d, 6 H, ³*J*_{HH} = 6.7 Hz, Me-Dipp), 1.30 (d, 6 H, ³*J*_{HH} = 6.8 Hz, Me-Dipp), 1.22 (d, 6 H, ²*J*_{HP} = 11.5 Hz, PMe₂), 1.06 (d, 6 H, ³*J*_{HH} = 6.8 Hz, Me-Dipp), 1.03 (d, 6 H, ³*J*_{HH} = 6.7 Hz, Me-Dipp) ppm.

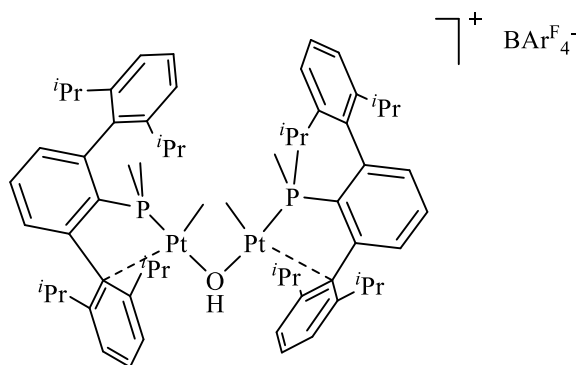
¹³C{¹H} NMR (125.7 MHz, 25 °C, CD₂Cl₂): δ 162.3 (q, BAR_F), 150.2 (s, *p*-Py), 150.14 (s, *o*-Py), 149.6 (s, *o*-Dipp), 147.5 (s, *o*-Dipp), 139.4 (s, *p*-C₆H₃), 136.0 (s, C_{ipso}-Dipp), 135.4 (s, *o*-BAR_F), 134.8 (d, ⁴*J*_{CP} = 2 Hz, *m*-Ph), 134.0 (d, ¹*J*_{CP} = 7 Hz, C_{ipso}-C₆H₃), 133.6 (s, *p*-Dipp), 132.3 (d, ³*J*_{CP} = 2 Hz, *m*-C₆H₃), 131.6 (s, *m*-C₆H₃), 130.6 (s, *p*-Dipp), 129.3 (s, *o*-Ph), 126.7 (s, *p*-Ph), 125.8 (s, *m*-Dipp), 125.5 (br, *p*-Py), 124.6 (br, *m*-Py), 123.7 (s, *m*-Dipp), 122.9 (d, ³*J*_{CP} = 5 Hz, C_{ipso}-Dipp), 118.0 (q, ³*J*_{CF} = 4 Hz, *p*-BAR_F),

33.4 (s, CH-Dipp), 31.9 (s, CH-Dipp), 26.5 (s, Me-Dipp), 25.4 (s, Me-Dipp), 24.4 (s, Me-Dipp), 21.8 (s, Me-Dipp), 13.3 (d, $^1J_{\text{CP}} = 45$ Hz, PMe_2) ppm.

$^{31}\text{P}\{^1\text{H}\}$ NMR (202.4 MHz, 25 °C, CD_2Cl_2): δ -4.6 (s, $^1J_{\text{PPt}} = 3757$ Hz) ppm.

Synthesis and Characterisation of $[\{\text{PtMe}(\text{PMe}_2\text{Ar}^{\text{Dipp}_2})\}_2(\mu\text{-OH})][\text{BAr}_\text{F}]$, **23**

In a young NMR tube, a solid mixture of $[\text{PtMe}_2(\text{PMe}_2\text{Ar}^{\text{Dipp}_2})]$, **8**, (20 mg, 0.03 mmol) and $[\text{PtMe}(\text{PMe}_2\text{Ar}^{\text{Dipp}_2})(\text{solvent})][\text{BAr}_\text{F}]$, **20·S**, (47 mg, 0.03 mmol) was dissolved in CD_2Cl_2 (0.5 mL) under nitrogen at room temperature. After removing all volatiles under vacuum the compound was isolated as a pale yellow solid.



HR-MS (ESI) m/z Calcd. for M^+ : 1353.60. **Expt.:** 1353.59.

^1H NMR (500 MHz, 25 °C, CD_2Cl_2): δ 7.73 (s, 8 H, $o\text{-BAr}_\text{F}$), 7.57 (s, 4 H, $p\text{-BAr}_\text{F}$), 7.53 (t, 2 H, $^3J_{\text{HH}} = 7.8$ Hz, $p\text{-Dipp}$), 7.50 (t, 2 H, $^3J_{\text{HH}} = 7.8$ Hz, $p\text{-C}_6\text{H}_3$), 7.46 (t, 2 H, $^3J_{\text{HH}} = 7.8$ Hz, $p\text{-Dipp}$), 7.30 (d, 4 H, $^3J_{\text{HH}} = 7.8$ Hz, $m\text{-Dipp}$), 7.27 (d, 2 H, $^3J_{\text{HH}} = 7.8$ Hz, $m\text{-Dipp}$), 7.22 (dd, 2 H, $^3J_{\text{HH}} = 7.5$ Hz, $^4J_{\text{HP}} = 2.3$ Hz, $m\text{-C}_6\text{H}_3$), 7.05 (d, 2 H, $^3J_{\text{HH}} = 7.8$ Hz, $m\text{-Dipp}$), 6.86 (dd, 2 H, $^3J_{\text{HH}} = 7.7$ Hz, $^4J_{\text{HP}} = 1.5$ Hz, $m\text{-C}_6\text{H}_3$), 2.43 (hept, 2 H, $^3J_{\text{HH}} = 6.8$ Hz, CH-Dipp), 2.37 (hept, 2 H, $^3J_{\text{HH}} = 6.7$ Hz, CH-Dipp), 2.35 (hept, 2 H, $^3J_{\text{HH}} = 6.7$ Hz, CH-Dipp), 2.33 (hept, 2 H, $^3J_{\text{HH}} = 6.8$ Hz, CH-Dipp), 1.72 (d, 6 H, $^3J_{\text{HH}} = 6.9$ Hz, Me-Dipp), 1.34 (d, 12 H, $^2J_{\text{HP}} = 11.0$ Hz, $^3J_{\text{HPt}} = 50.0$ Hz, PMe_2), 1.34 (d, 6 H, $^3J_{\text{HH}} = 6.8$ Hz, Me-Dipp), 1.31 (d, 6 H, $^3J_{\text{HH}} = 6.7$ Hz, Me-Dipp), 1.26 (d, 6 H, $^3J_{\text{HH}} = 6.8$ Hz, Me-Dipp), 1.07 (d, 6 H, $^3J_{\text{HH}} = 6.8$ Hz, Me-Dipp), 1.04 (d, 6 H, $^3J_{\text{HH}} = 6.7$ Hz, Me-Dipp), 0.97 (d, 6 H, $^3J_{\text{HH}} = 6.6$ Hz, Me-Dipp), 0.89 (d, 6 H, $^3J_{\text{HH}} = 6.9$ Hz, Me-Dipp), 0.50 (d, 6 H, $^3J_{\text{HP}} = 2.7$ Hz, $^2J_{\text{HPt}} = 78.0$ Hz, Pt-Me), -2.35 (t br, 1 H, $^2J_{\text{HPt}} = 23.5$ Hz, $^3J_{\text{HP}} = 1.5$ Hz, $\mu\text{-OH}$) ppm.

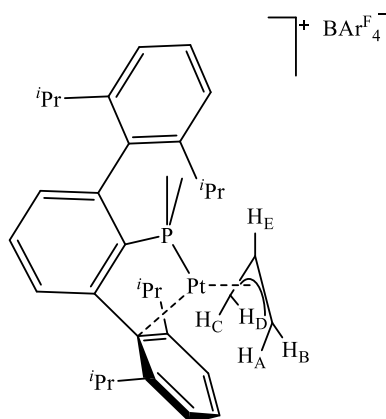
$^{13}\text{C}\{^1\text{H}\}$ NMR (125.7 MHz, 25 °C, CD_2Cl_2): δ 162.4 (q, $\text{C}_{\text{ipso}}\text{-BAr}_\text{F}$), 149.3 (s, $o\text{-Dipp}$), 147.6 (s, $o\text{-Dipp}$), 147.6 (s, $o\text{-Dipp}$), 146.8 (s, $o\text{-C}_6\text{H}_3$), 146.6 (s, $o\text{-C}_6\text{H}_3$), 146.4 (s, $o\text{-Dipp}$), 144.7 (s, $o\text{-C}_6\text{H}_3$), 135.4 (s, $m\text{-BAr}_\text{F}$), 133.6 (d, $^3J_{\text{CP}} = 7$ Hz, $m\text{-C}_6\text{H}_3$), 133.9 (s, $p\text{-Dipp}$), 132.9 (s, $p\text{-Dipp}$), 131.5 (s, $m\text{-$

C₆H₃), 131.4 (s, *m*-C₆H₃), 131.3 (s, *p*-C₆H₃), 131.3 (s, *p*-C₆H₃), 130.3 (s, *p*-Dipp), 124.5 (s, *m*-Dipp), 123.7 (s, *m*-Dipp), 123.6 (s, *m*-Dipp), 123.5 (s, *m*-Dipp), 118.1 (hept, ⁴*J*_{CF} = 4 Hz, *p*-BAr_F), 33.3 (s, CH-Dipp), 32.9 (s, CH-Dipp), 31.9 (s, CH-Dipp), 31.8 (s, CH-Dipp), 26.6 (s, Me-Dipp), 26.4 (s, Me-Dipp), 24.9 (s, Me-Dipp), 24.1 (s, Me-Dipp), 21.9 (s, Me-Dipp), 21.7 (s, Me-Dipp), 14.5 (d, ¹*J*_{CP} = 44 Hz, PMe₂), 14.1 (d, ¹*J*_{CP} = 45 Hz, PMe₂), -0.8 (t, ²*J*_{CP} = 3 Hz, Pt-Me) ppm.

³¹P{¹H} NMR (202.4 MHz, 25 °C, CD₂Cl₂): δ -3.2 (s, ¹*J*_{Pt} = 4270 Hz) ppm.

Synthesis and Characterisation of $[\text{Pt}(\eta^3\text{-C}_3\text{H}_5)(\text{PMe}_2\text{Ar}^{\text{Dipp}_2})][\text{BAr}_\text{F}^-]$, **24**

- 1) The cationic methyl complex **20·S** (50 mg, 0.032 mmol) was dissolved in CD_2Cl_2 (0.5 mL) under nitrogen at room temperature. The system was degassed (3 freeze-pump-thaw cycles) and charged with acetylene (2 bar). After 6 hours, the product formed with quantitative spectroscopic yield. After removing all volatiles under vacuum, the product was obtained as a pale yellow solid.
- 2) This synthetic procedure was performed in the absence of light. A solid mixture of the allyl bromide complex $[\text{Pt}(\text{PMe}_2\text{Ar}^{\text{Dipp}_2})(\eta^3\text{-C}_3\text{H}_5)\text{Br}]$, **14**, (55 mg, 0.07 mmol) and AgSbF_6 (24 mg, 0.07 mmol) was dissolved in dichloromethane (*c.a.* 3 mL) at room temperature. After 30 min stirring, the suspension was filtered and all volatiles were removing under vacuum, obtaining the product as a pale yellow solid. (56 mg, 85 %).



Anal. Calc. for $\text{C}_{67}\text{H}_{60}\text{BF}_{24}\text{PPt}$: C, 51.6; H, 3.9. **Found:** C, 51.4; H, 4.2.

^1H NMR (500 MHz, 25 °C, CD_2Cl_2): δ 7.73 (s, 8 H, *o*- BAr_F), 7.65 (t, 1 H, $^3J_{\text{HH}} = 7.5$ Hz, *p*-Dipp), 7.62 (t, 1 H, $^3J_{\text{HH}} = 7.6$ Hz, *p*- C_6H_3), 7.57 (s, 4 H, *p*- BAr_F), 7.51 (t, 1 H, $^3J_{\text{HH}} = 7.8$ Hz, *p*-Dipp), 7.37 (dd, 1 H, $^3J_{\text{HH}} = 7.6$ Hz, $^4J_{\text{HP}} = 2$ Hz, *m*- C_6H_3), 7.34 (d, 2 H, $^3J_{\text{HH}} = 7.4$ Hz, *m*-Dipp), 7.33 (d, 2 H, $^3J_{\text{HH}} = 7.0$ Hz, *m*-Dipp), 6.86 (dd, 1 H, $^3J_{\text{HH}} = 7.6$ Hz, $^4J_{\text{HP}} = 2.0$ Hz, *m*- C_6H_3), 5.08 (tt, 1 H, $^3J_{\text{HH}} = 6.7$ Hz, $^3J_{\text{HH}} = 12.7$ Hz, H_E), 3.22 (m, 1 H, $^2J_{\text{HH}} = 2.2$ Hz, $^3J_{\text{HH}} = 6.7$ Hz, $^3J_{\text{HP}} = 3$ Hz, H_A), 3.14 (dd, 1 H, $^3J_{\text{HH}} = 13.4$ Hz, $^3J_{\text{HP}} = 8.1$ Hz, H_D), 2.38 (hept, 2 H, $^3J_{\text{HH}} = 6.3$ Hz, CH-Dipp), 2.31 (hept, 2 H, $^3J_{\text{HH}} = 6.3$ Hz, CH-Dipp), 2.08 (d br, 1 H, $^3J_{\text{HH}} = 13$ Hz, H_B), 1.84 (br, 1 H, $^3J_{\text{HH}} = 7.5$ Hz, $^3J_{\text{HP}} = 7.0$ Hz, H_C), 1.61 (d, 3 H, $^2J_{\text{HP}} = 10.9$ Hz, $^3J_{\text{HPt}} =$

49.2 Hz, PMe), 1.48 (d, 3 H, $^2J_{\text{HP}} = 11.1$ Hz, $^3J_{\text{HPt}} = 52.6$ Hz, PMe), 1.32 (d, 6 H, $^3J_{\text{HH}} = 6.9$ Hz, Me-Dipp), 1.29 (d, 3 H, $^3J_{\text{HH}} = 6.8$ Hz, Me-Dipp), 1.28 (d, 3 H, $^3J_{\text{HH}} = 7.1$ Hz, Me-Dipp), 1.09 (d, 3 H, $^3J_{\text{HH}} = 6.8$ Hz, Me-Dipp), 1.04 (d, 3 H, $^3J_{\text{HH}} = 6.8$ Hz, Me-Dipp), 1.01 (d, 3 H, $^3J_{\text{HH}} = 6.9$ Hz, Me-Dipp), 0.95 (d, 3 H, $^3J_{\text{HH}} = 6.8$ Hz, Me-Dipp) ppm.

$^{13}\text{C}\{^1\text{H}\}$ NMR (125.7 MHz, 25 °C, CD_2Cl_2): δ 162.4 (q, *m*-BAr_F), 151.8 (s), 149.4 (s), 147.6 (s), 147.5 (s), 147.0 (s), 145.6 (s), 145.3 (s), 144.6 (s), 134.4 (d, $^3J_{\text{CP}} = 6$ Hz, *m*-C₆H₃), 133.3 (d, $^4J_{\text{CP}} = 3$ Hz, *p*-C₆H₃), 132.4 (s, *m*-Dipp), 132.3 (s, *m*-C₆H₃), 130.9 (s, *p*-Dipp), 129.5 (q, C_{*ipso*}-BAr_F), 128.3 (s, *p*-Dipp), 123.8 (s, *m*-Dipp), 118.1 (q, *o*-BAr_F), 115.1 (br, $^1J_{\text{CPt}} = 23$ Hz, CH₂-CH-CH₂), 94.5 (d, $^1J_{\text{CP}} = 28$ Hz, C_{CD}), 43.8 (S, $^1J_{\text{CPt}} = 259$ Hz, C_{AB}), 34.2 (s, CH-Dipp), 33.9 (s, CH-Dipp), 31.9 (s, CH-Dipp), 31.8 (s, CH-Dipp), 26.6 (s, Me-Dipp), 26.5 (s, Me-Dipp), 25.4 (s, Me-Dipp), 24.6 (s, Me-Dipp), 24.4 (s, Me-Dipp), 24.2 (s, Me-Dipp), 21.8 (s, Me-Dipp), 21.7 (s, Me-Dipp), 17.3 (d, $^1J_{\text{CP}} = 38$ Hz, PMe), 16.5 (d, $^1J_{\text{CP}} = 39$ Hz, PMe) ppm.

$^{31}\text{P}\{^1\text{H}\}$ NMR (202.4 MHz, 25 °C, CD_2Cl_2): δ 18.6 (s, $^1J_{\text{PPt}} = 4078$ Hz) ppm.

I.3.3. Kinetic Studies on the Cyclometallation of Complex 2

In a typical experiment, a pure sample of complex **2** was dissolved in benzene- d_6 , introduced into the NMR device, and heated at the desired temperature for about 2-3 hours, during which time the reaction was followed by $^{31}\text{P}\{^1\text{H}\}$ and ^1H NMR. The experiment was repeated at 40, 45, 50, 55, and 60 °C. The activation parameters ΔS^\ddagger and ΔH^\ddagger were calculated by means of an Eyring plot (temperature dependence of the rate constant).

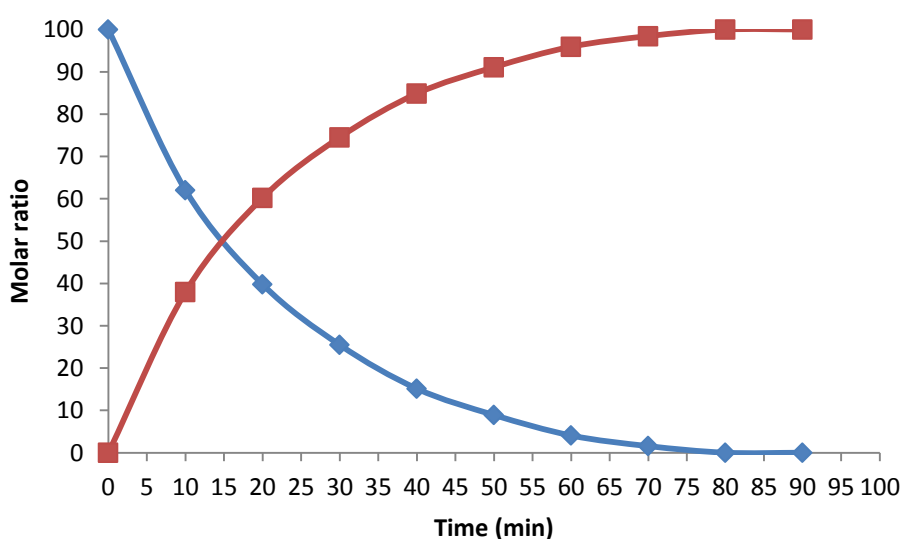


Figure 75: Time depending conversion of **2** (blue) into **3** (red) at 55 °C in C_6D_6 . Molar ratio was calculated based on the integrals of both species in the ^1H NMR spectra.

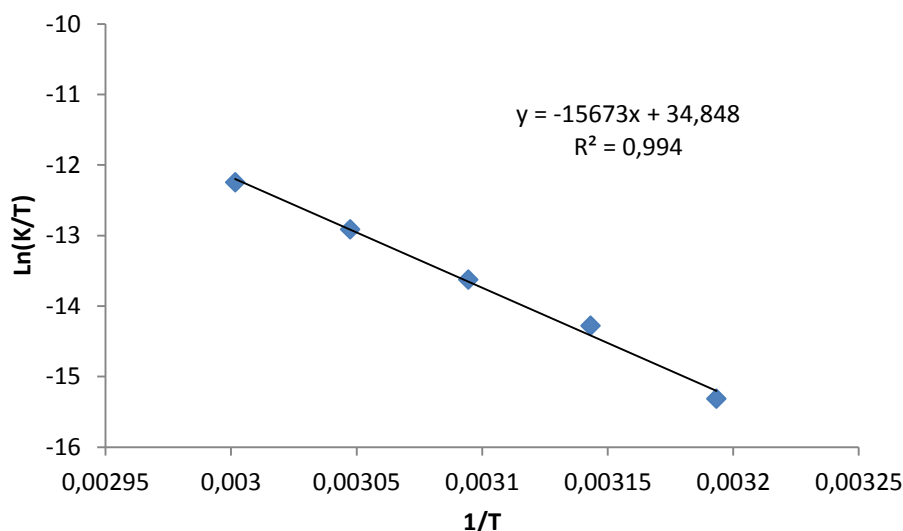


Figure 76: Eyring plot for the intramolecular cyclometallation reaction of **2**.

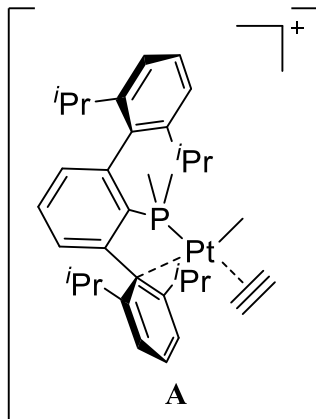
I.3.4. Reaction of complexes **2** and **3** with $[\text{H}(\text{Et}_2\text{O})_2][\text{BAr}_\text{F}]$

A solid mixture of the complex (**2** or **3**) (0.017 mmol) and $[\text{H}(\text{Et}_2\text{O})_2][\text{BAr}_\text{F}]$ (0.02 mmol) was placed in a Young NMR tube and dissolved in CD_2Cl_2 (0.5 mL) at $-80\text{ }^\circ\text{C}$. The reaction was followed by ^{31}P and ^1H NMR at different temperatures. Once at room temperature, the reaction mixture was heated in an oil bath at $50\text{ }^\circ\text{C}$.

I.3.5. Characterisation of detected intermediates in the formation of complex **24**

In Young NMR tube complex **20-S** (50 mg) was dissolved in CD_2Cl_2 (0.5 mL) under N_2 . The system was degassed (3 freeze-pump-thaw cycles) and bubbled with C_2H_2 at $-80\text{ }^\circ\text{C}$ for 1 min. The mixture of both detected intermediates (A: acetylene adduct and B: vinylidene derivative) were characterized at $-20\text{ }^\circ\text{C}$ in solution by NMR spectroscopy.

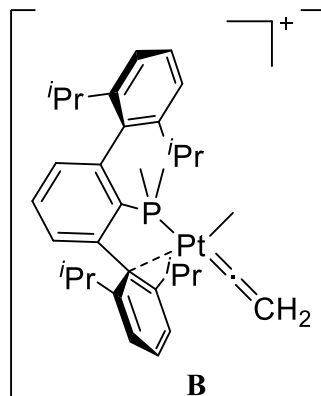
Intermediate A



^1H NMR (400 MHz, $-20\text{ }^\circ\text{C}$, CD_2Cl_2): δ 3.08 (d, $^3J_{\text{HP}} = 4.6\text{ Hz}$, $^2J_{\text{HPt}} = 50.0\text{ Hz}$, 2 H, C_2H_2), 0.60 (d, $^3J_{\text{HP}} = 3.8\text{ Hz}$, $^2J_{\text{HPt}} = 76\text{ Hz}$, 3 H, Pt- CH_3) ppm.

^{13}C NMR (100.6 MHz, $-20\text{ }^\circ\text{C}$, CD_2Cl_2): δ 77.7 (dd, $^1J_{\text{CH}} = 263.0\text{ Hz}$, $^2J_{\text{CH}} = 44.3\text{ Hz}$, $^2J_{\text{CP}} = 11.5\text{ Hz}$, C_2H_2), -3.2 (qd, $^1J_{\text{CH}} = 140\text{ Hz}$, $^2J_{\text{CP}} = 4.7\text{ Hz}$, Pt- CH_3) ppm.

$^{31}\text{P}\{^1\text{H}\}$ NMR (161.9 MHz, $-20\text{ }^\circ\text{C}$, CD_2Cl_2): δ 11.1 (s, $^1J_{\text{PPt}} = 4296\text{ Hz}$) ppm.

Intermediate **B**

^1H NMR (400 MHz, -20°C , CD_2Cl_2): δ 2.21 (s, 2 H, Pt-CCH₂), 0.44 (s, $^2J_{\text{CPt}} = 74$ Hz, 3 H, Pt-CH₃) ppm.

^{13}C NMR (100.6 MHz, -20°C , CD_2Cl_2): δ 221.2 (s, α -PtCCH₂), 33.7 (t, β -PtCCH₂), -6.6 (qd, $^1J_{\text{CH}} = 135.0$ Hz, $^2J_{\text{CP}} = 5.5$ Hz, Pt-CH₃) ppm.

$^{31}\text{P}\{^1\text{H}\}$ NMR (161.9 MHz, -20°C , CD_2Cl_2): δ -4.2 (s, $^1J_{\text{PPt}} = 4615$ Hz) ppm.

I.3.6. Reaction of 20-S with H₂ and D₂

In a Young NMR tube complex **20-S** (50 mg) was dissolved in CD_2Cl_2 (0.5 mL). The system was degassed (3 freeze-pump-thaw cycles) and charged with H₂ or D₂ (2 atm) at room temperature. The reaction was followed by ^1H and ^{31}P NMR spectroscopies.

I.3.7. Computational Details

Calculations were carried out at the DFT level with Gaussian 09 suite of programs,¹¹⁸ with Truhlar's hybrid meta-GGA functional M06.¹¹⁹ The Pt

¹¹⁸ M. J. Frisch, G. W. Trucks, G. E. Schlegel, G. E. Scuseria, M. A. Robb, J. R. Cheeseman, G. Scalmani, V. Barone, B. Mennucci, G. A. Petersson, H. Nakatsuji, M. Caricato, X. Li, H. P. Hratchian, A. F. Izmaylov, J. Bloino, G. Zheng, J. L. Sonnenberg, M. Hada, M. Ehara, K. Toyota, R. Fukuda, J. Hasegawa, M. Ishida, T. Nakajima, Y. Honda, O. Kitao, H. Nakai, T. Vreven, J. A. Montgomery, J. E. Peralta, F. Ogliaro, M. Bearpark, J. J. Heyd, E. Brothers, K. N. Kudin, V. N. Staroverov, R. Kobayashi, J. 246

atom was represented by the Stuttgart/Dresden Effective Core Potential and the associated basis set as implemented in Gaussian 09 (SDD).¹²⁰ The remaining H, C, O and P atoms were represented by means of the 6-31G(d,p) basis set.¹²¹ The geometries for all species described were optimized in the gas phase without symmetry restrictions. Frequency calculations were performed on the optimized structures at the same level of theory to characterize the stationary points, as well as for the calculation of gas-phase enthalpies (H), entropies (S) and Gibbs energies (G). The nature of the intermediates connected by a transition state was determined by Intrinsic Reaction Coordinate (IRC) calculations or by perturbing the transition states along the TS coordinate and optimizing to a minimum. The solvent effects (dichloromethane) were modelled with the SMD¹⁰⁹ continuum model by single point calculations on gas phase-optimized geometries and free optimizations in solution. The relative free energies in solution were calculated according to: $\Delta G^{\text{solution}} = \Delta E^{\text{solution}} + (\Delta G^{\text{gas}} - \Delta E^{\text{gas}})$, where $\Delta E^{\text{solution}}$ is the electronic energy plus the solvent entropy.¹²²

The delocalization energies are estimated as follows

Normand, K. Raghavachari, A. Rendell, J. C. Burant, S. S. Iyengar, J. Tomasi, M. Cossi, N. Rega, J. M. Millam, M. Klene, J. E. Knox, J. B. Cross, V. Bakken, C. Adamo, J. Jaramillo, R. Gomperts, R. E. Stratmann, O. Yazyev, A. J. Austin, R. Cammi, C. Pomelli, J. W. Ochterski, R. L. Martin, K. Morokuma, O. Zakrzewski, G. A. Voth, P. Salvador, J. J. Dannenberg, S. Dapprich, A. D. Daniels, Ö. Farkas, J. B. Foresman, J. V. Ortiz, J. Cioslowski, D. J. Fox, Gaussian, Inc., Wallingford CT, **2009**.

¹¹⁹ Y. Zhao, D. Truhlar, *Theor. Chim. Acta* **2008**, 120, 215.

¹²⁰ D. Andrae, U. H., M. Dolg, H. Stoll, H. Preul, *Theor. Chim. Acc.* **1990**, 123.

¹²¹ a) W. J. Hehre, R. Ditchfield, J. A. Pople, *J. Phys. Chem.* **1972**, 56, 2257; b) P. C. Hariharan, J. A. Pople, *Theor. Chim. Acta.* **1973**, 28, 213; c) M. M. Francl, W. J. Pietro, W. J. Hehre, J. S. Binkley, M. S. Gordon, D. J. Defrees, J. A. Pople, *J. Chem. Phys.* **1982**, 77, 3654.

¹²² A. A. C. Braga, G. Ujaque, F. Maseras, *Organometallics* **2006**, 25, 3647-3658.

$$\Delta E_{i,j} = q_i \frac{F(i,j)^2}{\varepsilon_i - \varepsilon_j}$$

Where $\Delta E_{i,j}$ is the stabilization energy associated with the donor –acceptor (i-j) interaction as obtained from second order perturbation theory analysis of the Fock matrix and:

q_i is the occupancy of the donor (i) orbital,

ε_i and ε_j are the corresponding diagonal elements (orbital energies) of the NBO Fock matrix and

$F(i,j)$ is the corresponding off-diagonal element of the NBO Fock Matrix.

I.3.8. 1D Selective EXSY experiments

a) Ethylene exchange on compound **20**•C₂H₄

Complex **20**•S (40 mg) was dissolved in 0.5 mL of CD₂Cl₂ in a Young NMR tube. Then, three vacuum/nitrogen cycles were performed and the solution was bubbled with C₂H₄ at room temperature for two minutes. Experiments were performed in the temperature range from 25 to 0 °C. A set of 1D Selective EXSY experiments with different mixing times was performed for each temperature by irradiation of the Pt-C₂H₄ signal with d 3.92 ppm (designated as A), which allowed for chemical exchange into free C₂H₄ signal (B). The two peaks in the 1D EXSY spectra were then integrated and the total integral intensity normalised to 100% at each temperature (tables 7-8). The representation of these values *vs.* mixing time is shown in Figures 76-81. Then, the spreadsheet entered into Excel (simulation ran out to a reaction time of first in order to fit all the experimental data) works in conjunction with the solver routine to minimise

the sum of the squares of the differences between the experimental and calculated values by varying the rate constant, k .

	Temperature (K)					
	298		293		288	
Mixing time (s)	A	B	A	B	A	B
0,01	75,97	24,03	83,83	16,17	-	-
0,015	-	-	-	-	87,62	12,38
0,02	56,12	43,88	-	-	-	-
0,025	-	-	65,36	34,64	79,60	20,40
0,03	40,66	59,34	-	-	-	-
0,035	-	-	55,66	44,34	71,25	28,75
0,05	25,36	74,64	43,31	56,69	63,54	36,46
0,07	-	-	32,70	67,30	-	-
0,08	18,94	81,06	-	-	-	-
0,1	16,08	83,92	22,26	77,74	41,00	59,00
0,12	-	-	19,44	80,56		
0,15	-	-	15,40	84,60	29,44	70,56
0,2	-	-	-	-	20,87	79,13
0,25	-	-	-	-	17,29	82,71

Table 7

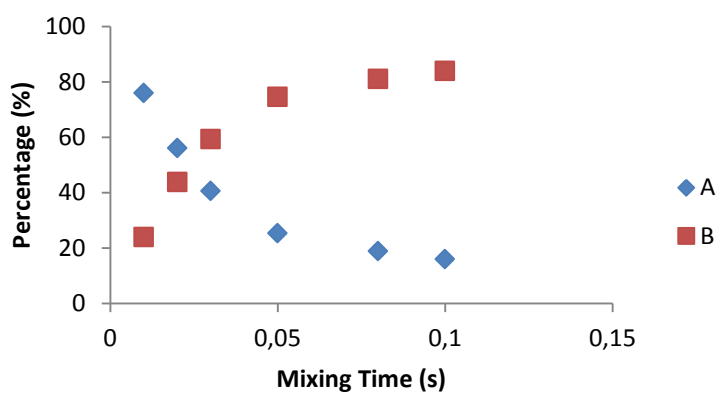
	Temperature (K)					
	283		278		273	
Mixing Time (s)	A	B	A	B	A	B
0,01	95,63	4,37	-	-	-	-
0,02	91,35	8,65	95,76	4,24	-	-
0,04	83,26	16,74	-	-	-	-
0,05	-	-	-	-	94,67	5,33
0,07	71,72	28,28	84,55	15,45	-	-
0,10	-	-	77,87	22,13	-	-
0,14	-	-	70,90	29,10	-	-
0,15	49,33	50,67	-	-	85,33	14,67
0,17	44,46	55,54	-	-	-	-
0,18			64,06	35,94	-	-
0,2	39,11	60,89	-	-	-	-
0,25	-	-	52,96	47,04	75,07	24,93
0,27	29,94	70,06	-	-	-	-

0,3	-	-	46,30	53,70	-	-
0,35	-	-	40,93	59,07	65,20	34,80
0,5	-	-	-	-	52,94	47,06
0,7	-	-	-	-	37,02	62,98
0,8	-	-	-	-	32,27	67,73
0,9	-	-	-	-	26,20	73,80

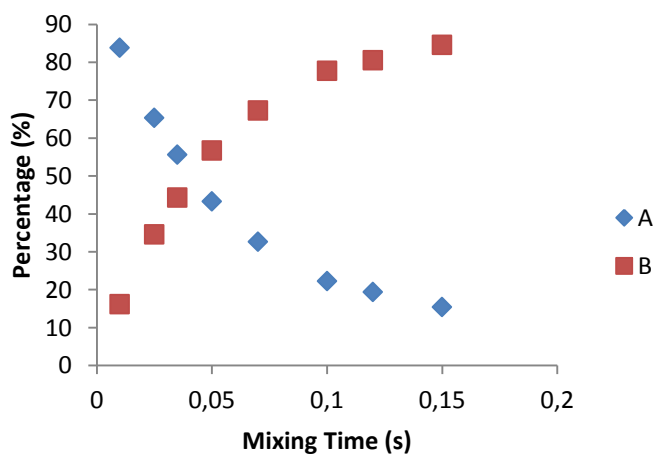
Table 8

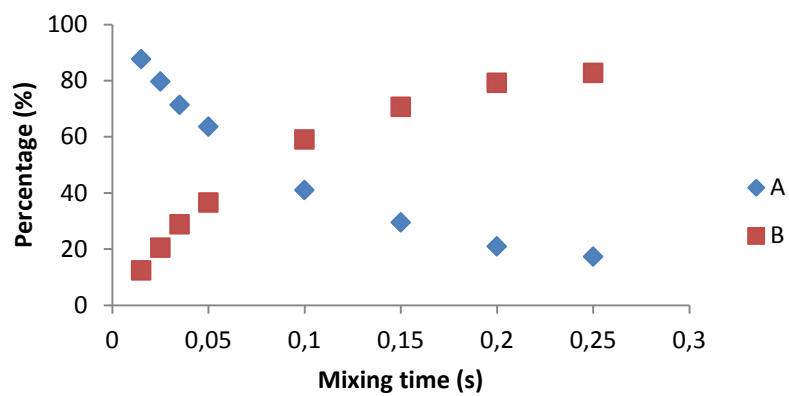
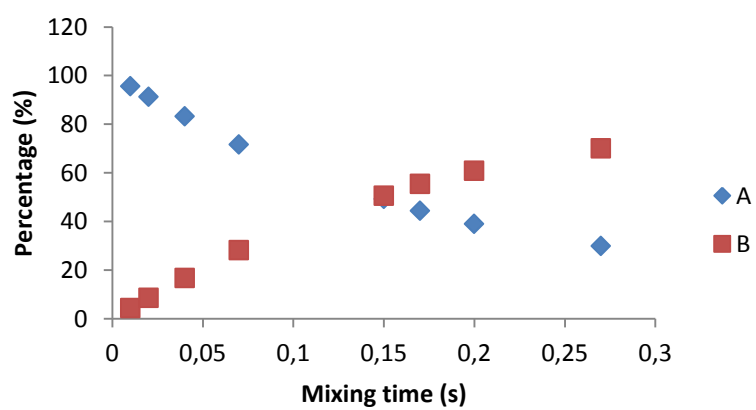
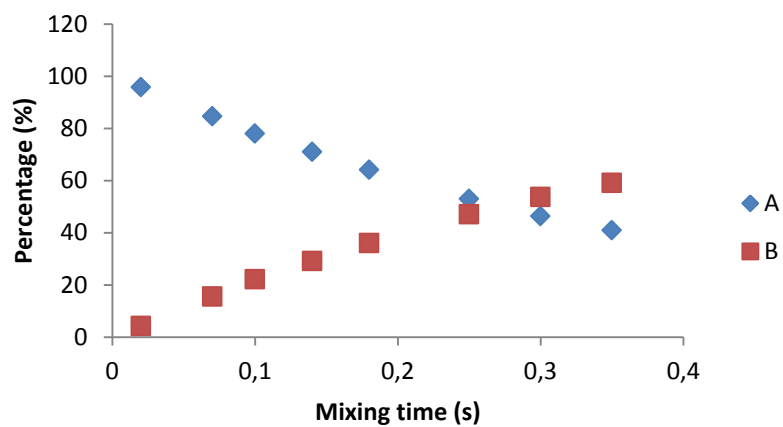
Figures 76-81 illustrate the representation of the data included in Tables 7-8.

· 25 °C (298 K)

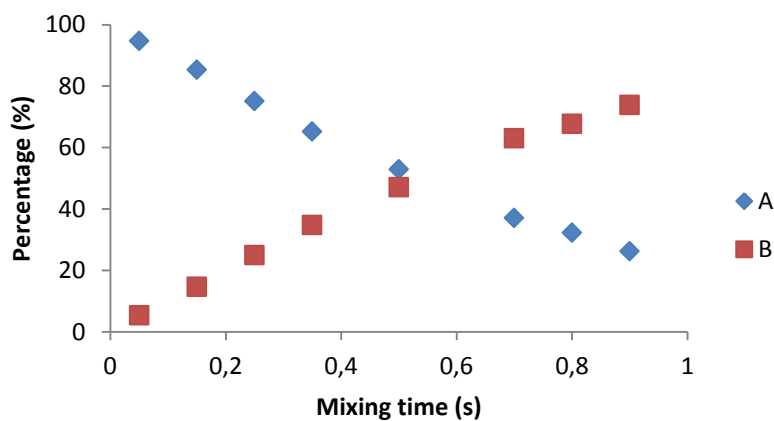


· 20 °C (293 K)



$-15\text{ }^{\circ}\text{C}$ (288 K) $-10\text{ }^{\circ}\text{C}$ (283 K) $5\text{ }^{\circ}\text{C}$ (278 K)

·0 °C (273 K)



Figures 76-81. Representation of the peak intensities (percentage) as a function of the exchange or reaction time.

The rate constants determined as described before were used to calculate the activation parameters. The resulting representation of the Eyring equation is illustrated in Figure 82.

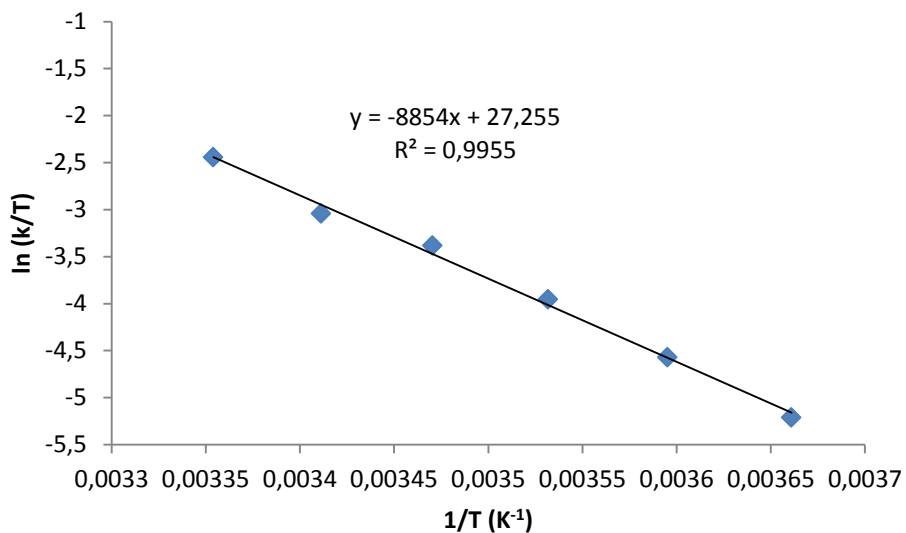


Figure 82: Eyring representation of the exchange rate constants obtained from the 1D Selective EXSY experiments for ethylene exchange on complex **20**·C₂H₄.

b) Acetylene exchange on compound **20·C₂H₂**

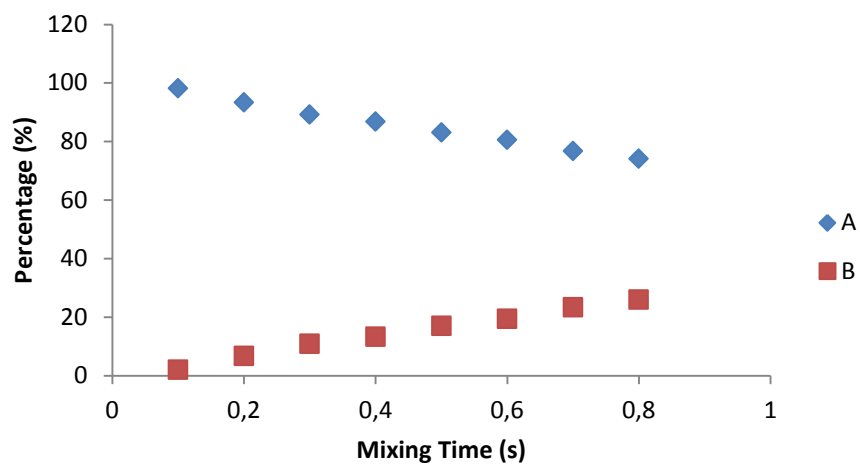
Complex **20·S** (40 mg) was dissolved in 0.5 mL of CD₂Cl₂ in a Young NMR tube. Then, three vacuum/nitrogen cycles were performed and the solution was bubbled with acetylene at -80 °C during 1 minute. Experiments were performed in the temperature range from -35 °C to -20 °C. A set of 1D EXSY experiments with different mixing times was performed for each temperature by irradiation of the Pt-C₂H₂ signal with δ 3.18 ppm (designated as A), which allowed for chemical exchange into free C₂H₂ signal (B). The two peaks in the 1D EXSY spectra were then integrated and the total integral intensity normalised to 100 % at each temperatures (Table 9). The representation of these values vs. mixing time is shown in Figures 83 to 87. The spreadsheet entered into Excel (simulation ran out to a reaction time of first in order to fit all experimental data) works in conjunction with the solver routine to minimise the sum of the squares of the differences between the experimental and calculated values by varying the rate constant, k.

Mixing time (s)	Temperature (K)							
	238		243		248		253	
	A	B	A	B	A	B	A	B
0,05	-	-	-	-	-	-	87,85	12,15
0,1	98,07	1,93	92,99	7,01	88,25	11,77	76,43	23,57
0,2	93,34	6,66	86,28	13,72	76,45	23,55	57,05	42,05
0,3	89,2	10,8	80,41	19,59	66,1	33,9	43,58	56,42
0,4	86,71	13,29	75,03	24,97	57,97	42,03	32,75	67,25
0,5	83,04	16,96	68,17	31,83	50,24	49,76	25,82	74,18
0,6	80,51	19,39	63,78	36,22	44,01	55,99	18,41	81,5
0,7	76,67	23,33	57,23	42,77	38,17	61,83	14,82	85,15
0,8	74,05	25,95	54,72	45,28	31,93	68,07	13,19	86,81

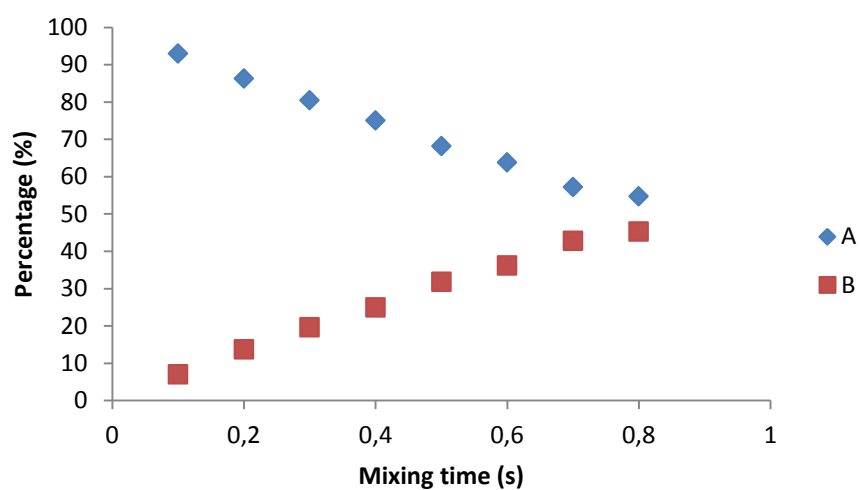
Table 9: Peak intensities (percentage) for the coordinated acetylene (A) and free acetylene (B).

Figures 83 to 87 illustrate the representation of the data included in table 9.

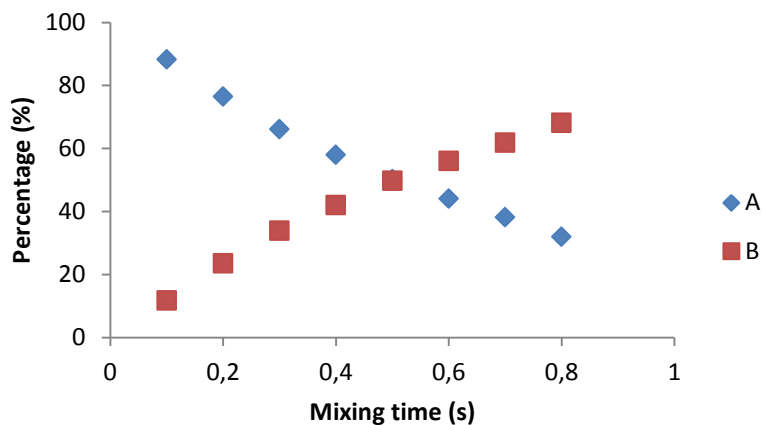
-35 °C (238 K)



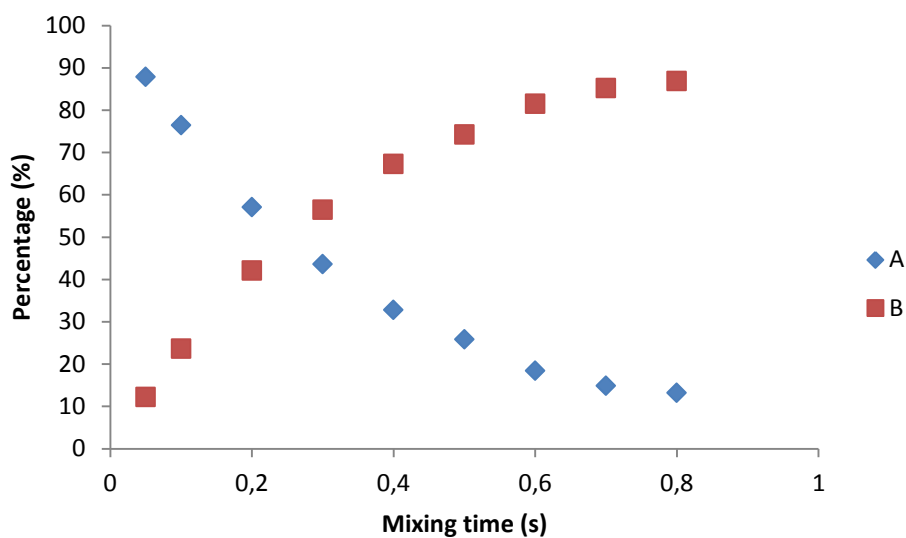
-30 °C (243 K)



-25 °C (248 K)



-20 °C (253 K)



Figures 83-87. Representation of the peak intensities (percentage) as a function of the exchange or reaction time.

The rate constants determined as described before were used to calculate the activation parameters. The resulting representation of the Eyring equation is illustrated in Figure 88.

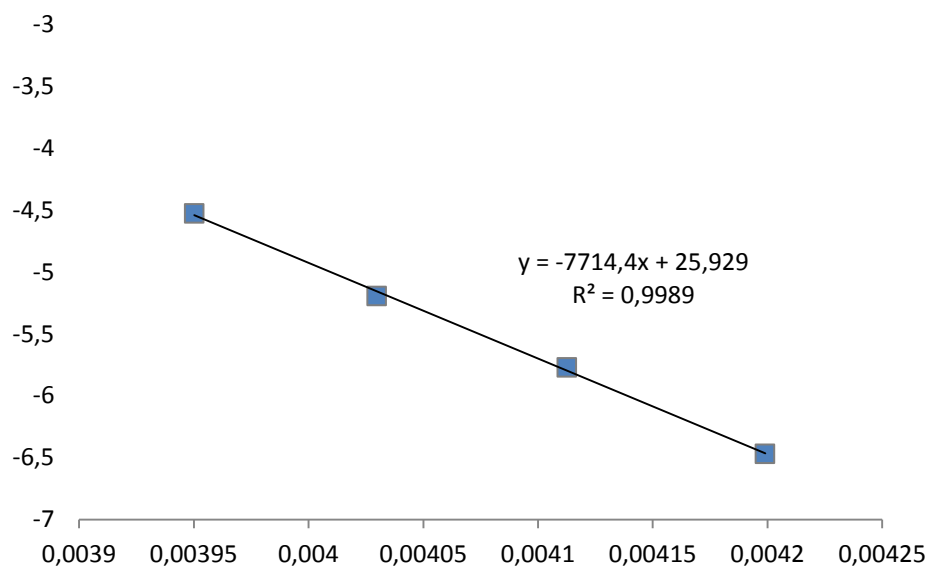


Figure 88: Eyring representation of the exchange rate constants obtained from the 1D Selective EXSY experiments for acetylene exchange on **22**·C₂H₂ complex.

I.3.9. General Method for Catalytic Hydroarylation of Alkynes

In a typical experiment, a Screw-cap NMR tube was charged with a mixture containing the alkyne (0.17 mmol), the indole (0.17 mmol), and 5 mol% of the catalytic mixture composed by **6** and Na[BAr_F] (2 eq with respect to Pt). The mixture was dissolved with CD₂Cl₂ (0.5 mL) and heated in an oil bath at 55 °C for a period of 24 h. The reaction progress was monitored by ¹H NMR spectroscopy.

I.3.10. General Method for Catalytic Hydroamination of Alkynes

In a typical experiment, a Screw-cap NMR tube was charged with a mixture containing the alkyne (0.13 mmol), the amine (0.13 mmol), 1,3,5-tris(*ter*-butyl)benzene (0.01 mmol, internal standard) and 0.5 mol% of **20**·**S**. The mixture was dissolved with CD₂Cl₂ (0.5 mL) and heated in an oil bath at 60 °C. The reaction progress was monitored by ¹H NMR spectroscopy.

I.4. BIBLIOGRAPHY

1. *Comprehensive Coordination Chemistry*, 2nd ed. (Eds.: J. A. McCleverty, T. J. Meyer), Elsevier, **2004**.
2. *Comprehensive Organometallic Chemistry*, 3rd ed. (Ed.: R. H. Crabtree), Elsevier, **2007**.
3. a) See *Historical Introduction* by J. Chatt in Chapter 1 of reference 3b.
b) L. H. Pignolet, *Homogeneous Catalysis with Metal Phosphine Complexes*, Ed. Plenum Press, New York, **1983**.
4. C. A. McAuliffe, W. Levason, *Phosphine, Arsine and Stibine Complexes of the Transition Elements*, Elsevier Scientific Pub. Co., Amsterdam, **1999**.
5. For an informative discussion on the development of phosphine metal complexes (also compounds with arsine and stibine ligands) focused on research from the 1950s and early 1960s, see: G. Booth, *Adv. Inorg. Chem. Radiochem.* **1964**, 6, 1-69.
6. a) M. J. S. Dewar, *Bull. Soc. Chim. Fr.* **1951**, 18, C71-C79; b) J. Chatt, L. A. Duncanson, *J. Chem. Soc.* **1953**, 2939-2947.
7. H. Werner, *Landmarks in Organo-Transition Metal Chemistry*, Springer, **2003**.
8. a) J. Chatt, B. L. Shaw, *J. Chem. Soc.* **1959**, 705-716; b) J. Chatt, B. L. Shaw, *J. Chem. Soc.* **1959**, 4020-4033.
9. a) T. G. Appleton, H. C. Clark, L. E. Manzer, *Coord. Chem. Rev.* **1973**, 10, 335-422; b) F. R. Hartley, *Chem. Soc. Rev.* **1973**, 2, 163-179; c) L. J. Manojlovic-Muir, K. W. Muir, *Inorg. Chim. Acta* **1974**, 10, 47-49.

10. a) A. J. Cheney, B. E. Mann, B. L. Shaw, R. M. Slade, *J. Chem. Soc., Chem. Commun.* **1970**, 1176-1177; b) A. J. Cheney, B. E. Mann, B. L. Shaw, R. M. Slade, *J. Chem. Soc., A* **1971**, 3833-3842; c) A. J. Cheney, B. L. Shaw, *J. Chem. Soc., Dalton Trans.* **1972**, 754-763.
11. See for example: J. Campos, L. Ortega-Moreno, S. Conejero, R. Peloso, J. López-Serrano, C. Maya, E. Carmona, *Chem. Eur. J.* **2015**, *21*, 8883-8896.
12. For leading references see: J. Campos, M. F. Espada, J. López-Serrano, E. Carmona, *Inorg. Chem.* **2013**, *52*, 6694-6704.
13. a) R. D. Cramer, E. L. Jenner, R. V. Lindsey, U. G. Stolberg, *J. Am. Chem. Soc.* **1963**, *85*, 1691-1692; b) E. Frankel, E. Emken, H. Itatani, J. J. Bailar, *J. Org. Chem.* **1967**, *32*, 1447-1452.
14. a) A. R. Chianese, S. J. Lee, M. R. Gagné, *Angew. Chem. Int. Ed.* **2007**, *46*, 4042-4059; b) A. Fürstner, P. W. Davies, *Angew. Chem. Int. Ed.* **2007**, *46*, 3410-3449.
15. a) M. Bochmann, *Organometallics and Catalysis. An Introduction.*, Oxford University Press, Oxford, UK, **2015**; b) R. H. Crabtree, *The Organometallic Chemistry of the Transition Metals*, 6th ed., John Wiley & Sons, Inc., Hoboken, **2014**; c) J. Hartwig, *Organotransition Metal Chemistry: From Bonding to Catalysis*, Sausalito, **2010**; d) R. H. Crabtree, *J. Organomet. Chem.* **2005**, *690*, 5451-5457; e) C. A. Tolman, *Chem. Rev.* **1977**, *77*, 313-348.
16. a) R. Noyori, *Angew. Chem. Int. Ed.* **2002**, *41*, 2008-2022; b) W. S. Knowles, *Angew. Chem. Int. Ed.* **2002**, *41*, 1998-2007.
17. a) J. Halpern, *Inorg. Chim. Acta* **1981**, *50*, 11-19; b) C. P. Casey, G. T. Whiteker, M. G. Melville, L. M. Petrovich, J. A. Gavney, D. R. Powell, *J. Am. Chem. Soc.* **1992**, *114*, 5535-5543; c) L. H. Shultz, D. J. Tempel, M. Brookhart, *J. Am. Chem. Soc.* **2001**, *123*, 11539-11555; d) Z. Liu, E. Somsook, C. B. White, K. A. Rosaaen, C. R. Landis, *J. Am. Chem. Soc.* **2001**, *123*, 11193-11207.
18. A. Zapf, A. Ehrentraut, M. Beller, *Angew. Chem. Int. Ed.* **2000**, *39*, 4153-4155.
19. a) J. P. Wolfe, R. A. Singer, B. H. Yang, S. L. Buchwald, *J. Am. Chem. Soc.* **1999**, *121*, 9550-9561; b) A. Aranyos, D. W. Old, A. Kiyomori, J. P. Wolfe, J. P. Sadighi, S. L. Buchwald, *J. Am. Chem. Soc.* **1999**, *121*, 4369-4378; c) J. P. Wolfe, S. Wagaw, J.-F. Marcoux, S. L. Buchwald, *Acc. Chem. Res.* **1998**, *31*, 805-818; d) R. Martin, S. L. Buchwald, *Acc. Chem. Res.* **2008**, *41*, 1461.
20. A. F. Littke, G. C. Fu, *Angew. Chem. Int. Ed.* **2002**, *41*, 4176-4211.

21. a) Q. Shelby, N. Kataoka, G. Mann, J. Hartwig, *J. Am. Chem. Soc.* **2000**, *122*, 10718-10719; b) G. Mann, C. Incarvito, A. L. Rheingold, J. F. Hartwig, *J. Am. Chem. Soc.* **1999**, *121*, 3224-3225; c) J. F. Hartwig, *Angew. Chem. Int. Ed.* **1998**, *37*, 2046-2067.
22. a) D. S. Surry, S. L. Buchwald, *Chem. Sci.* **2011**, *2*; b) T. J. Maimone, P. J. Milner, T. Kinzel, Y. Zhang, M. K. Takase, S. L. Buchwald, *J. Am. Chem. Soc.* **2011**, *133*, 18106-18109; c) B. P. Fors, D. A. Watson, M. R. Biscoe, S. L. Buchwald, *J. Am. Chem. Soc.* **2008**, *130*, 13552-13554; d) T. E. Barder, S. L. Buchwald, *J. Am. Chem. Soc.* **2007**, *129*, 12003-12010; e) T. E. Barder, S. D. Walker, J. R. Martinelli, S. L. Buchwald, *J. Am. Chem. Soc.* **2005**, *127*, 4685-4696.
23. a) P. Braunstein, F. Naud, *Angew. Chem. Int. Ed.* **2001**, *40*, 680-699; b) H. Grützmacher, *Angew. Chem. Int. Ed.* **2008**, *47*, 1814-1818; c) H. Werner, *Dalton Trans.* **2003**, 3829-3837; d) H. Werner, G. Canepa, K. Ilg, J. Wolf, *Organometallics* **2000**, *19*, 4756-4766.
24. a) A. R. O'Connor, W. Kaminsky, B. C. Chan, D. M. Heinekey, K. I. Goldberg, *Organometallics* **2013**, *32*, 4016-4019; b) A. R. O'Connor, W. Kaminsky, D. M. Heinekey, K. I. Goldberg, *Organometallics* **2011**, *30*, 2105-2116; c) A. DeAngelis, V. W. Shurtleff, O. Dmitrenko, J. M. Fox, *J. Am. Chem. Soc.* **2011**, *133*, 1650-1653; d) A. Grirrane, H. Garcia, A. Corma, E. Álvarez, *ACS Catal.* **2011**, *1*, 1647-1653; e) Y. Wang, K. Ji, S. Lan, L. Zhang, *Angew. Chem. Int. Ed.* **2012**, *51*, 1915-1918; f) E. Herrero-Gómez, C. Nieto-Oberhuber, S. López, J. Benet-Buchholz, A. M. Echavarren, *Angew. Chem. Int. Ed.* **2006**, *45*, 5455-5459.
25. a) R. J. Lundgren, M. Stradiotto, *Aldrichimica Acta* **2012**, *45*, 59-65; b) M. Albrecht, M. M. Lindner, *Dalton Trans.* **2011**, *40*, 8733-8744; c) C. A. Fleckenstein, H. Plenio, *Chem. Soc. Rev.* **2010**, *39*, 694-711; d) A. J. Kendall, C. A. Salazar, P. F. Martino, D. R. Tyler, *Organometallics* **2014**, *33*, 6171-6178; e) J. Keller, C. Schlierf, C. Nolte, P. Mayer, B. F. Straub, *Synthesis* **2006**, *2006*, 354-365.
26. a) J. J. Adams, A. Lau, N. Arulsamy, D. M. Roddick, *Inorg. Chem.* **2007**, *46*, 11328-11334; b) S. Basu, N. Arulsamy, D. M. Roddick, *Organometallics* **2008**, *27*, 3659-3665; c) J. J. Adams, N. Arulsamy, D. M. Roddick, *Organometallics* **2009**, *28*, 1148-1157; d) B. Thapaliya, S. Debnath, N. Arulsamy, D. M. Roddick, *Organometallics* **2015**, *34*, 4018-4022.
27. B. G. Anderson, J. L. Spencer, *Chem. Eur. J.* **2014**, *20*, 6421-6432.
28. a) C. Barthes, C. Lepetit, Y. Canac, C. Duhayon, D. Zargarian, R. Chauvin, *Inorg. Chem.* **2013**, *52*, 48-58; b) Y. Canac, C. Maaliki, I. Abdellah, R. Chauvin, *New J. Chem.* **2012**, *36*, 17-27.

29. a) Á. Kozma, T. Deden, J. Carreras, C. Wille, J. Petušková, J. Rust, M. Alcarazo, *Chem. Eur. J.* **2014**, *20*, 2208-2214; b) H. Tinnermann, C. Wille, M. Alcarazo, *Angew. Chem. Int. Ed.* **2014**, *53*, 8732-8736; c) J. Carreras, G. Gopakumar, L. Gu, A. Gimeno, P. Linowski, J. Petušková, W. Thiel, M. Alcarazo, *J. Am. Chem. Soc.* **2013**, *135*, 18815-18823; d) J. Carreras, M. Patil, W. Thiel, M. Alcarazo, *J. Am. Chem. Soc.* **2012**, *134*, 16753-16758; e) J. Petušková, M. Patil, S. Holle, C. W. Lehmann, W. Thiel, M. Alcarazo, *J. Am. Chem. Soc.* **2011**, *133*, 20758-20760; f) J. J. Weigand, K.-O. Feldmann, F. D. Henne, *J. Am. Chem. Soc.* **2010**, *132*, 16321-16323.
30. See for example: a) E. Carmona, F. Gonzalez, M. L. Poveda, J. L. Atwood, R. D. Rogers, *J. Chem. Soc., Dalton Trans.* **1980**, 2108-2116; b) E. Carmona, F. Gonzalez, M. L. Poveda, J. L. Atwood, R. D. Rogers, *J. Chem. Soc., Dalton Trans.* **1981**, 777-782.
31. See for example: a) E. Carmona, J. M. Marin, M. L. Poveda, J. L. Atwood, R. D. Rogers, *J. Am. Chem. Soc.* **1983**, *105*, 3014-3022; b) R. Alvarez, E. Carmona, M. L. Poveda, R. Sanchez-Delgado, *J. Am. Chem. Soc.* **1984**, *106*, 2731-2732.
32. a) M. Carrasco, I. Mendoza, E. Álvarez, A. Grirrane, C. Maya, R. Peloso, A. Rodríguez, A. Falceto, S. Álvarez, E. Carmona, *Chem. Eur. J.* **2015**, *21*, 410-421; b) M. Carrasco, I. Mendoza, M. Faust, J. López-Serrano, R. Peloso, A. Rodríguez, E. Álvarez, C. Maya, P. P. Power, E. Carmona, *J. Am. Chem. Soc.* **2014**, *136*, 9173-9180.
33. a) D. V. Partyka, M. P. Washington, J. B. Updegraff Iii, X. Chen, C. D. Incarvito, A. L. Rheingold, J. D. Protasiewicz, *J. Organomet. Chem.* **2009**, *694*, 1441-1446; b) R. C. Smith, R. A. Woloszynek, W. Chen, T. Ren, J. D. Protasiewicz, *Tetrahedron Lett.* **2004**, *45*, 8327-8330; c) B. Buster, A. A. Diaz, T. Graham, R. Khan, M. A. Khan, D. R. Powell, R. J. Wehmschulte, *Inorg. Chim. Acta* **2009**, *362*, 3465-3474; d) L. Ortega-Moreno, R. Peloso, C. Maya, A. Suarez, E. Carmona, *Chem. Commun.* **2015**, *51*, 17008-17011; e) M. F. Espada, J. Campos, J. López-Serrano, M. L. Poveda, E. Carmona, *Angew. Chem. Int. Ed.* **2015**, *54*, 15379-15384.
34. G. Berthon-Gelloz, B. de Bruin, B. Tinant, I. E. Markó, *Angew. Chem. Int. Ed.* **2009**, *48*, 3161-3164.
35. a) O. Rivada-Wheellaghan, M. A. Ortuño, J. Díez, A. Lledós, S. Conejero, *Angew. Chem.* **2012**, *124*, 4002-4005; b) O. Rivada-Wheellaghan, B. Donnadieu, C. Maya, S. Conejero, *Chem. Eur. J.* **2010**, *16*, 10323-10326; c) H. Braunschweig, K. Radacki, K. Uttinger, *Chem. Eur. J.* **2008**, *14*, 7858-7866; d) H. Braunschweig, K. Radacki, D. Rais, D. Scheschkewitz, *Angew. Chem. Int. Ed.* **2005**,

- 44, 5651-5654; e) M. J. Ingleson, M. F. Mahon, A. S. Weller, *Chem. Commun.* **2004**, 2398-2399; f) W. Baratta, S. Stoccoro, A. Doppiu, E. Herdtweck, A. Zucca, P. Rigo, *Angew. Chem. Int. Ed.* **2003**, *42*, 105-108; g) R. G. Goel, R. C. Srivastava, *Can. J. Chem.* **1983**, *61*, 1352-1359.
36. J. Campos, R. Peloso, E. Carmona, *Angew. Chem. Int. Ed.* **2012**, *51*, 8255-8258.
37. a) N. Carr, B. J. Dunne, L. Mole, A. G. Orpen, J. L. Spencer, *J. Chem. Soc., Dalton Trans.* **1991**, 863-871; b) L. Mole, J. L. Spencer, N. Carr, A. G. Orpen, *Organometallics* **1991**, *10*, 49-52.
38. a) T. G. Appleton, M. A. Bennett, *Inorg. Chem.* **1978**, *17*, 738-747; b) E. M. Shustorovich, M. A. Porai-Koshits, Y. A. Buslaev, *Coord. Chem. Rev.* **1975**, *17*, 1-98; c) K. F. Purcell, J. C. Kotz, in *Inorg. Chem.*, W. B. Saunders Co., Philadelphia, **1977**, Chapter 13.
39. a) R. H. Crabtree, *The Organometallic Chemistry of the Transition Metals, Vol. Chapter 10*, 1st ed., John Wiley & Sons, Inc., **1988**; b) R. K. Harris, *Can. J. Chem.* **1964**, *42*, 2275-2281; c) A. Ault, *J. Chem. Educ.* **1970**, *47*, 812; d) D. A. Redfield, L. W. Cary, J. H. Nelson, *Inorg. Chem.* **1975**, *14*, 50-59.
40. J. D. Scott, R. J. Puddephatt, *Organometallics* **1983**, *2*, 1643-1648.
41. See for example: a) R. J. Goodfellow, M. J. Hardy, B. F. Taylor, *J. Chem. Soc., Dalton Trans.* **1973**, 2450-2453; b) C. M. Haar, S. P. Nolan, W. J. Marshall, K. G. Moloy, A. Prock, W. P. Giering, *Organometallics* **1999**, *18*, 474-479.
42. L. Pauling, *The Nature of the Chemical Bond*, 3rd. ed., Cornell University Press, Cornell University, New York, **1960**.
43. For some early review articles, see: a) G. W. Parshall, *Acc. Chem. Res.* **1970**, *3*, 139-144; b) J. Dehand, M. Pfeffer, *Coord. Chem. Rev.* **1976**, *18*, 327-352; c) M. I. Bruce, *Angew. Chem. Int. Ed. Engl.* **1977**, *16*, 73-86; d) I. Omae, *Coord. Chem. Rev.* **1980**, *32*, 235-271.
44. a) A. D. Ryabov, *Chem. Rev.* **1990**, *90*, 403-424; b) M. E. van der Boom, D. Milstein, *Chem. Rev.* **2003**, *103*, 1759-1792; c) M. Albrecht, *Chem. Rev.* **2010**, *110*, 576-623; d) I. Omae, *Cyclometalation Reactions*, Springer, Japan, **2014**; e) Y.-F. Han, G.-X. Jin, *Chem. Soc. Rev.* **2014**, *43*, 2799-2823; f) F. Mohr, S. H. Privér, S. K. Bhargava, M. A. Bennett, *Coord. Chem. Rev.* **2006**, *250*, 1851-1888.
45. a) M. E. van der Boom, S.-Y. Liou, L. J. W. Shimon, Y. Ben-David, D. Milstein, *Organometallics* **1996**, *15*, 2562-2568; b) M. E. van der Boom, J. Ott, D. Milstein, *Organometallics* **1998**, *17*, 4263-4266; c)

- M. Montag, G. Leitus, L. J. W. Shimon, Y. Ben-David, D. Milstein, *Chem. Eur. J.* **2007**, *13*, 9043-9055.
46. a) J. Forniés, A. Martín, R. Navarro, V. Sicilia, P. Villarroya, *Organometallics* **1996**, *15*, 1826-1833; b) M. Sano, Y. Nakamura, *J. Chem. Soc., Dalton Trans.* **1991**, 417-424.
47. a) R. Romeo, M. R. Plutino, A. Romeo, *Helv. Chim. Acta* **2005**, *88*, 507-522; b) A. Marrone, N. Re, R. Romeo, *Organometallics* **2008**, *27*, 2215-2222.
48. a) W. Baratta, E. Herdtweck, P. Rigo, *Angew. Chem. Int. Ed.* **1999**, *38*, 1629-1631; b) W. Baratta, E. Herdtweck, P. Martinuzzi, P. Rigo, *Organometallics* **2001**, *20*, 305-308; c) W. Baratta, C. Mealli, E. Herdtweck, A. Ienco, S. A. Mason, P. Rigo, *J. Am. Chem. Soc.* **2004**, *126*, 5549-5562; d) W. Baratta, A. Del Zotto, G. Esposito, A. Sechi, M. Toniutti, E. Zangrando, P. Rigo, *Organometallics* **2004**, *23*, 6264-6272; e) W. Baratta, M. Ballico, A. Del Zotto, E. Zangrando, P. Rigo, *Chem. Eur. J.* **2007**, *13*, 6701-6709.
49. a) A. Zucca, G. L. Petretto, S. Stoccoro, M. A. Cinellu, G. Minghetti, M. Manassero, C. Manassero, L. Male, A. Albinati, *Organometallics* **2006**, *25*, 2253-2265; b) A. Zucca, G. L. Petretto, S. Stoccoro, M. A. Cinellu, M. Manassero, C. Manassero, G. Minghetti, *Organometallics* **2009**, *28*, 2150-2159; c) G. L. Petretto, J. P. Rourke, L. Maidich, S. Stoccoro, M. A. Cinellu, G. Minghetti, G. J. Clarkson, A. Zucca, *Organometallics* **2012**, *31*, 2971-2977; d) L. Maidich, G. Zuri, S. Stoccoro, M. A. Cinellu, M. Masia, A. Zucca, *Organometallics* **2013**, *32*, 438-448; e) L. Maidich, G. Zuri, S. Stoccoro, M. A. Cinellu, A. Zucca, *Dalton Trans.* **2014**, *43*, 14806-14815; f) A. Zucca, L. Maidich, L. Canu, G. L. Petretto, S. Stoccoro, M. A. Cinellu, G. J. Clarkson, J. P. Rourke, *Chem. Eur. J.* **2014**, *20*, 5501-5510.
50. G. Faraone, V. Ricevuto, R. Romeo, M. Trozzi, *Inorg. Chem.* **1969**, *8*, 2207-2211.
51. W. H. Bernskoetter, C. K. Schauer, K. I. Goldberg, M. Brookhart, *Science* **2009**, *326*, 553-556.
52. A. Falceto, E. Carmona, S. Alvarez, *Organometallics* **2014**, *33*, 6660-6668.
53. M. Black, R. H. B. Mais, P. G. Owston, *Acta Crystall. B* **1969**, *25*, 1753-1759.
54. a) P. S. Pregosin, *NMR in Organometallic Chemistry*, Wiley-VCH, Weinheim, **2012**; b) J. G. Verkade, *Phosphorus-31 NMR spectroscopy in stereochemical analysis: organic compounds and*

- metal complexes*, VCH, Deerfield Beach, FL, **1987**; c) S. O. Grim, R. L. Keiter, W. McFarlane, *Inorg. Chem.* **1967**, *6*, 1133-1137.
55. F. Allen, O. Kennard, *Chemical Design Automation News* **1993**, *8*, 31-37.
56. F. H. Allen, A. Pidcock, *J. Chem. Soc., A* **1968**, 2700-2704.
57. M.-E. Moret, P. Chen, *Organometallics* **2008**, *27*, 4903-4916.
58. J. Y. Corey, J. Braddock-Wilking, *Chem. Rev.* **1999**, *99*, 175-292.
59. F. Alonso, I. P. Beletskaya, M. Yus, *Chem. Rev.* **2002**, *102*, 4009-4092.
60. a) B. Marciniec, *Silicon Chemistry* **2002**, *1*, 155-174; b) A. K. Roy, in *Adv. Organomet. Chem., Vol. Volume 55* (Eds.: A. F. H. Robert West, J. F. Mark), Academic Press, **2007**, pp. 1-59; ; c) E. Calimano, T. D. Tilley, *J. Am. Chem. Soc.* **2009**, *131*, 11161-11173.
61. a) R. Malacea, R. Poli, E. Manoury, *Coord. Chem. Rev.* **2010**, *254*, 729-752; b) R. H. Morris, *Chem. Soc. Rev.* **2009**, *38*, 2282-2291.
62. I. E. Markó, S. Stérin, O. Buisine, G. Mignani, P. Branlard, B. Tinant, J. Declercq, *Science* **2002**, *298*, 204-206.
63. a) D. A. Rooke, E. M. Ferreira, *Angew. Chem. Int. Ed.* **2012**, *51*, 3225-3230; b) S. E. Parker, J. Börgel, T. Ritter, *J. Am. Chem. Soc.* **2014**, *136*, 4857-4860.
64. a) F. Ozawa, T. Hikida, T. Hayashi, *J. Am. Chem. Soc.* **1994**, *116*, 2844-2849; b) F. Ozawa, *J. Organomet. Chem.* **2000**, *611*, 332-342; c) F. Ozawa, T. Hikida, K. Hasebe, T. Mori, *Organometallics* **1998**, *17*, 1018-1024; d) K. Hasebe, J. Kamite, T. Mori, H. Katayama, F. Ozawa, *Organometallics* **2000**, *19*, 2022-2030.
65. D. Chan, S. B. Duckett, S. L. Heath, I. G. Khazal, R. N. Perutz, S. Sabo-Etienne, P. L. Timmins, *Organometallics* **2004**, *23*, 5744-5756.
66. R. Bau, M. H. Drabnis, *Inorg. Chim. Acta* **1997**, *259*, 27-50.
67. M. D. Butts, B. L. Scott, G. J. Kubas, *J. Am. Chem. Soc.* **1996**, *118*, 11831-11843.
68. a) H. A. Zhong, J. A. Labinger, J. E. Bercaw, *J. Am. Chem. Soc.* **2002**, *124*, 1378-1399; b) L. Johansson, O. B. Ryan, C. Rømming, M. Tilset, *J. Am. Chem. Soc.* **2001**, *123*, 6579-6590; c) S. Reinartz, P. S. White, M. Brookhart, J. L. Templeton, *Organometallics* **2000**, *19*, 3854-3866; d) J. C. Thomas, J. C. Peters, *Inorg. Chem.* **2003**, *42*, 5055-5073; e) S. Martínez-Salvador, B. Menjón, J. Forniés, A. Martín, I. Usón, *Angew. Chem. Int. Ed.* **2010**, *49*, 4286-4289; f) S. Martínez-Salvador, J. Forniés, A. Martín, B. Menjón, *Chem. Eur. J.* **2011**, *17*, 8085-8097.

69. F. Canziani, P. Chini, A. Quarta, A. Di Martino, *J. Organomet. Chem.* **1971**, *26*, 285-292.
70. C. Elschenbroich, *Organometallics*, 3rd ed., **2006**.
71. J. Forniés, E. Lalinde, in *Comprehensive Organometallic Chemistry III* (Ed.: R. H. Crabtree), Elsevier, Oxford, **2007**, 8.09. 611-673,
72. a) M. Lersch, M. Tilset, *Chem. Rev.* **2005**, *105*, 2471-2526; b) H. Heiberg, L. Johansson, O. Gropen, O. B. Ryan, O. Swang, M. Tilset, *J. Am. Chem. Soc.* **2000**, *122*, 10831-10845; c) N. Oberbeckmann-Winter, X. Morise, P. Braunstein, R. Welter, *Inorg. Chem.* **2005**, *44*, 1391-1403; d) P. Nilsson, G. Puxty, O. F. Wendt, *Organometallics* **2006**, *25*, 1285-1292.
73. a) D. Karstedt, A. T. Bell, T. D. Tilley, *Organometallics* **2004**, *23*, 4169-4171; b) D. Karstedt, A. T. Bell, T. D. Tilley, *J. Am. Chem. Soc.* **2005**, *127*, 12640-12646; c) J. L. McBee, A. T. Bell, T. D. Tilley, *J. Am. Chem. Soc.* **2008**, *130*, 16562-16571.
74. a) M. P. Brown, S. J. Cooper, A. A. Frew, L. Manojlovic-Muir, K. W. Muir, R. J. Puddephatt, K. R. Seddon, M. A. Thomson, *Inorg. Chem.* **1981**, *20*, 1500-1507; b) P. K. Monaghan, R. J. Puddephatt, *Organometallics* **1984**, *3*, 444-449; c) K. R. Pellarin, M. S. McCready, R. J. Puddephatt, *Dalton Trans.* **2013**, *42*, 10444-10453.
75. a) C. Hahn, *Organometallics* **2010**, *29*, 1331-1338; b) C. Hahn, P. Morvillo, E. Herdtweck, A. Vitagliano, *Organometallics* **2002**, *21*, 1807-1818; c) C. Hahn, M. E. Cucciolito, A. Vitagliano, *J. Am. Chem. Soc.* **2002**, *124*, 9038-9039; d) M. E. Cucciolito, A. D'Amor, A. Vitagliano, *Organometallics* **2005**, *24*, 3359-3361; e) M. E. Cucciolito, A. D'Amora, A. Tuzi, A. Vitagliano, *Organometallics* **2007**, *26*, 5216-5223; f) M. E. Cucciolito, A. Vitagliano, *Organometallics* **2008**, *27*, 6360-6363; g) W. D. Kerber, J. H. Koh, M. R. Gagné, *Org. Lett.* **2004**, *6*, 3013-3015; h) J. A. Feducia, A. N. Campbell, M. Q. Doherty, M. R. Gagné, *J. Am. Chem. Soc.* **2006**, *128*, 13290-13297; i) C. Hahn, *Chem. Eur. J.* **2004**, *10*, 5888-5899.
76. M. E. Cucciolito, A. D'Amora, A. Vitagliano, *Organometallics* **2010**, *29*, 5878-5884.
77. a) T. J. Williams, A. J. M. Caffyn, N. Hazari, P. F. Oblad, J. A. Labinger, J. E. Bercaw, *J. Am. Chem. Soc.* **2008**, *130*, 2418-2419; b) T. G. Driver, T. J. Williams, J. A. Labinger, J. E. Bercaw, *Organometallics* **2007**, *26*, 294-301; c) A. G. Wong-Foy, L. M. Henling, M. Day, J. A. Labinger, J. E. Bercaw, *J. Mol. Catal. A: Chem.* **2002**, *189*, 3-16.

78. J. Parmene, A. Krivokapic, M. Tilset, *Eur. J. Inorg. Chem.* **2010**, 2010, 1381-1394.
79. H. Braunschweig, P. Brenner, R. D. Dewhurst, J. O. C. Jimenez-Halla, T. Kupfer, D. Rais, K. Uttinger, *Angew. Chem. Int. Ed.* **2013**, 52, 2981-2984.
80. a) M. A. Bowring, R. G. Bergman, T. D. Tilley, *Organometallics* **2013**, 32, 5266-5268; b) M. A. Bowring, R. G. Bergman, T. D. Tilley, *J. Am. Chem. Soc.* **2013**, 135, 13121-13128.
81. G. R. Fulmer, A. J. M. Miller, N. H. Sherden, H. E. Gottlieb, A. Nudelman, B. M. Stoltz, J. E. Bercaw, K. I. Goldberg, *Organometallics* **2010**, 29, 2176-2179.
82. N. W. Alcock, A. W. G. Platt, P. G. Pringle, *J. Chem. Soc., Dalton Trans.* **1989**, 2069-2072.
83. a) Y. K. Kryshchenko, S. R. Seidel, D. C. Muddiman, A. I. Nepomuceno, P. J. Stang, *J. Am. Chem. Soc.* **2003**, 125, 9647-9652; b) M. Ito, M. Ebihara, T. Kawamura, *Inorg. Chim. Acta* **1994**, 218, 199-202.
84. a) S. D. Ittel, L. K. Johnson, M. Brookhart, *Chem. Rev.* **2000**, 100, 1169-1204; b) M. Bochmann, *Organometallics* **2010**, 29, 4711-4740; c) D. S. McGuinness, *Chem. Rev.* **2011**, 111, 2321-2341.
85. a) J. J. Verendel, O. Pàmies, M. Diéguez, P. G. Andersson, *Chem. Rev.* **2014**, 114, 2130-2169; b) G. S. Chen, J. A. Labinger, J. E. Bercaw, *PNAS* **2007**, 104, 6915-6920.
86. a) R. Dorel, A. M. Echavarren, *Chem. Rev.* **2015**, 115, 9028-9072; b) I. Braun, A. M. Asiri, A. S. K. Hashmi, *ACS Catal.* **2013**, 3, 1902-1907; c) C. Hahn, M. Miranda, N. P. B. Chittineni, T. A. Pinion, R. Perez, *Organometallics* **2014**, 33, 3040-3050.
87. a) R. Romeo, *Comments Inorg. Chem.* **2002**, 23, 79-100; b) R. Romeo, G. D'Amico, E. Sicilia, N. Russo, S. Rizzato, *J. Am. Chem. Soc.* **2007**, 129, 5744-5755; c) R. J. Puddephatt, *Coord. Chem. Rev.* **2001**, 219-221, 157-185; d) E. M. Prokopchuk, R. J. Puddephatt, *Organometallics* **2003**, 22, 787-796.
88. a) L. Johansson, M. Tilset, J. A. Labinger, J. E. Bercaw, *J. Am. Chem. Soc.* **2000**, 122, 10846-10855; b) J. S. Owen, J. A. Labinger, J. E. Bercaw, *J. Am. Chem. Soc.* **2006**, 128, 2005-2016; c) A. E. Shilov, G. B. Shul'pin, *Chem. Rev.* **1997**, 97, 2879-2932; d) U. Fekl, K. I. Goldberg, in *Adv. Inorg. Chem.*, Vol. Volume 54, Academic Press, **2003**, pp. 259-320,

89. a) S. H. Crosby, G. J. Clarkson, J. P. Rourke, *Organometallics* **2011**, 30, 3603-3609; b) O. Rivada-Wheelaghan, M. Roselló-Merino, M. A. Ortuño, P. Vidossich, E. Gutiérrez-Puebla, A. Lledós, S. Conejero, *Inorg. Chem.* **2014**, 53, 4257-4268; c) O. Rivada-Wheelaghan, M. Roselló-Merino, J. Díez, C. Maya, J. López-Serrano, S. Conejero, *Organometallics* **2014**, 33, 5944-5947; d) J. L. Spencer, G. S. Mhinzi, *J. Chem. Soc., Dalton Trans.* **1995**, 3819-3824.
90. a) J. Silvestre, R. Hoffmann, *Helv. Chim. Acta* **1985**, 68, 1461-1506; b) M. I. Bruce, *Chem. Rev.* **1991**, 91, 197-257; c) C. Bruneau, P. H. Dixneuf, *Angew. Chem. Int. Ed.* **2006**, 45, 2176-2203.
91. a) J. M. Lynam, *Chem. Eur. J.* **2010**, 16, 8238-8247; b) O. J. S. Pickup, I. Khazal, E. J. Smith, A. C. Whitwood, J. M. Lynam, K. Bolaky, T. C. King, B. W. Rawe, N. Fey, *Organometallics* **2014**, 33, 1751-1761; c) M. Jiménez-Tenorio, M. C. Puerta, P. Valerga, M. A. Ortuño, G. Ujaque, A. Lledós, *Inorg. Chem.* **2013**, 52, 8919-8932; d) H. Werner, *Coord. Chem. Rev.* **2004**, 248, 1693-1702.
92. For early work on mononuclear Pt(II) vinylidenes see: a) U. Belluco, R. Bertani, F. Meneghetti, R. A. Michelin, M. Mozzon, *J. Organomet. Chem.* **1999**, 583, 131-135; b) U. Belluco, R. Bertani, R. A. Michelin, M. Mozzon, *J. Organomet. Chem.* **2000**, 600, 37-55; c) M. Rashidi, R. J. Puddephatt, *J. Am. Chem. Soc.* **1986**, 108, 7111-7112.
93. a) S. S. Stahl, J. A. Labinger, J. E. Bercaw, *Inorg. Chem.* **1998**, 37, 2422-2431; b) K. Q. Almeida Lenero, Y. Guari, P. C. J. Kamer, P. W. N. M. van Leeuwen, B. Donnadiu, S. Sabo-Etienne, B. Chaudret, M. Lutz, A. L. Spek, *Dalton Trans.* **2013**, 42, 6495-6512; c) D. G. Gusev, J. U. Notheis, J. R. Rambo, B. E. Hauger, O. Eisenstein, K. G. Caulton, *J. Am. Chem. Soc.* **1994**, 116, 7409-7410.
94. a) J. Campos, S. Kundu, D. R. Pahls, M. Brookhart, E. Carmona, T. R. Cundari, *J. Am. Chem. Soc.* **2013**, 135, 1217-1220; b) J. R. Webb, C. Munro-Leighton, A. W. Pierpont, J. T. Gurkin, T. B. Gunnoe, T. R. Cundari, M. Sabat, J. L. Petersen, P. D. Boyle, *Inorg. Chem.* **2011**, 50, 4195-4211; c) D. Stern, M. Sabat, T. J. Marks, *J. Am. Chem. Soc.* **1990**, 112, 9558-9575.
95. R. N. Perutz, S. Sabo-Etienne, *Angew. Chem. Int. Ed.* **2007**, 46, 2578-2592.
96. J. Oddershede, J. Geertsen, G. E. Scuseria, *The Journal of Physical Chemistry* **1988**, 92, 3056-3059.
97. F. A. L. Anet, D. J. O'Leary, *Tetrahedron Lett.* **1989**, 30, 2755-2758.

98. a) S. S. Stahl, J. A. Labinger, J. E. Bercaw, *J. Am. Chem. Soc.* **1996**, *118*, 5961-5976; b) M. W. Holtcamp, L. M. Henling, M. W. Day, J. A. Labinger, J. E. Bercaw, *Inorg. Chim. Acta* **1998**, *270*, 467-478; c) J. A. Labinger, J. E. Bercaw, *Nature* **2002**, *417*, 507-514; d) R. Romeo, G. D'Amico, *Organometallics* **2006**, *25*, 3435-3446.
99. C. M. Morris, J. L. Templeton, in *Activation and Functionalization of C-H Bonds* (Eds.: K. I. Goldberg, A. S. Goldman), ACS Symposium Series 885, Washington, DC, **2004**, pp. 303-318,
100. J. Parmene, I. Ivanović-Burmazović, M. Tilset, R. van Eldik, *Inorg. Chem.* **2009**, *48*, 9092-9103.
101. a) M.-E. Moret, in *Higher Oxidation State Organopalladium and Platinum Chemistry* (Ed.: J. A. Canty), Springer Berlin Heidelberg, Berlin, Heidelberg, **2011**, pp. 157-184, ; b) D. Serra, M.-E. Moret, P. Chen, *J. Am. Chem. Soc.* **2011**, *133*, 8914-8926; c) M.-E. Moret, D. Serra, A. Bach, P. Chen, *Angew. Chem. Int. Ed.* **2010**, *49*, 2873-2877.
102. a) J. delPozo, D. Carrasco, M. H. Pérez-Temprano, M. García-Melchor, R. Álvarez, J. A. Casares, P. Espinet, *Angew. Chem. Int. Ed.* **2013**, *52*, 2189-2193; b) A. R. Petersen, R. A. Taylor, I. Vicente-Hernández, J. Heinzer, A. J. P. White, G. J. P. Britovsek, *Organometallics* **2014**, *33*, 1453-1461.
103. a) J. Holton, M. F. Lappert, R. Pearce, P. I. W. Yarrow, *Chem. Rev.* **1983**, *83*, 135-201; b) P. Braunstein, N. M. Boag, *Angew. Chem. Int. Ed.* **2001**, *40*, 2427-2433; c) J. C. Green, M. L. H. Green, G. Parkin, *Chem. Commun.* **2012**, *48*, 11481-11503; d) M. L. H. Green, G. Parkin, in *Struct. Bond.*, Springer, Berlin, Heidelberg, **2016**, pp. 1-61,
104. J. Campos, J. López-Serrano, R. Peloso, E. Carmona, *Chem. Eur. J.* **2016**.
105. a) U. Anandhi, P. R. Sharp, *Inorg. Chem.* **2004**, *43*, 6780-6785; b) U. Belluco, R. Bertani, S. Coppetti, R. A. Michelin, M. Mozzon, *Inorg. Chim. Acta* **2003**, *343*, 329-334.
106. a) T. L. Lohr, W. E. Piers, M. J. Sgro, M. Parvez, *Dalton Trans.* **2014**, *43*, 13858-13864; b) T. L. Lohr, W. E. Piers, M. Parvez, *Dalton Trans.* **2013**, *42*, 14742-14748; c) T. L. Lohr, W. E. Piers, M. Parvez, *Inorg. Chem.* **2012**, *51*, 4900-4902.
107. a) J. J. Li, W. Li, P. R. Sharp, *Inorg. Chem.* **1996**, *35*, 604-613; b) J. J. Li, P. R. Sharp, *Inorg. Chem.* **1994**, *33*, 183-184; c) J. J. Li, W. Li, A. J. James, T. Holbert, T. P. Sharp, P. R. Sharp, *Inorg. Chem.* **1999**, *38*, 1563-1572; d) S. Kannan, A. J. James, P. R. Sharp, *Polyhedron* **2000**, *19*, 155-163.

108. a) Y. Suzaki, K. Osakada, *Organometallics* **2006**, 25, 3251-3258; b) Y. Suzaki, K. Osakada, *Organometallics* **2004**, 23, 5081-5084.
109. A. V. Marenich, C. J. Cramer, D. G. Truhlar, *The Journal of Physical Chemistry B* **2009**, 113, 6378-6396.
110. A. E. Reed, L. A. Curtiss, F. Weinhold, *Chem. Rev.* **1988**, 88, 899-926.
111. a) T. Kitamura, *Eur. J. Org. Chem.* **2009**, 2009, 1111-1125; b) Y. Yamamoto, *Chem. Soc. Rev.* **2014**, 43, 1575-1600; c) P. d. Mendoza, A. M. Echavarren, *Pure Appl. Chem.* **2010**, 82, 801-820; d) C. Nevado, A. M. Echavarren, *Synthesis* **2005**, 2, 167-182.
112. a) S. Bhuvaneswari, M. Jeganmohan, C.-H. Cheng, *Chem. Eur. J.* **2007**, 13, 8285-8293; b) J. Oyamada, T. Kitamura, *Tetrahedron* **2009**, 65, 3842-3847.
113. a) C. Ferrer, H. M. A. Catelijne, A. M. Echavarren, *Chem. Eur. J.* **2007**, 13, 1358-1373; b) X. Hu, D. Martin, M. Melaimi, G. Bertrand, *J. Am. Chem. Soc.* **2014**, 136, 13594-13597; c) J. S. Yadav, B. V. S. Reddy, B. Padmavani, M. K. Gupta, *Tetrahedron Lett.* **2004**, 45, 7577-7579; d) T. Tsuchimoto, H. Matsubayashi, M. Kaneko, Y. Nagase, T. Miyamura, E. Shirakawa, *J. Am. Chem. Soc.* **2008**, 130, 15823-15835.
114. L. Huang, M. Arndt, K. Gooßen, H. Heydt, L. J. Gooßen, *Chem. Rev.* **2015**, 115, 2596-2697.
115. a) R. Severin, S. Doye, *Chem. Soc. Rev.* **2007**, 36, 1407-1420; b) T. E. Müller, K. C. Hultsch, M. Yus, F. Foubelo, M. Tada, *Chem. Rev.* **2008**, 108, 3795-3892.
116. a) J. M. Hoover, A. DiPasquale, J. M. Mayer, F. E. Michael, *J. Am. Chem. Soc.* **2010**, 132, 5043-5053; b) H. Qian, R. A. Widenhoefer, *Org. Lett.* **2005**, 7, 2635-2638; c) C. Liu, C. F. Bender, X. Han, R. A. Widenhoefer, *Chem. Commun.* **2007**, 3607-3618; d) C. Tsukano, S. Yokouchi, A.-L. Girard, T. Kuribayashi, S. Sakamoto, T. Enomoto, Y. Takemoto, *Organic & Biomolecular Chemistry* **2012**, 10, 6074-6086.
117. J.-J. Brunet, N. C. Chu, O. Diallo, S. Vincendeau, *J. Mol. Catal. A: Chem.* **2005**, 240, 245-248.
118. M. J. Frisch, G. W. Trucks, G. E. Schlegel, G. E. Scuseria, M. A. Robb, J. R. Cheeseman, G. Scalmani, V. Barone, B. Mennucci, G. A. Petersson, H. Nakatsuji, M. Caricato, X. Li, H. P. Hratchian, A. F. Izmaylov, J. Bloino, G. Zheng, J. L. Sonnenberg, M. Hada, M. Ehara, K. Toyota, R. Fukuda, J. Hasegawa, M. Ishida, T. Nakajima, Y. Honda, O. Kitao, H. Nakai, T. Vreven, J. A. Montgomery, J. E.

- Peralta, F. Ogliaro, M. Bearpark, J. J. Heyd, E. Brothers, K. N. Kudin, V. N. Staroverov, R. Kobayashi, J. Normand, K. Raghavachari, A. Rendell, J. C. Burant, S. S. Iyengar, J. Tomasi, M. Cossi, N. Rega, J. M. Millam, M. Klene, J. E. Knox, J. B. Cross, V. Bakken, C. Adamo, J. Jaramillo, R. Gomperts, R. E. Stratmann, O. Yazyev, A. J. Austin, R. Cammi, C. Pomelli, J. W. Ochterski, R. L. Martin, K. Morokuma, O. Zakrzewski, G. A. Voth, P. Salvador, J. J. Dannenberg, S. Dapprich, A. D. Daniels, Ö. Farkas, J. B. Foresman, J. V. Ortiz, J. Cioslowski, D. J. Fox, Gaussian, Inc., Wallingford CT, **2009**.
119. Y. Zhao, D. Truhlar, *Theor. Chim. Acta* **2008**, *120*, 215.
120. D. Andrae, U. H., M. Dolg, H. Stoll, H. Preul, *Theor. Chim. Acc.* **1990**, 123.
121. a) W. J. Hehre, R. Ditchfield, J. A. Pople, *J. Phys. Chem.* **1972**, *56*, 2257; b) P. C. Hariharan, J. A. Pople, *Theor. Chim. Acta.* **1973**, *28*, 213; c) M. M. Francl, W. J. Pietro, W. J. Hehre, J. S. Binkley, M. S. Gordon, D. J. Defrees, J. A. Pople, *J. Chem. Phys.* **1982**, *77*, 3654.
122. A. A. C. Braga, G. Ujaque, F. Maseras, *Organometallics* **2006**, *25*, 3647-3658.

CHAPTER II

II.1. PREFACE

This chapter describes the coordinative chemistry of platinum (0) towards the terphenylphosphines **L**₂ and **L**₃. To facilitate comprehensive reading these ligands are, once again, represented here in schematic form (see Figure 1).

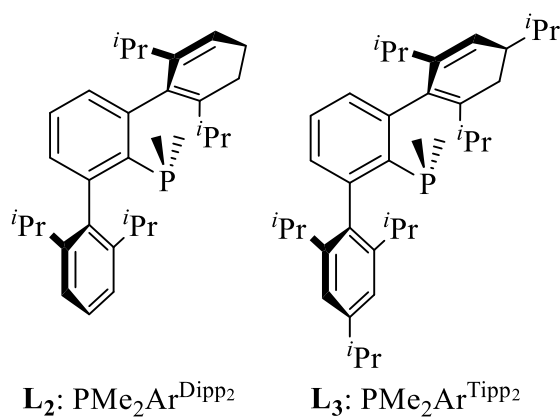


Figure 1: Dimethylterphenylphosphines **L**₂ and **L**₃.

The chemistry of Pt(0)—PR₃ complexes is one more chapter of the coordination and organometallic chemistry of this element, that is

historically relevant, for, as recalled in the general introduction that will follow this prologue, Pt—PR₃ complexes were among the first transition metal compounds in which the metal centre attained the zero oxidation state (leaving aside binary carbonyls such as [Ni(CO)₄] or [Fe(CO)₅], *vide infra*). The first Pt(0)—PR₃ complexes (and the Pd(0) analogues) were prepared by Malatesta and coworkers,¹ and included [Pt(EPh₃)₄] (E = P, As), [Pt(PPh₃)₃] and some mixed phosphine-carbonyl species such as [Pt(PPh₃)₃(CO)] and [Pt(PPh₃)₂(CO)₂], among other complexes.^{1b}

At the time, chemists were, however, reluctant to accept the concept that metals in the zero oxidation state could form stable molecular compounds. Thus, shortly afterwards, a *Nature* publication by Chopoorian, Lewis and Nyholm, proposed re-formulation of Malatesta's Pt(0)—PR₃ complexes as metal hydrides.² As remarked in the following section, in 1963 Malatesta and Ugo convincingly proved the real nature of their complexes.³

The general Introduction presented in the following section of this Thesis highlights the current importance of Pt(0)—PR₃ and related complexes, in particular, their capacity to act as a source of coordinative and electronically unsaturated [Pt(L)] and [PtL₂] fragments, capable to activate a variety of element-element bonds in stoichiometric and catalytic reactions. The interest shown by our research group in the last few years in the synthesis and coordination chemistry of terphenylphosphines PR₂Ar',⁴ where Ar' represents a terphenyl substituent of exceptional protecting steric features, like for instance Dipp and Tipp in Figure 1, led us to initiate

¹ a) L. Malatesta, M. Angoletta, *J. Chem. Soc.* **1957**, 1186-1188; b) L. Malatesta, C. Cariello, *J. Chem. Soc.* **1958**, 2323-2328.

² J. A. Chopoorian, J. Lewis, R. S. Nyholm, *Nature* **1961**, 190, 528-529.

³ L. Malatesta, R. Ugo, *J. Chem. Soc.* **1963**, 2080-2082.

⁴ L. Ortega-Moreno, M. F. Espada, J. J. Moreno, C. Navarro-Gilabert, J. Campos, S. Conejero, J. López-Serrano, C. Maya, R. Peloso, E. Carmona, *Polyhedron* **2016**, Accepted.

the study of Pt(0) complexes stabilised by coordination to these bulky phosphines.

It is worth anticipating that at variance with very bulky trialkylphosphine ligands, like PCy₃ or P^tBu₃, that form bis(phosphine), [Pt(PR₃)₂] compounds (see Section II.3.1) only mono(phosphine) platinum(0) complexes of PMe₂Ar^{Dipp}₂ and PMe₂Ar^{Tipp}₂ could be obtained in this work. In fact, the [Pt(PMe₂Ar')(olefin)_n] (n = 1,2) compounds described in this Thesis have been found to act as a source of the formally mono-coordinate, 12-electron fragments [Pt(PMe₂Ar')].

This chapter describes our first results in this area. It concentrated attention on Pt—PR₂Ar'—olefin complexes and in some stoichiometric and catalytic reactivity studies. Other closely related areas of research that nowadays attract considerable attention, such as the structure and reaction properties of Pt—PMe₂Ar'—L species derived from alkynes, N-heterocyclic carbenes, or bulk isocyanides, could not be considered within the time framework of this Thesis, and will hopefully be the subject of future work from our laboratories.

II.2. INTRODUCTION

Even after the correct structure of transition metal carbonyls such as Ni(CO)_4 or Fe(CO)_5 had been recognised, they were not considered as derivatives of M(0) metals because prior to 1942 molecular complexes of zerovalent transition metals were considered unlikely.

In 1942, Eastes and Burgess reported the synthesis of the alkylmetal cyanonickelates $\text{M}^{\text{I}}_4\text{Ni(CN)}_4$ and $\text{M}^{\text{I}}_2\text{Ni(CN)}_3$ but while for the latter they suggested that nickel appeared to be monovalent, no explanation of the state of valence of nickel in the former was offered.⁵ One year later, Burbage and Fernelius reported the synthesis of a zerovalent compound of palladium, $\text{K}_4[\text{Pd(CN)}_4]$ by reduction of $\text{K}_2[\text{Pd(CN)}_4]$ by potassium in liquid ammonia.⁶ These observations and the fact that $\text{K}_4[\text{Ni(CN)}_4]$ could be obtained from elemental nickel and KCN, in a reaction that occurred without a change in the oxidation state of the atoms involved, led chemists

⁵ J. W. Eastes, W. M. Burgess, *J. Am. Chem. Soc.* **1942**, *64*, 1187-1189.

⁶ J. J. Burbage, W. C. Fernelius, *J. Am. Chem. Soc.* **1943**, *65*, 1484-1486.

to consider the possibility that a metal in a complex might be in the oxidation state of zero.⁷

The importance of metal-to-ligand π -back donation in complexes of metals in a zero oxidation state was soon recognized although, it required many years of intense research to gather unambiguous experimental results in favour of such a bond.^{7,8} In fact, the most common ligands which allowed the isolation of metals in low oxidations states (see Table 1) did not include water, ammonia, halide ions and others commonly found in Werner complexes. These somewhat unusual at the time, Lewis bases were called π -acceptor or π -acid ligands and incorporated conspicuously phosphine and other P-donor ligands.⁸

Table 1: Most common ligands in compounds of metals in low oxidations (Adapted from Ref 3b)

CO	carbon monoxide
CN ⁻	cyanide ion
C ₂ R ⁻	acetylide ion
C ₅ H ₅ ⁻	cyclopentadienide ion
RCOR	alkylcarboxycarbenes
RCNR ₂	alkyldialkylaminocarbenes
C ₆ H ₆	benzene
C ₄ H ₄	cyclobutadiene
C ₃ H ₅	allyl
C ₂ R ₂	alkynes
C ₂ R ₄	alkenes
C _n H _(2n-2)	dienes
C _n H _(2n-2m)	polyenes
C ₆ H ₄ O ₂	<i>para</i> -benzoquinona
N ₂	nitrogen

⁷ a) Part 1 (pp 1-67) of Ref 7b; b) L. Malatesta, S. Cenini, in *Zerovalent Compounds of Metals* (Eds.: P. M. Maitlis, F. G. A. Stone, R. West), Academic Press Inc., London, **1974**,

⁸ J. G. Verkade, *Coord. Chem. Rev.* **1972**, 9, 1-106.

NO	nitric oxide
RCN	nitriles
C ₁₂ H ₈ N ₂	2,2'-bipyridyl
R ₂ N ₄	tetraazadienes
PR ₃	trihalogeno, triaryl and trialkyl phosphines
P(OR) ₃	triaryl and trialkyl phosphines
AsR ₃	triaryl and trialkyl arsines
SbR ₃	triarylstibines
SR ₂	dialkyl and diarylsulphides
SO ₂	sulphur dioxide
CS ₂	carbon disulphide

In the late 1950s, the group of Malatesta synthesised Pt(0) and Pt(0) complexes with phosphine and related ligands.⁹ These d¹⁰ systems had a great tendency to stabilise low-coordinate structures and contained electron rich metal centres. Once it was demonstrated that they were true zerovalent species¹⁰ interest grew on their use as models of the active centres of transition metal surfaces.

The large majority of the early Pt(0) complexes of P-donor ligands had coordination number four or three, *e.g.* Pt(PMe₃)₄ or PtPh₃.⁹ In the mid 1970s, two coordinated Pt(PR₃)₂ complexes attracted considerable interest,¹¹ which continued unabated up to the present time. Many catalytic cycles proposed for C—C and C—N cross-couplings and for other reactions that employ group 10 transition metal precatalysts involve [ML₂], or even [ML], reactive intermediates (M = Ni, Pd, Pt, L = biarylphosphines or other bulky phosphines or related ligands, *e.g.* NHCs) capable to induce

⁹ Part 2 of Ref. 7b (pp. 70-235).

¹⁰ R. Ugo, *Coord. Chem. Rev.* **1968**, 3, 319-344.

¹¹ a) A. Immirzi, A. Musco, P. Zambelli, G. Carturan, *Inorg. Chim. Acta* **1975**, 13, L13-L14; b) M. Green, J. A. Howard, J. L. Spencer, F. G. A. Stone, *J. Chem. Soc., Chem. Commun.* **1975**, 3-4; c) S. Otsuka, T. Yoshida, M. Matsumoto, K. Nakatsu, *J. Am. Chem. Soc.* **1976**, 98, 5850-5858; d) N. M. Boag, M. Green, D. M. Grove, J. A. K. Howard, J. L. Spencer, F. G. A. Stone, *J. Chem. Soc., Dalton Trans.* **1980**, 2170-2181.

the activation and the functionalization of a variety of C—X and other element-element bonds.

Recent reports have focused attention on N-heterocyclic carbene (NHC) complexes of Pt(0), since the chemistry of isolated complexes of composition $[\text{Pt}(\text{NHC})_2]$ is almost unexplored.¹² New 14-electron compounds of this type were investigated and their reactivity toward alkenes, alkynes, ketones and other unsaturated molecules analysed.¹³ Somewhat related complexes of π -accepting cyclic alkyl(amino) carbenes (cAACs), *i.e.* $[\text{Pt}(\text{cAAC})_2]$, have also been reported.^{13c} Mixed $[\text{Pt}(\text{PR}_3)(\text{NHC})]$ complexes were characterised by Braunschweig and coworkers and used as tuneable Lewis bases interactions with AlCl_3 and other metal halides, including ZrCl_4 , as the Lewis acid (Scheme 1).^{12d,14a}

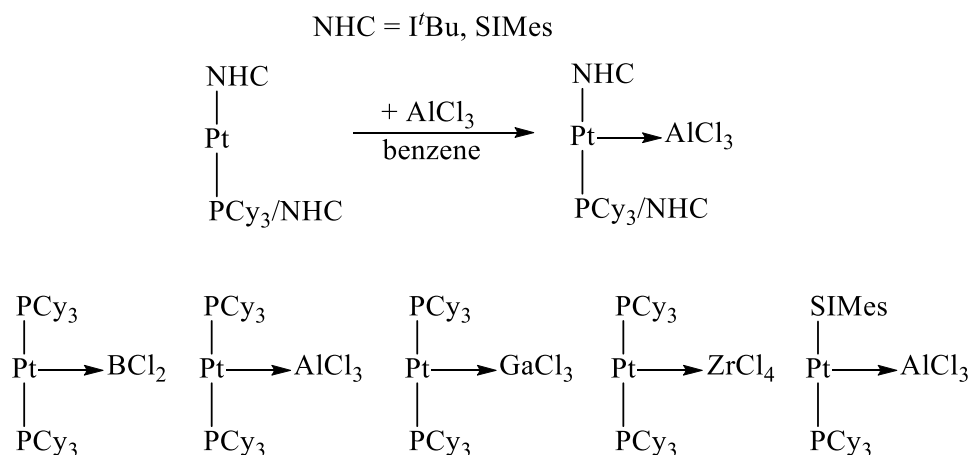
The same group studied the formation of the Pt(0) carbonyl complexes $[\text{Pt}(\text{PCy}_3)_2(\text{CO})]$ and $[\text{Pt}(\text{PCy}_3)_2(\text{CO})_2]$, the former representing the first structurally characterised Pt(0) monocarbonyl derivative.^{14b} Related complexes of platinum(0), *e.g.* $(\text{PCy}_3)_2\text{Pt} \rightarrow \text{MX}_2$ ($\text{M} = \text{Zn}, \text{Cd}$; $\text{X} = \text{Br}, \text{I}$), were described by Stasch and Jones.¹⁵

¹² a) A. J. Arduengo, S. F. Gamper, J. C. Calabrese, F. Davidson, *J. Am. Chem. Soc.* **1994**, *116*, 4391-4394; b) P. L. Arnold, F. G. N. Cloke, T. Geldbach, P. B. Hitchcock, *Organometallics* **1999**, *18*, 3228-3233; c) G. C. Fortman, N. M. Scott, A. Linden, E. D. Stevens, R. Dorta, S. P. Nolan, *Chem. Commun.* **2010**, *46*, 1050-1052; d) J. Bauer, H. Braunschweig, P. Brenner, K. Kraft, K. Radacki, K. Schwab, *Chem. Eur. J.* **2010**, *16*, 11985-11992.

¹³ a) F. Hering, J. Nitsch, U. Paul, A. Steffen, F. M. Bickelhaupt, U. Radius, *Chem. Sci.* **2015**, *6*, 1426-1432; b) F. Hering, U. Radius, *Organometallics* **2015**, *34*, 3236-3245; c) S. Roy, K. C. Mondal, J. Meyer, B. Niepötter, C. Köhler, R. Herbst-Irmer, D. Stalke, B. Dittrich, D. M. Andrada, G. Frenking, H. W. Roesky, *Chem. Eur. J.* **2015**, *21*, 9312-9318.

¹⁴ a) J. Bauer, R. Bertermann, H. Braunschweig, K. Gruss, F. Hupp, T. Kramer, *Inorg. Chem.* **2012**, *51*, 5617-5626; b) S. Bertsch, H. Braunschweig, M. Forster, K. Gruss, K. Radacki, *Inorg. Chem.* **2011**, *50*, 1816-1819.

¹⁵ M. Ma, A. Sidiropoulos, L. Ralte, A. Stasch, C. Jones, *Chem. Commun.* **2013**, *49*, 48-50.



Scheme 1: Metal-only Lewis Pairs from refs 12d and 14a.

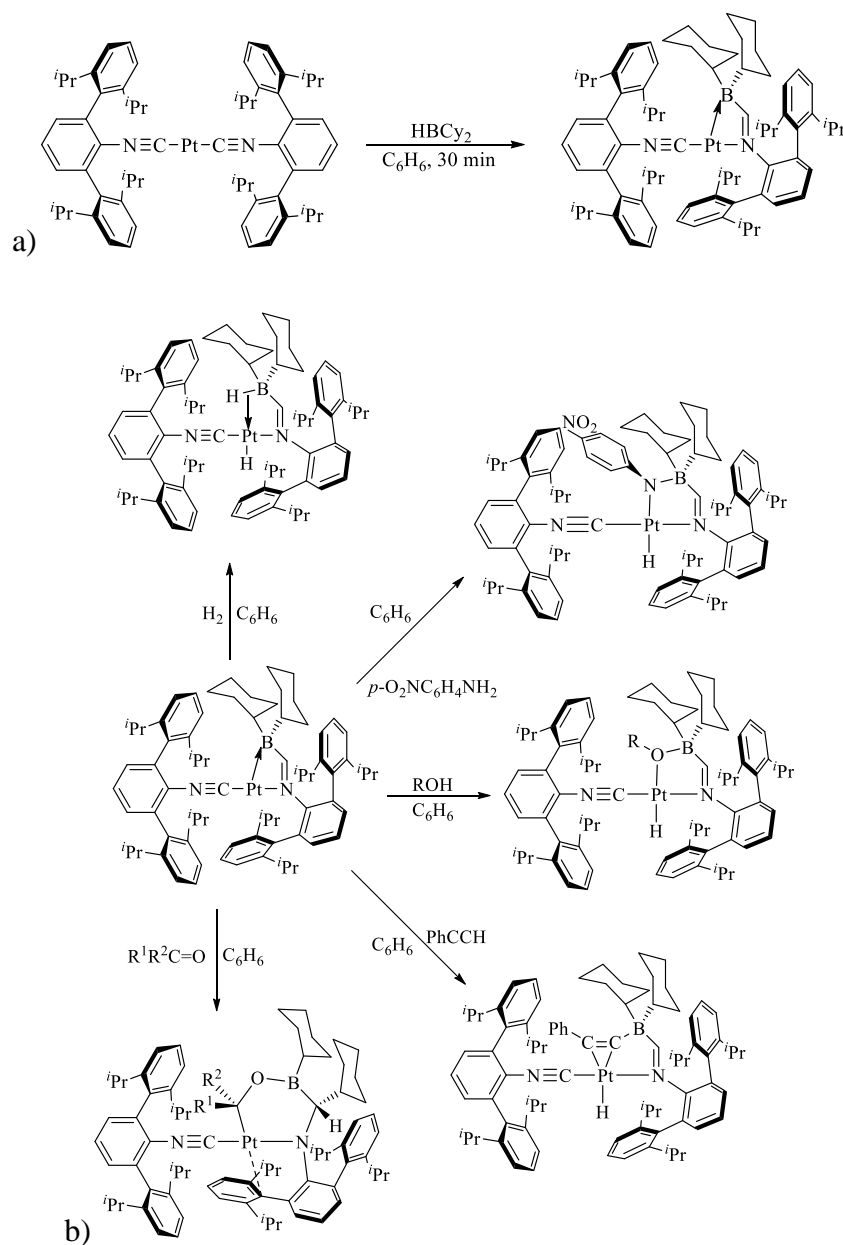
C—F and C—O bonds can be readily activated by $[\text{Pt}(\text{PR}_3)_2]$ complexes, as demonstrated by work developed by the group of Perutz.¹⁶ Using $[\text{Pt}(\text{PCyp}_3)_2]$ (Cyp = cyclopentyl), a variety of fluorinated aromatic methyl ethers underwent $\text{Me}-\text{OAr}^{\text{F}}$ cleavage in preference to $\text{MeO}-\text{Ar}^{\text{F}}$, to afford corresponding *trans*- $[\text{PtMe}(\text{OAr}^{\text{F}})(\text{PCyp}_3)_2]$ complexes.^{16a}

There are other novel contemporary results that deserve being highlighted. Firstly, the zero-valent bis (*m*-terpehnylisocyanide) platinum complex $[\text{Pt}(\text{CNAr}^{\text{Dipp}_2})_2]$ was found to react with HBCy_2 with formation of complex **1** of Scheme 2a, that features a bidentate “LZ” (boryl)iminomethane ligand, with significant platinum-to-borane dative σ -interaction.¹⁷ As represented in Scheme 2b, this complex reacts readily with a variety of substrates (H_2 , methanol, *p*-nitroanyline, $\text{PhC}\equiv\text{CH}$, acetone, etc.) giving rise to products that result from the activation of H-X

¹⁶ a) N. A. Jasim, R. N. Perutz, B. Procacci, A. C. Whitwood, *Chem. Commun.* **2014**, 50, 3914-3917; b) A. Nova, S. Erhardt, N. A. Jasim, R. N. Perutz, S. A. Macgregor, J. E. McGrady, A. C. Whitwood, *J. Am. Chem. Soc.* **2008**, 130, 15499-15511; c) E. Clot, O. Eisenstein, N. Jasim, S. A. Macgregor, J. E. McGrady, R. N. Perutz, *Acc. Chem. Res.* **2011**, 44, 333-348.

¹⁷ B. R. Barnett, C. E. Moore, A. L. Rheingold, J. S. Figueroa, *J. Am. Chem. Soc.* **2014**, 136, 10262-10265.

bonds by the Pt \rightarrow B linkage in a manner reminiscent of Frustrated Lewis Pairs (FLPs).¹⁸



Scheme 2: Bond activation reactions resulting from cooperative transition metal/Lewis acid pairs (adapted from Ref. 17).

¹⁸ P. A. Chase, T. Jurca, D. W. Stephan, *Chem. Commun.* **2008**, 1701-1703.

To complete this section, some catalytic applications of Pt(0) complexes should be mentioned. In particular, recent results related to hydrosilylation and carbonylation reactions will be considered. Species implicated in these transformations keep close resemblance with some of the complexes described in this chapter. (and also in Chapter I).

One of the most important industrial reactions catalysed by Pt(0) is the hydrosilylation, the addition of a Si-H unit to a C—C double bond to form an alkyl silane.¹⁹ This process enables the production of silicon polymers of wide applications. Methods for the hydrosilylation of terminal alkynes have also been developed for the preparation of *cis*- and *trans*-alkenylsilanes. As mentioned previously, a variety of metal salts, supported metal and transition metal complexes can be used with platinum compounds finding numerous utilisations.²⁰

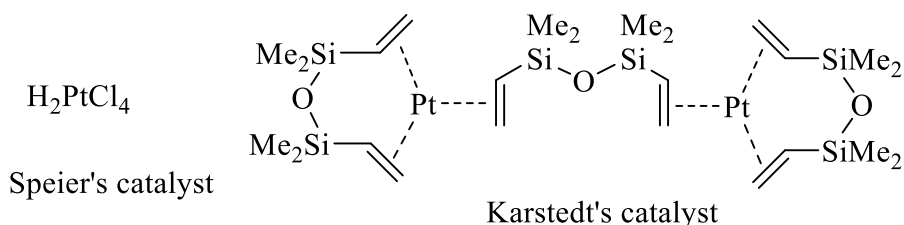
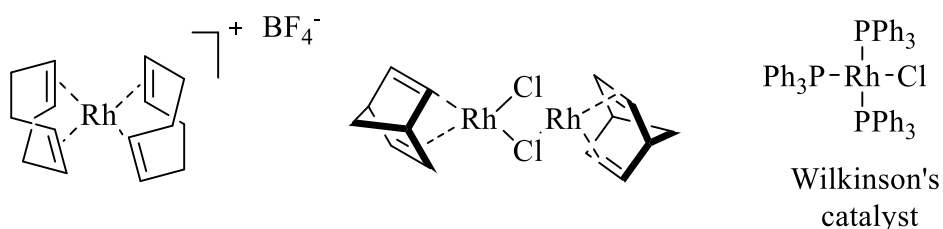
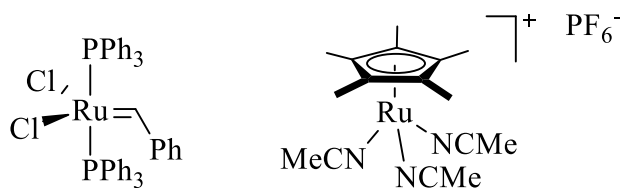
Classical platinum catalysis (Speier's and Karstedt's catalyst, as well as some recently developed variants²⁰), along with rhodium precatalysts²¹ constitute powerful methods for the synthesis of useful silicon-containing materials. Besides, ruthenium-based catalysts²² (Figure 2) allow access to *cis*- β -alkenylsilanes. In general, the stereo- and regioselectivity of the hydrosilylation of alkynes is highly dependent on the alkyne, silane and solvent.

¹⁹ K. Yamamoto, T. Hayashi, in *Transition Metals for Organic Synthesis*, Wiley-VCH Verlag GmbH, **2008**, pp. 167-191.

²⁰ a) I. E. Markó, S. Stérin, O. Buisine, G. Mignani, P. Branlard, B. Tinant, J. Declercq, *Science* **2002**, 298, 204-206; b) O. Buisine, G. Berthon-Gelloz, J.-F. Briere, S. Sterin, G. Mignani, P. Branlard, B. Tinant, J.-P. Declercq, I. E. Marko, *Chem. Commun.* **2005**, 3856-3858; c) G. Berthon-Gelloz, J.-M. Schumers, G. De Bo, I. E. Markó, *J. Org. Chem.* **2008**, 73, 4190-4197.

²¹ a) R. Takeuchi, S. Nitta, D. Watanabe, *J. Org. Chem.* **1995**, 60, 3045-3051; b) R. Takeuchi, N. Tanouchi, *J. Chem. Soc., Perkin Trans. 1* **1994**, 2909-2913; c) A. Sato, H. Kinoshita, H. Shinokubo, K. Oshima, *Org. Lett.* **2004**, 6, 2217-2220.

²² Y. Na, S. Chang, *Org. Lett.* **2000**, 2, 1887-1889.

Pt-based catalysts**Rh-based catalysts****Ru-based catalysts****Figure 2:** Examples of hydrosilylation catalysts.

Alkene hydrosilylation by Kardstedt catalyst suffers from some drawbacks, in particular the generation of important quantities of side-products. Markó and coworkers found^{20a} that although the addition of tertiary phosphines to Karstedt catalysts (structure **A**, Figure 3) resulted in smaller amounts of bi-products, catalysis occurred at lower rate and colloidal platinum was still produced. By contrast the more robust σ -donor NHC complexes **B** reduced greatly the amounts of undesired side-products. Moreover, the new NHC catalysts were found to exhibit high chemoselectivity and tolerance towards reactive functionalities like alcohols, ketones, esters or epoxides.^{20a} Subsequently, the same group of

researchers found that complexes of type **B** containing the bis(allyl) ether diolefin ligand was highly active for the regioselective hydrosilylation of terminal and internal alkynes.^{20c}

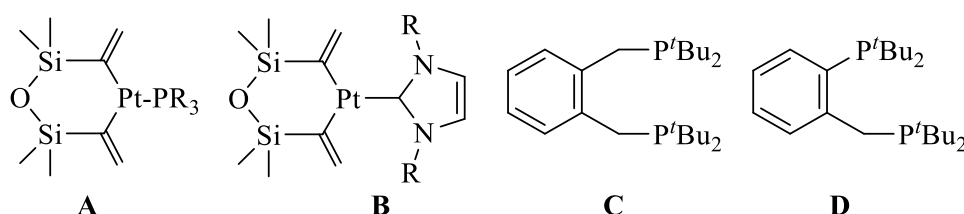


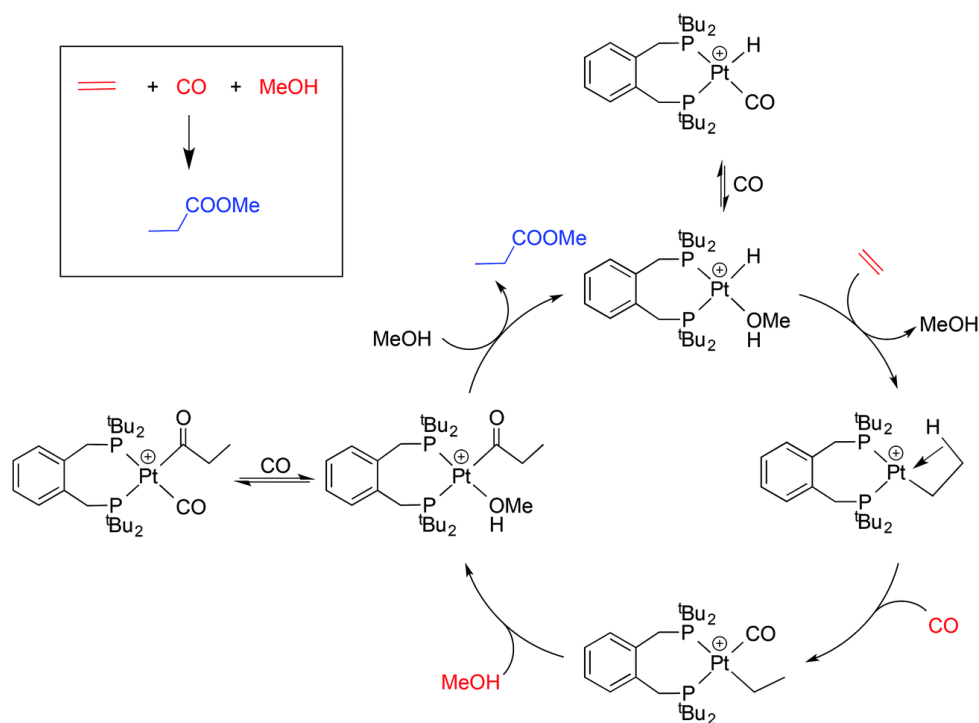
Figure 3: Molecular structure of selected compounds from Ref. 20c and 23.

Platinum(0) complexes are also relevant as models for the Pd-catalysed ethane hydromethoxycarbonylation reaction that converts C_2H_4 , CO and MeOH into an acrylic ester, $\text{CH}_3\text{CH}_2\text{C}(\text{O})\text{OMe}$, in the *Lucite Process*.²³ The commercialised Pd-catalyst contains the diphosphine ligand **C**, first reported Shaw in 1976.²⁴ Spencer *et al.* later reported the first examples of β -agostic of $\text{Pt-CH}_2\text{CH}_3$ complexes by protonation of the $[\text{Pt}(\text{P}^{\wedge}\text{P})(\text{C}_2\text{H}_4)]$ complex of ligand **C**.²⁵ The proposed mechanism for the Pt-catalysed formation of $\text{CH}_3\text{CH}_2\text{C}(\text{O})\text{OMe}$ from C_2H_4 , MeOH and CO is shown in Scheme 3, and includes two non-productive exocyclic equilibrium implicating cationic Pt(II) carbonyl complexes.

²³ S. J. K. Forrest, P. G. Pringle, H. A. Sparkes, D. F. Wass, *Dalton Trans.* **2014**, 43, 16335-16344.

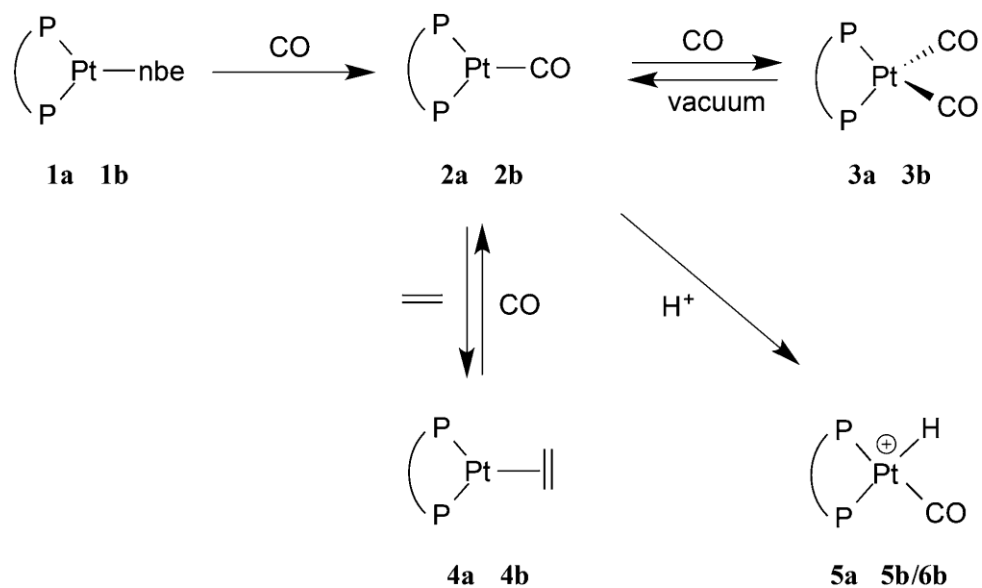
²⁴ C. J. Moulton, B. L. Shaw, *J. Chem. Soc., Chem. Commun.* **1976**, 365-366.

²⁵ a) N. Carr, B. J. Dunne, A. G. Orpen, J. L. Spencer, *J. Chem. Soc., Chem. Commun.* **1988**, 926-928; b) L. Mole, J. L. Spencer, N. Carr, A. G. Orpen, *Organometallics* **1991**, 10, 49-52.



Scheme 3: Outline of the mechanism of Pt-catalysed hydromethoxycarbonylation of ethane including two exocyclic equilibria.

Recent work from Pringle, Wass *et al.*²³ has provided evidence for the rapid formation and interconversion of the mono- and dicarbonylplatinum(0) complexes **2** and **3** of Scheme X, that contain ligands **C** and **D** (denoted with **a** and **b**, respectively in Scheme 4). Furthermore, they demonstrated the feasibility of cationic Pt(II) carbonylhydrides of type **5**, with the structural characterisation by X-ray crystallography of complex **5a** of ligand **C** above.²³

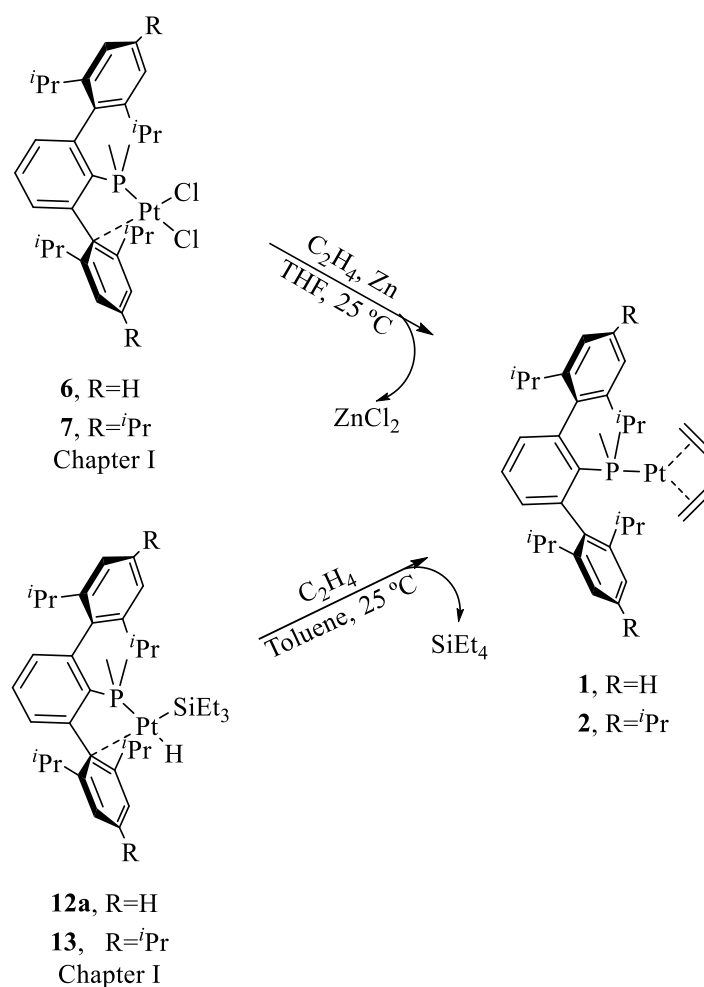
**Scheme 4:** Reaction scheme from Ref 23.

II.3. RESULTS AND DISCUSSION

II.3.1. Synthesis of Pt(0)-olefin complexes

A widely used procedure for the synthesis of Pt(0)-PR₃-olefin complexes consists in reductive processes that make use of readily available Pt(II) precursors. A variety of reducing agents may be used, including alkali metals, hydrazine, sodium borohydride and others.^{9,26} We found that platinum(II) complexes *cis*-[PtCl₂(PMe₂Ar')] (Ar' = Ar^{Dipp}₂, **6**; Ar^{Tipp}₂, **7** from Chapter I) could be reduced by Na, K, sodium amalgam, etc. under an atmosphere of C₂H₄ (1.5 bar) to afford the desired complexes [Pt(C₂H₄)₂(PMe₂Ar')], that contained two coordinated molecules of the olefin. From an experimental point of view, Zn powder proved to be the most convenient reductant (Scheme 5) and yielded complexes **1** and **2** after stirring the reaction mixture at room temperature for about 14 h, employing THF as the solvent. As an alternative procedure, compounds **1** and **2** could also be obtained from the corresponding hydride silyl derivatives, **12a** and **13**, respectively, by formal reductive elimination of HSiEt₃ induced by C₂H₄ (2 bar).

²⁶ J. Forniés, E. Lalinde, in *Comprehensive Organometallic Chemistry III* (Ed.: R. H. Crabtree), Elsevier, Oxford, **2007**, pp. 611-673,



Scheme 5. Synthesis of the bis(ethylene) Pt(0) complexes **1** and **2**.

Compounds **1** and **2** were isolated as air-sensitive brown solids and were characterized by microanalysis and NMR spectroscopy in solution. Additionally, the solid-state molecular structure of **1** was determined by X-ray diffraction. Before discussing their structural characterisation, some comments on their formation from the corresponding hydride-silyl precursors **12a** and **13**, respectively appear pertinent. Although we did not consider necessary studying in detail the mechanism of the reaction, some comments on its course are appropriate, however speculative they might appear. A reasonable reaction path could involve ethylene substitution of

the highly labile $\text{Pt}\cdots\text{C}_{\text{ar}}$ interaction in complex **13a**, which is *trans* to the high *trans*-effect $-\text{SiEt}_3$ ligand.²⁷ As represented in Scheme 6a, this could be followed by migratory insertion reactivity, to afford a transient platinum(II)-ethyl-silyl-phosphine intermediate, stabilised either by a β -agostic ethyl (not shown) or an $\eta^1\text{-C}_{\text{ar}}$ interaction. Such a sterically congested intermediate would render the observed $[\text{Pt}(\text{C}_2\text{H}_4)_2(\text{PMe}_2\text{Ar}^{\text{Dipp}})_2]$ and SiEt_4 products, by reductive elimination of the silane induced by excess of ethylene.

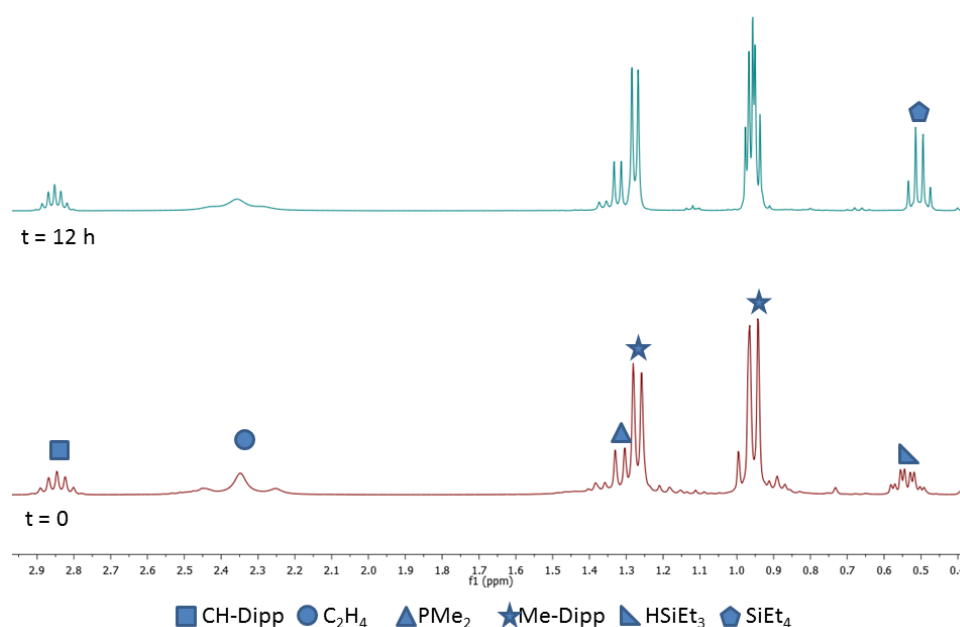
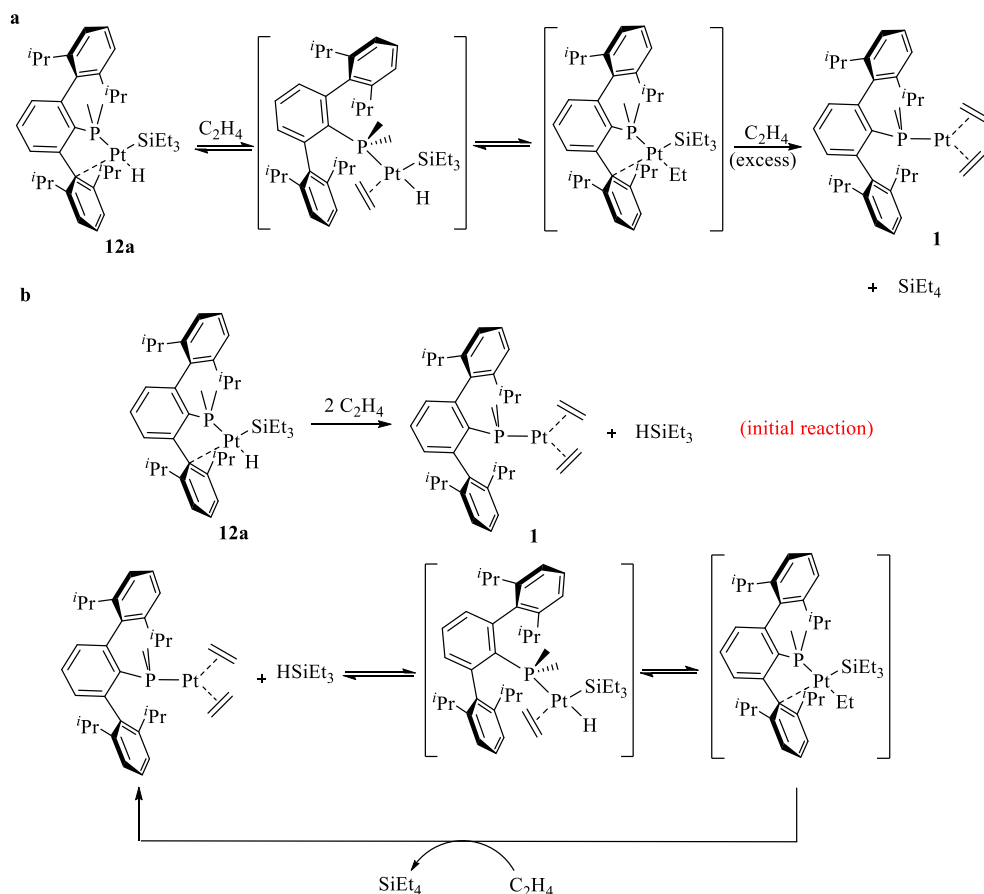


Figure 4. Aliphatic zone of ^1H NMR spectrum of the reaction between complex **12a** (Chapter I) and C_2H_4 (2 bar) on the moment of reaction (bottom, C_6D_6 , 25 °C, 300 MHz) and after *c.a.* 12 hours (top, C_6D_6 , 25 °C, 400 MHz).

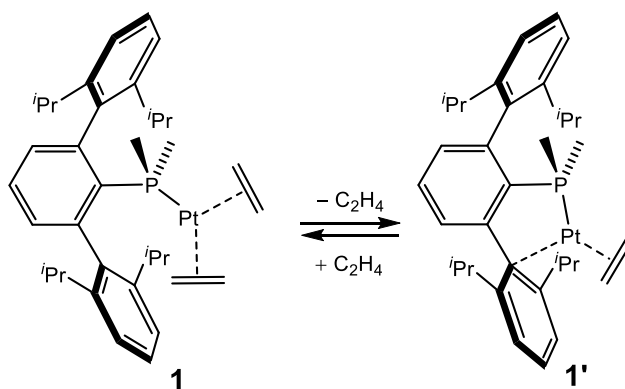
²⁷ a) T. G. Appleton, H. C. Clark, L. E. Manzer, *Coord. Chem. Rev.* **1973**, 10, 335-422; b) F. R. Hartley, *Chem. Soc. Rev.* **1973**, 2, 163-179; c) L. J. Manojlovic-Muir, K. W. Muir, *Inorg. Chim. Acta* **1974**, 10, 47-49.



Scheme 6: Possible mechanistic routes for the conversion of complex **12a** and C_2H_4 into complex **1** plus SiEt_4 depicted in the bottom reaction of Scheme 5. See text for details.

^1H NMR monitoring of this transformation (Figure 4, $t = 0$) demonstrated, however, that complex $[\text{Pt}(\text{C}_2\text{H}_4)_2(\text{PMe}_2\text{Ar}^{\text{Dipp}_2})]$ (**1**) and HSiEt_3 formed (top of Scheme 6b) at the very early stages of the reaction (mixing of the reactants in an NMR tube and intermediate recording of the ^1H NMR spectrum) and that the hydrosilane slowly converted into SiEt_4 , probably by C_2H_4 hydrosilylation catalysed by complex **1** (top spectrum in Figure 4, recorded after 12 hours).

Although the bis(ethylene) complex **1** formed cleanly under the reaction conditions, that included the use of an excess of C_2H_4 , as represented in Scheme 7, solutions of isolated complex **1** maintained under an atmosphere of dinitrogen slowly underwent C_2H_4 dissociation with formation of the apparently two coordinate monoethylene complex $[\text{Pt}(\text{C}_2\text{H}_4)(\text{PMe}_2\text{Ar}^{\text{Dipp}_2})]$ (**1'**). In solid state, ethylene dissociation from **1** was very slow under ambient conditions and required around three months under a N_2 or Ar atmosphere (inside the globe-box). At 50°C under high vacuum (10^{-4} torr) several days were needed for the conversion of **1** into **1'**. Considerable decomposition took, however, place during the heating process. Convincing evidence for the dynamic equilibrium between complexes **1** and **1'** was provided by quantitative conversion of solution equilibrium mixtures of the two compounds into exclusively the bis(ethylene) adduct **1** upon treatment with excess C_2H_4 . This permitted isolation of this complex in analytically pure form and as single crystals suitable for X-ray studies.

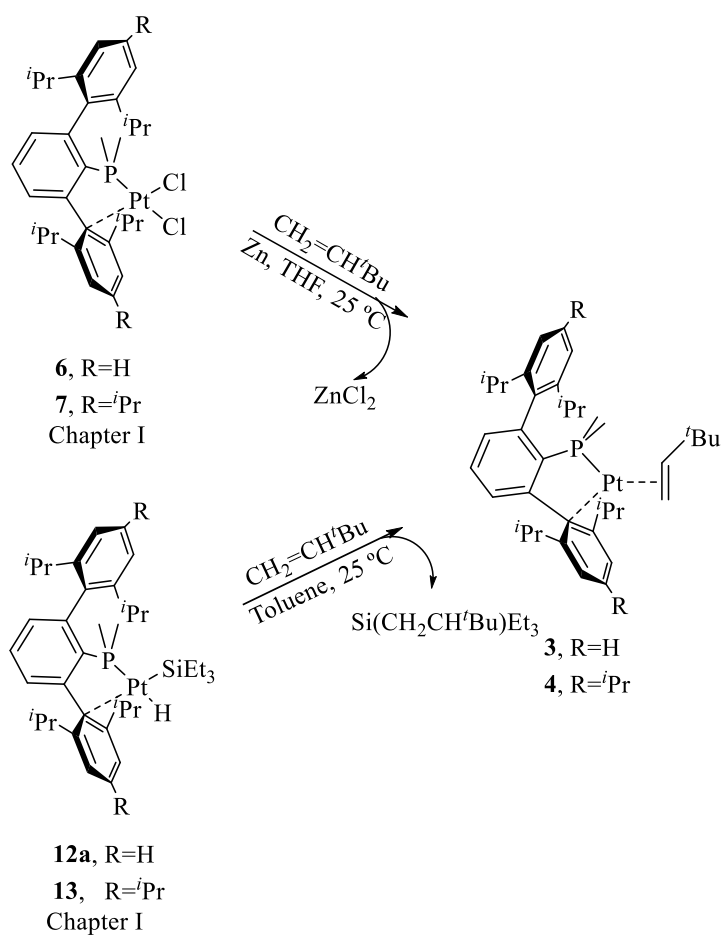


Scheme 7: Equilibrium between mono- and bis(ethylene) adducts, **1'** and **1** respectively.

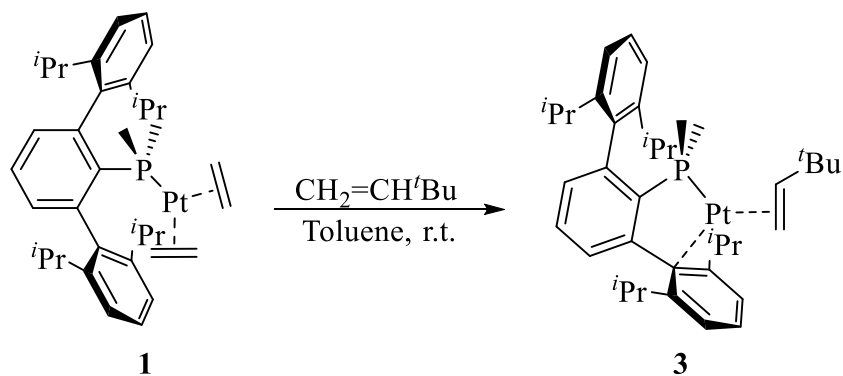
Even though two-coordinate $\text{Pt}(0)$ complexes are known, stable compounds, contain bulky PR_3 , NHC or related ligands (see II.2. Introduction). Internal alkynes with bulky substituents also give rise to

[Pt(alkyne)₂] complexes with thermal stability depending markedly upon the size of the R-C≡C-R R groups.^{11d} To our knowledge, complexes of the [Pt(PR₃)(alkene)] are presently unknown, and accordingly the experimental evidence gained for the existence of compound **1'** that will be completed later in this section prompted us to explore the possibility of preparing a stable, formally two coordinate Pt(0)-phosphine-alkene complex, with the introduction of a sterically demanding substituent in the olefin molecular framework. Such a substituent would be expected to impede the coordination of a second molecule of the olefin, thereby forcing the desired two-ligand structure.

Tert-butylethylene (tbe) was the olefin of choice and led selectively and cleanly to the targeted complex **3** and **4**, with the structures suggested in Scheme 8. Similarly to the related C₂H₄ complexes, the new compounds could be obtained by: (i) Zn powder reduction of the PtCl₂-precursors **6** and **7** or, alternatively, (ii) reductive elimination reactions of the hydrido-silyls **12a** and **13** promoted by the olefin. Additionally (Scheme 9), the PMe₂Ar^{Dipp}₂ derivative **3** was also prepared from complex **1** (or from **1/1'** mixtures) by action of an excess of tbe.

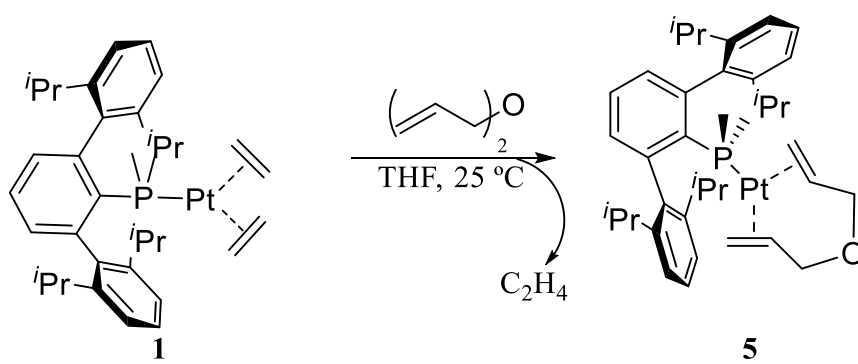


Scheme 8. Synthesis of *tert*-butylethylene Pt(0) complexes **3** and **4** from Pt(II) precursors.



Scheme 9: Synthesis of complex **3** from **1**.

To complete these synthetic studies, we also deemed pertinent to prepare a related complex of a diene ligand, $[\text{Pt}(\eta^4\text{-diene})(\text{PMe}_2\text{Ar}')]]$. The Dipp-substituted phosphine was chosen as the P-donor ligand and bis(allyl)ether, $(\text{CH}_2=\text{CH}-\text{CH}_2)_2\text{O}$ (usually designated allyl ether) as the diene. It was found that treatment of the bis(ethylene) derivative **1** with an excess of allyl ether, at room temperature, in THF afforded complex **5** as a light brown solid in good isolated yields (Scheme 10).



Scheme 10. Synthesis of Pt(0) complex **5**.

In summary, the synthetic chemistry described in the foregoing paragraphs allowed the isolation of new Pt(0)-phosphine-olefin complexes of composition $[\text{Pt}(\text{PMe}_2\text{Ar}')(\text{olefin})]$ and $[\text{Pt}(\text{PMe}_2\text{Ar}')(\text{olefin})_2]$. The new compounds were fully characterized by microanalytical data and by NMR spectroscopy. The NMR studies that will be detailed later suggest classical, monodentate coordination of the terphenyl phosphine in the bis(olefin) complexes and bidentate, $\kappa^2\text{-P,C}$ binding in the mono(olefin) derivatives. These structural proportions were confirmed by single-crystal X-ray studies performed with complexes $[\text{Pt}(\text{C}_2\text{H}_4)_2(\text{PMe}_2\text{Ar}^{\text{Dipp2}})]$ (**1**) and $[\text{Pt}(\text{CH}_2=\text{CH}-t\text{Bu})(\text{PMe}_2\text{Ar}^{\text{Dipp2}})]$ (**3**). Before we describe the NMR and X-ray results collected for the new compounds, some commentaries on previous work on complexes of this kind seem suitable. Mono-olefin complexes $[\text{Pt}(\text{PR}_3)_2(\text{olefin})]$ have long been known for both mono- and

bidentate ($P^{\wedge}P$) phosphine ligands.⁹ They have always been considered of interest as a source of $Pt(PR_3)_2$ species, highly valuable for the activation of diverse element-element bonds. The structure of $[Pt(PPh_3)_3(C_2H_4)]$ was determined by X-ray crystallography in 1972 and led to a C-C distance for the coordination ethylene ligand of 1.434(13) Å, *in accord with that found when transition elements form metallo-cyclopropanes*.²⁸ More than 15 years later, the structure of $[Pt(PCy_3)_2(C_2H_4)]$, which exists in solution in equilibrium with $Pt(PCy_3)_2$ and C_2H_4 , was disclosed, the results suggesting weak coordination of ethylene, with Pt—C and C—C bond distances of 2.173(7) and 1.440(7) Å, respectively. Despite the time elapsed, $[Pt(PR_3)_2(olefin)]$ complexes attract the attention of many researchers. In a recent study, the group of Ruhland reported the synthesis of 48 new bis(triphenylphosphine) complexes of substituted cinnamic acid esters, that were investigated *to examine electronic and steric influences on their behavior as inhibited precatalysts* (mainly for hydrosilylation reactions).²⁹ The authors aimed to find a cinnamate ligand which binds tightly to Pt(0) inhibiting catalysis, but could be cleaved off via photoassistance.²⁹

By contrast with the above complexes those containing only one PR_3 ligated to Pt(0) and two olefinic ligands are very rare, naturally with the exception of those derived from diolefin ligands. A series of $[Pt(C_2H_4)_2(PR_3)complexes]$ was prepared by Stone and co-workers^{30a} with the purpose of using them as a source of the “ $Pt(PR_3)$ ” fragment. Different alkyl and aryl phosphines were utilized and $[Pt(C_2H_4)(PCy_3)_2]$ was found to react with C_2F_4 to afford the mixed-olefin complex $[Pt(C_2H_4)(C_2F_4)(PCy_3)]$. The 16-electron complexes exhibited dynamic

²⁸ P. T. Cheng, S. C. Nyburg, *Can. J. Chem.* **1972**, 50, 912-916.

²⁹ M. R. Buchner, B. Bechlars, B. Wahl, K. Ruhland, *Organometallics* **2013**, 32, 1643-1653.

³⁰ a) N. C. Harrison, M. Murray, J. L. Spencer, F. G. A. Stone, *J. Chem. Soc., Dalton Trans.* **1978**, 1337-1342; b) J. A. K. Howard, P. Mitprachachon, A. Roy, *J. Organomet. Chem.* **1982**, 235, 375-381.

behavior in solution with rotation of the ethylene ligands. Variable temperature NMR studies pointed at a planar molecular structure that was subsequently confirmed by X-ray crystallographic studies on the above mixed C₂H₄/C₂F₄ complex.^{30b} The mean Pt—C(C₂H₄) and Pt—C(C₂F₄) separations were found at 2.027(10) and 2.173(9) Å respectively.

Platinum(0) complexes of composition [Pt(η⁴-diene)(PR₃)] are also relevant molecules, in particular those containing η⁴-1,6-diene ligands. Pörschke and co-workers reported in 1999 a series of homoleptic Pd(0) and Pt(0) of some 1,6-diene ligands, that encompass allyl ether and 1,3divinyl-1,1,3,3-tetramethyldisiloxane (dvds).³¹ As discussed in the Introduction some Pt(0)-NHC-diolefin complexes of this kind, notably [Pt(dvds)(NHC)] derivatives^{20a} are highly selective and efficient hydrosilylation catalysts.^{20a,32}

The ¹H NMR spectrum of complex **1** is shown in Figure 5 and will be discussed in detail. The ¹H NMR spectrum of complex **2** features analogous characteristics, both in terms of molecular symmetry and chemical shifts, with the evident differences that arise from the presence of the aliphatic signals of the 4-*iso*-propyl groups. The hydrogen atoms of the *i*-propyl substituents of complex **1** resonate as two doublets at 0.95 and 1.95ppm (CH₃ groups) and one septet at 2.84 ppm (CH), reflecting the equivalence of the two flanking aryl groups. The olefinic protons appear as a broad singlet at 2.34 ppm (²J_{HPt} = 53.1 Hz), whereas the corresponding carbon nuclei appear as a singlet at 38.5 ppm (¹J_{CPt} = 153 Hz) in the ¹³C{¹H} NMR spectrum, as a consequence of the symmetry and fast rotation around the Pt-alkene bonds. The ³¹P nuclei give rise to a singlet at

³¹ J. Krause, G. Cestarc, K. Haack, K. Seevogel, W. Storm, K. Pörschke, *J. Am. Chem. Soc.* **1999**, *121*, 9807-9823.

³² a) G. Berthon-Gelloz, J. Schumers, F. Lucaccioni, B. Tinant, J. Wouters, I. E. Markó, *Organometallics* **2007**, *26*, 5731-5734; b) G. Berthon-Gelloz, B. de Bruin, B. Tinant, I. E. Markó, *Angew. Chem. Int. Ed.* **2009**, *48*, 3161-3164.

$\delta -16.2$ ppm ($^1J_{\text{PPt}} = 3265$ Hz), with a strong high-frequency shift compared with the free phosphine ligand (-41.3 ppm).

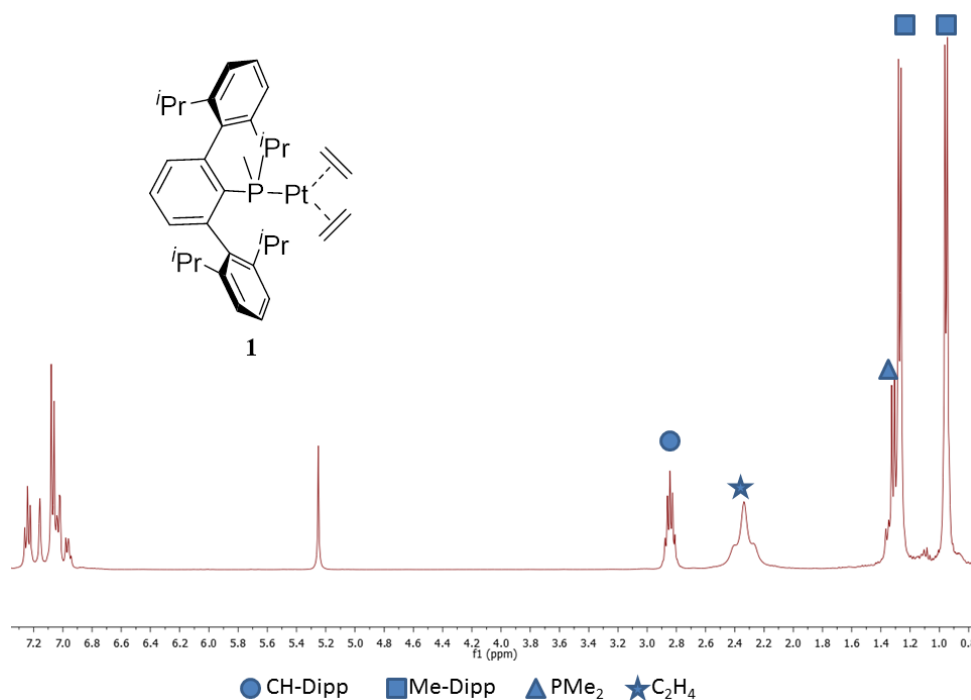


Figure 5. ^1H NMR spectrum of complex **1** (400 MHz, C_6D_6 , 25 °C).

These data are not in agreement with a rigid structure of the kind represented in Scheme 5 and Figure 5, for which the methylene groups of each C_2H_4 ligand occupy two non-equivalent molecular sites. The ^1H and $^{13}\text{C}\{^1\text{H}\}$ NMR spectra of complex **1** were therefore examined in the temperature interval from +25 to -50 °C (see Figure 6 for variable temperature ^1H and $^{13}\text{C}\{^1\text{H}\}$ NMR spectra) and revealed the expected variations of line shape. Thus, at 0 °C the broad, 25 °C signal centred at 2.35 ppm ($^2J_{\text{HPt}} = 54$ Hz) became practically hidden into the base line, to emerge as two very broad resonances at *ca.* 1.97 and 2.91 ppm, the latter accidentally superimposed with the resonance attributed to the methane protons of the terphenyl radical *i*-propyl substituents. At the coalescence

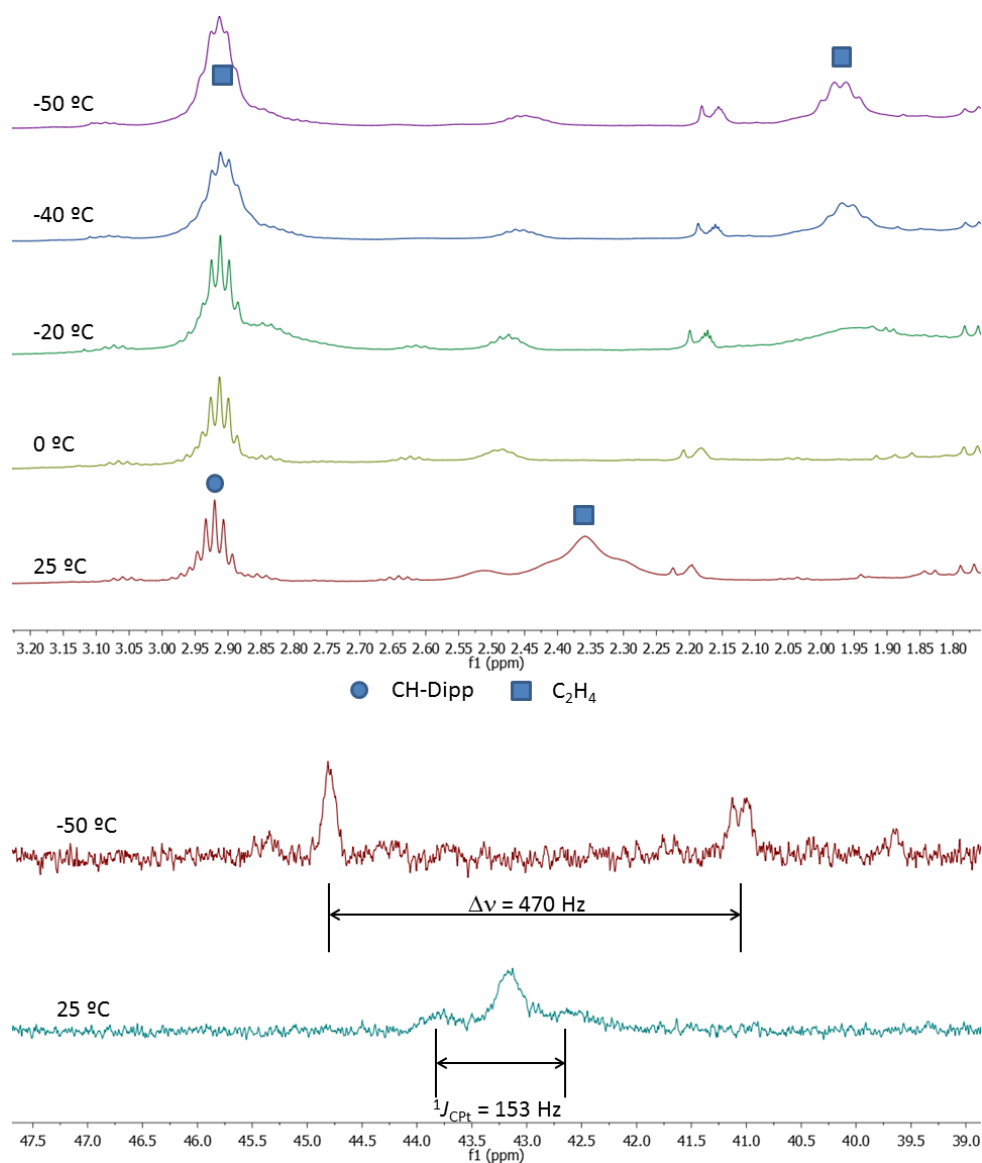


Figure 6: Variable temperature ^1H (top) and $^{13}\text{C}\{^1\text{H}\}$ (bottom) NMR spectrum of complex **1** ($\text{Tol-}d_8$, 500 MHz, 125.7 MHz).

temperature (0 °C) the exchange rate was $\kappa = 926 \text{ s}^{-1}$, leaving to an activation energy for ethylene rotation of $13.4 \text{ kcal}\cdot\text{mol}^{-1}$. In the low-temperature limit, the four protons of each ethylene ligand gave rise to broad several-line patterns, further complicated by the ^{195}Pt -satellites. The poor resolution did not allow for a computer analysis of the spectrum.

Similar variations were recorded in the $^{13}\text{C}\{^1\text{H}\}$ NMR spectrum (Figure 6, bottom), where the room temperature singlet at 43.2 ppm converted into two singlets at 41.1 and 44.8 ppm. Of note is the remarkable similarity between the activation energy determined for complex **1** and the values of *ca.* 13 kcal·mol⁻¹ reported for both $[\text{Pt}(\text{C}_2\text{H}_4)_2(\text{PCy}_3)]^{30\text{a}}$ and $[\text{Pt}(\text{C}_2\text{H}_4)_2(\text{PMe}_3)]$. This resemblance hints that steric factors are not implicated.

Room temperature NMR spectra of mixtures of the bis- and mono-olefin complexes **1** and **1'** revealed the presence of the two types of coordinated alkene molecules. For example, in the ^1H NMR spectrum, besides the 2.35 ppm signal of **1** there is another resonance at 2.20 ppm ($^2J_{\text{HPt}} = 68$ Hz) assigned to the mono-ethylene complex **1'**. This signal has an associated $^{13}\text{C}\{^1\text{H}\}$ resonance at 42.5 ppm ($^2J_{\text{CPt}} = 270$ Hz). In the $^{31}\text{P}\{^1\text{H}\}$ NMR spectrum (Figure 7), the molecules of **1'** provide a resonance at 24.1 ppm, further characterised by a $^1J_{\text{PPt}}$ coupling constant of 4333 Hz. These data are strikingly similar to those recorded for the structurally characterised complex **3** (23.9 ppm, 4457 Hz) and therefore support strongly the bidentate $\kappa^1\text{-P}$, η -arene coordination proposed for **1'** in Scheme 7.

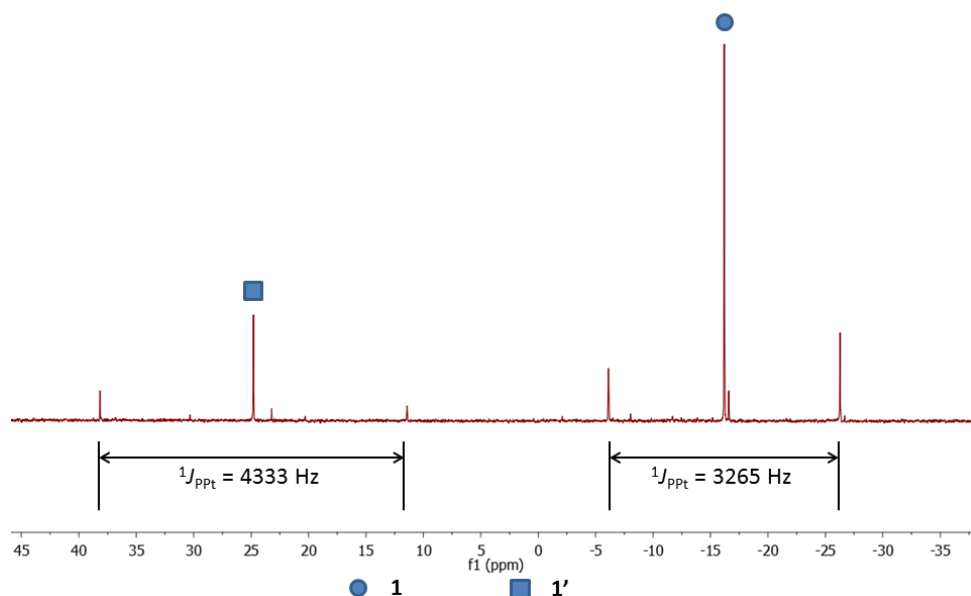


Figure 7: $^{31}\text{P}\{^1\text{H}\}$ NMR spectrum of a solution mixture of **1** and **1'** (C_6D_6 , 161.9 MHz, 25 °C).

The $\text{CH}_2=\text{CH}'\text{Bu}$ complexes **3** and **4** (Scheme 8) exhibit NMR parameters which are markedly different from those recorded for the bis(ethylene) compounds **1** and **2**. The dissimilarities are mostly associated with resonances due to the terphenylphosphine ligand and denote its bidentate coordination through the P and a C_{ar} donor atom. Figure 8 depicts the room temperature ^1H NMR spectrum of **3**, revealing the presence of two sets of signals for the flanking aryl rings of the terphenyl substituent, is in agreement with the interaction of one of them with the metal centre. Likewise, the presence of a substituent on the coordinated alkene reduces further the symmetry of this species, removing the symmetry plane, as demonstrated by the diastereotopic nature of the methyl groups directly bound to the P atom, which resonate with chemical shifts of 1.45 and 1.38 ppm for complex **3**, and 1.45 and 1.50 ppm for complex **4**. Nevertheless, fast rotation at room temperature along the P–Pt bond of the ligand, probably with temporary disengagement of the weak $\text{Pt}\cdots\text{C}_{\text{ar}}$ interaction, makes isochronous the isopropyl protons of the same ring (Figure 9). The

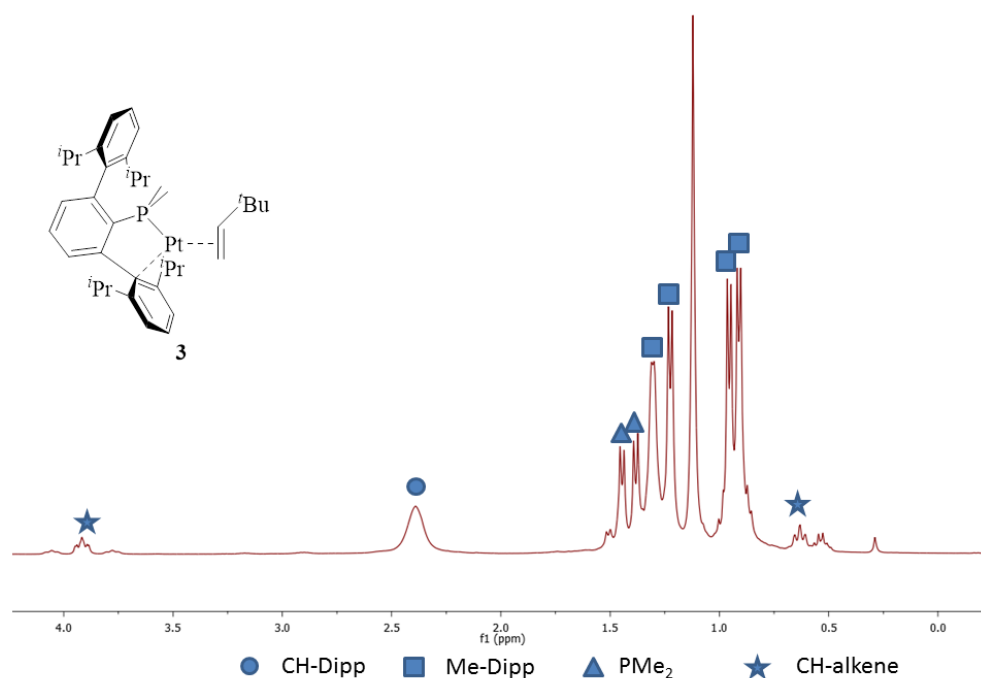


Figure 8. Aliphatic area of ¹H NMR spectrum of complex **3**
(400 MHz, C₆D₆, 25 °C).

¹³C{¹H} resonances for the olefinic nuclei of complex **3** appear at 78.0 (¹J_{CPt} = 460 Hz, ²J_{CP} = 4 Hz) and 45.6 (²J_{CP} = 38 Hz) ppm. As this complex has a low coordination number, the ¹J_{Pt} value (4457 Hz) found in ³¹P{¹H} NMR spectra is significantly larger than those found for complexes **1** and **2** (3265 Hz). As mentioned before, the ³¹P nucleus of **3** resonates at 23.9 ppm, and features a one-bond coupling constant to the ¹⁹⁵Pt nucleus of 4457 Hz.

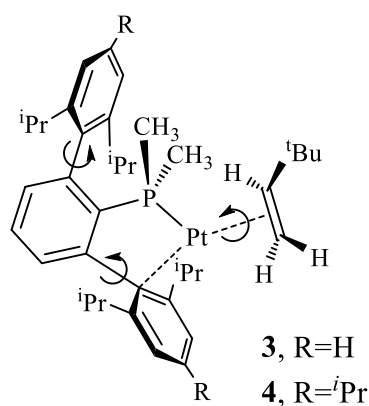


Figure 9: Fluxional behaviour in solution at room temperature of complexes **3** and **4**.

Variable temperature NMR studies shed more light on the fluxional behaviour of **3** and **4** in solution. As observed in Figure 10 for complex **3**, the ^1H NMR resonances due to the phosphine ligand experience relevant changes. For example, at room temperature only one broad resonance for all methine CHMe_2 protons of the *iso*-propyl substituents is observed, whereas at $-40\text{ }^\circ\text{C}$ four signals are clearly detected, with chemical shifts 1.84, 1.93, 2.41 and 2.42 ppm. The analysis of the resonances pertaining to the two Dipp phosphine substituents in complex **3** indicates a fluxional process that exchanges the two rings. An approximate ΔG^\ddagger value of $12.6\text{ kcal}\cdot\text{mol}^{-1}$ can be estimated for this rearrangement from the calculated rate at the coalescence temperature (*ca.* $0\text{ }^\circ\text{C}$). The temperature dependence of these resonances can be ascribed to a fast rotation around the $\text{P}-\text{C}_{\text{aryl}}$ bond (Scheme 11) that switches the coordinated and the free flanking aryl substituents.

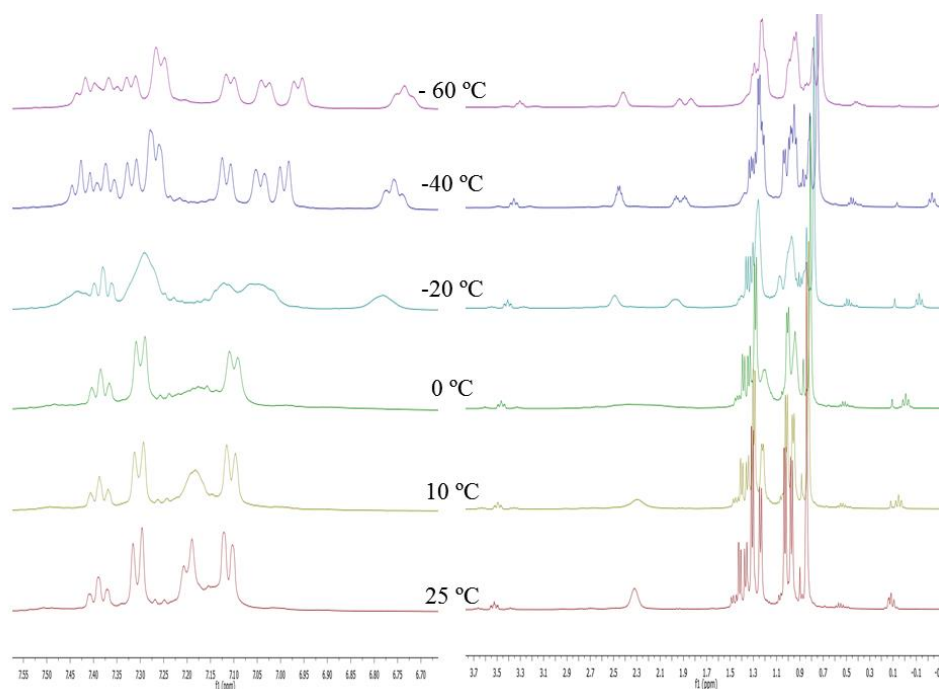
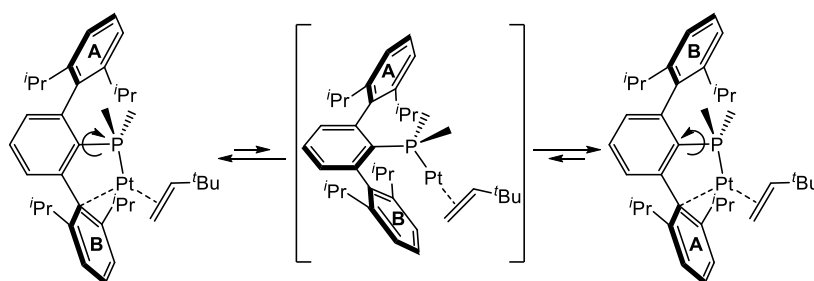


Figure 10. Variable temperature ^1H NMR (left: aromatic area, right: aliphatic region) of complex **3** (CD_2Cl_2 , 400 MHz).



Scheme 11. Proposed mechanism for the fast exchange of the flanking aryl rings of complex **3** (C_6D_6 at 25 °C).

The X-ray studies carried out with complex **3** demonstrate the existence of two diastereomers, **A** and **B**, in the crystal lattice (see below). In solution, however, only one stereomer of **3** exists between -80 and 25 °C. It seems probable that the two stereomers exist in solution at 25 °C in a fast equilibrium on the laboratory time scale that favours strongly one of them. Unfortunately, NOESY experiments did not permit discriminating

the solution structure. To close this discussion, it should be remarked that the observation for the olefinic ^1H and $^{13}\text{C}\{^1\text{H}\}$ resonances of coupling to the ^{31}P and ^{195}Pt nuclei between -80 and 25 °C rules out any dissociative mechanism for the observed site exchanges.

The platinum(0) allyl ether complex **5** (Scheme 10) features the expected monodentate P-coordination of the $\text{PMe}_2\text{Ar}^{\text{Dipp}_2}$ ligand. Unenivocal proof for this type of ligation is provided by NMR data. For instance the $^{31}\text{P}\{^1\text{H}\}$ NMR spectrum is a singlet at -18.7 ppm, with ^{195}Pt satellites that afford a 1JPt value of 3532 Hz. These parameters are strikingly similar to those recorded for the structurally characterised $[\text{Pt}(\text{C}_2\text{H}_4)_2(\text{PMe}_2\text{Ar}^{\text{Dipp}_2})]$ complex **1** (-16.2 ppm, 3265 Hz) and markedly different from data characteristic for $[\text{Pt}(\text{CH}_2=\text{CH}^t\text{Bu})(\text{PMe}_2\text{Ar}^{\text{Dipp}_2})]$ (**3**), which contains a bidentate, $\kappa^2\text{-P,C}$ -bound phosphine ligand (23.9 ppm, 4457 Hz). Besides, the ^1H NMR spectrum of compound **5** (Figure 11), contains one septet and two doublets for the CHMe_2 and CHMe_2 protons of the terphenyl *iso*-propyl substituents, along with one doublet for the two methyl groups bonded to phosphorus. Regarding the olefinic termini, the two are chemically equivalent but the three protons of each alkene unit are non-equivalent and give rise to corresponding multiplets centred at 4.02 ($^2J_{\text{HPt}} = 23.6$ Hz), 2.66 and 1.81 ppm. The observed many-line pattern results from $^1\text{H}\text{-}^1\text{H}$ and $^1\text{H}\text{-}^{31}\text{P}$ couplings and is further complicated by platinum satellites. Naturally, it simplifies considerably upon ^{31}P -decoupling (see Figure 12). The calculated NMR parameters are collected in the Experimental Section.

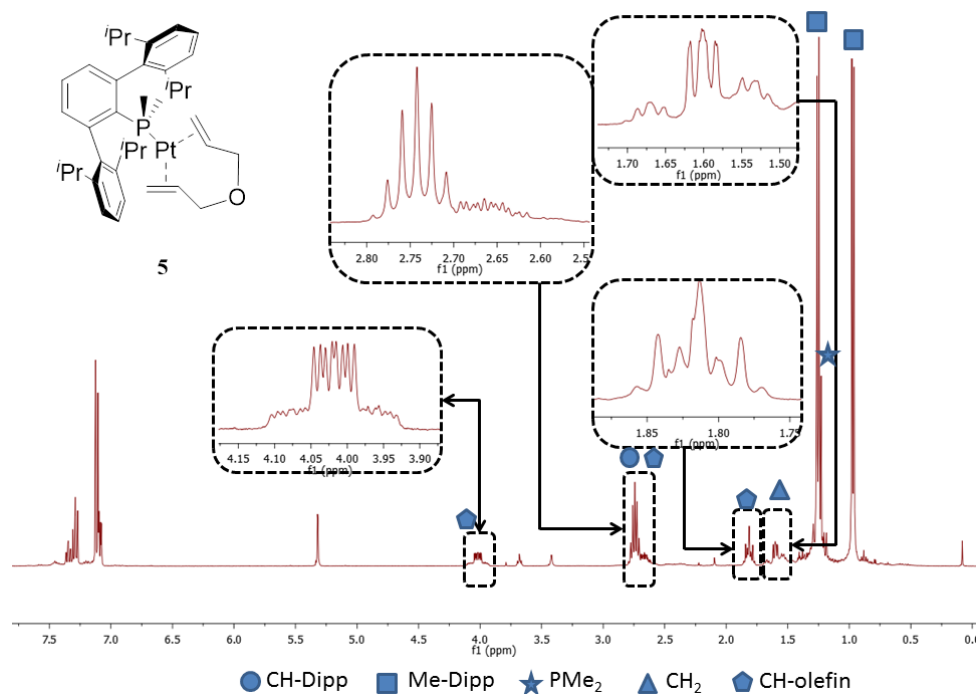


Figure 11. ^1H NMR spectra of complex **5** (400 MHz, CD_2Cl_2 , 25 °C).

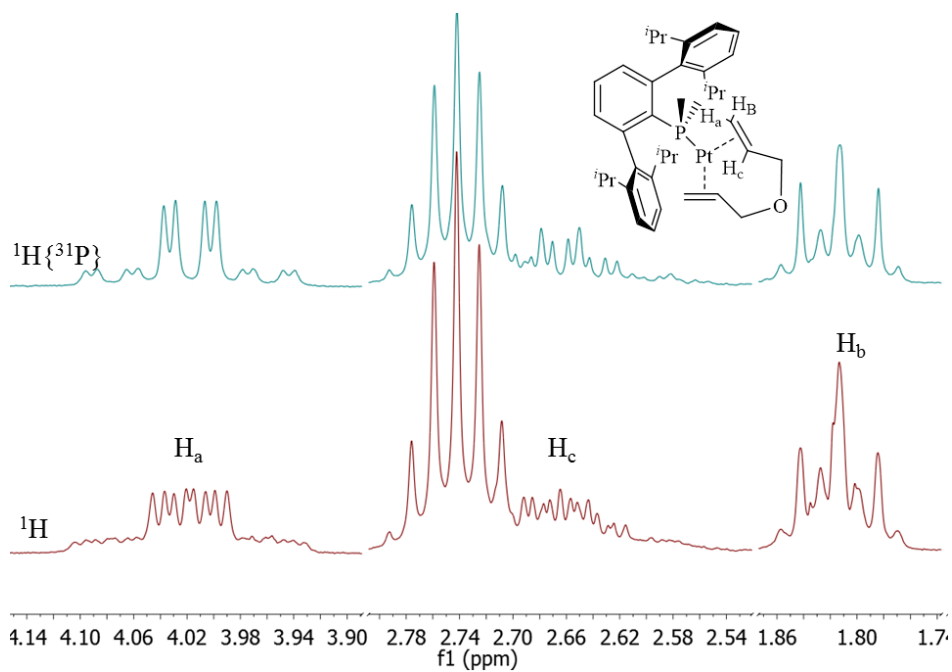


Figure 12: Selected areas of ^1H (bottom) and $^1\text{H}\{^{31}\text{P}\}$ (top) NMR spectra of compound **5** (CD_2Cl_2 , 25 °C, 400MHz).

The solid-state molecular structures of two of the newly reported Pt(0)-PMe₂Ar'-olefin complexes, **1** and **3**, were determined by X-ray crystallography and are presented in the form of ORTEP views in Figures 13 and 14. Complex **1** is an example of a three-ligand species, *i.e.* PMe₂Ar^{Dipp₂} plus two molecules of C₂H₄, whereas complex **3** is a case of a two-ligand derivative, for in addition to the phosphine it accommodates only one molecule of the alkene CH₂=CH^tBu. Although bis(phosphine)-, bis(NHC)-, bis(alkyne)- and mixed phosphine-NHC platinum(0) complexes are known (see section II.2. Introduction), to our knowledge no [Pt(PR₃)(olefin)] complexes have, so far, been reported.

In complex **1** (Figure 13) the Pt(0) centre lies in a distorted trigonal planar coordination environment, the three coordination positions being occupied by two C=C double bonds and the phosphorus atom of the phosphine ligand. Notice that, in spite of the high steric demands of the PMe₂Ar' ligand, the coordination angle between the two ethylene ligands at 132.7(1)° is significantly larger than the two P-Pt-alkene centroid angles of 113.8 (1) and 113.22(8)°, probably to minimize C₂H₄...C₂H₄ contacts that would arise from the disposition of the four carbon atoms in the coordination plane. Notwithstanding the presence of two p-acceptor olefin ligands, the coordinated C=C bonds are relatively long, 1.425(5) (C1—C2) and 1.415(4) Å (C3—C4), only slightly shorter than the C=C bond of the single olefin ligand in [Pt(C₂H₄)(PPh₃)₂] (1.434(13) Å)²⁸ and [Pt(C₂H₄)(PCy₃)₂] (1.440(7) Å)³³. The four Pt—C bonds are nearly identical, as they cluster in the very narrow range 2.115(3)-2.121(2) Å. They are slightly longer than in the above PPh₃ derivative (2.106(8) and 2.116(9) Å)²⁸, but somewhat shorter than in the PCy₃ complex analogue (2.137(1) Å).³³ Comparison of the metric parameters found for **1** with

³³ H. C. Clarkt, G. Ferguson, M. J. Hampden-Smith, B. Kaitner, H. Ruegger, *Polyhedron* **1988**, 7, 1349-1353.

those reported for $[\text{Pt}(\text{C}_2\text{H}_4)(\text{C}_2\text{F}_4)(\text{PCy}_3)]^{30\text{b}}$ is also appropriate. The Pt—P bond length of 2.2866(6) Å in **1** is significantly shorter than in the mixed $\text{C}_2\text{H}_4/\text{C}_2\text{F}_4$ complex, viz.: 2.343(2) Å. In the latter complex the coordinated $\text{CH}_2=\text{CH}_2$ and $\text{CF}_2=\text{CF}_2$ bonds have lengths of 1.35(2) and 1.45(2) Å, respectively, these differences reflecting the higher π donor and π^* acceptor capacity of C_2F_4 relative to C_2H_4 . Accordingly, the Pt—C(F) separations (*ca.* 2.03 Å) are shorter than the Pt—C(H) ones of *ca.* 2.17 Å.^{30b} Back bonding to the π^* orbital of the C_2H_4 becomes reduced by the presence of the better π -acceptor C_2F_4 and this variation is also manifested in the reduction in the barrier to C_2H_4 rotation by approximately 3 $\text{kcal}\cdot\text{mol}^{-1}$ relative to the bis(ethylene) analogue $[\text{Pt}(\text{C}_2\text{H}_4)_2(\text{PCy}_3)]$ (9.8 vs. 12.8 $\text{kcal}\cdot\text{mol}^{-1}$).^{30a} In complex **1** back donation from the Pt(0) centre is divided between two C_2H_4 ligands, leading therefore, as already discussed, to shorter Pt—C(H) bonds (*ca.* 2.12 Å), longer C=C bonds (*ca.* 1.42 Å) and higher rotation barriers (13.4 $\text{kcal}\cdot\text{mol}^{-1}$).

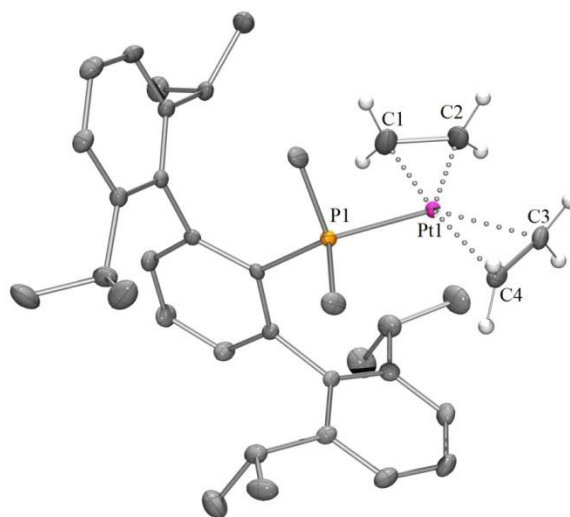


Figure 13. ORTEP view of the complex **1**; selected hydrogen atoms are excluded for clarity and thermal ellipsoids are set to 50% level probability. Selected bond distances(Å) and angles(°): Pt1-P1 2.2866(6), Pt1-C1 2.117(4), Pt1-C2 2.115(3), Pt1-C3 2.121(2), Pt1-C4 2.115(3), C1-C2 1.425(5), C3-C4 1.415(4), P1-Pt1-centroid(C1-C2) 113.8(1), P1-Pt1-centroid(C3-C4) 113.22(8), centroid(C1-C2)-Pt1-centroid(C3-C4) 132.7(1).

The X-ray of $[\text{Pt}(\text{CH}_2=\text{CH}^t\text{Bu})(\text{PMe}_2\text{Ar}^{\text{Dipp}_2})]$ (**3**) is presented in Figure 14. All $\text{Pt}(0)\text{L}_2$ compounds listed in the Cambridge Structural Database (CSD) contain phosphine or NHC ligands.³⁴ Furthermore, only a handful of transition metal complexes of *tert*-butylethylene have been characterised by X-ray crystallography.³⁵ They include a $\text{Pt}(\text{II})$ derivative^{35d} but no $\text{Pt}(0)$ species. The X-ray data collected for single crystals of **3** revealed the presence of two diastereomers in the crystal lattice. Figure 14 contains data for the molecules arbitrarily designated as **A** and **B**. Molecules **A** approach a two-coordinate geometry with a $\text{Pt}-\text{P}$ bond that is shorter than in the trigonal planar complex **1** (2.193(2) vs. 2.2866(6) Å) and it is in the lower end of the range of the $\text{Pt}-\text{PR}_3$ distances for compounds listed in the CSD.³⁴ Olefin coordination in **3** is characterised by nearly identical $\text{Pt}-\text{C}$ bonds (*ca.* 2.08 Å, *av.* value), once more shorter than in **1** (roughly 2.12 Å) and by a $\text{C}-\text{C}$ bond of length 1.40(1) Å, comparable to that found in other $\text{CH}_2=\text{CH}^t\text{Bu}$ transition metal complexes.³⁵ However, at variance with the linearity expected for a two coordinated complex, the angle subtended by the phosphorus atom and olefin centroid at platinum is of nearly 142°. This deviation is caused by the existence of a weak $\text{Pt}\cdots\text{C}_{\text{arene}}$ interaction with C27 (2.314(4) Å) that counterbalances in part the coordinative and electronic unsaturation of the $\text{Pt}(0)$ centre. Since the next shortest platinum contact (to C32) spans 2.627(6) Å, the $\text{Pt}\cdots\text{C}_{\text{arene}}$ electronic interaction can be defined as η^1 .³⁶ In molecules **B**, the prochiral olefin binds to platinum through the other face. $\text{Pt}-\text{C}$ distances within the $\text{Pt}-\text{C}_2\text{H}_3^t\text{Bu}$ linkage are nonetheless similar,

³⁴ Cambridge Structural Database (Version 5.36). F. Allen, O. Kennard, *Chemical Design Automation News* **1993**, 8, 31-37.

³⁵ a) E. Molinos, S. K. Brayshaw, G. Kociok-Kohn, A. S. Weller, *Dalton Trans.* **2007**, 4829-4844; b) S. Gatard, C. Guo, B. M. Foxman, O. V. Ozerov, *Organometallics* **2007**, 26, 6066-6075; c) D. L. Coombs, S. Aldridge, A. Rossin, C. Jones, D. J. Willock, *Organometallics* **2004**, 23, 2911-2926; d) U. Fekl, W. Kaminsky, K. I. Goldberg, *J. Am. Chem. Soc.* **2003**, 125, 15286-15287.

³⁶ A. Falceto, E. Carmona, S. Alvarez, *Organometallics* **2014**, 33, 6660-6668.

but the coordination of the phosphine becomes noticeably different. Not only the Pt1—P1 bond distance becomes longer (2.276(2) vs. 2.193(2) Å) but, moreover, one of the lateral aryl rings becomes η^2 -coordinated through C27 (2.257(4) Å) and C32 (2.2893(1) Å).

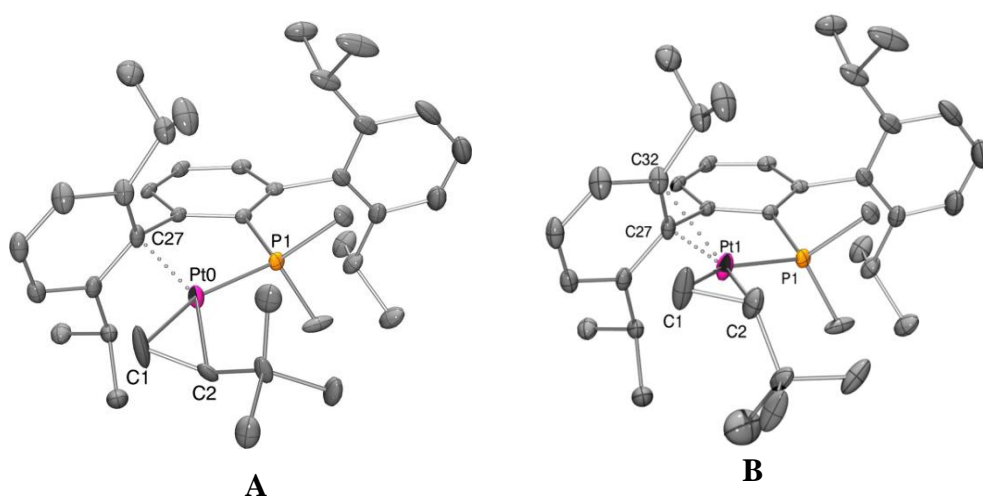
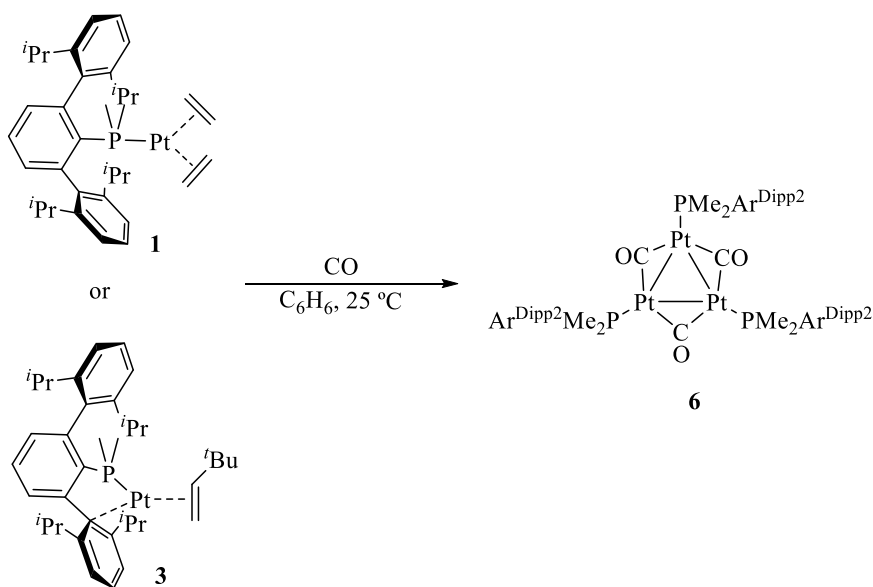


Figure 14. ORTEP view of the solid structure of **3** (molecule **A** left, molecule **B** right) with ellipsoids drawn at the 30% probability level. Selected bond distances [Å] and angles [°]: Molecule A: Pt0—P1 2.193(2), Pt0—C1 2.10(1), Pt0—C2 2.063(8), Pt0—C27 2.314(4), C1—C2 1.40(1); P1—Pt0-centroid(C1—C2) 141.6, C27—Pt0-centroid(C1—C2) 135.1, C27—Pt0—P1 83.1(1); Molecule B: Pt1—P1 2.276(2), Pt1—C1 2.11(1), Pt1—C2 2.14(1), Pt1—C27 2.257(4), Pt1—C32 2.2893(1), C1—C2 1.40(1); P1—Pt1-centroid(C1—C2) 134.9, centroid(C27—C32)—Pt1—centroid(C1—C2) 129.9, centroid(C27—C32)—Pt1—P1 92.7.

II.3.2. Reactivity of Pt(0)-olefin complexes

II.3.2.1. Reactivity towards CO

Aiming to explore the possibility of substituting the weak Pt-arene interaction described in the previous section with a different neutral Lewis base, we essayed the reactivity of complexes **1** and **3** towards carbon monoxide. Although Pt(P[^]P)(olefin) complexes were reported to undergo reversible CO/alkene exchange,²³ *in situ* generation of the coordinatively unsaturated Pt(PMe₂Ar^{Dipp2}) fragment was expected to lead instead to a trinuclear Pt₃(μ-CO)₃(PMe₂Ar^{Dipp2})₃ 42-electron cluster.³⁷ In accordance with these expectations, bubbling CO into a benzene solution of complexes **1** or **3** at 25 °C, rapidly resulted in the formation of an orange precipitate that was identified by spectroscopy and X-ray crystallography as the triplatinum cluster **6** represented in Scheme 12.



Scheme 12. Synthesis of the cluster **6**.

³⁷ a) E. Poverenov, M. Gandelman, L. J. W. Shimon, H. Rozenberg, Y. Ben-David, D. Milstein, *Organometallics* **2005**, 24, 1082-1090; b) K. H. Dahmen, A. Moor, R. Naegeli, L. M. Venanzi, *Inorg. Chem.* **1991**, 30, 4285-4286; c) C. M. Lukehart, G. P. Torrence, *Inorg. Chim. Acta* **1977**, 22, 131-134.

In agreement with the proposed C_{3h} molecular symmetry, only one IR band was recorded in CH_2Cl_2 at 1780 cm^{-1} due to the stretching vibration of the bridging CO ligands, which are also responsible for a weak ^{13}C NMR resonance at 182.6 ppm. Owing to fast rotation along the P-Pt bond, this complex shows fluxional behavior in dichloromethane solution, as observed by the variable temperature ^1H NMR study showed in Figure 16A. The most characteristic NMR feature of **4** is its intricate $^{31}\text{P}\{^1\text{H}\}$ NMR spectrum (Figure 16B) that exhibits the expected complexity inherent to the mixture of isotopologues (Figure 15) foreseen for this formulation, as accurately described many years ago by Moor, Pregosin, and Venanzi³⁸.

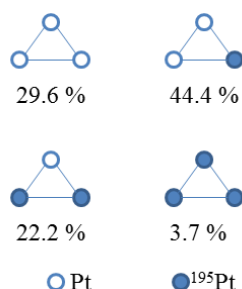


Figure 15: Possible isotopologues for a Pt_3 cluster with their relative abundances.

As commented above the molecular structure of this cluster was ascertained by X-ray diffraction studies. As shown in Figure 17, the cluster exhibits a C_{3h} symmetry. Pt and P atoms, and CO ligands lie the same plane. The Pt-Pt distance in this structure is shorter than the sum of Van der Waals atomic radii, due to the covalent bond between them (2.6462 (2) vs. 3.50 Å). Because of the π -back donation from the Pt nuclei to the CO ligand, the C-O bond distance is longer than the analogous bond length in the free molecule (1.153 vs. 1.128 Å). As the CO acts as a μ^2 bridging

³⁸ A. Moor, P. S. Pregosin, L. M. Venanzi, *Inorg. Chim. Acta* **1981**, 48, 153-157.

ligand, and the existence of a Pt-Pt bond is evidenced, the phosphine shows a κ^1 -P coordination mode.

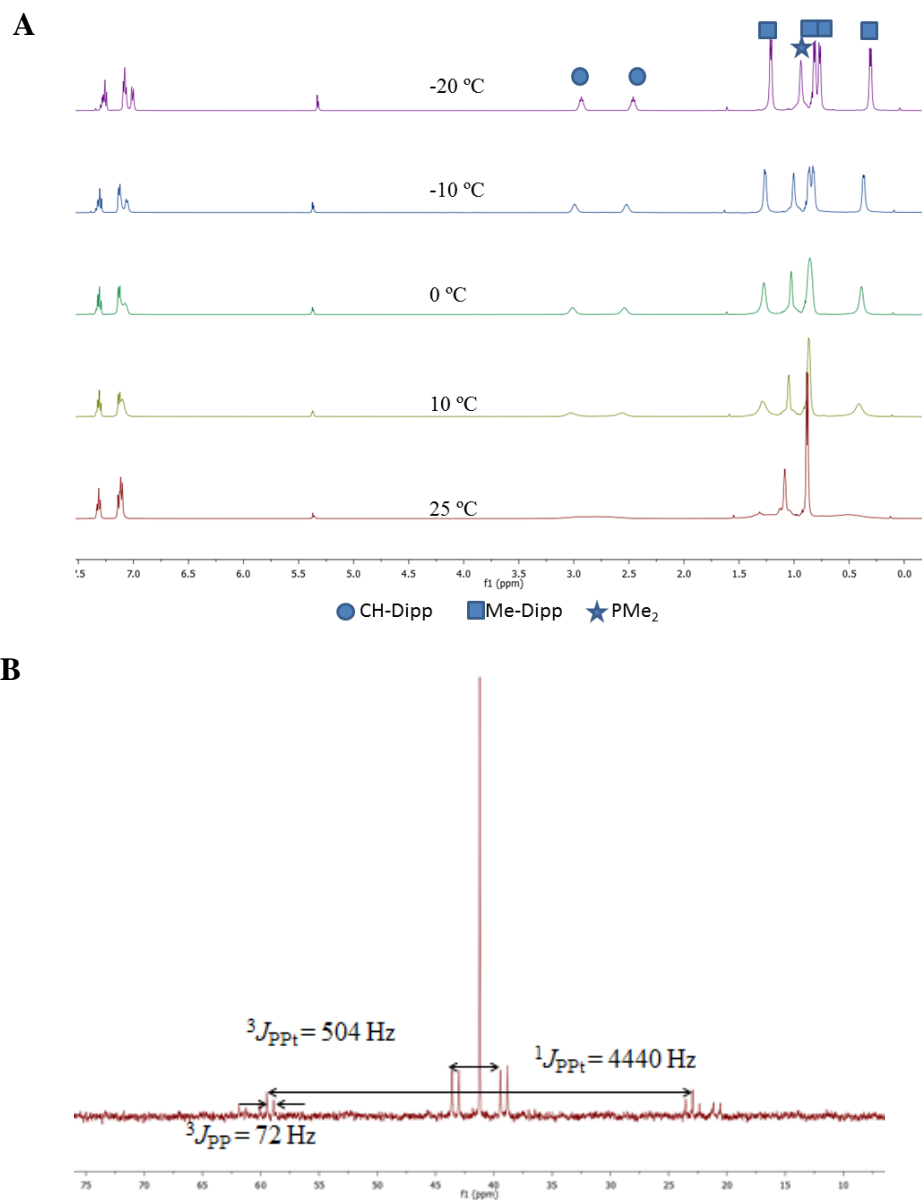


Figure 16. Spectroscopic data of cluster **6** (top: variable temperature ^1H NMR spectra, 500 MHz; bottom: $^{31}\text{P}\{^1\text{H}\}$ NMR spectrum, CH_2Cl_2 , 25 °C).

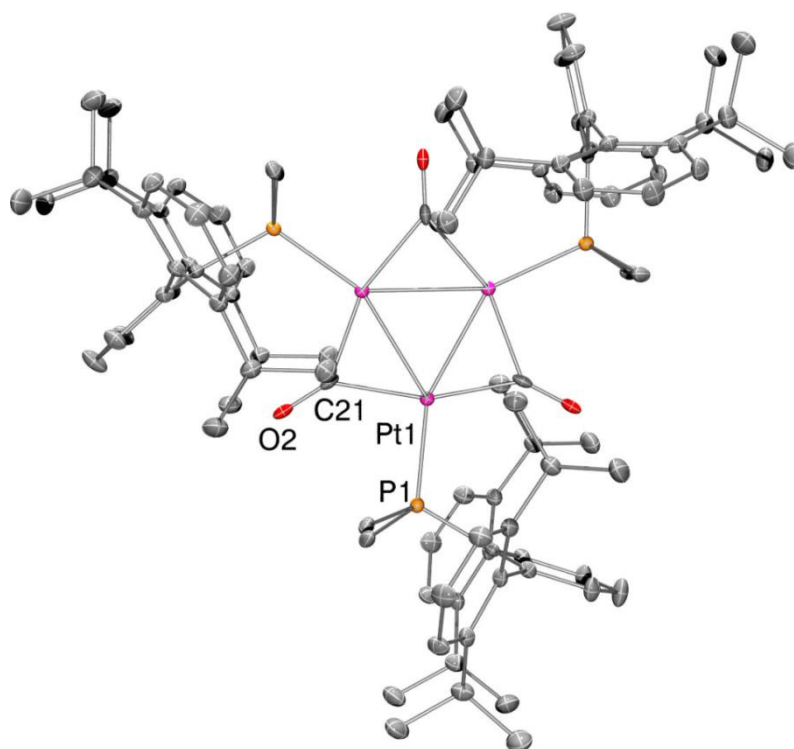
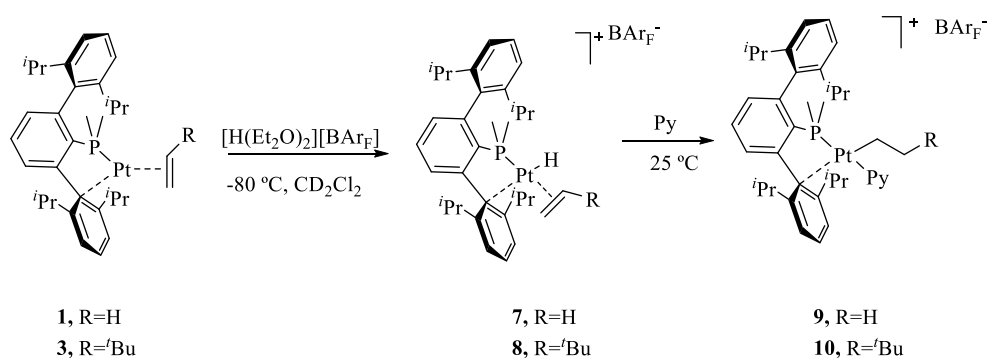


Figure 17. ORTEP view of cluster **6**; hydrogen atoms are excluded for clarity and thermal ellipsoids are set at 30 % level of probability. Selected bond distances (Å) and angles (°): Pt1–P1 2.258(1), Pt1–C21 2.076(4), Pt1–C21' 2.036(4), Pt1–Pt1' 2.6462(2), C21–Pt1–Pt1' 109.3(1), C21–Pt1–Pt1'' 49.3(1), C21–Pt1–P1 94.4(1), C21'–Pt1–P1 105.7(1), Pt1'–Pt1–Pt1'' 60.0.

II.3.2.2. Reactivity towards protonation

Protonation of complexes **1** and **3** with equimolar amounts of $[\text{H}(\text{Et}_2\text{O})_2][\text{BAr}_\text{F}]$ ($\text{BAr}_\text{F} = [\text{B}(3,5\text{-(CF}_3)_2\text{C}_6\text{H}_3)_4]$) were studied. These investigations were carried out monitoring the evolution of the reactions by ^1H and ^{31}P NMR spectroscopy from low ($-80\text{ }^\circ\text{C}$) to room temperature (Scheme 13).



Scheme 13. Protonation of complexes **1** and **3**.

As observed by ^1H NMR at low temperature, the proton adds to the Pt(0) centre forming a hydride-alkene Pt(II) intermediate, **7** or **8**, which is stable only at low temperature. The most characteristic NMR feature of this intermediates is its highly upfield hydride resonance at *c.a.* -19 ppm with a large ^1H - ^{195}Pt coupling constant value of 1660 Hz (Figure 18). The ^1H and $^{13}\text{C}\{^1\text{H}\}$ NMR spectra also evidence the asymmetric coordination mode, reasonably of the $\kappa^1\text{-P}$, $\eta^1\text{-C}_{\text{arene}}$ type, of the phosphine ligand. Intermediates **7** and **8** also contain a coordinated alkene molecule, whose characteristic resonances are found in the ^1H NMR spectra at 3.95 ppm and 4.91, and 3.66 ppm for complexes **7** and **8**, respectively.

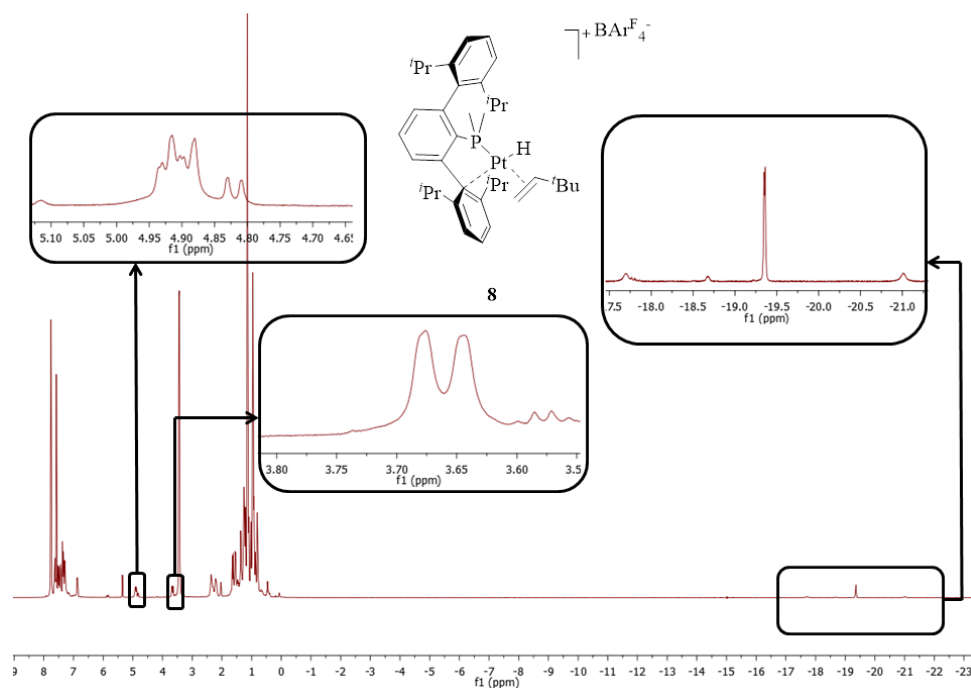


Figure 18. ^1H NMR spectra of complex **8** (500 MHz, CD_2Cl_2 , -50°C).

On warming the reaction mixture to room temperature, the coordinated alkene molecule inserts into the Pt-H bond to form the corresponding three coordinate 14-electron alkyl cationic complexes. Interestingly, the derivative converts regioselectively into the less hindered alkyl species. Both complexes show fluxional behaviour in solution and were characterized by NMR spectroscopy as the corresponding pyridine adducts, **9** and **10** (Scheme 13). The molecular structure of **10** has been determined by X-ray diffraction studies.

Again, NMR studies in solution of the pyridine adducts **9** and **10** are in agreement with the presence of an interaction between the metal centre and the terphenyl fragment which partially compensate the unsaturation of these organometallic species. Although the Pt—CH₂ proton resonances cannot be clearly observed because they overlap with other aliphatic signals, the methyl protons of the ethyl fragment resonates as a

triplet at 0.53 ppm showing a ^1H - ^{195}Pt coupling constant value of 90.1 Hz (Figure 19). In the aromatic area of the spectra, diagnostic signals of coordinated pyridine molecule are detected at 8.52, 7.86 and 7.43 ppm. The carbon atom directly bound to the platinum centre resonates at 10.6 ppm ($^1J_{\text{C}_{\text{Pt}}} = 776$ Hz) for **9** and at 7.0 ppm for **10** in the $^{13}\text{C}\{^1\text{H}\}$ spectra, while ^{13}C nucleus in β position appears at 44.5 ppm ($^2J_{\text{C}_{\text{Pt}}} = 37$ Hz) and 15.3 ppm for **9** and **10**, respectively.

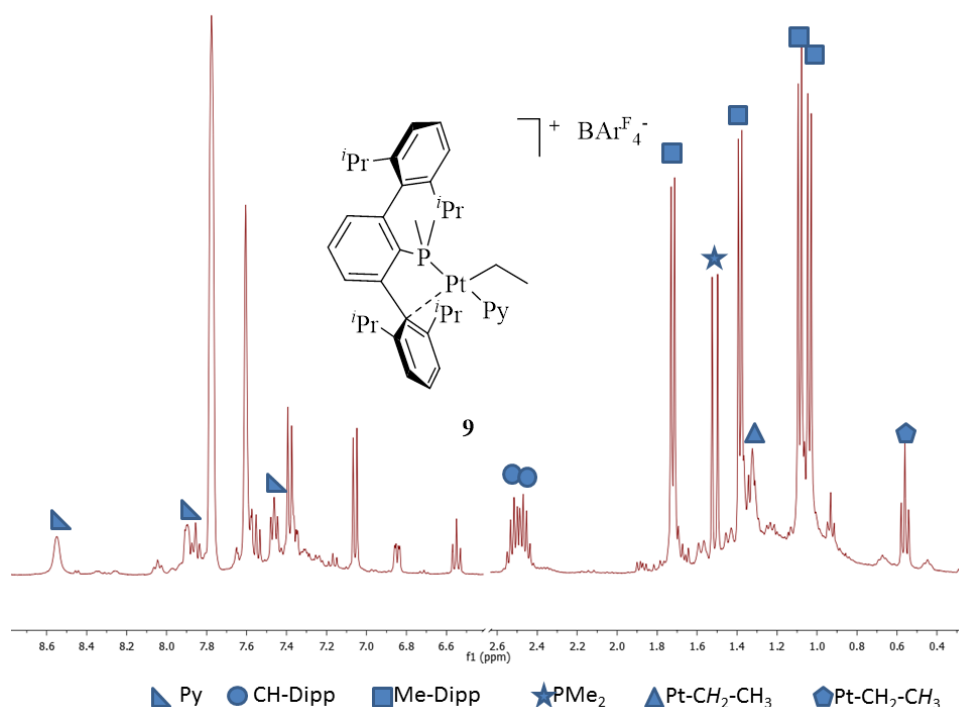


Figure 19. ^1H NMR spectra of adduct **9** (400 MHz, CD_2Cl_2 , 25 °C).

The solid state structure of complex **10** was confirmed by single crystal X-ray diffraction studies. The molecular structure of the cationic complex of **10** is depicted in Figure 20. The square-planar coordination environment of the metal is constituted by two neutral and one anionic ligands, which formally provide 5 electrons to the covalent electron-count. The fourth coordination site is occupied by a weak bonding interaction with the *ipso*-carbon atom of the lateral ring of the terphenyl group with a

Pt-C distance of 2.387(6) Å. The alkyl ligand is in the *trans* position with respect to the secondary interaction, possibly due to the minor *trans* influence comparing with the P atom.

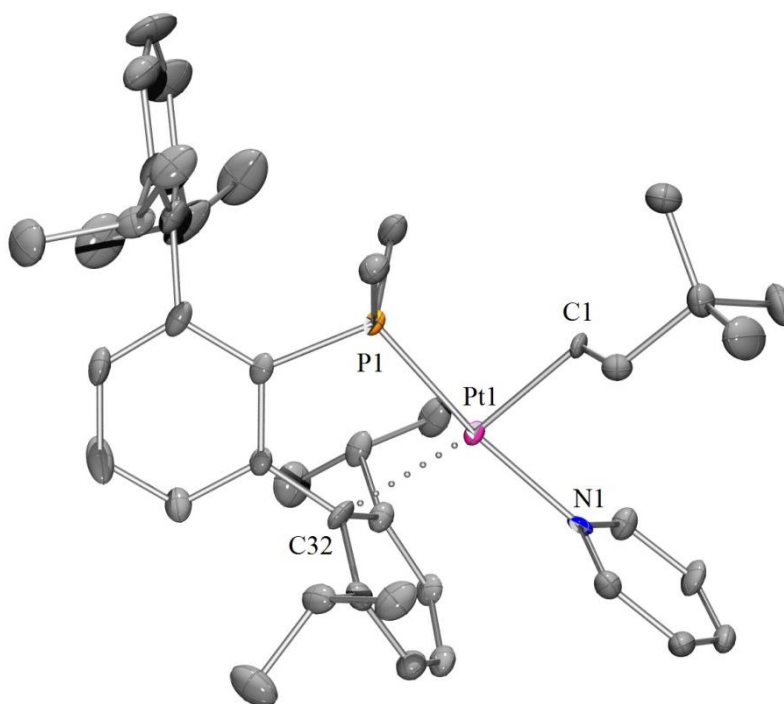
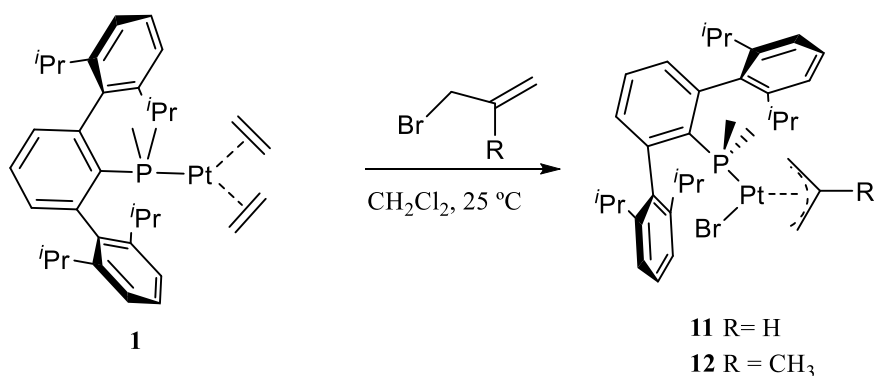


Figure 20. ORTEP view of the cation of complex **10**; hydrogen and BAr_F atoms are excluded for clarity and thermal ellipsoids are set to 50% level probability. Selected bond distances (Å) and angles (°): Pt1-P1 2.214(2), Pt1-C1 2.080(6), Pt1-N1 2.094(7), Pt1-C32 2.387(6), P1-Pt1-C1 89.1(1), C1-Pt1-N1 83.8(2), N1-Pt1-C32 105.4(2), C32-Pt1-P1 81.7(1).

II.3.2.3. Oxidative addition of allylbromides

Treatment of complex **1** with the allylhalides, 3-bromopropene and 3-bromo-2-methylpropene, yielded the neutral η^3 -allyl complexes **11** and **12**, respectively, resulting from the oxidative addition of the Br—C bond to the Pt(0) centre (Scheme 14). Complex **11** was alternatively obtained by treatment of *cis*-[Pt(PMe₂Ar^{Dipp})Cl₂] with allylmagnesiumbromide (Chapter I).



Scheme 14. Synthesis of complexes **11** and **12**.

Both compounds were characterized by microanalysis and NMR spectroscopy. As expected, in these 16-electron complexes the phosphine acts as a $\kappa^1\text{-P}$ ligand. The existence of only two CH isopropyllic resonances in their ^1H NMR spectra is in accordance with a fast rotation of the Pt-P bond or the P-arene bond in a molecule which lacks a symmetry plane, considering the coordination of the allyl ligand is asymmetric with respect to the coordination plane. As mentioned above the coordination of the allyl fragment is η^3 , as evidenced by ^1H and $^{13}\text{C}\{^1\text{H}\}$ resonances showing coupling with ^{195}Pt and ^{31}P nuclei (Figure 21). For complex **11** the $^{13}\text{C}\{^1\text{H}\}$ allylic resonances appear at 108.3, 64.3 and 44.7 ppm showing coupling constants with the ^{195}Pt nucleus from 47 Hz to 259 Hz. The ^{31}P nucleus resonate at *c.a.* -10 ppm with $^1J_{\text{PPt}}$ values of 4370 and 4241 Hz for complexes **11** and **12**, respectively.

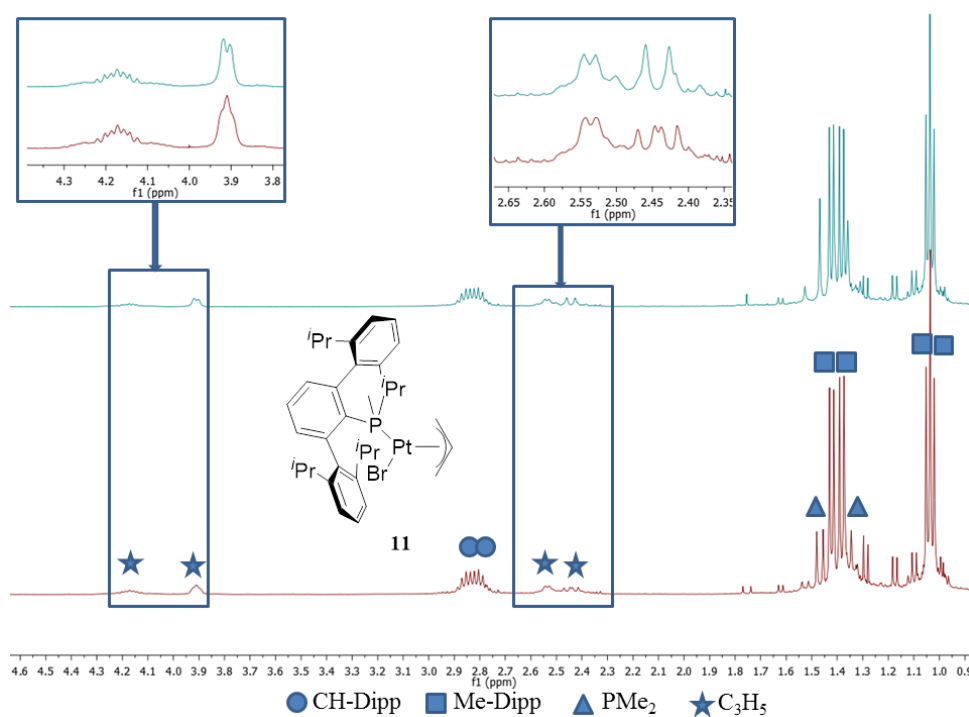
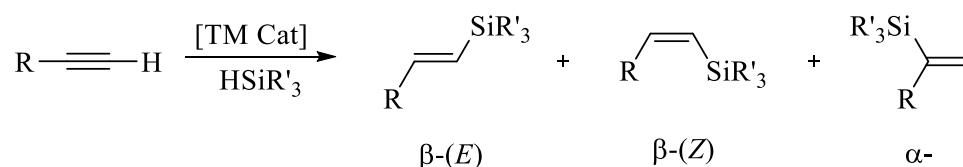


Figure 21. $^1\text{H}\{^{31}\text{P}\}$ NMR spectrum (top) and ^1H NMR spectrum (bottom) of complex **11** (CD_2Cl_2 , 400 MHz, 25 °C).

II.3.3. Catalytic Hydrosilylation of Alkynes

The transition-metal catalysed hydrosilylation of unsaturated C-C bonds provides a simple and atom-economical method for the preparation of organosilicon compounds³⁹. For example, the addition of hydrosilanes to alkynes yields alkenylsilanes, which are versatile reagents in organic synthesis⁴⁰. Also, the hydrosilylation of alkynes is a useful reaction for the synthesis of silicon polymers. The major concern in this transformation is selectivity. Hydrosilylation of terminal alkynes may give a mixture of three isomeric alkenylsilanes, namely, the β -(*E*), β -(*Z*) and α -alkenyl silanes depicted in Scheme 15.



Scheme 15: Catalytic Hydrosilylation of terminal Alkynes.

Classical hydrosilylation Pt catalysts such as Speier (H_2PtCl_6) and Karstedt ($\text{Pt}_2(\text{dvds})_3$, $\text{dvds} = [(\text{H}_2\text{C}=\text{CH})\text{Me}_2\text{Si}]\text{O}$) complexes provide high catalytic activity, although low-to-moderate selectivity towards the β -(*E*) isomer and formation of platinum colloids is commonly observed⁴¹.

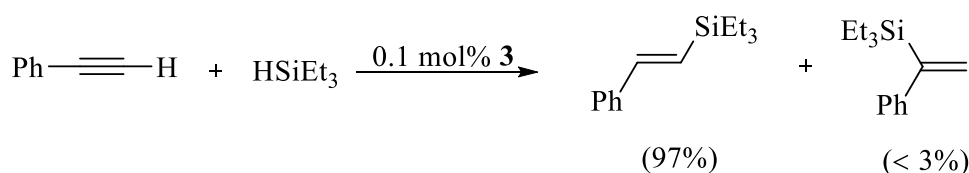
³⁹ a) B. Marciniec, *Hydrosilylation. Advances in Silicon Science.*, Springer, **2009**; b) A. K. Roy, *Adv. Organomet. Chem.* **2008**, *55*, 1-59.

⁴⁰ a) E. Langkopf, D. Schinzer, *Chem. Rev.* **1995**, *95*, 1375-1408; b) I. Fleming, A. Barbero, D. Walter, *Chem. Rev.* **1997**, *97*, 2063-2192; c) T. A. Blumenkopf, L. E. Overman, *Chem. Rev.* **1986**, *86*, 857-873; d) G. R. Jones, Y. Landais, *Tetrahedron* **1996**, *52*, 7599-7662; e) T. Hiyama, E. Shirakawa, *Top. Curr. Chem.* **2002**, *219*, 61-85; f) I. Fleming, J. Dunogues, R. Smithers, *Org. React.* **1989**, *37*, 57-575; g) S. E. Denmark, M. H. Ober, *Aldrichimica Acta* **2003**, *36*, 75-85; h) S. E. Denmark, R. F. Sweis, *Acc. Chem. Res.* **2002**, *35*, 835-846.

⁴¹ a) J. L. Speier, in *Adv. Organomet. Chem.*, Vol. Volume 17 (Eds.: F. G. A. Stone, W. Robert), Academic Press, **1979**, pp. 407-447, ; b) M. P. Doyle, K. G. High, C. L. Nesloney, T. W. Clayton, J. Lin, *Organometallics* **1991**, *10*, 1225-1226; c) L. N. Lewis, K. G. Sy, G. L. Bryant, P. E. Donahue, *Organometallics* **1991**, *10*, 3750-3759.

Following seminal studies by Stone and Tsipis⁴², platinum catalysts based on bulky (highly basic) phosphines⁴³, as well as other 2-electron neutral donors such as *N*-heterocyclic carbenes^{11d,20c,44-45}, were tested in the hydrosilylation of alkynes leading to improved catalytic systems for the regioselective synthesis of *E*-vinylsilanes.

Based on these precedents, we examined the catalytic behaviour of our platinum(0) complex **3** in the addition of hydrosilanes to terminal alkynes (Scheme 16).



Scheme 16: Hydrosilylation of phenylacetylene with HSiEt₃ (see Table 1 for reaction conditions).

Initial catalytic tests were performed using the benchmark reaction of phenylacetylene with triethylsilane (Table 1). Scheme 16 shows that complex **3** attained high selectivity towards the β -(*E*) vinylsilane, accompanied by minor amounts of the α isomer, using 0.5 mol% of catalyst in different solvents (entries 1-3). Higher catalytic activities were

⁴² a) M. Green, J. L. Spencer, F. G. A. Stone, C. A. Tsipis, *J. Chem. Soc., Dalton Trans.* **1977**, 1525-1529; b) C. A. Tsipis, *J. Organomet. Chem.* **1980**, 187, 427-446.

⁴³ a) P. J. Murphy, J. L. Spencer, G. Procter, *Tetrahedron Lett.* **1990**, 31, 1051-1054; b) T. Kyoko, M. Tatsuya, O. Yoshio, H. Tamejiro, *Tetrahedron Lett.* **1993**, 34, 8263-8266; c) S. E. Denmark, Z. Wang, *Org. Lett.* **2001**, 3, 1073-1076; d) K. Itami, K. Mitsudo, A. Nishino, J.-i. Yoshida, *J. Org. Chem.* **2002**, 67, 2645-2652; e) M. Blug, X.-F. Le Goff, N. Mézailles, P. Le Floch, *Organometallics* **2009**, 28, 2360-2362; f) A. Hamze, O. Provot, J.-D. Brion, M. Alami, *Tetrahedron Lett.* **2008**, 49, 2429-2431; g) W. Wu, C.-J. Li, *Chem. Commun.* **2003**, 1668-1669; h) H. Aneetha, W. Wu, J. G. Verkade, *Organometallics* **2005**, 24, 2590-2596.

⁴⁴ a) G. De Bo, G. Berthon-Gelloz, B. Tinant, I. E. Markó, *Organometallics* **2006**, 25, 1881-1890; b) G. F. Silvestri, J. C. Flores, E. de Jesús, *Organometallics* **2012**, 31, 3355-3360.

⁴⁵ S. Dierick, E. Vercruysse, G. Berthon-Gelloz, I. E. Markó, *Chem. Eur. J.* **2015**, 21, 17073-17078.

observed in CD₃CN and C₆D₆, although a better selectivity in the latter solvent was found. Interestingly, at 80 °C catalyst loading could be lowered to 0.1 mol% without erosion of the selectivity, thus allowing for a minimum TOF of 4000 h⁻¹ (entry 4). Also, this catalytic precursor provided a higher (*E*)-selectivity than the more encumbered complex **4** (entry 5). However, use of lower loadings of complex **3** significantly retarded the reaction and gave poorer *E*-selectivity (entry 6). This effect may be ascribed to the formation in the presence of a large excess of alkyne of less selective catalytic species lacking a coordinated phosphine^{11d,20c}. In fact, when the same reaction was carried out in the presence of 1.5 additional equivalents of the terphenyl phosphine the selectivity was reestablished (entry 7). Also, it should be noted that addition of Hg to the reaction did not affect the catalytic activity and selectivity of the catalyst, in agreement with the occurrence of a homogeneously catalyzed process⁴⁶⁻⁴⁷.

⁴⁶ Formation of nanoparticles has previously been observed for the unmodified Karstedt catalyst: a) L. N. Lewis, N. Lewis, *J. Am. Chem. Soc.* **1986**, *108*, 7228-7231; b) L. N. Lewis, *J. Am. Chem. Soc.* **1990**, *112*, 5998-6004; c) L. N. Lewis, R. J. Uriarte, *Organometallics* **1990**, *9*, 621-625; d) L. N. Lewis, R. J. Uriarte, N. Lewis, *J. Catal.* **1991**, *127*, 67-74.

⁴⁷ For selected examples of heterogeneous Pt catalysts: a) M. Chauhan, B. J. Hauck, L. P. Keller, P. Boudjouk, *J. Organomet. Chem.* **2002**, *645*, 1-13; b) F. Alonso, R. Buitrago, Y. Moglie, J. Ruiz-Martínez, A. Sepúlveda-Escribano, M. Yus, *J. Organomet. Chem.* **2011**, *696*, 368-372; c) R. Cano, M. Yus, D. J. Ramón, *ACS Catal.* **2012**, *2*, 1070-1078.

Table 1. Catalytic hydrosilylation of phenylacetylene with Et₃SiH.^a

Entry	Cat. (mol%)	Solvent	T (°C)	Conv. (%)	% <i>E</i> selectivity
1	3 (0.5)	CD ₂ Cl ₂	50	78 (2 h)	98
2 ^b	3 (0.1)	CD ₃ CN	50	>99 (0.5 h)	84
3	3 (0.5)	C ₆ D ₆	50	98 (2 h)	98
4	3 (0.1)	C ₆ D ₆	80	>99 (0.25 h)	97
5	4 (0.1)	C ₆ D ₆	80	>99 (1 h)	88
6	3 (0.02)	C ₆ D ₆	80	>99 (4.5 h)	82
7 ^c	3 (0.02)	C ₆ D ₆	80	42 (45 h)	98

^aReactions were carried out using 1.35 mmol of phenylacetylene, 1.35 mmol of Et₃SiH and 0.07 mmol of hexamethylbenzene as internal standard. [Phenylacetylene] = 2.7 M. Conversion and selectivity were determined by ¹H NMR spectroscopy. Only formation of *β*-(*E*) and *α* isomers were observed. ^bConversion and selectivity were determined by GC-MS. ^cIn the presence of 1.5 equivalents of terphenylphosphine with respect to complex **3**.

Next, other hydrosilanes were studied in the hydrosilylation of phenylacetylene under the previous reaction conditions (Table 2). For example, complex **3** completed the reaction of phenylacetylene with HSiPhMe₂ in less than 15 min with an *E*-selectivity of 91% (entry 1). Also, the reaction of a dihydrosilane, H₂SiPh₂, with phenylacetylene in a 1:1 ratio produced the corresponding *E*-monovinylsilane with a notable level of selectivity, whereas the use of two equivalents of alkyne yielded the (*E,E*)-divinylsilane with 80% selectivity (entries 2 and 3). Since alkenylalcoxy-silanes and -siloxanes are interesting substrates for Hiyama C-C couplings,^{40g-h} the catalytic activity of **3** in the hydrosilylation with HSi(OEt)₃ and HSi(OTMS)₃ was studied (entries 4 and 5). These silicon derivatives added to phenylacetylene to yield the *β*-(*E*)-isomers with 83

and 77% selectivity respectively, although a lower catalytic activity was found. Finally, the reaction of HSiCl_3 with phenylacetylene was tested, providing the corresponding β -(*E*)-vinylsilane with 88% selectivity (entry 6).

Table 2. Catalytic hydrosilylation of phenylacetylene with silanes catalysed by **3**.^a

Entry	Silane	Conv. (%)	% <i>E</i> selectivity
1	HSiPhMe_2	>99 (0.5 h)	91
2	H_2SiPh_2	>99 (0.5 h)	70 ^[b]
3	H_2SiPh_2	>99 (1.25 h)	80 ^[c]
4	HSi(OEt)_3	>99 (5 h)	83
5	HSi(OTMS)_3	87 (22 h)	77
6	HSiCl_3	>99 (4 h)	88

^a Reactions were carried out at 80 °C in C_6D_6 using 1.35 mmol of phenylacetylene, 1.35 mmol of silane, 0.07 mmol of hexamethylbenzene (internal standard) and 0.1 mol% of **3**. [Phenylacetylene] = 2.7 M. Conversion and selectivity were determined by ^1H NMR spectroscopy. Only formation of β -(*E*) and α isomers were observed. ^b Referred to the silane:alkyne 1:1 addition product. ^c A silane/alkyne = 2 ratio was employed. *E* selectivity refers to the (*E,E*)-divinylsilane.

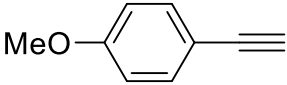
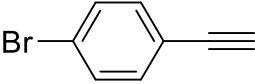
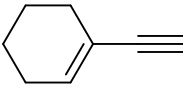
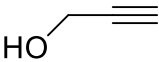
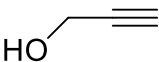
As an additional assay, a series of alkynes were hydrosilylated with HSiEt_3 in the presence of complex **3** (Table 3). In the case of arylacetylenes, a significant dependence of the catalytic activity with the electronic effects of the para-substituents was evidenced (entries 1 and 2). Thus, the reaction rate of the (*p*-bromophenyl)acetylene was significantly slower than that of the phenyl- and (*p*-methoxyphenyl)acetylene. On the other hand, hydrosilylation of alkyl-substituted terminal alkynes was accomplished with high activity and *E*-selectivity (entries 3 and 4), whereas a notable selectivity was obtained in the addition of HSiEt_3 to

trimethylsilylacetylene (entry 5). The hydrosilylation of alkynes containing a additional C=C bond was also examined (entry 6). Selective Si-H addition to the acetylenic bond took place leaving the C=C functionality untouched. Finally, complex **3** was also active in the hydrosilylation of ethyl propiolate, although a reduced activity was found. In addition, the α -isomer was formed predominantly, probably as a consequence of the strongly electron-withdrawing character of the carboxylate group (entry 7)^{42b,20c,43a,48}. Finally, at variance with previous reports with other Pt catalysts, the hydrosilylation of propargyl alcohol with Et₃SiH did not proceed (entry 8).^{43a,43h} Alternatively, use of a more reactive silane, HSiMe₂Ph, yielded the corresponding α - and β -(*E*)-vinylsilanes although with poor regioselectivity (entry 9).

In summary, complex **3** is an efficient catalyst for the hydrosilylation of a broad range of alkynes, standing among the most effective Pt(0) systems based on bulky NHC and phosphorus ligands for alkyne hydrosilylation.

⁴⁸ For other examples of electronic effects on selectivity: D. A. Rooke, E. M. Ferreira, *Angew. Chem. Int. Ed.* **2012**, *51*, 3225-3230., and references therein.

Table 3. Catalytic hydrosilylation of acetylenes with Et₃SiH catalysed by **3**.^a

Entry	Alkyne	Conv. (%)	% <i>E</i> selectivity
1		>99 (15 min)	96
2		>99 (4 h)	80
3	1-Hexyne	>99 (15 min)	95
4	<i>t</i> Bu—C≡C—	>99 (15 min)	98
5	Me ₃ Si—C≡C—	>99 (2 h)	78
6		>99 (15 min)	92
7	EtO ₂ C—C≡C—	>99 (23 h)	44
8		0 (22 h)	-
9 ^b		>99 (2.5 h)	62

^a Reactions were carried out at 80 °C in C₆D₆ using 1.35 mmol of alkyne, 1.35 mmol of Et₃SiH, 0.07 mmol of hexamethylbenzene (internal standard) and 0.1 mol% of **3**. [alkyne]= 2.7 M. Conversion and selectivity were determined by ¹H NMR. Only formation of *E* and α isomers were observed. ^b HSiMe₂Ph was used.

II.4. EXPERIMENTAL SECTION

II.4.1. General Considerations

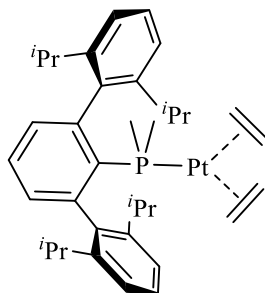
All operations were performed under a nitrogen atmosphere using standard Schlenk techniques, employing dry solvents and glassware. Microanalyses were performed by the Microanalytical Service of the Instituto de Investigaciones Químicas. Infrared spectra were recorded on a Bruker Vector 22 spectrometer.

The NMR instruments used were Bruker DRX-500, DRX-400, Avance^{III}-400/R and DRX-300 spectrometers. Spectra were referenced to external SiMe₄ (δ : 0 ppm) using residual proton solvent peaks as internal standards (¹H NMR experiments), or the characteristic resonances of the solvent nuclei (¹³C NMR experiments), while ³¹P was referenced to external H₃PO₄. Spectral assignments were made by routine one- and two-dimensional NMR experiments (¹H, ¹H{³¹P}, ¹³C, ¹³C{¹H}, COSY, NOESY, HSQC, and HMBC).

II.4.2. Synthesis and Characterisation of the New Complexes Obtained

Synthesis and Characterisation of $[\text{Pt}(\text{PMe}_2\text{Ar}^{\text{Dipp}_2})(\text{C}_2\text{H}_4)_2]$, **1**

Complex $[\text{Pt}(\text{PMe}_2\text{Ar}^{\text{Dipp}_2})\text{Cl}_2]$ (**6** from Chapter I) (40 mg, 0.06 mmol) was dissolved in THF (5 mL) and the solution treated with an excess of Zn powder (50 mg, 0.76 mmol) at room temperature. The resulting suspension was kept under C_2H_4 atmosphere (1.5 atm) overnight and filtered. After evaporation of the volatiles under reduced pressure, the product was obtained as a dark brown solid, which was purified by crystallization from a saturated pentane solution at -23°C . Yield: 25 mg (64%). The product was obtained in a *ca.* 1:1 mixture of **1** and **1'**.



Anal. Calc. for $\text{C}_{36}\text{H}_{51}\text{PPt}$: C, 60.9; H, 7.2. **Found:** C, 61.2; H, 7.6 %.

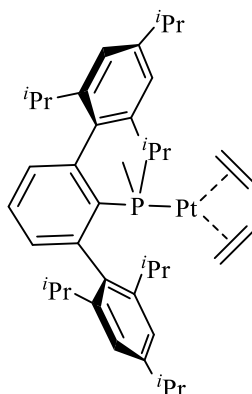
^1H NMR (400 MHz, 25°C , C_6D_6): δ 7.24 (t, 2 H, $^3J_{\text{HH}} = 7.5$ Hz, *p*-Dipp), 7.07 (d, 4 H, $^3J_{\text{HH}} = 7.3$ Hz, *m*-Dipp), 7.00 – 7.05 (m, 2 H, *m*- C_6H_3), 6.96 (t, 1 H, $^3J_{\text{HH}} = 7.7$ Hz, *p*- C_6H_3), 2.84 (sept, 4 H, $^3J_{\text{HH}} = 7.0$ Hz, CH-Dipp), 2.34 (br s, 8 H, $^2J_{\text{HPt}} = 53.1$ Hz, C_2H_4), 1.32 (d, 6 H, $^2J_{\text{HP}} = 7.7$ Hz, $^3J_{\text{HPt}} = 32.2$ Hz, PMe_2), 1.27 (d, 12 H, $^3J_{\text{HH}} = 6.6$ Hz, Me-Dipp), 0.95 (d, 12H, $^3J_{\text{HH}} = 6.6$ Hz, Me-Dipp) ppm.

$^{13}\text{C}\{^1\text{H}\}$ NMR (100.6 MHz, 25°C , C_6D_6): δ 147.1 (s, *o*-Dipp), 143.5 (d, $^2J_{\text{CP}} = 9$ Hz, $^3J_{\text{CPt}} = 13$ Hz, *o*- C_6H_3), 140.9 (d, $^3J_{\text{CP}} = 3$ Hz, C_{ipso} -Dipp), 135.1 (d, $^1J_{\text{CP}} = 24$ Hz, $^2J_{\text{CPt}} = 36$ Hz, C_{ipso} - C_6H_3), 133.6 (s, $^3J_{\text{CP}} = 6$ Hz, *m*- C_6H_3), 128.9 (s, *p*-Dipp), 126.6 (d, $^4J_{\text{CP}} = 1$ Hz, *p*- C_6H_3), 123.0 (s, *m*-Dipp), 38.5 (br s, $^1J_{\text{CPt}} = 153$ Hz, C_2H_4), 31.3 (s, CH-Dipp), 25.9 (s, Me-Dipp), 22.8 (s, Me-Dipp), 20.6 (d, $^1J_{\text{CP}} = 30$ Hz, $^2J_{\text{CPt}} = 40$ Hz, PMe_2) ppm.

$^{31}\text{P}\{^1\text{H}\}$ NMR (161.9 MHz, 25°C , C_6D_6): δ -16.2 (s, $^1J_{\text{PPt}} = 3265$ Hz) ppm.

Synthesis and Characterisation of $[\text{Pt}(\text{C}_2\text{H}_4)_2(\text{PMe}_2\text{Ar}^{\text{Tipp}_2})]$, **2**

Complex *cis*- $[\text{PtH}(\text{SiEt}_3)(\text{PMe}_2\text{Ar}^{\text{Tipp}_2})]$ (**14** from Chapter I) (0.158 mg, 0.18 mmol) was dissolved in C_6H_6 (5 mL) in a pressure-resistant flask. The reaction system was charged with an ethylene pressure of 2 bar and stirred overnight. All volatiles were removed under vacuum giving product and its monoalkene derivative in a *ca.*1:1 mixture as a dark brown solid. Yield: 67 mg (46%).



Anal. Calc. for $\text{C}_{42}\text{H}_{63}\text{PPt}$: C, 63.5; H, 8.0. **Found:** C, 63.3; H, 8.3 %.

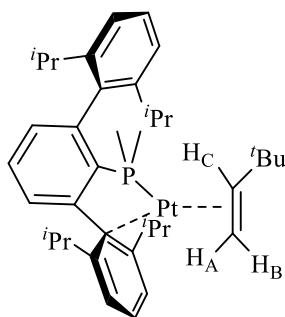
^1H NMR (400 MHz, CD_2Cl_2 , 25 °C): δ 7.30 (td, 1 H, $^3J_{\text{HH}} = 7.6$ Hz, $^5J_{\text{HP}} = 1.1$ Hz, *p*- C_6H_3), 7.08 (dd, 2 H, $^3J_{\text{HH}} = 7.6$ Hz, $^4J_{\text{HP}} = 2.6$ Hz, *m*- C_6H_3), 6.98 (s, 4 H, *m*-Tipp), 2.90 (sept, 2 H, $^3J_{\text{HH}} = 6.9$ Hz, *p*-CH-Tipp), 2.67 (sept, 4 H, $^3J_{\text{HH}} = 6.8$ Hz, *o*-CH-Tipp), 1.87 (s br, 8 H, C_2H_4), 1.28 (d, 12 H, $^3J_{\text{HH}} = 6.9$ Hz, *o*- CH_3 -Tipp), 1.26 (d, 12 H, $^3J_{\text{HH}} = 6.8$ Hz, *p*-Me-Tipp), 1.21 (d, 6 H, $^3J_{\text{HH}} = 7.8$ Hz, PMe_2), 0.97 (d, 12 H, $^3J_{\text{HH}} = 6.7$ Hz, *o*-Me-Tipp) ppm.

$^{13}\text{C}\{^1\text{H}\}$ NMR (96.6 MHz, 25 °C, CD_2Cl_2): δ 149.3 (s, *p*-Tipp), 147.2 (s, *o*-Tipp), 143.8 (d, $^2J_{\text{CP}} = 9$ Hz, *o*- C_6H_3), 138.6 (s, C_{ipso} -Tipp), 133.9 (d, $^3J_{\text{CP}} = 6$ Hz, *m*- C_6H_3), 126.9 (s, *p*- C_6H_3), 121.0 (s, *m*-Tipp), 38.0 (br, C_2H_4), 35.0 (s, *p*-CH-Tipp), 31.5 (s, *o*-CH-Tipp), 26.1 (s, *o*-Me-Tipp), 24.6 (s, *o*-Me-Tipp), 22.9 (s, *p*-Me-Tipp), 20.6 (d, $^1J_{\text{CP}} = 30$ Hz, PMe_2) ppm.

$^{31}\text{P}\{^1\text{H}\}$ NMR (161.9 MHz, 25 °C, CD_2Cl_2) δ : -17.3 (s, $^1J_{\text{PPt}} = 3260$ Hz) ppm.

Synthesis and Characterisation of $[\text{Pt}(\text{CH}_2=\text{CH}^i\text{Bu})(\text{PMe}_2\text{Ar}^{\text{Dipp}_2})]$, **3**

To a THF (5 mL) solution of complex $[\text{Pt}(\text{PMe}_2\text{Ar}^{\text{Dipp}_2})\text{Cl}_2]$ (**6** from Chapter I) (100 mg, 0.14 mmol) Zn powder (0.090 g, 1.4 mmol) and 3,3-dimethyl-1-butene (0.27 mL, 2.07 mmol) were added at room temperature. The reaction mixture was stirred for 48 hours. The resulting suspension was filtered and all volatiles were removed under vacuum. The dark brown residue was washed with pentane at -80°C . For further purification the product can be crystallized from a saturated pentane solution at -23°C . Yield: 64 mg (62%).



Anal. Calc. for $\text{C}_{38}\text{H}_{55}\text{PPt}$: C, 61.9; H, 7.5. **Found:** C, 61.5; H, 7.8.

^1H NMR (400 MHz, 25°C , C_6D_6): δ 7.23 (br, 2 H, H_{ar}), 7.11 (br, 4 H, H_{ar}), 6.95 (br, 3 H, H_{ar}), 3.92 (ddd, 1 H, $^3J_{\text{HH}} = 10$ Hz, $^3J_{\text{HH}} = 12$ Hz, $^3J_{\text{HP}} = 3.3$ Hz, $^2J_{\text{HPt}} = 110.8$ Hz, H_C), 2.39 (br, 4 H, CH-Dipp), 1.45 (d, 3 H, $^2J_{\text{HP}} = 7.1$ Hz, $^3J_{\text{HPt}} = 49.8$ Hz, PMe), 1.38 (d, 3 H, $^2J_{\text{HP}} = 7.6$ Hz, $^3J_{\text{HPt}} = 57.6$ Hz, PMe), 1.30 (br, 7 H, Me-Dipp and H_A), 1.22 (d, 6 H, $^3J_{\text{HH}} = 6.8$ Hz, Me-Dipp), 1.12 (s, 9 H, ^iBu), 0.96 (d, 6 H, $^3J_{\text{HH}} = 6.7$ Hz, Me-Dipp), 0.91 (d, 6 H, $^3J_{\text{HH}} = 6.7$ Hz, Me-Dipp), 0.63 (t, 1 H, $^3J_{\text{HH}} = 9.7$ Hz, $^3J_{\text{HH}} = 9.0$ Hz, $^2J_{\text{HPt}} = 18.4$ Hz, H_B) ppm.

^1H NMR (400 MHz, -40°C , CD_2Cl_2): δ 7.38 (t, 1 H, $^3J_{\text{HH}} = 7.8$ Hz, p -Dipp), 7.32 (t, 1 H, $^3J_{\text{HH}} = 7.4$ Hz, p - C_6H_3), 7.27 (d, 1 H, $^3J_{\text{HH}} = 7.9$ Hz, m -Dipp c), 7.22 (d, 2 H, $^3J_{\text{HH}} = 7.3$ Hz, m -Dipp), 7.07 (d, 1 H, $^3J_{\text{HH}} = 7.4$ Hz, m - C_6H_3), 6.99 (d, 1 H, $^3J_{\text{HH}} = 7.7$ Hz, m - C_6H_3), 6.94 (d, 1 H, $^3J_{\text{HH}} = 7.5$ Hz, m -Dipp c), 6.71 (t, 1 H, $^3J_{\text{HH}} = 7.6$ Hz, p -Dipp c), 3.31 (td, 1 H, $^3J_{\text{HH}} = 10.6$ Hz, $^3J_{\text{HP}} = 3.0$ Hz, $^2J_{\text{HP}} = 109.1$ Hz, H_C), 2.41 (sept, 1 H, $^3J_{\text{HH}} = 6.5$ Hz, CH-Dipp), 2.40 (sept, 1 H, $^3J_{\text{HH}} = 6.5$ Hz, CH-Dipp), 1.91 (sept, 1 H, $^3J_{\text{HH}} = 6.7$ Hz, CH-Dipp), 1.84 (sept, 1 H, $^3J_{\text{HH}} = 6.7$ Hz, CH-Dipp), 1.33 (d, 3 H, $^2J_{\text{HP}} = 7.2$ Hz, $^3J_{\text{HPt}} = 48.4$ Hz, PMe), 1.25 (d, 3 H, $^2J_{\text{HP}} = 8.2$ Hz, $^3J_{\text{HPt}} = 56.2$ Hz, PMe), 1.20 (d, 6 H, $^3J_{\text{HH}} = 6.4$ Hz, Me-Dipp), 1.17 (d, 3 H, $^3J_{\text{HH}} = 6.8$ Hz, Me-Dipp), 0.98 (d, 3 H, $^3J_{\text{HH}} = 6.8$ Hz, Me-Dipp), 0.94 (d, 3 H, 332

$^3J_{\text{HH}} = 6.5$ Hz, Me-Dipp), 0.91 (d, 3 H, $^3J_{\text{HH}} = 7.7$ Hz, Me-Dipp), 0.89 (d, 3 H, $^3J_{\text{HH}} = 7.4$ Hz, Me-Dipp), 0.77 (m, 7 H, Me-Dipp and H_A), 0.70 (s, 9 H, ^tBu), -0.28 (t, 1 H, $^3J_{\text{HP}} = 9.3$ Hz, $^3J_{\text{HH}} = 9.3$ Hz, $^2J_{\text{HPt}} = 28$ Hz, H_B) ppm.

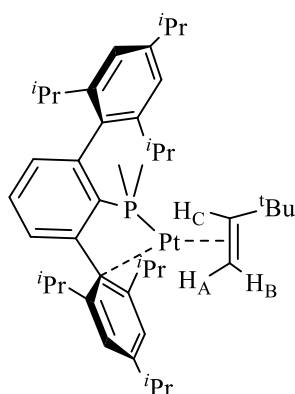
$^{13}\text{C}\{^1\text{H}\}$ NMR (96.6 MHz, -40 °C, CD₂Cl₂) δ : 147.4 (d, $^2J_{\text{CP}} = 41$ Hz, *o*-C₆H₃), 147.1 (s, *o*-Dipp), 146.9 (s, *o*-Dipp), 144.8 (s, *o*-C₆H₃), 143.9 (d, $^1J_{\text{CP}} = 33$ Hz, C_{ipso}-C₆H₃), 139.1 (s, *o*-Dipp'), 137.7 (s, C_{ipso}-Dipp), 131.8 (s, *m*-C₆H₃), 131.4 (s, *m*-C₆H₃), 128.9 (s, *p*-Dipp), 128.7 (s, *p*-C₆H₃), 125.9 (s, *o*-Dipp'), 124.2 (s, *m*-Dipp'), 122.6 (s, *m*-Dipp), 122.5 (s, *m*-Dipp), 121.5 (s, *m*-Dipp'), 121.0 (s, *p*-Dipp'), 117.0 (s, C_{ipso}-Dipp'), 78.0 (d, $^1J_{\text{CPt}} = 460$ Hz, $^2J_{\text{CP}} = 4$ Hz, C_H), 45.6 (d, $^2J_{\text{CP}} = 38$ Hz, C_{AB}), 34.7 (s, (Me)₃C), 31.6 (s, $^2J_{\text{CPt}} = 63$ Hz, (Me)₃C), 33.0 (s, CH-Dipp), 32.1 (s, CH-Dipp), 31.1 (s, CH-Dipp), 31.0 (s, CH-Dipp), 26.2 (s, Me-Dipp), 26.1 (s, Me-Dipp), 24.7 (s, Me-Dipp), 24.6 (s, Me-Dipp), 23.8 (s, Me-Dipp), 22.2 (s, Me-Dipp), 21.4 (s, Me-Dipp), 21.4 (s, Me-Dipp), 18.25 (d, $^1J_{\text{CP}} = 26$ Hz, PMe), 17.6 (d, $^1J_{\text{CP}} = 26$ Hz, PMe) ppm.

$^{31}\text{P}\{^1\text{H}\}$ NMR (161.9 MHz, 25 °C, C₆D₆): δ 23.9 (s, $^1J_{\text{PPt}} = 4457$ Hz) ppm.

$^{31}\text{P}\{^1\text{H}\}$ NMR (161.9 MHz, -40 °C, CD₂Cl₂): δ 23.7 (s, $^1J_{\text{PPt}} = 4414$ Hz) ppm.

Synthesis and Characterisation of [Pt(CH₂=CH^{*i*}Bu)(PMe₂Ar^{Tipp}₂)], 4

To a toluene solution (10 mL) of complex [PtMe₂(PMe₂Ar^{Tipp}₂)] (**10** from Chapter I) (0.4 g, 0.52 mmol) SiHET₃ (0.175 mL, 1.04 mmol) was added at room temperature. After one hour 3,3-dimethyl-1-butene was added (3.4 mL, 26 mmol) and the reaction mixture was stirred overnight. The volatiles were removed under high vacuum (10⁻⁴ bar) at 50 °C for several hours, yielding the compound as a dark brown solid (265 mg, 62 %).



Anal. Calc. for C₄₄H₆₇PPt: C, 64.3; H, 8.2. **Found:** C, 63.9; H, 8.0.

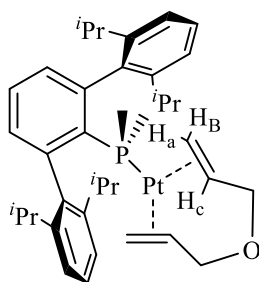
¹H NMR (500 MHz, 25 °C, C₆D₆) δ: 7.27 (br, 2 H, *m*-Tipp'), 7.18 (s, 2 H, *m*-Tipp), 6.87-7.00 (m, 3 H, C₆H₃), 3.86 (ddd, 1 H, ³*J*_{HH} = 9.8 Hz, ³*J*_{HH} = 11.7 Hz, ³*J*_{HP} = 2.9 Hz, ²*J*_{HPt} = 110.5 Hz, H_C), 2.87 (sept, 2H, *p*-CH-Tipp), 2.47 (br, 4 H, *o*-CH-Tipp), 1.50 (d, 3 H, ²*J*_{HP} = 7.0 Hz, PMe), 1.44 (d, 3 H, ²*J*_{HP} = 7.6 Hz, PMe), 1.39 (br, 6 H, *o*-Me-Tipp), 1.34 (d, 12 H, ³*J*_{HH} = 6.8 Hz, *p*-Me-Tipp), 1.31 (d, 6 H, ³*J*_{HH} = 6.9 Hz, *o*-Me-Tipp), 1.25 (m, 1 H, H_B), 1.12 (s, 9 H, ^{*t*}Bu), 1.01 (d, 6 H, ³*J*_{HH} = 6.6 Hz, *o*-Me-Tipp), 0.97 (d, 6 H, ³*J*_{HH} = 6.6 Hz, *o*-Me-Tipp), 0.75 (t, 1 H, ³*J*_{HH} = 9.4 Hz, H_A) ppm.

¹³C{¹H} NMR (125.72 MHz, 25 °C, C₆D₆) δ: 147.0 (br), 146.9 (s), 145.3 (d, ¹*J*_{CP} = 32 Hz, C_{ipso}-C₆H₃), 132.3 (s, *m*-C₆H₃), 132.3 (s, *m*-C₆H₃), 128.7 (d, ⁴*J*_{CP} = 2 Hz, *p*-C₆H₃), 121.3 (br, *m*-Tipp), 120.7 (s, *m*-Tipp), 78.5 (d, ²*J*_{CP} = 5 Hz, ¹*J*_{CPt} = 468 Hz, CH_C), 44.2 (d, ²*J*_{CP} = 39 Hz, CH_AH_B), 35.1 (d, ³*J*_{CP} = 2 Hz, C(Me)₃), 34.7 (s, *p*-CH-Tipp), 32.4 (s, C(CH₃)₃), 32.1 (br, *o*-CH-Tipp), 25.5 (br, *o*-Me-Tipp and *p*-Me-Tipp), 22.6 (br, *o*-Me-Tipp), 18.9 (d, ¹*J*_{CP} = 26 Hz, PMe), 18.2 (d, ¹*J*_{CP} = 25 Hz, PMe) ppm.

³¹P{¹H} NMR (202.4 MHz, 25 °C, C₆D₆): δ 24.0 (s, ¹*J*_{Pt} = 4419 Hz) ppm.

Synthesis and Characterisation of [Pt(PMe₂Ar^{Dipp2})(CH₂=CH-CH₂)₂O], 5

[Pt(C₂H₄)₂(PMe₂Ar^{Dipp2})], **1**, (20 mg, 0.03 mmol) was dissolved in THF (2 mL). Protected from light, allyl ether (5 μ L, 1.5 eq) was added at room temperature and the reaction mixture was stirred overnight. All volatiles were removed under vacuum. The complex was washed with pentane (3 x 1 mL) at –80°C obtaining the complex as a dark brown solid. Yield: 17 mg (78%).



Anal. Calc. for C₃₈H₅₃OPPt: C, 61.3; H, 7.0. **Found:** C, 61.2; H, 7.2.

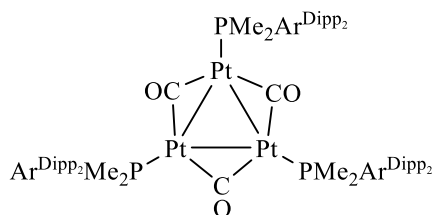
¹H NMR (400 MHz, 25 °C, CD₂Cl₂): δ 7.35 (td, 1 H, ³*J*_{HH} = 7.6 Hz, ⁵*J*_{HP} = 1.5 Hz, *p*-C₆H₃), 7.29 (t, 2 H, ³*J*_{HH} = 7.7, *p*-Dipp), 7.12 (d, 4 H, ³*J*_{HH} = 7.8 Hz, *m*-Dipp), 7.09 (dd, 2 H, ³*J*_{HH} = 7.7 Hz, ⁴*J*_{HP} = 2.6 Hz, *m*-C₆H₃), 4.02 (ddd, 2 H, ⁴*J*_{HH} = 12.3 Hz, ³*J*_{HH} = 3.6 Hz, ³*J*_{HP} = 6.5 Hz, ²*J*_{HPt} = 23.6 Hz, H_a), 2.74 (sept, 4 H, ³*J*_{HH} = 6.8 Hz, CH-Dipp), 2.66 (m, 2 H, ³*J*_{HH} = 3.4 Hz, ³*J*_{HH} = 8.0 Hz, ²*J*_{HPt} = 22 Hz, H_c), 1.81 (m, 2 H, ³*J*_{HH} = 11.5 Hz, ²*J*_{HPt} = 11.6 Hz, H_b), 1.60 (ddd, 2 H, ³*J*_{HH} = 8.2 Hz, ⁴*J*_{HH} = 1 Hz, ⁴*J*_{HP} = 6 Hz, ³*J*_{HPt} = 54.8 Hz, CH₂-O), 1.25 (d, 12 H, ³*J*_{HH} = 6.9 Hz, Me-Dipp), 1.23 (d, 6 H, ²*J*_{HP} = 7.9 Hz, ³*J*_{HPt} = 17.4 Hz, PMe₂), 1.21 (dd, 2 H, ³*J*_{HH} = 11.4 Hz, ⁴*J*_{HP} = 7.8 Hz, ³*J*_{HPt} = 36.6 Hz, CH₂-O), 0.97 (d, 12 H, ³*J*_{HH} = 6.7 Hz, Me-Dipp) ppm.

¹³C{¹H} NMR (96.6 MHz, 25 °C, CD₂Cl₂): δ 147.3 (s, *o*-Dipp), 143.4 (d, ²*J*_{CP} = 9 Hz, *o*-C₆H₃), 141.2 (s, C_{ipso}-Dipp), 133.8 (d, ³*J*_{CP} = 6 Hz, *m*-C₆H₃), 128.6 (s, *p*-Dipp), 127.2 (s, *p*-C₆H₃), 123.1 (s, *m*-Dipp), 70.0 (d, ²*J*_{PC} = 15 Hz, =CH), 56.4 (d, ²*J*_{PC} = 5 Hz, CH₂=), 37.0 (s, CH₂-O), 31.5 (s, CH-Dipp), 25.9 (s, Me-Dipp), 23.0 (s, Me-Dipp), 21.3 (d, ¹*J*_{CP} = 31 Hz, ²*J*_{CPt} = 42 Hz, PMe₂) ppm.

³¹P{¹H} NMR (161.9 MHz, 25 °C, CD₂Cl₂): δ –18.7 (s, ¹*J*_{Pt} = 3532 Hz) ppm.

Synthesis and Characterisation of [Pt(PMe₂Ar^{Dipp}₂)(μ-CO)]₃, 6

[Pt(C₂H₄)₂(PMe₂Ar^{Dipp}₂)], **1**, (0.1 g, 0.14 mmol) was dissolved in C₆H₆ (5 mL). CO was bubbled through the solution for 5 minutes at room temperature causing the product to precipitate as an orange solid, which was filtered and washed with hexane. Yield: 68 mg (71%).



Anal. Calc. for C₉₉H₁₂₉O₃P₃Pt₃: C, 58.1; H, 6.4. **Found:** C, 58.4; H, 6.8.

IR (Nujol): $\bar{\nu}(\text{CO}) = 1780 \text{ cm}^{-1}$.

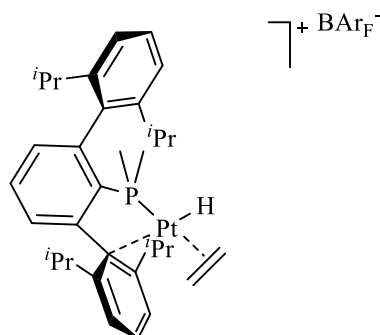
¹H NMR (500 MHz, −10 °C, CD₂Cl₂): δ 7.28 (t, 3 H, ³J_{HH} = 7.4 Hz, *p*-C₆H₃), 7.26 (t, 6 H, ³J_{HH} = 7.8 Hz, *p*-Dipp), 7.08 (d, 6 H, ³J_{HH} = 6.8 Hz, *m*-C₆H₃), 7.07 (d, 6 H, ³J_{HH} = 6.8 Hz, *m*-Dipp), 7.01 (d, 6 H, ³J_{HH} = 7.8 Hz, *m*-Dipp), 2.93 (sept, 6 H, ³J_{HH} = 6.6 Hz, CH-Dipp), 2.46 (sept, 6 H, ³J_{HH} = 6.7 Hz, CH-Dipp), 1.21 (d, 18 H, ³J_{HH} = 6.5 Hz, Me-Dipp), 0.94 (br, 18 H, PMe₂), 0.81 (d, 18 H, ³J_{HH} = 6.5 Hz, Me-Dipp), 0.77 (d, 18 H, ³J_{HH} = 6.5 Hz, Me-Dipp), 0.31 (d, 18 H, ³J_{HH} = 6.5 Hz, Me-Dipp) ppm.

¹³C{¹H} NMR (125.72 MHz, −10 °C, CD₂Cl₂): δ 182.6 (s, CO), 147.6 (s, C_{ipso}-Dipp), 146.7 (s, C_{ipso}-Dipp), 142.8 (m, *o*-C₆H₃), 140.3 (s, *o*-Dipp), 135.5 (m, C_{ipso}-C₆H₃), 131.8 (s, *m*-C₆H₃), 128.3 (*p*-Dipp), 126.9 (*p*-C₆H₃), 123.2 (s, *m*-Dipp), 122.2 (s, *m*-Dipp), 30.8 (s, CH-Dipp), 30.0 (s, CH-Dipp), 25.6 (s, Me-Dipp), 25.3 (s, Me-Dipp), 24.3 (s, Me-Dipp), 22.0 (s, Me-Dipp), 18.2 (m, PMe₂) ppm.

³¹P{¹H} NMR (121.44 MHz, 25 °C, CD₂Cl₂): δ 41.2 (s, ²J_{PPt} = 504 Hz, ³J_{PP} = 72 Hz, ¹J_{PPt} = 4440 Hz) ppm.

Synthesis and Characterisation of $[\text{PtH}(\text{C}_2\text{H}_4)(\text{PMe}_2\text{Ar}^{\text{Dipp}_2})][\text{BAr}_\text{F}]$, **7**

In a Young NMR tube complex $[\text{Pt}(\text{C}_2\text{H}_4)_2(\text{PMe}_2\text{Ar}^{\text{Dipp}_2})]$, **1** (50 mg, 0.07 mmol) and $[\text{H}(\text{Et}_2\text{O})_2][\text{BAr}_\text{F}]$ (74.2 mg, 0.07 mmol) were dissolved in CD_2Cl_2 (0.7 mL) at -80°C . The reaction was monitored by ^1H and $^{31}\text{P}\{^1\text{H}\}$ NMR spectroscopy and the product was characterized at -40°C with a quantitative spectroscopic yield.



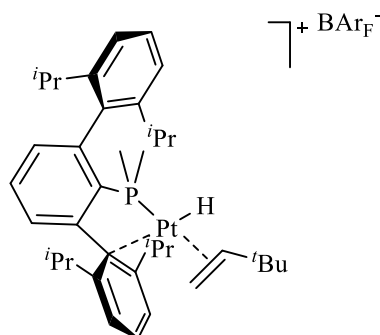
^1H NMR (500 MHz, -50°C , CD_2Cl_2): δ -19.18 (s, 1 H, $^1J_{\text{HPt}} = 1668.9$ Hz, Pt-H), 0.99 (d, 6 H, $^3J_{\text{HH}} = 6.7$ Hz, Me-Dipp), 1.01 (d, 6 H, $^3J_{\text{HH}} = 6.7$ Hz, Me-Dipp), 1.28 (d, 6 H, $^3J_{\text{HH}} = 6.7$ Hz, Me-Dipp), 1.31 (d, 6 H, $^3J_{\text{HH}} = 6.7$ Hz, Me-Dipp), 1.63 (d, 6 H, $^2J_{\text{HP}} = 11.5$ Hz, $^3J_{\text{HPt}} = 72.4$ Hz, PMe_2), 2.26 (sept, 2 H, $^3J_{\text{HH}} = 6.7$ Hz, CH-Dipp), 2.33 (sept, 2 H, $^3J_{\text{HH}} = 6.8$ Hz, CH-Dipp), 3.95 (s br, 4 H, $^2J_{\text{HPt}} = 35.0$ Hz, C_2H_4), 6.92 (m, 1 H, H_{ar}), 7.15-7.55 (m, 8 H, H_{ar}) ppm.

$^{13}\text{C}\{^1\text{H}\}$ NMR (96.6 MHz, -40°C , CD_2Cl_2): δ 147.4 (s), 146.9 (d, $J_{\text{CP}} = 21$ Hz), 133.5 (s), 133.1 (s), 132.2 (s), 131.7 (d, $J_{\text{CP}} = 16$ Hz), 130.3 (s), 125.9 (s), 125.6 (s), 123.3 (s), 120.5 (s), 96.4 (d, $^2J_{\text{CP}} = 10$ Hz, C_2H_4), 32.9 (s, CH-Dipp), 31.4 (s, CH-Dipp), 26.1 (s, Me-Dipp), 24.0 (s, Me-Dipp), 23.8 (s, Me-Dipp), 21.2 (s, Me-Dipp), 18.0 (d, $^1J_{\text{CP}} = 43.2$ Hz, PMe_2) ppm.

$^{31}\text{P}\{^1\text{H}\}$ NMR (161.9 MHz, -40°C , CD_2Cl_2): δ 11.0 (s, $^1J_{\text{PPt}} = 3679$ Hz) ppm.

Synthesis and Characterisation of $[\text{PtH}(\text{CH}_2=\text{CHBu}^t)(\text{PMe}_2\text{Ar}^{\text{Dipp}_2})][\text{BAr}_\text{F}]$, **8**

In a Young NMR tube complex $[\text{Pt}(\text{CH}_2=\text{CH}^t\text{Bu})(\text{PMe}_2\text{Ar}^{\text{Dipp}_2})]$ (30 mg, 0.04 mmol) and $[\text{H}(\text{Et}_2\text{O})_2][\text{BAr}_\text{F}]$ (41.2 mg, 0.04 mmol) were dissolved in CD_2Cl_2 (0.7 mL) at -80°C . The reaction was monitored by ^1H and $^{31}\text{P}\{^1\text{H}\}$ NMR spectroscopy and the product was characterized at -50°C with a quantitative spectroscopic yield.



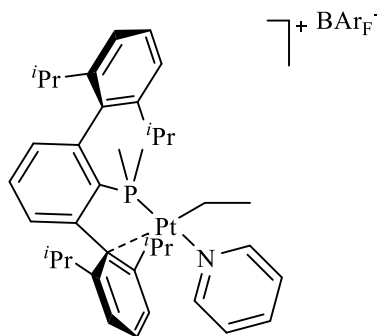
^1H NMR (500 MHz, -50°C , CD_2Cl_2): δ 7.76 (s, 8 H, *o*- BAr_F), 7.60-7.66 (m, 2 H, H_{ar}), 7.57 (s, 4 H, *p*- BAr_F), 7.52 (d, 1 H, $^3J_{\text{HH}} = 7.6$ Hz, H_{ar}), 7.49 (t, 1 H, $^3J_{\text{HH}} = 6.7$ Hz, H_{ar}), 7.43 (d, 1 H, $^3J_{\text{HH}} = 7.8$ Hz, H_{ar}), 7.31-7.38 (m, 2 H, H_{ar}), 7.29 (d, 1 H, $^3J_{\text{HH}} = 7.2$ Hz, H_{ar}), 6.87 (d, 1 H, $^3J_{\text{HH}} = 7.0$ Hz, H_{ar}), 4.91 (m, 1 H, CH-alkene), 3.66 (d, 1 H, $^3J_{\text{HH}} = 15.9$ Hz, CH_2), 2.37 (sept, 1 H, $^3J_{\text{HH}} = 6.5$ Hz, CH-Dipp), 2.35 (sept, 1 H, $^3J_{\text{HH}} = 6.5$ Hz, CH-Dipp), 2.22 (sept, 1 H, $^3J_{\text{HH}} = 6.5$ Hz, CH-Dipp), 2.19 (sept, 1 H, $^3J_{\text{HH}} = 6.5$ Hz, CH-Dipp), 2.04 (dd, 1 H, $^3J_{\text{HH}} = 8.8$ Hz, $^3J_{\text{HP}} = 4.3$ Hz, CH_2), 1.63 (d, 3 H, $^2J_{\text{HP}} = 11.5$ Hz, PMe), 1.54 (d, 3 H, $^2J_{\text{HP}} = 11.5$ Hz, PMe), 1.36 (d, 3 H, $^3J_{\text{HH}} = 6.9$ Hz, Me-Dipp), 1.27 (d, 3 H, $^3J_{\text{HH}} = 6.6$ Hz, Me-Dipp), 1.25 (d, 3 H, $^3J_{\text{HH}} = 6.9$ Hz, Me-Dipp), 1.21 (d, 3 H, $^3J_{\text{HH}} = 6.9$ Hz, Me-Dipp), 1.10 (d, 3 H, $^3J_{\text{HH}} = 6.6$ Hz, Me-Dipp), 1.03 (d, 3 H, $^3J_{\text{HH}} = 6.5$ Hz, Me-Dipp), 0.95 (s, 9 H, Bu^t), 0.79 (d, 3 H, $^3J_{\text{HH}} = 7.0$ Hz, Me-Dipp), 0.93 (d, 3 H, $^3J_{\text{HH}} = 6.4$ Hz, Me-Dipp), -19.35 (d, 1 H, $^2J_{\text{HP}} = 6.6$ Hz, $^1J_{\text{HPt}} = 1657$ Hz, Pt-H) ppm.

$^{13}\text{C}\{^1\text{H}\}$ NMR (125.7 MHz, -50°C , CD_2Cl_2) δ : 161.8 (q, $\text{C}_{\text{ipso}}\text{-BAr}_\text{F}$), 134.7 (s, *o*- BAr_F), 128.7 (q, $\text{CF}_3\text{-BAr}_\text{F}$), 117.6 (s, *p*- BAr_F), 89.9 (d, $^2J_{\text{CP}} = 12$ Hz, CH_2), 33.1 (s, CH-Dipp), 36.9 (s, CMe_3), 32.8 (s, CH-Dipp), 31.4 (s, CH-Dipp), 31.3 (s, CH-Dipp), 28.7 (s, CMe_3), 26.3 (s, Me-Dipp), 25.9 (s, Me-Dipp), 25.5 (s, Me-Dipp), 24.6 (s, Me-Dipp), 23.5 (s, Me-Dipp), 22.1 (s, Me-Dipp), 21.2 (s, Me-Dipp), 21.1 (s, Me-Dipp), 18.5 (d, $^1J_{\text{CP}} = 44$ Hz, PMe), 17.6 (d, $^1J_{\text{CP}} = 42$ Hz, PMe) ppm.

$^{31}\text{P}\{^1\text{H}\}$ NMR (202.4 MHz, -50°C , CD_2Cl_2): δ 9.5 (s, $^1J_{\text{PPt}} = 3595$ Hz) ppm.

Synthesis and Characterisation of [PtEt(Py)(PMe₂Ar^{Dipp2})] [BAr_F], **9**

A solution of [H(Et₂O)₂][BAr_F] (0.214 mg, 0.21 mmol) in dichloromethane (*ca.* 5 mL) at -80°C was added to a solution of [Pt(C₂H₄)₂(PMe₂Ar^{Dipp2})], **1**, (150 mg, 0.21 mmol) in the same solvent (*ca.* 5 mL). The reaction mixture was allowed to warm slowly to the room temperature while stirring overnight. Pyridine (0.1 mL) was added to the reaction mixture and all volatiles were removed under vacuum, obtaining the product as a yellow solid. For further purification, this complex can be crystallized by slow diffusion of pentane into a CH₂Cl₂ solution at -20°C (1:1 by vol). Yield: 245 mg (72%).



Anal. Calc. for C₃₉H₅₃NPt: C, 61.5; H, 7.0. **Found:** C, 61.3; H, 7.2.

¹H NMR (500 MHz, 25 °C, CD₂Cl₂): δ 8.52 (br, 1 H, *p*-Py), 7.86 (br, 2 H, *o*-Py), 7.74 (s, 8 H, *o*-BAr_F), 7.57 (s, 4 H, *p*-BAr_F), 7.55 (t, 1 H, *p*-C₆H₃), 7.52 (t, 1 H, ³*J*_{HH} = 7.8 Hz, *p*-Dipp), 7.43 (t, 2 H, ³*J*_{HH} = 6.9 Hz, *m*-Py), 7.35 (d, 2 H, ³*J*_{HH} = 8.0 Hz, *m*-Dipp), 7.32 (dd, 1 H, ³*J*_{HH} = 7.6 Hz, ⁴*J*_{HP} = 2.7 Hz, *m*-C₆H₃), 7.02 (d, 2 H, ³*J*_{HH} = 7.9 Hz, *m*-Dipp'), 6.81 (dd, 1 H, ³*J*_{HH} = 7.6 Hz, ⁴*J*_{HP} = 2.7 Hz, *m*-C₆H₃), 6.52 (t, 1 H, ³*J*_{HH} = 7.8 Hz, *p*-Dipp'), 2.48 (sept, 1 H, ³*J*_{HH} = 6.7 Hz, CH-Dipp), 2.43 (sept, 1 H, ³*J*_{HH} = 6.7 Hz, CH-Dipp), 1.69 (d, 6 H, ³*J*_{HH} = 7.1 Hz, Me-Dipp), 1.47 (d, 6 H, ²*J*_{HP} = 11.0 Hz, ³*J*_{HPt} = 54.6 Hz, PMe₂), 1.35 (d, 6 H, ³*J*_{HH} = 6.8 Hz, Me-Dipp), 1.29 (m, 2 H, CH₃-CH₂-Pt), 1.05 (d, 6 H, ³*J*_{HH} = 6.7 Hz, CH₃-Dipp), 1.01 (d, 6 H, ³*J*_{HH} = 7.0 Hz, CH₃-Dipp), 0.53 (t, 3 H, ³*J*_{HH} = 7.4 Hz, ³*J*_{HPt} = 90.1 Hz, CH₃-CH₂-Pt) ppm.

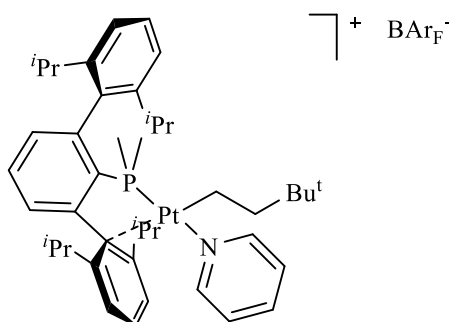
¹³C{¹H} NMR (125.7 MHz, 25 °C, CD₂Cl₂): δ 161.7 (q, ¹*J*_{CB} = 50 Hz, C_{ipso}-BAr_F), 148.4 (s, *o*-Dipp'), 147.0 (s, *o*-Dipp), 145.4 (s, *o*-C₆H₃), 145.2 (s, *o*-C₆H₃), 144.7 (s, C_{ipso}-C₆H₃), 135.7 (d, ³*J*_{CP} = 6 Hz, C_{ipso}-Dipp), 134.8 (s, *o*-BAr_F), 133.4 (d, ³*J*_{CP} = 7 Hz, *m*-C₆H₃), 132.4 (s, *p*-Dipp'), 131.4 (d, ⁴*J*_{CP} = 3 Hz, *p*-C₆H₃), 131.0 (d, ³*J*_{CP} = 13 Hz, *m*-C₆H₃), 130.0 (s, *p*-Dipp),

128.9 (qq, CF₃-BAr_F), 125.9 (s, *m*-Py), 124.5 (s, *m*-Dipp'), 123.2 (s, C_{ipso}-Dipp'), 123.2 (s, *m*-Dipp), 120.5 (s, *m*-BAr_F), 117.4 (sept, ³J_{HF} = 4 Hz, *p*-BAr_F), 32.7 (s, CH-Dipp), 31.3 (s, CH-Dipp), 25.9 (s, Me-Dipp), 24.1 (s, Me-Dipp), 23.9 (s, Me-Dipp), 21.2 (s, Me-Dipp), 15.3 (s, Pt-CH₂-CH₃), 12.3 (d, ¹J_{CP} = 43 Hz, PMe₂), 7.0 (d, ²J_{CP} = 4 Hz, Pt-CH₂-CH₃) ppm.

³¹P{¹H} NMR (202.4 MHz, 25 °C, CD₂Cl₂): δ -1.0 (s, ¹J_{PPt} = 4005 Hz) ppm.

Synthesis and Characterisation of $[\text{Pt}(\text{CH}_2\text{-CH}_2\text{-Bu}^t)\text{Py}(\text{PMe}_2\text{Ar}^{\text{Dipp}_2})][\text{BAr}_\text{F}]$, 10

In a Young NMR tube complex $[\text{Pt}(\text{CH}_2=\text{CHBu}^t)(\text{PMe}_2\text{Ar}^{\text{Dipp}_2})]$ (50 mg, 0.068 mmol) and $[\text{H}(\text{Et}_2\text{O})_2][\text{BAr}_\text{F}]$ (75.5 mg, 0.074 mmol) were dissolved in CH_2Cl_2 (3 mL) at -80°C . The reaction mixture was allowed to warm up slowly to the room temperature while stirring overnight. Pyridine (0.1 mL) was added to the resulting solution and all volatiles were removed under vacuum obtaining the product as a brown solid. Yield: 79 mg (70 %).



Anal. Calc. for $\text{C}_{75}\text{H}_{73}\text{BF}_{24}\text{NPt}\cdot\text{CH}_2\text{Cl}_2$: C, 51.68; H, 4.28. **Found:** C, 51.2; H, 4.4.

^1H NMR (400 MHz, 25°C , CD_2Cl_2): δ 8.56 (s br, 1 H, *p*-Py), 7.99 (t br, 1 H, $^3J_{\text{HH}} = 7.3$ Hz, *p*- C_6H_3), 7.88 (m, 2 H, *o*-Py), 7.77 (s, 8 H, *o*- BAr_F), 7.59 (s, 4 H, *p*- BAr_F), 7.56 (dd, 1 H, $^3J_{\text{HH}} = 7.5$ Hz, $^4J_{\text{HP}} = 1.8$ Hz, *m*- C_6H_3), 7.51 (t, 1 H, $^3J_{\text{HH}} = 7.8$ Hz, *p*-Dipp'), 7.41 (t, 2 H, $^3J_{\text{HH}} = 6.8$ Hz, *m*-Py), 7.35 (d, 2 H, $^3J_{\text{HH}} = 7.8$ Hz, *m*-Dipp'), 7.04 (d, 2 H, $^3J_{\text{HH}} = 7.8$ Hz, *m*-Dipp), 6.83 (dd, 1 H, $^3J_{\text{HH}} = 7.7$ Hz, $^4J_{\text{HP}} = 2.8$ Hz, *m*- C_6H_3), 6.54 (t, 1 H, $^3J_{\text{HH}} = 7.8$ Hz, *p*-Dipp), 2.49 (d, 2 H, $^3J_{\text{HH}} = 7.0$ Hz, CH-Dipp), 2.45 (d, 2 H, $^3J_{\text{HH}} = 7.0$ Hz, CH-Dipp), 1.69 (d, 6 H, $^3J_{\text{HH}} = 7.0$ Hz, Me-Dipp), 1.50 (d, 6 H, $^2J_{\text{HP}} = 10.9$ Hz, $^3J_{\text{HPt}} = 52.2$ Hz, PMe_2), 1.36 (d, 6 H, $^3J_{\text{HH}} = 6.8$ Hz, Me-Dipp), 1.32 (m, 2 H, Pt- CH_2), 1.06 (d, 6 H, $^3J_{\text{HH}} = 6.5$ Hz, Me-Dipp), 1.01 (d, 6 H, $^3J_{\text{HH}} = 6.7$ Hz, Me-Dipp), 0.86 (m, 2 H, $\text{CH}_2\text{-}^t\text{Bu}$), 0.50 (s, 9 H, ^tBu) ppm.

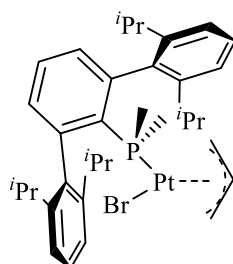
$^{13}\text{C}\{^1\text{H}\}$ NMR (96.6 MHz, 25°C , CD_2Cl_2): δ 10.6 (d, $^2J_{\text{CP}} = 4$ Hz, $^1J_{\text{CPt}} = 776$ Hz, Pt- CH_2), 13.0 (d, $^1J_{\text{CP}} = 43$ Hz, $^2J_{\text{CPt}} = 52$ Hz, PMe_2), 21.8 (s, Me-Dipp), 24.5 (s, Me-Dipp), 24.7 (s, Me-Dipp), 26.6 (s, Me-Dipp), 28.8 (s, CMe_3), 31.6 (s, CMe_3), 32.0 (s, CH-Dipp), 33.8 (s, CH-Dipp), 44.5 (s, $^2J_{\text{CPt}} = 37$ Hz, $\text{CH}_2\text{-}^t\text{Bu}$), 123.8 (s, *m*-Dipp), 125.0 (s, *o*- C_6H_3), 125.1 (s, *m*-

Dipp), 126.6 (s, *m*-Py), 130.7 (s, *p*-Dipp), 131.6 (d, $^3J_{\text{CP}} = 11$ Hz, *m*-C₆H₃), 132.1 (d, $^3J_{\text{CP}} = 3$ Hz, *m*-C₆H₃), 133.2 (s, *p*-Dipp), 140.9 (br, *p*-C₆H₃), 146.9 (br, *p*-Py), 147.7 (s, *o*-Dipp), 149.1 (s, *o*-Dipp), 151.1 (s, *o*-Py) ppm.

$^{31}\text{P}\{^1\text{H}\}$ NMR (161.9 MHz, 25 °C, CD₂Cl₂): δ -1.4 (s, $^1J_{\text{PPt}} = 3985$ Hz) ppm.

Synthesis and Characterisation of [Pt(η^3 -C₃H₅)Br(PMe₂Ar^{Dipp2})], 11

- a) The Pt(II) dichloride complex [PtCl₂(PMe₂Ar^{Dipp2})] (**6** from Chapter I) (0.1 g, 0.14 mmol) was dissolved in toluene (10 mL) and added dropwise with Mg(C₃H₅)Br (1 M in Et₂O, 0.17 mL) –50 °C. The reaction mixture was allowed to warm up slowly to the room temperature while stirring overnight. The suspension was filtered and the volatiles were removed in vacuo. The resulting solid residue was extracted in pentane (2 x 5 mL), giving a yellow solid after evaporation of the solvent. Yield: 48 mg (44%).
- b) To a dichloromethane (5 mL) solution of complex [Pt(C₂H₄)₂(PMe₂Ar^{Dipp2})], **1**, (0.1 g, 0.14 mmol), allylbromide (12 μ L, 0.14 mmol) was added, avoiding the light, and the reaction mixture was stirred overnight at room temperature. After removing all volatiles under vacuum, the product was extracted in pentane (2 x 5mL), to yield a yellow solid after removal of the solvent under vacuum. Yield: 68 mg (62%).



Anal. Calc. for C₃₅H₄₈BrPPt: C, 52.4; H, 5.9. **Found:** C, 52.1; H, 6.4.

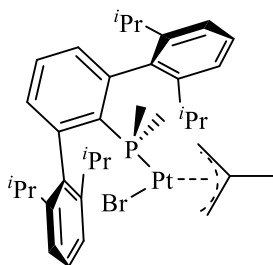
¹H NMR (400 MHz, 25 °C, CD₂Cl₂): δ 7.46 (td, 1 H, $^5J_{\text{HP}} = 1.7$ Hz, $^3J_{\text{HH}} = 7.8$ Hz, *p*-C₆H₃), 7.40 (t, 2 H, $^3J_{\text{HH}} = 7.8$ Hz, *p*-Dipp), 7.28 (d br, 2 H, $^3J_{\text{HH}} = 7.1$ Hz, *m*-Dipp), 7.26 (d, br, 2 H, $^3J_{\text{HH}} = 7.2$ Hz, *m*-Dipp), 7.22 (dd, 2 H, $^4J_{\text{HP}} = 3.0$ Hz, $^3J_{\text{HH}} = 7.7$ Hz, *m*-C₆H₃), 4.17 (m, 1 H, CH-allyl), 3.91 (t br, 1 H, $^3J_{\text{HH}} = 6.3$ Hz, $^3J_{\text{HP}} = 5.3$ Hz, CH₂), 2.85 (sept, 2 H, $^3J_{\text{HH}} = 6.7$ Hz, CH-Dipp), 2.80 (sept, 2 H, $^3J_{\text{HH}} = 6.7$ Hz, CH-Dipp), 2.54 (m, 1 H, $^3J_{\text{HH}} = 6.5$ Hz, CH₂), 2.44 (dd, 1 H, $^3J_{\text{HH}} = 13.2$ Hz, $^3J_{\text{HP}} = 9.5$ Hz, CH₂), 1.47 (d, 3 H, $^2J_{\text{HP}} = 10.5$ Hz, $^2J_{\text{HPt}} = 46$ Hz, PMe), 1.42 (d, 6 H, $^3J_{\text{HH}} = 6.7$ Hz, Me-Dipp), 1.38 (d, 6 H, $^3J_{\text{HH}} = 6.7$ Hz, Me-Dipp), 1.35 (d, 3 H, $^2J_{\text{HP}} = 10.8$ Hz, $^3J_{\text{HPt}} = 39.5$ Hz, PMe), 1.34 (m, 1 H, CH₂), 1.05 (d, 6 H, $^3J_{\text{HH}} = 6.3$ Hz, Me-Dipp), 1.03 (d, 6 H, $^3J_{\text{HH}} = 6.2$ Hz, Me-Dipp) ppm.

$^{13}\text{C}\{^1\text{H}\}$ NMR (96.6 MHz, 25 °C, CD_2Cl_2): δ 147.8 (s, *o*-Dipp), 147.7 (s, *o*-Dipp), 144.8 (d, $^2J_{\text{CP}} = 10$ Hz, $^3J_{\text{CPt}} = 21$ Hz, *o*- C_6H_3), 140.6 (d, $^3J_{\text{CP}} = 3$ Hz, C_{ipso} -Dipp), 133.8 (d, $^3J_{\text{CP}} = 8$ Hz, *m*- C_6H_3), 130.8 (d, $^1J_{\text{CP}} = 43$ Hz, C_{ipso} -P), 129.3 (s, *p*-Dipp), 128.2 (s, *p*- C_6H_3), 123.4 (s, *m*-Dipp), 123.3 (s, *m*-Dipp), 108.3 (s, $^1J_{\text{CPt}} = 47$ Hz, CH-allyl), 64.3 (d, $^2J_{\text{CP}} = 35$ Hz, $^1J_{\text{CPt}} = 53$ Hz, CH_2), 44.7 (s, $^1J_{\text{CPt}} = 259$ Hz, CH_2), 31.6 (s, CH-Dipp), 31.4 (s, CH-Dipp), 26.3 (s, Me-Dipp), 26.3 (s, Me-Dipp), 23.6 (s, Me-Dipp), 23.5 (s, Me-Dipp), 19.4 (d, $^1J_{\text{CP}} = 37$ Hz, $^2J_{\text{CPt}} = 56$ Hz, PMe), 19.1 (d, $^1J_{\text{CP}} = 36$ Hz, $^2J_{\text{CPt}} = 37$ Hz, PMe) ppm.

$^{31}\text{P}\{^1\text{H}\}$ NMR (161.9 MHz, 25 °C, CD_2Cl_2): δ -10.0 (s, $^1J_{\text{PPt}} = 4370$ Hz) ppm.

Synthesis and Characterisation of [Pt(η^3 -CH₂C(Me)CH₂)Br(PMe₂Ar^{Dipp2})], 12

To a dichloromethane (*ca.* 2 mL) solution of complex [Pt(C₂H₄)₂(PMe₂Ar^{Dipp2})], **1**, (0.03 g, 0.04 mmol) 2-methylallyl bromide (5 μ L, 0.05 mmol), was added, avoiding the light, and the reaction mixture was stirred overnight at room temperature. After removing the volatiles under vacuum, the product was extracted with pentane at -30 °C, and isolated as a pale yellow solid. Yield: 26 mg (72%).



Anal. Calc. for C₃₆H₅₀BrPPt: C, 54.8; H, 6.4. **Found:** C, 54.6; H, 6.9.

¹H NMR (500 MHz, 25 °C, CD₂Cl₂): δ 7.41 (td, 1 H, ³*J*_{HH} = 7.7 Hz, ⁵*J*_{HP} = 1.7 Hz, *p*-C₆H₃), 7.32 (t, 2 H, ³*J*_{HH} = 7.7 Hz, *p*-Dipp), 7.22 (d, 2 H, ³*J*_{HH} = 7.7 Hz, *m*-Dipp), 7.15-7.19 (m, 4 H, *m*-C₆H₃ and *m*-Dipp), 3.64 (dd, 1 H, ³*J*_{HP} = 3 Hz, ²*J*_{HH} = 3 Hz, CH₂), 2.83 (sept, 4 H, ³*J*_{HH} = 6.9 Hz, CH-Dipp), 2.43 (dt, 1 H, ²*J*_{HH} = 2.5 Hz, ³*J*_{HP} = 2.5 Hz, ²*J*_{HPt} = 18.6 Hz, CH₂), 2.11 (d, 1 H, ³*J*_{CP} = 10.6 Hz, ²*J*_{HPt} = 21.7 Hz, CH₂), 1.69 (s, 3 H, ³*J*_{HPt} = 73.8 Hz, Me-allyl), 1.53 (d, 3 H, ²*J*_{HP} = 9.6 Hz, ³*J*_{HPt} = 48 Hz, PMe), 1.38 (d, 6 H, ³*J*_{HH} = 6.7 Hz, Me-Dipp), 1.35 (d, 6 H, ³*J*_{HH} = 6.7 Hz, Me-Dipp), 1.10 (d, 3 H, ²*J*_{HP} = 10 Hz, ³*J*_{HPt} = 40 Hz, PMe), 1.01 (d, 6 H, ³*J*_{HH} = 6.7 Hz, Me-Dipp), 0.97 (d, 6 H, ³*J*_{HH} = 6.7 Hz, Me-Dipp), 0.72 (d, 1 H, ²*J*_{HH} = 2.1 Hz, CH₂) ppm.

¹³C{¹H} NMR (125.72 MHz, 25 °C, CD₂Cl₂): δ 147.8 (s, *o*-Dipp), 144.8 (d, ²*J*_{HP} = 9 Hz, *o*-C₆H₃), 140.9 (d, ³*J*_{CP} = 4 Hz, C_{ipso}-Dipp), 134.0 (s, *m*-C₆H₃), 133.9 (s, *m*-C₆H₃), 131.6 (d, ¹*J*_{CP} = 51 Hz, C_{ipso}-C₆H₃), 129.2 (s, *p*-Dipp), 128.0 (s, *p*-C₆H₃), 123.5 (s, *m*-Dipp), 123.3 (s, *m*-Dipp), 63.6 (d, ¹*J*_{CP} = 38 Hz, CH₂), 46.8 (s, ¹*J*_{CPt} = 264 Hz, CH₂), 31.5 (s, CH-Dipp), 31.4 (s, CH-Dipp), 26.2 (s, Me-Dipp), 24.2 (s, ²*J*_{CPt} = 70 Hz, Me-allyl), 23.9 (s, Me-Dipp), 23.6 (s, CMe-allyl), 23.4 (s, Me-Dipp), 20.6 (d, ¹*J*_{CP} = 36 Hz, PMe), 19.2 (d, ¹*J*_{CP} = 37 Hz, PMe) ppm.

³¹P{¹H} NMR (202.4 MHz, 25 °C, CD₂Cl₂): δ -10.2 (s, ¹*J*_{PPt} = 4241 Hz) ppm.

II.4.3. General Method for Catalytic Hydrosilylation of Alkynes

In a NMR tube the alkyne (1.35 mmol), the silane (1.35 mmol), hexamethylbenzene (0.07 mmol, internal standard) and **3** (1.35 μ mol) were dissolved in C_6D_6 (0.5 mL). The reaction was heated at 80 °C. Selectivity and conversions were determined by 1H NMR spectroscopy and GC-MS analysis.

II.5. Bibliography

1. a) L. Malatesta, M. Angoletta, *J. Chem. Soc.* **1957**, 1186-1188; b) L. Malatesta, C. Cariello, *J. Chem. Soc.* **1958**, 2323-2328.
2. J. A. Chopoorian, J. Lewis, R. S. Nyholm, *Nature* **1961**, *190*, 528-529.
3. L. Malatesta, R. Ugo, *J. Chem. Soc.* **1963**, 2080-2082.
4. L. Ortega-Moreno, M. F. Espada, J. J. Moreno, C. Navarro-Gilabert, J. Campos, S. Conejero, J. López-Serrano, C. Maya, R. Peloso, E. Carmona, *Polyhedron* **2016**, Accepted.
5. J. W. Eastes, W. M. Burgess, *J. Am. Chem. Soc.* **1942**, *64*, 1187-1189.
6. J. J. Burbage, W. C. Fernelius, *J. Am. Chem. Soc.* **1943**, *65*, 1484-1486.
7. a) Part 1 (pp 1-67) of Ref 7b; b) L. Malatesta, S. Cenini, in *Zerovalent Compounds of Metals* (Eds.: P. M. Maitlis, F. G. A. Stone, R. West), Academic Press Inc., London, **1974**,
8. J. G. Verkade, *Coord. Chem. Rev.* **1972**, *9*, 1-106.
9. Part 2 of Ref. 7b (pp. 70-235).
10. R. Ugo, *Coord. Chem. Rev.* **1968**, *3*, 319-344.
11. a) A. Immirzi, A. Musco, P. Zambelli, G. Carturan, *Inorg. Chim. Acta* **1975**, *13*, L13-L14; b) M. Green, J. A. Howard, J. L. Spencer, F. G. A. Stone, *J. Chem. Soc., Chem. Commun.* **1975**, 3-4; c) S. Otsuka, T. Yoshida, M. Matsumoto, K. Nakatsu, *J. Am. Chem. Soc.* **1976**, *98*, 5850-5858; d) N. M. Boag, M. Green, D. M. Grove, J. A. K. Howard, J. L. Spencer, F. G. A. Stone, *J. Chem. Soc., Dalton Trans.* **1980**, 2170-2181.

12. a) A. J. Arduengo, S. F. Gamper, J. C. Calabrese, F. Davidson, *J. Am. Chem. Soc.* **1994**, *116*, 4391-4394; b) P. L. Arnold, F. G. N. Cloke, T. Geldbach, P. B. Hitchcock, *Organometallics* **1999**, *18*, 3228-3233; c) G. C. Fortman, N. M. Scott, A. Linden, E. D. Stevens, R. Dorta, S. P. Nolan, *Chem. Commun.* **2010**, *46*, 1050-1052; d) J. Bauer, H. Braunschweig, P. Brenner, K. Kraft, K. Radacki, K. Schwab, *Chem. Eur. J.* **2010**, *16*, 11985-11992.
13. a) F. Hering, J. Nitsch, U. Paul, A. Steffen, F. M. Bickelhaupt, U. Radius, *Chem. Sci.* **2015**, *6*, 1426-1432; b) F. Hering, U. Radius, *Organometallics* **2015**, *34*, 3236-3245; c) S. Roy, K. C. Mondal, J. Meyer, B. Niepötter, C. Köhler, R. Herbst-Irmer, D. Stalke, B. Dittrich, D. M. Andrada, G. Frenking, H. W. Roesky, *Chem. Eur. J.* **2015**, *21*, 9312-9318.
14. a) J. Bauer, R. Bertermann, H. Braunschweig, K. Gruss, F. Hupp, T. Kramer, *Inorg. Chem.* **2012**, *51*, 5617-5626; b) S. Bertsch, H. Braunschweig, M. Forster, K. Gruss, K. Radacki, *Inorg. Chem.* **2011**, *50*, 1816-1819.
15. M. Ma, A. Sidiropoulos, L. Ralte, A. Stasch, C. Jones, *Chem. Commun.* **2013**, *49*, 48-50.
16. a) N. A. Jasim, R. N. Perutz, B. Procacci, A. C. Whitwood, *Chem. Commun.* **2014**, *50*, 3914-3917; b) A. Nova, S. Erhardt, N. A. Jasim, R. N. Perutz, S. A. Macgregor, J. E. McGrady, A. C. Whitwood, *J. Am. Chem. Soc.* **2008**, *130*, 15499-15511; c) E. Clot, O. Eisenstein, N. Jasim, S. A. Macgregor, J. E. McGrady, R. N. Perutz, *Acc. Chem. Res.* **2011**, *44*, 333-348.
17. B. R. Barnett, C. E. Moore, A. L. Rheingold, J. S. Figueroa, *J. Am. Chem. Soc.* **2014**, *136*, 10262-10265.
18. P. A. Chase, T. Jurca, D. W. Stephan, *Chem. Commun.* **2008**, 1701-1703.
19. K. Yamamoto, T. Hayashi, in *Transition Metals for Organic Synthesis*, Wiley-VCH Verlag GmbH, **2008**, pp. 167-191,
20. a) I. E. Markó, S. Stérin, O. Buisine, G. Mignani, P. Branlard, B. Tinant, J. Declercq, *Science* **2002**, *298*, 204-206; b) O. Buisine, G. Berthon-Gelloz, J.-F. Briere, S. Sterin, G. Mignani, P. Branlard, B. Tinant, J.-P. Declercq, I. E. Marko, *Chem. Commun.* **2005**, 3856-3858; c) G. Berthon-Gelloz, J.-M. Schumers, G. De Bo, I. E. Markó, *J. Org. Chem.* **2008**, *73*, 4190-4197.
21. a) R. Takeuchi, S. Nitta, D. Watanabe, *J. Org. Chem.* **1995**, *60*, 3045-3051; b) R. Takeuchi, N. Tanouchi, *J. Chem. Soc., Perkin Trans. 1*

- 1994**, 2909-2913; c) A. Sato, H. Kinoshita, H. Shinokubo, K. Oshima, *Org. Lett.* **2004**, 6, 2217-2220.
22. Y. Na, S. Chang, *Org. Lett.* **2000**, 2, 1887-1889.
23. S. J. K. Forrest, P. G. Pringle, H. A. Sparkes, D. F. Wass, *Dalton Trans.* **2014**, 43, 16335-16344.
- 24 C. J. Moulton, B. L. Shaw, *J. Chem. Soc., Chem. Commun.* **1976**, 365-366.
25. a) N. Carr, B. J. Dunne, A. G. Orpen, J. L. Spencer, *J. Chem. Soc., Chem. Commun.* **1988**, 926-928; b) L. Mole, J. L. Spencer, N. Carr, A. G. Orpen, *Organometallics* **1991**, 10, 49-52.
26. J. Forniés, E. Lalinde, in *Comprehensive Organometallic Chemistry III* (Ed.: R. H. Crabtree), Elsevier, Oxford, **2007**, pp. 611-673,
27. a) T. G. Appleton, H. C. Clark, L. E. Manzer, *Coord. Chem. Rev.* **1973**, 10, 335-422; b) F. R. Hartley, *Chem. Soc. Rev.* **1973**, 2, 163-179; c) L. J. Manojlovic-Muir, K. W. Muir, *Inorg. Chim. Acta* **1974**, 10, 47-49.
28. P. T. Cheng, S. C. Nyburg, *Can. J. Chem.* **1972**, 50, 912-916.
29. M. R. Buchner, B. Bechlars, B. Wahl, K. Ruhland, *Organometallics* **2013**, 32, 1643-1653.
30. a) N. C. Harrison, M. Murray, J. L. Spencer, F. G. A. Stone, *J. Chem. Soc., Dalton Trans.* **1978**, 1337-1342; b) J. A. K. Howard, P. Mitprachachon, A. Roy, *J. Organomet. Chem.* **1982**, 235, 375-381.
31. J. Krause, G. Cestarc, K. Haack, K. Seevogel, W. Storm, K. Pörschke, *J. Am. Chem. Soc.* **1999**, 121, 9807-9823.
32. a) G. Berthon-Gelloz, J. Schumers, F. Lucaccioni, B. Tinant, J. Wouters, I. E. Markó, *Organometallics* **2007**, 26, 5731-5734; b) G. Berthon-Gelloz, B. de Bruin, B. Tinant, I. E. Markó, *Angew. Chem. Int. Ed.* **2009**, 48, 3161-3164.
33. H. C. Clark, G. Ferguson, M. J. Hampden-Smith, B. Kaitner, H. Ruegger, *Polyhedron* **1988**, 7, 1349-1353.
34. Cambridge Structural Database (Version 5.36). F. Allen, O. Kennard, *Chemical Design Automation News* **1993**, 8, 31-37.
35. a) E. Molinos, S. K. Brayshaw, G. Kociok-Kohn, A. S. Weller, *Dalton Trans.* **2007**, 4829-4844; b) S. Gatard, C. Guo, B. M. Foxman, O. V. Ozerov, *Organometallics* **2007**, 26, 6066-6075; c) D. L. Coombs, S. Aldridge, A. Rossin, C. Jones, D. J. Willock, *Organometallics* **2004**, 23, 2911-2926; d) U. Fekl, W. Kaminsky, K. I. Goldberg, *J. Am. Chem. Soc.* **2003**, 125, 15286-15287.

36. A. Falceto, E. Carmona, S. Alvarez, *Organometallics* **2014**, *33*, 6660-6668.
37. a) E. Poverenov, M. Gandelman, L. J. W. Shimon, H. Rozenberg, Y. Ben-David, D. Milstein, *Organometallics* **2005**, *24*, 1082-1090; b) K. H. Dahmen, A. Moor, R. Naegeli, L. M. Venanzi, *Inorg. Chem.* **1991**, *30*, 4285-4286; c) C. M. Lukehart, G. P. Torrence, *Inorg. Chim. Acta* **1977**, *22*, 131-134.
38. A. Moor, P. S. Pregosin, L. M. Venanzi, *Inorg. Chim. Acta* **1981**, *48*, 153-157.
39. a) B. Marciniec, *Hydrosilylation. Advances in Silicon Science.*, Springer, **2009**; b) A. K. Roy, *Adv. Organomet. Chem.* **2008**, *55*, 1-59.
40. a) E. Langkopf, D. Schinzer, *Chem. Rev.* **1995**, *95*, 1375-1408; b) I. Fleming, A. Barbero, D. Walter, *Chem. Rev.* **1997**, *97*, 2063-2192; c) T. A. Blumenkopf, L. E. Overman, *Chem. Rev.* **1986**, *86*, 857-873; d) G. R. Jones, Y. Landais, *Tetrahedron* **1996**, *52*, 7599-7662; e) T. Hiyama, E. Shirakawa, *Top. Curr. Chem.* **2002**, *219*, 61-85; f) I. Fleming, J. Dunogues, R. Smithers, *Org. React.* **1989**, *37*, 57-575; g) S. E. Denmark, M. H. Ober, *Aldrichimica Acta* **2003**, *36*, 75-85; h) S. E. Denmark, R. F. Sweis, *Acc. Chem. Res.* **2002**, *35*, 835-846.
41. a) J. L. Speier, in *Adv. Organomet. Chem., Vol. Volume 17* (Eds.: F. G. A. Stone, W. Robert), Academic Press, **1979**, pp. 407-447, ; b) M. P. Doyle, K. G. High, C. L. Nesloney, T. W. Clayton, J. Lin, *Organometallics* **1991**, *10*, 1225-1226; c) L. N. Lewis, K. G. Sy, G. L. Bryant, P. E. Donahue, *Organometallics* **1991**, *10*, 3750-3759.
42. a) M. Green, J. L. Spencer, F. G. A. Stone, C. A. Tsipis, *J. Chem. Soc., Dalton Trans.* **1977**, 1525-1529; b) C. A. Tsipis, *J. Organomet. Chem.* **1980**, *187*, 427-446.
43. a) P. J. Murphy, J. L. Spencer, G. Procter, *Tetrahedron Lett.* **1990**, *31*, 1051-1054; b) T. Kyoko, M. Tatsuya, O. Yoshio, H. Tamejiro, *Tetrahedron Lett.* **1993**, *34*, 8263-8266; c) S. E. Denmark, Z. Wang, *Org. Lett.* **2001**, *3*, 1073-1076; d) K. Itami, K. Mitsudo, A. Nishino, J.-i. Yoshida, *J. Org. Chem.* **2002**, *67*, 2645-2652; e) M. Blug, X.-F. Le Goff, N. Mézailles, P. Le Floch, *Organometallics* **2009**, *28*, 2360-2362; f) A. Hamze, O. Provot, J.-D. Brion, M. Alami, *Tetrahedron Lett.* **2008**, *49*, 2429-2431; g) W. Wu, C.-J. Li, *Chem. Commun.* **2003**, 1668-1669; h) H. Aneetha, W. Wu, J. G. Verkade, *Organometallics* **2005**, *24*, 2590-2596.

-
44. a) G. De Bo, G. Berthon-Gelloz, B. Tinant, I. E. Markó, *Organometallics* **2006**, *25*, 1881-1890; b) G. F. Silbestri, J. C. Flores, E. de Jesús, *Organometallics* **2012**, *31*, 3355-3360.
45. S. Dierick, E. Vercruysse, G. Berthon-Gelloz, I. E. Markó, *Chem. Eur. J.* **2015**, *21*, 17073-17078.
46. Formation of nanoparticles has previously been observed for the unmodified Karstedt catalyst: a) L. N. Lewis, N. Lewis, *J. Am. Chem. Soc.* **1986**, *108*, 7228-7231; b) L. N. Lewis, *J. Am. Chem. Soc.* **1990**, *112*, 5998-6004; c) L. N. Lewis, R. J. Uriarte, *Organometallics* **1990**, *9*, 621-625; d) L. N. Lewis, R. J. Uriarte, N. Lewis, *J. Catal.* **1991**, *127*, 67-74.
47. For selected examples of heterogeneous Pt catalysts: a) M. Chauhan, B. J. Hauck, L. P. Keller, P. Boudjouk, *J. Organomet. Chem.* **2002**, *645*, 1-13; b) F. Alonso, R. Buitrago, Y. Moglie, J. Ruiz-Martínez, A. Sepúlveda-Escribano, M. Yus, *J. Organomet. Chem.* **2011**, *696*, 368-372; c) R. Cano, M. Yus, D. J. Ramón, *ACS Catal.* **2012**, *2*, 1070-1078.
48. For other examples of electronic effects on selectivity: D. A. Rooke, E. M. Ferreira, *Angew. Chem. Int. Ed.* **2012**, *51*, 3225-3230.

CONCLUSIONES

1. Las características estructurales dilucidadas en este trabajo para los complejos de Pt(II) y Pt(0) que se han investigado y los estudios de reactividad química con ellos desarrollados, permiten concluir que los ligandos fosfina de tipo $\text{PMe}_2\text{Ar}'$, donde Ar' simboliza un radical terfenilo voluminoso, tienen excelentes propiedades de coordinación, fruto de su elevada capacidad para donar densidad electrónica, y permiten además estabilizar estructuras de alta insaturación, tanto electrónica como de coordinación, gracias de una parte a su gran tamaño, y de otra a su capacidad para establecer interacciones electrónicas secundarias, relativamente débiles, mediante el sistema aromático de uno de los anillos laterales del grupo terfenilo.
2. Las fosfinas de terfenilo más voluminosas utilizadas ($\text{PMe}_2\text{Ar}^{\text{Dipp}_2}$, L_2 y $\text{PMe}_2\text{Ar}^{\text{Tipp}_2}$, L_3) son capaces de estabilizar por sí solas complejos tricoordinados de Pt(II), $[\text{PtX}_2(\text{L})]$ o $[\text{Pt}(\text{X})(\text{Y})\text{L}]$ donde X e Y representan ligandos monoaniónicos como CH_3^- , Ph^- , H^- , SiR_3^- , y Cl^- , gracias a una interacción secundaria $\text{Pt}\cdots\text{C}_{\text{ar}}$ cuya fuerza depende de la *influencia-trans* del ligando X o Y que ocupa la posición de coordinación opuesta, como se infiere de modo inequívoco de los estudios estructurales y de reactividad realizados. Uno, o los dos ligandos aniónicos, X e Y, de estos complejos se pueden eliminar de estas estructuras, originando especies mono y dicatiónicas, $[\text{Pt}(\text{X})(\text{L})]^+$ y $[\text{Pt}(\text{L})]^{2+}$, respectivamente, que presentan una elevada electrofilia, como consecuencia de su carácter insaturado.

3. Una de tales especies, $cis-[PtMe(S)(PMe_2Ar^{Dipp2})]^+$ ($S = H_2O, Et_2O$ u otra molécula de escasa capacidad donadora) se escogió como modelo para desarrollar estudios de reactividad química que corroboran la anterior hipótesis acerca de su marcada electrofilia. De este modo, se encontró que al reemplazar S por CO la banda correspondiente a la vibración $\bar{\nu}(CO)$ aparece a 2127 cm^{-1} , valor próximo al de esta molécula libre, y que al reaccionar con H_2 se originan complejos catiónicos $\sigma-H_2$ y $\sigma-CH_4$, que aunque inestables, perviven el tiempo suficiente para experimentar intercambios isotópicos de protio y de deuterio con el grupo metilo coordinado, $Pt-CH_3$. Muy en especial, se ha demostrado de forma concluyente que el catión $[PtMe(PMe_2Ar^{Dipp2})]^+$ posee capacidad de inducir la tautomería de una molécula de acetileno coordinada, $[Pt-C_2H_2]^+$, a vinilideno, $[Pt=C=CH_2]^+$, y la consiguiente formación de un nuevo enlace $C-C$ con el grupo metilo coordinado.

4. En la química del platino en estado de oxidación cero, las fosfinas de terfenilo han permitido aislar complejos de composición $[Pt(olefina)_2(PMe_2Ar')]$ y $[Pt(olefina)(PMe_2Ar')]$, asimismo insaturados en su coordinación y en sus requerimientos electrónicos, los cuales se comportan en disolución como fuentes del fragmento $[Pt(PMe_2Ar')]$, de gran interés por su capacidad para inducir la activación de enlaces $H-X$ o $C-X$. Dicho fragmento se genera, por ejemplo, en la reacción de los complejos anteriores con CO , que origina un clúster trinuclear $[Pt_3(\mu-CO)_3(PMe_2Ar')_3]$.

5. Además de una notable actividad química en reacciones estequiométricas de diversa naturaleza, los nuevos complejos de Pt(0) y Pt(II) de estos ligandos terfenilfosfina poseen una destacada actividad catalítica en reacciones de hidrosililación, hidroaminación o hidroarilación de alquinos. En particular, el complejo $[\text{Pt}(\text{CH}_2=\text{CH}'\text{Bu})(\text{PMe}_2\text{Ar}^{\text{Dipp}_2})]$ cataliza la hidrosililación de alquinos terminales como el fenilacetileno con conversiones próximas al 100% y elevada selectividad hacia la formación del correspondiente β -*E*-alquenilsilano, en condiciones de temperaturas moderadas (50-80 °C) y con bajas concentraciones de catalizador (0.02-0.1 mol%).